GENE EXPRESSION, BONE REMODELLING, AND MICRODAMAGE IN THE HUMAN PROXIMAL FEMUR: A MOLECULAR HISTOMORPHOMETRIC ANALYSIS OF OSTEOARTHRITIC BONE

A thesis submitted for the degree of

Doctor of Philosophy

by

JULIA SUZANNE KULIWABA

Department of Pathology

The University of Adelaide

and

Division of Tissue Pathology

Institute of Medical and Veterinary Science

Adelaide, Australia

January 2003

TABLE OF CONTENTS

CHAPTER 1
INTRODUCTION

CHAPTER 2

EXPERIMENTAL MATERIALS AND METHODS

CHAPTER 3

STABILITY OF RNA ISOLATED FROM HUMAN TRABECULAR BONE AT POSTMORTEM AND SURGERY

CHAPTER 4

mRNA EXPRESSION OF BONE CELL MARKERS AND REGULATORY FACTORS OF BONE REMODELLING IN HUMAN TRABECULAR BONE FROM THE ILIAC CREST AND PROXIMAL FEMUR

CHAPTER 5

mRNA EXPRESSION OF CYTOKINES, BONE CELL MARKERS, AND REGULATORY FACTORS OF OSTEOCLASTOGENESIS, IN TRABECULAR BONE FROM THE HUMAN PROXIMAL FEMUR

CHAPTER 8
TRABECULAR BONE MICRODAMAGE IN THE HUMAN PROXIMAL FEMUR: REGIONAL DISTRIBUTION AND THE INFLUENCE OF AGE AND OSTEOARTHRITIS ON DAMAGE MORPHOLOGY

ERRATA

Page 10, paragraph 2, line 13	Remove: "which are bipedal"
Page 90, line 21	Replace: "inactive" with "inactivate"
Figure 6.18, legend, line 3	Replace: "RANKL/OPG" with "RANK/OPG"
Page 170, paragraph 2, line 8	Replace: "cells types" with "cell types"
Figures 7.1-7.4, legend, line 2	Replace: "controls individuals" with "control individuals"

SUMMARY

Osteoarthritis (OA) is a common, age-related skeletal disease affecting both men and women, which causes significant morbidity and immobility. It is characterised by progressive degenerative damage to the articular joint cartilage, and is associated with a conservation of bone mass and a different, more rigid structure of the subchondral bone. The subchondral bone changes may therefore exacerbate the disease by transferring more of the load to the articular surface. Similar bone changes are also found at sites distal to the joint articular surface, in the proximal femur and in the iliac crest, suggesting that they are not simply reactive to the joint pathology. Thus, the bone changes may precede the joint degeneration of OA, or may arise secondarily to the joint pathology, or indeed may occur in parallel with the cartilage damage. Whichever of these is the case, in order to devise effective treatments for OA, it is clearly important to consider the bony component of this disease and to develop an understanding of the cellular and molecular processes that lead to the bony changes. Moreover, the cytokines and growth factors that regulate the differentiation and activity of the cell types that are directly responsible for the remodelling of bone, the osteoblast and osteoclast, have been studied extensively in cell culture systems and in animal models. Relatively little is known about the expression and production of these molecular factors in the local microenvironment of normal human bone, or in different bone pathologies, such as OA.

Therefore, this thesis has focused on trabecular bone remodelling, from both a molecular and histomorphometric perspective, at a skeletal site distal to the subchondral bone, the intertrochanteric region of the proximal femur, from OA patients undergoing joint

replacement surgery for primary OA of the hip, and age-matched adults, at autopsy, without any overt/known joint disease or any medical condition predicted to affect their bone turnover status.

Contiguous trabecular bone samples were analysed for messenger RNA (mRNA) expression of a selection of molecular factors involved in the regulation of bone remodelling, together with the histomorphometric quantitation of static indices of bone turnover, bone structural parameters, and microdamage parameters (microscopic cracks in the bone matrix targeted for repair by bone remodelling). High quality undegraded RNA was extracted from trabecular bone retrieved surgically (OA) and at autopsy (control), and semi-quantitative reverse transcription-polymerase chain reaction (RT-PCR) analysis was performed using a panel of oligonucleotides designed to amplify mRNA encoding a number of skeletally active molecules.

At first, it was established that total RNA and specific mRNA transcripts were relatively stable in bone tissues stored at 4°C up to 3.5 days postmortem. Secondly, the mRNA expression pattern of a number of bone cell markers and regulatory molecules of bone remodelling was not different between the proximal femur (intertrochanteric and femoral neck regions) and iliac crest, for a cohort of postmortem individuals. This finding was unexpected, given the known heterogeneity of bone turnover and architecture in the human skeleton.

Striking differences were observed in gene expression between OA and control trabecular bone at the intertrochanteric region of the proximal femur. OA bone showed significantly reduced interleukin (IL)-6 and IL-11 mRNA expression, two cytokines with predominantly

pro-resorptive roles in the bone microenvironment. In contrast, an age-dependent elevation in the mRNA expression of an osteoblastic cell marker, osteocalcin (OCN), was observed in OA bone compared with control bone. This finding is consistent with a reported increase in OCN protein in OA iliac crest bone, and also that at the intertrochanteric region there is maintenance of trabecular bone volume in OA.

Osteoclast differentiation requires direct contact between osteoclast precursors and osteoblastic cells, resulting from an essential interaction between receptor activator of nuclear factor kappa B (RANK) ligand, expressed on the surface of osteoblastic cells, and its receptor, RANK, located on the surface of osteoclast precursor cells and mature osteoclasts. A naturally occurring antagonist of RANKL, termed osteoprotegerin (OPG) can inhibit both the formation and activity of mature osteoclasts. There is extensive evidence from cell culture experiments that the local ratio of RANKL to OPG determines the effective activity of RANKL to promote osteoclast formation. The RANKL/OPG mRNA ratio was significantly lower in OA bone compared to controls. This finding suggests that osteoclast formation may be reduced in OA, and is consistent with the lower expression levels of mRNA encoding the osteoclastogenic cytokines IL-6 and IL-11 in OA bone. Furthermore, the bone resorption index, eroded surface (ES/BS), relative to the bone formation index, osteoid surface (OS/BS), was significantly reduced in OA bone compared to controls, consistent with reports of lower bone turnover in OA.

Intriguingly, when the histomorphometric and molecular analyses on contiguous bone samples were combined, there was a strong positive correlation between ES/BS and the RANKL/OPG mRNA ratio, independent of age, in controls. This finding suggests that, as more RANKL becomes available to promote osteoclast formation, there is an increase in

bone resorption. Further, trabecular bone volume (BV/TV) was inversely correlated to the ratio of RANKL/OPG mRNA. In addition, a strong positive association was found between OS/BS and the ratio of RANKL/OPG mRNA in the controls. This is the first direct evidence that RANKL and OPG are involved in human bone remodelling, consistent with the roles of RANKL and OPG in osteoclast development established from *in vitro* murine and human cell systems and *in vivo* murine gene deletion studies. Moreover, RANKL has been shown to be of central importance in determining the trabecular bone volume and turnover in the human bone microenvironment of the proximal femur. These relationships between the RANKL/OPG mRNA ratio and ES/BS, BV/TV, and OS/BS, observed in controls, were not evident in trabecular bone from severe primary OA, suggesting that bone turnover in the proximal femur may be regulated differently in this disease. Further, it can be speculated that the trabecular bone structures in OA arise by subversion of the physiological RANKL-controlled mechanisms.

Recent reports have shown that OA bone is less mineralised and the matrix collagen is disorganised, which could potentially significantly weaken the biomechanical properties of the bone matrix, resulting in collagen overproduction and thickening of the bone. Interestingly, the length and type of microscopic cracks in the bone matrix, specifically bone microdamage, differed between OA and control bone sampled from the intertrochanteric region of the proximal femur. Intriguingly, the proportion of bone matrix containing diffuse microdamage, focal collections of very fine microcracks, was higher in OA bone. Bone microdamage is targeted for repair, and thus subsequent removal, by stimulating a local bone remodelling response, *via* an unknown molecular mechanism. As the length of the microcracks increased, for the pooled OA and control data, there was an associated elevation in the mRNA expression of the pro-resorptive cytokine IL-11,

measured in contiguous bone samples. This finding is consistent with an increased stimulus for bone resorption in response to microdamage.

The experimental approach of *molecular histomorphometry*, to compare gene expression with trabecular bone structure and bone turnover, has provided the first description of the molecular events in the local bone microenvironment in OA. The data presented in this thesis support, but do not prove, the hypothesis that altered bone architecture may be the cause of primary OA. Furthermore, the experimental approach has great potential to uncover the mechanisms of normal bone turnover and of those that lead to the altered bone structures found in OA. If OA is caused or exacerbated by altered bone structure, it may be possible to find ways to modify or prevent the bone changes and thus delay joint degeneration. Such a finding would have important implications for the current treatment of OA, which is the surgical replacement of diseased joints.

DECLARATION

This work contains no material which has been accepted for the award of any degree or diploma in any university or other tertiary institution and, to the best of my knowledge, contains no material previously published or written by another person, except where due reference has been made in the text.

I give consent to this copy of my thesis, when deposited in the University Library, being available for loan and photocopying.

Julia S Kuliwaba

31 January, 2003

ACKNOWLEDGEMENTS

This study was supported by the Arthritis Foundation of Australia in the form of the Mary Paxton Gibson Scholarship.

I would like to express my sincere gratitude to my supervisors Associate Professor Nick L Fazzalari (Division of Tissue Pathology, Institute of Medical and Veterinary Science) and Associate Professor David M Findlay (Department of Orthopaedics and Trauma, The University of Adelaide), for allowing me to undertake my PhD in the Department of Pathology, The University of Adelaide, and in the Division of Tissue Pathology, the Institute of Medical and Veterinary Science, Adelaide. I would like to thank Assoc Prof Nick Fazzalari and Assoc Prof David Findlay, for your expert guidance, support, supervision, and constant enthusiasm.

I would like to thank Dr Mark R Forwood (Department of Anatomy and Developmental Biology, University of Queensland, Brisbane), for your expertise and time involved in collecting the data for the bone microdamage component of this thesis.

I would like to thank all of the families who generously donated postmortem bone tissues for research.

Thanks to the theatre staff at the Royal Adelaide Hospital, for their support and cooperation in the collection of surgical bone tissues, and to the mortuary staff of the Division of Tissue Pathology, for their support and cooperation in the collection of the invaluable postmortem bone tissues.

Thanks to the databank staff of the Department of Orthopaedics and Trauma, for their support in the collection of surgical case details.

I would like to thank Dr Gerald J Atkins, for your expertise and advice in helping me to develop my molecular techniques in the Orthopaedic and Trauma Bone Cell Laboratory, Hanson Institute, Adelaide.

Thanks to Mr Peter McNeil, for your technical expertise and advice on bone histology (Adelaide Centre for Spinal Research, Adelaide).

I would like to thank all of my fellow researchers in the Bone and Joint Research Laboratory and the Orthopaedic and Trauma Bone Cell Laboratory, for your technical advice and most importantly, moral support.

And, finally, I would like to express my special thanks and sincere gratitude to my parents for their endless support, encouragement, and generosity.

PUBLICATIONS ARISING

Kuliwaba J.S., Findlay D.M., Atkins G.J., Forwood M.R., and Fazzalari N.L. (2000) Enhanced expression of osteocalcin mRNA in human osteoarthritic trabecular bone of the proximal femur is associated with decreased expression of interleukin-6 and interleukin-11 mRNA. *Journal of Bone and Mineral Research* 15: 332-341.

Fazzalari N.L., **Kuliwaba J.S.**, Atkins G.J., Forwood M.R., and Findlay D.M. (2001) The ratio of messenger RNA levels of receptor activator of nuclear factor κB ligand to osteoprotegerin correlates with bone remodeling indices in normal human cancellous bone but not in osteoarthritis. *Journal of Bone and Mineral Research* 16: 1015-1027.

Fazzalari N.L., **Kuliwaba J.S.**, and Forwood M.R. (2002) Cancellous bone microdamage in the proximal femur: influence of age and osteoarthritis on damage morphology and regional distribution. *Bone* 31: 697-702.

PUBLISHED ABSTRACTS

Kuliwaba J.S., Forwood M.R., Findlay D.M., Fazzalari NL. (2002) Microdamage and cytokine messenger RNA expression in trabecular bone of the human proximal femur: a comparison between osteoarthritic and control bone. *Osteoarthritis and Cartilage* 10(Suppl A): S20.

Fazzalari N.L., **Kuliwaba J.S.**, Forwood M.R., Findlay D.M. (2002) Trabecular bone architecture in primary osteoarthritis. *Osteoarthritis and Cartilage* 10(Suppl A): S20-S21.

Kuliwaba J.S., Findlay D.M., Atkins G.J., Forwood M.R., Fazzalari N.L. (2001) Gene expression in human cancellous bone is similar between skeletal sites. *Journal of Bone and Mineral Research* 16(Suppl 1): S327.

Fazzalari N.L., **Kuliwaba J.S.**, Findlay D.M., Forwood M.R. (2001) Microdamage distribution and altered messenger RNA gene expression in the proximal femur. *Bone* 28(5) Suppl: S105.

Fazzalari N.L., **Kuliwaba J.S.**, Atkins G.J., Forwood M.R., Findlay D.M. (2001) Osteoclast differentiation factor is dominant in controlling the extent of bone resorption. *Bone* 28(5) Suppl: S160.

Findlay D.M., **Kuliwaba J.S.**, Atkins G.J., Fazzalari N.L. (2001) The ratio of ODF/RANKL to OPG increased with age in human cancellous bone. *Journal of Bone and Joint Surgery - British Volume* 83-B(Suppl III): 311.

Kuliwaba J.S., Findlay D.M., Atkins G.J., Forwood M.R., Fazzalari N.L. (2000) The role of osteoclast differentiation factor in determining trabecular bone structure in the human bone microenvironment. *Bone* 27(4) Suppl: S14.

Fazzalari N.L., **Kuliwaba J.S.**, Findlay D.M., Forwood M.R. (2000) Microdamage, IL-6 and CTR mRNA gene expression. *Bone* 27(4) Suppl: S18.

Fazzalari N.L., **Kuliwaba J.S.**, Findlay D.M., Forwood M.R. (2000) Microdamage distribution and IL-6 and CTR mRNA gene expression in the proximal femur. *Proceedings of the 12th Conference of the European Society of Biomechanics Dublin 2000*. p 44.

Kuliwaba J.S., Findlay D.M., Atkins G.J., Forwood M.R., Fazzalari N.L. (1999) Bone remodelling in osteoarthritic cancellous bone - a molecular histomorphometric study. *Journal of Bone and Mineral Research* 14(Suppl 1): S464.

Kuliwaba J.S., Findlay D.M., Atkins G.J., Forwood M.R., Fazzalari N.L. (1999) Gene expression in osteoarthritic cancellous bone is consistent with osteoarthritis being a disease of the skeleton. *SIROT 99: Papers presented at the International Meeting of the International Research Society of Orthopaedic Surgery and Traumatology*. Freund Publishing House, London, pp 437-441.

SCIENTIFIC COMMUNICATIONS

Kuliwaba J.S., Forwood M.R., Findlay D.M., Fazzalari N.L. Interleukin-11 messenger RNA expression and regional distribution of cancellous bone microdamage in the human proximal femur. *12th Annual Scientific Meeting of the Australian and New Zealand Bone and Mineral Society (ANZBMS)*. Adelaide, Australia, 6-9 October, 2002.

Kuliwaba J.S., Forwood M.R., Findlay D.M., Fazzalari N.L. Microdamage and cytokine messenger RNA expression in trabecular bone of the human proximal femur: a comparison between osteoarthritic and control bone. *7th World Congress of the Osteoarthritis Research Society International (OARSI)*. Sydney, Australia, 22-25 September, 2002.

Fazzalari N.L., **Kuliwaba J.S.**, Forwood M.R., Findlay D.M. Trabecular bone architecture in primary osteoarthritis. *7th World Congress of the OARSI*. Sydney, Australia, 22-25 September, 2002.

Kuliwaba J.S., Findlay D.M., Atkins G.J., Forwood M.R., Fazzalari N.L. Gene expression in human cancellous bone is similar between skeletal sites. *Annual Scientific Meeting of the Australian Society for Medical Research (ASMR) (South Australian Division)*. Adelaide, Australia, 30 May, 2002.

Kuliwaba J.S., Forwood M.R., Findlay D.M., Fazzalari N.L. Regional distribution of cancellous bone microdamage in the human proximal femur. *International Society for Fracture Repair Meeting: "Fracture and Bone Repair: Pushing the Boundaries"*. Clare, South Australia, Australia, 10-14 March, 2002.

Kuliwaba J.S., Findlay D.M., Atkins G.J., Forwood M.R., Fazzalari N.L. Differential gene expression in the human bone microenvironment of the hip: a comparison between osteoarthritic and control bone. *23rd Annual Lorne Genome Conference*. Lorne, Victoria, Australia, 17-21 February, 2002.

Kuliwaba J.S., Findlay D.M., Atkins G.J., Forwood M.R., Fazzalari N.L. Gene expression in human cancellous bone is similar between skeletal sites. *23rd Annual Lorne Genome Conference*. Lorne, Victoria, Australia, 17-21 February, 2002.

Kuliwaba J.S., Findlay D.M., Atkins G.J., Forwood M.R., Fazzalari N.L. Gene expression in human cancellous bone is similar between skeletal sites. *23rd Annual Meeting of the American Society for Bone and Mineral Research (ASBMR)*. Phoenix, Arizona, USA, 12-16 October, 2001.

Kuliwaba J.S., Findlay D.M., Atkins G.J., Forwood M.R., Fazzalari N.L. Gene expression in human cancellous bone is similar between skeletal sites. *11th Annual Scientific Meeting of the ANZBMS*. Auckland, New Zealand, 7-10 October, 2001.

Kuliwaba J.S., Findlay D.M., Atkins G.J., Forwood M.R., Fazzalari N.L. Gene expression in human cancellous bone is similar between skeletal sites. *7th Annual Scientific Meeting of the Australian and New Zealand Orthopaedic Research Society (ANZORS)*. Sydney, Australia, 5-6 October, 2001.

Kuliwaba J.S., Forwood M.R., Findlay D.M., Atkins G.J., Fazzalari N.L. Microdamage and cytokine messenger RNA expression in trabecular bone of the human proximal femur. *Annual Scientific Meeting of the ASMR (South Australian Division)*. Adelaide, Australia, 8 June, 2001.

Fazzalari N.L., **Kuliwaba J.S.**, Findlay D.M., Forwood M.R. Microdamage distribution and altered messenger RNA gene expression in the proximal femur. *1st Joint Meeting of the International Bone and Mineral Society (IBMS) and the European Calcified Tissue Society*. Madrid, Spain, 5-10 June, 2001.

Fazzalari N.L., **Kuliwaba J.S.**, Atkins G.J., Forwood M.R., Findlay D.M. Osteoclast differentiation factor is dominant in controlling the extent of bone resorption. *1st Joint Meeting of the IBMS and the European Calcified Tissue Society*. Madrid, Spain, 5-10 June, 2001.

Fazzalari N.L., **Kuliwaba J.S.**, Findlay D.M., Forwood M.R. Microdamage distribution and altered messenger RNA gene expression in the proximal femur. *4th Combined Meeting of the Orthopaedic Research Societies of the USA, Canada, Europe and Japan*. Rhodes, Greece, 1-3 June, 2001.

Fazzalari N.L., **Kuliwaba J.S.**, Atkins G.J., Forwood M.R., Findlay D.M. The ratio of messenger RNA levels of osteoclast differentiation factor (ODF) to osteoprotegerin (OPG) correlates with bone remodeling indices in normal human cancellous bone but not in osteoarthritis. *4th Combined Meeting of the Orthopaedic Research Societies of the USA, Canada, Europe and Japan*. Rhodes, Greece, 1-3 June, 2001.

Kuliwaba J.S., Findlay D.M., Atkins G.J., Forwood M.R., Fazzalari N.L. Differential gene expression in the human bone microenvironment of the hip; comparison between control and osteoarthritis. *13th Triennial Congress of the Asia Pacific Orthopaedic Association*. Adelaide, Australia, 1-6 April, 2001.

Kuliwaba J.S., Findlay D.M., Atkins G.J., Forwood M.R., Fazzalari N.L. The role of osteoclast differentiation factor in determining trabecular bone structure in the human bone microenvironment. *10th Annual Scientific Meeting of the ANZBMS: International Bone and Hormone Meeting*. Hamilton Island, Australia, 4–7 November, 2000.

Fazzalari N.L., **Kuliwaba J.S.**, Findlay D.M., Forwood M.R. Microdamage, IL-6 and CTR mRNA gene expression. *10th Annual Scientific Meeting of the ANZBMS: International Bone and Hormone Meeting*. Hamilton Island, Australia, 4–7 November, 2000.

Kuliwaba J.S., Findlay D.M., Atkins G.J., Forwood M.R., Fazzalari N.L. Differential gene expression in the human bone microenvironment of the hip; comparison between control and osteoarthritis. *11th Annual Scientific and Clinical Meeting of the Australian Rheumatology Association (ARA) (South Australian Branch)*. Adelaide, Australia, 20 October, 2000.

Findlay D.M., **Kuliwaba J.S.**, Atkins G.J., Fazzalari N.L. The ratio of ODF/RANKL to OPG increased with age in human cancellous bone. *6th Annual Meeting of the ANZORS*. Hobart, Australia, 13 October, 2000.

Fazzalari N.L., **Kuliwaba J.S.**, Findlay D.M., Forwood M.R. Microdamage distribution and IL-6 and CTR mRNA gene expression in the proximal femur. *12th Conference of the European Society of Biomechanics*. Dublin, Ireland, 27-30 August, 2000.

Kuliwaba J.S., Findlay D.M., Atkins G.J., Forwood M.R., Fazzalari N.L. The role of osteoclast differentiation factor in determining trabecular bone structure in the human bone microenvironment. *Annual Scientific Meeting of the Australian Orthopaedic Association (AOA) (South Australian Branch)*. Adelaide, Australia, 30 June, 2000.

Kuliwaba J.S., Findlay D.M., Atkins G.J., Forwood M.R., Fazzalari N.L. Gene expression of the osteoclastogenic factors ODF, OPG and RANK determines trabecular bone structure in the human bone microenvironment. *Annual Meeting of the ASMR (South Australian Division)*. Adelaide, Australia, 9 June, 2000.

Atkins G.J., **Kuliwaba J.S.**, Fazzalari N.L., Forwood M.R., Findlay D.M. The ratio of ODF/RANKL to OPG mRNA increases with age in human cancellous bone; comparison between osteoarthritic and control bone. *8th Workshop on Cell Biology of Bone and Cartilage in Health and Disease*. Davos, Switzerland, 1-4 April, 2000.

Kuliwaba J.S., Findlay D.M., Atkins G.J., Forwood M.R., Fazzalari N.L. Gene expression of the osteoclastogenic factors ODF, OPG and RANK determines trabecular bone structure in the human bone microenvironment. *An Academy of Science Boden 2000 Conference "The Human Skeleton – from molecules to structure and function"*. Clare, Australia, 26-29 March, 2000.

Findlay D.M., **Kuliwaba J.S.**, Atkins G.J., Forwood M.R., Fazzalari N.L. Bone cell signalling and regulation. *An Academy of Science Boden 2000 Conference "The Human Skeleton – from molecules to structure and function"*. Clare, Australia, 26-29 March, 2000.

Kuliwaba J.S., Findlay D.M., Atkins G.J., Forwood M.R., Fazzalari N.L. Bone remodelling in osteoarthritic cancellous bone - a molecular histomorphometric study. *10th Annual Scientific and Clinical Meeting of the ARA (South Australian Branch)*. Adelaide, Australia, 22 October, 1999.

Kuliwaba J.S., Findlay D.M., Atkins G.J., Forwood M.R., Fazzalari N.L. Bone remodelling in osteoarthritic cancellous bone. *5th Annual Meeting of the ANZORS.* Brisbane, Australia, 15 October, 1999.

Kuliwaba J.S., Findlay D.M., Atkins G.J., Forwood M.R., Fazzalari N.L. A molecular histomorphometric study of osteoarthritic cancellous bone. *8th World Congress of the International Society of Bone Morphometry.* Scottsdale, Arizona, USA, 6-10 October, 1999.

Kuliwaba J.S., Findlay D.M., Atkins G.J., Forwood M.R., Fazzalari N.L. Bone remodelling in osteoarthritic cancellous bone - a molecular histomorphometric study. *21st Annual Meeting of the ASBMR.* St Louis, Missouri, USA, 30 September – 4 October, 1999.

Kuliwaba J.S., Findlay D.M., Atkins G.J., Forwood M.R., Fazzalari N.L. Bone remodelling in osteoarthritic cancellous bone. *Annual Scientific Meeting of the AOA (South Australian Branch).* Adelaide, Australia, 13 August, 1999.

Kuliwaba J.S., Findlay D.M., Atkins G.J., Forwood M.R., Fazzalari N.L. Bone remodelling in osteoarthritic cancellous bone. *9th Annual Scientific Meeting of the ANZBMS.* Cairns, Australia, 30 June - 2 July, 1999.

Kuliwaba J.S., Findlay D.M., Atkins G.J., Forwood M.R., Fazzalari N.L. Bone remodelling in osteoarthritic cancellous bone. *Annual Meeting of the ASMR (South Australian Division).* Adelaide, Australia, 4 June, 1999.

Kuliwaba J.S., Findlay D.M., Atkins G.J., Forwood M.R., Fazzalari N.L. Gene expression in osteoarthritic cancellous bone is consistent with osteoarthritis being a disease of the skeleton. *International Meeting of the International Research Society of Orthopaedic Surgery and Traumatology.* Sydney, Australia, 16-19 April, 1999.

AWARDS

The following awards were received for original work in this thesis:

The Promega Student Award at the 23rd Annual Lorne Genome Conference. Lorne, Victoria, Australia, 18 February, 2002.

The Philip Alpers Award at the 11th Annual Scientific and Clinical Meeting of the Australian Rheumatology Association (South Australian Branch). Adelaide, Australia, 20 October, 2000.

The Royal Adelaide Hospital Medical Staff Society Research Prize. Adelaide, Australia, 27 June, 2000.

ABBREVIATIONS

bp	Base pair
cDNA	Complementary deoxyribonucleic acid
cm	Centimetre
CTR	Calcitonin receptor
DEPC	Diethyl pyrocarbonate
1,25-$(OH)_2D_3$	1,25-dihydroxyvitamin D_3
EDTA	Ethylenediaminetetra-acetic acid
GAPDH	Glyceraldehyde-3-phosphate dehydrogenase
H&E	Haematoxylin and eosin
IL-6	Interleukin-6
IL-11	Interleukin-11
kb	Kilobase pair
µg	Microgram
µl	Microlitre
µm	Micrometre
mg	Milligram
ml	Millilitre
mm	Millimetre
mM	Millimolar
mRNA	Messenger ribonucleic acid
M	Molar

OA	Osteoarthritis
OCN	Osteocalcin
OPG	Osteoprotegerin
OPN	Osteopontin
PCR	Polymerase chain reaction
PMI	Postmortem interval
PMIS	Sum of the postmortem and storage intervals
RANK	Receptor activator of nuclear factor kappa B
RANKL	Receptor activator of nuclear factor kappa B ligand
RNase	Ribonuclease
rRNA	Ribosomal ribonucleic acid
RT-PCR	Reverse transcription-polymerase chain reaction
SDS	Sodium dodecyl sulphate
SSC	Saline-sodium citrate
TAE	Tris-acetate EDTA
TGF-β	Transforming growth factor beta
TNF-α	Tumour necrosis factor alpha
TRAP	Tartrate-resistant acid phosphatase
UV	Ultraviolet
v/v	Volume per volume
w/v	Weight per volume

CHAPTER 1

INTRODUCTION

1.1 OSTEOARTHRITIS (OA)

1.1.1 Introduction

Osteoarthritis (OA) is a common age-related joint disease in both men and women. OA is characterised by relatively non-inflammatory degeneration of the articular cartilage and bony changes in the synovial joint. Symptoms of OA are localised to the affected joint, and include considerable pain, stiffness, and limitation of motion. OA is a major cause of incapacity, economic loss, and social disadvantage throughout the world's aged Caucasian populations. The aetiology of OA is undetermined and there are no proven treatments to reduce the severity or slow progression of this disease. For many sufferers of hip and knee OA, symptoms become sufficiently severe to require resolution by joint replacement surgery.

1.1.2 Classification

OA is classified as primary or idiopathic when it occurs in the absence of any known underlying predisposing factor. In contrast, secondary OA is where joint degenerative change is superimposed on a preceding abnormality such as local trauma, congenital dysplasia, calcium deposition disease, aseptic necrosis or osteopetrosis (Flores and Hochberg, 1998). Although the late stage pathological and radiological features are very similar in both primary and secondary OA (section 1.1.6), it is likely that different mechanisms are involved in the initiation of the disease.

1.1.3 Articular joints affected by OA

OA shows a predilection for lower extremity weight-bearing articular joints, such as the knee, hip, and spine. OA of the hand, specifically of the distal interphalangeal (Heberden's nodes) and first carpometacarpal joints, is more common in women than in men (Felson,

1998). Primary generalised OA is characterised by the familial development of hand OA and the premature degeneration of the articular cartilage of multiple joints, which may include the knee, hip, and cervical and lumbosacral spine (Kellgren and Moore, 1952).

1.1.4 Epidemiology

The reported epidemiological data for OA predominantly pertain to knee and hip OA. A number of systemic and local factors have been identified as putative risk factors for the development of OA. Systemic vulnerability factors include age, gender, racial characteristics, inherited susceptibility to OA (section 1.1.5), bone density (section 1.2.2), and oestrogen loss after menopause (Dequeker *et al.*, 1996; Hart *et al.*, 1999; Felson *et al.*, 1998; Felson and Zhang, 1998; Nevitt *et al.*, 1995; Spector *et al.*, 1996a; Van Saase *et al.*, 1989). OA has a higher prevalence, and more often exhibits a generalised distribution, in women than in men (Malchau *et al.*, 2002; Oliveria *et al.*, 1995; Van Saase *et al.*, 1989). A low prevalence of hip OA has been found in African black, American Indian, and Asian populations (Felson and Zhang, 1998). Local factors such as joint injury (major joint trauma and repetitive joint use), body mass index (BMI; strong relationship with knee OA), joint developmental deformity, and muscle weakness may alter the biomechanical environment of the joint and thus increase the joint's susceptibility to OA (Dougados *et al.*, 1992; Felson *et al.*, 1997; Gelber *et al.*, 2000; Hadler *et al.*, 1978; Felson *et al.*, 1991; Kujala *et al.*, 1995; Neyret *et al.*, 1993; Sharma *et al.*, 2001; Slemenda *et al.*, 1998; Solomon, 1976; Spector *et al.*, 1994; Spector *et al.*, 1996b; Zhang *et al.*, 1996).

1.1.5 Genetics

Family and twin studies on subsets of patients with OA of the hands (Heberden's nodes), hip and/or knee, have shown a significant genetic contribution to OA, which is

independent of environmental and confounding factors such as gender, age, and BMI (Demissie *et al.*, 2002; Hirsch *et al.*, 1998; Ingvarsson, 2000; Felson *et al.*, 1998; Lanyon *et al.*, 2000; Lindberg, 1986; Spector *et al.*, 1996a). Chitnavis *et al.* (1997) reported that siblings, relative to a control group, had nearly twice the risk of total hip replacement and nearly five times the risk of total knee replacement for primary OA. In addition, this group reported that 27% and 31% of the disease variance of OA of the hip and knee, respectively, is likely to be genetically determined (Chitnavis *et al.*, 1997). A twin study in females demonstrated that 39% of the variance of knee OA, graded radiographically for osteophytes and joint space narrowing (section 1.1.6.3), was attributable to genetic factors, independent of known environmental or demographic confounders (Spector *et al.*, 1996a). Studies of potential candidate genes for OA have included polymorphisms of the 1,25-dihydroxyvitamin D_3 (1,25-$(OH)_2D_3$) receptor (VDR) locus in association with knee and hip OA (Aerssens *et al.*, 1998; Keen *et al.*, 1997; Uitterlinden *et al.*, 1997), the type II procollagen (COL2A1) gene (Aerssens *et al.*, 1998; Vikkula *et al.*, 1993), and the insulin-like growth factor type I (IGF-I) gene in association with radiographically identified OA of the hip (Meulenbelt *et al.*, 1998). Collectively, these studies indicate that individuals with primary OA are likely to have a significant genetic component, which is independent of environmental and demographic factors.

1.1.6 Pathology of OA

It is possible that the different presentations of OA, with different spectra of joints involved, indicate that OA is actually a cluster of diseases, with the common feature of relatively non-inflammatory degeneration of the articular cartilage. Further, it is likely that different pathophysiological mechanisms are involved in the initiation of the disease

process. However, advanced or end-stage OA, regardless of the initiating event, shows similar pathological and radiological features.

1.1.6.1 Articular cartilage degeneration

Articular cartilage is a highly specialised and uniquely designed bio-material that forms the smooth, gliding surface of the diarthrodial joints. It is an avascular, aneural, and alymphatic matrix, which is synthesised by the sparsely distributed chondrocyte cells (Muir, 1995). The cartilage matrix consists of a dense scaffold of insoluble collagen fibres and soluble proteoglycan molecules; the major proteoglycan is aggrecan. The proteoglycans (primarily aggrecan) associate with water, generating a swelling pressure that is resisted by the collagen fibres resulting in a tissue that is able to absorb compression and shock (Carney and Muir, 1988; Maroudas, 1976). In normal adult cartilage, chondrocytes maintain a balance between synthesis and degradation of extracellular matrix components. However, in OA, new matrix synthesis is outweighed by the breakdown of matrix components, resulting in the degeneration and gradual loss of articular cartilage. The degradation of cartilage matrix components in OA has been shown to be due to an increased synthesis and activation of extracellular proteinases, such as the matrix metalloproteinases (MMPs) and the recently identified aggrecanases (Arner *et al.*, 1999; Billinghurst *et al.*, 1997; Cawston *et al.*, 1999; Tetlow *et al.*, 2001). The pathological features of the articular cartilage in advanced OA include the total loss of cartilage from large areas of the joint surface, with eburnation of the exposed bone (i.e., the bone surface becomes smooth and burnished). Most of the remaining cartilage is fibrillated and fissured, and there is a loss of joint surface congruity (Collins, 1949). Variable degrees of synovial inflammation are seen in advanced OA, which is a response to an increased release of cartilage degradation products into the synovial fluid, such as fragments of aggrecan,

cartilage oligomeric matrix protein (COMP), and type II collagen C-propeptide (Lohmander and Felson, 1998).

1.1.6.2 Subchondral bone changes

The articular cartilage is supported, and separated from the underlying subchondral trabecular bone, by the subchondral plate. The subchondral plate, consisting of calcified cartilage and subchondral cortical bone, transmits loads from the cartilage into the trabecular bone beneath. This underlying subchondral trabecular or cancellous bone is composed of thin plates and rods, or trabeculae, oriented in a lattice structure. The interstices between the trabeculae are filled with cellular marrow. Bone is vascularised, metabolically active, and a highly organised tissue consisting of a mineral phase of hydroxyapatite and calcium phosphate crystals deposited in an organic matrix. The mineral component of bone makes the tissue hard and rigid, whilst the organic component gives bone its flexibility and resilience. Bone is constantly remodelled or renewed (by the coupled processes of bone resorption and bone formation; section 1.3.2) to maintain the mechanical integrity of the skeleton and for the maintenance of calcium homeostasis (section 1.3.3). The pathological features of the subchondral bone in advanced OA include sclerosis, with increased trabecular thickness and decreased inter-trabecular spacing (Fazzalari *et al.*, 1985; Fazzalari *et al.*, 1992), which appears to be a result of increased bone remodelling activity (Grynpas *et al.*, 1991; Jeffery, 1973). However, it is not known whether adaptational bone formation or bone modelling (i.e., bone formation in the absence of bone resorption) is involved in the subchondral bone sclerosis in advanced OA. In addition, the subchondral bone develops cysts, and osteophytic outgrowths at the joint margins (Collins, 1949). The development of bony osteophytes occurs by endochondral ossification (i.e., calcified cartilage that is remodelled into bone; Jeffery, 1973). The

altered trabecular architecture of OA subchondral bone is associated with altered mechanical properties, such that the tissue is rendered more rigid and less able to absorb shock (Li and Aspden, 1997b). These changes in the subchondral bone may therefore exacerbate the disease by transferring more of the load to the articular surface (Radin *et al.*, 1972).

1.1.6.3 Radiographic grading of OA

Currently, diagnosis of OA is based on clinical examination, symptoms, and radiographic assessment. OA is defined radiographically by joint space narrowing, loss and fibrosis of articular cartilage, subchondral bone sclerosis, cyst formation, and bony osteophytes at the joint margins (Kellgren and Lawrence, 1963). The onset of OA is usually insidious, occurring long before it can be detected with current clinical and radiographic methods. Thus, permanent and irreversible damage to the joint structure has often occurred by the time the clinical diagnosis is made. The development of sensitive and reliable methods for early diagnosis of OA, and for monitoring disease progression, is essential for the implementation of preventative treatment strategies, which may avoid the need for joint replacement surgery (Buckwalter *et al.*, 2001). Recently, Beuf *et al.* (2002) have reported on the use of high-resolution magnetic resonance imaging (MRI) for the characterisation of subchondral trabecular bone changes in different stages of knee OA. In addition, MRI can be used to evaluate articular cartilage volume, thickness, and degeneration (Disler *et al.*, 1996; Eckstein *et al.*, 1997; Stammberger *et al.*, 1999). Beuf *et al.* (2002) have suggested that MRI is an emerging clinical modality that allows investigation of the clinical relationship between bone and cartilage and the onset and progression of OA. Many reports have described the increased release of markers of cartilage (eg., fragments of aggrecan, COMP, and type II collagen C-propeptide), bone (eg., bone sialoprotein,

osteocalcin), or synovial (eg., hyaluronic acid, MMPs) metabolism into the synovial fluid, serum, and urine in OA (reviewed in Lohmander and Felson, 1998). Potentially, assays for these biochemical markers could be used to detect and/or monitor development of OA. However, most biochemical marker assays are still at the level of research.

1.2 THE ROLE OF BONE IN THE PATHOGENESIS OF OA

An understanding of all the joint structures involved in OA, including the cartilage, bone, joint capsule, synovial membrane, ligaments, and tendons, will help to develop sensitive and reliable methods for early diagnosis, and to devise preventative and treatment strategies to avoid the need for joint replacement surgery. Research into the aetiology of OA has predominantly focussed on understanding the mechanism of breakdown and loss of articular cartilage. Furthermore, OA has been considered primarily to be a cartilaginous disorder (Bland and Cooper, 1984). However, there is now substantial evidence in spontaneous OA animal models (section 1.2.1) that there is a change in the density and metabolism of bone, particularly of subchondral bone, before any evidence of cartilage fibrillation (Dequeker and Luyten, 2000). Furthermore, alterations in bone density, trabecular bone structure, bone mineralisation, bone growth factor content, and osteoblast cell activity have been observed in primary human OA (sections 1.2.2-1.2.7). These observations lend support to the hypothesis that primary OA may primarily be a bone disorder, in which more dense bone, with less shock absorbing capacity, would transfer the stress of loading directly to the articular surface, promoting degeneration in the cartilage, as first proposed by Radin *et al.* (1972).

1.2.1 Early subchondral bone changes in spontaneous OA animal models

Studies of animals, which naturally develop medial compartment knee OA with age (i.e., spontaneous OA animal models), have shown that early changes are evident in the subchondral bone before any fibrillation of the cartilage occurs. All of these spontaneous OA animal models show OA pathology similar to that seen in human OA. Of the three OA animal models discussed below, the spontaneous OA guinea pig model is emerging as the leading animal model for studying the pathogenesis of primary OA and the potential effectiveness of new drug therapies (Billingham, 1998).

1.2.1.1 STR/ORT mouse

Spontaneous OA occurs in the medial tibiofemoral compartment of the knee in STR/ORT mice (Sokoloff, 1956; Walton, 1977a; Walton, 1977b). The incidence and severity of knee OA is greater in male than in female STR/ORT mice (Collins *et al.*, 1994; Walton, 1977a; Walton, 1977b). An MRI study has shown early calcification of the patellar tendon before any evidence of articular cartilage damage (Munasinghe *et al.*, 1995). However, other studies have shown that the first indication of articular cartilage degeneration occurs at the junction of the cartilage with the cruciate ligament on the medial tibial condyle (Walton, 1977a; Walton, 1977b). Anderson-MacKenzie *et al.* (1999) have shown that collagen metabolism in the cruciate ligament is up-regulated before any OA cartilage degeneration or subchondral bone changes are evident. Consequently, the cruciate ligament is weaker in male STR/ORT mice, which may destabilise the knee joint, alter the load, and trigger the OA cartilage degeneration and subchondral bone remodelling (Anderson-MacKenzie *et al.*, 1999). Interestingly, medial tibial articular cartilage degeneration and subchondral bone thickening are closely related pathologically and chronologically in male STR/ORT mice (Walton and Elves, 1979). Walton and Elves (1979) reported that the subchondral bone

sclerosis in male STR/ORT mice was due to reduced osteoclastogenesis (i.e., reduced numbers of osteoclasts, the bone-resorbing cells; section 1.3.1.1), rather than increased osteoblastic activity (i.e., the bone-forming cells; section 1.3.1.2). Thus, the authors concluded that bone turnover was abnormally low in male STR/ORT mice (Walton and Elves, 1979).

1.2.1.2 Dunkin Hartley guinea pig

Spontaneous OA occurs in the medial compartment of the knee in male Dunkin Hartley guinea pigs (Bendele and Hulman, 1988; Meacock *et al.*, 1990). MRI studies of the Dunkin Hartley guinea pig have shown that subchondral bone changes are evident prior to any obvious articular cartilage degeneration (Watson *et al.*, 1996). Recently, Anderson-MacKenzie *et al.* (2002) have shown that metabolic bone remodelling is increased in the subchondral bone of the Dunkin Hartley guinea pig before any changes in bone density or cartilage pathology are detected. The Strain 13 guinea pig displays less severe spontaneous OA in comparison to the Dunkin Hartley guinea pig (Huebner *et al.*, 2002). The Dunkin Hartley guinea pig has increased bone metabolism (increased serum markers of bone resorption and formation) at a young age, with persistence of a greater rate of bone formation at 12 months of age when OA is severe (Huebner *et al.*, 2002). Interestingly, the Dunkin Hartley guinea pig also demonstrated higher knee bone mineral density (an absorptiometric estimate of the total amount of bone mineral; BMD) at 12 months of age, compared with the Strain 13 guinea pig (Huebner *et al.*, 2002). Young *et al.* (2002) recently described the deposition of fibrocartilage in the cruciate ligament of the Dunkin Hartley guinea pig before any cartilage degeneration or subchondral bone changes were evident. The authors suggest that cruciate ligament stiffening could precede, and thus provide a stimulus for, the early subchondral bone changes, or alternatively, that the

chondrogenesis in the ligament may be a response to bone remodelling processes already occurring (Young *et al.*, 2002). Quasnichka *et al.* (2002) also reported increased collagen metabolism in the cruciate ligament of the Dunkin Hartley guinea pig, which was associated with an increased laxity of the ligament.

1.2.1.3 Cynomolgus monkey

Spontaneous OA occurs in the medial compartment of the knee in male and female cynomolgus monkeys (Carlson *et al.*, 1994; Carlson *et al.*, 1995; Carlson *et al.*, 1996). The earliest histological change in the medial tibial plateau was a thickening of the subchondral bone plate, which was followed by fibrillation of the cartilage (Carlson *et al.*, 1994). In addition, Carlson *et al.* (1996) have shown that cartilage degenerative changes were not evident until the subchondral bone had thickened to a significant degree. As the disease progressed and increased in severity, subchondral bone thickened in the lateral tibial plateau and femoral condyles (Carlson *et al.*, 1994). The prevalence and severity of OA increased with age, but were independent of gender and weight (Carlson *et al.*, 1996). Interestingly, as in humans, OA in cynomolgus monkeys can occur in young individuals and spares certain older individuals (Carlson *et al.*, 1996). The advantage of this spontaneous OA animal model is that the OA occurs in middle-aged animals (average age of 12 years), which are bipedal. However, the disadvantages of this animal model are that it is long-term and expensive.

1.2.2 Bone mineral density in OA patients

A number of reports have described hip and knee OA individuals to have a better preserved bone mass (measured as hip and spine bone mineral density; BMD) compared to age- and sex-matched controls, independent of BMI (Gotfredsen *et al.*, 1990; Lethbridge-

Cejku *et al.*, 1996; Nevitt *et al.*, 1995). Two recent reports have shown that bone changes may precede cartilage changes in the onset and progression of primary OA (Bruno *et al.*, 1999; Goker *et al.*, 2000). Bruno *et al.* (1999) reported that proximal femur BMD is elevated when there are early radiographic signs of hip OA. Goker *et al.* (2000) reported that elevated local and remote BMD is associated with a subsequent accelerated joint space narrowing rate of the hip. Interestingly, the rare congenital disorder, osteopetrosis, is characterised by a marked increase in bone density and early-onset OA in patients who reach adulthood (Milgram and Jasty, 1982). Intriguingly, primary OA and osteoporosis are rarely both seen in the same patient, and clinical reports and epidemiological studies have suggested that there is a negative association between the two age-related diseases (Cooper *et al.*, 1991; Dequeker *et al.*, 1993a; Dequeker *et al.*, 1996; Soloman *et al.*, 1982; Verstraeten *et al.*, 1991). Osteoporosis is characterised by a reduced amount of bone, leading to a fragile skeleton, which is more susceptible to fracture. The more supple bone in osteoporosis may be a better shock absorber in synovial joints and therefore may spare the cartilage and protect against OA. Hart *et al.* (2002) recently reported that women with previous fractures had a reduced risk of subsequently developing knee OA, which was independent of BMD status. The mechanism to explain the inverse relationship between primary OA and osteoporosis remains unclear.

1.2.3 Trabecular bone architecture at distal skeletal sites

Subchondral bone in advanced primary hip OA is sclerotic, with increased trabecular bone volume due to increased trabecular thickness and decreased inter-trabecular spacing, compared to age-matched controls (Crane *et al.*, 1990; Fazzalari *et al.*, 1985; Fazzalari *et al.*, 1992). It has been postulated that such changes are due to alteration of loading through the joint because of the articular disease (Bland and Cooper, 1984) or, alternatively that

they are secondary to pathology within the joint. However, similar trabecular bone structural changes are also present at sites distal to the joint articular surface, in the proximal femur (at the intertrochanteric region, more than 15 cm from the joint surface) and in the iliac crest (Crane *et al.*, 1990; Fazzalari *et al.*, 1992). In addition, Gevers *et al.* (1989a) have reported increased iliac crest trabecular bone volume and trabecular thickness in individuals with OA of the hands. Iliac crest bone has been studied in OA as a skeletal site distal from the affected joint structures, as it is not subject to loading abnormalities or joint pathological changes. The observation of altered trabecular bone architecture at distal skeletal sites suggests that these architectural changes are not merely reactive to the joint pathology.

1.2.4 Hypomineralised bone

The trabecular bone structural changes in OA (section 1.2.3) may develop to compensate for an altered bone matrix structure and composition in OA. A number of reports have described OA subchondral femoral head and femoral neck trabecular bone to be hypomineralised (i.e., less mineralised; Brown *et al.*, 2002; Grynpas *et al.*, 1991; Helliwell *et al.*, 1996; Li and Aspden, 1997a; Li and Aspden, 1997b; Mansell and Bailey, 1998). Type I collagen forms approximately 90% of the organic mass of bone. The triple helix of type I collagen is composed of two $\alpha 1$ chains and one $\alpha 2$ chain of type I collagen (van der Rest and Garrone, 1991). The ability of bone collagen to provide a strong framework and to fully mineralise depends on the very precise alignment of the type I collagen molecules in the collagen fibre (Kielty *et al.*, 1994). Interestingly, a recent study has shown that subchondral bone osteoblasts, from individuals with hip OA, produce a molecularly distinct collagen, type I collagen homotrimer (i.e., three $\alpha 1$ chains of type I collagen; Bailey *et al.*, 2002). A decreased enthalpy (i.e., the energy required to denature the triple

helix) of the type I collagen homotrimer fibre indicated that the homotrimer molecules are more loosely packed in the fibre (Bailey *et al.*, 2002). Furthermore, the collagen fibres appeared to be narrower and aligned in a disorganised manner in OA subchondral bone (Bailey *et al.*, 2002). The type I collagen homotrimer is suggested to be mechanically weaker and less mineralised in bone (McBride *et al.*, 1998; Misof *et al.*, 1997).

1.2.5 Biomechanical properties of OA bone

Subchondral and femoral neck trabecular bone from hip OA subjects has been reported to be materially weaker (i.e., less stiff and dense) compared with age-matched controls (Li and Aspden, 1997a). However, biomechanical studies of OA subchondral and femoral neck trabecular bone cores have shown the bone to be stiffer or more rigid (Li and Aspden, 1997a; Li and Aspden, 1997b; Martens *et al.*, 1983). The biomechanical properties of a trabecular bone core are influenced by the bone matrix composition and trabecular bone architecture. The more rigid subchondral trabecular bone in OA is associated with trabecular bone architectural changes, such as increased trabecular bone volume, and altered trabecular size and spacing (section 1.2.3; Crane *et al.*, 1990; Fazzalari *et al.*, 1992). Interestingly, in individuals with hand OA, increased trabecular bone volume and trabecular thickness at the iliac crest is associated with increased biomechanical stiffness (Gevers *et al.*, 1989b). Since the more rigid subchondral bone would have a reduced ability to absorb shock, it has been postulated that the bone changes in OA might exacerbate the disease or could even precede and be causative of the cartilage degeneration (Radin *et al.*, 1972; Radin *et al.*, 1978; Radin *et al.*, 1991).

1.2.6 Bone matrix growth factor composition

Consistent with the concept of generalised bone changes in OA (sections 1.2.2-1.2.5), bone matrix from the iliac crest of individuals with hand OA has been found to contain a higher content of the growth factors, insulin-like growth factor types I and II (IGF-I and IGF-II) and transforming growth factor (TGF)-β, compared with that in control subjects (Dequeker *et al.*, 1993b). These anabolic growth factors are thought to be locally released and activated during the bone resorption phase, acting to link bone resorption to bone formation in the remodelling cycle (Hayden *et al.*, 1995; Linkhart *et al.*, 1996). The higher concentrations of these growth factors in OA iliac crest bone may act to maintain bone mass in OA individuals (section 1.2.2). In addition, OA iliac crest bone matrix has significantly increased osteocalcin (OCN) content, compared with that in control subjects (Dequeker *et al.*, 1993b; Gevers and Dequeker, 1987; Raymaekers *et al.*, 1992). OCN is a major non-collagenous protein of the bone matrix and it is utilised as an indicator of bone formation as it is one of the marker genes for the progression of osteoblastic differentiation (Stein and Lian, 1993). OCN has been implicated to play a role in the regulation of bone mineral turnover (Boskey *et al.*, 1998). However, the biological function of OCN in the bone microenvironment has not been precisely defined. Interestingly, vitamin K, which is needed for gamma-carboxylation of OCN, has been reported to be increased in iliac crest bone and in serum from OA patients, compared to osteoporotic patients (Wakabayashi *et al.*, 2000).

1.2.7 An altered OA osteoblast phenotype

Biochemical studies have shown an increase in the metabolism of subchondral bone collagen in individuals with hip OA, compared to age-matched controls (Mansell *et al.*, 1997; Mansell and Bailey, 1998). Dequeker *et al.* (1993b) postulated that there may be an

increased biosynthetic activity of osteoblasts in OA, a possibility supported by Hilal *et al.* (1998) showing that bone explants and osteoblasts from OA medial tibial subchondral bone produced more IGF-I and alkaline phosphatase (a bone formation marker) than controls. Furthermore, Hilal *et al.* (1998) have shown an increase in *de novo* OCN synthesis, in response to 1,25-$(OH)_2D_3$ stimulation, by OA osteoblasts *in vitro*. Given that the phenotypic alterations in the OA subchondral osteoblast-like cells were observed in *ex vivo* and *in vitro* experiments, Hilal *et al.* (1998) have suggested that the altered OA osteoblast phenotype may be caused by a primary defect in these cells, rather than a secondary response to local chemical and/or systemic factors *in vivo*. Intriguingly, Westacott *et al.* (1997) have shown that the secretory products of OA subchondral osteoblasts are capable of altering cartilage matrix metabolism. Specifically, the co-culture of OA subchondral osteoblast-like cells, derived from individuals with knee and hip OA, with non-OA cartilage explants resulted in enhanced cartilage matrix degradation (Westacott *et al.*, 1997). The specific cellular and molecular interaction between bone and cartilage in OA has not been defined. Furthermore, it is not known whether an interaction between bone and cartilage occurs during the initiation and/or progression of the OA disease process.

1.3 BONE REMODELLING

1.3.1 Cells of bone

1.3.1.1 The Osteoclast

The unique bone-resorbing cell, the osteoclast, is a large motile cell often displaying multinucleation with irregular cytoplasmic branches. Osteoclasts are formed by the fusion of mononuclear progenitor cells of the monocyte-macrophage lineage (Suda *et al.*, 1997). The resorption of mineralised bone matrix is accomplished by the osteoclast attaching to

the bone surface (mediated by integrin receptors) and creating a "sealing zone" to isolate the bone area to be resorbed from the extracellular environment. The osteoclast then secretes proteolytic enzymes (such as cathepsin K) into the space between the bone and the osteoclast plasma membrane (the resorption lacunae), which removes the osteoid and exposes the bone mineral. The osteoclast pumps acid (*via* the activities of carbonic anhydrase II and the vacuolar proton ATPase) into the resorption lacunae *via* the ruffled border, an osteoclast-specific organelle, which dissolves the bone mineral leaving a pit in the bone surface (Roodman, 1996). In trabecular bone, these pits appear as shallow, scalloped bays in the surface of the bone and are termed Howship's lacunae. Resorption activity of the osteoclast can be rapidly terminated by the binding of calcitonin to the calcitonin receptor on the cell surface, which is used experimentally as an osteoclast marker (Hattersley and Chambers, 1989). Another osteoclast marker is the enzyme tartrate-resistant acid phosphatase (Minkin, 1982).

Considerable progress has been made towards an understanding of the mechanisms responsible for the formation and activation of osteoclasts. A large number of hormones and cytokines have been identified that can stimulate the development of osteoclasts from their haematopoietic precursors (Martin and Ng, 1994; Martin *et al.*, 1998; Martin and Udagawa, 1998). Cell-to-cell contact between cells of the osteoblast lineage and haemopoietic cells is necessary for inducing differentiation of osteoclasts (Martin and Udagawa, 1998). A cell-surface member of the tumour necrosis factor (TNF)-ligand family, termed receptor activator of nuclear factor kappa B ligand (RANKL), was shown to be central in osteoclast development and activity (Lacey *et al.*, 1998; Wong *et al.*, 1997; Yasuda *et al.*, 1998b). Agents that induce bone resorption, including 1,25-$(OH)_2D_3$, parathyroid hormone (PTH), prostaglandin E_2 (PGE_2), and interleukin (IL)-11, have been

shown to induce the presentation of RANKL on the surface of osteoblastic cells, which are then able to promote osteoclast formation (Horwood *et al.*, 1998; Udagawa *et al.*, 1999; Yasuda *et al.*, 1998b). RANKL binds to a TNF-receptor superfamily member, RANK (Anderson *et al.*, 1997; Hsu *et al.*, 1999), which is expressed on the surface of osteoclasts and their precursors (Hsu *et al.*, 1999). RANK has been shown to be essential for osteoclast formation; anti-RANK antibodies inhibit osteoclast formation *in vitro* (Nakagawa *et al.*, 1998), and RANK-deficient mice exhibit profound osteopetrosis and lack osteoclasts (Dougall *et al.*, 1999; Li *et al.*, 2000). In addition, over-expression of soluble RANK in transgenic mice resulted in osteopetrosis, decreased numbers of osteoclasts, and decreased bone resorption (Hsu *et al.*, 1999). Furthermore, mice deficient in RANKL lack osteoclasts and develop osteopetrosis (Kong *et al.*, 1999). Likewise, a natural RANKL antagonist, a soluble TNF-receptor family member, termed osteoprotegerin (OPG), can inhibit osteoclast formation and bone resorption (Simonet *et al.*, 1997). Over-expression of OPG in mice resulted in an osteopetrotic phenotype and decreased numbers of osteoclasts (Simonet *et al.*, 1997), while mice in which the OPG gene is deleted develop extensive osteoporosis and increased numbers of osteoclasts (Bucay *et al.*, 1998; Mizuno *et al.*, 1998). Furthermore, administration of recombinant murine OPG protects against ovariectomy-associated bone loss in rats, *via* a reduction in osteoclast number and subsequent increase in bone volume (Simonet *et al.*, 1997). OPG is expressed by a wide variety of cell types, including osteoblasts, in which its expression is down-regulated by many of the same factors that promote bone resorption and RANKL expression (Hofbauer *et al.*, 1999b). Thus, there is now good evidence that the local amount of RANKL, relative to OPG, is important in osteoclast formation (Hofbauer *et al.*, 2000).

1.3.1.2 The Osteoblast

The bone-forming cell, the osteoblast, is derived from the multipotent mesenchymal stem cell, which also gives rise to fibroblasts, bone marrow stromal cells, chondrocytes, muscle cells, and adipocytes (Manolagas and Jilka, 1995). The differentiation of osteoblasts is dependent on the expression of the osteoblast-specific transcription factor, core binding factor a1 (Cbfa1; Ducy *et al.*, 1997). Cbfa1-deficient mice lack osteoblasts and osteoclasts, and develop with a normally patterned skeleton that is made exclusively of cartilage (Komori *et al.*, 1997). The bone morphogenetic proteins (BMPs) are capable of initiating osteoblastogenesis from mesenchymal progenitors (Rosen *et al.*, 1996). A number of growth factors, including fibroblast growth factors (FGFs), IGFs, platelet-derived growth factor, and TGF-β, are able to stimulate the proliferation and differentiation of committed osteoblast progenitors toward the osteoblastic lineage (Centrella *et al.*, 1994; Hayden *et al.*, 1995; Mundy, 1996). Osteoblasts are identified morphologically by their cuboidal appearance and by their association with newly synthesised bone matrix (osteoid) at sites of active bone formation. The plasma membrane of the osteoblast is rich in alkaline phosphatase, which is used as a biochemical marker of bone formation (Calvo *et al.*, 1996). The osteoblasts produce and secrete proteins that constitute the bone matrix. These bone-associated matrix proteins include type I collagen, osteocalcin (OCN), osteonectin, osteopontin (OPN), and bone sialoprotein (Karsenty, 1999). All of these proteins have been implicated in the regulation of the mineralisation process (i.e., the process of deposition of hydroxyapatite; Boskey, 1996).

OCN and OPN are both marker genes for the progression of osteoblastic differentiation (Denhardt and Noda, 1998; Stein and Lian, 1993). However, OPN is also expressed at high levels in osteoclasts (Dodds *et al.*, 1995). The biological function of OCN and OPN in the

bone microenvironment has not been precisely defined. Mice deficient in OCN have increased bone density, cortical thickness, and bone formation (Ducy *et al.*, 1996). However, osteoblast number was not altered in OCN deficient mice, suggesting that the role of OCN in the bone microenvironment is an inhibitor of osteoblast function (Ducy *et al.*, 1996). Subsequently, those investigators reported that bone mineral maturation was impaired in OCN-deficient mice, suggesting that OCN is involved in the regulation of bone mineral turnover (Boskey *et al.*, 1998). Interestingly, there were significantly more osteoclasts per unit surface in the OCN-deficient mice than in the wild-type mice (Ducy *et al.*, 1996). Conversely, OCN has been shown to be important for osteoclast recruitment both in *in vitro* and in animal models (Chenu *et al.*, 1994; DeFranco *et al.*, 1991; Glowacki *et al.*, 1989; Glowacki *et al.*, 1991; Ingram *et al.*, 1994; Liggett *et al.*, 1994). For instance, OCN may act in combination with other non-collagenous proteins, such as OPN, as a signal for osteoclastic bone resorption (Reinholt *et al.*, 1990; Ritter *et al.*, 1992). *In vitro*, OPN has been shown to be an extracellular signalling molecule for osteoclasts and endothelial cells, *via* binding of OPN to the cell surface $\alpha_v\beta_3$ integrin (Denhardt and Noda, 1998; Liaw *et al.*, 1995). Furthermore, OPN has been shown to be required for vascularisation by endothelial cells and subsequent osteoclastic bone resorption in an ectopic bone-resorbing model, in which wild-type and OPN-deficient bone discs were implanted into wild-type and OPN knockout mice (Asou *et al.*, 2001).

1.3.1.3 The Osteocyte

Osteocytes are terminally differentiated osteoblasts that have become buried within lacunae of the mineralised bone matrix. The osteocyte is the most abundant cell type in bone tissue; there are approximately 10 times as many osteocytes as osteoblasts (Parfitt, 1977). Osteocytes have a stellate shape with long cytoplasmic processes that extend

through small canals (canaliculi) in the bone matrix to connect with, and enable communication with, adjacent osteocytes and bone lining surface cells (Nijweide *et al.*, 1996). *In situ* hybridisation and immunohistochemical studies have shown that osteocytes express a range of bone-matrix proteins, including type I collagen, osteocalcin, osteonectin, and osteopontin (Mason *et al.*, 1996; Nijweide *et al.*, 1996).

The osteocytes collectively form a mechanosensory system, which is sensitive to mechanical stress (Burger and Klein-Nulend, 1999). Mechanical stress in bone causes deformation (strain) of the bone matrix, which is thought to initiate the mechanotransduction pathway in the osteocytic canalicular network (Forwood and Turner, 1995). The strain causes interstitial fluid to flow through the osteocytic canalicular network (Weinbaum *et al.*, 1994). *In vitro*, fluid flow has been shown to greatly affect osteocyte metabolism. Osteocytes are affected by direct fluid shear stress and by the movement of ions over their cell surface, which modulates the production of signalling molecules, such as nitric oxide and prostaglandins (such as PGE_2; Klein-Nulend *et al.*, 1995; Klein-Nulend *et al.*, 1997; Pitsillides *et al.*, 1995). These factors in turn may act to stimulate other factors, such as IGF-I and OPN, that regulate bone formation and bone resorption by osteoblasts and osteoclasts, respectively (Lean *et al.*, 1995; Terai *et al.*, 1999). In addition to sensing mechanical strain, it has been proposed that osteocytes may also detect microdamage within bone and direct its removal through their apoptosis (section 1.3.3.1; Verborgt *et al.*, 2000). However, the molecular mechanism(s) of the activation of osteoclasts and osteoblasts, which lead to site-specific bone remodelling after the osteocytic detection of mechanical stress or microdamage, have not been fully elucidated.

1.3.2 The bone remodelling cycle

Bone remodelling or bone turnover is the coordinated process whereby small packets of bone are eroded and replaced with new bone by an organised group of cells, the basic multicellular unit (BMU; Parfitt, 1994). Remodelling is a dynamic process occurring constantly throughout the mature skeleton, replacing approximately 10% of the skeleton per year (Parfitt, 1994). This process enables hypermineralised and/or damaged bone to be replaced, structural alterations to be made, and mineral homeostasis to be maintained. There are four distinct phases in the remodelling cycle: activation, resorption, reversal, and formation. These processes are temporally and spatially distinct, occurring sequentially at any single site, and occurring simultaneously at different locations, respectively (Parfitt, 1994).

Activation is the process that converts a quiescent bone surface into an active remodelling surface. Osteoclasts are activated at specific focal sites on the bone surface by mechanisms that are not well understood. In some circumstances, this site-specific activation of osteoclasts may involve bone matrix microdamage (section 1.3.3.1). The activation phase involves resorption of the thin layer of osteoid covering the bone surface, by the resident bone lining cells (Chambers *et al.*, 1985), and their retraction to expose the mineralised surface to osteoclasts. This is followed by fusion of the mononuclear osteoclasts and the tight attachment of the osteoclast to the mineralised surface. Resorption is a dynamic process, with multinucleated osteoclasts working in teams producing a moving resorption front. In cortical bone this results in a cutting cone burrowing through the tissue. In trabecular bone this results in an irregular scalloped cavity on the surface of the bone (Howship's lacunae). The reversal phase is characterised by the disappearance of multinucleated osteoclasts (osteoclast apoptosis; Hughes *et al.*, 1996) and the appearance

of mononuclear cells, which may be of the macrophage lineage. The majority of resorption results from the action of multinuclear osteoclasts. However, it has been suggested that mononuclear cells, found in resorption pits after the departure of multinuclear osteoclasts, are responsible for up to one third of resorption (Eriksen, 1986). During this period the resorbed surface is smoothed, a non-collagenous cement layer is laid down, and a thin layer of collagen is deposited by bone lining cells (Everts *et al.*, 2002). The initiation of bone formation involves the chemotactic attraction of osteoblast precursors to the site of previous resorption. This process is likely mediated by local factors produced during bone resorption, with evidence from *in vitro* studies of the chemotactic effect of BMP-2, IGFs, osteopontin, and TGF-β (Dodds *et al.*, 1995; Hayden *et al.*, 1995; Lind *et al.*, 1996; Pfeilschifter *et al.*, 1990b). Once attracted to the site of previous resorption, osteoblast precursors proliferate and differentiate into mature osteoblasts, influenced by local growth factors released from the bone matrix during resorption, such as the IGFs and TGF-β (Hayden *et al.*, 1995; Mundy, 1999). The assembled team of osteoblasts begins production of new matrix, in the form of osteoid, which is subsequently mineralised. As the resorption front proceeds, so does the formation front, with newly exposed portions of the Howship's lacunae occupied by newly differentiated osteoblasts. Formation occurs at a much slower rate than resorption (approximately 3 months versus 2 weeks; Parfitt, 1994), resulting in osteoblasts rather than osteoclasts, representing a larger proportion of the cells active on bone at any time. As formation continues, osteoblasts are incorporated into the matrix and differentiate into osteocytes, connecting with other osteocytes in the newly synthesised section of bone (Parfitt, 1994).

1.3.3 Functions of bone remodelling

Bone remodelling fulfils metabolic functions, replacing bone matrix in a stochastic fashion throughout the skeleton in response to a systemic requirement for calcium. Superimposed on this is targeted remodelling of bone as a response to microdamage (section 1.3.3.1; Burr, 2002). Thus, some BMUs may be "targeted" at (i.e., initiated by, and in proximity to) microdamage, while others serve purposes through "stochastic" or "random" remodelling (Burr, 2002; Martin, 2000; Parfitt, 2002). The proportion of total bone remodelling that is stochastic and that is targeted is not known. This proportionality is likely to differ between skeletal regions given the heterogeneity of the human skeleton (Parfitt, 1996). Furthermore, it is not known whether similar or independent mechanisms are involved in the regulation of stochastic and targeted remodelling.

1.3.3.1 The repair of bone microdamage by targeted bone remodelling

Mechanical strain is an important stimulus for the maintenance of normal bone metabolism (Frost, 2000). However, repetitive loading causes skeletal fatigue or microdamage, resulting in the microscopic cracking of the ultra-structural bone matrix (Burr *et al.*, 1997). The accumulation of microdamage in bone has been shown to contribute to the loss of bone quality or biomechanical properties (Burr *et al.*, 1997; Carter *et al.*, 1981; Carter and Hayes, 1977; Forwood and Parker, 1989; Mashiba *et al.*, 2000; Pattin *et al.*, 1996; Schaffler *et al.*, 1989). *In vivo*, microdamage may accumulate in a bone faster than the bone's capacity to repair that damage. Microdamage is thought to play an important role in fractures attributed to aging or osteoporosis (Burr *et al.*, 1997).

Mori and Burr (1993) first demonstrated that microdamage initiates its repair by targeted bone remodelling, by fatigue loading dog long bones and observing a subsequent increase

in osteoclastic resorption. Bentolila *et al.* (1998) tested the hypothesis that bone fatigue loading *in vivo*, which induces *in vivo* microdamage, can activate the remodelling process in adult rat long bones, in which haversian remodelling (i.e., cortical bone remodelling) characteristically does not occur. Ten days after fatigue loading of adult rat ulnae, intracortical resorption was activated (Bentolila *et al.* 1998). Moreover, numerical microcrack density was reduced by almost 40% by ten days after fatigue loading. Intriguingly, intracortical resorption was associated with both bone microdamage and regions of altered osteocyte and canalicular integrity (Bentolila *et al.* 1998). Subsequently, those investigators reported that microdamage induced osteocyte apoptosis, which may provide an important local signal to remodel a damaged area of bone (Verborgt *et al.*, 2000; Verborgt *et al.*, 2002). However, at this time, the nature and mechanism of the stimulus to recruit osteoclasts to begin the targeted bone remodelling process, to remove the bone microdamage, is unknown.

1.3.4 Molecular factors involved in the regulation of bone remodelling

Bone mass is preserved in the healthy skeleton by a tight balance between the amount of bone resorbed and formed during each cycle of remodelling. The strict regulation of bone remodelling is achieved by the coordinated actions of a variety of systemic and local factors, identified *in vitro* and in animal models, which act either directly or indirectly on bone cells.

1.3.4.1 Systemic regulation

The two principal calcium-regulating hormones, PTH and the active metabolite of vitamin D_3, 1,25-$(OH)_2D_3$, are involved in the regulation of bone turnover. PTH is a potent stimulator of osteoclastic bone resorption and has biphasic effects on bone formation

(Roodman, 1999). There is an acute inhibition of collagen synthesis with high concentrations of PTH, but prolonged intermittent administration of PTH produces increased bone formation (Dempster *et al.*, 1993). This latter property of PTH has been explored clinically (reviewed in Crandall, 2002), and PTH has recently been approved as an anabolic agent for the treatment of established osteoporosis in postmenopausal women who are at high risk of a fracture. 1,25-$(OH)_2D_3$ is a potent stimulator of bone resorption and osteoclast formation, and is also involved in bone formation (Roodman, 1999). The stimulatory effects of PTH and 1,25-$(OH)_2D_3$ on osteoclastic bone resorption appear to be mediated by the induction of RANKL expression on marrow stromal/osteoblastic cells (Horwood *et al.*, 1998; Lee and Lorenzo, 1999; Yasuda *et al.*, 1998b). Oestrogen deficiency in postmenopausal women results in an increase in bone remodelling, in which resorption exceeds formation and thus bone mass decreases. The mechanism responsible for the increased bone turnover with oestrogen deficiency is not fully understood, but the pro-resorptive cytokines IL-1, IL-6, IL-7, and TNF-α have been implicated in this process (Jilka, 1998; Manolagas, 1995; Manolagas and Jilka, 1995; Pacifici, 1998; Weitzmann *et al.*, 2002). Other systemic factors involved in the regulation of bone turnover include the prostaglandins (particularly PGE_2), calcitonin, androgen, growth hormone (acting through IGF production), thyroid hormone, and the glucocorticoids (Roodman, 1999).

1.3.4.2 Local regulation

Signals that promote osteoclast differentiation appear to act *via* receptors expressed by cells of the osteoblast lineage (Martin and Ng, 1994), suggesting that *in situ,* localised activation of osteoclastogenesis leads to site-directed bone remodelling. RANKL, RANK, and OPG are key molecular regulators of osteoclast biology and bone metabolism (section 1.3.1.1). RANKL is expressed on the cell surface of stromal/osteoblastic cells and

promotes osteoclast development by binding to its cognate receptor, RANK, which is expressed on the surface of osteoclasts and their precursors, with the required presence of macrophage colony stimulating factor (M-CSF; Anderson *et al.*, 1997; Hsu *et al.*, 1999; Lacey *et al.*, 1998; Nakagawa *et al.*, 1998; Wong *et al.*, 1997; Yasuda *et al.*, 1998b). OPG is a natural antagonist for RANKL and inhibits osteoclast formation and bone resorption (Simonet *et al.*, 1997). Extensive bone marrow cell culture studies have shown that RANKL, OPG, and to a lesser extent, RANK, are modulated by cytokines, growth factors, and hormones known to affect bone metabolism (Hofbauer *et al.*, 2000; Hofbauer and Heufelder, 2001; Horowitz *et al.*, 2001; Suda *et al.*, 1999). These modulators include PTH, 1,25-$(OH)_2D_3$, oestrogen, glucocorticoids, TGF-β, BMP-2, basic FGF, PGE_2, and the pro-resorptive cytokines IL-1, IL-6, IL-11, and TNF-α (Hofbauer *et al.*, 2000; Hofbauer and Heufelder, 2001; Horowitz *et al.*, 2001; Suda *et al.*, 1999).

IL-6 and IL-11 are two cytokines that share many biological properties, including the ability to stimulate osteoclast development from their haematopoietic precursors (Martin *et al.*, 1998). IL-6 is produced by a number of cell types in the bone microenvironment, including marrow stromal cells, monocyte-macrophages, osteoblasts, and osteoclasts (Girasole *et al.*, 1992; Kishimoto, 1989; Linkhart *et al.*, 1991; O'Keefe *et al.*, 1997). The reported effects of IL-6 on RANKL-RANK-promoted osteoclast development are conflicting (Brandstrom *et al.*, 1998; Hofbauer *et al.*, 1998; Hofbauer *et al.*, 1999b; Nakashima *et al.*, 2000; O'Brien *et al.*, 1999; Vidal *et al.*, 1998). It has been suggested that IL-6 may attenuate calcium sensing and thus enhance bone resorption by a direct effect on mature osteoclast activity (Adebanjo *et al.*, 1998). Interestingly, while expression of IL-6 mRNA in the bone is contributed by several cell types, IL-11 mRNA is likely to be expressed predominantly by cells of mesenchymal origin, namely, cells of the osteoblast

lineage (Paul *et al.*, 1990). IL-11 has been suggested to play a critical role in the hierarchy of osteoclastogenic factors, since *in vitro* its expression is induced by a number of hormone and local activators of osteoclast formation (Manolagas, 1995; Romas *et al.*, 1996; Yang and Yang, 1994). In addition, neutralisation of IL-11 has been shown *in vitro* to suppress osteoclast development induced by 1,25-$(OH)_2D_3$, PTH, IL-1, and TNF-α (Girasole *et al.*, 1994). The effects of IL-11 on osteoclast differentiation appear to be mediated by inducing RANKL expression on marrow stromal/osteoblastic cells (Nakashima *et al.*, 2000; Yasuda *et al.*, 1998b). Furthermore, the bone-resorptive effect of IL-11 in neonatal mouse calvarial bone cultures resulted in dose-dependent increases in RANKL and OPG mRNA (Ahlen *et al.*, 2002). However, in contrast to observations in mouse bone marrow cultures (Girasole *et al.*, 1994; Romas *et al.*, 1996), Ahlen *et al.* (2002) have demonstrated that IL-11 did not play an important role in the resorptive effects of PTH and 1,25-$(OH)_2D_3$ in the mouse calvarial bone culture experimental system. IL-6 and IL-11 have also been implicated as suppressors of osteoblastic synthetic activity (Hughes and Howells, 1993a; Hughes and Howells, 1993b). However, a recent report of over-expression of IL-11 in transgenic mice suggests that this cytokine functions as an anabolic factor for bone *in vivo* (Takeuchi *et al.*, 2002). The full role of these pleiotropic cytokines in the bone microenvironment is not completely understood.

1.4 SUMMARY AND AIMS OF THESIS

Evidence from spontaneous OA animal models suggest that a change in the density and metabolism of subchondral bone occurs before any signs of cartilage fibrillation (section 1.2.1). In addition, there have been numerous reports of alterations in bone density, trabecular bone structure, bone mineralisation, bone growth factor content, and osteoblast cell activity in subchondral bone, and at skeletal sites distal to the joint articular surface, in

primary human OA individuals (sections 1.2.2-1.2.7). Collectively, these studies suggest that the bone changes may precede the joint degeneration of OA, or may arise secondarily to the joint pathology, or indeed may occur in parallel with the cartilage damage, driven by the same causative agent(s) that lead to cartilage disease. Whichever of these is the case, in order to devise effective treatments for OA, it is clearly important to consider the bony component of this disease and to develop an understanding of the cellular and molecular processes that lead to the bony changes. Moreover, the cytokines and growth factors that regulate the differentiation and activity of the cell types that are directly responsible for the remodelling of bone, the osteoclast and osteoblast, have been studied extensively in cell culture systems and in animal models. Relatively little is known about the expression and production of these molecular factors in the local microenvironment of normal human bone, or in different bone pathologies, such as OA.

Therefore, this thesis has focused on trabecular bone remodelling, from both a molecular and histomorphometric perspective, at a skeletal site distal to the subchondral bone, the intertrochanteric region of the proximal femur, from OA patients undergoing joint replacement surgery for primary OA of the hip, and age-matched adults, at autopsy, without any overt/known joint disease or any medical condition predicted to affect their bone turnover status.

The general aims of this thesis are listed below:

- To investigate the stability of total RNA and bone-specific mRNAs in human postmortem and surgical trabecular bone tissues (Chapter 3).

- To investigate whether there are skeletal site differences in the mRNA expression of bone cell markers and factors known to have important regulatory roles in bone remodelling, in human postmortem trabecular bone sampled from the iliac crest, and femoral neck and intertrochanteric regions of the proximal femur (Chapter 4).

- To describe and compare the pattern of mRNA expression of factors known to have important regulatory roles in bone remodelling in trabecular bone sampled from the intertrochanteric region of the proximal femur, between individuals with primary hip OA and a postmortem non-diseased/control group (Chapters 5 and 6).

- To describe and compare the histomorphometric parameters describing trabecular structure and bone turnover, in trabecular bone sampled from the intertrochanteric region, between individuals with primary hip OA and a postmortem non-diseased/control group (Chapter 7).

- To examine and compare the relationships between the histomorphometric parameters describing trabecular structure and bone turnover, and the levels of expression of mRNA corresponding to factors known to have important regulatory roles in bone remodelling, measured in contiguous bone samples from the intertrochanteric region,

between individuals with primary hip OA and a postmortem non-diseased/control group (Chapter 7).

- To describe and compare the morphometric parameters describing the extent of bone microdamage, in trabecular bone sampled from the intertrochanteric region, between individuals with primary hip OA and a postmortem non-diseased/control group (Chapter 8).

CHAPTER 2

EXPERIMENTAL MATERIALS AND METHODS

2.1 MATERIALS

2.1.1 General chemicals and reagents

2.1.1.1 Chemicals supplied by BDH Laboratory Supplies

The following chemicals and reagents were obtained from BDH Laboratory Supplies, MERCK, Kilsyth, VIC, Australia.

Acetone

Basic Fuchsin

Ethanol

Ethylenediaminetetra-acetic acid (EDTA)

Ethylene glycol monoethyl ether

Chloroform

Formaldehyde 40% solution

Glycerol

Isoamyl alcohol

Isopropanol

Methyl methacrylate

Bis (4-tert-butyl cyclohexyl) peroxydicarbonate (perkadox 16)

Polyethyleneglycol 400 (PEG-400)

Sarkosyl NL30

Sodium hydroxide

Xylene

2.1.1.2 Chemicals supplied by ICN Biomedicals Inc.

The following chemicals and reagents were obtained from ICN Biomedicals Inc., Aurora, OH, USA.

Diethyl pyrocarbonate (DEPC)

Formamide

Guanidine thiocyanate

3-[N'-morpholino] propane-sulphonic acid (MOPS)

2.1.1.3 Chemicals supplied by Sigma Chemical Company Ltd.

The following chemicals and reagents were obtained from Sigma Chemical Co. Ltd., St Louis, MO, USA.

Bromophenol blue
Dextran sulphate
Dithiothreitol (DTT)
Ethidium bromide
Herring sperm DNA
β-mercaptoethanol
Phenol
Sephadex G_{50}
Sodium acetate
Sodium chloride
Sodium citrate
Sodium dodecyl sulphate (SDS)
Tris [hydroxymethyl] aminomethane (Tris)-HCl

2.1.1.4 Sources of other routinely used chemicals

Agarose DNA grade Low melt agarose	Progen Industries, QLD, Australia
DNA 100 bp ladder	GeneWorks, SA, Australia
Deoxyribonucleotide triphosphates (dNTP's)	Amersham Pharmacia Biotech, Uppsala, Sweden
Random hexamers	GeneWorks, SA, Australia
SYBR® Gold nucleic acid gel stain	Molecular Probes, Eugene, OR, USA

2.1.2 Enzymes

The enzymes were obtained from the following companies:

AmpliTaq Gold® DNA polymerase	Applied Biosystems, Foster City, CA, USA
Superscript™ II reverse transcriptase	Invitrogen, Life Technologies, Carlsbad, CA, USA

2.1.3 Radionucleotides

[α-^{32}P] deoxycytidine triphosphate (dCTP), 3000Ci/mM	GeneWorks, SA, Australia

2.1.4 Kits

Oligolabelling of DNA (Gigaprime kit)	GeneWorks, SA, Australia
Purification of PCR products (Wizard PCR preps DNA purification system)	Promega Biosciences, Madison, WI, USA

2.1.5 Buffers and solutions

All solutions were prepared in RNase-free glassware, using either DEPC-treated and autoclaved water or Milli-Q purified water. The DEPC-treated water was prepared by treating Milli-Q water with 0.1% (v/v) DEPC, a potent inhibitor of RNases, for a minimum of 12 hours at 37°C, and then autoclaved. The autoclave treatment is important, as it removes all traces of DEPC. Any residual DEPC may modify purine residues in RNA by carboxymethylation.

DNA loading buffer (6X)	0.25% bromophenol blue, 40% (w/v) sucrose in water
MOPS buffer (10X)	0.2 M MOPS, 50 mM sodium acetate, 10 mM EDTA, (pH 8.0)
RNA loading buffer (2X)	50% formamide, 6.2% formaldehyde, 10% glycerol, 30 μg/ml ethidium bromide, 1 X MOPS buffer
RNA lysis buffer	4 M guanidine thiocyanate, 25 mM sodium citrate (pH 7.0), 0.5% sarkosyl, 100 mM β-mercaptoethanol
SSC (20X)	3 M sodium chloride, 0.3 M sodium citrate, (pH 7.0)
TAE	40 mM Tris-acetate, 1 mM EDTA, (pH 8.0)
TE	10 mM Tris-HCl, 1 mM EDTA, (pH 8.0)

2.1.6 Synthetic oligonucleotides

RT-PCR oligonucleotide primers GeneWorks, SA, Australia

(Refer to Table 2.1 for primer sequences)

2.1.7 Miscellaneous

Hybond™-N^+ nucleic acid transfer membrane	Amersham Pharmacia Biotech, Buckinghamshire, UK

2.2 METHODS

2.2.1 Human bone tissue samples

The profiles of the human postmortem cases and surgical primary osteoarthritis (OA) of the hip cases, from which the trabecular bone tissues were sampled, are described in detail in the methods section of each relevant chapter. The following sections, 2.2.1.1 and 2.2.1.2, provide a generalised description of the human postmortem and surgical OA cases, in particular the skeletal sites from which the trabecular bone was sampled and the initial processing and storage of the bone tissue samples, before subsequent RNA isolation and/or histological analysis.

2.2.1.1 Human postmortem bone tissue

Proximal femurs and for a subset of cases, the iliac crest, were obtained from routine autopsies performed at the Royal Adelaide Hospital, Adelaide, SA, Australia. The postmortem case details, including age, gender, anatomical side, postmortem interval, and cause of death, are listed in Tables 3.1, 3.2, 4.1, and 5.1. With the exception of the experiments described in Chapters 3 and 4, which investigate the stability of RNA isolated from human postmortem bone tissues and skeletal site differences in mRNA expression, respectively, the postmortem cases were selected using the following criteria: no known history of any chronic condition or disease, which may have affected bone status (such as renal dysfunction or endocrine disease affecting bone metabolism); no known history of any medication which may have affected bone turnover; admitted to hospital less than 3

days before death; and on macroscopic and radiological assessment of the proximal femur showed no significant sign of joint degeneration, according to the criteria of Collins (1949). Based upon these exclusion criteria, the postmortem cases were thus categorized as *control* cases in this thesis. Further, pertaining to all postmortem cases, cases were excluded if there was any evidence of hepatitis or HIV; from patient history and a blood test of arterial blood taken at autopsy.

2.2.1.1.1 Sampling of trabecular bone from the proximal femur

Trabecular bone was sampled from the intertrochanteric region of the proximal femur for each postmortem case (Figure 2.1). In addition, for a subset of cases, trabecular bone was sampled from the subchondral principal compressive and medial principal compressive regions (for microdamage assessment, Chapter 8; Figure 2.3), or the femoral neck region (for investigation of stability of RNA isolated from human postmortem bone tissues, Chapter 3; and for assessment of skeletal site differences in mRNA expression, Chapter 4; Figure 2.1) of the proximal femur. Initially, each proximal femur was sectioned in the coronal plane using a band saw, which had been cleaned with DEPC-treated water, to allow access to trabecular bone for sampling from the femoral neck and intertrochanteric regions, which are enclosed within the femoral cortex. Using sterile bone cutters, the trabecular bone tissue was sampled as small fragments from an approximate 1.5 x 1.0 cm^2 area, to a specimen depth of 0.5 cm, from the femoral neck and intertrochanteric regions. The trabecular bone tissue fragments were rinsed briefly in DEPC-treated water (the rinsed material contained trabecular bone and bone marrow) and then immersed in RNA lysis buffer (4 M guanidine isothiocyanate solution, section 2.1.5; 2 ml/250 mg wet weight), and stored at -70°C until RNA isolation. The remaining coronal half of each proximal femur was stored frozen until required for undecalcified histological analysis (section 2.2.3).

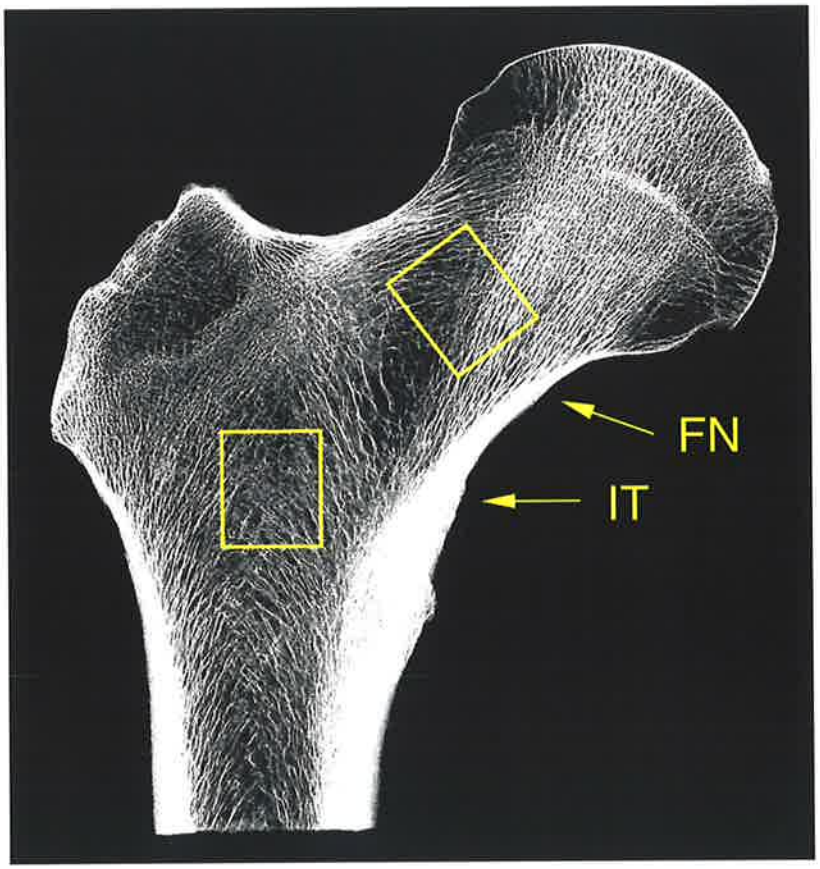

Figure 2.1: X-ray of a 5 mm-thick para-coronal slice through a human proximal femur which shows the regions of trabecular bone sampling for RNA isolation and histomorphometric analysis; femoral neck (FN) and intertrochanteric (IT).

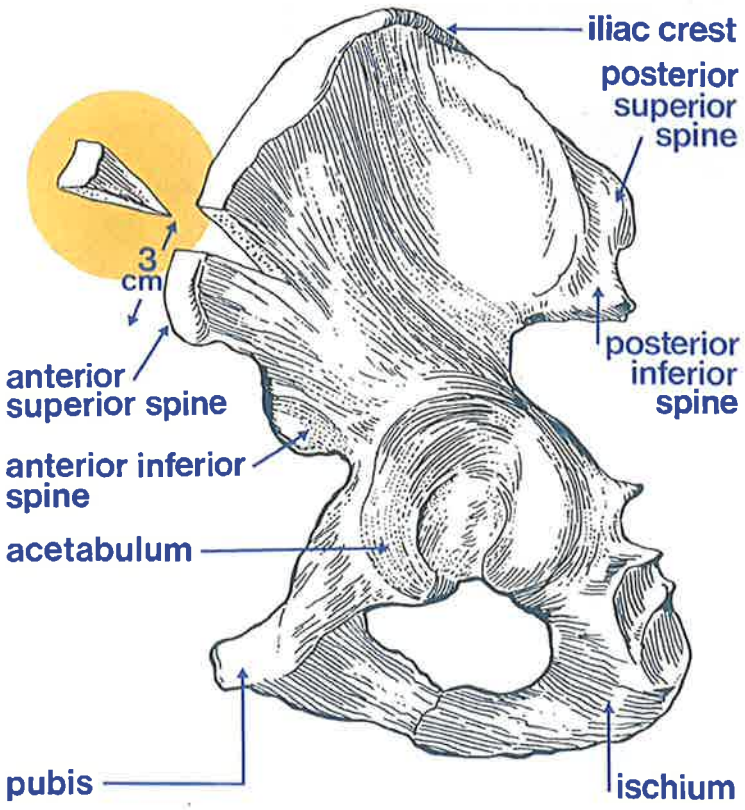

Figure 2.2: A wedge of bone was sampled from the iliac crest at a point 3 cm posterior to the antero-superior iliac spine from postmortem cases.

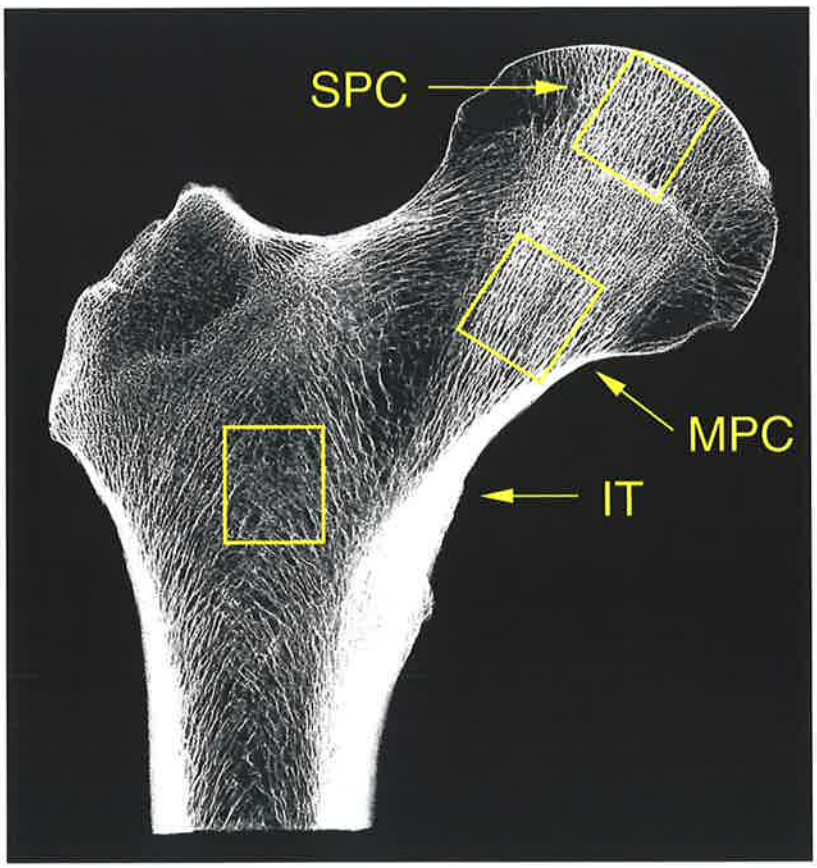

Figure 2.3: X-ray of a 5 mm-thick para-coronal slice through a human proximal femur which shows the regions of trabecular bone sampling for microdamage assessment; subchondral principal compressive (SPC), medial principal compressive (MPC), and intertrochanteric (IT).

2.2.1.1.2 Sampling of trabecular bone from the iliac crest

Trabecular bone was sampled from the iliac crest for a subset of postmortem cases (for investigation of stability of RNA isolated from human postmortem bone tissues, Chapter 3; and for assessment of skeletal site differences in mRNA expression, Chapter 4). The iliac crest was sampled as a wedge of bone at a point 3 cm posterior to the antero-superior iliac spine (Figure 2.2; Crane *et al.*, 1990; Fazzalari *et al.*, 1992). Each iliac crest bone sample was bisected longitudinally, in an antero-posterior plane, using a band saw, which had been cleaned with DEPC-treated water, to access the trabecular bone enclosed within the cortical shell. Using sterile bone cutters, the trabecular bone tissue was sampled as small fragments from an approximate 1.0 x 1.0 cm^2 area, to a specimen depth of 0.5 cm. The trabecular bone tissue fragments, consisting of trabecular bone and the encased bone marrow, were rinsed briefly in DEPC-treated water and then immersed in RNA lysis buffer (4 M guanidine isothiocyanate solution, section 2.1.5; 2 ml/250 mg wet weight), and stored at -70°C until RNA isolation.

2.2.1.2 Human surgical OA bone tissue

Proximal femur surgical specimens were obtained from patients undergoing total hip arthroplasty for advanced primary OA at the Royal Adelaide Hospital. The surgical OA case details, including age, gender, anatomical side, and macroscopic grade of the femoral head and acetabulum, are listed in Table 6.1. The clinical diagnosis of OA is based on radiological investigation (Kellgren and Lawrence, 1963), and patient history determines whether the OA is classified as primary in nature. In addition, the orthopaedic surgeon graded the macroscopic appearance of the femoral head and acetabulum at surgery by assessment of the location and degree of fibrillation and degeneration, according to the criteria of Collins (1949). For all OA cases selected in this thesis, the macroscopic grade of

the femoral head and acetabulum at surgery was severe, characterised by cartilage loss, eburnation of bone, osteophytes, and remodelling of the articular contour (Table 6.1). Patients suspected of having secondary OA, inflammatory joint disease, Paget's disease, drug-induced disease or other conditions, which may have affected the trabecular bone architecture and quality, were excluded.

2.2.1.2.1 Sampling of trabecular bone from the intertrochanteric region of the OA proximal femur

At total hip arthroplasty surgery, a 10 mm internal diameter tube saw was used to take a trabecular bone core biopsy of the intertrochanteric region (Figure 2.1), taken in line with the femoral medullary canal (Fazzalari *et al.*, 1998b), from OA patients. The intertrochanteric region was chosen for sampling for the following reasons: the trabecular architecture in this region depends upon stresses in the proximal femoral shaft while being remote from the subchondral bone that undergoes well-characterised secondary changes in severe OA (Fazzalari *et al.*, 1985; Fazzalari *et al.*, 1992); the region has previously been shown to be structurally different between OA and control bone (Crane *et al.*, 1990); and a trabecular bone core biopsy from this region is easily obtainable during total hip arthroplasty surgery, as this region is reamed and the bone usually discarded. The intertrochanteric bone core biopsies, 10 mm in diameter and 3-5 cm in length, were placed in cold (4°C) sterile RNase-free 0.85% saline and transported directly to the laboratory. Within 12 hours after retrieval at surgery, RNA was extracted from the bone samples as follows: trabecular bone tissue was sampled as small fragments from an approximate tube saw length of 1-2 cm, using sterile bone cutters and/or a sterile scalpel blade. The trabecular bone tissue fragments were rinsed briefly in DEPC-treated water (the rinsed material contained trabecular bone and bone marrow) and then immersed in RNA lysis

buffer (4 M guanidine isothiocyanate solution, section 2.1.5; 2 ml/250 mg wet weight), and stored at -70°C until RNA isolation (section 2.2.2.1). The remaining contiguous pieces of the intertrochanteric trabecular bone samples, 10 mm in diameter and 2-3 cm in length, were stored frozen until required for undecalcified histological analysis (section 2.2.3).

2.2.1.3 Ethical considerations

Ethical approval for the collection of surgical and postmortem bone specimens from the Royal Adelaide Hospital was granted by the Royal Adelaide Hospital Human Ethics Committee (Ethical approval number: 970418b). Informed consent for collection and use of bone tissues was obtained prior to the patient undergoing surgery and from the next-of-kin prior to autopsy.

2.2.2 Isolation and analysis of RNA

Disposable plasticware that was sterile was considered to be essentially free of RNases, and was used for the preparation and storage of RNA without any pre-treatment. Filter tips, which were manufacturer-certified RNase-free, were used for RNA isolation and subsequent Northern blot and RT-PCR analyses.

2.2.2.1 Isolation of total RNA from human trabecular bone

Total RNA was isolated from human postmortem and surgical trabecular bone tissue using an adaptation of the protocol for rat femoral cortical bone described by Davey *et al.* (2000), which takes into account the large amount of extracellular matrix and mineral present in skeletal tissue samples. The trabecular bone tissue fragments had been rinsed briefly in DEPC-treated water (the rinsed material contained trabecular bone and bone marrow), immersed in RNA lysis buffer (4 M guanidine isothiocyanate solution; 2 ml/250

mg wet weight), and stored at -70°C. The trabecular bone tissue fragments in RNA lysis buffer (section 2.1.5; Chomzynski and Sacchi, 1987) were homogenised using an Ultra-Turrax (TP 18-10; Janke and Kunkel, Staufen, Germany). The homogenised sample was clarified by centrifugation (1000 x *g* for 5 minutes at 4°C) to separate the lysate from the bone mineral. To remove the DNA and proteins, the lysate was vortexed in 0.1 volume of 2 M sodium acetate, pH 4.0, and then extracted with 1 volume of phenol and 0.2 volume of chloroform/isoamylalcohol (49:1), incubated on ice for 15 minutes, and centrifuged (4000 x *g* for 45 minutes at 4°C) to recover the aqueous layer containing the RNA. The RNA was precipitated with 1 volume of isopropanol overnight at -20°C. The RNA was recovered by centrifugation (4000 x *g* for 45 minutes at 4°C); the RNA pellet was drained and air-dried for 5 minutes. The RNA was resuspended in 1 X TE buffer containing 0.1 volume of 3 M sodium acetate, pH 5.2, then re-extracted with 0.5 volume phenol, followed by 0.5 volume chloroform/isoamylalcohol (49:1) to remove any phenol remaining in the aqueous layer. To remove contaminating proteoglycans, 3 volumes of 4M sodium acetate, pH 7.0, was added to the aqueous phase, and precipitated at -20°C overnight. Total RNA was recovered by centrifugation, washed with 75% v/v cold ethanol, and air-dried. RNA was dissolved in an appropriate volume of DEPC-treated water (50-200 µl) and stored at -70°C until required for Northern blot and RT-PCR analyses.

Total RNA was also isolated from cultured human osteoblasts, obtained by outgrowth from trabecular chips, which were treated for 48 hours with 10^{-8} M 1,25-$(OH)_2D_3$ as described previously (Gronthos *et al.*, 1999), and stromal and multinucleated cells sub-fractionated from human giant cell tumour cultures (Atkins *et al.*, 2000). These RNA samples provided positive controls for amplification of CTR, IL-6, IL-11, OCN, OPG, OPN, RANK, RANKL, TGF-β, TNF-α, and TRAP mRNA (results not shown).

Before use for Northern blot analysis and/or RT-PCR analysis, RNA purity and integrity of the 28S and 18S ribosomal RNA (rRNA) bands were assessed on ethidium bromide-stained 1% w/v agarose-formaldehyde gels. Briefly, 6 µl of the total RNA sample was added to 6 µl of 2 X RNA loading buffer (section 2.1.5), denatured at 68°C for 2 minutes, snap-cooled on ice, and separated in a 1% w/v agarose gel containing 2.2 M formaldehyde in 1 X MOPS (section 2.1.5) running buffer by electrophoresis. The gel was viewed under UV light to check the integrity of the RNA by the presence and intensity of the rRNA bands. A 2:1 ratio of the 28S to the 18S rRNA bands indicates that the RNA is undegraded (Sambrook and Russell, 2001).

2.2.2.1.1 Spectrophotometric quantification of RNA

Each total RNA sample was quantified by measuring the absorbance of a 1 in 100 dilution of RNA in DEPC-treated water on a UV spectrophotometer (Beckman Coulter Inc., Fullerton, CA, USA) at wavelengths of 260 and 280 nm. The concentration of RNA was calculated using the following formula:

RNA concentration (µg/µl) = Absorbance at 260 nm x 40 x dilution factor (100).

The purity of the RNA was assessed by calculating the ratio of absorbance at 260 nm to absorbance at 280 nm. Pure RNA has a 260/280 absorbance ratio of 2.0 (Sambrook and Russell, 2001). This RNA isolation method consistently yielded high quality total RNA from human trabecular bone tissue, with 260/280 ratios of 1.6 to 2.0.

2.2.2.2 Northern blot analysis

2.2.2.2.1 Separation of RNA on a denaturing gel and transfer to nylon membrane

Total RNA (3 μg per lane), prepared in 2 X RNA loading buffer (section 2.1.5), was denatured and size-separated by electrophoresis on 1% w/v agarose gels containing 2.2 M formaldehyde and 1 X MOPS buffer (section 2.1.5). Following electrophoresis, the ethidium bromide-stained 28S (5 kb) and 18S (1.8 kb) rRNA bands were visualised with UV light and the gels scanned using a FluorImager (Molecular Dynamics, Sunnyvale, CA, USA) to assess the integrity of the RNA. RNA samples were transferred, by downward capillary blotting, to Hybond™-N^+ nucleic acid transfer nylon membranes (Amersham Pharmacia Biotech), using 10 X SSC (Section 2.1.5) as the transfer buffer. Briefly, the nylon membrane was cut to the size of the gel, and both the gel and nylon membrane were rinsed in milli-Q water and placed in transfer buffer for 5 minutes. The downward transfer of the RNA was carried out using a 3 cm-thick stack of paper towels onto which three Whatman 3MM filters, cut to the size of the gel, were positioned on top. The top two filters were soaked in transfer buffer. The nylon membrane was placed on top of these filters followed by the gel. Three Whatman 3MM filters were soaked in transfer buffer and placed on top of the gel followed by a stack of soft towelling wipes, also soaked in transfer buffer. The RNA was transferred to the nylon membrane for 2 hours. The nylon membrane was rinsed in 2 X SSC buffer for 5 minutes after the transfer, blotted dry using filter paper, and the RNA was immobilised on the membrane by UV cross-linking (1200 μJ/cm^2 for 18 seconds; Spectrolinker XL-1000 UV Crosslinker, Spectronics Corp., Lincoln, NE, USA). Membranes were scanned using a FluorImager (Molecular Dynamics) to enable the position of the 28S and 18S rRNA bands to be marked on the membranes. The membranes were stored at 4°C between sheets of Whatman 3MM filter paper until required.

2.2.2.2.2 Labelling of DNA probe with ^{32}P

The 415 bp PCR-generated DNA fragment of human glyceraldehyde-3-phosphate dehydrogenase (GAPDH; Table 2.1), purified by the Wizard PCR preps DNA purification system (Promega), was radiolabelled with [α-^{32}P]dCTP (GeneWorks), by random priming using the Gigaprime DNA labelling kit (GeneWorks), according to the manufacturer's recommended protocol. The labelled probe was purified from unincorporated nucleotides through a Sephadex G_{50} column. The labelled probe was monitored for ^{32}P incorporation efficiency using a radiation monitor before and after column treatment.

2.2.2.2.3 Pre-hybridisation, hybridisation, and washing of nylon membrane

Membranes were pre-hybridised for at least 4 hours at 43°C in hybridisation glass bottles in a rotary incubator, in a solution consisting of 1 M NaCl, 1% SDS, 10% dextran sulphate, 50% formamide, and 100 μg/ml of sheared and heat-denatured herring sperm DNA. After pre-hybridisation, the purified ^{32}P-labelled 415 bp PCR-generated DNA fragment of human GAPDH was denatured by heating to 100°C for 5 minutes, snap-cooled on ice, and added directly to the hybridisation bottle containing the pre-hybridisation solution. The membrane and ^{32}P-labelled probe hybridised overnight at 43°C. The membranes were washed twice with a stringency of 2 X SSC, 0.1% SDS, at 60°C for 10 minutes, and to a final stringency of 1 X SSC, 0.1% SDS, at 60°C for 10 minutes. The membranes were wrapped in cling film, exposed to a Storage Phosphor Screen (Molecular Dynamics), and bound probe was quantified using a PhosphorImager (Molecular Dynamics) and the volume integration function of ImageQuant v.3.3 software (Molecular Dynamics). Northern blot analysis was performed twice, yielding reproducible results for the quantitation of the relative density of the GAPDH mRNA bands.

2.2.2.3 Reverse transcription-polymerase chain reaction (RT-PCR) amplification of RNA

2.2.2.3.1 Synthesis of complementary DNA (cDNA)

First-strand complementary DNA (cDNA) was synthesized from 1 μg of total RNA, isolated from human trabecular bone samples, in a reverse transcription reaction mixture containing 200 U of SuperScript™ II reverse transcriptase (Invitrogen), 0.5 μg random hexamer primers (GeneWorks), 1 mM dNTP's (Amersham Pharmacia Biotech), 10 mM DTT, and 1 X First-Strand Buffer (Invitrogen). cDNA was synthesized from the RNA samples for each group (either control or OA) at the same time, to limit differences between RNA samples within the same group in the efficiency of cDNA synthesis.

2.2.2.3.2 Polymerase chain reaction amplification of cDNA

cDNA was amplified by polymerase chain reaction (PCR) to generate products corresponding to mRNA encoding human CTR, IL-6, IL-11, OCN, OPG, OPN, RANK, RANKL, TGF-β1, TNF-α, TRAP, and the housekeeping gene GAPDH. Amplification of GAPDH served as an internal positive control for the integrity of the extraction/reverse transcription and PCR processes, and ensured that the various mRNA levels were normalised against the total mRNA content in the samples. The 20 μl amplification mixture contained 1 μl of cDNA, 1 U of AmpliTaq Gold® DNA polymerase (Applied Biosystems), 100 ng each of the sense and antisense primers (Table 2.1), 0.2 mM dNTP's (Amersham Pharmacia Biotech), 1.5 mM $MgCl_2$, 1 X PCR reaction buffer (Applied Biosystems), and sterile DEPC-treated water. PCR was performed for 23-37 cycles for the primer pairs specified in Table 2.1 in a DNA thermal cycler (PC-960C cooled thermal cycler; Corbett Research, Melbourne, VIC, Australia). After an initial step at 95°C for 9 minutes to activate the polymerase, each cycle consisted of 1 minute of denaturation at

94°C, 1 minute of annealing at 62°C for all primer pairs, except for an annealing temperature of 60°C for GAPDH, and 1 minute of extension at 72°C. This cycle was followed by an additional extension step at 72°C for 1 minute.

Human mRNA-specific oligonucleotide primers were designed, on the basis of published sequences available in GenBank for CTR, IL-6, IL-11, OCN, OPG, OPN, RANK, RANKL, TGF-β1, TNF-α, TRAP, and GAPDH (GeneWorks), in the Department of Orthopaedics and Trauma Bone Cell Laboratory (Hanson Institute, Adelaide, SA, Australia). To prevent amplification of genomic DNA, all of the primers were mRNA-specific in that the recognition sites of the upstream and downstream primers resided in separate exons or at intron/exon boundaries in the genomic sequence. Primer sequences, GenBank accession numbers, and predicted PCR product sizes are shown in Table 2.1.

To show that there were no false-positive results, PCR reactions were carried out using non-reverse transcribed RNA, and on reaction mixtures to which no RNA was added. Positive controls, including human cell line-derived cDNAs, were used to confirm the activity of each primer pair (Atkins *et al.* 2000; described in section 2.2.2.1). The specificity of the PCR reactions had been confirmed previously in the Department of Orthopaedics and Trauma Bone Cell Laboratory (Hanson Institute) by Southern blot transfer onto a nylon membrane and hybridisation with a digoxigenin (DIG)-labelled internal detecting oligonucleotide probe (Atkins *et al.* 2000).

2.2.2.3.3 Semi-quantification of PCR products

To allow semi-quantification of the PCR products, preliminary experiments were performed to ensure that the PCR amplification cycle number, for each set of primers, was

Table 2.1 RT-PCR oligonucleotide primers and expected PCR product sizes for the specific amplification of human mRNA.

Target gene	Sense [a]	Primer sequence (5' – 3')	PCR product size (bp)	GenBank accession number
GAPDH	S	CATGGAGAAGGCTGGGGCTC	415	M33197
	AS	CACTGACACGTTGGCAGTGG		
CTR	S	GCAATGCTTTCACTCCTGAGAAACT	780/732 [b]	X69920/ L00587
	AS	AGTGCATCACGTAATCATATATC		
IL-6	S	ATGAACTCCTTCTCCACAAG	544	M54894
	AS	GTGCCTGCAGCTTCGTCAGCA		
IL-11	S	GACATGAACTGTGTTTGCCGCCTGG	289	M57765
	AS	TTGTCAGCACACCTGGGAGCTGTAG		
OCN	S	ATGAGAGCCCTCACACTCCTCG	255	X53698
	AS	GTCAGCCAACTCGTCACAGTCC		
OPG	S	TGCTGTTCCTACAAAGTTTACG	433	U94332
	AS	CTTTGAGTGCTTTAGTGCGTG		
OPN	S	AGCCGTGGGAAGGACAGTTATG	472	X13694
	AS	GAGTTTCCATGAAGCCACAAAC		
RANK	S	CCTACGCACAAGGCGAAGATGC	702	AF018253
	AS	CGTAGACCACGATGATGTCGCC		
RANKL	S	ATAGAATATCAGAAGATGGCACTC	665	NM_003701
	AS	TAAGGAGGGGTTGGAGACCTCG		
TGF-β1	S	CTAGACCCTTTCTCCTCCAGGAGACG	224	X02812
	AS	GCTGGGGGTCTCCCGGCAAAAGGT		
TNF-α	S	TCAGATCATCTTCTCGAACC	359	M10988
	AS	CAGATAGATGGGCTCATACC		
TRAP	S	CTGGCTGATGGTGCCACCCCTG	470	NM_001611
	AS	CTCTCAGGCTGCTGGCTGAGG		

[a] S, "sense" primer; AS, "antisense" primer.
[b] Bands corresponding to the calcitonin receptor insert-positive and insert-negative isoforms, respectively (Kuestner *et al.*, 1994).

within the log-linear range of amplification. An example of a PCR amplification curve is shown in Figure 2.4 for OCN mRNA. This was achieved by performing 6 PCR reactions for the same cDNA synthesized from intertrochanteric trabecular bone, from an OA case, and removing one PCR tube after 24, 26, 28, 30, 32, and 34 cycles. The number of PCR cycles required for linear amplification of OCN mRNA in human trabecular bone, from the intertrochanteric region of the proximal femur, was 27 cycles (Figure 2.4).

PCR amplification products (10 μl of each PCR product) were resolved by electrophoresis on 2% w/v agarose gels in 1 X TAE (section 2.1.5) running buffer and post-stained with SYBR® Gold (Cat. No. S-11494; Molecular Probes). The molecular weight of the PCR products (size in bp; Table 2.1) was estimated visually by comparison with DNA 100 bp ladder markers (GeneWorks). The relative amounts of the PCR products were determined by quantitating the intensity of bands using a FluorImager and the volume integration function of ImageQuant v.3.3 software (Molecular Dynamics). Amplified product corresponding to CTR, IL-6, IL-11, OCN, OPG, OPN, RANK, RANKL, TGF-β1, TNF-α, and TRAP mRNA are represented as a ratio of the respective PCR product/GAPDH PCR product. It was found to be important for this semi-quantitative method that all samples for a given mRNA species amplified were electrophoresed in a single gel, and good inter-assay variability was obtained by adhering to this procedure.

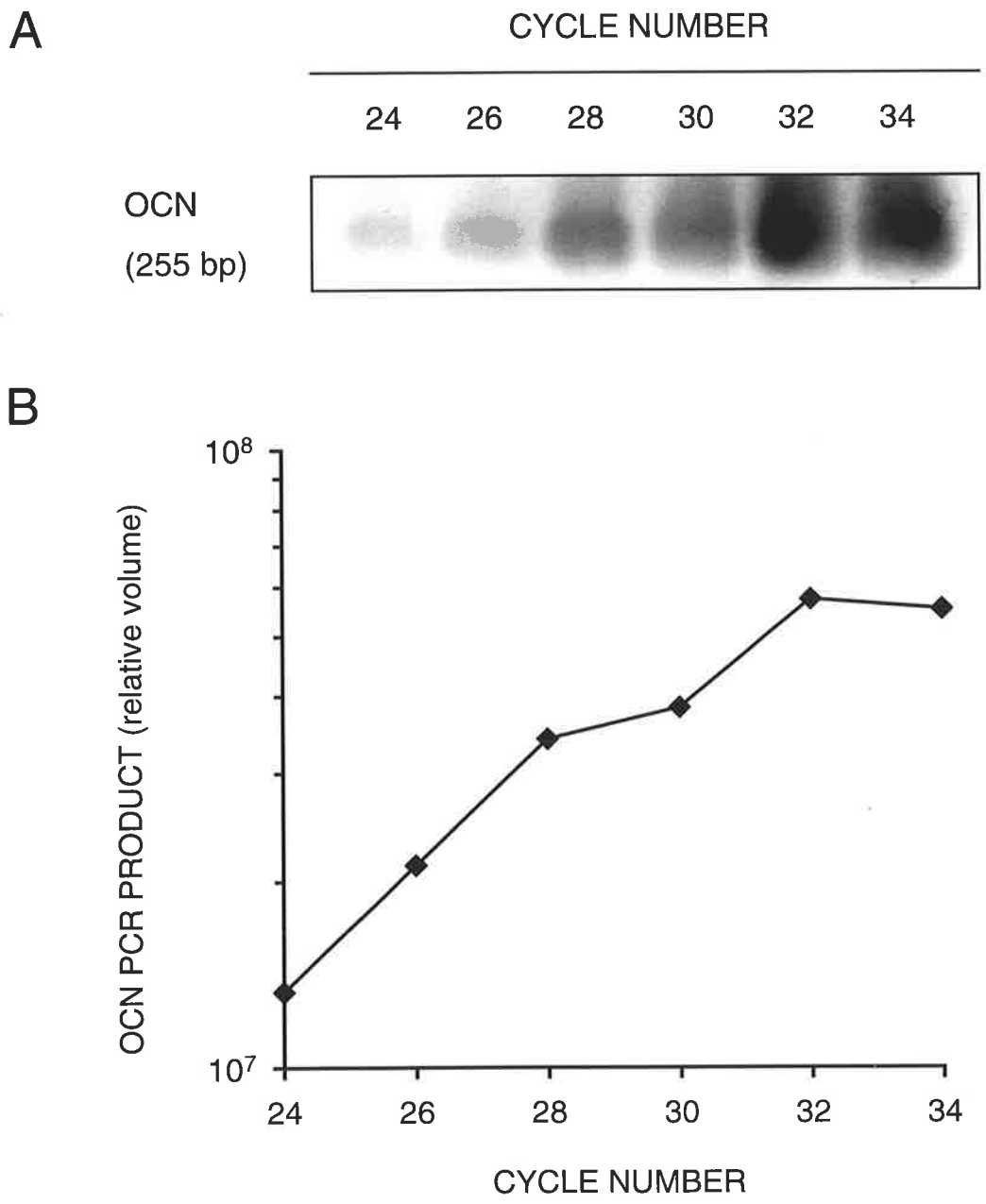

Figure 2.4: (A) PCR cycle course of OCN mRNA expression in total RNA extracted from intertrochanteric trabecular bone from a 80-year-old female undergoing total hip arthroplasty surgery for primary osteoarthritis. PCR product representing OCN mRNA (255 bp) is visualised on a SYBR® Gold-stained 2% agarose gel. (B) Relationship between PCR product (relative volume) and number of PCR cycles for OCN mRNA, as determined by RT-PCR.

2.2.3 Bone histomorphometry

2.2.3.1 Human bone tissue samples

2.2.3.1.1 Sampling of trabecular bone from the proximal femur of human postmortem cases

Each autopsy proximal femur had been sectioned in the coronal plane using a band saw, to allow sampling access to trabecular bone from the intertrochanteric region, and the femoral neck region for a subset of cases, for subsequent RNA isolation (section 2.2.1.1.1). Two 5 mm-thick coronal slices were cut from the remaining coronal half of each proximal femur, using a diamond blade on the Exakt saw (Exakt Apparatebau GmbH & Co. KG, Norderstedt, Germany). In a study comparing the diamond blade on the Exakt saw, the diamond wire saw (Ahlburg Technical Equipment, Norcross, GA, USA), and the band saw, in cutting 5 mm-thick coronal slices from a femoral head, the amount of microdamage, including discrete microcracks and diffuse staining (Figures 2.7A and 2.7B; Chapter 2.2.3.6.2), was qualitatively higher from the band saw (results not shown). Moreover, there was no difference in the amount of microdamage between the Exakt saw and wire saw (results not shown). Contact X-ray images of the 5 mm-thick coronal slices were taken using a Faxitron X-ray cabinet (Hewlett-Packard, McMinville, OR, USA) and Min-R film (Eastman Kodak, Rochester, NY, USA). The X-ray images were used to enable reproducible sampling of trabecular bone from the intertrochanteric region for one coronal slice (for undecalcified bone histology, Chapter 7), and to sample trabecular bone from the intertrochanteric, subchondral principal compressive, and medial principal compressive regions for the other coronal slice (for microdamage assessment, Chapter 8; Figure 2.3). Trabecular bone was sampled as a 1.0 x 1.0 cm^2 block of tissue from the intertrochanteric, subchondral principal compressive, and medial principal compressive regions of the 5 mm-thick coronal slices using an Isomet 11-1180 low-speed diamond saw

(Buehler Ltd., Evanston, IL, USA). The trabecular bone tissue blocks (1.0 x 1.0 x 0.5 cm^3) were immediately fixed in 70% ethanol for 24 hours at room temperature.

2.2.3.1.2 Sampling of trabecular bone from the intertrochanteric region of the human OA proximal femur

Intertrochanteric bone core biopsies, 10 mm in diameter and 3-5 cm in length, were obtained from patients undergoing total hip arthroplasty surgery for advanced primary OA (section 2.2.1.2.). Trabecular bone tissue was sampled from an approximate tube saw length of 1-2 cm from each OA case (section 2.2.1.2.1), for subsequent RNA isolation. The remaining contiguous intertrochanteric trabecular bone samples, 10 mm in diameter and 2-3 cm in length, were X-rayed (Faxitron X-ray cabinet; Hewlett-Packard) before sampling for undecalcified histological analysis, to ensure the exclusion of any damaged tissue (particularly the ends of the biopsy). Each undamaged tube saw biopsy, approximately 1-1.5 cm in length, was bisected lengthwise using an Isomet low-speed diamond saw (Buehler Ltd.). One half of the tube saw was processed for microdamage assessment (section 2.2.3.2) and the other half processed for undecalcified bone histology (section 2.2.3.3). The trabecular bone tissue samples were immediately fixed in 70% ethanol for 24 hours at room temperature.

2.2.3.2 Basic fuchsin bulk-staining of bone tissue

Trabecular bone samples for microdamage assessment, from the intertrochanteric region for OA cases, and from the intertrochanteric, subchondral principal compressive, and medial principal compressive regions for autopsy cases, were fixed in 70% ethanol (sections 2.2.3.1.1 and 2.2.3.1.2). These trabecular bone samples were bulk-stained in basic fuchsin according to the protocols of Burr and Hooser (1995) and Fazzalari *et al.* (1998b).

Briefly, bone samples were dehydrated through a series of graded ethanols (70%, 2 X 85%, 2 X 95%, 3 X 100%) containing 1% basic fuchsin, each for at least 4 hours under vacuum, for uniform tissue dehydration and staining, and then embedded in methyl methacrylate (MMA; section 2.2.3.3).

2.2.3.3 Processing bone tissue undecalcified into resin

Trabecular bone samples for microdamage assessment, from the intertrochanteric region for OA cases, and from the intertrochanteric, subchondral principal compressive, and medial principal compressive regions for autopsy cases, were bulk-stained in basic fuchsin (section 2.2.3.2). In addition, trabecular bone samples for undecalcified bone histology, from the intertrochanteric region for both OA and autopsy cases were fixed in 70% ethanol (sections 2.2.3.1.1 and 2.2.3.1.2). All of these trabecular bone samples were embedded, undecalcified, in MMA. Briefly, bone samples for undecalcified bone histology, were dehydrated through a series of graded ethanols (70%, 2 X 85%, 2 X 95%, 3 X 100%), each for at least 4 hours under vacuum, for uniform tissue dehydration. All of the bone samples (for undecalcified bone histology and microdamage assessment) were rinsed in 100% ethanol (2 X), dehydrated in 100% acetone under vacuum overnight, and transferred into MMA monomer under vacuum for 3-5 days. The bone samples were then placed in MMA monomer containing 10% w/v PEG-400 (hardener) under vacuum overnight. The final 3-4 ml embedding mixture contained MMA monomer, 10% w/v PEG-400 (hardener) and 0.4% w/v perkadox 16 (initiator). The mixture was poured into a 25 ml polypropylene tube and the bone sample immersed, with the low-speed saw cut surface (for OA cases) or the Exakt saw cut surface (for autopsy cases) facing downwards (as thin sections were sampled from this surface). The tubes were tightly capped and transferred to a 37°C waterbath for 1-2 days polymerisation. The bone samples, once embedded in MMA, were cut from the tubes

using a band saw, and fixed to aluminium block holders with epoxy glue (Selleys, Sydney, NSW, Australia).

2.2.3.4 Undecalcified resin embedded bone tissue sectioning

2.2.3.4.1 Microtome sectioning

Following embedding in MMA, the bone samples were trimmed to expose the sample area by removing and discarding 10 μm-thick sections with a Jung K motorised microtome (Reichert, Heidelberg, Germany). Once the sample area was exposed, the block surface was moistened with tap water and two 5 μm-thick sections were cut. MMA sections were immersed in a 30:70 mixture of ethylene glycol monoethyl ether (Merck) and 70% ethanol heated to 65-70°C, and flattened onto gelatinised slides. The section was then covered with polyethylene plastic and filter paper, clamped, and adhered to the slide overnight in a 37°C oven.

2.2.3.4.2 Wire saw sectioning

A diamond wire saw (Ahlburg Technical Equipment) was used to cut two 70 μm-thick sections from each of the basic fuchsin bulk-stained, resin embedded, bone samples. Sections were mounted on glass slides.

2.2.3.5 von Kossa and haematoxylin and eosin staining of undecalcified bone tissue sections

Prior to staining of 5 μm-thick bone sections (section 2.2.3.4.1), MMA was removed by a 10 minute immersion in 100% acetone. Undecalcified bone sections were impregnated with silver by the von Kossa technique (Drury and Wallington, 1980), and counterstained with haematoxylin and eosin (H&E) to distinguish between the mineralised bone, the

osteoid, and the cellular components of the marrow. Following staining, sections were dehydrated in ethanol (3 X 100%), cleared in xylene (3 X 100%), and mounted in a xylene based mountant, Depex. Undecalcified 5μm-thick sections of human trabecular bone stained with von Kossa/H&E showing osteoclastic bone resorption and osteoblastic bone formation are shown in Figures 2.5A and 2.5B, respectively.

2.2.3.6 Quantitative histomorphometry

2.2.3.6.1 Manual quantitation of trabecular bone structure and bone turnover indices

The von Kossa and H&E stained 5 μm-thick undecalcified bone sections were used for the manual quantitation, by point and intersection counting (for volume and surface measurements, respectively), of bone structural parameters and static indices of bone turnover (Fazzalari *et al.*, 1992; Parfitt *et al.*, 1987). Two sections per case, each section representing approximately 1 x 1 cm^2 of bone tissue, were quantitated. This involved using an ocular-mounted Zeiss II Integration 100 point (10 x 10) graticule in a X10 eye-piece and an objective magnification of X10 on an Olympus BH-2 light microscope (Olympus, Tokyo, Japan). At this magnification, the total length of a single grid line was 1.2 mm and the length of a single partition 0.12 mm (Figure 2.6). The following standard histomorphometric parameters (Parfitt *et al.*, 1987) were calculated using formulae from Recker (1983):

Trabecular bone structural parameters:

(1) Percentage of mineralised bone tissue volume BV/TV

(2) Surface density of bone in mm^2/mm^3 BS/TV

(3) Specific surface of bone in mm^2/mm^3 BS/BV

A

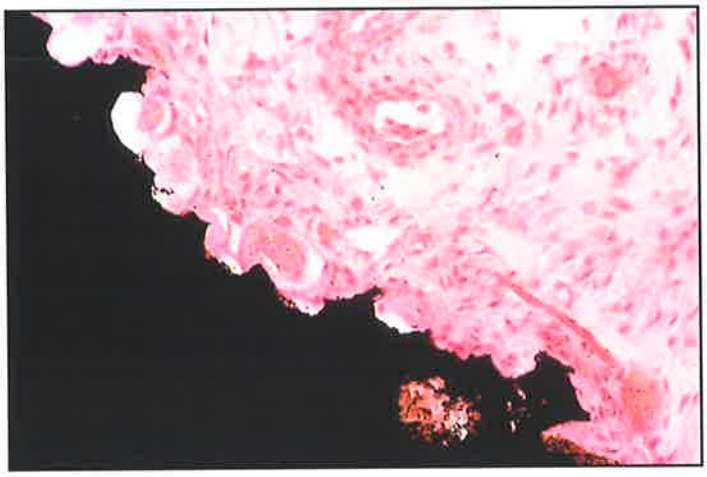

B

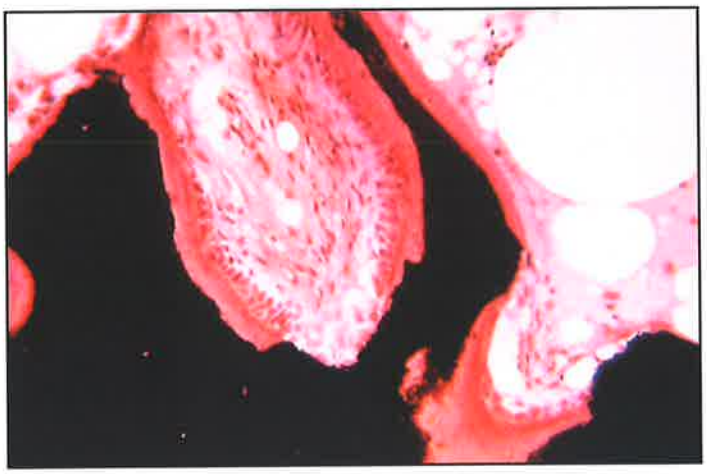

Figure 2.5: Undecalcified 5µm-thick sections of human trabecular bone stained with von Kossa/H&E showing (A) osteoclasts resorbing bone, and (B) osteoblasts laying down osteoid.

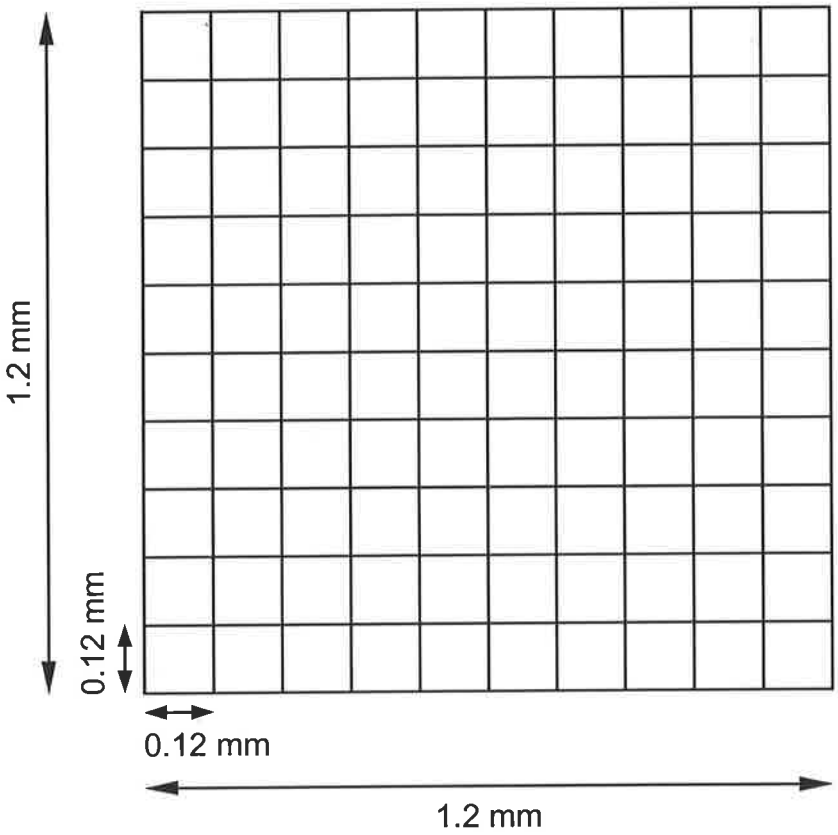

Figure 2.6: Diagrammatic representation of the Zeiss II Integration 100 point graticule field used for histomorphometric analysis. The total length of a single grid line was 1.2 mm and the length of a single partition 0.12 mm.

(4)	Trabecular thickness in μm	Tb.Th
(5)	Trabecular separation in μm	Tb.Sp
(6)	Trabecular number per mm	Tb.N

Static indices of bone turnover:

(1)	Percentage of osteoid volume	OV/TV
(2)	Percentage of osteoid volume	OV/BV
(3)	Percentage of osteoid surface	OS/BS
(4)	Percentage of eroded surface	ES/BS

To assess reproducibility of the manual histoquantitation, 8 cases were selected at random (including both OA and control cases), and were re-quantitated by the same single observer and by a different observer. The mean difference and standard deviation of the mean difference of each parameter between either the single observer (intra-observer variability) or different observers (inter-observer variability), were calculated. These represent the bias and random error, respectively, between the two group estimates (Grubbs, 1948). Intra-observer and inter-observer variability were not statistically significant for any of the histomorphometric parameters (bias and random error were less than 10%).

2.2.3.6.2 Quantitation of bone microdamage parameters

The basic fuchsin bulk-stained 70 μm-thick undecalcified bone sections were used for the quantitation of bone microdamage parameters (Fazzalari *et al.*, 1998b; Forwood *et al.*, 1995). Microdamage is identified histologically by discrete microcracks (basic fuchsin staining through the depth of a crack, sharp edges, some depth of field, and permeation of the stain into the walls of the crack), cross-hatch staining (a series of crossed darkly stained

lines), and diffuse staining (amorphous flooding of basic fuchsin on the trabeculae; Burr and Stafford, 1990; Fazzalari *et al.*, 1998b; Figures 2.7A and 2.7B). Two sections per case, each section representing approximately 1 x 1 cm^2 of bone tissue, were quantitated. To avoid edge artifacts, only microdamage further than 1 mm from the edge of the sample was measured (Fyhrie and Schaffler, 1994). The following morphometric parameters, describing the extent of microdamage, were measured using a Nikon Optiphot II microscope (Nikon, Tokyo, Japan) at X250 magnification by point counting and a semi-automated digitizing system (Bioquant, R & M Biometrics, Nashville, TN, USA):

Microdamage parameters:

(1) Trabecular bone area in mm^2 B.Ar

(2) Total tissue area in mm^2 TT.Ar

(3) Number of microcracks Cr.N

(4) Mean microcrack length in μm Cr.Le

(5) Area of trabecular bone damage in mm^2 Dx.Ar

The above measurements were used to calculate the following morphometric parameters describing the extent of microdamage:

Morphometric parameters describing the extent of microdamage:

(1) Percentage of mineralised bone tissue volume BV/TV

BV/TV = B.Ar/TT.Ar

(2) Numerical microcrack density in number/mm^2 Cr.Dn

Cr.Dn = Cr.N/B.Ar

A

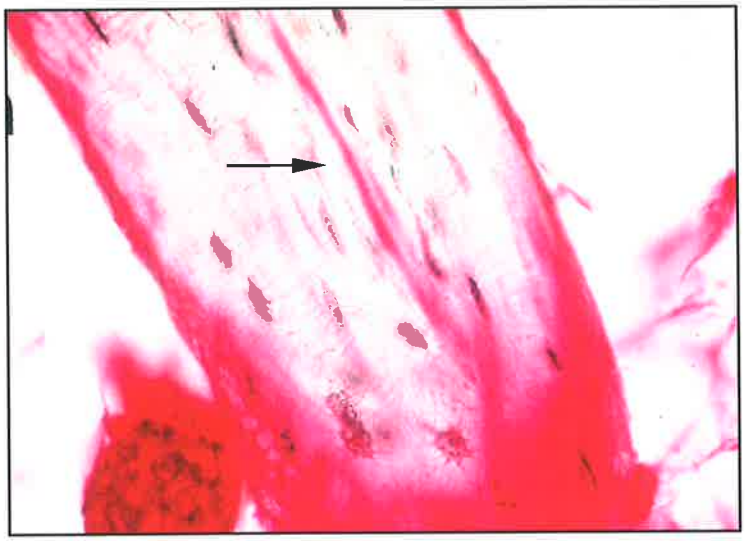

B

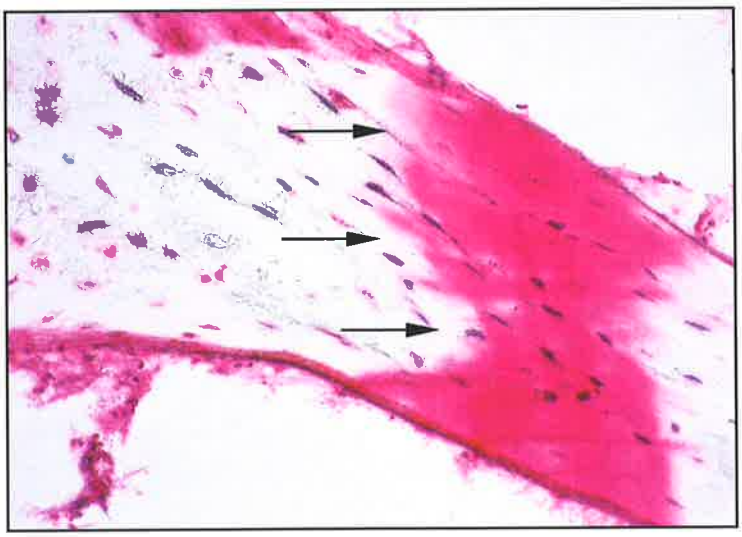

Figure 2.7: Photomicrographs of human femoral 70 μm-thick sections of trabecular bone bulk-stained with basic fuchsin to show microdamage. Arrows identify (A) a microcrack, and (B) cross-hatching embedded in diffuse staining (objective magnification: X20).

(3) Microcrack surface density in μm/mm^2 Cr.S.Dn

Cr.S.Dn = Cr.Le*Cr.Dn

(4) Percentage of damaged bone volume DxV/BV

DxV/BV = Dx.Ar/B.Ar

(5) Percentage of damaged bone volume DxV/TV

DxV/TV = Dx.Ar/TT.Ar

2.2.4 Statistical analyses

2.2.4.1 Statistical analysis of mRNA expression data

RT-PCR reactions were performed twice, from duplicate cDNA syntheses, which confirmed that repeated RT-PCR analysis of the same RNA samples yielded reproducible results. In addition, to minimise inter-assay variability between each bone sample for either the comparison of time-points in the RNA stability studies (Chapter 3), or the comparison between skeletal sites (Chapter 4), or the comparison of OA and control cases (Chapter 6), all PCR products for a given mRNA species ($n \leq 30$), were electrophoresed in a single 2% agarose gel.

Regression analysis, both linear and exponential, was used to examine the relationship between the relative mRNA expression levels and storage intervals of the bone tissue, for both the Northern blot and RT-PCR analyses for the RNA stability studies (Chapter 3). Pearson's correlation coefficient was used to examine the relationship between postmortem variables and relative intensities of the rRNA bands and GAPDH mRNA for the RNA stability studies (Chapter 3; Excel; Microsoft Corp., Redmond, WA, USA).

The Shapiro-Wilk statistic was used to test the semi-quantitative RT-PCR data for normality (PC-SAS software; SAS Institute, Cary, NC, USA); for the skeletal site comparisons (Chapter 4) and for the comparison of OA and control cases (Chapters 5 and 6). The semi-quantitative RT-PCR data were found to be both normally and non-normally distributed. Therefore, both parametric and non-parametric statistical methods were used to analyse the data (Excel; Microsoft Corp.; PC-SAS software; SAS Institute).

Differences in mRNA expression between the iliac crest and proximal femur regions (femoral neck and intertrochanteric), for postmortem cases, were tested by one-way analysis of variance (ANOVA) for the means (parametric) or by the Kruskal-Wallis one-way ANOVA by ranks for the medians (non-parametric; Chapter4). The statistical significance of differences in mRNA expression between females and males, and between the autopsy control and OA groups, were determined by Student's *t*-test (parametric) or the Mann-Whitney *U*-test (non-parametric). The F-test was used to analyse differences in the variance of mRNA expression between females and males, and between the control and OA groups. Linear regression analysis was used to describe age-related changes, and to examine the relationship between PCR products representing specific mRNA species. The Spearman rank correlation (r_s) was used to test for an association between two specific PCR products when the data were non-normally distributed. Student's *t*-test was used to compare the slopes and intercepts of significant linear regressions between the OA and control groups. If there was more than one significant independent factor associated with a specific mRNA species, multiple regression was performed to determine the contribution of each independent factor. Parametric mRNA expression data is quoted as mean ± standard deviation and non-parametric mRNA expression data quoted as the median (quartiles). The critical value for significance was chosen as $p = 0.05$.

2.2.4.2 Statistical analysis of histomorphometric data

The Shapiro-Wilk statistic was used to test the histomorphometric data (bone structural parameters, static indices of bone turnover, and microdamage parameters) for normality (PC-SAS software; SAS Institute). The histomorphometric data for bone structural parameters and static indices of bone turnover was found to be normally distributed, and parametric statistical methods were used to analyse the data (Chapter 7). The morphometric parameters describing the extent of bone microdamage were found to be both normally and non-normally distributed (Chapter 8). Therefore, both parametric and non-parametric statistical methods were used to analyse the microdamage data (Excel; Microsoft Corp.; PC-SAS software; SAS Institute).

Differences in the microdamage morphometric parameters between the proximal femur regions (intertrochanteric, subchondral principal compressive, and medial principal compressive) were tested by one-way analysis of variance (ANOVA) for the means (parametric) or by the Kruskal-Wallis one-way ANOVA by ranks for the medians (non-parametric). If significant differences were indicated, comparison between proximal femur region means or medians was tested by Student's *t*-test (parametric) or the Mann-Whitney *U*-test (non-parametric), respectively. The statistical significance of differences between females and males, and between the autopsy control and OA groups, were determined by Student's *t*-test or the Mann-Whitney *U*-test. The F-test was used to analyse differences in the variance of the histomorphometric parameters between females and males. Linear regression analysis was used to describe age-related changes. Regression analysis was used to examine the relationship between bone microdamage morphometric parameters, and between histomorphometric parameters. The Spearman rank correlation (r_s) was used to test for an association between two non-normally distributed microdamage parameters.

Regression analysis was used to examine the relationship between PCR products representing specific mRNA species (Chapters 5 and 6) and bone microdamage and histomorphometric variables (Chapters 7 and 8), measured in contiguous trabecular bone tissue samples. Student's *t*-test was used to compare the slopes and intercepts of significant linear regressions between the OA and control groups. If there was more than one significant independent factor associated with a specific histomorphometric variable, multiple regression was performed to determine the contribution of each independent factor. Parametric histomorphometric data is quoted as mean ± standard deviation and non-parametric histomorphometric data quoted as the median (quartiles). The critical value for significance was chosen as $p = 0.05$.

CHAPTER 3

STABILITY OF RNA ISOLATED FROM HUMAN TRABECULAR BONE AT POSTMORTEM AND SURGERY

3.1 INTRODUCTION

The extensive knowledge of systemic and local regulation of bone remodelling has been developed primarily from studies utilising *in vitro* cell culture systems, human and predominantly murine, and animal studies such as the effects of gene deletion studies in mice (reviewed in Ducy *et al.*, 2000; Hofbauer and Heufelder, 2001; Raisz, 1999; Roodman, 1999; Suda *et al.*, 1999). There is limited information regarding the pattern of gene expression corresponding to specific molecules, with regulatory roles in bone turnover, in normal human bone tissue or their role in skeletal disease. The advantage of investigating the mRNA expression of skeletally active genes in the local human bone microenvironment, over cell culture techniques, is that paracrine factors/mediators of bone turnover can be analysed with their local regulatory mechanisms intact. Furthermore, Lin *et al.* (1999) emphasized that the analysis of mRNA expression patterns in human tissues can provide significant insight into the spatio-temporal activities of gene transcription in a tissue, and further provide important information on physiology and pathology at a molecular level.

It is not known how a pattern of gene expression in normal human bone may be altered in musculoskeletal pathologies such as osteoarthritis (OA) and osteoporosis, and further, how this may support mechanisms of disease. Insight may also be gained from changes in mRNA levels in tissues specifically affected by disease; for example the bone adjacent to an OA articular joint, where the structural parameters and turnover indices of trabecular bone are known (Crane *et al.*, 1990; Fazzalari *et al.*, 1992). Human pathological bone tissue is readily available from joint replacement surgery, including OA, rheumatoid arthritic, and fractured neck of femur cases. It is difficult, or rarely possible, to obtain suitable non-diseased bone tissues at surgery. A valuable resource of skeletal site-matched

control tissue is postmortem bone tissue. However, the disadvantage in using postmortem tissues for molecular studies is the time interval between death and the postmortem examination. This postmortem interval (PMI) is variable and often uncontrollably delayed due to the time of the death, autopsy consent being obtained, and a number of other hospital protocols. Recovering intact RNA from postmortem tissues is complicated by the activity of both targeted and generalised ribonuclease enzymes (RNases) that cause degradation of mRNA molecules. Therefore, to determine the reliability of gene expression studies in postmortem bone tissue, it is important to evaluate the stability of total RNA and specific mRNA species isolated from such tissues, as a function of the PMI.

The isolation and stability of total RNA and specific mRNA species from human postmortem tissues has been widely reported for neurological tissues (reviewed in Bahn *et al.*, 2001; Yasojima *et al.*, 2001). A number of these studies have demonstrated the importance of controlling postmortem variables, such as minimising the time between death and refrigeration of the body at 4°C, the PMI, and the storage interval of the tissue before RNA isolation. Moreover, the storage temperature of the body has been reported to be more important than the PMI (Bahn *et al.*, 2001). Human brain-specific mRNAs are generally stable up to 48 hours postmortem at 4°C, as assessed by Northern blotting and RT-PCR (Burke *et al.*, 1991; Leonard *et al.*, 1993; Ross *et al.*, 1992). In addition, biologically stable total RNA and tissue-specific mRNAs have been isolated from a number of other human postmortem tissues, including the adrenal glands, heart, kidney, liver, lung, muscle, pancreas, spleen, stomach, and temporal bone soft tissues (Eikmans *et al.*, 2001; Humphreys-Beher *et al.*, 1986; Larsen *et al.*, 1992; Lin *et al.*, 1999; Stuart *et al.*, 1999). The optimal PMI for obtaining undegraded RNA from these tissue types was found to vary considerably. RNA isolated from the stomach and pancreas, tissues that are known

to produce abundant RNases, degraded after a PMI of 2 hours (Humphreys-Beher *et al.*, 1986). In contrast, Larsen *et al.* (1992) isolated RNA from human adrenal glands, brain, heart, kidney, lung, liver, and spleen, which was preserved and undegraded up to 50 hours postmortem. The integrity of the total RNA samples was shown by the presence of ribosomal (r)RNA bands in ethidium bromide-stained gels and Northern blotting analysis of β-actin and retinoblastoma transcripts (Larsen *et al.*, 1992). The variation between these reports in the PMI for obtaining undegraded RNA may be associated with the type of soft tissue analysed, differences in the inherent stability of mRNA transcripts, and the sensitivity of the techniques used for assessment and quantitation of mRNA integrity.

The stability of total RNA isolated from human postmortem skeletal tissues is unknown. Marchuk *et al.* (1998) isolated intact rRNA and specific mRNA species, such as type I collagen and transforming growth factor (TGF)-β1, up to 96 hours postmortem from rabbit connective tissues such as ligament, cartilage, and tendon at 4°C. Furthermore, type I collagen and TGF-β1 mRNA were stable in these hypocellular tissues up to 48 hours postmortem at room temperature. However, the RT-PCR protocol used in this study was not designed for either semi-quantitative or quantitative analysis, and therefore may not have been sensitive enough to detect subtle loss of mRNA transcripts with increased postmortem time. Marchuk *et al.* (1998) suggest that cellular RNases are either maintained in sequestered intracellular sites or maintained in an inactive state up to 96 hours postmortem at 4°C. Larsen *et al.* (1992) demonstrated that RNA stability is strongly dependent on the temperature, at which the tissue is stored before RNA isolation. Mouse lung tumour rRNA bands and mRNA Northern blot signals for c-*raf*-1 and c-*myc* genes indicated undegraded RNA in tissue kept at 4°C up to 72 hours. However, RNA began to degrade in tissue kept at 20°C for 48 hours (Larsen *et al.*, 1992). Importantly, stability of

specific mRNA transcripts postmortem was not dependent on the *in vivo* mRNA half-lives. Similar rates of mRNA degradation in mouse postmortem small cell lung cancer tumour tissue kept at 20°C, for times up to 72 hours, were observed for c-*myc* mRNA, which has a short *in vivo* half-life of 10 to 20 minutes, compared to β-actin, which has an approximate half-life of 6 to 12 hours (Larsen *et al.*, 1992).

This chapter describes investigation of the optimal postmortem conditions, that is the PMI and tissue processing conditions, required to isolate undegraded total RNA from human postmortem trabecular bone tissues. In addition, the influence of different bone tissue storage conditions, such as temperature and time, on the stability of total RNA and bone-specific mRNAs, was investigated in surgical trabecular bone tissues. The data presented in this chapter were used to define the sampling conditions described in Chapters 2, 4, 5, and 6, for the isolation of total RNA from human postmortem and surgical trabecular bone tissues, for semi-quantitative RT-PCR analysis. This information was necessary to validate comparison of the expression of mRNA species in OA bone obtained at surgery with their expression in skeletal site-matched non-OA bone obtained postmortem (Chapter 6).

3.2 CHAPTER AIMS

- To investigate the optimal postmortem conditions, that is the PMI and tissue processing conditions, required to isolate undegraded total RNA from human femoral and iliac crest postmortem trabecular bone tissues.

- To investigate whether differences in bone tissue storage conditions, such as temperature and time, influence the stability of total RNA and bone-specific mRNAs in surgical femoral trabecular bone tissues.

3.3 METHODS

3.3.1 Human postmortem bone tissue

3.3.1.1 Postmortem case profiles

Proximal femurs and iliac crest samples were obtained from 18 routine autopsies performed at the Royal Adelaide Hospital (Table 3.1). The postmortem cases had a PMI range, the time between death and the postmortem examination, of 4 to 84 hours (mean ± SD [standard deviation]; 39.0 ± 20.5 hours; Table 3.2). The proximal femurs and iliac crest samples were stored at 4°C between 0 and 30 hours (9.2 ± 10.0 hours), after removal at autopsy, and before sampling trabecular bone tissue for RNA isolation. The combined PMI and bone tissue storage interval at 4°C (PMIS) ranged from 12 to 108 hours (48.2 ± 23.2 hours; Table 3.2). The age of the postmortem cases, comprising 10 women (aged 43-83 years) and 8 men (aged 44-81 years), varied between 43 and 83 years (64.4 ± 12.6 years). There was no correlation between PMI or PMIS and the age of the individual. Informed consent from next-of-kin was obtained for the collection of these postmortem specimens, with approval by the Royal Adelaide Hospital Human Ethics Committee.

3.3.1.2 Sampling of trabecular bone from the iliac crest and proximal femur

Trabecular bone was sampled from the intertrochanteric region of the proximal femur for each postmortem case (Figure 2.1). In addition, trabecular bone was sampled from the femoral neck, and iliac crest at a point 3 cm posterior to the antero-superior iliac spine, for

Table 3.1 Profiles of autopsy cases examined.

Case	Age *(years)*	Gender	Skeletal regions	Cause of death
A1	50	Male	FN, IT	Chronic renal failure
A2	61	Female	IC, IT	Non-Hodgkins lymphoma
A3	60	Male	IT	Pneumonia
A4	64	Male	FN, IT	Sepsis
A5	50	Male	FN, IT	Liver failure
A6	57	Female	IC, IT	CML/sepsis
A7	43	Female	IT	Liver failure
A8	72	Female	IT	Respiratory failure/pulmonary oedema
A9	83	Female	FN, IT	Cardiac arrest
A10	83	Female	FN, IT	#NOF
A11	71	Male	FN, IT	Lupus erythematosus
A12	73	Male	IT	Cerebrovascular disease
A13	68	Female	IT	Sepsis
A14	75	Female	IT	Pneumonia
A15	44	Male	IT	Sepsis/pneumonia
A16	68	Female	IT	Post CABG
A17	81	Male	IT	GI haemorrhage
A18	57	Female	IT	Abdominal sepsis

A, autopsy case.
Total RNA was isolated from trabecular bone sampled from the following skeletal regions: FN, femoral neck; IC, iliac crest; IT, intertrochanteric region of the proximal femur.
Abbreviations for cause of death: CABG, coronary artery bypass surgery; CML, chronic myelogenous leukaemia; GI, gastrointestinal; #NOF, femoral neck fracture.

Table 3.2 Postmortem and bone tissue storage intervals for autopsy cases examined.

Case	PMI *(hours)*	Storage interval *(hours)*	PMIS *(hours)*
A1	4	8	12
A2	16	4	20
A3	29	7	36
A4	27	3	30
A5	34	2	36
A6	37	0	37
A7	38	10	48
A8	44	4	48
A9	45	3	48
A10	45	3	48
A11	37	11	48
A12	24	24	48
A13	37	23	60
A14	30	30	60
A15	67	5	72
A16	84	0	84
A17	80	28	108
A18 [a]	24	0	24
Mean ± SD	39.0 ± 20.5	9.2 ± 10.0	48.2 ± 23.2

[a] Case A18 was used for a time-course analysis, incubating the bone tissue at 4°C from the 24 hour PMI time-point, with additional 24 hour increments, up to 96 hours.
A, autopsy case; SD, standard deviation.
PMI, postmortem interval, refers to the time between death and autopsy.
Storage interval, refers to the time the bone tissue has been stored at 4°C between removal of the tissue at autopsy and subsequent RNA isolation.
PMIS, refers to the sum of the postmortem and storage intervals.

a subset of postmortem cases (Figures 2.1 and 2.2; Table 3.1). Immediately after removal from storage at 4°C, each proximal femur was sectioned in the coronal plane using a band saw, which had been cleaned with DEPC-treated water, to allow access to trabecular bone for sampling from the femoral neck and intertrochanteric skeletal regions, which are enclosed within the femoral cortex. The iliac crest bone samples were bisected longitudinally, in an antero-posterior plane, to access the trabecular bone enclosed within the cortical shell. Using sterile bone cutters, the trabecular bone tissue was sampled as small fragments from an approximate 1.5 x 1.0 cm^2 area, to a specimen depth of 0.5 cm, from the femoral neck and intertrochanteric regions, and from an approximate 1.0 x 1.0 cm^2 area, to a specimen depth of 0.5 cm, from the iliac crest. The trabecular bone tissue fragments were rinsed briefly in DEPC-treated water (the rinsed material contained trabecular bone and bone marrow) and then immersed in RNA lysis buffer (4 M guanidine isothiocyanate solution, Chapter 2.1.5; 2 ml/250 mg wet weight).

To investigate the effect of the PMI or the storage interval at 4°C on the integrity of specific mRNA species, trabecular bone tissue from the intertrochanteric region of postmortem case A18 (57-year-old female; Tables 3.1 and 3.2) was further divided into four samples of equivalent tissue weight (approximately 250 mg wet weight of trabecular bone tissue, including bone marrow). Total RNA was isolated from one sample to represent a 24 hour PMI time-point. The remaining three samples were kept in sterile RNase-free 0.85% saline at 4°C, and RNA was sequentially isolated at 24 hour intervals up to 96 hours.

3.3.2 Human surgical bone tissue

3.3.2.1 Surgical case profiles

Trabecular bone samples obtained at surgery were used to investigate the effect of storage temperature and storage time on the integrity of total RNA and specific mRNA species in human bone tissue. The samples were obtained from 7 patients (4 females, 3 males, aged 70.3 ± 11.5 years) undergoing total hip arthroplasty surgery for either severe OA of the hip or subcapital femoral neck fracture (Table 3.3). Trabecular bone tissue from the proximal tibia was obtained from one surgical case S1 (71-year-old female) undergoing a tibial osteotomy. Informed consent was obtained for the collection of these surgical specimens, with approval by the Royal Adelaide Hospital Human Ethics Committee.

3.3.2.2 Sampling of trabecular bone from the proximal femur and tibia

At total hip arthroplasty surgery, a 10 mm internal diameter tube saw was used to take a trabecular bone core biopsy of the intertrochanteric region (Figure 2.1), taken in line with the femoral medullary canal (Fazzalari *et al.*, 1998b), from OA and subcapital femoral neck fracture patients. In addition, trabecular bone was sampled from the femoral neck region for case S5 (81-year-old female; Table 3.3). Trabecular bone tissue from the proximal tibia was obtained from surgical case S1 (71-year-old female; Table 3.3). All of the fresh surgical bone samples were placed in cold sterile RNase-free 0.85% saline and transported directly to the laboratory. Samples were separated into small fragments using sterile bone cutters and/or a sterile scalpel blade. The trabecular bone tissue fragments were rinsed briefly in DEPC-treated water (the rinsed material contained trabecular bone and bone marrow) and then immersed in RNA lysis buffer (4 M guanidine isothiocyanate solution; 2 ml/250 mg wet weight).

Table 3.3 Profiles of surgical cases examined.

Case	Age *(years)*	Gender	Skeletal regions	Skeletal disease
S1	71	Female	PT	Early knee OA
S2	49	Female	IT	Severe hip OA
S3	69	Male	IT	Severe hip OA
S4	77	Male	IT	OP/#NOF
S5	81	Female	FN, IT	#NOF
S6 [a]	80	Female	IT	Severe hip OA
S7 [b]	62	Male	IT	Severe hip OA
S8 [c]	74	Female	IT	#NOF

[a,b,c] Cases used for time-course analyses; the bone tissue was incubated in sterile saline at 4°C, room temperature (22°C ± 1°C), or 37°C, for cases S6, S7, or S8, respectively. RNA was isolated at 0 hours and at 2, 4, 8, 16, 24, 48, and 72 hours.
S, surgical case.
Total RNA was isolated from trabecular bone from the following skeletal regions: FN, femoral neck; IT, intertrochanteric region of the proximal femur; PT, proximal tibia.
All patients were undergoing hip arthroplasty surgery, with the exception of patient S1, who underwent a tibial osteotomy.
Abbreviations for skeletal disease: OA, osteoarthritis; OP, osteoporosis; #NOF, subcapital femoral neck fracture.

Trabecular bone tissues from the intertrochanteric region of surgical cases S6 (80-year-old female), S7 (62-year-old male), and S8 (74-year-old female), were used to investigate the effect of storage temperature and storage time on the integrity of total RNA and specific mRNA species (Table 3.3). Tube saw core biopsies, 10 mm in diameter, from cases S6, S7, and S8 were 4 cm, 5.5 cm, and 4.5 cm in length, respectively. These were divided, using a sterile scalpel blade, into eight pieces of approximately equivalent tissue weight (350 mg, 650 mg, and 250 mg wet weight, for cases S6, S7, and S8, respectively). Total RNA was isolated from the bone tissue sampled from one end of the tube saw to represent a 0 hour time-point. The remaining seven bone samples were kept in sterile RNase-free 0.85% saline at 4°C or room temperature (22°C ± 1°C) or 37°C, for cases S6, S7, and S8, respectively, and RNA was isolated from contiguous bone samples at 2, 4, 8, 16, 24, 48, and 72 hour time-points.

3.3.3 Isolation of total RNA from human postmortem and surgical trabecular bone

Total RNA was isolated from the postmortem and surgical trabecular bone tissue fragments (described in Chapter 2.2.2.1). RNA concentration and the 260/280 absorbance ratio were determined by UV spectrophotometric readings at 260 and 280 nm (Chapter 2.2.2.1.1) for each total RNA sample. The trabecular bone tissue for each time-point from the surgical cases S6, S7, and S8, used for a time-course analysis of RNA integrity, were weighed prior to RNA extraction. The RNA yields were derived from the spectrophotometric RNA concentration and are listed in Table 3.5. Before use for Northern blot analysis and/or RT-PCR analysis, RNA purity and integrity of the 28S and 18S rRNA bands were assessed on ethidium bromide-stained 1% w/v agarose-formaldehyde gels (Chapter 2.2.2.1).

3.3.4 Northern blot analysis of human GAPDH mRNA in total RNA isolated from human postmortem and surgical trabecular bone

Total RNA isolated from human postmortem and surgical trabecular bone (3 μg per lane), prepared in a loading buffer containing ethidium bromide (Chapter 2.1.5), was denatured and size-separated by electrophoresis on 1% w/v agarose-formaldehyde gels. Following electrophoresis, the ethidium bromide-stained 28S (5 kb) and 18S (1.8 kb) rRNA bands were identified on the gels using a FluorImager (Molecular Dynamics) to assess the integrity of the RNA (Chapter 2.2.2.2.1). The gels were transferred to a nylon membrane, and hybridised with a ^{32}P-labelled GAPDH probe to detect human GAPDH mRNA (1.28 kb; Chapter 2.2.2.2). Bound probe was quantified using a PhosphorImager (Molecular Dynamics) and the volume integration function of ImageQuant v.3.3 software (Molecular Dynamics). The relative intensity data of the 28S and 18S rRNA bands from ethidium bromide-stained 1% agarose-formaldehyde gels, and the GAPDH mRNA bands from Northern blots, are expressed per mg of bone tissue for the surgical cases S6 and S7. The relative half-life (T_{50}), the incubation time required for 28S and 18S rRNA, and GAPDH mRNA, to decrease to 50% of the starting value at 0 hours for cases S6 and S7, has been derived from the exponential regression of the relative intensity of 28S and 18S rRNA, and GAPDH mRNA, per mg bone tissue versus the storage interval (hours).

3.3.5 Semi-quantitative RT-PCR of total RNA isolated from human postmortem and surgical trabecular bone

cDNA was synthesized from 1 μg of total RNA from each sample (4 time-points from postmortem case A18, 8 time-points from surgical case S7, and 7 time-points from surgical cases S6 and S8; Chapter 2.2.2.3.1). cDNA was synthesized from each time-point RNA

sample for each case at the same time, to limit differences between time-point RNA samples in the efficiency of cDNA synthesis. cDNA was then amplified by PCR, using human-specific oligonucleotide primer pairs (Table 2.1), to generate products corresponding to mRNA encoding human calcitonin receptor (CTR), interleukin (IL)-6, osteocalcin (OCN), osteoprotegerin (OPG), receptor activator of nuclear factor kappa B (RANK), RANK ligand (RANKL), TGF-β1, and the housekeeping gene GAPDH (Chapter 2.2.2.3.2). To allow semi-quantification of the PCR products, to compare the mRNA expression between time-points, preliminary experiments were performed to ensure that the PCR amplification cycle number, for each set of primers, was within the log-linear range of amplification (Chapter 2.2.2.3.3). PCR amplification products were resolved by electrophoresis in 2% w/v agarose gels and post-stained with SYBR® Gold (Molecular Probes). The relative amounts of the PCR products were determined by quantitating the intensity of bands using a FluorImager (Molecular Dynamics) and the volume integration function of ImageQuant v.3.3 software (Molecular Dynamics). Semi-quantitative RT-PCR, involving verification and quantitation of PCR products by hybridisation with ^{32}P-labelled internal oligonucleotide probes, has been previously used by our group to determine the half-life of CTR mRNA in mouse osteoclast-like cells (Wada *et al.*, 1997).

The relative mRNA expression data (i.e., the relative amounts of the PCR products) are expressed as percentages of the respective mRNA level at 24 hours postmortem for the postmortem case A18. The relative half-life (T_{50}), the incubation time required for mRNA to decrease to 50% of the starting value at 24 hours postmortem, of each mRNA analysed for case A18, has been derived from the exponential regression of the percentage of mRNA at 24 hours postmortem versus the storage interval (hours). The relative mRNA expression data (i.e., the relative amounts of the PCR products) are expressed per mg of

bone tissue for the surgical cases S6, S7, and S8. The relative half-life (T_{50}), the incubation time required for mRNA to decrease to 50% of the starting value at 2 hours for S6, and 0 hours for S7 and S8, for each mRNA analysed, has been derived from the exponential regression of the relative mRNA level per mg bone tissue versus the storage interval (hours). RT-PCR data was not available for the 0 hour time-point from case S6 (bone tissue stored at 4°C) or the 72 hour time-point from case S8 (bone tissue stored at 37°C) due to small quantities of total RNA recovered.

3.3.6 Statistical analysis of Northern blot and RT-PCR data

Northern blot analysis was performed twice, yielding reproducible results for the quantitation of the relative density of the GAPDH mRNA bands. For each time-point, from postmortem case A18, and surgical cases S6, S7, and S8, RT-PCR reactions were performed twice, from duplicate cDNA syntheses, which confirmed that repeated RT-PCR analysis of the same RNA samples yielded reproducible results. In addition, to minimise inter-assay variability for the comparison of time-points within a single case, all PCR products, for each case, for a given mRNA species, were electrophoresed in a single 2% agarose gel. Each data point for the statistical analyses represented the mean of two separate RT-PCR reactions. Regression analysis, both linear and exponential, was used to examine the relationship between the relative mRNA expression levels and storage intervals of the bone tissue, for both the Northern blot and RT-PCR analyses. Pearson's correlation coefficient was used to examine the relationship between postmortem variables and relative intensities of the rRNA bands and GAPDH mRNA (Excel; Microsoft Corp.). The critical value for significance was chosen as $p = 0.05$.

3.4 RESULTS

3.4.1 Stability of total RNA isolated from human postmortem trabecular bone

Total RNA was isolated from femoral and iliac crest trabecular bone tissues, from 17 routine postmortem cases with a PMI range of 4 to 84 hours (Tables 3.1 and 3.2). Total RNA integrity was assessed by the relative abundance of the 28S and 18S rRNA bands, which were visualised, under UV light, on ethidium bromide-stained 1% agarose-formaldehyde gels (Figure 3.1). Total RNA samples were loaded into the gel according to increasing PMIS. Although an equivalent amount of total RNA was loaded per lane (3 μg), Figure 3.1 shows that there is considerable variability in the intensity of the 28S (5 kb) and 18S (1.8 kb) rRNA bands. The 260/280 absorbance ratio for these samples was on average 1.7 ± 0.2. When the relative intensities of the 28S and 18S rRNA bands were quantitated, no significant correlation was found between the relative intensities of 28S, 18S, or the 28S/18S ratio and the postmortem variables, which included the age of the individual, PMI, storage interval at 4°C, and PMIS.

Human GAPDH mRNA, a housekeeping gene used as a referent in mRNA expression analyses, was detected as a 1.28 kb band in these postmortem trabecular bone RNA samples by Northern blot analysis (Figure 3.1). A tailing or smearing of GAPDH mRNA below the 1.28 kb band was observed in several cases, which suggests partial degradation of the GAPDH mRNA. This band tailing effect has been previously observed for GAPDH mRNA on Northern blots of rabbit postmortem connective tissue RNA (Marchuk *et al.*, 1998). Interestingly, a GAPDH mRNA 1.28 kb band was still detectable up to 84 hours postmortem (Figure 3.1). The relative intensity of the GAPDH mRNA band did not

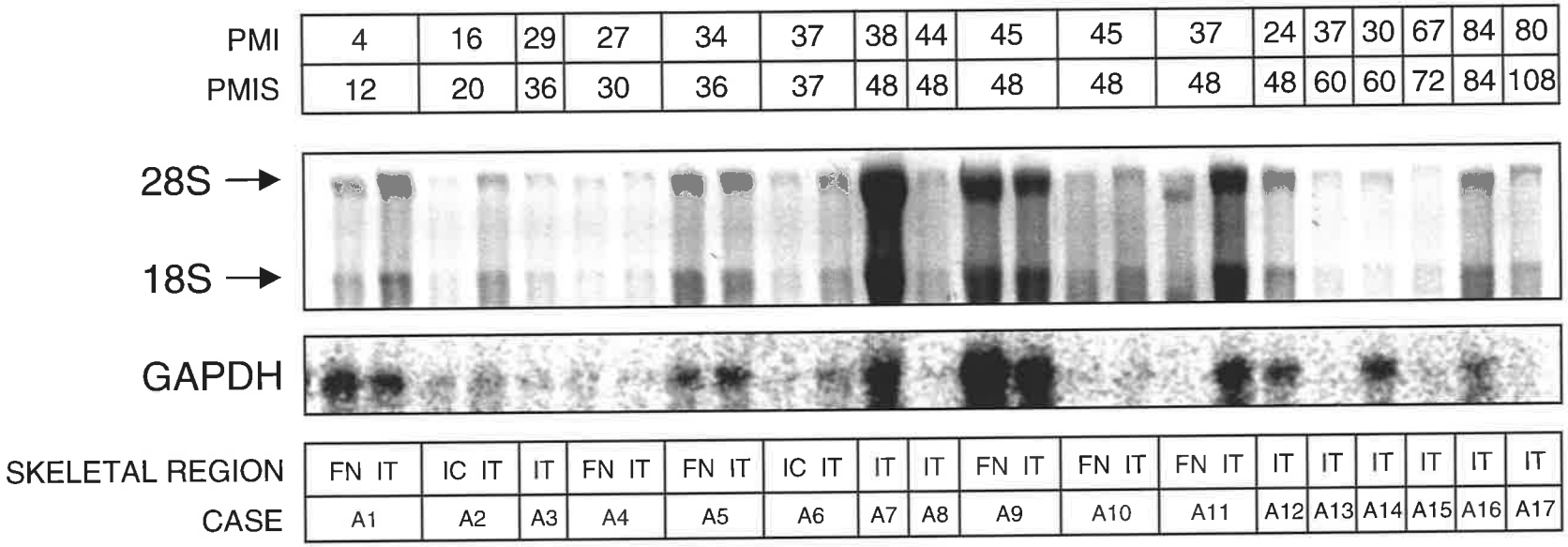

Figure 3.1: Total RNA isolated from human postmortem trabecular bone, 3 µg per lane, was electrophoresed through a 1% agarose-formaldehyde gel, stained with ethidium bromide to visualise the 28S (5 kb) and 18S (1.8 kb) rRNA bands, transferred to a nylon membrane, and hybridised with a ^{32}P-labelled GAPDH probe (Chapter 2.2.2.2) to detect human GAPDH mRNA (1.28 kb). PMI, postmortem interval (hours); PMIS, sum of the postmortem and bone tissue storage at 4°C intervals (hours); skeletal regions: FN, femoral neck; IC, iliac crest; IT, intertrochanteric region of the proximal femur; for case profiles refer to Table 3.1.

correlate with the postmortem variables, which included the age of the individual, PMI, storage interval at 4°C, and PMIS.

A significant positive correlation was observed between the relative intensities of the 28S and 18S rRNA bands for all of these postmortem trabecular bone RNA samples (n = 25; 28S vs. 18S: r = 0.95, p < 0.0001). In addition, significant positive correlations were observed between the relative intensity of the GAPDH mRNA band and the relative intensity of both the 28S and 18S rRNA bands for all of these samples (n = 25; GAPDH vs. 28S: r = 0.65, p < 0.0005; GAPDH vs. 18S: r = 0.60, p < 0.001). Collectively, these observations suggest that, irrespective of the postmortem variables for each case, there are similar relationships between the relative intensities of 28S rRNA, 18S rRNA, and GAPDH mRNA, for each case. Furthermore, the data suggest that the RNA stability of 28S rRNA, 18S rRNA, and GAPDH mRNA is comparable in human postmortem trabecular bone tissues up to 84 hours postmortem at 4°C. When RNA was isolated from two different skeletal regions from the same postmortem case, with the exception of case A11, significant positive correlations were observed between the two skeletal regions for the relative intensity of the 28S rRNA band, 18S rRNA band, and GAPDH mRNA band (n = 7; 28S: r = 0.91, p < 0.001; 18S: r = 0.74, p < 0.03; GAPDH: r = 0.98, p < 0.0001). This suggests that the relative intensity of each of the 28S rRNA, 18S rRNA, and GAPDH mRNA bands is similar between skeletal regions for each case. In addition, the data further suggest that the bone tissue processing conditions for RNA isolation are unlikely to be influencing variation in the relative intensity of the 28S rRNA, 18S rRNA, and GAPDH mRNA bands between cases.

Total RNA was also isolated from femoral and tibial trabecular bone tissues from 5 surgical cases (Table 3.3), to assess the integrity of rRNA and GAPDH mRNA in bone tissues which were processed immediately for RNA isolation after their retrieval at surgery, without a storage interval. The 260/280 absorbance ratio for these surgical bone RNA samples was on average 1.7 ± 0.2, which was comparable to the postmortem bone RNA samples. The assessment of rRNA integrity, on ethidium bromide-stained 1% agarose-formaldehyde gels, and GAPDH mRNA integrity, by Northern blot analysis, is shown in Figure 3.2. Variability in the appearance of the 28S and 18S rRNA bands for an equivalent quantity of total RNA loaded per lane (3 μg), as observed for the postmortem bone tissue RNA, was evident for these surgical samples (Figure 3.2). A significant positive correlation was observed between the relative intensities of the 28S and 18S rRNA bands for these surgical samples (n = 6; 28S vs. 18S: r = 0.99, p < 0.0002), consistent with the postmortem bone RNA. No correlation was observed between the relative intensity of the GAPDH mRNA band and the relative intensity of either the 28S or 18S rRNA band for the surgical bone RNA. Further, the band tailing effect for GAPDH mRNA, which was evident for some of the postmortem bone RNA samples (Figure 3.1), was not observed for any of the surgical bone RNA samples (Figure 3.2).

3.4.2 Stability of various mRNA species in human postmortem trabecular bone

To investigate the effect of the PMI, or the storage interval at 4°C, on the integrity of specific mRNA species in human postmortem bone, total RNA was isolated from intertrochanteric trabecular bone sampled from a postmortem case with a 24 hour PMI (case A18; Table 3.1), and at further 24 hour intervals, up to 96 hours, after storage of the

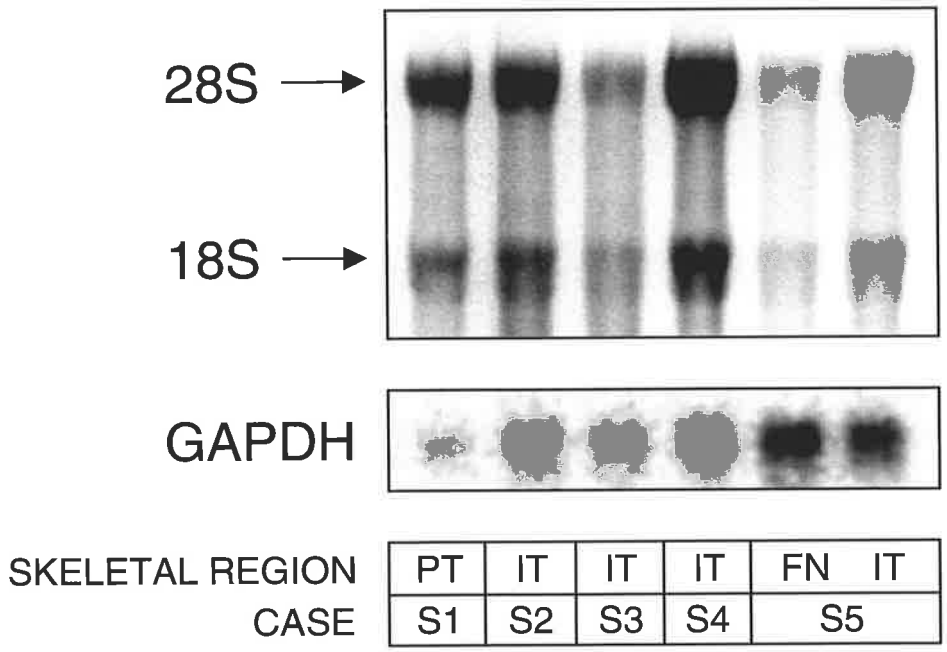

Figure 3.2: Total RNA isolated from human surgical trabecular bone, 3 μg per lane, was electrophoresed through a 1% agarose-formaldehyde gel, stained with ethidium bromide to visualise the 28S (5 kb) and 18S (1.8 kb) rRNA bands, transferred to a nylon membrane, and hybridised with a ^{32}P-labelled GAPDH probe (Chapter 2.2.2.2) to detect human GAPDH mRNA (1.28 kb). Skeletal regions: FN, femoral neck; IT, intertrochanteric region of the proximal femur; PT, proximal tibia; for case profiles refer to Table 3.3.

bone tissue at 4°C (section 3.3.1.2). These time-course total RNA samples had an average 260/280 absorbance ratio of 1.8 ± 0.1. Semi-quantitative RT-PCR (section 3.3.5) was used to assess the relative abundance of mRNA encoding the key osteoclast differentiation factor, RANKL; the soluble decoy receptor for RANKL, OPG; IL-6, a recognised skeletally-active cytokine capable of promoting osteoclast formation; the abundant bone matrix growth factor, TGF-β1; and the housekeeping gene, GAPDH, in these time-course RNA samples. The relative expression of OPG, TGF-β1, and GAPDH mRNA was observed to decline with the time the postmortem bone tissue was stored at 4°C (Figure 3.3). RANKL mRNA appeared to follow this pattern of decline up to 72 hours, although RANKL mRNA was abundant at the 96 hour time-point (Figure 3.3). IL-6 mRNA did not appear to decline with bone tissue storage time at 4°C. The relative half-life (T_{50}), for each mRNA analysed, was derived from the exponential regression of the percentage of mRNA at 24 hours postmortem versus the storage interval at 4°C (hours; section 3.3.5). The relative T_{50} for OPG, TGF-β1, and GAPDH mRNA was 64, 35, and 88 hours, respectively (Table 3.4). The relative T_{50} for RANKL and IL-6 mRNA could not be determined as the data is not described by a significant exponential regression.

There was no change in the relative ratios of RANKL/GAPDH, OPG/GAPDH, and IL-6/GAPDH mRNA with bone tissue storage time. However, the relative ratio of TGF-β1/GAPDH mRNA declined with bone tissue storage time at 4°C (n = 4; exponential regression: r = -0.83, $p < 0.05$), suggesting that TGF-β1 mRNA degraded at a faster rate compared to the referent mRNA, GAPDH, in this postmortem bone tissue. Furthermore, the relative T_{50} for TGF-β1 mRNA (35 hours) was 2.5 fold less than for GAPDH mRNA (88 hours; Table 3.4).

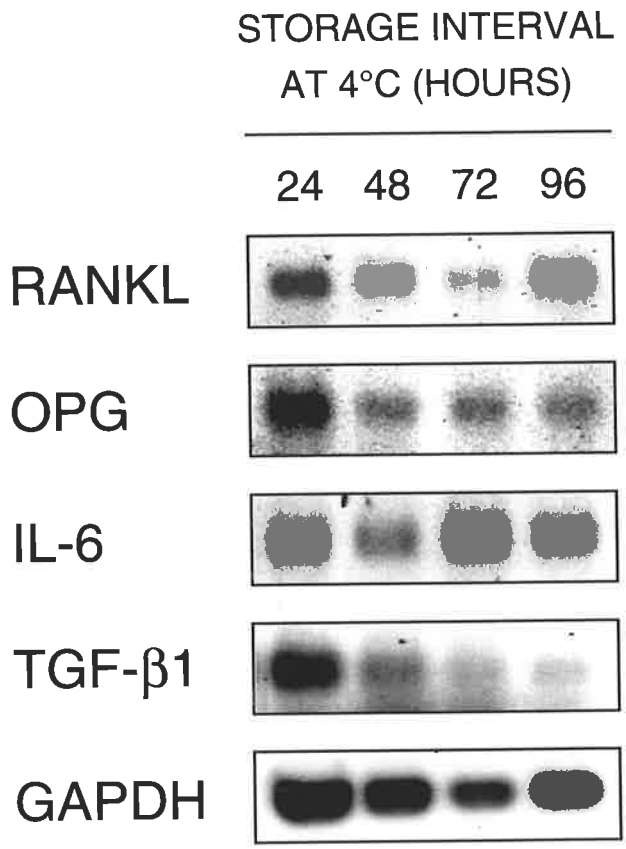

Figure 3.3: Expression of RANKL (665 bp), OPG (433 bp), IL-6 (544 bp), TGF-β1 (224 bp), and GAPDH (415 bp) mRNA in total RNA isolated from human postmortem intertrochanteric trabecular bone sampled from case A18 (PMI of 24 hours; Table 3.1). Trabecular bone tissue was stored in sterile saline at 4°C and total RNA was isolated at 24 hour increments, up to 96 hours, for RT-PCR analysis of specific mRNA expression. PCR products representing each mRNA species were visualised on SYBR® Gold-stained 2% agarose gels.

Table 3.4 Relative T_{50} for specific mRNA species in human postmortem intertrochanteric trabecular bone tissue sampled from case A18 (PMI of 24 hours). The bone tissue had been stored in sterile saline at 4°C and total RNA was isolated at 24 hour increments, up to 96 hours, for RT-PCR analysis of specific mRNA expression. Relative values for each specific mRNA were determined using ImageQuant on FluorImager (Molecular Dynamics) scanned SYBR® Gold-stained 2% agarose gels, and expressed as percentages of the respective mRNA level at 24 hours postmortem.

mRNA	T_{50} *(hours)*
RANKL	Indeterminate
OPG	63.6
IL-6	Indeterminate
TGF-β1	34.5
GAPDH	87.7

Relative half-life (T_{50}), refers to the incubation time required for mRNA to decrease to 50% of the starting value at 24 hours postmortem.
Indeterminate, refers to the relative T_{50} could not be determined as the data is not described by a significant exponential regression.

3.4.3 Effect of storage temperature and time on the stability of total RNA isolated from human surgical trabecular bone

Trabecular bone samples from the intertrochanteric region (sampled as 10 mm diameter tube saw core biopsies; section 3.3.2.2) of surgical cases S6, S7, and S8 (Table 3.3), were used to investigate the effect of storage temperature and storage time on the integrity of total RNA and specific mRNA species in human bone tissue. Total RNA was isolated from an eighth of each bone sample, immediately after their retrieval at surgery, to represent a 0 hour time-point. The remaining bone samples were stored in sterile saline at 4°C, room temperature (22°C ± 1°C), or 37°C, for cases S6, S7, and S8, respectively, and total RNA

was isolated at 2, 4, 8, 16, 24, 48, and 72 hour time-points (section 3.3.2.2). The storage temperatures investigated were chosen for the following reasons: 4°C replicates the storage temperature of the body before the postmortem examination, and subsequent bone tissue retrieval and RNA isolation; room temperature replicates the stabilised body temperature before refrigeration; and 37°C replicates the average core body temperature before death (Henssge, 1995), and allows the RNA degradation rate to be assessed at a temperature at which endogenous and introduced RNases are likely to be active. The total RNA yield (μg RNA/mg wet weight) was calculated for each time-point for each of the three cases (section 3.3.3; Table 3.5). There was no significant decline with time in the total RNA yield or 260/280 absorbance ratio for the bone samples stored at 4°C or room temperature (Table 3.5). However, total RNA yield declined rapidly with time for the bone samples stored at 37°C ($n = 8$; linear regression: $r = -0.81$, $p < 0.005$; exponential regression: $r = -0.86$, $p < 0.002$). The 260/280 absorbance ratio also decreased with the time the bone samples were stored at 37°C ($n = 8$; linear regression: $r = -0.89$, $p < 0.001$; exponential regression: $r = -0.91$, $p < 0.001$). The total RNA yield from the 37°C stored bone tissues was not sufficient in quantity for Northern blot analysis.

Total RNA integrity for the 4°C and room temperature time-course bone tissue RNA samples was assessed by the relative abundance of the 28S and 18S rRNA bands on ethidium bromide-stained 1% agarose-formaldehyde gels (Figures 3.4 and 3.5). The relative intensity data of the 28S and 18S rRNA bands were expressed per mg of bone tissue to correct for differences in sample tissue weight. A negative exponential correlation was observed between the relative intensities of 28S rRNA, 18S rRNA, and the 28S/18S ratio, and the storage interval at 4°C, but not at room temperature (Table 3.6). There may be more variability between time-points in the relative intensity of the 28S and 18S rRNA

Table 3.5 Yield of total RNA (μg RNA/mg wet weight) isolated from human surgical intertrochanteric trabecular bone sampled from cases S6, S7, and S8. Trabecular bone tissue was stored in sterile saline at 4°C (S6), room temperature (RT; S7), or 37°C (S8), for 0, 2, 4, 8, 16, 24, 48, and 72 hours and total RNA isolated at these time-points.

Time *(hours)*	**Total RNA yield** *(μg RNA/mg wet weight)* **Storage temperature**		
	4°C	**RT (22°C)**	**37°C**
0	0.044	0.221	0.067
2	0.106	0.086	0.064
4	0.057	0.119	0.042
8	0.044	0.087	0.052
16	0.074	0.047	0.024
24	0.149	0.094	0.009
48	0.054	0.126	0.013
72	0.045	0.089	0.007

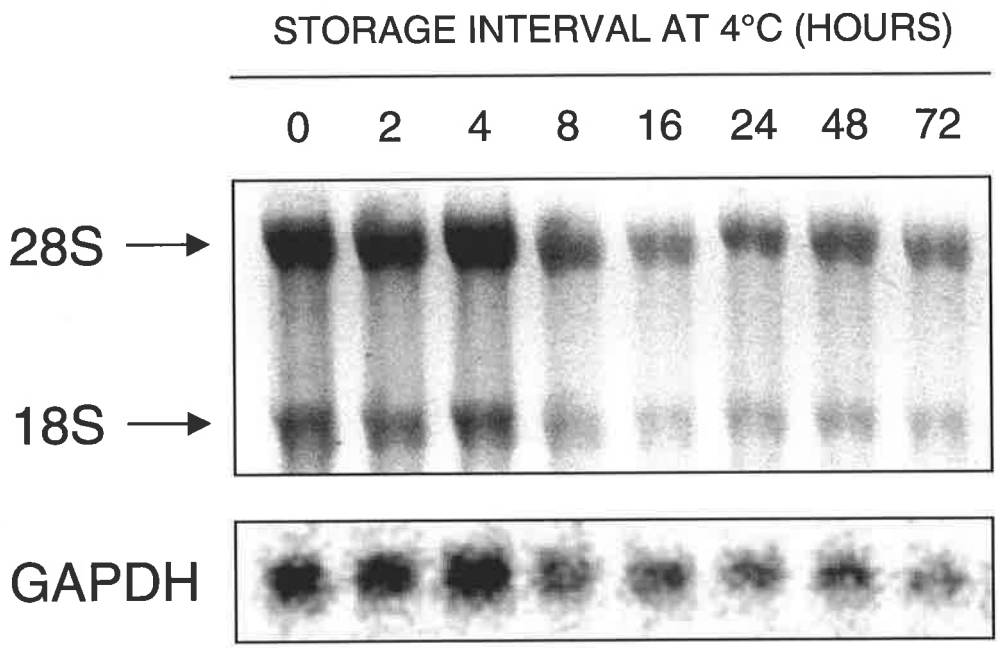

Figure 3.4: Total RNA isolated from human surgical intertrochanteric trabecular bone sampled from case S6 (Table 3.3), 3 μg per lane, was electrophoresed through a 1% agarose-formaldehyde gel, stained with ethidium bromide to visualise the 28S (5 kb) and 18S (1.8 kb) rRNA bands, transferred to a nylon membrane, and hybridised with a ^{32}P-labelled GAPDH probe (Chapter 2.2.2.2) to detect human GAPDH mRNA (1.28 kb). Trabecular bone tissue was stored in sterile saline at 4°C for 0, 2, 4, 8, 16, 24, 48, and 72 hours and total RNA isolated at these time-points.

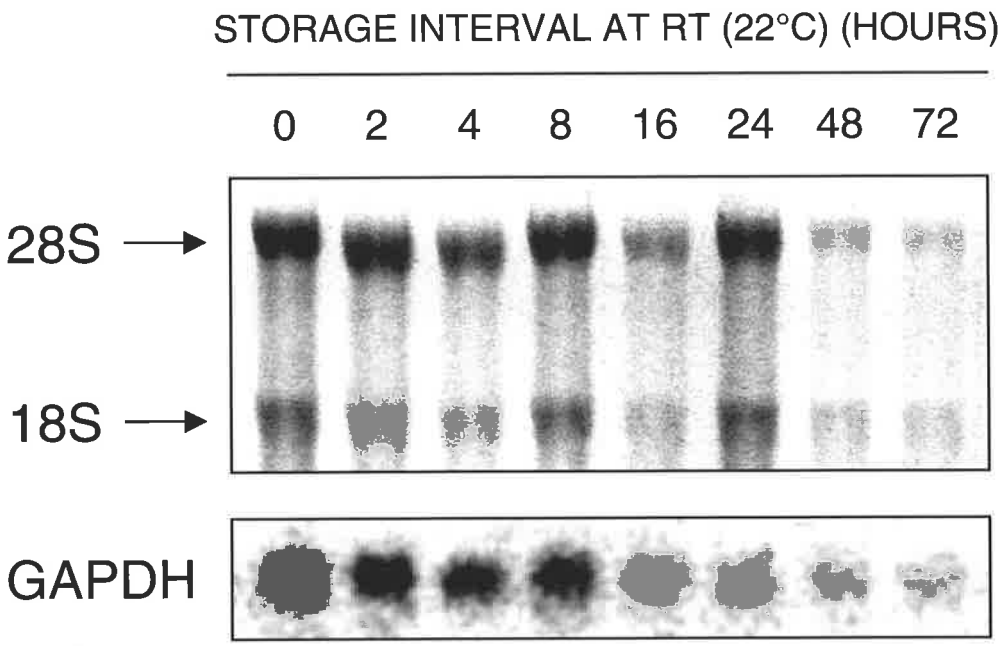

Figure 3.5: Total RNA isolated from human surgical intertrochanteric trabecular bone sampled from case S7 (Table 3.3), 3 µg per lane, was electrophoresed through a 1% agarose-formaldehyde gel, stained with ethidium bromide to visualise the 28S (5 kb) and 18S (1.8 kb) rRNA bands, transferred to a nylon membrane, and hybridised with a ^{32}P-labelled GAPDH probe (Chapter 2.2.2.2) to detect human GAPDH mRNA (1.28 kb). Trabecular bone tissue was stored in sterile saline at RT (room temperature; 22°C ± 1°C) for 0, 2, 4, 8, 16, 24, 48, and 72 hours and total RNA isolated at these time-points.

Table 3.6 Relative intensity values of 28S and 18S rRNA, and GAPDH mRNA, were determined using ImageQuant on FluorImager (Molecular Dynamics) scanned 1% agarose-formaldehyde gels and PhosphorImager (Molecular Dynamics) scanned Northern blots, respectively, and expressed per mg of bone tissue. Total RNA was isolated from human surgical intertrochanteric trabecular bone sampled from cases S6 and S7. Trabecular bone tissue was stored in sterile saline at 4°C (S6) or room temperature (RT; S7) for 0, 2, 4, 8, 16, 24, 48, and 72 hours and total RNA isolated at these time-points.

RNA ($n = 8$)	Storage temperature			
	4°C		RT (22°C)	
	Linear	*Exponential*	*Linear*	*Exponential*
28S rRNA	$r = -0.65$ $p < 0.05$	$r = -0.80$ $p < 0.005$	$r = -0.46$ NS	$r = -0.46$ NS
18S rRNA	$r = -0.60$ NS	$r = -0.70$ $p < 0.03$	$r = -0.50$ NS	$r = -0.52$ NS
28S/18S rRNA	$r = -0.63$ NS	$r = -0.69$ $p < 0.03$	$r = -0.19$ NS	$r = -0.15$ NS
GAPDH mRNA	$r = -0.55$ NS	$r = -0.65$ $p < 0.05$	$r = -0.61$ NS	$r = -0.70$ $p < 0.03$

The linear and exponential correlation coefficients between the time the bone tissue was stored at 4°C or RT, and levels of 28S and 18S rRNA, and GAPDH mRNA, are shown. The two-tailed p value for each correlation is given; NS, not significant.

bands in bone tissue stored at room temperature in comparison to 4°C, due to small fluctuations in the temperature during the time-course (i.e., 22°C ± 1°C; compare Figures 3.4 and 3.5). The stability of GAPDH mRNA in the 4°C and room temperature time-course bone tissue RNA samples was assessed by Northern blot analysis (Figures 3.4 and 3.5, respectively), and the relative intensity data of the GAPDH mRNA bands were expressed per mg of bone tissue. The relative intensity of the human GAPDH mRNA band negatively correlated with the storage interval at both 4°C and room temperature by an exponential regression (Figures 3.6A and 3.6B, respectively; Table 3.6).

The relative T_{50} was derived from the exponential regression of the relative intensity of 28S and 18S rRNA, and GAPDH mRNA, per mg bone tissue versus the storage interval (hours; section 3.3.4). The relative T_{50} for 28S and 18S rRNA at 4°C was 26 and 39 hours, respectively (Table 3.7). The 28S and 18S rRNA relative T_{50} at room temperature could not be determined as the data is not described by a significant exponential regression. The relative T_{50} for GAPDH mRNA at 4°C and room temperature was 48 and 39 hours, respectively (Table 3.7). Interestingly, at both 4°C and room temperature, there was no change in the relative ratio of GAPDH mRNA/28S rRNA or GAPDH mRNA/18S rRNA with increasing bone tissue storage time. This suggests that there is no difference between the degradative rates of GAPDH mRNA and rRNA in surgical trabecular bone tissue stored in sterile saline at either 4°C or room temperature.

Figure 3.6: Effect of storage temperature and time on stability of GAPDH mRNA in total RNA isolated from human surgical intertrochanteric trabecular bone sampled from cases S6 (4°C; A) and S7 (room temperature {RT; 22°C ± 1°C}; B; Table 3.3), as determined by Northern blot analysis (Chapter 2.2.2.2). Trabecular bone tissue was stored in sterile saline at 4°C or RT for 0, 2, 4, 8, 16, 24, 48, and 72 hours and total RNA was isolated at these time-points. Relative intensity values of GAPDH mRNA were determined using ImageQuant on PhosphorImager (Molecular Dynamics) scanned Northern blots, and expressed per mg of bone tissue. The relative intensity value at the first time-point was set to one. Relative intensity values at other time-points are shown relative to the first time-point. There was a significant exponential decline in the relative intensity of GAPDH mRNA with storage time at both 4°C ($y = 1.59e^{-0.01x}$; $r = -0.65$ and $p < 0.05$) and RT ($y = 0.47e^{-0.02x}$; $r = -0.70$ and $p < 0.03$).

GAPDH mRNA

A

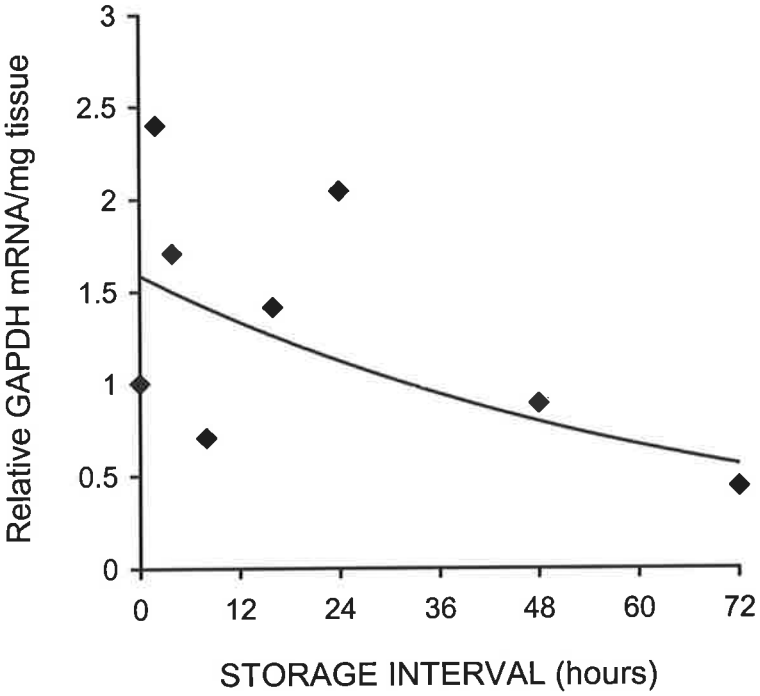

4°C

B

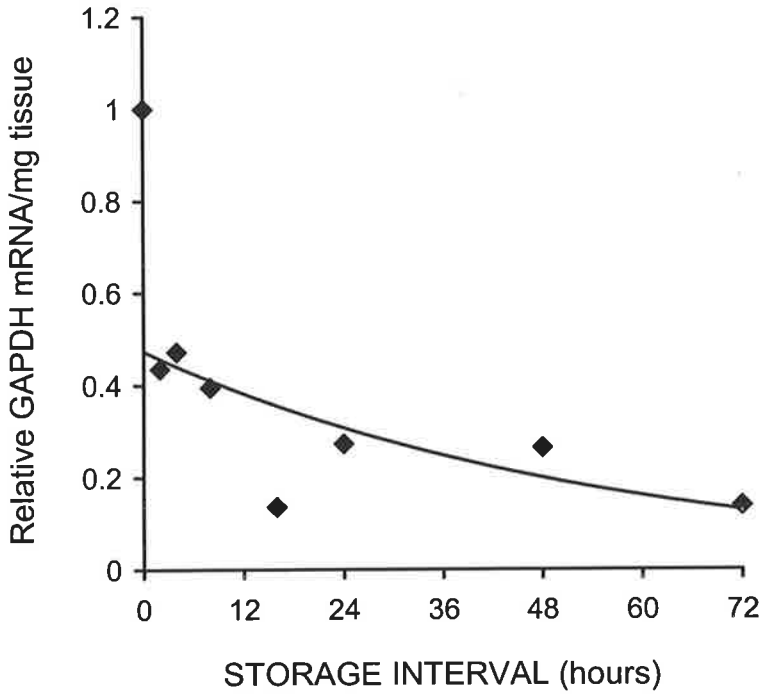

RT (22°C)

Table 3.7 Relative T_{50} for 28S and 18S rRNA, and GAPDH mRNA, in human surgical intertrochanteric trabecular bone tissue sampled from cases S6 and S7, which had been stored in sterile saline at 4°C (S6) or room temperature (RT; S7) for 0, 2, 4, 8, 16, 24, 48, and 72 hours. Total RNA was isolated from each of these time-points. Relative intensity values of 28S and 18S rRNA, and GAPDH mRNA, were determined using ImageQuant on FluorImager (Molecular Dynamics) scanned 1% agarose-formaldehyde gels and PhosphorImager (Molecular Dynamics) scanned Northern blots, respectively, and expressed per mg of bone tissue.

RNA	T_{50} *(hours)* Storage temperature	
	4°C	RT (22°C)
28S rRNA	26.4	Indeterminate
18S rRNA	38.7	Indeterminate
GAPDH mRNA	47.8	38.5

Relative half-life (T_{50}), refers to the incubation time required for RNA to decrease to 50% of the starting value at 0 hours.
Indeterminate, refers to the relative T_{50} could not be determined as the data is not described by a significant exponential regression.

3.4.4 Effect of storage temperature and time on the stability of various mRNA species in human surgical trabecular bone

Time-courses of RNA isolation from trabecular bone tissues sampled from surgical cases S6, S7, and S8, where the bone tissue was stored at either 4°C, room temperature, or 37°C, respectively, were used to investigate the effect of storage temperature and storage time on the integrity of specific mRNA species in human bone tissue (section 3.3.2.2). Semi-quantitative RT-PCR (section 3.3.5) was used to assess the relative abundance of mRNA encoding RANKL; OPG; the cognate receptor of RANKL, RANK; the osteoclastic cell marker, CTR; the osteoblastic cell marker, OCN; IL-6; TGF-β1; and GAPDH, in these

time-course RNA samples. In general, the relative expression of these mRNA species declined significantly by 48 hours in bone tissue stored at 4°C from a 2 hour time-point up to 72 hours (Figure 3.7). The 0 hour time-point for this surgical case (S6), where the bone tissue was stored at 4°C, was not included in the RT-PCR analysis as all specific mRNA species, excluding GAPDH mRNA, were very low in abundance. However, the relative abundance of the 28S and 18S rRNA bands, and Northern blot analysis for GAPDH mRNA were not significantly low for this 4°C 0 hour time-point compared to the 4°C 2 hour time-point (Figure 3.4). The low expression of bone-specific mRNA species for the 4°C 0 hour time-point may be due to the bone tissue being sampled from the end of the tube saw specimen, and a subsequent loss of marrow elements due to inadequate harvesting and/or processing techniques.

For the bone tissue stored at room temperature from a 0 hour time-point up to 72 hours, RANKL, OPG, RANK, CTR, and TGF-β1 mRNA expression had declined significantly by 24 hours (Figure 3.8). The PCR cycle number for the human GAPDH mRNA-specific oligonucleotide primer set was within the log-linear range of amplification. The expression of GAPDH mRNA, assessed by semi-quantitative RT-PCR for the 4°C (S7) and room temperature (S8) time-courses (Figures 3.7 and 3.8, respectively), appeared to only decline slightly up to 72 hours, which is in contrast with the significant exponential decline in GAPDH mRNA observed with Northern blot analysis for both the 4°C and room temperature time-courses (Figures 3.4 and 3.5, respectively; Figures 3.6A and 3.6B, respectively). Northern blot analysis detects full-length GAPDH mRNA transcripts (1.28 kb) using a ^{32}P-labelled probe of the 415 bp GAPDH fragment amplified by PCR (Chapter 2.2.2.2). RT-PCR analysis utilises oligonucleotide primers specific to human GAPDH mRNA, which amplify a 415 bp fragment between the exon 4/5 boundary and within exon

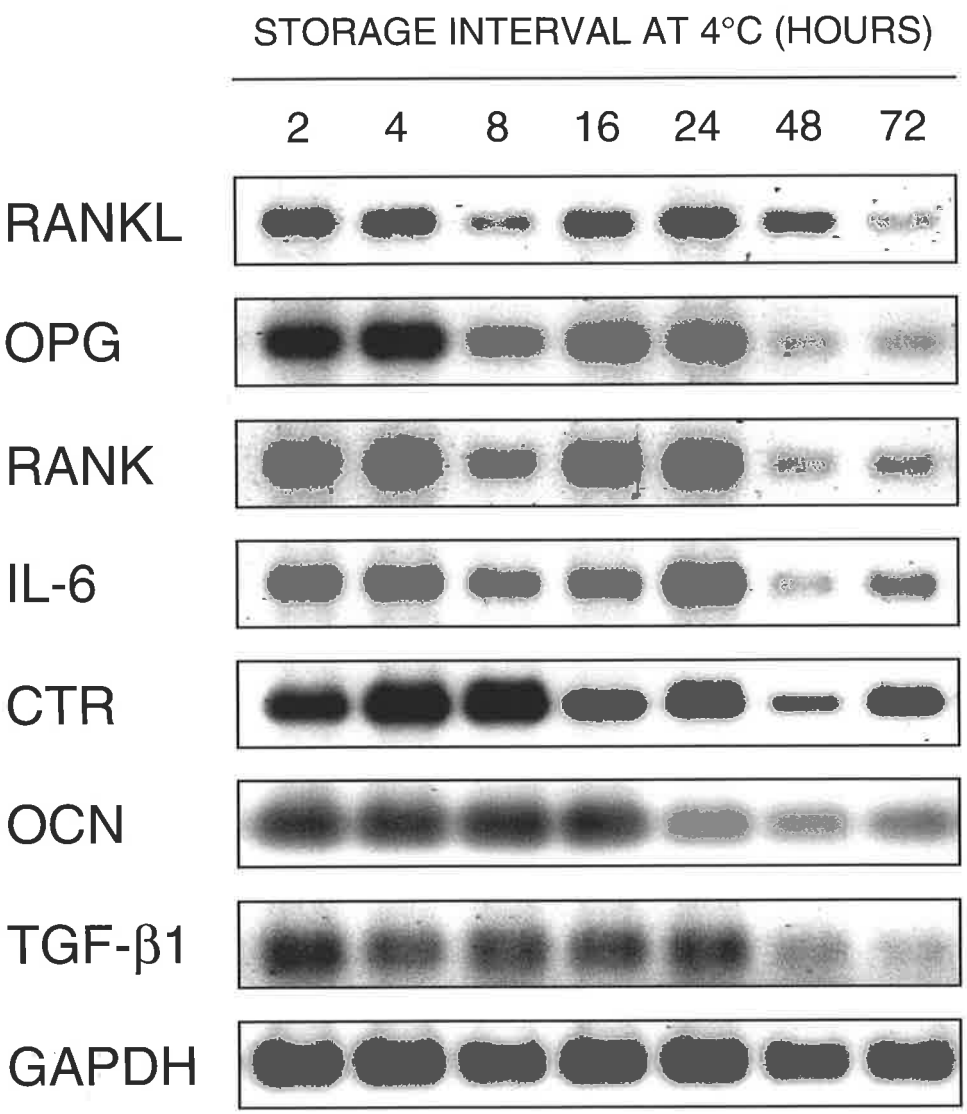

Figure 3.7: Expression of RANKL (665 bp), OPG (433 bp), RANK (702 bp), IL-6 (544 bp), CTR isoforms (780/732 bp), OCN (255 bp), TGF-β1 (224 bp), and GAPDH (415 bp) mRNA in total RNA isolated from human surgical intertrochanteric trabecular bone sampled from case S6 (Table 3.3). Trabecular bone tissue was stored in sterile saline at 4°C for 2, 4, 8, 16, 24, 48, and 72 hours, total RNA was isolated at these time-points, for RT-PCR analysis of specific mRNA expression. PCR products representing each mRNA species were visualised on SYBR® Gold-stained 2% agarose gels.

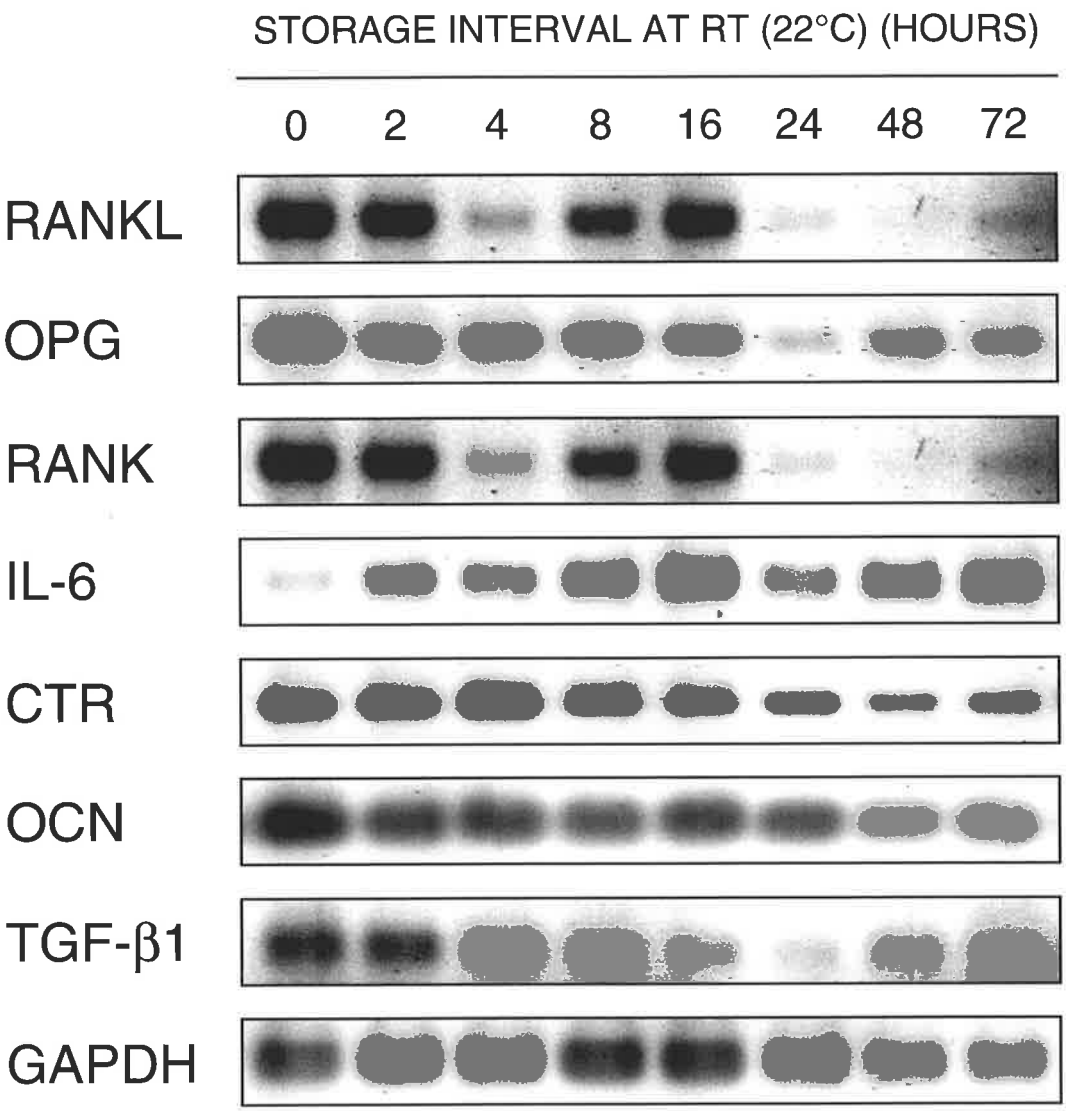

Figure 3.8: Expression of RANKL (665 bp), OPG (433 bp), RANK (702 bp), IL-6 (544 bp), CTR isoforms (780/732 bp), OCN (255 bp), TGF-β1 (224 bp), and GAPDH (415 bp) mRNA in total RNA isolated from human surgical intertrochanteric trabecular bone sampled from case S7 (Table 3.3). Trabecular bone tissue was stored in sterile saline at RT (room temperature; 22°C ± 1°C) for 0, 2, 4, 8, 16, 24, 48, and 72 hours, total RNA was isolated at these time-points, for RT-PCR analysis of specific mRNA expression. PCR products representing each mRNA species were visualised on SYBR® Gold-stained 2% agarose gels.

7 (Table 2.1). The RT-PCR analysis for GAPDH mRNA would be amplifying both full-length and partially degraded GAPDH mRNA transcripts, degraded from the 3' end up to within exon 7 and/or degraded from the 5' end up to exon 5. The discrepancy between the Northern blot and RT-PCR analysis, for the 4°C and room temperature time-courses, suggests that full-length GAPDH mRNA partially degraded with storage time, either from the 3' end or 5' end, with relatively much less cleavage occurring in the region of sequence being amplified by PCR.

The expression of all the mRNA species declined to almost no detectable PCR product by 48 hours in bone tissue stored at 37°C from a 0 hour time-point up to 48 hours (Figure 3.9). There was an insufficient quantity of total RNA recovered from the 72 hour time-point, from the 37°C time-course, for RT-PCR analysis.

The relative mRNA expression data for the 4°C, room temperature, and 37°C time-courses were expressed per mg of bone tissue to correct for differences in sample tissue weight, and to allow the calculation of relative half-lives (T_{50}) of each mRNA species (section 3.3.5). The relative expression of OPG, CTR, OCN, and TGF-β1 mRNA declined significantly in bone tissue stored at 4°C with an exponential regression yielding relative T_{50} values of 21, 35, 41, and 21 hours, respectively (Table 3.8). At room temperature, the expression of RANK and CTR mRNA significantly declined with an exponential regression yielding relative T_{50} values of 18 and 45 hours, respectively (Table 3.8). The RT-PCR data for the mRNA species listed in Table 3.8 without a relative T_{50}, for the 4°C and room temperature time-courses, could not be described by a significant exponential regression. All of the mRNA species rapidly degraded in bone tissue stored at 37°C, with the relative T_{50} ranging from 4 hours (RANK and OCN mRNA) to 14 hours (GAPDH

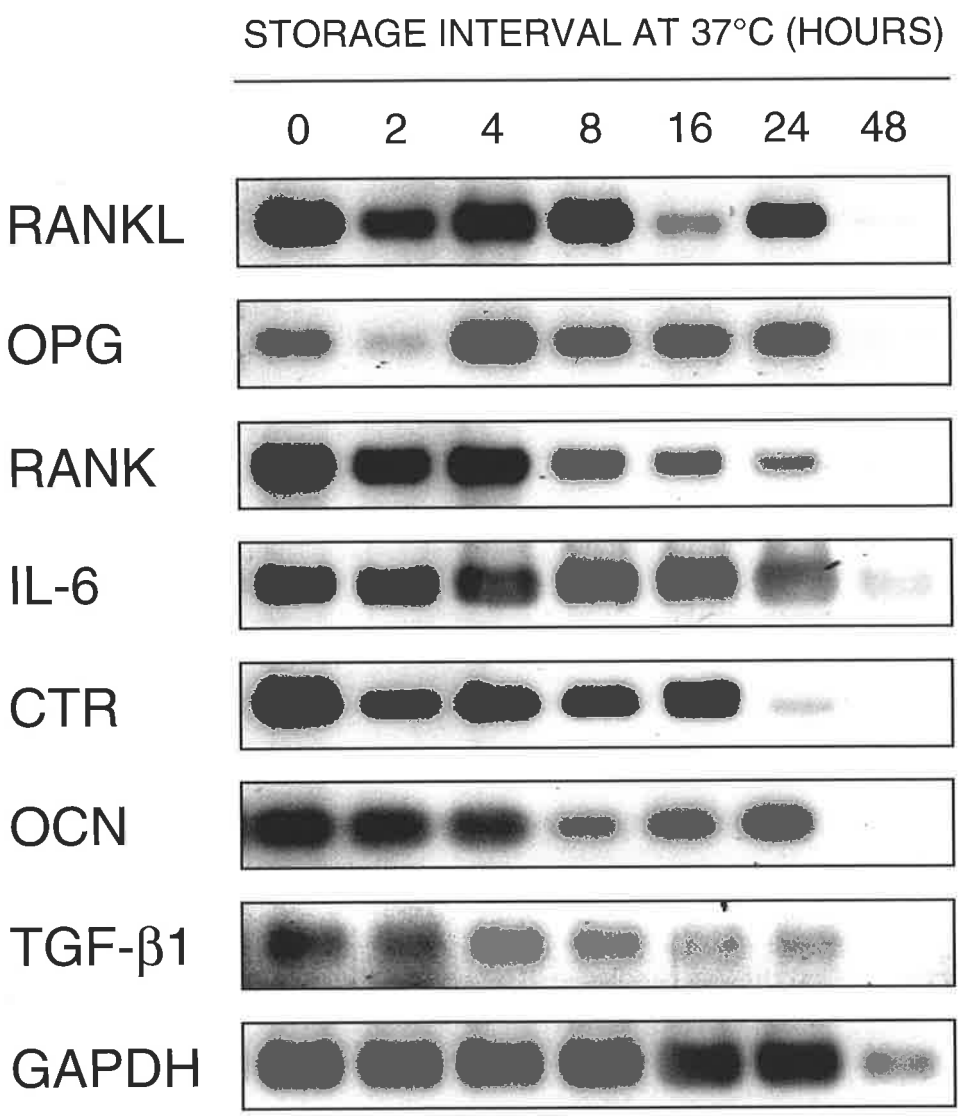

Figure 3.9: Expression of RANKL (665 bp), OPG (433 bp), RANK (702 bp), IL-6 (544 bp), CTR isoforms (780/732 bp), OCN (255 bp), TGF-β1 (224 bp), and GAPDH (415 bp) mRNA in total RNA isolated from human surgical intertrochanteric trabecular bone sampled from case S8 (Table 3.3). Trabecular bone tissue was stored in sterile saline at 37°C for 0, 2, 4, 8, 16, 24, and 48 hours, total RNA was isolated at these time-points, for RT-PCR analysis of specific mRNA expression. PCR products representing each mRNA species were visualised on SYBR® Gold-stained 2% agarose gels.

Table 3.8 Relative T_{50} for specific mRNA species in human surgical intertrochanteric trabecular bone tissue sampled from cases S6, S7, and S8. The bone tissue had been stored in sterile saline at 4°C (S6), room temperature (RT; S7), or 37°C (S8) for 0, 2, 4, 8, 16, 24, 48, and 72 hours. Total RNA was isolated from each of these time-points for RT-PCR analysis of specific mRNA expression. RT-PCR data was not available for the 4°C 0 hour time-point or the 37°C 72 hour time-point due to small quantities of total RNA recovered. Relative values for each specific mRNA were determined using ImageQuant on FluorImager (Molecular Dynamics) scanned SYBR® Gold-stained 2% agarose gels, and expressed per mg of bone tissue.

mRNA	T_{50} *(hours)* Storage temperature		
	4°C	**RT (22°C)**	**37°C**
RANKL	Indeterminate	Indeterminate	6.3
OPG	20.8	Indeterminate	7.0
RANK	Indeterminate	18.0	3.9
IL-6	Indeterminate	Indeterminate	9.6
CTR	34.5	45.3	4.4
OCN	40.5	Indeterminate	3.7
TGF-β1	20.9	Indeterminate	7.1
GAPDH	Indeterminate	Indeterminate	14.3

Relative half-life (T_{50}), refers to the incubation time required for mRNA to decrease to 50% of the starting value at 2 hours for 4°C, and 0 hours for RT and 37°C.
Indeterminate, refers to the relative T_{50} could not be determined as the data is not described by a significant exponential regression.

mRNA; Table 3.8). This rapid degradation of mRNA in bone tissue stored at 37°C is clearly demonstrated in Figures 3.10 and 3.11 as a comparison to bone tissue stored at 4°C, for CTR and OCN mRNA, respectively.

At 4°C, the relative ratios of OPG/GAPDH, RANK/GAPDH, OCN/GAPDH, and TGF-β1/GAPDH mRNA declined with bone tissue storage time (n = 7; exponential regression: OPG: r = -0.93, $p < 0.001$; RANK: r = -0.71, $p < 0.04$; OCN: r = -0.84, $p < 0.005$; TGF-β1: r = -0.91, $p < 0.001$), suggesting that OPG, RANK, OCN, and TGF-β1 mRNA degraded at a faster rate compared to the referent mRNA, GAPDH, in bone tissue stored at 4°C. At room temperature, the relative ratios of RANK/GAPDH and CTR/GAPDH mRNA declined with bone tissue storage time (n = 8; exponential regression: RANK: r = -0.72, $p < 0.03$; CTR: r = -0.67, $p < 0.05$), suggesting that RANK and CTR mRNA degraded at a faster rate compared to GAPDH mRNA. The relative ratio of all of the mRNA species/GAPDH mRNA declined significantly with bone tissue storage time at 37°C, suggesting that the degradative rate of all of these mRNA species was faster than GAPDH mRNA.

3.5 DISCUSSION

The analysis of mRNA expression patterns in human bone tissues can provide significant insight into the spatio-temporal activities of gene transcription, and furthermore, important information on physiology and pathology at a molecular level. Human pathological bone tissue is readily obtainable from surgery, but it is rarely possible to obtain suitable non-diseased bone tissues at surgery. Human postmortem bone tissue is a valuable resource of skeletal site-matched control tissue, although the stability of total RNA and specific mRNA species isolated from postmortem bone tissue is not known. The aim of the work

Figure 3.10: Effect of storage temperature and time on stability of CTR mRNA in total RNA isolated from human surgical intertrochanteric trabecular bone sampled from cases S6 (4°C) and S8 (37°C; Table 3.3), as determined by semi-quantitative RT-PCR analysis (Chapter 2.2.2.3). Trabecular bone tissue was stored in sterile saline at 4°C for 2, 4, 8, 16, 24, 48, and 72 hours, and at 37°C for 0, 2, 4, 8, 16, 24, and 48 hours, and total RNA was isolated at these time-points. The 37°C 48 hour time-point is not shown as the relative value for CTR mRNA was zero. Relative values of CTR mRNA were determined using ImageQuant on FluorImager (Molecular Dynamics) scanned SYBR® Gold-stained 2% agarose gels, and expressed per mg of bone tissue. The relative value at the first time-point was set to one. Relative values at other time-points are shown relative to the first time-point. There was a significant exponential decline in the relative value of CTR mRNA with storage time at both 4°C ($y = 0.94e^{-0.02x}$; $r = -0.69$ and $p < 0.05$ {solid line}) and 37°C ($y = 0.92e^{-0.16x}$; $r = -0.92$ and $p < 0.002$ {broken line}).

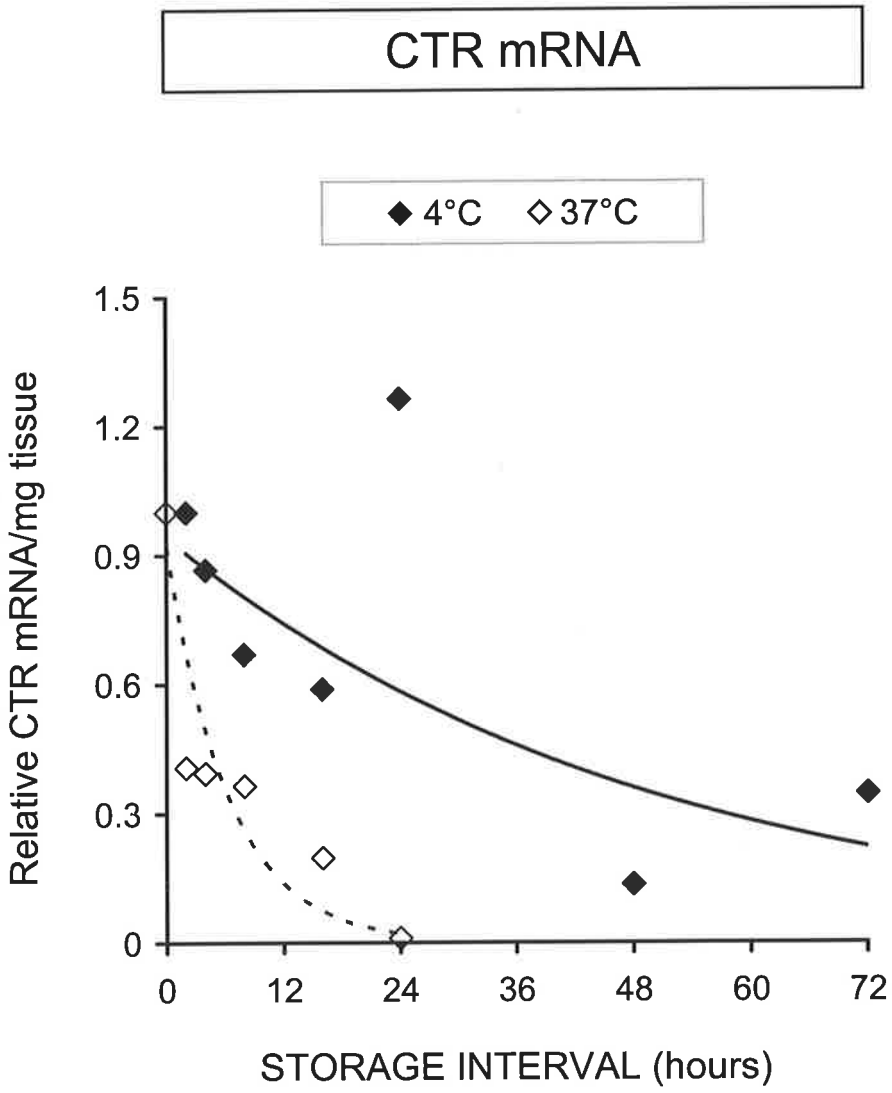
CTR mRNA
◆ 4°C ◇ 37°C
Relative CTR mRNA/mg tissue
1.5
1.2
0.9
0.6
0.3
0
0
12
24
36
48
60
72
STORAGE INTERVAL (hours)

Figure 3.11: Effect of storage temperature and time on stability of OCN mRNA in total RNA isolated from human surgical intertrochanteric trabecular bone sampled from cases S6 (4°C) and S8 (37°C; Table 3.3), as determined by semi-quantitative RT-PCR analysis (Chapter 2.2.2.3). Trabecular bone tissue was stored in sterile saline at 4°C for 2, 4, 8, 16, 24, 48, and 72 hours, and at 37°C for 0, 2, 4, 8, 16, 24, and 48 hours, and total RNA was isolated at these time-points. Relative values of OCN mRNA were determined using ImageQuant on FluorImager (Molecular Dynamics) scanned SYBR® Gold-stained 2% agarose gels, and expressed per mg of bone tissue. The relative value at the first time-point was set to one. Relative values at other time-points are shown relative to the first time-point. There was a significant exponential decline in the relative value of OCN mRNA with storage time at both 4°C ($y = 0.76e^{-0.02x}$; $r = -0.73$ and $p < 0.03$ {solid line}) and 37°C ($y = 1.96e^{-0.19x}$; $r = -0.95$ and $p < 0.001$ {broken line}).

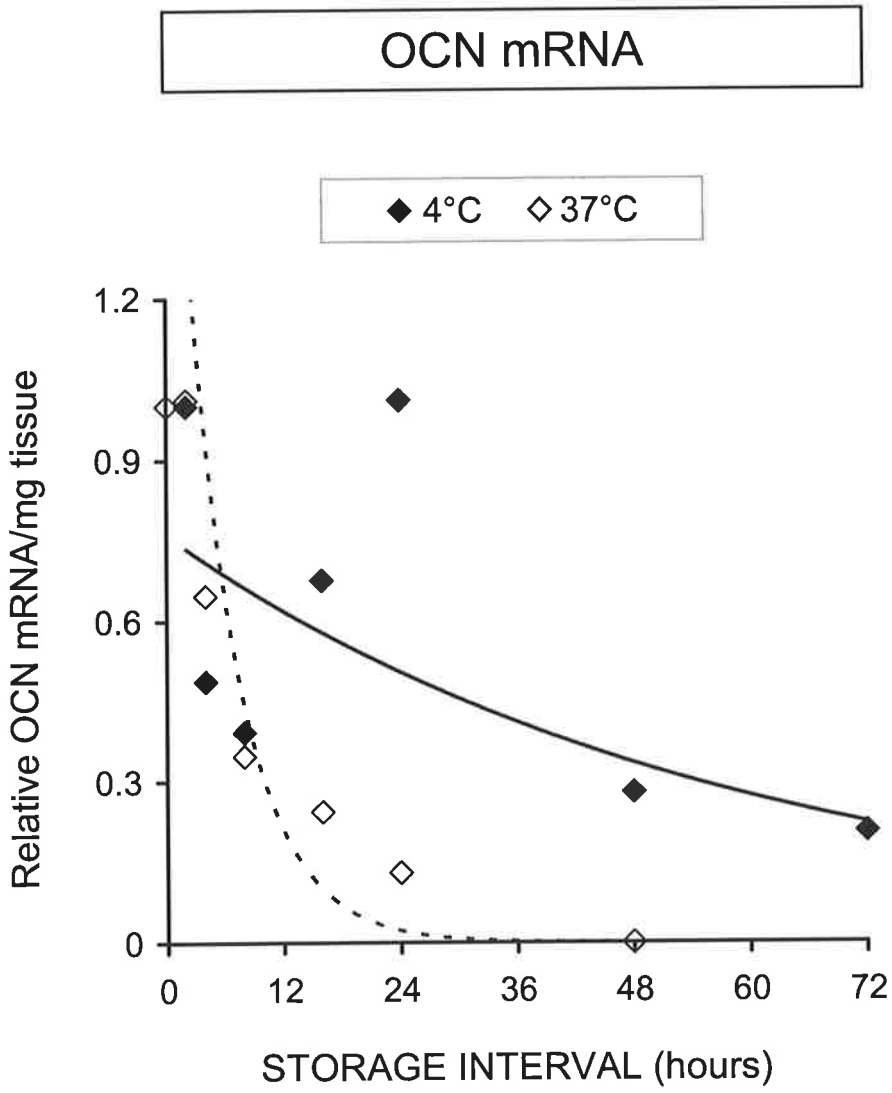
OCN mRNA
4°C
37°C
Relative OCN mRNA/mg tissue
1.2
0.9
0.6
0.3
0
0
12
24
36
48
60
72
STORAGE INTERVAL (hours)

described in this chapter was to investigate the stability of total RNA isolated from human postmortem bone tissues with a PMI range of 4 to 84 hours, and further, to examine the influence of different bone tissue storage conditions, such as temperature and time, on the stability of total RNA and bone-specific mRNAs in human surgical bone tissues.

3.5.1 Stability of total RNA and tissue-specific mRNA species in human postmortem tissues other than bone: a review of the literature

Yasojima *et al.* (2001) found negligible deterioration in total RNA and specific mRNAs in human postmortem brain tissue obtained up to 96 hours, provided the body had been kept at 4°C. There was no difference in the mRNA degradation rate between the highly stable housekeeping gene cyclophilin, and the highly labile (relatively unstable and transient) COX-2 mRNA, which has a half-life of 30 minutes *in vivo*. The techniques used in this study of postmortem RNA decay included the examination of the appearance of the rRNA bands on ethidium bromide-stained agarose-formaldehyde gels, and semi-quantitative RT-PCR amplification (Yasojima *et al.*, 2001), similar to the techniques used for the work described in this chapter pertaining to human postmortem bone tissues. A number of studies have found a variety of human brain-specific mRNAs, such as the G protein subunits, $G_{s\alpha}$, $G_{\beta 1}$, and $G_{\beta 2}$, fibroblast growth factor (FGF) receptor, basic FGF, and amyloid precursor protein, to be generally stable up to 48 hours postmortem at 4°C, when measured by Northern blotting and RT-PCR (Burke *et al.*, 1991; Leonard *et al.*, 1993; Ross *et al.*, 1992). The use of real-time RT-PCR analysis, for quantitation of mRNA levels, has shown that collagen α1(IV) and GAPDH mRNA levels exponentially decline at a similar rate when human postmortem kidney tissue, obtained at 7 hours postmortem, is incubated up to 48 hours at 4°C (Eikmans *et al.*, 2001). Eikmans *et al.* (2001) concluded that as the collagen α1(IV)/GAPDH mRNA ratio did not change with increasing tissue

storage time, which represents increasing PMI, this ratio was reliable for subsequent analyses of 18 postmortem kidneys with a range of 4 to 21 hours between death of the individual and storage of the renal tissue at -70°C. Real-time RT-PCR has also been used to quantitate pulmonary surfactant apoprotein A mRNA in human lung tissue specimens obtained from cases up to 96 hours postmortem (Ishida *et al.*, 2000). Human skeletal muscle tissues have been obtained within a postmortem interval of 24 hours and used for a time-course RNase protection assay analysis of the disappearance of quantifiable mRNA for the glucose transporter isoforms (GLUT) 3 and 4 (Stuart *et al.*, 1999). These muscle-specific mRNAs degraded rapidly in human postmortem muscle tissue stored at room temperature (20°C; Stuart *et al.*, 1999). There was a 50% decrease in GLUT 3 and GLUT 4 mRNA by 24 and 7 hours, respectively, at 4°C. GAPDH mRNA decreased by 50% by 17 hours at 4°C, and 2 hours at 20°C (Stuart *et al.*, 1999). Lin *et al.* (1999) have shown that RNA isolated from human temporal bone soft tissues, obtained up to 6 hours postmortem, is reliable for Northern blot analysis and *in situ* hybridisation analysis of both "stable" (low molecular weight; β-actin) and "unstable" (high molecular weight; MUC5B mucin gene) mRNA species.

3.5.2 Stability of total RNA in human postmortem trabecular bone

Overall degradation in total RNA isolated from trabecular bone from 17 postmortem cases was assessed by the integrity of the 28S and 18S rRNA bands on ethidium bromide-stained agarose-formaldehyde gels, and GAPDH mRNA expression by Northern blotting (Figure 3.1). There appeared to be a loss of higher molecular weight rRNA (28S and 18S), which is indicative of degradation, in some postmortem cases. However, there was no correlation between the relative rRNA band intensities, or GAPDH mRNA band intensity, and the PMI up to 84 hours. These observations are consistent with the report of well-preserved

RNA in rabbit connective tissues in carcasses stored at 4°C up to 96 hours postmortem (Marchuk *et al.*, 1998). Although there was no correlation between rRNA degradation and the PMI, there was considerable variability in the quality of the RNA recovered between cases with differing PMIs. This may be due to variability between the cases in a number of unrecorded premortem and postmortem variables; such as the time between death and storage of the body in the mortuary fridge at 4°C; and different body cooling rates due to different medical conditions prior to death, including sepsis (which may maintain or raise the body temperature for a short time after death), hypotension, local ischaemia from thromboembolic disease, and general nutritional status (Kleiner *et al.*, 1995). In addition, the body cooling rate after death will be affected by the individual's physique and build, as adipose tissue acts as an insulator and therefore loss of internal heat will be slower in an overweight individual, and conversely, a thin individual will lose heat quicker as the surface area is greater in relation to the total tissue volume (Henssge, 1995). The PMI depends on a number of uncontrolled factors, such as the time of day that the individual died, how quickly consent is obtained from the next-of-kin for tissue donation, if the individual died at the hospital, or if the body is transported between institutions the PMI is lengthened by 1 or 2 days (Kleiner *et al.*, 1995).

Different cell types and certain mRNA species, in the case of human postmortem brain tissue RNA, may be more susceptible than others to various premortem and postmortem factors (Burke *et al.*, 1991). Burke *et al.* (1991) found different effects of premortem variables, such as hypoxia and seizure activity, on human postmortem brain mRNA expression levels. In addition, brain pH has been shown to significantly associate with the abundance of several brain-specific mRNAs in human postmortem brain tissues (Harrison *et al.*, 1995). Brain tissues with low pH (pH < 6.0) had fragmented or absent mRNAs, and

a strong correlation between tissue pH and mRNA quality was demonstrated (Bahn *et al.*, 2001).

The Northern blot of GAPDH mRNA for some cases, for a selection of bone RNA samples from human postmortem cases (Figure 3.1), showed a tailing effect below the 1.28 kb band, which is suggestive of partial GAPDH mRNA degradation. This band tailing effect was also observed for GAPDH mRNA on Northern blots of rabbit postmortem connective tissue RNA (Marchuk *et al.*, 1998). A similar effect was observed for G protein mRNA in human postmortem brain tissues obtained up to 19 hours postmortem (Ross *et al.*, 1992); β-actin mRNA in [poly(A)$^+$]-RNA isolated from human postmortem brain tissues up to 43 hours postmortem (Leonard *et al.*, 1993); and MUC5B mucin gene and β-actin mRNA detected by Northern blotting in RNA isolated from human postmortem temporal bone soft tissues obtained up to 6 hours postmortem (Lin *et al.*, 1999). The difference between the study of Lin *et al.* (1999) and the data for human postmortem bone tissue, described in this chapter, is the time-dependent downshift in Northern blot hybridising signals for β-actin and MUC5B mRNA, indicating loss of intact mRNA transcripts (Lin *et al.*, 1999). Both intact and partially degraded GAPDH mRNA transcripts were observed in the Northern blot of the selection of postmortem cases in Figure 3.1. The similar rate of RNA degradation, found between different skeletal sites from the same case for 7 individuals (section 3.4.1), has been reported for different regions of the human postmortem brain from the same subject, for 28S rRNA integrity analysed by Northern blotting (Ross *et al.*, 1992).

Autolysis, the destruction of tissues or cells by the action of endogenous enzymes (RNases), occurs at different rates in different human tissue types after death. Tissues rich

in digestive enzymes are most readily subject to autolytic changes. After death, the autolytic process begins in the gastrointestinal tract, with the digestion of the stomach, lower oesophagus, and intestine by digestive enzymes. These digestive enzymes then seep into the pleural (lung) cavity. Cessation of blood circulation causes oxygen tension in the tissues to fall rapidly, resulting in no further aerobic activity (Madea *et al.*, 1995). Anaerobic metabolism in muscles may attain a high level post-death with the production of lactic acid from glycogen. Nearly all the muscle glycogen is broken down during the first hours after death. Up to 104 hours postmortem, muscle cells in frozen muscle pulp can react on ATP administration with a strong contraction (Madea *et al.*, 1995). Studies of bone marrow cytology in postmortem cases in the 1960s showed that bone marrow cells, particularly leukocytes, from the sternum and ilium were still motile in tissue culture up to 50 hours postmortem (Perry *et al.*, 1960; Porteous, 1961). Bone marrow cells aspirated from the sternum from 123 cadavers, stored at various times at 4°C up to 10 days after death, were shown to be surprisingly viable, by a vital dye exclusion test, despite the general assumption that autolytic changes proceed rapidly at the cellular level (Laiho and Penttila, 1981).

3.5.3 Isolation of undegraded total RNA from human postmortem trabecular bone: optimal tissue processing conditions

Positive correlations were found between RNA isolated from two different skeletal regions from the same postmortem case for the intensities of the 28S and 18S rRNA bands, and GAPDH mRNA (section 3.4.1). These data suggest that the processing of the bone tissues for RNA isolation was unlikely to be influencing the variation in the relative intensity of the rRNA and GAPDH mRNA bands between cases (Figure 3.1). Moreover, the bone tissue processing for RNA isolation was not resulting in any further RNA degradation. To

consistently recover high concentrations of intact RNA from postmortem bone tissue, and other tissues, it is important to mimimize the possible introduction of exogenous RNases during tissue processing and dissection. RNase contamination can be minimised during tissue processing to isolate RNA by: wearing gloves for all procedures, using tips and tubes that have been certified RNase-free, treating water and buffers with DEPC (which inactivates RNases by alkylation of histidine residues in the enzyme active site), and treating surfaces with RNase decontamination solution or with a detergent that denatures RNases such as 10% SDS. In addition, all tissues, including bone tissues, contain endogenous RNases, thus it is very important to rapidly process samples into a strong denaturant buffer, such as guanidine isothiocyanate, to inactivate these nucleases.

The RNA degradation seen in surgical bone tissues stored at 4°C, room temperature, and 37°C, up to 72 hours (Figures 3.4-3.11; Tables 3.5-3.8), may be due to the introduction of exogenous RNases during the processing of the tissue and/or more endogenous RNases from the bone tissue becoming free in solution with a longer storage time. The surgical trabecular bone tissue samples used for the time-course analyses were initially divided, and each sample separately stored at the study temperature in sterile saline (section 3.3.2.2). An alternative approach would be to retain the tube saw bone sample intact in sterile saline and cut or section contiguous pieces of bone tissue as each time-point arises. This approach would result in less initial exposure of the tissue to potential exogenous RNases. In addition, the cutting or sectioning action (i.e., mechanical action and/or generation of heat) may be damaging cell membranes at the borders of the tissue sample, resulting in damage to lysosomes (the cell organelles housing the RNases), and thus releasing endogenous RNases into the storage solution. This may explain the rapid mRNA degradation observed for surgical bone tissue stored at 37°C, an optimal activity

temperature for RNases, in sterile saline (Figures 3.10 and 3.11; Table 3.8). Minimising lysosomal damage could prevent rapid degradation of RNA in postmortem tissues. Experimentally controlled freeze/thawing of rat brain tissues in comparison with increasing PMI indicated that the RNA began to show signs of degradation at 48 hours in rats stored at 4°C up to 72 hours postmortem. When the brain tissues where frozen and then thawed at room temperature (20°C) up to 1 hour before RNA isolation there was rapid degradation of both 28S rRNA and specific mRNA species (Ross *et al.*, 1992). Rapid freezing of tissues causes damage to the membrane structures within the cell, in particular to the lysosomes, and thus results in the release of RNases into the cytoplasm. Upon thawing of these tissues these RNases can result in rapid RNA degradation.

3.5.4 Stability of specific mRNA species in human surgical trabecular bone: mRNA degradation rates

Cell culture studies have been the model system used to study the *in vivo* stability of specific mRNA types. mRNA half-lives vary from a few minutes for labile species, such as c-*fos*, up to 24 hours or more for stable species, such as the globins (Yasojima *et al.*, 2001). Degradation rates of specific mRNAs *in vivo* are largely determined by destabilising sequences. The most important destabilising sequences are found in the 3' untranslated region (UTR), and this includes the series of AUUUA pentamers. The greater the number of A+U rich elements (AREs) in the 3' UTR, the greater the vulnerability for the mRNA to decay. The initial steps in mRNA degradation include progressive deadenylation of the poly(A) tail, in the model described by Sachs (1993). This exposes the remaining adenosine nucleotides to attack by endoribonucleases and exoribonucleases, as the poly(A)-binding protein can no longer attach to the mRNA. Yasojima *et al.* (2001) proposed that these same pathways of mRNA degradation, for each mRNA in premortem

degradation, would occur but at a slower rate postmortem. The *in vivo* half-lives of some of the mRNA species described in this chapter have been analysed in cell culture studies. OCN mRNA has a half-life of 7 hours in clonal osteoblast cells (Mosavin and Mellon, 1996). CTR mRNA has a half-life of 14 hours in mature mouse osteoclast-like cells (Wada *et al.*, 1997). The 3' UTR of the human CTR mRNA contains 5 copies of the AUUUA motif, as well as other AREs, which are known to destabilise mRNAs (Wada *et al.*, 1997). CTR and OCN mRNA rapidly degraded in surgical trabecular bone tissue stored at 37°C, a temperature at which endogenous and introduced RNases are likely to be active, with a similar relative half-live (T_{50}) of approximately 4 hours for both mRNA species (Figures 3.10 and 3.11, respectively; Table 3.8).

Tong *et al.* (1997) described a study where total RNA isolated from human breast cancer cell lines was degraded to varying extents by treatment with different amounts of RNase A. Competitive RT-PCR was used to show that specific mRNA species, such as oestrogen receptor, p53, and GAPDH, were degraded to a similar extent depending on the degree of the degradation of the total RNA. Tong *et al.* (1997) suggest that in degraded total RNA samples the expression of specific mRNAs, measured by competitive RT-PCR, should be normalised to a constitutively expressed gene, such as GAPDH, to allow correct relative mRNA quantification. This approach would also correct erroneous results caused by any incorrect spectrophotometric determinations of RNA concentrations (Tong *et al.*, 1997). And thus, the comparison of gene expression in RNA samples with varying integrity is possible.

Time-courses of RNA isolation from surgical trabecular bone tissues stored at either 4°C, room temperature, or 37°C, were used to investigate the effect of storage temperature and

storage time on the integrity of specific mRNA species, as determined by semi-quantitative RT-PCR, in human bone tissue. In general, the relative expression of mRNA species corresponding to a number of skeletally active molecules, RANKL, OPG, RANK, IL-6, CTR, OCN, and TGF-β1, declined significantly by 48 hours and 24 hours in bone tissue stored at 4°C and room temperature (22°C ± 1°C), respectively (Figures 3.7 and 3.8, respectively). All of the specific mRNA species rapidly degraded in bone tissue stored at 37°C, with an average relative T_{50} of 6 hours (Table 3.8). The relative ratio of each specific mRNA/GAPDH mRNA was analysed as a function of bone tissue storage time at each temperature. At 4°C and room temperature, some mRNA species appeared to degrade at a faster rate than the referent mRNA, GAPDH (section 3.4.4). At 37°C, the degradative rate of all of the mRNA species appeared to be faster than GAPDH mRNA. Given that there appear to be differences in mRNA degradation rates for some mRNA species in human bone tissues stored at 4°C, it is important that the storage interval before RNA isolation from bone tissues retrieved postmortem or at surgery is kept to a minimum (i.e., less than 12 hours). Further, the expression of specific mRNA species in human postmortem and surgical bone tissues should be normalised to GAPDH mRNA expression to reduce the impact of bone tissue sampling time.

Some variability in the RT-PCR analysis of bone-specific mRNA expression was observed between the time-points for each time-course temperature (Figures 3.3, 3.7-3.9). This may be due to a difference in the abundance of particular cell types expressing these bone-specific mRNA species between the contiguous trabecular bone pieces for each time-point. For example, RT-PCR assessment of RANKL mRNA for the postmortem case A18 shows a decline in RANKL mRNA expression for the 24, 48, and 72 hour time-points, similar to that seen for OPG, TGF-β1, and GAPDH mRNA (Figure 3.3). However, the 96 hour time-

point shows abundant RANKL mRNA. This inconsistency in RANKL mRNA expression is most likely due to tissue sampling variation, as outlined above, and highly unlikely to be due to an induction of RANKL mRNA transcription while the tissue is stored at 4°C. This variation was not apparent between the time-points, for the 4°C and room temperature time-courses, for the assessment of the 28S and 18S rRNA and GAPDH mRNA integrity (Figures 3.4 and 3.5). The assessment of rRNA and GAPDH mRNA integrity is a representative measure of RNA stability from all cell types in the tissue homogenate. However, there may be more variability between time-points in the relative intensity of the 28S and 18S rRNA bands in bone tissue stored at room temperature in comparison to 4°C, due to small fluctuations in the temperature during the time-course (i.e., 22°C ± 1°C).

3.5.5 Conclusions

Total RNA isolated from different skeletal sites from human postmortem cases shows signs of partial degradation up to 84 hours postmortem at 4°C. There is a mixture of both intact and partially degraded GAPDH mRNA transcripts up to 84 hours postmortem on a Northern blot (Figure 3.1). This suggests that RT-PCR analysis is the preferred technique for the analysis of gene expression in human postmortem bone tissues, as it tolerates partial RNA degradation. Postmortem cases should be selected with an optimal PMI of 72 hours or less for gene expression studies in bone tissue, and the time the bone tissue is stored at 4°C after retrieval at autopsy must be kept to a minimum. The time-course storage analysis of a postmortem bone tissue sample at 4°C, with a 24 hour PMI, demonstrated that bone-specific mRNAs begin to degrade in sterile saline solution after 24 hours of storage. In addition, processing of the postmortem bone tissues must be controlled to minimise introduction of exogenous RNases. The optimal temperature for any storage and transport of the bone tissue before RNA isolation is 4°C. If RNA is isolated from pathological bone tissues retrieved from surgery, this bone tissue should be processed and handled as for the postmortem bone tissue (i.e., the optimal temperature for any short-term storage is 4°C). The data described in this chapter have identified a 50% reduction in the relative abundance of some bone-specific mRNAs in surgical bone tissues stored at 4°C by 24 hours. This suggests that surgical bone tissues should be processed for the reliable isolation of intact total RNA within 12 hours after retrieval. Furthermore, once any sectioning or cutting of the bone tissue has occurred the samples should be immersed into a strong denaturant buffer, to inactive any released endogeneous RNases. These sampling conditions have been utilised for isolation of total RNA from human postmortem and surgical trabecular bone tissues to study the *ex vivo* pattern of gene expression (using semi-

quantitative RT-PCR analysis) from non-diseased individuals (postmortem) and from patients with severe primary hip OA (surgery; Chapters 4, 5, and 6).

CHAPTER 4

mRNA EXPRESSION OF BONE CELL MARKERS AND REGULATORY FACTORS OF BONE REMODELLING IN HUMAN TRABECULAR BONE FROM THE ILIAC CREST AND PROXIMAL FEMUR

4.1 INTRODUCTION

The adult human skeleton is considerably heterogeneous in terms of trabecular bone architecture, bone matrix properties, and the rate at which bone is turned over. This heterogeneity is a reflection of the mechanical and metabolic functions of each skeletal region (Parfitt, 1996). Amling *et al.* (1996) and Hildebrand *et al.* (1999) described architectural differences in trabecular bone from the calcaneus, femoral neck, iliac crest, lumbar spine, and intertrochanteric region of the femur. Histomorphometric assessment of trabecular bone architecture between the iliac crest, a number of femoral head regions (subchondral and medial principal compressive regions, subchondral principal tensile region), and the intertrochanteric region of the femur, demonstrated that the subchondral principal tensile region most closely represented the iliac crest (Fazzalari *et al.*, 1989). Differences in the mineralisation profile of trabecular bone between the calcaneus, femoral neck, iliac crest, and lumbar spine have been reported for a cohort of postmortem cases (Aerssens *et al.*, 1997). In addition, skeletal site differences in the bone matrix content of osteocalcin (OCN) and insulin-like growth factor type I (IGF-I) were reported in the same study (Aerssens *et al.*, 1997). Specifically, the trabecular bone matrix concentration of OCN and IGF-I was higher at the femoral neck and lumbar spine than at the calcaneus and iliac crest (Aerssens *et al.*, 1997). Furthermore, Pfeilschifter *et al.* (1998) reported regional differences in the trabecular bone matrix concentration of transforming growth factor (TGF)-β1 and TGF-β2 between the femoral head, lumbar spine, and iliac crest for postmenopausal women. Ampe *et al.* (1986) described differences in the trabecular bone matrix composition of collagen and non-collagenous proteins between the subchondral and central regions of the femoral head, for 5 postmortem cases. Histomorphometry has shown that the rate of bone turnover is higher at the iliac crest compared to appendicular skeletal sites (Parfitt, 1996). Eventov *et al.* (1991) described a reduction in the proportion of

haematopoietic marrow and lower numbers of osteoclasts and osteoblasts in femoral neck trabecular bone, in comparison to the iliac crest, for patients with femoral neck fractures. In addition, lower bone turnover was reported in tetracycline-labelled bone biopsies from the distal radius in comparison to iliac crest bone biopsies (Schnitzler *et al.*, 1996). Furthermore, the proportion of haematopoietic marrow was reduced in trabecular bone from the distal radius (Schnitzler *et al.*, 1996). Similarly, Burkhardt *et al.* (1987) reported lower bone turnover, increased fatty marrow, and reduced vascularity at the distal radius in comparison to the iliac crest. Differential rates of bone turnover between skeletal regions may be related to the differentiation potential and activity of the bone cell populations derived from different skeletal sites. For instance, the expression of TGF-β mRNA was more abundant in iliac crest-derived human osteoblastic cells compared to osteoblastic cells derived from the mandible (Kasperk *et al.*, 1995).

The extensive knowledge of systemic and local regulation of bone remodelling has been developed primarily from studies utilising *in vitro* cell culture systems, human and predominantly murine, and animal studies such as the effects of gene deletion studies in mice (reviewed in Ducy *et al.*, 2000; Hofbauer and Heufelder, 2001; Raisz, 1999; Roodman, 1999; Suda *et al.*, 1999). However, few studies, in the context of normal human bone physiology, have addressed the expression of molecular regulators of bone turnover *in situ* in the local human bone microenvironment, where paracrine mediators of bone turnover can be measured with their local regulatory mechanisms intact. Furthermore, there is a lack of information regarding the pattern of gene expression corresponding to markers of bone cells and specific molecules, with regulatory roles in bone turnover, in different skeletal sites from the same individual.

Therefore, this chapter describes investigation of mRNA expression levels of bone cell markers and a number of skeletally active molecules in trabecular bone sampled from the iliac crest, femoral neck, and intertrochanteric region of the proximal femur, for a cohort of postmortem individuals. The iliac crest was chosen for investigation as histomorphometric studies have described the trabecular bone architecture and bone turnover at this skeletal site for normal individuals and individuals with skeletal disease. In addition, the iliac crest is a skeletal site accessible for bone biopsy. Trabecular bone was sampled from the femoral neck, as low bone volume and associated changes in trabecular architecture are evident in patients with femoral neck fractures (Fazzalari *et al.*, 1985). The intertrochanteric region of the proximal femur was included in the investigation, as striking differences were observed at this skeletal site in the pattern of mRNA expression, corresponding to a number of skeletally active molecules, between patients with severe primary hip osteoarthritis (OA) and non-diseased postmortem individuals (described in Chapter 6). Trabecular bone in the intertrochanteric region has previously been shown to be structurally different between OA and non-OA individuals (Crane *et al.*, 1990). Moreover, the intertrochanteric region is remote from the subchondral bone that undergoes well-characterised secondary changes in severe OA (Fazzalari *et al.*, 1992).

The skeletally active molecules in this investigation include the key regulators of osteoclast biology and bone metabolism, RANKL, RANK, and OPG (as detailed in Chapter 5.1), interleukin (IL)-6 and tumour necrosis factor alpha (TNF-α), both of which are recognised skeletally active cytokines capable of promoting osteoclast formation (Azuma *et al.*, 2000; Komine *et al.*, 2001; Martin *et al.*, 1998), and the abundant bone matrix growth factor, TGF-β1, proposed to be one of the key factors involved in coupling bone formation to previous bone resorption (Pfeilschifter and Mundy, 1987). In addition, the osteoblastic cell

markers, OCN and osteopontin (OPN), and the bone osteoclastic cell markers, the calcitonin receptor (CTR) and tartrate-resistant acid phosphatase (TRAP), were included in the investigation.

4.2 CHAPTER AIMS

- To investigate whether there are skeletal site differences in the mRNA expression of bone cell markers and factors known to have important regulatory roles in bone remodelling, in human postmortem trabecular bone sampled from the iliac crest, and femoral neck and intertrochanteric regions of the proximal femur.

- To seek gender or age-related differences in the pattern of mRNA expression in human postmortem trabecular bone sampled from the iliac crest, and femoral neck and intertrochanteric regions of the proximal femur.

- To examine associations between the mRNA expression of skeletally active molecules in human postmortem trabecular bone tissue sampled from the iliac crest, and femoral neck and intertrochanteric regions of the proximal femur.

4.3 METHODS

4.3.1 Case selection

Proximal femurs, 7 from the left and 2 from the right anatomical side, were obtained from 9 routine autopsies performed at the Royal Adelaide Hospital (Table 4.1). The age of the postmortem cases, comprising 6 women (aged 57-85 years; mean ± SD [standard deviation] age, 69.8 ± 12.1 years) and 3 men (aged 42-60 years; 53.7 ± 10.1 years), varied

Case	Age *(years)*	Gender	Skeletal regions	Anatomical side	PMI *(hours)*	Cause of death
PM1	57	Female	IC, IT	Left	37	CML/sepsis
PM2	61	Female	IC, IT	Left	16	Non-Hodgkins lymphoma
PM3	61	Female	FN, IC, IT	Left	70	Lymphoma/chronic renal failure
PM4	72	Female	FN, IC, IT	Right	54	Ruptured duodenal ulcer
PM5	83	Female	FN, IC, IT	Left	67	MVA chest trauma
PM6	85	Female	IC, IT	Right	40	Cardiac arrest
PM7	42	Male	FN, IC, IT	Left	36	Chronic renal failure
PM8	59	Male	IC, IT	Left	72	Sepsis/pneumonia/post # pelvis
PM9	60	Male	FN, IC, IT	Left	58	Chronic renal failure

PM, postmortem case.
Total RNA was isolated from trabecular bone sampled from the following skeletal regions: FN, femoral neck; IC, iliac crest; IT, intertrochanteric region of the proximal femur.
PMI, postmortem interval, refers to the time between death and autopsy.
Abbreviations for cause of death: CML, chronic myelogenous leukaemia; #, fractured; MVA, motor vehicle accident.

Table 4.1 Profiles of postmortem cases examined.

between 42 and 85 years (64.4 ± 13.5 years). There was no difference in the mean age between females and males. The postmortem cases had a postmortem interval (PMI) range, the time between death and the postmortem examination, of 16 to 72 hours, which was an average of 2 days (50.0 ± 19.0 hours). There was no correlation between PMI and the age of the individual. Informed consent from next-of-kin was obtained for the collection of these postmortem specimens, with approval by the Royal Adelaide Hospital Human Ethics Committee.

4.3.2 Sampling of trabecular bone from the iliac crest and proximal femur

Trabecular bone was sampled from the iliac crest (IC), at a point 3 cm posterior to the antero-superior iliac spine (Figure 2.2), and the intertrochanteric (IT) region of the proximal femur (Figure 2.1) for each postmortem case. In addition, trabecular bone was sampled from the femoral neck (FN) region of the proximal femur for a subset of postmortem cases (Figure 2.1; Table 4.1). Each IC bone sample was bisected longitudinally, in an antero-posterior plane, using a band saw, which had been cleaned with DEPC-treated water, to access the trabecular bone enclosed within the cortical shell. Each proximal femur was sectioned in the coronal plane using a band saw to allow access to trabecular bone for sampling from the FN and IT skeletal regions, which are enclosed within the femoral cortex. Using sterile bone cutters, the trabecular bone tissue was sampled as small fragments from an approximate 1.0 x 1.0 cm^2 area, to a specimen depth of 0.5 cm, from the IC, and from an approximate 1.5 x 1.0 cm^2 area, to a specimen depth of 0.5 cm, from the FN and IT regions. The trabecular bone tissue fragments were rinsed briefly in DEPC-treated water (the rinsed material contained trabecular bone and bone marrow) and then immersed in RNA lysis buffer (4 M guanidine isothiocyanate solution, Chapter 2.1.5; 2 ml/250 mg wet weight).

4.3.3 Semi-quantitative RT-PCR of total RNA isolated from human trabecular bone

Total RNA was isolated from the postmortem IC, FN, and IT trabecular bone tissue fragments (Chapter 2.2.2.1). cDNA was synthesized from all the RNA samples (n = 23) at the same time, to limit differences between RNA samples in the efficiency of cDNA synthesis. cDNA was then amplified by PCR, using the human-specific oligonucleotide primer pairs listed in Table 2.1, to generate products corresponding to mRNA encoding human RANKL, OPG, RANK, IL-6, TNF-α, CTR, TRAP, OCN, OPN, TGF-β1, and the housekeeping gene GAPDH (Chapter 2.2.2.3.2). To allow semi-quantification of the PCR products, preliminary experiments were performed to ensure that the PCR amplification cycle number, for each set of primers, was within the log-linear range of amplification (Chapter 2.2.2.3.3). Amplified PCR products corresponding to RANKL, OPG, RANK, IL-6, TNF-α, CTR, TRAP, OCN, OPN, and TGF-β1 mRNA are represented as a ratio of the respective PCR product/GAPDH PCR product. There was no correlation between PMI and the relative ratios of PCR product/GAPDH for any of the mRNA species.

4.3.4 Statistical analysis of mRNA expression data

RT-PCR reactions were performed twice, from duplicate cDNA syntheses, which confirmed that repeated RT-PCR analysis of the same RNA samples yielded reproducible results. In addition, to minimise inter-assay variability for the comparison of skeletal regions, all PCR products for a given mRNA species (n = 23), were electrophoresed in a single 2% agarose gel. The Shapiro-Wilk statistic was used to test the semi-quantitative RT-PCR data for normality (PC-SAS software; SAS Institute). The semi-quantitative RT-PCR data were found to be both normally and non-normally distributed. Therefore, both parametric and non-parametric statistical methods were used to analyse the data (Excel;

Microsoft Corp.; PC-SAS software; SAS Institute). The statistical significance of differences in mRNA expression between females and males were determined by Student's *t*-test (parametric) or the Mann-Whitney *U*-test (non-parametric). The F-test was used to analyse differences in the variance of mRNA expression between females and males. Differences in mRNA expression between the skeletal regions, IC, FN, and IT, were tested by one-way analysis of variance (ANOVA) for the means (parametric) or by the Kruskal-Wallis one-way ANOVA by ranks for the medians (non-parametric). Linear regression analysis was used to describe age-related changes, and to examine the relationship between PCR products representing specific mRNA species. If there was more than one significant independent factor associated with a specific mRNA species, multiple regression was performed to determine the contribution of each independent factor. The Spearman rank correlation (r_s) was used to test for an association between two specific PCR products when the data were non-normally distributed. Parametric data is quoted as mean ± standard deviation and non-parametric data quoted as the median (quartiles). The critical value for significance was chosen as $p = 0.05$.

4.4 RESULTS

Semi-quantitative RT-PCR was employed to examine the expression of RANKL, OPG, RANK, IL-6, TNF-α, CTR, TRAP, OCN, OPN, and TGF-β1 mRNA in postmortem trabecular bone sampled from the iliac crest (IC), and femoral neck (FN) and intertrochanteric (IT) regions of the proximal femur (Figures 2.1 and 2.2). There were 5 postmortem cases where mRNA expression data was available from all three skeletal sites (IC, FN, and IT), and 4 cases where mRNA expression data was available from the IC and IT regions (Table 4.1). The mRNA species RANKL, OPG, and RANK were chosen for their central regulatory roles in controlling osteoclast development and activity (as detailed

in Chapter 5.1). IL-6 and TNF-α are skeletally active cytokines capable of promoting osteoclast formation (Azuma *et al.*, 2000; Komine *et al.*, 2001; Martin *et al.*, 1998). CTR and TRAP, and OCN and OPN, were chosen as markers for the presence of osteoclasts and osteoblasts, respectively (Denhardt and Noda, 1998; Hattersley and Chambers, 1989; Minkin, 1982; Stein and Lian, 1993). However, it is important to note that OPN is also expressed at high levels in osteoclasts (Dodds *et al.*, 1995; Merry *et al.*, 1993). The growth factor TGF-β1 is abundant in the bone matrix and has been proposed to be one of the key factors involved in coupling bone formation to previous bone resorption (Pfeilschifter and Mundy, 1987). The number of PCR cycles employed for each of these mRNA transcripts was within the exponential phase of the amplification curve, enabling comparison of mRNA expression between bone samples. Relative levels of RANKL, OPG, RANK, IL-6, TNF-α, CTR, TRAP, OCN, OPN, and TGF-β1 mRNA were determined by normalising values to the GAPDH mRNA level determined for each sample.

4.4.1 Comparison of mRNA expression between females and males

The semi-quantitative RT-PCR data for specific mRNA species at each skeletal site (IC, FN, and IT) in postmortem individuals were found to be both normally (TRAP, OCN, OPN, and TGF-β1) and non-normally (RANKL, OPG, RANK, IL-6, TNF-α, and CTR) distributed (the Shapiro-Wilk statistic; PC-SAS software; SAS Institute). Therefore, the student's *t*-test or the Mann-Whitney *U*-test was used to assess whether there were any gender differences in the mRNA expression levels of RANKL, OPG, RANK, IL-6, TNF-α, CTR, TRAP, OCN, OPN, and TGF-β1 in postmortem trabecular bone sampled from the IC, and FN and IT regions of the proximal femur. No significant differences were observed between females and males for the mean or median mRNA expression of each PCR product/GAPDH ratio, at each skeletal site (IC, FN, and IT; results not shown). Based on

these comparisons between females and males at each skeletal site, and the fact that the sample sizes are small (IC, n = 9; FN, n = 5; IT, n = 9), further analyses of the mRNA expression data were made independent of gender.

The statistical significance of differences in mRNA expression between females and males were also assessed in the pooled IC, FN, and IT data (females, n = 15; males, n = 8), as no statistical differences in mRNA expression were observed between these skeletal sites (described in the following section 4.4.2). RANK/GAPDH mRNA expression was significantly higher in the pooled skeletal site data for females compared to males ($p <$ 0.05; Table 4.2). In the local bone microenvironment, RANK is primarily expressed on the surface of osteoclasts and their precursors (Hsu *et al.*, 1999). However, is it is not known whether the measured RANK mRNA is representative of immature and/or mature osteoclasts in these human bone samples, or whether the RANK mRNA expression is representative of the number of osteoclasts and/or the number of RANK receptors on each osteoclast. The only other difference between females and males for the pooled skeletal site data was for mean OCN/GAPDH mRNA expression, which was significantly higher in females compared to males ($p < 0.02$; Table 4.2). In addition, the variance in OCN/GAPDH mRNA in females was significantly higher than in males (F-statistic = 11.1, representing the ratio of the female variance to male variance, $p < 0.002$; Table 4.2), suggesting that the females are a more heterogeneous group with respect to OCN mRNA expression. It is acknowledged that the number of male cases is small (n = 3; Table 4.1), and increased cases are required to confirm these gender differences. OCN is utilised as an indicator of bone formation as it is one of the marker genes for the progression of osteoblastic differentiation (Stein and Lian, 1993). Minisola *et al.* (1997) reported an age-related increase in serum OCN levels in women aged 25 to 75 years. All of the females in the

Table 4.2 Female and male RT-PCR product/GAPDH ratios in the pooled skeletal site data for iliac crest, femoral neck, and intertrochanteric trabecular bone sampled from postmortem individuals aged 42-85 years.

Ratio	Female (n = 15)	Male (n = 8)
RANKL/GAPDH	0.15 (0.09-0.42)	0.20 (0.14-0.71)
OPG/GAPDH	0.09 (0.04-0.37)	0.06 (0.05-0.28)
RANK/GAPDH	0.17 (0.07-0.30)	0.01 (0.01-0.14) [a]
IL-6/GAPDH	0.35 (0.03-1.31)	0.10 (0-0.96)
TNF-α/GAPDH	0.55 (0.34-0.97)	0.47 (0.32-0.72)
CTR/GAPDH	0.04 (0.02-0.23)	0.10 (0.01-0.21)
TRAP/GAPDH	0.39 ± 0.20	0.30 ± 0.13
OCN/GAPDH	0.53 ± 0.44	0.19 ± 0.13 [b]
OPN/GAPDH	0.37 ± 0.27	0.37 ± 0.30
TGF-β1/GAPDH	0.23 ± 0.09	0.17 ± 0.04

Parametric data reported as mean ± standard deviation, and non-parametric data as median (quartiles).
[a] $p < 0.05$; [b] $p < 0.02$.

pooled skeletal site data group are postmenopausal (aged 57-85 years, cases PM1 to PM6; Table 4.1), who may have had an increased bone remodelling rate due to oestrogen deficiency. In contrast, no difference in OCN protein concentration was observed at the femoral neck and iliac crest between females and males (Aerssens *et al.*, 1997; Boonen *et al.*, 1997). Further, Vanderschueren *et al.* (1990) reported that the concentration of OCN protein in iliac crest bone was more abundant in males than in females. However, the age range of the postmortem individuals in these studies was broad (aged 23-92 years, Aerssens *et al.*, 1997, Boonen *et al.*, 1997; aged 19-90 years, Vanderschueren *et al.*, 1990).

4.4.2 Comparison of mRNA expression between the iliac crest, and femoral neck and intertrochanteric regions of the proximal femur

Relative mRNA expression levels of RANKL, OPG, RANK, IL-6, TNF-α, CTR, TRAP, OCN, OPN, and TGF-β1 were measured in postmortem trabecular bone sampled from the IC, and FN and IT regions of the proximal femur. Differences in bone turnover, bone matrix properties, and trabecular bone architecture have been reported between these skeletal sites (Aerssens *et al.*, 1997; Amling *et al.*, 1996; Fazzalari *et al.*, 1989; Parfitt, 1996). Thus, it was hypothesised that the levels of mRNA corresponding to bone cell markers and regulatory factors of bone remodelling would differ between the IC, FN, and IT regions. One-way analysis of variance (ANOVA) for the means or Kruskal-Wallis one-way ANOVA by ranks for the medians was used to assess whether there were any differences in the mRNA expression levels of RANKL, OPG, RANK, IL-6, TNF-α, CTR, TRAP, OCN, OPN, and TGF-β1 between the three skeletal sites.

Intriguingly, no significant differences were observed for mean or median RANKL, OPG, RANK, IL-6, TNF-α, CTR, TRAP, OCN, OPN, and TGF-β1 mRNA expression between

the IC, FN, and IT skeletal sites (Table 4.3). This suggests that the steady state mRNA expression levels for these skeletally active molecules are similar between the three skeletal regions. However, it is not known whether the gene expression patterns are representative of the corresponding protein levels in the trabecular bone tissue. For instance, the trabecular bone matrix concentration of OCN was higher at the femoral neck than at the iliac crest for postmortem individuals (Aerssens *et al.*, 1997).

Table 4.3 RT-PCR product/GAPDH ratios in iliac crest, femoral neck, and intertrochanteric trabecular bone sampled from postmortem individuals aged 42-85 years.

Ratio	IC ($n = 9$)	FN ($n = 5$)	IT ($n = 9$)
RANKL/GAPDH	0.17 (0.09-0.20)	0.09 (0.04-0.43)	0.22 (0.11-0.41)
OPG/GAPDH	0.07 (0.05-0.09)	0.36 (0.06-0.51)	0.06 (0.05-0.34)
RANK/GAPDH	0.11 (0.02-0.15)	0.21 (0.01-0.30)	0.11 (0.01-0.28)
IL-6/GAPDH	0.05 (0.01-0.96)	0.53 (0.35-1.10)	0.32 (0.01-0.94)
TNF-α/GAPDH	0.39 (0.15-0.75)	0.66 (0.39-0.81)	0.53 (0.41-0.74)
CTR/GAPDH	0.05 (0.01-0.19)	0.12 (0.04-0.23)	0.03 (0.01-0.18)
TRAP/GAPDH	0.32 ± 0.16	0.39 ± 0.24	0.38 ± 0.19
OCN/GAPDH	0.41 ± 0.29	0.53 ± 0.64	0.35 ± 0.36
OPN/GAPDH	0.38 ± 0.16	0.42 ± 0.47	0.34 ± 0.26
TGF-β1/GAPDH	0.21 ± 0.08	0.23 ± 0.11	0.20 ± 0.06

Total RNA was isolated from trabecular bone sampled from the following skeletal regions: IC, iliac crest; FN, femoral neck; IT, intertrochanteric region of the proximal femur.
Parametric data reported as mean ± standard deviation, and non-parametric data as median (quartiles).

4.4.3 Age-related changes in mRNA expression in human trabecular bone

To investigate whether there are any age-related changes in the mRNA expression levels in trabecular bone sampled from the IC, FN, and IT sites, each PCR product/GAPDH mRNA ratio, for each skeletal site, was plotted as a function of increasing age in years, and analysed by linear regression analysis. There were no relationships with age for any of the specific mRNA species, RANKL, OPG, RANK, IL-6, TNF-α, CTR, TRAP, OCN, OPN, and TGF-β1, at the FN or IT regions of the proximal femur (results not shown). The TGF-β1/GAPDH mRNA ratio increased with age at the IC, when analysed by linear regression (n = 9; r = 0.64, $p < 0.05$; results not shown). In contrast, in a previous study, the bone matrix concentration of TGF-β1 at the iliac crest did not change with age in postmenopausal women (Pfeilschifter *et al.*, 1998). The expression of RANKL, OPG, RANK, IL-6, TNF-α, CTR, TRAP, OCN, and OPN mRNA showed no dependence on age at the IC (results not shown).

Age-related changes in the mRNA expression levels were also assessed for the pooled IC, FN, and IT trabecular bone samples (n = 23), as no significant differences in mRNA expression were observed between these skeletal sites (Table 4.3; described in the previous section 4.4.2). The RANKL/GAPDH mRNA ratio declined with age for the pooled skeletal site samples, when analysed by linear regression (n = 23; r = -0.59, $p < 0.003$; results not shown). This is consistent with *in situ* hybridisation analysis of RANKL mRNA in 8-week-old and 2.5-year-old male rat distal femur bones which showed a trend for an age-related reduction in RANKL mRNA expression (Ikeda *et al.*, 2001). In contrast, the RANKL/GAPDH mRNA ratio increased with age in trabecular bone sampled from the IT region for a non-diseased autopsy cohort of 12 individuals (Figure 5.13; Chapter 5.4.4); although this relationship was dependent on inclusion of two young individuals. These

non-diseased postmortem cases were selected using criteria described in Chapter 5.3.1, which included no history of any chronic condition or disease which may have affected bone status (such as renal dysfunction or endocrine disease affecting bone metabolism). The postmortem cases for the skeletal site comparison of mRNA expression included 3 cases with a history of renal disease (cases PM3, PM7, and PM9; Table 4.1). Patients with end-stage renal disease often have increased rates of bone turnover leading to increased bone resorption (Hruska and Teitelbaum, 1995). Interestingly, a recent report identified increased RANKL mRNA expression, detected by *in situ* hybridisation, associated with increased bone resorption in iliac crest bone biopsies, from individuals with renal disease (Langub and Malluche, 2002). The differences in the selection of postmortem cases may account for the opposing relationships between RANKL/GAPDH mRNA expression and age. Furthermore, the age range of the non-diseased autopsy cohort was wider (aged 20-85 years; Chapter 5), in comparison to the postmortem cases described in this chapter (aged 42-85 years). There were no relationships with age for any of the other specific mRNA species, OPG, RANK, IL-6, TNF-α, CTR, TRAP, OCN, OPN, and TGF-β1, for the pooled skeletal site data (results not shown).

4.4.4 Associations between expression of specific mRNA transcripts in human trabecular bone

Linear regression analysis was used to investigate whether there are any relationships between amounts of PCR product representing specific mRNA species in the pooled skeletal site data (n = 23), and in the individual skeletal regions, the IC (n =9), and FN (n = 6) and IT (n = 9) regions of the proximal femur, from postmortem individuals. The Spearman rank correlation (r_s) was used to test for an association between two specific PCR products when the data were non-normally distributed.

In the bone microenvironment, the CTR, TRAP, and RANK are expressed by the same cell types, namely osteoclasts and their precursors (Hattersley and Chambers, 1989; Hsu *et al.*, 1999; Minkin, 1982; Quinn *et al.*, 1999). Interestingly, significant positive associations were observed between CTR/GAPDH and TRAP/GAPDH mRNA expression ($r = 0.48$, $p < 0.02$; Figure 4.1; Table 4.4), RANK/GAPDH and TRAP/GAPDH mRNA expression ($r = 0.67$, $p < 0.001$; Figure 4.2; Table 4.4), and CTR/GAPDH and RANK/GAPDH mRNA expression ($r_s = 0.53$, $p < 0.01$; Table 4.4), in the pooled skeletal site data. The positive associations between CTR/GAPDH and TRAP/GAPDH mRNA expression and CTR/GAPDH and RANK/GAPDH mRNA expression were not observed at each skeletal site (Table 4.4). However, the positive association between RANK/GAPDH and TRAP/GAPDH mRNA expression in the pooled skeletal site data was maintained when the skeletal sites were analysed individually (IC, $r = 0.68$, $p < 0.03$; FN, $r = 0.77$, $p < 0.05$; IT, $r = 0.61$, $p < 0.05$; Table 4.4). Taken together, these observations are consistent with the expression of CTR, TRAP, and RANK by osteoclast-like cells in the bone microenvironment, and further suggest that the cell types expressing these factors in the bone RNA samples are predominantly osteoclasts and their precursors.

Both RANK/GAPDH and IL-6/GAPDH mRNA positively associated with TNF-α/GAPDH mRNA expression ($r_s = 0.53$, $p < 0.009$; $r_s = 0.51$, $p < 0.02$; respectively; Table 4.5) in the pooled skeletal site data. The positive association between RANK/GAPDH and TNF-α/GAPDH mRNA expression was maintained at the IC ($r_s = 0.72$, $p < 0.03$; Table 4.5), but not at the FN or IT regions of the proximal femur (Table 4.5). This association between RANK and TNF-α mRNA expression is consistent with induction of RANK mRNA expression by TNF-α treatment of rodent pre-osteoclast cells (Komine *et al.*,

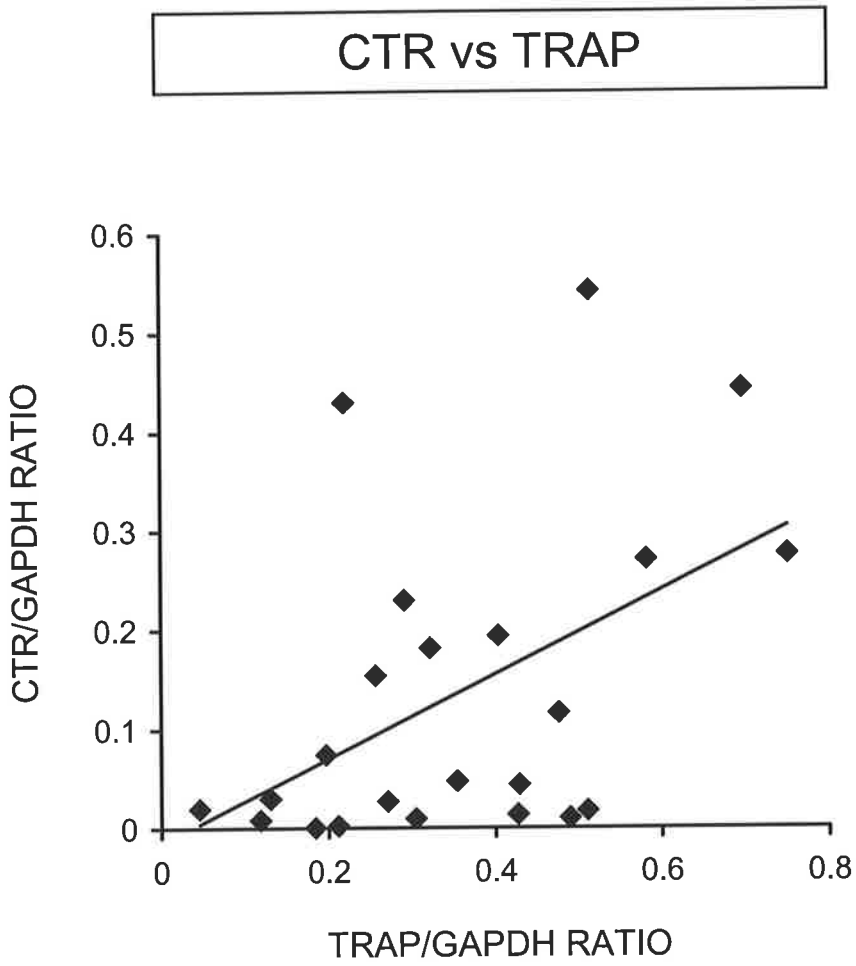

Figure 4.1: A positive association was observed between the relative ratio of CTR/GAPDH mRNA and TRAP/GAPDH mRNA in trabecular bone for the pooled skeletal site data from postmortem individuals (n = 23; CTR/GAPDH = 0.43*TRAP/GAPDH - 0.02; $r = 0.48$ and $p < 0.02$).

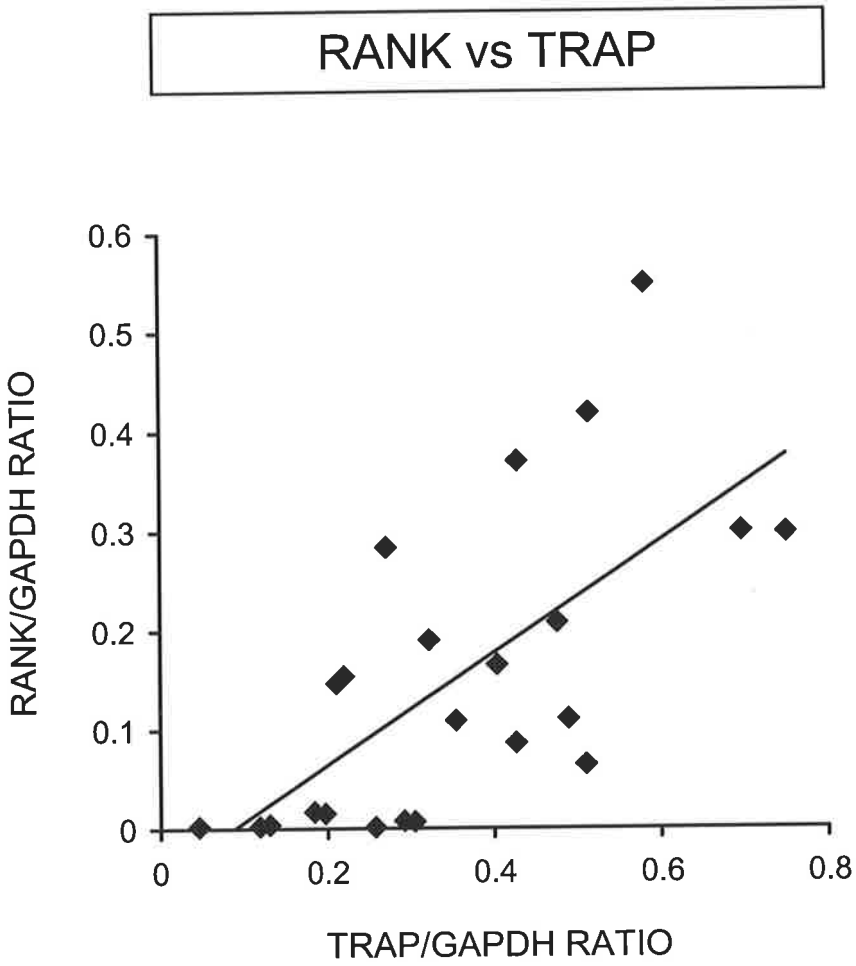

Figure 4.2: A positive association was observed between the relative ratio of RANK/GAPDH mRNA and TRAP/GAPDH mRNA in trabecular bone for the pooled skeletal site data from postmortem individuals (n = 23; RANK/GAPDH = 0.57*TRAP/GAPDH - 0.05; $r = 0.67$ and $p < 0.001$).

Table 4.4 Associations between RT-PCR product/GAPDH ratios for CTR, TRAP, and RANK mRNA in the pooled skeletal site data, and in trabecular bone sampled from the individual skeletal sites, the iliac crest, femoral neck, and intertrochanteric regions, for postmortem individuals aged 42-85 years.

Association	Pooled ($n = 23$)	IC ($n = 9$)	FN ($n = 5$)	IT ($n = 9$)
CTR/GAPDH vs TRAP/GAPDH	$r = 0.48$ $p < 0.02$	$r = 0.22$ $p =$ NS	$r = 0.72$ $p =$ NS	$r = 0.53$ $p =$ NS
RANK/GAPDH vs TRAP/GAPDH	$r = 0.67$ $p < 0.001$	$r = 0.68$ $p < 0.03$	$r = 0.77$ $p < 0.05$	$r = 0.61$ $p < 0.05$
CTR/GAPDH vs RANK/GAPDH	$r_s = 0.53$ $p < 0.01$	$r_s = 0.57$ $p =$ NS	$r_s = 0.30$ $p =$ NS	$r_s = 0.62$ $p =$ NS

Total RNA was isolated from trabecular bone sampled from the following skeletal regions: IC, iliac crest; FN, femoral neck; IT, intertrochanteric region of the proximal femur.
r, linear regression analysis; r_s, Spearman rank correlation; NS, not significant.

2001), and the overall synergy between the RANKL-RANK system of osteoclast development and TNF-α (Komine *et al.*, 2001). Furthermore, a key causal role for TNF-α in bone loss induced by oestrogen deficiency has been demonstrated *in vivo*, since bone loss is not seen in ovariectomised TNF-deficient mice (Roggia *et al.*, 2001). The positive association between IL-6/GAPDH and TNF-α/GAPDH mRNA expression in the pooled skeletal site data was not observed when the skeletal sites were analysed individually (Table 4.5). However, the positive association between IL-6 and TNF-α mRNA, in the pooled skeletal site data, is consistent with the finding that TNF-α treatment of murine osteoblastic cells resulted in a dose-dependent induction of IL-6 mRNA (Ishimi *et al.*, 1990; Kurokouchi *et al.*, 1998). In addition, the data suggest the co-regulation of these pro-osteoclastic cytokines in the local human bone microenvironment. Interestingly, a positive association was observed between RANK/GAPDH and IL-6/GAPDH mRNA expression in the pooled skeletal site data ($r_s = 0.59$, $p < 0.003$; Table 4.5), which was maintained at the IC ($r_s = 0.73$, $p < 0.03$; Table 4.5), but not at the FN and IT regions (Table 4.5). In contrast, a recent report of the effects of IL-6 in combination with soluble IL-6R in neonatal mouse calvarial bone cultures demonstrated enhanced RANKL and OPG mRNA expression and protein levels, but decreased RANK mRNA expression (Palmqvist *et al.*, 2002). However, *in vivo* studies suggest that IL-6 may play a central role in bone loss induced by oestrogen deficiency, since bone loss in ovariectomised mice can be reduced with anti-IL-6 antibodies, and bone loss is not seen in ovariectomised IL-6-deficient mice (Jilka *et al.*, 1992; Poli *et al.*, 1994).

Table 4.5 Associations between RT-PCR product/GAPDH ratios for RANK, TNF-α, and IL-6 mRNA in the pooled skeletal site data, and in trabecular bone sampled from the individual skeletal sites, the iliac crest, femoral neck, and intertrochanteric regions, for postmortem individuals aged 42-85 years.

Association	Pooled ($n = 23$)	IC ($n = 9$)	FN ($n = 5$)	IT ($n = 9$)
RANK/GAPDH vs TNF-α/GAPDH	$r_s = 0.53$ $p < 0.009$	$r_s = 0.72$ $p < 0.03$	$r_s = 0.80$ $p =$ NS	$r_s = 0.08$ $p =$ NS
IL-6/GAPDH vs TNF-α/GAPDH	$r_s = 0.51$ $p < 0.02$	$r_s = 0.63$ $p =$ NS	$r_s = 0.70$ $p =$ NS	$r_s = 0.25$ $p =$ NS
RANK/GAPDH vs IL-6/GAPDH	$r_s = 0.59$ $p < 0.003$	$r_s = 0.73$ $p < 0.03$	$r_s = 0.30$ $p =$ NS	$r_s = 0.52$ $p =$ NS

Total RNA was isolated from trabecular bone sampled from the following skeletal regions: IC, iliac crest; FN, femoral neck; IT, intertrochanteric region of the proximal femur.
r_s, Spearman rank correlation. NS, not significant.

Extensive bone marrow cell culture studies have shown that RANKL, OPG, and to a lesser extent, RANK, are modulated by growth factors, cytokines, peptide and steroid hormones, and drugs known to affect bone metabolism (Hofbauer *et al.*, 2000; Hofbauer and Heufelder, 2001; Horowitz *et al.*, 2001; Suda *et al.*, 1999). Therefore, the results for RANKL and OPG mRNA, RANK and OPG mRNA, and RANKL and RANK mRNA were analysed by the Spearman rank correlation to identify whether any relationships exist in the human bone microenvironment. No associations were observed between RANKL/GAPDH mRNA with either OPG/GAPDH or RANK/GAPDH mRNA expression in the pooled skeletal site data or when the skeletal sites were analysed individually (Table 4.6). In contrast, positive associations were observed between RANKL mRNA with both OPG and RANK mRNA expression in trabecular bone sampled from the IT region for a non-diseased autopsy cohort of 12 individuals (Figures 5.6 and 5.7, respectively; Chapter

5.4.3). However, a positive association was observed between RANK/GAPDH mRNA and OPG/GAPDH mRNA expression in the pooled skeletal site data (r_s = 0.68, p < 0.0005; Table 4.6), which was maintained at the IC (r_s = 0.75, p < 0.02; Table 4.6), but not at the FN and IT regions (Table 4.6). This association was not observed in the non-diseased autopsy cohort for the co-plot of RANK/GAPDH mRNA and OPG/GAPDH mRNA expression (Figure 5.8; Chapter 5.4.3). The differences in the associations between RANKL, OPG, and RANK mRNA between the postmortem cases described in this chapter (Table 4.6) and the non-diseased autopsy cohort described in Chapter 5, may be accounted for by the difference in postmortem case selection and the age range of the cases (as described in section 4.4.3).

Table 4.6 Associations between RT-PCR product/GAPDH ratios for RANKL, OPG, and RANK mRNA in the pooled skeletal site data, and in trabecular bone sampled from the individual skeletal sites, the iliac crest, femoral neck, and intertrochanteric regions, for postmortem individuals aged 42-85 years.

Association	Pooled (n = 23)	IC (n = 9)	FN (n = 5)	IT (n = 9)
RANKL/GAPDH vs OPG/GAPDH	r_s = 0.32 p = NS	r_s = 0.27 p = NS	r_s = 0.80 p = NS	r_s = 0.18 p = NS
RANK/GAPDH vs OPG/GAPDH	r_s = 0.68 p < 0.0005	r_s = 0.75 p < 0.02	r_s = 0.60 p = NS	r_s = 0.60 p = NS
RANKL/GAPDH vs RANK/GAPDH	r_s = 0.26 p = NS	r_s = 0.13 p = NS	r_s = 0.60 p = NS	r_s = -0.02 p = NS

Total RNA was isolated from trabecular bone sampled from the following skeletal regions: IC, iliac crest; FN, femoral neck; IT, intertrochanteric region of the proximal femur.
r_s, Spearman rank correlation; NS, not significant.

The growth factor TGF-β1 and the non-collagenous proteins, OCN and OPN, are abundant in the bone matrix. Both OCN/GAPDH and OPN/GAPDH mRNA positively associated with TGF-β1/GAPDH mRNA expression ($r = 0.70$, $p < 0.001$; Figure 4.3; $r = 0.51$, $p < 0.01$; Figure 4.4; respectively; Table 4.7) in the pooled skeletal site data. The positive association between OCN/GAPDH mRNA and TGF-β1/GAPDH mRNA expression was maintained at the FN ($r = 0.99$, $p < 0.001$; Table 4.7), but not at the IC and IT regions (Table 4.7). In contrast, a number of reports have demonstrated that TGF-β inhibits the mRNA expression and synthesis of OCN in osteoblast-like cells (Harris *et al.*, 1994; Lai and Cheng, 2002; Pirskanen *et al.*, 1994). Further, the positive association between OPN/GAPDH mRNA and TGF-β1/GAPDH mRNA expression was maintained at the IC ($r = 0.64$, $p < 0.05$; Table 4.7), but not at the FN and IT regions (Table 4.7). This association between OPN mRNA and TGF-β1 mRNA is consistent with a report of TGF-β treatment of rat osteoblastic cells resulting in an up-regulation of OPN mRNA expression (Sodek *et al.*, 1995). Finally, there was a positive correlation between OCN/GAPDH mRNA and OPN/GAPDH mRNA expression in the pooled skeletal site data ($r = 0.65$, $p < 0.001$; Figure 4.5; Table 4.7), which was maintained at the IC and IT regions ($r = 0.92$, $p < 0.001$; $r = 0.81$, $p < 0.003$; respectively; Table 4.7), but not at the FN region (Table 4.7), when the skeletal sites where analysed individually. Interestingly, OCN and OPN have been shown to form protein complexes *in vitro* (Ritter *et al.*, 1992).

As detailed in Chapter 1.3.1.2, OCN and OPN are both marker genes for the progression of osteoblastic differentiation (Denhardt and Noda, 1998; Stein and Lian, 1993). However, OPN is also expressed at high levels in osteoclasts (Dodds *et al.*, 1995; Merry *et al.*, 1993). The biological function of OCN and OPN in the bone microenvironment has not been precisely defined. OCN has been suggested to play a role in the regulation of bone mineral

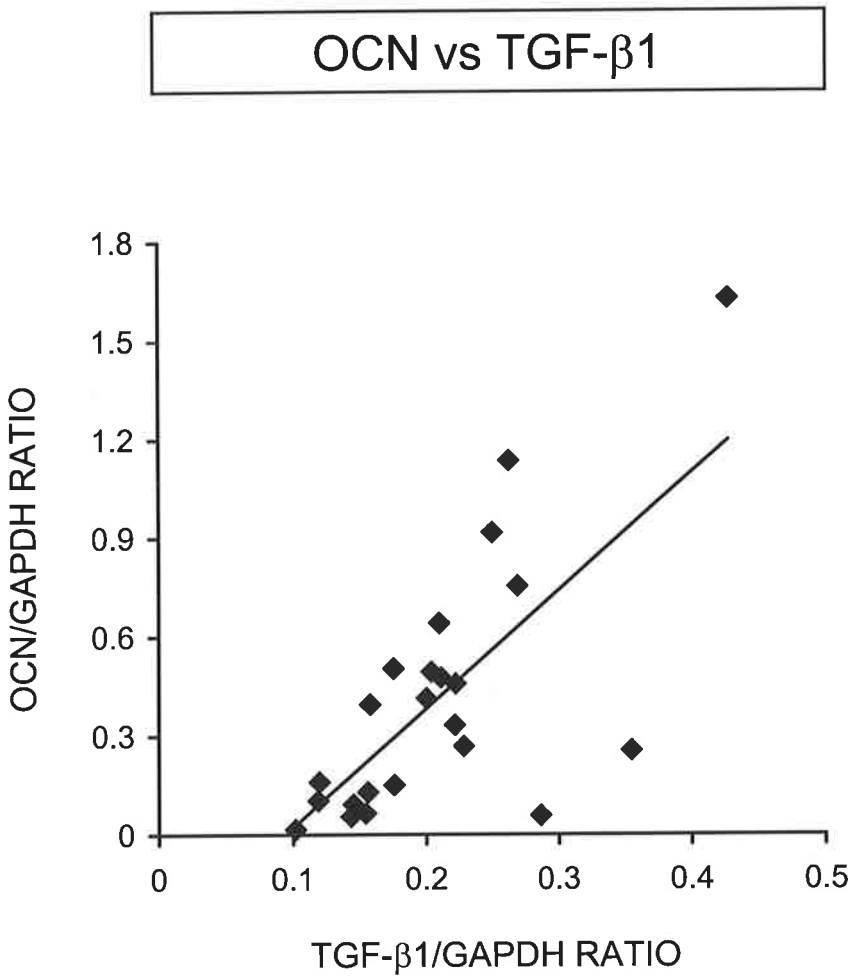

Figure 4.3: A positive association was observed between the relative ratio of OCN/GAPDH mRNA and TGF-β1/GAPDH mRNA in trabecular bone for the pooled skeletal site data from postmortem individuals (n = 23; OCN/GAPDH = 3.59*/TGF-β1GAPDH - 0.34; $r = 0.70$ and $p < 0.001$).

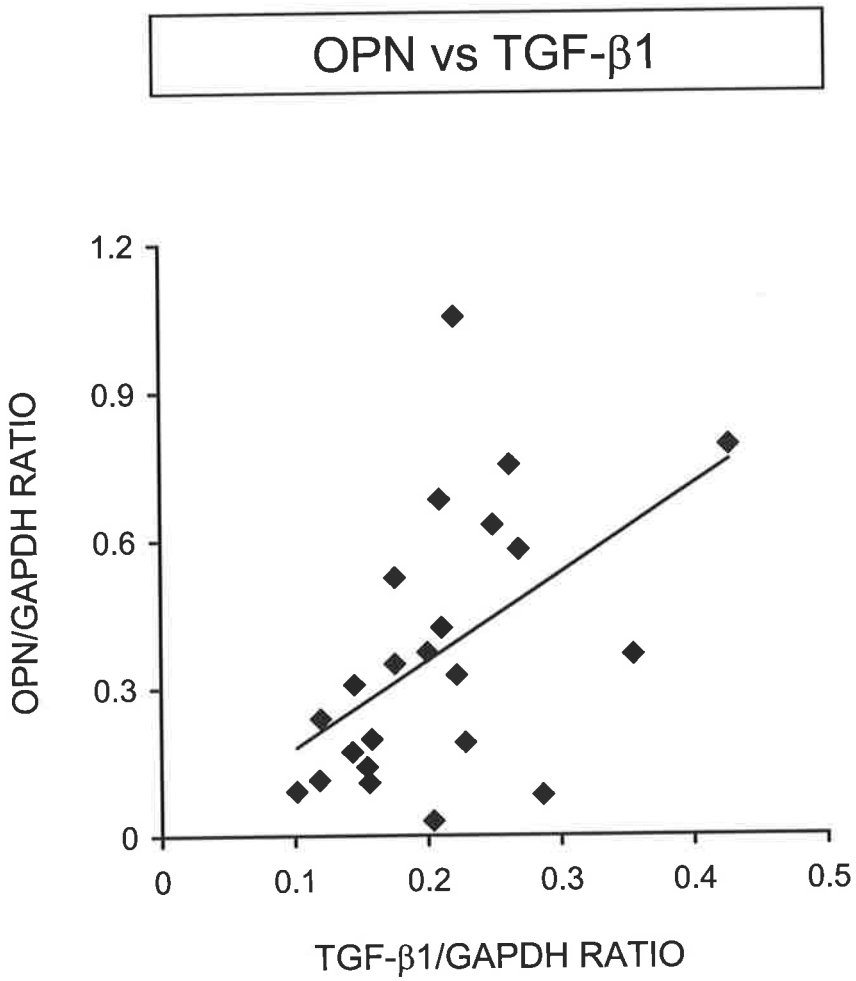

Figure 4.4: A positive association was observed between the relative ratio of OPN/GAPDH mRNA and TGF-β1/GAPDH mRNA in trabecular bone for the pooled skeletal site data from postmortem individuals (n = 23; OPN/GAPDH = 1.79*TGF-β1/GAPDH - 0.002; $r = 0.51$ and $p < 0.01$).

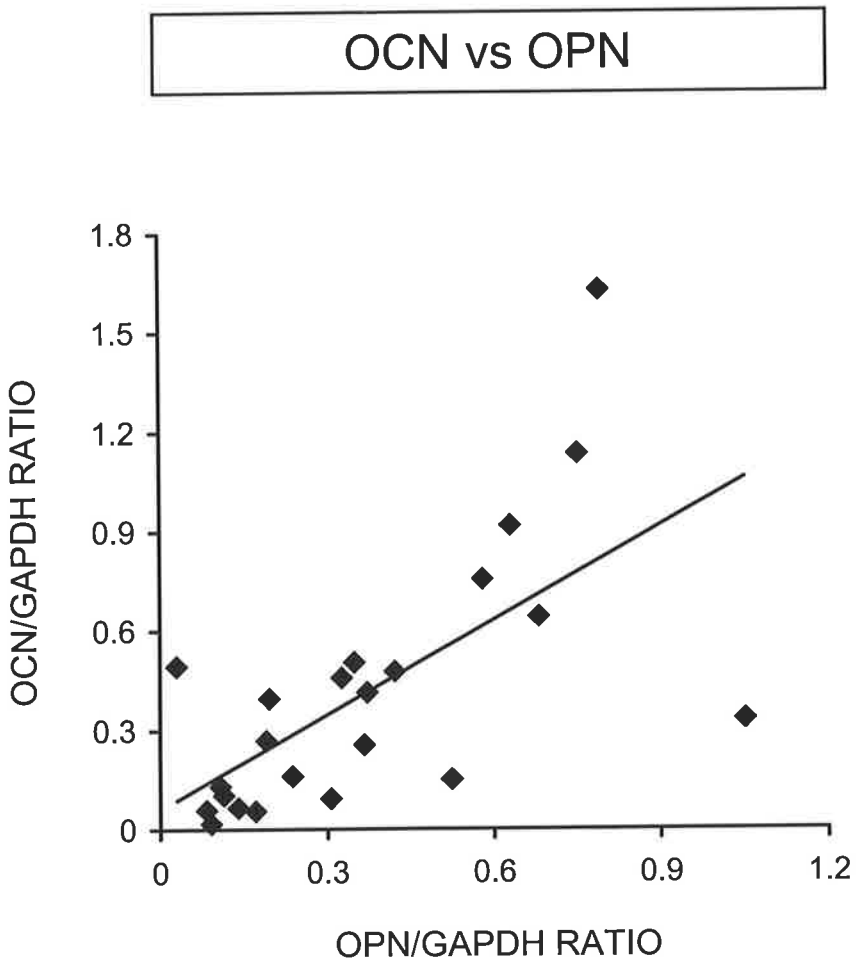

Figure 4.5: A positive association was observed between the relative ratio of OCN/GAPDH mRNA and OPN/GAPDH mRNA in trabecular bone for the pooled skeletal site data from postmortem individuals (n = 23; OCN/GAPDH = 0.95*OPN/GAPDH + 0.06; $r = 0.65$ and $p < 0.001$).

Table 4.7 Associations between RT-PCR product/GAPDH ratios for OCN, TGF-β1, and OPN mRNA in the pooled skeletal site data, and in trabecular bone sampled from the individual skeletal sites, the iliac crest, femoral neck, and intertrochanteric regions, for postmortem individuals aged 42-85 years.

Association	Pooled ($n = 23$)	IC ($n = 9$)	FN ($n = 5$)	IT ($n = 9$)
OCN/GAPDH vs TGF-β1/GAPDH	$r = 0.70$ $p < 0.001$	$r = 0.48$ $p =$ NS	$r = 0.99$ $p < 0.001$	$r = 0.46$ $p =$ NS
OPN/GAPDH vs TGF-β1/GAPDH	$r = 0.51$ $p < 0.01$	$r = 0.64$ $p < 0.05$	$r = 0.58$ $p =$ NS	$r = 0.32$ $p =$ NS
OCN/GAPDH vs OPN/GAPDH	$r = 0.65$ $p < 0.001$	$r = 0.92$ $p < 0.001$	$r = 0.47$ $p =$ NS	$r = 0.81$ $p < 0.003$

Total RNA was isolated from trabecular bone sampled from the following skeletal regions: IC, iliac crest; FN, femoral neck; IT, intertrochanteric region of the proximal femur.
r, linear regression analysis; NS, not significant.

turnover, as mineral maturation was impaired in OCN-deficient mice (Boskey *et al.*, 1998). In addition, OCN may act in combination with other non-collagenous proteins, such as OPN, as a signal for osteoclastic bone resorption (Reinholt *et al.*, 1990; Ritter *et al.*, 1992). *In vitro*, OPN has been shown to be an extracellular signalling molecule for osteoclasts and endothelial cells, *via* binding of OPN to the cell surface $\alpha_v\beta_3$ integrin (Denhardt and Noda, 1998; Liaw *et al.*, 1995).

Positive associations were observed between OPG/GAPDH mRNA with both OCN/GAPDH and OPN/GAPDH mRNA expression in the pooled skeletal site data (r = 0.61, $p < 0.002$; Figure 4.6; $r = 0.71$, $p < 0.001$; Figure 4.7; respectively; Table 4.8). The positive association between OPG/GAPDH and OPN/GAPDH mRNA expression in the pooled skeletal site data was maintained when the skeletal sites were analysed individually (IC, $r = 0.72$, $p < 0.02$; FN, $r = 0.77$, $p < 0.05$; IT, $r = 0.81$, $p < 0.003$; Table 4.8). However, the positive association between OPG/GAPDH and OCN/GAPDH mRNA expression was maintained at the IC ($r = 0.73$, $p < 0.02$; Table 4.8), but not at the FN and IT regions (Table 4.8). Further, as both OCN and OPN mRNA expression were significantly associated with OPG mRNA expression in the pooled skeletal site data (Figures 4.6 and 4.7, respectively), a multiple regression analysis was performed to determine the contribution of OCN and OPN mRNA expression to OPG mRNA expression. OPG mRNA expression was dependent on OPN and not OCN mRNA expression ($p < 0.02$). Interestingly, OPG mRNA expression and protein synthesis was induced by $\alpha_v\beta_3$ integrin ligation by OPN in endothelial cells (Malyankar *et al.*, 2000). *In vitro*, the $\alpha_v\beta_3$ integrin is involved in inhibition of endothelial cell death *via* an NF-κB-mediated pathway (Scatena *et al.*, 1998). OPG-deficient mice develop severe arterial calcification, in addition to the development of extensive osteoporosis (Bucay *et al.*, 1998;

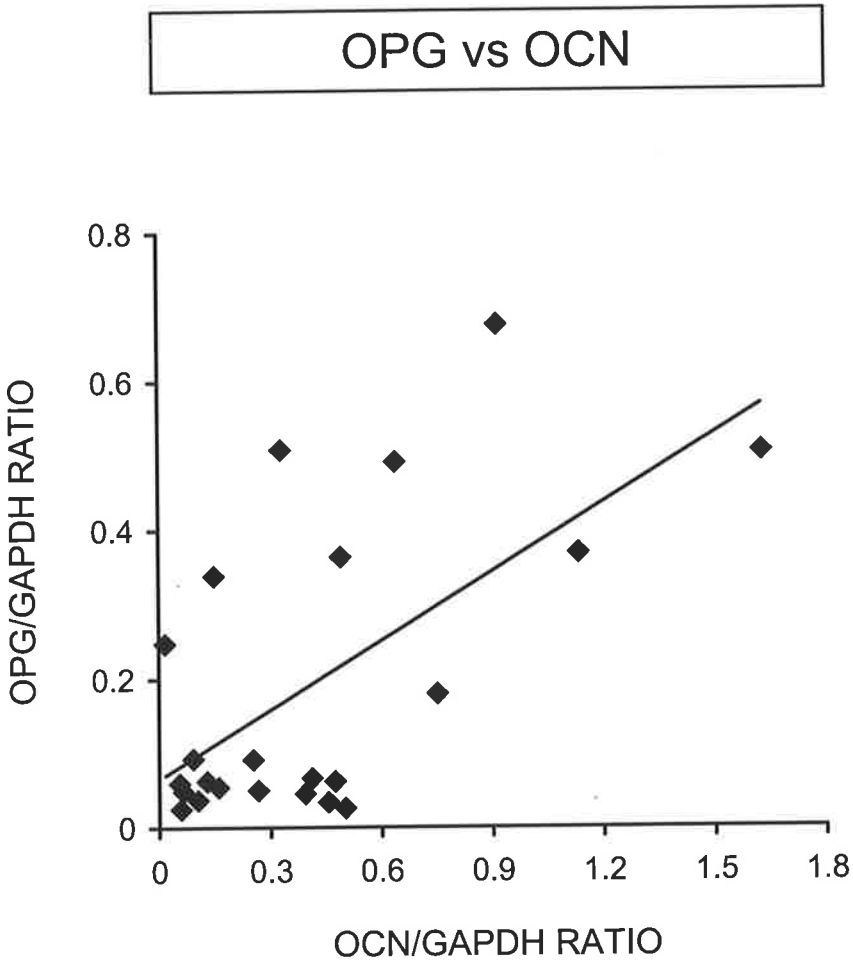

Figure 4.6: A positive association was observed between the relative ratio of OPG/GAPDH mRNA and OCN/GAPDH mRNA in trabecular bone for the pooled skeletal site data from postmortem individuals (n = 23; OPG/GAPDH = 0.31*OCN/GAPDH + 0.07; $r = 0.61$ and $p < 0.002$).

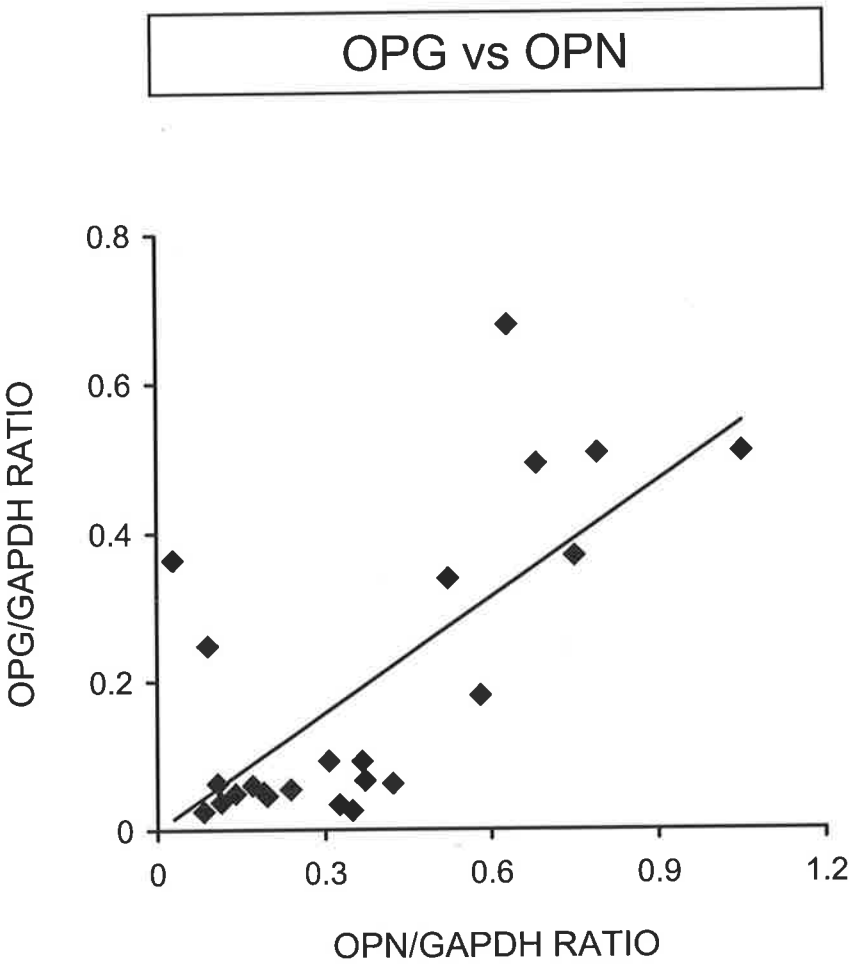

Figure 4.7: A positive association was observed between the relative ratio of OPG/GAPDH mRNA and OPN/GAPDH mRNA in trabecular bone for the pooled skeletal site data from postmortem individuals (n = 23; OPG/GAPDH = 0.52*OPN/GAPDH - 0.0002; $r = 0.71$ and $p < 0.001$).

Mizuno *et al.*, 1998). Thus, the biological function of OPG may not only be to inhibit bone resorption, but may also be a protective role in the vascular system (Bucay *et al.*, 1998; Malyankar *et al.*, 2000; Mizuno *et al.*, 1998), perhaps with a role also for OPN. It is important to note that the cellular origin(s) of the measured OPG, OCN, and OPN mRNA expression in these human trabecular bone samples are not known. Thus, it is not known whether the relationship between OPG and OPN exists for osteoblasts.

Table 4.8 Associations between RT-PCR product/GAPDH ratios for OPG, OCN, and OPN mRNA in the pooled skeletal site data, and in trabecular bone sampled from the individual skeletal sites, the iliac crest, femoral neck, and intertrochanteric regions, for postmortem individuals aged 42-85 years.

Association	Pooled ($n = 23$)	IC ($n = 9$)	FN ($n = 5$)	IT ($n = 9$)
OPG/GAPDH vs OCN/GAPDH	$r = 0.61$ $p < 0.002$	$r = 0.73$ $p < 0.02$	$r = 0.68$ $p =$ NS	$r = 0.49$ $p =$ NS
OPG/GAPDH vs OPN/GAPDH	$r = 0.71$ $p < 0.001$	$r = 0.72$ $p < 0.02$	$r = 0.77$ $p < 0.05$	$r = 0.81$ $p < 0.003$

Total RNA was isolated from trabecular bone sampled from the following skeletal regions: IC, iliac crest; FN, femoral neck; IT, intertrochanteric region of the proximal femur.
r, linear regression analysis; NS, not significant.

4.5 DISCUSSION

There is heterogeneity in the architecture, bone matrix properties, and bone turnover rates of trabecular bone throughout the human skeleton. However, there is a lack of information regarding the pattern of gene expression corresponding to markers of bone cells and specific molecules, with regulatory roles in bone turnover, in different skeletal sites from the same individual. Thus, the aim of the work described in this chapter was to investigate

mRNA gene expression in trabecular bone sampled from the iliac crest, femoral neck, and intertrochanteric region of the proximal femur, for a cohort of postmortem individuals. The purpose of describing the pattern of mRNA expression between these three skeletal regions was to establish whether there were any skeletal site differences in the steady state mRNA levels of the skeletally active molecules. These data were of particular interest as striking differences in the pattern of mRNA expression, of a similar selection of skeletally active molecules, were observed at the intertrochanteric region between patients with severe primary hip osteoarthritis (OA) and non-diseased postmortem individuals (described in Chapter 6). The select group of skeletally active molecules chosen for investigation included the factors with central regulatory roles in controlling osteoclast development and activity, namely RANKL, OPG, and RANK, two recognised skeletally active cytokines capable of promoting osteoclast formation, IL-6 and TNF-α, the abundant bone matrix growth factor TGF-β1, the osteoblastic cell markers, OCN and OPN, and the osteoclastic cell markers, the CTR and TRAP.

4.5.1 The mRNA expression pattern of bone cell markers and regulatory factors of bone remodelling is similar between iliac crest, femoral neck, and intertrochanteric trabecular bone

Differences in trabecular bone architecture, bone matrix properties, and bone turnover have been reported between the iliac crest, femoral neck, and intertrochanteric region of the proximal femur, for non-diseased individuals (Aerssens *et al.*, 1997; Amling *et al.*, 1996; Fazzalari *et al.*, 1989; Parfitt, 1996). Amling *et al.* (1996) described a greater degree of trabecular interconnection at the femoral neck compared to the iliac crest and intertrochanteric region. Histomorphometric assessment of trabecular bone architecture and bone turnover between the iliac crest and the region medial to the greater trochanter

(MGT), which is medially adjacent to the intertrochanteric region, identified differences between these skeletal sites (Fazzalari *et al.*, 1989). Specifically, the structural parameters BS/TV and BS/BV were lower, trabecular spacing was increased, and trabecular bone volume did not differ, at the MGT region in comparison to the iliac crest (Fazzalari *et al.*, 1989). Further, the histomorphometric parameters representative of bone formation, osteoid volume and osteoid surface, were lower at the MGT region in comparison to the iliac crest. However, eroded bone surface, representative of bone resorption, was not different between the MGT region and the iliac crest (Fazzalari *et al.*, 1989). Aerssens *et al.* (1997) reported that trabecular bone from the femoral neck was more mineralised compared to iliac crest trabecular bone. In addition, the trabecular bone matrix concentration of OCN and IGF-I was higher at the femoral neck than at the iliac crest (Aerssens *et al.*, 1997). Static and kinetic histomorphometry have shown that the rate of bone turnover is higher at the iliac crest compared to appendicular skeletal sites (Parfitt, 1996; Schnitzler *et al.*, 1996). However, there is limited information on the rate of bone turnover, specifically between the iliac crest, femoral neck, and intertrochanteric region, for the same non-diseased individual.

It was hypothesised that the mRNA expression levels of bone cell markers and regulatory factors of bone remodelling would differ between the iliac crest, femoral neck, and intertrochanteric regions. Intriguingly, the levels of mRNA corresponding to the bone cell markers, CTR, OCN, OPN, and TRAP, and the skeletally active molecules, RANKL, OPG, RANK, IL-6, TNF-α, and TGF-β1, were not significantly different between trabecular bone sampled from the iliac crest, femoral neck, and intertrochanteric region, for a cohort of postmortem individuals (Table 4.3). This finding suggests that the steady state mRNA expression levels for these skeletally active molecules are similar between the three skeletal

regions. Furthermore, this finding is even more unexpected given the diverse cellular expression and function of these mRNA species in the local bone microenvironment. However, a generalised observation was that for some individuals there was some skeletal site variation for a number of mRNA species (with visual assessment of the pattern of mRNA expression between skeletal sites for an individual case (i.e., a radial plot); results not shown).

Histomorphometry has been used to show differential rates of bone turnover between specific skeletal sites (Parfitt, 1996). The histomorphometric calculation of activation frequency, which in trabecular bone refers to the probability that a new cycle of remodelling will be initiated at any point on the bone surface, is a two-dimensional, not a three-dimensional, concept (Parfitt *et al.*, 1987). However, the calculation of activation frequency depends upon both the birth-rate of new basic multicellular units (BMUs) and the distance that each one moves (i.e., the lifespan of the BMU; Parfitt, 2002). Therefore, the histomorphometric estimation of activation frequency and other histomorphometric parameters describing the extent of bone formation and resorption, measured in 5μm-thick sections of trabecular bone, may not be directly comparable to the steady state mRNA expression levels of skeletally active molecules, measured in 1.0 x 1.0 x 0.5 cm^3 trabecular bone tissue, from the same skeletal region. However, a strong positive association was observed between eroded bone surface, ES/BS, and the ratio of RANKL/OPG mRNA, measured in contiguous trabecular bone samples from the intertrochanteric region of the proximal femur, for non-diseased individuals (Figure 7.8; Chapter 7.4.3). The RANKL/OPG ratio is hypothesised to be the main determinant of the pool size of active osteoclasts in the local bone microenvironment (Hofbauer *et al.*, 2000).

The similarity in the steady state mRNA expression levels of the skeletally active molecules between the iliac crest, femoral neck, and intertrochanteric region, for a cohort of postmortem individuals (Table 4.3), is of particular interest as striking differences in the pattern of mRNA expression, of a similar selection of skeletally active molecules, were observed at the intertrochanteric region between patients with severe primary hip osteoarthritis (OA) and non-diseased postmortem individuals (described in Chapter 6). It remains to be established whether the different pattern of mRNA expression in trabecular bone at the intertrochanteric region for OA patients is a local or constitutive skeletal site phenomenon. Based upon the similarity in the pattern of mRNA expression between the iliac crest and intertrochanteric region, for a cohort of postmortem individuals, it can be hypothesised that the differences in mRNA expression at the intertrochanteric region between OA patients and controls will also be observed at the iliac crest. It is important to ascertain whether the pattern of mRNA expression for OA patients is different at the iliac crest, for a number of reasons. Firstly, the iliac crest is a skeletal site accessible for bone biopsy and is the accepted bone biopsy site for histomorphometric assessment of skeletal change (Parfitt, 1983). Secondly, the iliac crest is not subject to loading abnormalities or joint pathological changes. Finally, the trabecular bone structure and bone matrix biochemistry of the iliac crest have been described in OA (Crane *et al.*, 1990; Dequeker *et al.*, 1993b; Fazzalari *et al.*, 1992; Gevers and Dequeker, 1987). For instance, the bone matrix from the iliac crest of OA subjects has been found to contain a higher content of the growth factors IGF-I, IGF-II, and TGF-β, and an increased concentration of OCN, compared with that in control subjects (Dequeker *et al.*, 1993b; Gevers and Dequeker, 1987). The potential use of gene expression profiles in trabecular bone biopsies for predicting development of OA is discussed in Chapters 6.5.4 and 7.5.4.

4.5.2 Associations between specific mRNA transcripts in human trabecular bone from the iliac crest, femoral neck, and intertrochanteric regions

The current knowledge of systemic and local regulation of bone remodelling has been developed primarily from studies utilising *in vitro* cell culture systems, predominantly murine, and animal studies such as the effects of gene deletion studies in mice (reviewed in Ducy *et al.*, 2000; Hofbauer and Heufelder, 2001; Raisz, 1999; Roodman, 1999; Suda *et al.*, 1999). Human bone cell studies *in vitro* involve culturing cells from trabecular bone tissues obtained at surgery. The cells are cultured in a medium enriched with serum growth factors, but this may not represent the paracrine and autocrine factors that are produced in the local bone microenvironment. Thus, the morphology and behaviour of human bone cells in culture may not exactly mimic their behaviour or function *in vivo*. Therefore, it is important to investigate the mRNA expression of skeletally active genes in the local human bone microenvironment, where paracrine mediators of bone turnover can be measured with their local regulatory mechanisms intact.

A number of significant associations between specific mRNA species, with known regulatory roles in bone remodelling, were observed in human trabecular bone sampled from the iliac crest, femoral neck, and intertrochanteric region, for a cohort of postmortem individuals (Figures 4.1-4.7; Tables 4.4-4.8). For example, significant positive associations were observed between CTR/GAPDH, TRAP/GAPDH, and RANK/GAPDH mRNA expression in the pooled skeletal site data (Figures 4.1 and 4.2; Table 4.4). These associations are consistent with the expression of CTR, TRAP, and RANK by the same cell types, namely osteoclasts and their precursors, in the bone microenvironment (Hattersley and Chambers, 1989; Hsu *et al.*, 1999; Minkin, 1982; Quinn *et al.*, 1999). Interestingly, there was a positive association between IL-6/GAPDH and TNF-α/GAPDH

mRNA expression in the pooled skeletal site data (Table 4.5). This association is consistent with the finding that TNF-α treatment of murine osteoblastic cells resulted in a dose-dependent induction of IL-6 mRNA (Ishimi *et al.*, 1990; Kurokouchi *et al.*, 1998). In addition, the data suggest the co-regulation of these pro-osteoclastic cytokines in the local human bone microenvironment. *In vivo* studies suggest that both IL-6 and TNF-α play a key role in bone loss induced by oestrogen deficiency, since bone loss is not seen in ovariectomised IL-6-deficient and TNF-deficient mice (Jilka *et al.*, 1992; Poli *et al.*, 1994; Roggia *et al.*, 2001).

The growth factor TGF-β1 and the non-collagenous proteins, OCN and OPN, are abundant in the bone matrix. TGF-β has been shown to be released from the bone matrix as a consequence of bone resorption (Pfeilschifter *et al.*, 1990a). A number of roles for TGF-β in the bone microenvironment have been described, including a role in enhancing osteoclast apoptosis (Hughes *et al.*, 1996), and TGF-β has been shown to be chemotactic for osteoblasts (Pfeilschifter *et al.*, 1990b). Furthermore, TGF-β1 has been proposed to be one of the key factors involved in coupling bone formation to previous bone resorption (Pfeilschifter and Mundy, 1987). *In vivo*, TGF-β1 has been shown to stimulate bone formation in rodents (Marcelli *et al.*, 1990; Noda and Camilliere, 1989). As detailed in Chapter 1.3.1.2, OCN and OPN are both marker genes for the progression of osteoblastic differentiation (Denhardt and Noda, 1998; Stein and Lian, 1993). However, OPN is also expressed at high levels in osteoclasts (Dodds *et al.*, 1995; Merry *et al.*, 1993). The biological function of OCN and OPN in the bone microenvironment has not been precisely defined. OCN has been suggested to play a role in the regulation of bone mineral turnover, as mineral maturation was impaired in OCN-deficient mice (Boskey *et al.*, 1998). In addition, OCN may act in combination with other non-collagenous proteins, such as OPN,

as a signal for osteoclastic bone resorption (Reinholt *et al.*, 1990; Ritter *et al.*, 1992). *In vitro*, OPN has been shown to be an extracellular signalling molecule for osteoclasts and endothelial cells, *via* binding of OPN to the cell surface $\alpha_v\beta_3$ integrin (Denhardt and Noda, 1998; Liaw *et al.*, 1995). Interestingly, OPG mRNA expression and protein synthesis was induced by $\alpha_v\beta_3$ integrin ligation by OPN in endothelial cells (Malyankar *et al.*, 2000). OPG-deficient mice develop severe arterial calcification, in addition to the development of extensive osteoporosis (Bucay *et al.*, 1998; Mizuno *et al.*, 1998). Thus, the biological function of OPG may not only be to inhibit bone resorption, but may also be a protective role in the vascular system (Bucay *et al.*, 1998; Malyankar *et al.*, 2000; Mizuno *et al.*, 1998), perhaps with a role also for OPN. Intriguingly, a significant positive association was observed between OPG/GAPDH and OPN/GAPDH mRNA expression in the pooled skeletal site data (Figure 4.7; Table 4.8), which was maintained when the skeletal sites were analysed individually (Table 4.8).

Interestingly, significant positive associations were observed between OCN/GAPDH, OPN/GAPDH, and TGF-β1/GAPDH mRNA expression in the pooled skeletal site data (Figures 4.3-4.5; Table 4.7). These associations may be related to the biological function of these factors in the bone microenvironment. For example, the association between OPN mRNA and TGF-β1 mRNA is consistent with a report of TGF-β treatment of rat osteoblastic cells resulting in an up-regulation of OPN mRNA expression (Sodek *et al.*, 1995). Further, the association between OCN mRNA and OPN mRNA is consistent with a previous report which showed OCN and OPN form protein complexes *in vitro* (Ritter *et al.*, 1992). However, the associations between OCN, OPN, and TGF-β1 mRNA in human trabecular bone may relate to the expression of these mRNA species by similar cell types, namely osteoblasts, osteoclasts, and osteocytes, in the bone microenvironment. One

limitation of semi-quantitative RT-PCR analysis of mRNA expression in bone tissue is that the data provide no information about the cellular origin of each mRNA transcript. A second limitation is that it is not known whether the gene expression patterns are representative of the corresponding protein levels in the trabecular bone tissue.

4.5.3 Conclusions

There is considerable heterogeneity in the architecture, bone matrix properties, and bone turnover rates of trabecular bone throughout the human skeleton. However, a similar pattern of mRNA expression for markers of bone cells (CTR, OCN, OPN, and TRAP) and specific molecules, with regulatory roles in bone turnover (RANKL, OPG, RANK, IL-6, TNF-α, and TGF-β1), was observed between trabecular bone sampled from the iliac crest, femoral neck, and intertrochanteric region, for a cohort of postmortem individuals. This finding was unexpected given the diverse cellular expression and function of these mRNA species in the local bone microenvironment. Interestingly, a number of significant associations were observed between specific mRNA species, with known regulatory roles in bone remodelling, in trabecular bone sampled from the three skeletal regions. Although the semi-quantitative RT-PCR data provide no information about the cellular origin of each mRNA transcript, and it is not known whether the gene expression patterns are representative of the corresponding protein levels in the trabecular bone tissue, the advantage of this experimental approach over cell culture techniques is that factors/mediators can be analysed with their local regulatory mechanisms intact.

CHAPTER 5

mRNA EXPRESSION OF CYTOKINES, BONE CELL MARKERS, AND REGULATORY FACTORS OF OSTEOCLASTOGENESIS, IN TRABECULAR BONE FROM THE HUMAN PROXIMAL FEMUR

5.1 INTRODUCTION

Few studies, in the context of normal human bone physiology, have addressed the expression of molecular regulators of bone remodelling *in situ* in the local human bone microenvironment. The current knowledge of systemic and local regulation of bone remodelling has been developed primarily from studies utilising *in vitro* cell culture systems, predominantly murine, and animal studies such as the effects of gene deletion studies in mice (reviewed in Ducy *et al.*, 2000; Hofbauer and Heufelder, 2001; Raisz, 1999; Roodman, 1999; Suda *et al.*, 1999). Human bone cell studies *in vitro* involve culturing cells from trabecular bone tissues obtained at surgery, predominantly joint replacement surgery, for diseased and/or arthritic joints. The cells are cultured in a medium enriched with serum growth factors, but this may not represent the paracrine and autocrine factors that are produced in the local bone microenvironment. Thus, the morphology and behaviour of human bone cells in culture may not exactly mimic their behaviour or function *in vivo*. Therefore, there is a need to investigate the mRNA expression of skeletally active genes in the local human bone microenvironment where mediators of bone turnover can be related to bone structural parameters.

Analysis of the steady-state levels of gene transcription in human bone has been performed in studies of cytokine mRNA in iliac crest bone biopsies from postmenopausal women (Abrahamsen *et al.*, 2000; Ralston, 1994). These studies did not include any analysis of age-related changes in cytokine mRNA expression. Lin *et al.* (1999) emphasized that the analysis of mRNA expression patterns in human tissues can provide significant insight into the spatio-temporal activities of gene transcription in a tissue, and further provide important information on physiology and pathology at a molecular level.

As detailed in Chapter 1.3.1.1, considerable progress has been made towards an understanding of the mechanisms responsible for the formation and activation of osteoclasts. A large number of hormones and cytokines have been identified that can stimulate the development of osteoclasts from their haematopoietic precursors (Martin and Ng, 1994; Martin *et al.*, 1998; Martin and Udagawa, 1998). A cell-surface member of the tumour necrosis factor (TNF)-ligand family, termed receptor activator of nuclear factor kappa B ligand (RANKL), was shown to be central in osteoclast development and activity (Lacey *et al.*, 1998; Wong *et al.*, 1997; Yasuda *et al.*, 1998b). Agents that induce bone resorption, including 1,25-dihydroxyvitamin D_3 (1,25-$(OH)_2D_3$), parathyroid hormone (PTH), prostaglandin E_2 (PGE_2), and interleukin (IL)-11, have been shown to induce the presentation of RANKL on the surface of osteoblastic cells, which are then able to promote osteoclast formation (Horwood *et al.*, 1998; Udagawa *et al.*, 1999; Yasuda *et al.*, 1998b). RANKL binds to a TNF-receptor superfamily member, RANK (Anderson *et al.*, 1997; Hsu *et al.*, 1999), which is expressed on the surface of osteoclasts and their precursors (Hsu *et al.*, 1999). RANK has been shown to be essential for osteoclast formation; anti-RANK antibodies inhibit osteoclast formation *in vitro* (Nakagawa *et al.*, 1998), and RANK-deficient mice exhibit profound osteopetrosis and lack osteoclasts (Dougall *et al.*, 1999; Li *et al.*, 2000). In addition, over-expression of soluble RANK in transgenic mice resulted in osteopetrosis, decreased numbers of osteoclasts, and decreased bone resorption (Hsu *et al.*, 1999). Furthermore, mice deficient in RANKL lack osteoclasts and develop osteopetrosis (Kong *et al.*, 1999). Likewise, a natural RANKL antagonist, a soluble TNF-receptor family member, termed osteoprotegerin (OPG), can inhibit osteoclast formation and bone resorption (Simonet *et al.*, 1997). Over-expression of OPG in mice resulted in an osteopetrotic phenotype and decreased numbers of osteoclasts (Simonet *et al.*, 1997), while mice in which the OPG gene is deleted develop extensive osteoporosis and increased

numbers of osteoclasts (Bucay *et al.*, 1998; Mizuno *et al.*, 1998). Furthermore, administration of recombinant murine OPG protects against ovariectomy-associated bone loss in rats, *via* a reduction in osteoclast number and subsequent increase in bone volume (Simonet *et al.*, 1997). OPG is being considered for use clinically as an anti-resorptive agent to treat a variety of bone disorders characterised by increased osteoclast activity, such as osteoporosis, osteolytic bone tumours, rheumatoid arthritis, and periodontal disease. Indeed, a preliminary study involving treatment of 52 postmenopausal women with a single dose of human recombinant OPG resulted in a rapid and sustained decrease in urinary biochemical markers of bone resorption (Bekker *et al.*, 2001). OPG is expressed by a wide variety of cell types, including osteoblasts, in which its expression is down-regulated by many of the same factors that promote bone resorption and RANKL expression (Hofbauer *et al.*, 1999b). Thus, there is now good evidence that the local amount of RANKL, relative to OPG, is important in osteoclast formation (Hofbauer *et al.*, 2000).

As detailed in Chapter 1.3.4.2, IL-6 and IL-11 are two cytokines that share many biological properties, including the ability to stimulate osteoclast development from their haematopoietic precursors (Martin *et al.*, 1998). Both of these cytokines signal *via* a receptor system that consists of a unique ligand-binding domain and the common 130-kDa subunit (gp130; Kishimoto *et al.*, 1995). IL-6 can be produced by a number of cell types in the bone microenvironment, including marrow stromal cells, monocyte-macrophages, osteoblasts, and osteoclasts (Girasole *et al.*, 1992; Kishimoto, 1989; Linkhart *et al.*, 1991; O'Keefe *et al.*, 1997). The reported effects of IL-6 on RANKL-RANK-promoted osteoclast development are conflicting. IL-6 has been shown to induce RANKL mRNA expression, and conversely reduce OPG mRNA expression, in murine osteoblastic cell lines (Nakashima *et al.*, 2000; O'Brien *et al.*, 1999). In contrast, RANKL mRNA

expression was not affected by IL-6 in human marrow stromal/osteoblastic cells (Hofbauer *et al.*, 1999b), and further, IL-6 had no effect on OPG production in these stromal/osteoblastic cells (Brandstrom *et al.*, 1998; Hofbauer *et al.*, 1998; Vidal *et al.*, 1998). It has been suggested that IL-6 may attenuate calcium sensing and thus enhance bone resorption by a direct effect on mature osteoclast activity (Adebanjo *et al.*, 1998). Interestingly, while expression of IL-6 mRNA in the bone is contributed by several cell types, IL-11 mRNA is likely to be expressed predominantly by cells of mesenchymal origin, namely, cells of the osteoblast lineage (Paul *et al.*, 1990). IL-11 has been suggested to play a critical role in the hierarchy of osteoclastogenic factors, since *in vitro* its expression is induced by a number of hormone and local activators of osteoclast formation (Manolagas, 1995; Romas *et al.*, 1996; Yang and Yang, 1994). In addition, neutralisation of IL-11 has been shown *in vitro* to suppress osteoclast development induced by 1,25-$(OH)_2D_3$, PTH, IL-1, and TNF-α (Girasole *et al.*, 1994). The effects of IL-11 on osteoclast differentiation appear to be mediated by inducing RANKL expression on marrow stromal/osteoblastic cells (Nakashima *et al.*, 2000; Yasuda *et al.*, 1998b). Furthermore, the bone-resorptive effect of IL-11 in neonatal mouse calvarial bone cultures resulted in dose-dependent increases in RANKL and OPG mRNA (Ahlen *et al.*, 2002). However, in contrast to observations in mouse bone marrow cultures (Girasole *et al.*, 1994; Romas *et al.*, 1996), Ahlen *et al.* (2002) have demonstrated that IL-11 did not play an important role in the resorptive effects of PTH and 1,25-$(OH)_2D_3$ in the mouse calvarial bone culture experimental system.

There is a lack of information regarding the pattern of gene expression corresponding to specific molecules, with regulatory roles in bone turnover, in normal human bone tissue or indeed, their role in skeletal disease. Furthermore, it has not been determined whether there

is any change in the gene expression of these skeletally active molecules with aging in normal human bone tissues. Therefore, this chapter describes investigation of the expression of mRNA corresponding to the key osteoclast differentiation factor, RANKL, together with its cognate receptor, RANK, and the soluble decoy receptor for RANKL, OPG, in normal human trabecular bone. In addition, expression of mRNA encoding the cytokines IL-6 and IL-11, both of which are involved in the regulation of the RANKL-RANK-OPG system of osteoclast development was investigated in normal human trabecular bone. The osteoblastic cell marker, osteocalcin (OCN), and the calcitonin receptor (CTR), which in bone is exclusively expressed by osteoclasts, were also studied. The skeletal site chosen for investigation was from the proximal femur, with samples derived from a cohort of autopsy individuals, who had not suffered from conditions thought to affect their bone turnover status. The mRNA expression data presented in this chapter describes characterisation of a control group, to which data from osteoarthritic (OA) bone is compared in Chapter 6. The specific skeletal site that the trabecular bone was sampled from was the intertrochanteric region of the proximal femur, as this region has previously been shown to be structurally different between OA and control bone (Crane *et al.*, 1990). Further, the intertrochanteric region is remote from the subchondral bone that undergoes well-characterised secondary changes in severe OA (Fazzalari *et al.*, 1992).

5.2 CHAPTER AIMS

- To describe the steady state mRNA expression, of factors known to have important regulatory roles in bone remodelling, in non-diseased human trabecular bone tissue sampled from the intertrochanteric region of the proximal femur (a skeletal site which

displays a similar pattern of mRNA gene expression to the iliac crest and femoral neck in postmortem human bone, described in Chapter 4).

- To investigate whether there are gender differences in the mRNA expression levels in non-diseased human trabecular bone from the proximal femur.

- To investigate whether there are age-related changes in the mRNA expression levels in non-diseased human trabecular bone from the proximal femur.

5.3 METHODS

5.3.1 Case selection

Proximal femurs, 12 from the left and 2 from the right anatomical side, were obtained from 14 routine autopsies performed at the Royal Adelaide Hospital (Table 5.1). The age of the postmortem cases, comprising 7 women (aged 20-83 years; mean ± SD [standard deviation] age, 61.3 ± 22.0 years) and 7 men (aged 24-85 years; 61.9 ± 20.8 years), varied between 20 and 85 years (61.6 ± 20.6 years). There was no difference in the mean age between females and males. The postmortem cases had a postmortem interval (PMI) range, the time between death and the postmortem examination, of 24 to 72 hours, which was an average of 2 days (48.2 ± 19.1 hours). There was no correlation between PMI and the age of the individual. These postmortem cases, which are categorized as *control* cases in this thesis, were selected from routine autopsies using the following criteria: no known history of any chronic condition or disease, which may have affected bone status (such as renal dysfunction or endocrine disease affecting bone metabolism); no known history of any medication which may have affected bone turnover; admitted to hospital less than 3 days before death; and on macroscopic and radiological assessment of the proximal femur showed no significant sign of joint degeneration, according to the criteria of Collins

(1949). Informed consent from next-of-kin was obtained for the collection of these postmortem specimens, with approval by the Royal Adelaide Hospital Human Ethics Committee.

Table 5.1 Profiles of autopsy cases comprising the control group.

Case	Age *(years)*	Gender	Anatomical side	PMI *(hours)*	Cause of death
C1	20	Female	Left	24	Cardiac arrest
C2	43	Female	Left	38	Liver failure
C3	68	Female	Right	37	Sepsis
C4	68	Female	Left	70	Cardiac arrest/IHD
C5	72	Female	Left	44	Respiratory failure/pulmonary oedema
C6	75	Female	Left	30	Pneumonia
C7	83	Female	Left	45	Cardiac arrest
C8	24	Male	Left	72	MVA # ribs
C9	44	Male	Left	67	Sepsis/pneumonia
C10	65	Male	Left	69	MI
C11	69	Male	Right	57	Pneumonia
C12	73	Male	Left	24	Cerebrovascular disease
C13	73	Male	Left	26	Metastatic liver carcinoma
C14	85	Male	Left	72	Pulmonary embolism/bowel cancer

C, autopsy control case.
PMI, postmortem interval, refers to the time between death and autopsy.
Abbreviations for cause of death: #, fractured; IHD, ischaemic heart disease; MI, myocardial infarction; MVA, motor vehicle accident.

5.3.2 Sampling of trabecular bone from the intertrochanteric region of the human proximal femur

Trabecular bone was sampled from the intertrochanteric region of the proximal femur for each postmortem case. Each proximal femur was sectioned in the coronal plane using a band saw, which had been cleaned with DEPC-treated water, to allow access to trabecular bone for sampling from the intertrochanteric site, which is enclosed within the femoral cortex (Figure 2.1). Using sterile bone cutters, the trabecular bone tissue was sampled as small fragments from an approximate 1.5 x 1.0 cm^2 area, to a specimen depth of 0.5 cm, from the intertrochanteric region. The trabecular bone tissue fragments were rinsed briefly in DEPC-treated water (the rinsed material contained trabecular bone and bone marrow) and then immersed in RNA lysis buffer (4 M guanidine isothiocyanate solution; 2 ml/250 mg wet weight). In addition, for each proximal femur, an intertrochanteric trabecular bone sample (1.0 x 1.0 x 1.0 cm^3), contiguous with the bone sampled for RNA isolation, was processed for undecalcified bone histomorphometry and microdamage assessment (Chapters 7 and 8).

5.3.3 Semi-quantitative RT-PCR of total RNA isolated from human trabecular bone

Total RNA was isolated from the intertrochanteric trabecular bone tissue fragments (Chapter 2.2.2.1) for each postmortem case. Semi-quantitative RT-PCR (Chapter 2.2.2.3), using the human-specific oligonucleotide primer pairs listed in Table 2.1 and primer conditions described in Chapter 2.2.2.3.2, was used to determine the relative expression levels of IL-6, IL-11, CTR, OCN, RANKL, OPG, and RANK mRNA in these bone RNA samples. Amplified PCR products corresponding to IL-6, IL-11, CTR, OCN, RANKL, OPG, and RANK mRNA are represented as a ratio of the respective PCR product/GAPDH PCR product. There was no correlation between PMI and the relative ratios of PCR product/GAPDH for any of the mRNA species. RT-PCR data for RANKL, OPG, and

RANK mRNA could not be obtained for cases C10 (65-year-old male) and C13 (73-year-old male) due to small quantities of total RNA recovered.

5.3.4 Statistical analysis of mRNA expression data

RT-PCR reactions were performed twice, from duplicate cDNA syntheses, which confirmed that repeated RT-PCR analysis of the same RNA samples yielded reproducible results. In addition, to minimise inter-assay variability between each bone sample, all PCR products for a given mRNA species ($n \leq 14$), were electrophoresed in a single 2% agarose gel. The Shapiro-Wilk statistic was used to test the semi-quantitative RT-PCR data for normality (PC-SAS software; SAS Institute). The semi-quantitative RT-PCR data were found to be normally distributed. Therefore, parametric statistical methods were used to analyse the data (Excel; Microsoft Corp.). Student's *t*-test was used to analyse differences in mRNA expression between females and males. Linear regression analysis was used to describe age-related changes, and to examine the relationship between PCR products representing specific mRNA species. If there was more than one significant independent factor associated with a specific mRNA species, multiple regression was performed to determine the contribution of each independent factor. The mRNA expression data is quoted as mean ± standard deviation. The critical value for significance was chosen as $p = 0.05$.

5.4 RESULTS

5.4.1 Pattern of mRNA expression in non-diseased trabecular bone from the human proximal femur

Semi-quantitative RT-PCR was employed to examine the expression of IL-6, IL-11, CTR, OCN, RANKL, OPG, and RANK mRNA in trabecular bone sampled from the intertrochanteric region of the proximal femur of autopsy individuals. These mRNA

species were chosen because they represent, in the case of IL-6 and IL-11, recognised skeletally-active cytokines capable of promoting osteoclast formation. CTR and OCN were chosen as specific markers of the presence of osteoclasts and osteoblasts, respectively. RANKL, OPG, and RANK were chosen for their central regulatory roles in controlling osteoclast development and activity. These autopsy individuals did not suffer from any disease likely to affect the skeleton, and in particular, macroscopic examination of the femoral head showed no significant sign of joint degeneration, according to the criteria of Collins (1949). These individuals are thus categorized as *control* cases in this thesis.

Expression of mRNA corresponding to each of these seven mRNA species was found in all trabecular bone samples analysed from the proximal femur. A typical pattern of mRNA expression for IL-6, IL-11, the CTR isoforms, OCN, RANKL, OPG, and RANK is shown in Figure 5.1. The PCR products were authenticated by comparison with the expected product size and by hybridisation to an internal detecting oligonucleotide probe (Atkins *et al.*, 2000). In the case of the CTR, two bands were obtained, 780 bp and 732 bp PCR products, corresponding to the expected sizes of the insert-positive and insert-negative isoforms of the human CTR (Kuestner *et al.*, 1994). The two CTR isoforms differ from one another by the presence or absence of a 16-amino acid insert, generated by alternative splicing, in the first intracellular loop of the seven transmembrane domain (Moore *et al.*, 1995). The insert-negative isoform of the CTR was consistently more abundant than the insert-positive isoform in these bone samples, as seen in most tissues (Kuestner *et al.*, 1994).

The number of PCR cycles employed for each of these mRNA transcripts was within the exponential phase of the amplification curve, enabling comparison of mRNA expression

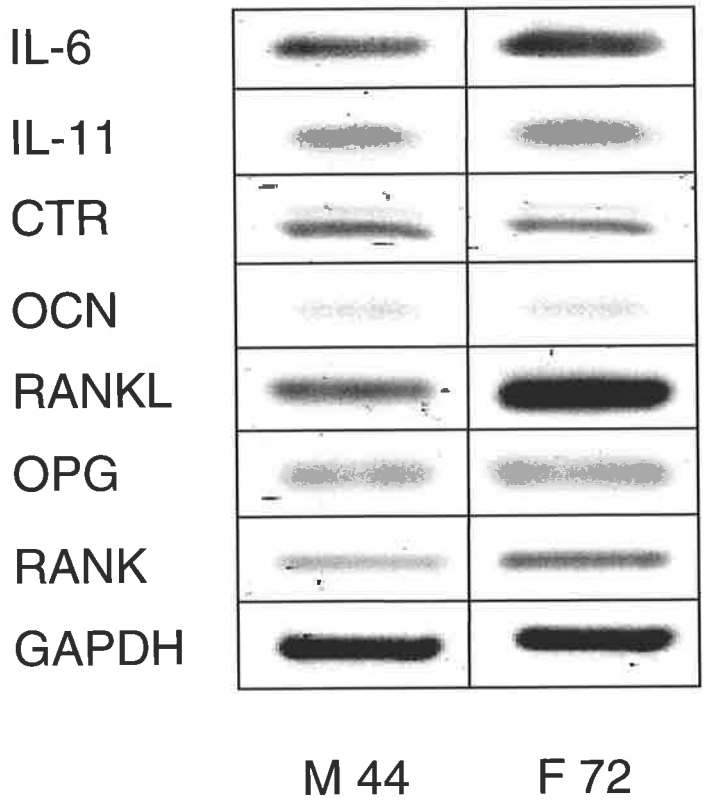

Figure 5.1: Expression of IL-6 (544 bp), IL-11 (289 bp), CTR isoforms (780/732 bp), OCN (255 bp), RANKL (665 bp), OPG (433 bp), RANK (702 bp), and GAPDH (415 bp) mRNA in total RNA extracted from intertrochanteric trabecular bone, as determined by RT-PCR (Chapter 2.2.2.3). Specimens were obtained from a 44-year-old male (M44) and a 72-year-old female (F72), without any bone-related disease, at autopsy. PCR products representing each mRNA species were visualised on SYBR® Gold-stained 2% agarose gels.

between bone samples. Relative levels of IL-6, IL-11, CTR, OCN, RANKL, OPG, and RANK mRNA were determined by normalising values to the GAPDH mRNA level determined for each sample. The distribution of the individual values obtained for IL-6, IL-11, CTR, OCN, RANKL, OPG, and RANK mRNA, expressed as a ratio to GAPDH, is shown in Figures 5.2 and 5.3. The two younger cases in this control cohort, cases C1 (20-year-old female) and C8 (24-year-old male), are indicated in Figures 5.2-5.8, as comparisons are made for this data between the controls and an OA group, aged over 49 years, in Chapter 6.

5.4.2 Comparison of mRNA expression between females and males

The student's *t*-test was used to assess whether there were any gender differences in the mean mRNA expression levels of IL-6, IL-11, CTR, OCN, RANKL, OPG, RANK, and the RANKL/OPG ratio in non-diseased human trabecular bone from the proximal femur. RANKL and OPG are important downstream signals of osteoclast biology, onto which many hormonal, chemical, and biochemical signals converge (Hofbauer and Heufelder, 2001). Hofbauer *et al.* (2000) hypothesised that the ratio of RANKL to OPG is the main determinant of the pool size of active osteoclasts in the local bone microenvironment, acting as a final effector system to modulate differentiation, activation, and apoptosis of osteoclasts. All of the mRNA species chosen for analysis, except for OCN, are involved in the regulation of osteoclastic bone resorption. Further, the 7 females in the control cohort comprise 5 postmenopausal females, who may have had an increased bone remodelling rate due to oestrogen deficiency. Thus, it was hypothesised that there may be an increased mRNA expression level of IL-6, IL-11, CTR, RANKL, RANK, and RANKL/OPG in the females compared to the males.

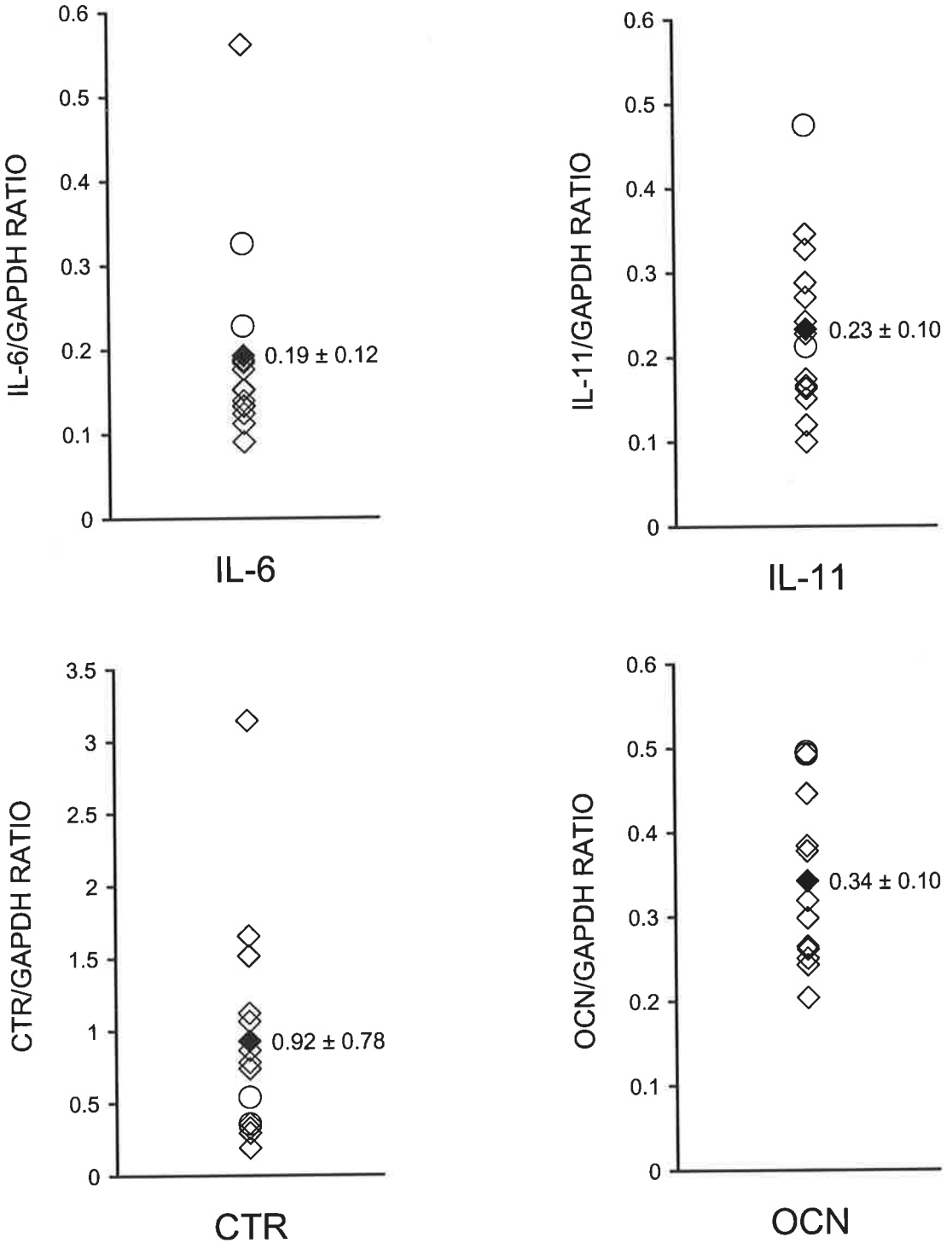

Figure 5.2: Relative ratios of PCR product/GAPDH for IL-6, IL-11, CTR, and OCN mRNA expression in intertrochanteric trabecular bone from control individuals (n = 14). Two cases, <40 years old, are indicated (○). The means are indicated (◆). Values are mean ± standard deviation.

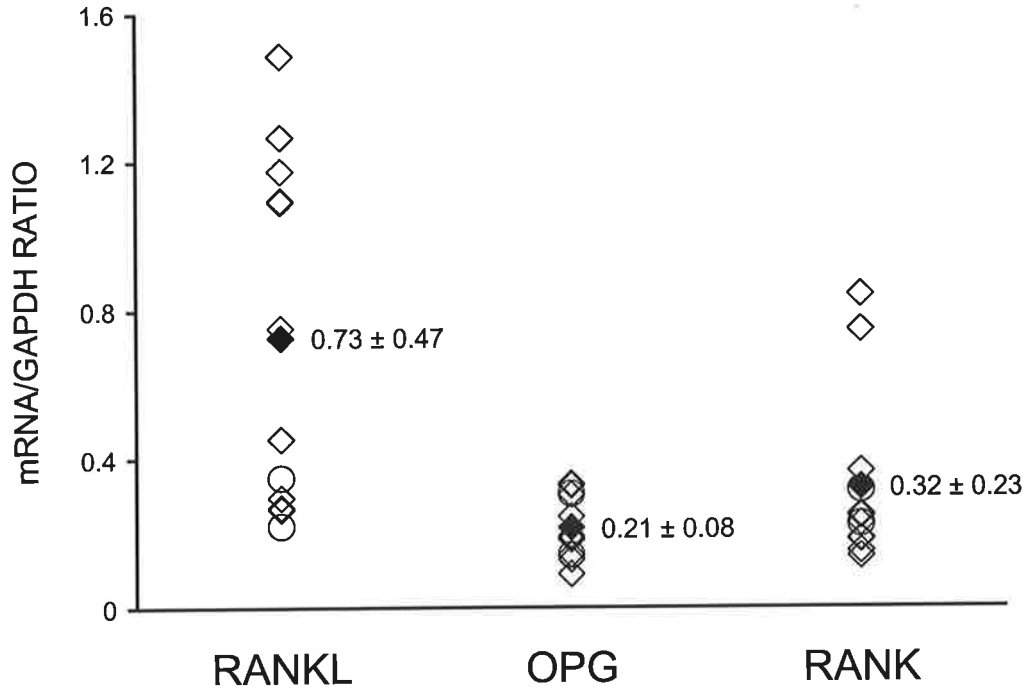

Figure 5.3: Relative ratios of PCR product/GAPDH for RANKL, OPG, and RANK mRNA expression in intertrochanteric trabecular bone from control individuals (n = 12). Two cases, <40 years old, are indicated (○). The means are indicated (◆). Values are mean ± standard deviation.

No significant differences were observed between females and males for the mean mRNA expression of IL-6/GAPDH, IL-11/GAPDH, OCN/GAPDH, RANKL/GAPDH, OPG/GAPDH or RANK/GAPDH (Table 5.2). These data compare with *in vitro* studies of human marrow stromal/osteoblastic cells, which found that the gender of the donor did not influence the mRNA expression of IL-6 or IL-11 (Shur *et al.*, 2001). Additionally, there was no difference in OCN protein concentration at the femoral neck between females and males (Boonen *et al.*, 1997). On the other hand, Vanderschueren *et al.* (1990) reported that the concentration of OCN protein in iliac crest bone was more abundant in males than in females. The RANKL/OPG mRNA ratio was significantly higher in the females than in the males ($p < 0.05$; Table 5.2), as expected. This suggests that the pool size of active osteoclasts may be greater in females than males at the intertrochanteric region of the proximal femur. Interestingly, a recent study has found no difference in the expression of RANKL and OPG mRNA or the RANKL/OPG mRNA ratio, in human iliac crest bone tissue, between premenopausal and postmenopausal women (Seck *et al.*, 2001). The only other difference between females and males was for CTR/GAPDH mRNA expression, which was significantly lower in females compared with males ($p < 0.05$; Table 5.2). As the CTR is expressed on the surface of mononuclear osteoclast precursor cells and multinuclear osteoclasts in bone (Hattersley and Chambers, 1989; Quinn *et al.*, 1999), it is not known whether immature and/or mature osteoclast cells are representative of the measured CTR mRNA, nor whether the CTR mRNA expression is representative of the number of osteoclasts and/or the number of calcitonin receptors on each osteoclast. Based on these comparisons between females and males for mRNA gene expression, and the fact that the sample size for the control cohort is small, further analyses of the data were made independent of gender.

Table 5.2 Female and male RT-PCR product/GAPDH ratios in intertrochanteric trabecular bone from control individuals.

Ratio	Female (n = 7)	Male (n = 7)
IL-6/GAPDH	0.23 ± 0.16	0.15 ± 0.04
IL-11/GAPDH	0.28 ± 0.12	0.18 ± 0.05
CTR/GAPDH	0.46 ± 0.23	1.39 ± 0.88 [a]
OCN/GAPDH	0.37 ± 0.11	0.32 ± 0.10
RANKL/GAPDH	0.88 ± 0.49	0.51 ± 0.38; n = 5
OPG/GAPDH	0.20 ± 0.09	0.23 ± 0.09; n = 5
RANK/GAPDH	0.32 ± 0.20	0.32 ± 0.29; n = 5
RANKL/OPG	4.28 ± 2.04	2.20 ± 0.94 [a]; n = 5

Values are mean ± standard deviation.
[a] $p < 0.05$.

5.4.3 Associations between expression of specific mRNA transcripts

As IL-6 and IL-11 are two cytokines that share many biological properties, including the ability to stimulate osteoclast development from their haematopoietic precursors (Martin *et al.*, 1998), the IL-6/GAPDH and IL-11/GAPDH mRNA ratios were co-plotted, and analysed by linear regression analysis. Intriguingly, a significant positive association was observed between IL-6/GAPDH and IL-11/GAPDH mRNA expression ($r = 0.49$, $p < 0.05$; Figure 5.4), although this association was dependent on inclusion of the two younger cases. This finding suggests the coordinated regulation of these two cytokines in the local human bone microenvironment. Further, when the outlier, case C5 (72-year-old female), was removed, the positive association between IL-6 and IL-11 mRNA was statistically

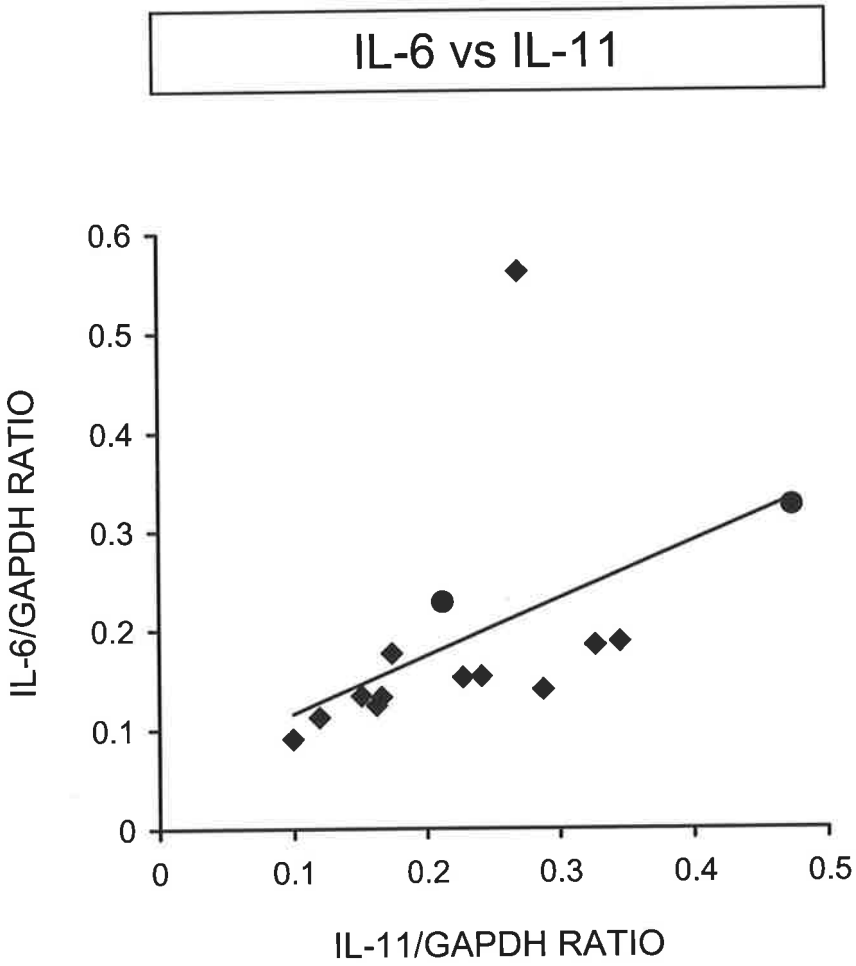

Figure 5.4: A positive association was observed between the relative ratio of IL-6/GAPDH mRNA and IL-11/GAPDH mRNA in intertrochanteric trabecular bone from control individuals (n = 14; IL-6/GAPDH = 0.58*IL-11/GAPDH + 0.06; r = 0.49 and p < 0.05; n = 13 (without outlier); IL-6/GAPDH = 0.47*IL-11/GAPDH + 0.06; r = 0.83 and p < 0.001). Two cases, <40 years old, are indicated (●).

more significant ($r = 0.83$, $p < 0.001$), which was maintained after exclusion of the two younger cases ($n = 11$; $r = 0.81$, $p < 0.001$).

OCN, the major non-collagenous protein of bone matrix, is utilised as an indicator of bone formation as it is one of the marker genes for the progression of osteoblastic differentiation (Stein and Lian, 1993). The CTR in bone is uniquely expressed on the surface of mononuclear osteoclast precursor cells and multinuclear osteoclasts (Hattersley and Chambers, 1989; Quinn *et al.*, 1999). The plot of CTR/GAPDH versus OCN/GAPDH mRNA expression might be regarded as an index of the balance of resorption to formation in these bone samples. However, no relationship was found between CTR/GAPDH and OCN/GAPDH mRNA expression in this cohort of bone samples (Figure 5.5). Using CTR/GAPDH mRNA as a marker of bone resorption in these bone samples is ambiguous, as it is not known whether immature and/or mature osteoclast cells are representative of the measured CTR mRNA, nor whether the CTR mRNA expression is representative of the number of osteoclasts and/or the number of calcitonin receptors on each osteoclast. Furthermore, there was no association between the mRNA expression of the pro-resorptive cytokines, IL-6 and IL-11, and CTR mRNA expression in these bone samples (results not shown). Despite the fact that RANK is expressed on the surface of the same cell types as the CTR in bone, namely osteoclasts and their precursors (Hsu *et al.*, 1999), no association was observed between CTR/GAPDH and RANK/GAPDH mRNA expression (Figure 6.12).

The stimulatory effects of IL-11 on osteoclast differentiation appear to be mediated by inducing RANKL expression on marrow stromal/osteoblastic cells (Nakashima *et al.*, 2000; Yasuda *et al.*, 1998b). However, the reported effects of IL-6 on RANKL-RANK-

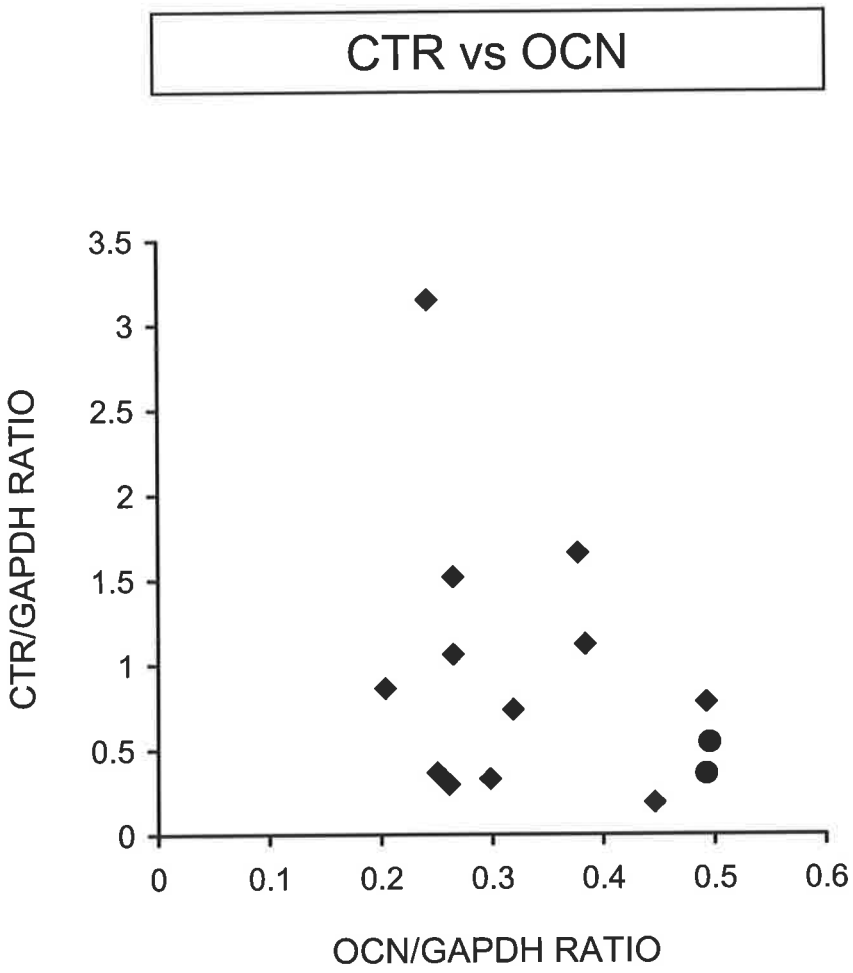

Figure 5.5: No association was observed between the relative ratio of CTR/GAPDH mRNA and OCN/GAPDH mRNA in intertrochanteric trabecular bone from control individuals (n = 14; CTR/GAPDH = -2.44*OCN/GAPDH + 1.76; r = -0.32 and p = NS). Two cases, <40 years old, are indicated (●). NS = not significant.

promoted osteoclast development are conflicting (Brandstrom *et al.*, 1998; Hofbauer *et al.*, 1998; Hofbauer *et al.*, 1999b; Nakashima *et al.*, 2000; O'Brien *et al.*, 1999; Vidal *et al.*, 1998). No associations were observed when the IL-6/GAPDH or IL-11/GAPDH mRNA ratios were co-plotted with the RANKL/GAPDH, OPG/GAPDH or RANK/GAPDH mRNA ratios for these bone samples (results not shown).

Extensive bone marrow cell culture studies have shown that RANKL, OPG, and to a lesser extent, RANK, are modulated by growth factors, cytokines, peptide and steroid hormones, and drugs known to affect bone metabolism (Hofbauer *et al.*, 2000; Hofbauer and Heufelder, 2001; Horowitz *et al.*, 2001; Suda *et al.*, 1999). Therefore, the results for RANKL and OPG mRNA, RANKL and RANK mRNA, and RANK and OPG mRNA were co-plotted to identify whether any relationships exist in the local human bone microenvironment of the proximal femur. Firstly, a significant positive association was observed between RANKL/GAPDH mRNA and OPG/GAPDH mRNA ($r = 0.55, p < 0.05$; Figure 5.6), which was maintained after exclusion of the two younger cases ($n = 10$; $r = 0.68$, $p < 0.02$). This finding suggests that the same stimuli/stimulus up-regulate/s both RANKL and OPG mRNA expression in these bone samples. Secondly, when the RANKL/GAPDH mRNA levels were plotted versus RANK/GAPDH mRNA, the level of RANKL gene expression increased as the level of RANK gene expression increased ($r = 0.66, p < 0.01$; Figure 5.7). Furthermore, this association was maintained after exclusion of the two younger cases ($n = 10$; $r = 0.69$, $p < 0.02$). This finding suggests that either the same stimulus regulates the expression of both RANKL and RANK mRNA, or, more likely, that the same stimulus up-regulates RANKL and causes recruitment of RANK-expressing osteoclast precursor cells. Finally, no association was observed in the co-plot of RANK/GAPDH mRNA and OPG/GAPDH mRNA expression (Figure 5.8).

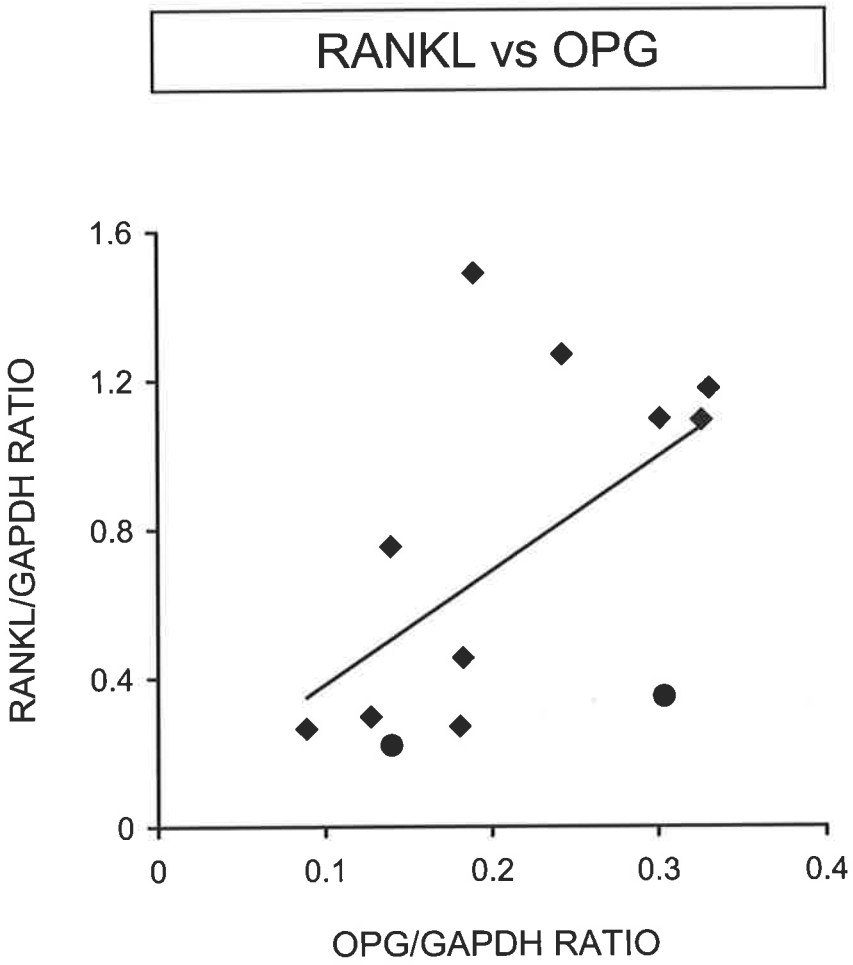

Figure 5.6: A positive association was observed between the relative ratio of RANKL/GAPDH mRNA and OPG/GAPDH mRNA in intertrochanteric trabecular bone from control individuals (n = 12; RANKL/GAPDH = 3.06*OPG/GAPDH + 0.08; r = 0.55 and $p < 0.05$). Two cases, <40 years old, are indicated (●).

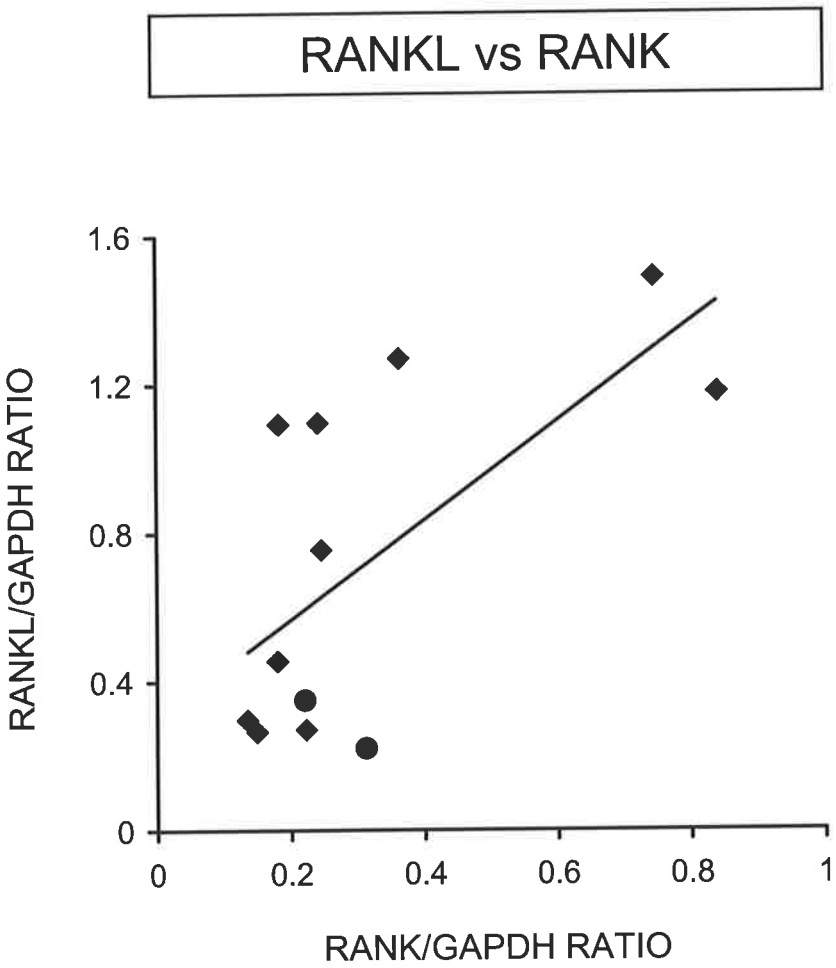

Figure 5.7: A positive association was observed between the relative ratio of RANKL/GAPDH mRNA and RANK/GAPDH mRNA in intertrochanteric trabecular bone from control individuals (n = 12; RANKL/GAPDH = 1.34*RANK/GAPDH + 0.30; r = 0.66 and $p < 0.01$). Two cases, <40 years old, are indicated (●).

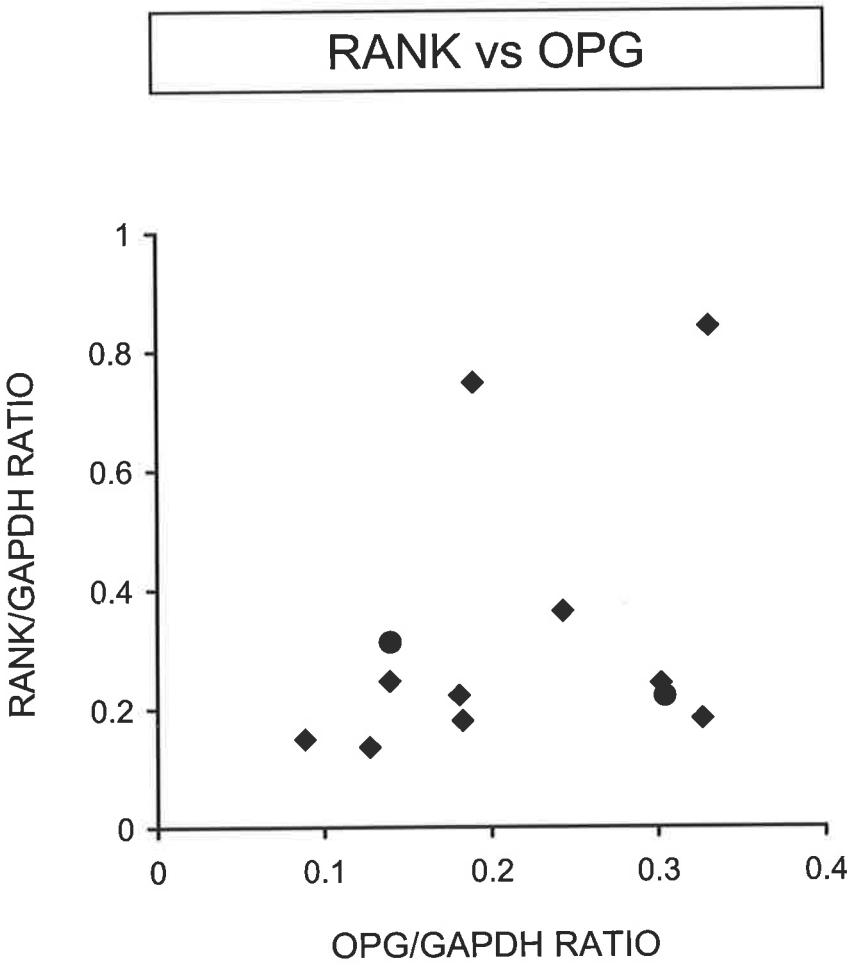

Figure 5.8: No association was observed between the relative ratio of RANK/GAPDH mRNA and OPG/GAPDH mRNA in intertrochanteric trabecular bone from control individuals (n = 12; RANK/GAPDH = 0.90*OPG/GAPDH + 0.13; r = 0.33 and p = NS). Two cases, <40 years old, are indicated (●). NS = not significant.

5.4.4 Age-related changes in mRNA expression in non-diseased trabecular bone from the human proximal femur

To investigate whether there are any age-related changes in the mRNA expression levels in non-diseased human trabecular bone from the proximal femur, each PCR product/GAPDH mRNA ratio was plotted as a function of increasing age in years, and analysed by linear regression analysis. IL-6/GAPDH mRNA expression showed no statistical dependence on age in these bone samples (Figure 5.9). However, when the outlier, case C5 (72-year-old female), was removed, the IL-6/GAPDH mRNA expression ratio significantly declined with age (r = -0.78, $p < 0.001$). The outlier, case C5, has a high relative expression level of IL-6/GAPDH mRNA in comparison with the IL-11/GAPDH mRNA expression level (Figure 5.4). In contrast to these bone mRNA expression levels, serum IL-6 levels in women, aged 24 to 87 years, have been shown to positively correlate with age (McKane *et al.*, 1994). However, it is not clear how serum cytokine levels relate to localised bone cytokine levels. The IL-11/GAPDH mRNA ratio declined with age, when analysed by linear regression (r = -0.60, $p < 0.02$; Figure 5.10), although this relationship was dependent on inclusion of the two younger cases. As both age and IL-6 mRNA expression were significantly associated with IL-11 mRNA expression (Figures 5.10 and 5.4, respectively), a multiple regression analysis was performed to determine the contribution of age and IL-6 mRNA expression to IL-11 mRNA expression. IL-11 mRNA expression was dependent on age and not IL-6 mRNA expression ($p < 0.05$), suggesting that the effect of IL-11 to stimulate osteoclast development may decline with age.

There was no relationship with age for CTR/GAPDH mRNA expression (Figure 5.11). Interestingly, when the OCN/GAPDH mRNA results were plotted against age, there was a

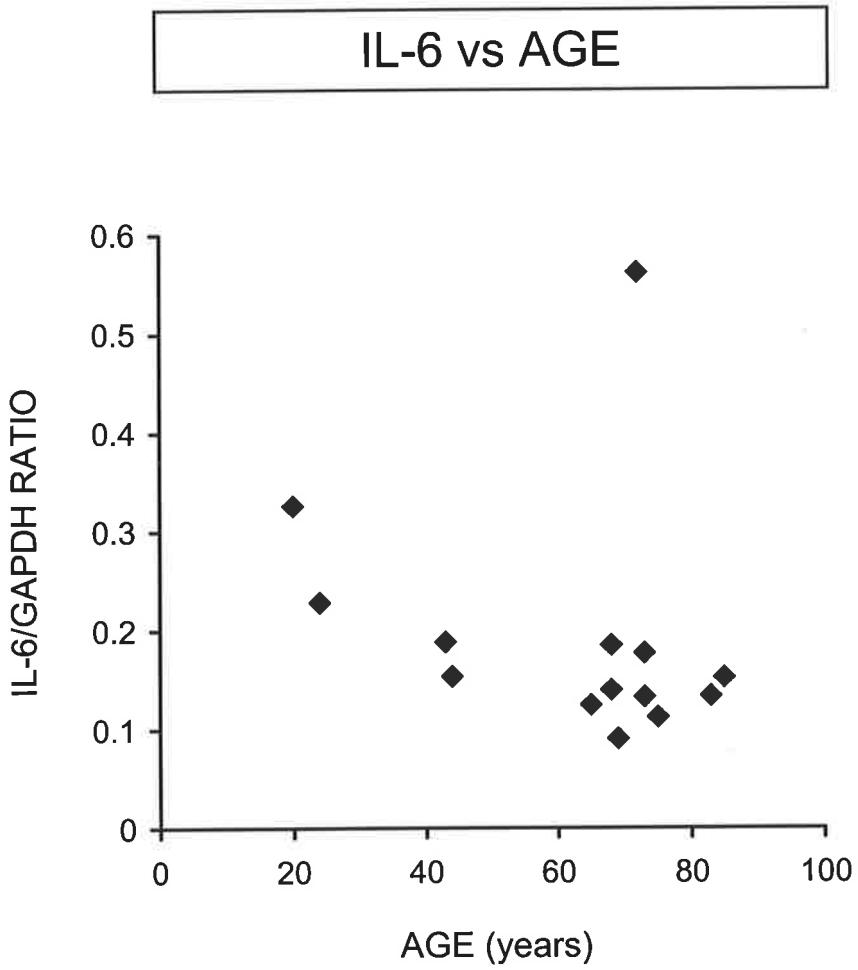

Figure 5.9: There was no significant change in IL-6/GAPDH mRNA with age in intertrochanteric trabecular bone from control individuals (n = 14; IL-6/GAPDH = -0.001*AGE + 0.28; r = -0.24 and p = NS; n = 13 (without outlier); IL-6/GAPDH = -0.002*AGE + 0.30; r = -0.78 and $p < 0.001$). NS = not significant.

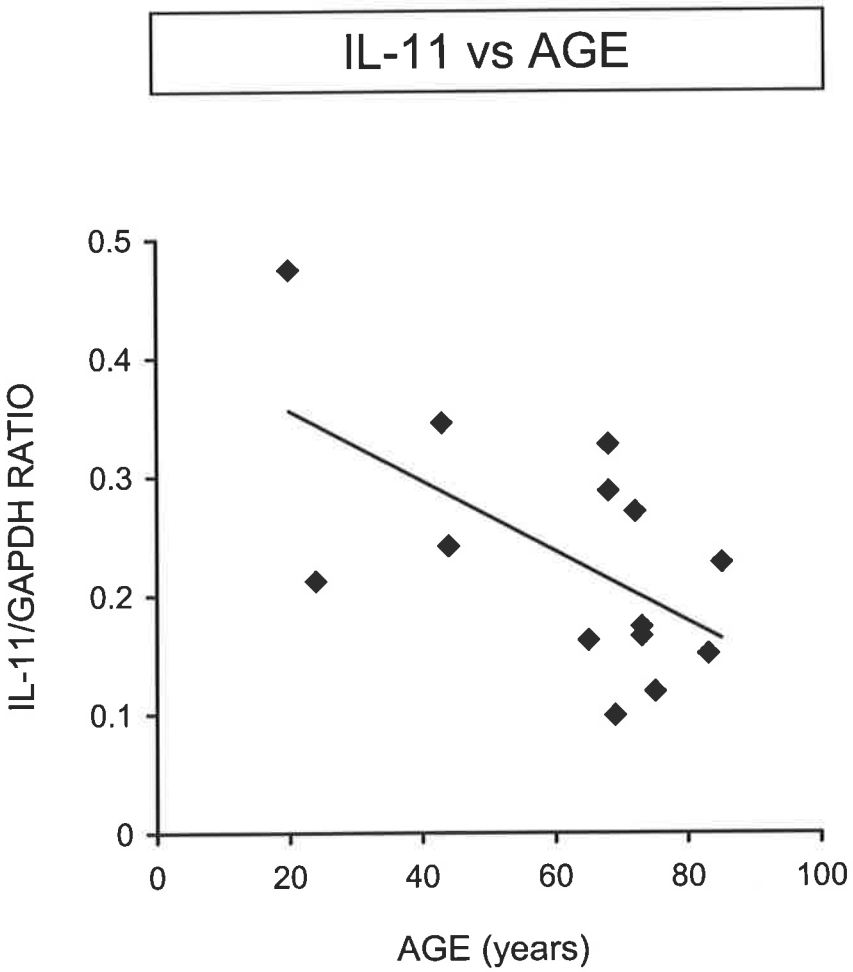

Figure 5.10: There was a significant decline in IL-11/GAPDH mRNA with age in intertrochanteric trabecular bone from control individuals (n = 14; IL-11/GAPDH = -0.003*AGE + 0.41; r = -0.60 and $p < 0.02$).

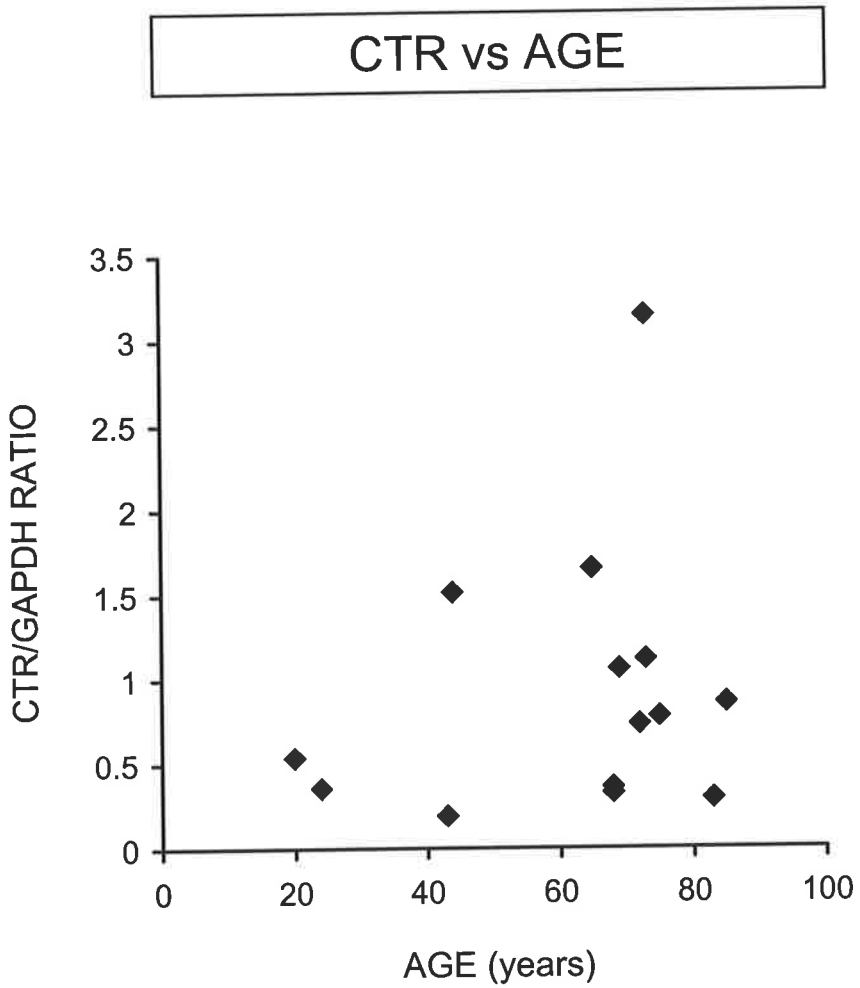

Figure 5.11: There was no significant change in CTR/GAPDH mRNA with age in intertrochanteric trabecular bone from control individuals (n = 14; CTR/GAPDH = 0.01*AGE + 0.42; r = 0.22 and p = NS). NS = not significant.

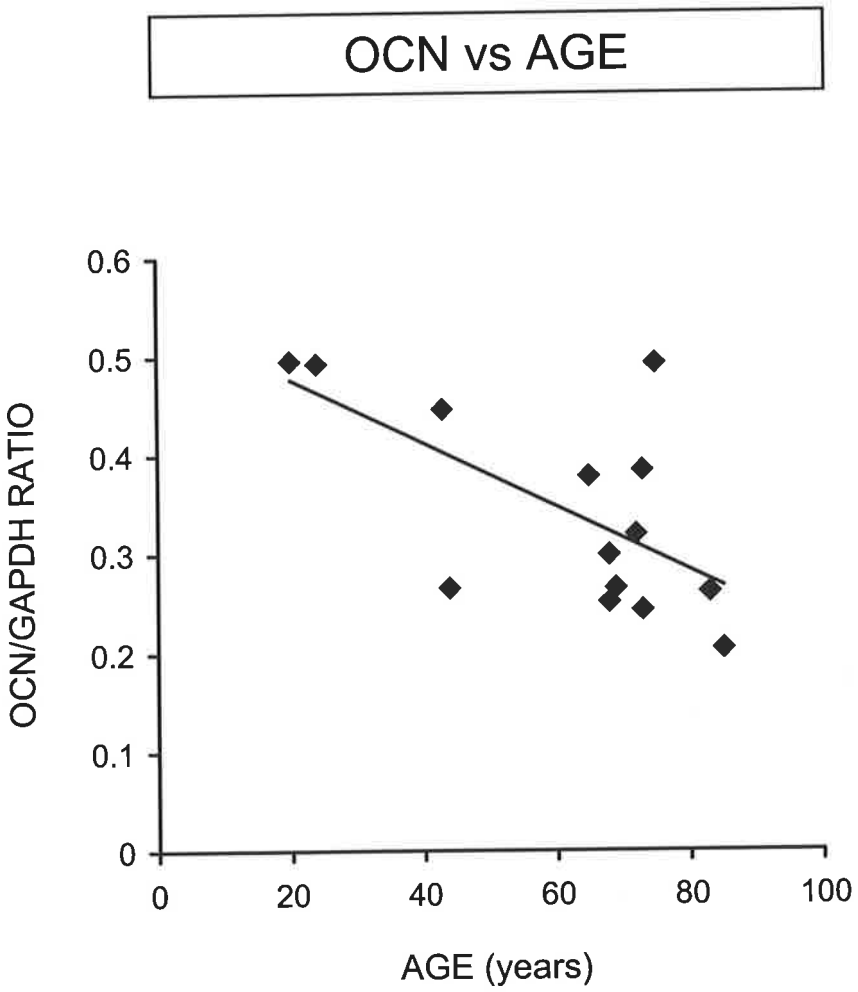

Figure 5.12: There was a significant decline in OCN/GAPDH mRNA with age in intertrochanteric trabecular bone from control individuals (n = 14; OCN/GAPDH = -0.003*AGE + 0.54; r = -0.64 and $p < 0.01$).

negative association (r = -0.64, $p < 0.01$; Figure 5.12), describing an age-related decrease in OCN mRNA expression. This age-related decline in OCN mRNA was dependent on inclusion of the two younger cases. This finding is consistent with a reported decrease in OCN protein with age at the femoral neck, for both cortical and trabecular bone, and at the iliac crest (Boonen *et al.*, 1997; Vanderschueren *et al.*, 1990). As OCN is regarded as an indicator of bone formation and a molecular marker for osteoblasts (Stein and Lian, 1993), this age-related decline in OCN mRNA in bone suggests an associated decrease in bone formation and/or osteoblastic activity with age in normal individuals.

The values corresponding to mRNA levels for RANKL, OPG, and RANK in non-diseased human trabecular bone from the proximal femur were plotted as a function of age. The RANKL/GAPDH mRNA ratio increased with age (r = 0.62, $p < 0.02$; Figure 5.13), although this relationship was dependent on inclusion of the two younger cases. OPG/GAPDH mRNA expression remained relatively constant with aging (Figure 5.14). In contrast, serum OPG levels have been shown to increase with age in women and men (Arrighi *et al.*, 2000; Szulc *et al.*, 2001; Yano *et al.*, 1999). As OPG is expressed by a wide variety of cell types including vascular endothelial cells (Collin-Osdoby *et al.* 2001; Kwon *et al.*, 1998; Simonet *et al.*, 1997; Tan *et al.*, 1997; Yasuda *et al.*, 1998b), systemic serum OPG levels are unlikely to reflect changes in OPG mRNA expression in the local bone microenvironment. The expression of RANK/GAPDH mRNA showed no dependence on age (Figure 5.15).

Since, based upon a large amount of evidence, the ratio of RANKL to OPG has been hypothesised to be the main determinant of the pool size of active osteoclasts in the local bone microenvironment (Hofbauer *et al.*, 2000), it was of great interest to investigate this

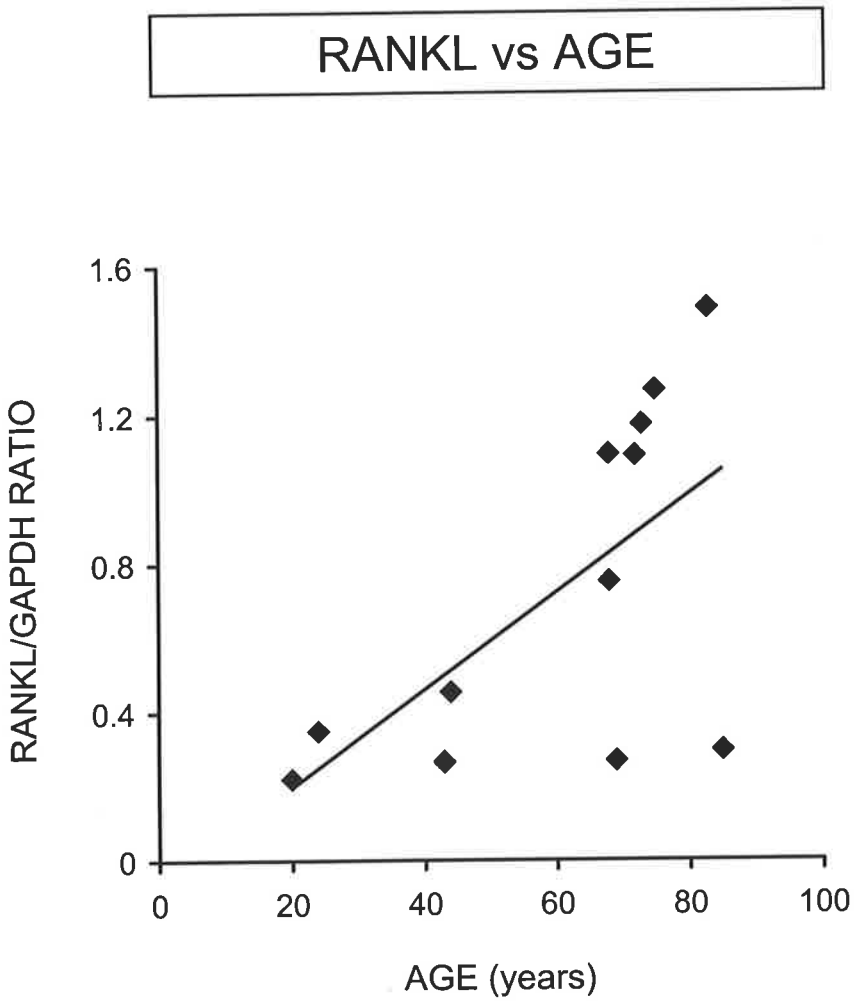

Figure 5.13: There was a significant increase in RANKL/GAPDH mRNA with age in intertrochanteric trabecular bone from control individuals (n = 12; RANKL/GAPDH = 0.01*AGE - 0.07; $r = 0.62$ and $p < 0.02$).

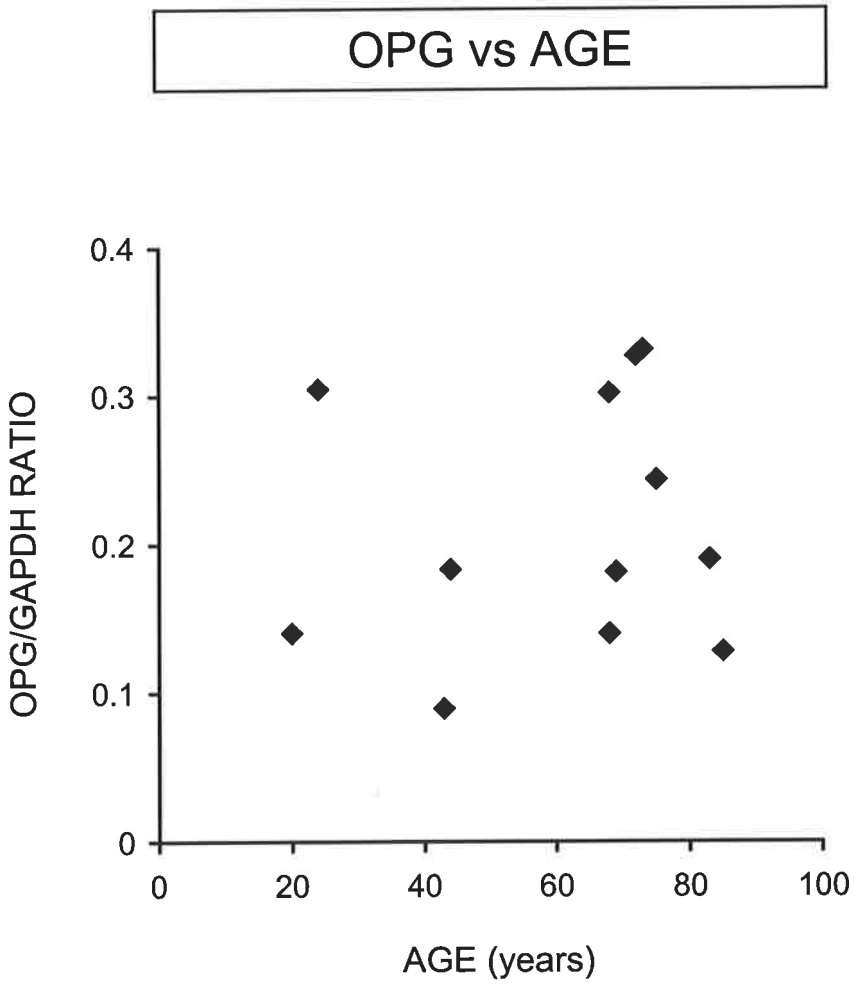

Figure 5.14: There was no significant change in OPG/GAPDH mRNA with age in intertrochanteric trabecular bone from control individuals (n = 12; OPG/GAPDH = 0.0005*AGE + 0.18; r = 0.13 and p = NS). NS = not significant.

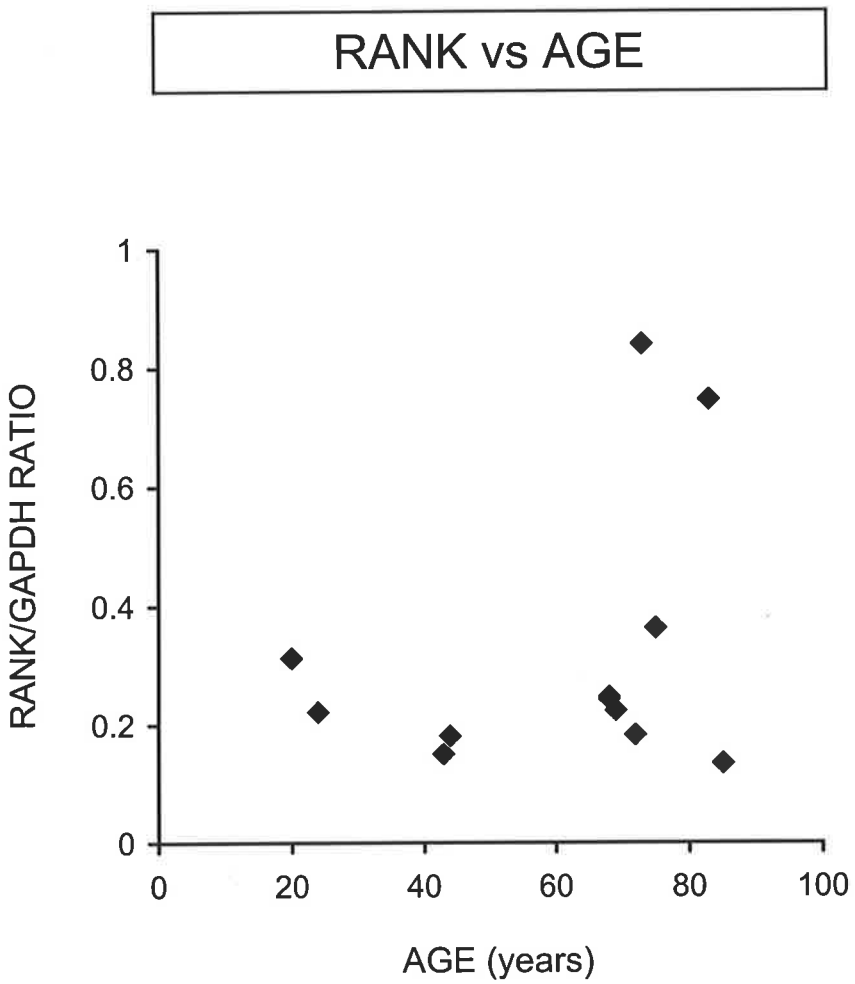

Figure 5.15: There was no significant change in RANK/GAPDH mRNA with age in intertrochanteric trabecular bone from control individuals (n = 12; RANK/GAPDH = 0.003*AGE + 0.12; r = 0.32 and p = NS). NS = not significant.

relationship during aging. It was found that the ratio of RANKL/OPG mRNA levels increased with age (r = 0.60, p < 0.03; Figure 5.16), although this relationship was dependent on inclusion of the two younger cases. This suggests that the effective activity of RANKL to promote osteoclast formation, and thus increase the pool size of active osteoclasts at the intertrochanteric region of the proximal femur, may be increased with age in normal individuals. Neither the RANKL/RANK nor RANK/OPG mRNA ratios were dependent on age in these bone samples (Figure 5.17 and results not shown).

5.5 DISCUSSION

There is limited information regarding the pattern of gene expression corresponding to specific molecules, with regulatory roles in bone turnover, in normal human bone tissue or indeed, their role in skeletal disease. The aim of the work described in this chapter was to investigate mRNA gene expression in the local human trabecular bone microenvironment of individuals without any evidence of joint disease or any known medical condition predicted to affect the skeletal status. The purpose of describing the pattern of mRNA gene expression of a select group of skeletal regulatory molecules in non-diseased proximal femur bone was to establish the base line or normal steady state mRNA levels of these factors so that a comparison could be made with skeletal site-matched bone tissue from individuals suffering from severe primary OA of the hip (Chapter 6). The select group of skeletal regulatory molecules chosen for investigation included two recognised skeletally-active cytokines capable of promoting osteoclast formation, IL-6 and IL-11, the CTR and OCN, as specific markers of the presence of osteoclasts and osteoblasts, respectively, and factors with central regulatory roles in controlling osteoclast development and activity, namely RANKL, OPG, and RANK.

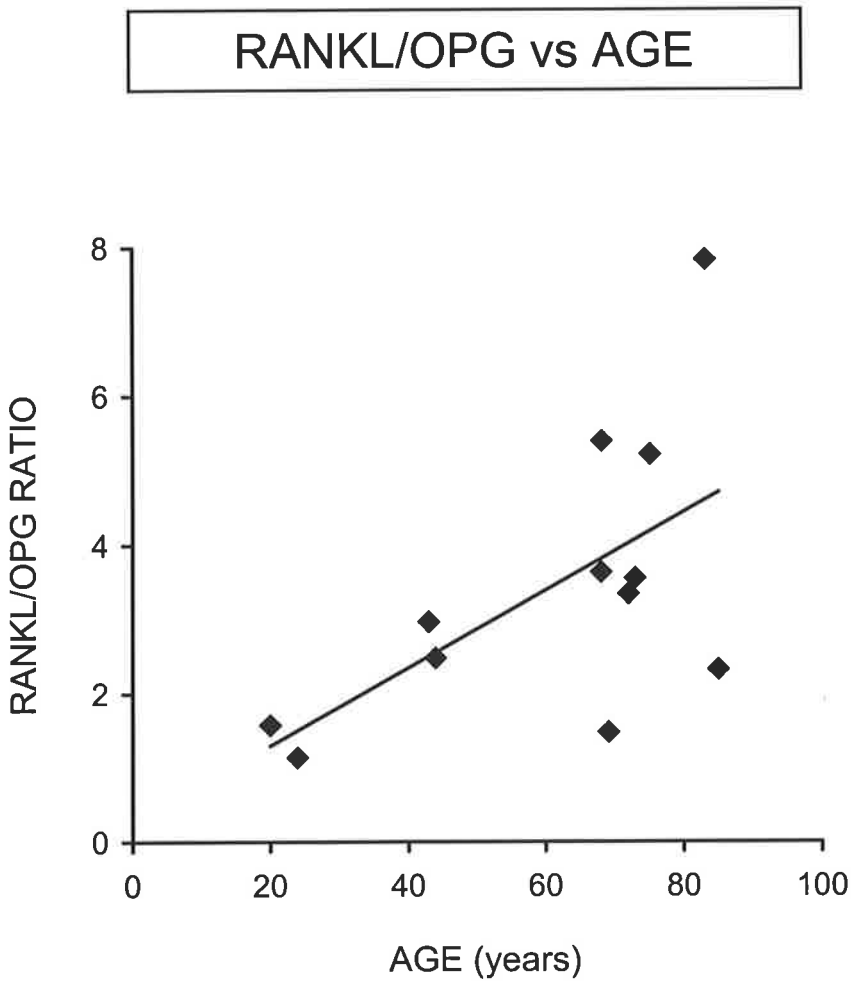

Figure 5.16: There was a significant increase in the RANKL/OPG mRNA ratio with age in intertrochanteric trabecular bone from control individuals (n = 12; RANKL/OPG = 0.05*AGE + 0.25; r = 0.60 and $p < 0.03$).

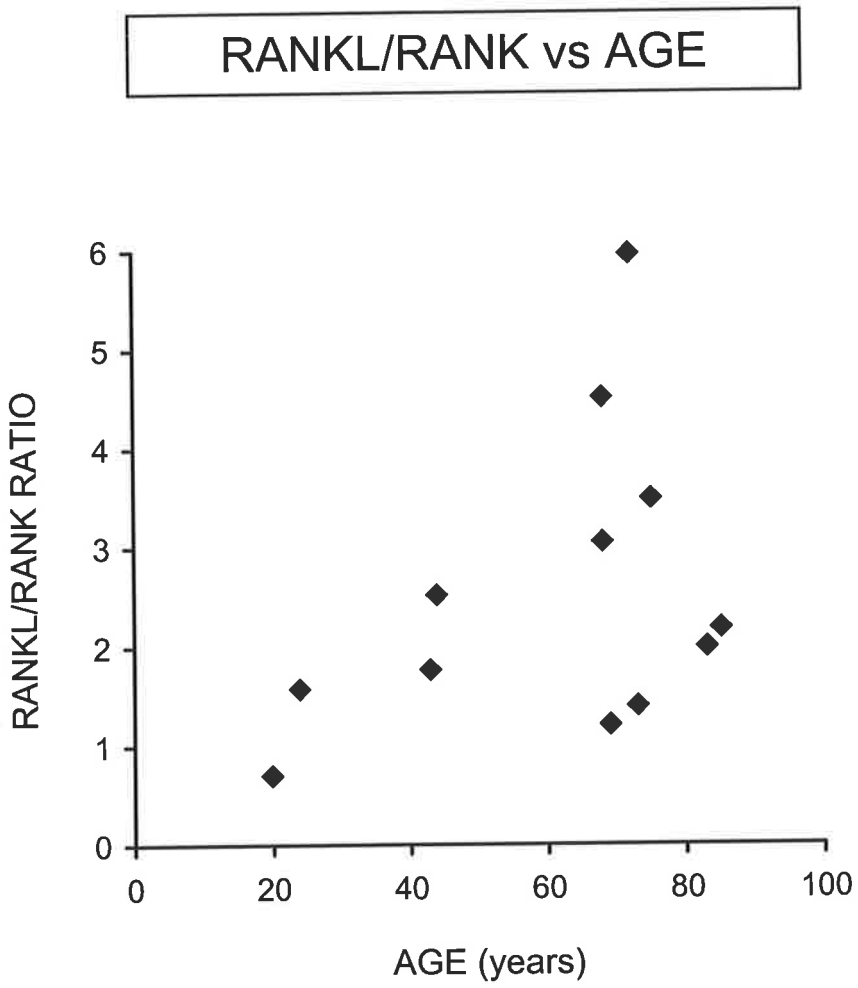

Figure 5.17: There was no significant change in the RANKL/RANK mRNA ratio with age in intertrochanteric trabecular bone from control individuals (n = 12; RANKL/RANK = 0.03*AGE + 0.86; r = 0.40 and p = NS). NS = not significant.

5.5.1 IL-6 and IL-11 mRNA expression in non-diseased human trabecular bone from the proximal femur: coordinated and age-dependent expression

IL-6 and IL-11 are two cytokines that share many biological properties, including the ability to stimulate osteoclast development from their haematopoietic precursors (Martin *et al.*, 1998). Both of these cytokines signal *via* a receptor system that consists of a unique ligand-binding domain and the common 130-kDa subunit (gp130; Kishimoto *et al.*, 1995). A positive correlation was found between IL-6 and IL-11 mRNA levels in normal human bone tissue, suggesting the coordinated regulation of these two cytokines in the local bone microenvironment (Figure 5.4). There is no *a priori* reason why this should be the case, and there are experimental examples of both coordinated and divergent regulation of IL-6 and IL-11 (Kim *et al.*, 1997; Nakchbandi *et al.*, 2001). However, Nakchbandi *et al.* (2001) reported a down-regulation of IL-11 by IL-6, both *in vitro* and *in vivo*, and further, that this negative regulatory effect of IL-6 on IL-11 is post-transcriptional. Nonetheless, the positive correlation between IL-6 and IL-11 mRNA (Figure 5.4) would be consistent with similar activities of the two cytokines in this skeletal site from the proximal femur.

A trend towards a decline with age was observed for IL-6 mRNA, but this did not reach statistical significance (Figure 5.9). However, when an outlier data point was removed, IL-6 mRNA declined significantly with age. In contrast, serum IL-6 levels in women have been shown to positively correlate with age, although not with any serum or urinary markers for bone turnover (McKane *et al.*, 1994). It is difficult to compare studies of cytokine levels in localised bone with systemic serum measurements of cytokines, due to the *in vivo* autocrine/paracrine action of cytokines. Further, as IL-6 can be produced by a number of cell types in the bone microenvironment, including marrow stromal cells, monocyte-macrophages, osteoblasts, and osteoclasts (Girasole *et al.*, 1992; Kishimoto,

1989; Linkhart *et al.*, 1991; O'Keefe *et al.*, 1997), it is not known which cell types are contributing to the IL-6 mRNA levels measured in these normal human bone samples. As detailed in section 5.1, the reported effects of IL-6 on RANKL-RANK-promoted osteoclast development are conflicting. For instance, IL-6 has been shown to induce RANKL mRNA expression, and conversely reduce OPG mRNA expression, in murine osteoblastic cell lines (Nakashima *et al.*, 2000; O'Brien *et al.*, 1999). In contrast, RANKL mRNA expression was not affected by IL-6 in human marrow stromal/osteoblastic cells (Hofbauer *et al.*, 1999b), and further, IL-6 had no effect on OPG production in these stromal/osteoblastic cells (Brandstrom *et al.*, 1998; Hofbauer *et al.*, 1998; Vidal *et al.*, 1998). Furthermore, it has been suggested that IL-6 may attenuate calcium sensing and thus enhance bone resorption by a direct effect on mature osteoclast activity (Adebanjo *et al.*, 1998). IL-6 has been implicated as playing a pathogenetic role in several conditions characterised by excessive osteoclastic bone resorption, rather than a major involvement in normal physiological osteoclast development. Conditions characterised by excessive bone resorption that IL-6 has been implicated in include: osteoporosis caused by loss of gonadal function, multiple myeloma, Paget's disease, rheumatoid arthritis, and hyperparathyroidism (Grey *et al.*, 1996; Kotake *et al.*, 1996; Manolagas and Jilka, 1995; Roodman *et al.*, 1992; Roodman, 1995).

There was a significant decline with age in the expression of IL-11 mRNA (Figure 5.10). A multiple regression analysis found that IL-11 mRNA expression was statistically dependent on age and not IL-6 mRNA expression ($p < 0.05$), suggesting that the effect of IL-11 to stimulate osteoclast development may decline with age. Interestingly, while expression of IL-6 mRNA in the bone is contributed by several cell types, IL-11 mRNA is likely to be expressed predominantly by cells of mesenchymal origin, namely, cells of the

osteoblast lineage (Paul *et al.*, 1990). However, the cellular origin(s) of the measured IL-6 and IL-11 mRNA expression in these human trabecular bone samples are not known. This can be resolved by the use of *in situ* hybridisation in combination with immunohistochemistry for the bone tissue localisation of IL-6 and IL-11 at the mRNA and protein level, respectively. As detailed in section 5.1, IL-11 has been suggested to play a critical role in the hierarchy of osteoclastogenic factors, since *in vitro*, its expression is induced by a number of hormone and local activators of osteoclast formation (Manolagas, 1995; Romas *et al.*, 1996; Yang and Yang, 1994). In addition, neutralisation of IL-11 has been shown *in vitro* to suppress osteoclast development induced by 1,25-$(OH)_2D_3$, PTH, IL-1, and TNF-α (Girasole *et al.*, 1994). The effects of IL-11 on osteoclast differentiation appear to be mediated by inducing RANKL expression on marrow stromal/osteoblastic cells (Nakashima *et al.*, 2000; Yasuda *et al.*, 1998b). Furthermore, the bone-resorptive effect of IL-11 in neonatal mouse calvarial bone cultures resulted in dose-dependent increases in RANKL and OPG mRNA (Ahlen *et al.*, 2002). Interestingly, IL-11 mRNA expression did not correlate with RANKL, OPG or RANK mRNA expression in normal human bone from the proximal femur. Although the evidence to date suggests one major role for IL-11 in bone is to act as an upstream stimulatory signal for osteoclast differentiation (Martin *et al.*, 1998), the full role of this pleiotropic cytokine in the bone microenvironment is not completely understood. IL-11 has also been implicated as a suppressor of osteoblastic synthetic activity. For example, IL-11 dose-dependently inhibited nodule formation and reduced alkaline phosphatase expression in rat calvarial cell cultures (Hughes and Howells, 1993b). Conversely, a recent report of over-expression of IL-11 in transgenic mice suggests that this cytokine functions as an anabolic factor for bone *in vivo* (Takeuchi *et al.*, 2002).

In bone marrow, adipocytes develop from bone marrow stromal cells, namely the same lineage that osteoblasts are derived from (Beresford *et al.*, 1992). IL-11 was originally identified as a potent inhibitor of the differentiation of adipocytes from marrow stromal cells (Kawashima *et al.*, 1991; Paul *et al.*, 1990). The decrease in bone volume associated with age-related osteopenia is accompanied by an increase in marrow adipose tissue (Burkhardt *et al.*, 1987; Parfitt *et al.*, 1995). Further, the number and size of marrow adipocytes has been shown to increase in a linear manner with age (Rozman *et al.*, 1989). In this thesis trabecular bone was also sampled for undecalcified bone histomorphometry from the intertrochanteric region of each proximal femur, contiguous to the site from which bone was sampled for RNA isolation and subsequent mRNA expression analysis. The undecalcified bone sections were quantified for trabecular bone structural parameters and static indices of bone turnover (data presented in Chapter 7). In performing this work, a generalised observation (not quantified) was an increase in bone marrow adipose tissue with age in these non-diseased human trabecular bone samples. The decrease in IL-11 mRNA expression with age in the human bone samples may be associated with this age-related increase in bone marrow adipose tissue. Moreover, Kodama *et al.* (1998) reported reduced IL-11 protein and mRNA expression in marrow stromal cells from senescence-accelerated mice (SAMP6). The SAMP6 mice exhibit an early decrease in bone mass, enhanced adipogenesis, with a reduction in bone remodelling, due to suppressed osteoblastogenesis and osteoclastogenesis (Kodama *et al.* 1998). Administration of recombinant IL-11 to SAMP6 mice enhanced the formation of osteoblasts and osteoclasts, and suppressed the enhanced adipogenesis (Kodama *et al.*, 1998).

5.5.2 CTR and OCN mRNA expression in non-diseased human trabecular bone from the proximal femur: age-dependent expression

OCN, the major non-collagenous protein of bone matrix, is utilised as an indicator of bone formation as it is one of the marker genes for the progression of osteoblastic differentiation (Stein and Lian, 1993). The circulating hormone, calcitonin, which is a potent inhibitor of osteoclastic bone resorption, binds to its receptor, the CTR, which in bone is uniquely expressed on the surface of mononuclear osteoclast precursor cells and multinuclear osteoclasts (Hattersley and Chambers, 1989; Quinn *et al.*, 1999). The plot of CTR versus OCN mRNA expression might be regarded as an index of the balance of resorption to formation in these bone samples. However, no association was found between CTR/GAPDH and OCN/GAPDH mRNA expression in these non-diseased human trabecular bone samples (Figure 5.5). Using CTR/GAPDH mRNA as a marker of osteoclasts or bone resorption in these bone samples is ambiguous as it is not known whether immature and/or mature osteoclast cells are representative of the measured CTR mRNA, nor whether the CTR mRNA expression is representative of the number of osteoclasts and/or the number of calcitonin receptors on each osteoclast. There are few reports on the regulation of the expression of CTR mRNA in human osteoclasts. Treatment of human osteoclast-like cells with calcitonin dose-dependently reduced CTR mRNA expression (Samura *et al.* 2000). Further, Wada *et al.* (2001) reported that glucocorticoids increase CTR mRNA expression in human osteoclast-like cells, which was shown to reflect an increase in the number of calcitonin receptors on individual osteoclast-like cells. Despite the fact that RANK is expressed on the surface of the same cell types as the CTR in bone, namely osteoclasts and their precursors (Hsu *et al.*, 1999; Myers *et al.* 1999), no association was observed between CTR and RANK mRNA expression in these human bone samples. Further, there was no relationship with age for CTR mRNA expression

(Figure 5.11). The data for CTR mRNA should be substantiated with the analysis of other osteoclast cell markers, including carbonic anhydrase II, cathepsin K, and TRAP, which are highly expressed by osteoclasts (Martin and Udagawa, 1998). Importantly, a significant positive association was observed between CTR and TRAP mRNA expression levels in the study comparing mRNA expression in different skeletal sites (iliac crest, femoral neck, and intertrochanteric region) for a cohort of postmortem individuals (Figure 4.1; Table 4.4; Chapter 4.4.4).

There was an age-related decline in OCN mRNA in these non-diseased human trabecular bone samples (Figure 5.12), which is consistent with a reported decrease in OCN protein with age at the femoral neck, for both cortical and trabecular bone, and at the iliac crest (Boonen *et al.*, 1997; Vanderschueren *et al.*, 1990). Furthermore, *in situ* hybridisation studies found an age-related reduction in osteoblastic OCN mRNA expression in rat bone tissues (Ikeda *et al.*, 1995). Frenkel *et al.* (1997) have shown an age-related decline in rat osteocalcin promoter activity in the bone of mice. In contrast, serum OCN levels increased linearly with age in women aged 25 to 75 years (Minisola *et al.*, 1997). It is important to note that the circulating OCN levels are unlikely to reflect the concentration of OCN at a specific skeletal site. As OCN is regarded as an indicator of bone formation and a molecular marker for osteoblasts (Stein and Lian, 1993), this age-related decline in OCN mRNA in human bone (Figure 5.12) suggests an associated decrease in bone formation and/or osteoblastic activity with age in normal individuals. D'Ippolito *et al.* (1999) reported an age-related decrease in the number of mesenchymal stem cells with osteogenic potential, cultured from human thoracic and lumbar spine bone marrow. Furthermore, the proliferative capacity, but not the number, of mesenchymal stem cells from the human femur, rib, and spine declined with age (Oreffo *et al.* 1998b). Oreffo *et al.* (1998b)

proposed that the reduction in bone formation associated with aging is not a consequence of reduced numbers of early osteoprogenitor cells, but rather an alteration of osteoprogenitor proliferation and differentiation. Furthermore, this altered differentiation potential of osteoprogenitor cells may involve differentiation into other stromal lineages, such as adipocytes.

5.5.3 RANKL, OPG, and RANK mRNA expression in non-diseased human trabecular bone from the proximal femur: coordinated and age-dependent expression

RANKL, RANK, and OPG are key regulators of osteoclast biology and bone metabolism. RANKL is expressed on the cell surface of stromal/osteoblastic cells and promotes osteoclast development by binding to its cognate receptor, RANK, which is expressed on the surface of osteoclasts and their precursors, with the required presence of macrophage colony stimulating factor (M-CSF; Anderson *et al.*, 1997; Hsu *et al.*, 1999; Lacey *et al.*, 1998; Nakagawa *et al.*, 1998; Wong *et al.*, 1997; Yasuda *et al.*, 1998b). OPG is a natural antagonist for RANKL and inhibits osteoclast formation and bone resorption (Simonet *et al.*, 1997). Mice deficient in OPG develop extensive osteoporosis, associated with increased numbers of osteoclasts (Bucay *et al.*, 1998; Mizuno *et al.*, 1998). Likewise, RANKL-deficient mice are severely osteopetrotic and lack osteoclasts (Kong *et al.*, 1999). Extensive bone marrow cell culture studies have shown that RANKL, OPG, and to a lesser extent, RANK, are modulated by growth factors, cytokines, peptide and steroid hormones, and drugs known to affect bone metabolism (Hofbauer *et al.*, 2000; Hofbauer and Heufelder, 2001; Horowitz *et al.*, 2001; Suda *et al.*, 1999).

In the local human bone microenvironment of the proximal femur a significant positive association was observed between RANKL and OPG mRNA (Figure 5.6). This finding suggests that the same stimuli/stimulus up-regulate/s both RANKL and OPG mRNA expression in these bone samples. Takami *et al.* (2000) have shown that treatment of murine stromal/osteoblastic cells with intracellular calcium-elevating compounds, or an activator of protein kinase C, stimulated the expression of both RANKL and OPG mRNA, which resulted in osteoclast formation in co-cultures of primary osteoblasts and bone marrow cells. Further, the pro-resorptive cytokines IL-1β and TNF-α induced the expression of both RANKL and OPG mRNA in human marrow stromal cells (Hofbauer *et al.*, 1999b). However, it is important to note that it is not known whether the same cell type(s) (eg., stromal/osteoblastic cells) are contributing to the measured RANKL and OPG mRNA expression in these human bone samples. A significant positive association was also observed between the expression of RANKL and RANK mRNA in non-diseased human trabecular bone from the proximal femur (Figure 5.7). This finding suggests that either the same stimulus regulates the expression of both RANKL and RANK mRNA, or, more likely, that the same stimulus up-regulates RANKL and causes recruitment of RANK-expressing osteoclast precursor cells. Treatment of murine bone marrow cultures with 1,25-$(OH)_2D_3$ resulted in the up-regulation of both RANKL and RANK mRNA expression, a reduction in OPG mRNA expression, and the formation of TRAP-positive multinucleated osteoclast-like cells (Mukohyama *et al.*, 2000). When these bone marrow cultures were treated with the neuropeptide vasoactive intestinal peptide, in addition to 1,25-$(OH)_2D_3$, the stimulatory effect of 1,25-$(OH)_2D_3$ on RANKL and RANK mRNA expression decreased, and the inhibitory effect on OPG mRNA expression was reversed (Mukohyama *et al.*, 2000). IL-1 has been shown to both up-regulate RANKL and OPG mRNA expression in human osteoblast-like cell lines (Hofbauer *et al.*, 1999b; Vidal *et al.*,

1998) and to potentiate the survival, fusion, and activation of pre-osteoclast cells in culture in the absence of stromal/osteoblastic cells (Jimi *et al.*, 1999). Based upon these observations, IL-1 is a potential stimulus that could up-regulate RANKL in stromal/osteoblastic cells and also recruit RANK-expressing osteoclast precursor cells, to effectively induce the development of mature bone-resorbing osteoclasts.

RANKL and OPG are important downstream signals of osteoclast biology, onto which many hormonal, chemical, and biochemical signals converge (Hofbauer and Heufelder, 2001). Hofbauer *et al.* (2000) hypothesised that the ratio of RANKL to OPG is the main determinant of the pool size of active osteoclasts in the local bone microenvironment, acting as a final effector system to modulate differentiation, activation, and apoptosis of osteoclasts. The data described in this chapter show that the ratio of RANKL/OPG mRNA is positively associated with age (Figure 5.16), and that this is largely driven by the changing RANKL mRNA levels (compare Figures 5.13 and 5.14). This suggests that the effective activity of RANKL to promote osteoclast formation and thus increase the pool size of active osteoclasts, at the intertrochanteric region of the proximal femur, may be increased with age in normal individuals. Moreover, the histomorphometric bone resorption index, eroded surface, ES/BS, was found to increase as the RANKL/OPG mRNA ratio increased, in contiguous trabecular bone samples from non-diseased individuals (Figure 7.8; Chapter 7.4.3). The changes in the magnitude of this RANKL/OPG mRNA ratio can be the result of changes in the magnitude of RANKL and OPG, independently or linked. Experiments *in vitro,* in which bone marrow stromal cells and osteoblast-like cells were treated with pro-resorptive agents, have shown concomitant up-regulation of RANKL mRNA and down-regulation of OPG mRNA, or up-regulation of RANKL with no change or even an increase in OPG, with the end result in each case an

increase in the RANKL/OPG mRNA ratio (Hofbauer *et al.*, 1999a; Hofbauer *et al.*, 2001; Horwood *et al.*, 1998; Lee and Lorenzo, 1999; Nakashima *et al.*, 2000; Takai *et al.*, 1998; Takami *et al.* 2000; Takeshita *et al.*, 2001; Udagawa *et al.*, 1999). In interpreting *in vivo* results, it is important to note that, while RANKL is expressed by a relatively restricted number of cell types, including stromal/osteoblastic cells and T cells, OPG is expressed more widely by several cell types, including vascular endothelial cells (Collin-Osdoby *et al.* 2001; Kwon *et al.*, 1998; Simonet *et al.*, 1997; Tan *et al.*, 1997; Yasuda *et al.*, 1998b).

The osteoclastogenic capacity of the stromal/osteoblast cell, albeit in murine cell lines, has been shown to depend upon the expression ratio of RANKL/OPG, reflecting the differentiation stage of the cell (Deyama *et al.*, 2000; Gori *et al.*, 2000; Nagai and Sato, 1999). Undifferentiated or pre-osteoblastic or bone marrow stromal cells have been reported to express abundant RANKL and low levels of OPG, and, further, the increased RANKL/OPG ratio correlates with the cells capacity to support osteoclast formation and activation. Conversely, the RANKL/OPG ratio is lower in mature osteoblasts and their capacity to support osteoclast development is suppressed or lost (Deyama *et al.*, 2000; Gori *et al.*, 2000; Nagai and Sato, 1999). This suggests that the increase in RANKL/OPG mRNA with age in non-diseased human trabecular bone (Figure 5.16) may be associated with an age-related increase in the number of stromal/osteoblast cells with an osteoclastogenic capacity. Interestingly, *in situ* hybridisation analysis of 8-week-old and 2.5-year-old male rat distal femur bones showed a trend for an age-related reduction in RANKL, OPG, and RANK mRNA expression (Ikeda *et al.*, 2001).

5.5.4 Conclusions

The extensive knowledge of systemic and local regulation of bone remodelling has been developed primarily from studies utilising *in vitro* cell culture systems, and animal studies such as the effects of gene deletion studies in mice (reviewed in Ducy *et al.*, 2000; Hofbauer and Heufelder, 2001; Raisz, 1999; Roodman, 1999; Suda *et al.*, 1999). The work described in this chapter is the first direct demonstration that mRNA corresponding to IL-6, IL-11, CTR, OCN, RANKL, OPG, and RANK is expressed locally in human trabecular bone from the intertrochanteric region of the proximal femur. Furthermore, coordinated and age-dependent expression of particular mRNA species has been described. One limitation of semi-quantitative RT-PCR analysis of mRNA expression in bone tissue is that the data provide no information about the cellular origin(s) of each mRNA transcript. Another limitation is that it is not known whether the gene expression patterns are representative of the corresponding protein levels in the bone tissue. Conversely, the advantage of this experimental approach over cell culture techniques is that factors/mediators can be analysed with their local regulatory mechanisms intact. Finally, the way in which the expression of these molecules relates to events in the human bone microenvironment needs to be established. Indeed, these data enabled the identification of a number of correlations between mRNA expression and trabecular bone volume and bone turnover indices, measured in contiguous human bone tissues sampled from the proximal femur. These results are presented in Chapter 7.

CHAPTER 6

DIFFERENTIAL mRNA EXPRESSION IN CONTROL AND OSTEOARTHRITIC TRABECULAR BONE FROM THE HUMAN PROXIMAL FEMUR

6.1 INTRODUCTION

Osteoarthritis (OA) is a common age-related skeletal disease characterised by progressive degenerative damage to the articular joint cartilage, and is associated with a conservation of bone mass and a different, more rigid structure of the subchondral bone (reviewed in Dequeker and Luyten, 2000). The aetiology of this disease is poorly understood, although it has both heritable and environmental components (Chitnavis *et al.*, 1997; Felson *et al.*, 1998; Spector *et al.*, 1996a). A number of gene loci have been linked to various forms of OA (Keen *et al.*, 1997; Meulenbelt *et al.*, 1998; Uitterlinden *et al.*, 1997). Although OA is accompanied by a well-defined set of changes in the trabecular bone of the joint, it has been considered primarily to be a cartilaginous disorder (Bland and Cooper, 1984). Fazzalari *et al.* (1992) have investigated the structural parameters of the trabecular bone in the proximal femur adjacent to OA hips. Typically, the subchondral bone is sclerotic, with increased trabecular bone volume, and altered trabecular size and spacing, compared to age-matched controls (Crane *et al.*, 1990; Fazzalari *et al.*, 1992). It has been postulated that such changes are due to alteration of loading through the joint because of the articular disease (Bland and Cooper, 1984) or, alternatively that they are secondary to pathology within the joint. However, similar structural changes are also present at sites distal to the joint articular surface, in the proximal femur and in the iliac crest (Crane *et al.*, 1990; Fazzalari *et al.*, 1992), suggesting that they are not merely reactive to the joint pathology. The different bone structure in hip OA is accompanied by a reduced incidence of trabecular microfracture (Fazzalari *et al.*, 1987), and altered mechanical properties, with a more rigid trabecular bone in the femoral neck (Li and Aspden, 1997b; Martens *et al.*, 1983). Since this more rigid bone would have a reduced ability to absorb shock, it has been postulated that the bone changes in OA might exacerbate the disease or could even precede and be causative of the cartilage degeneration (Radin *et al.*, 1972; Dequeker *et al.*, 1996).

Consistent with this concept of generalised bone structural changes in OA, bone matrix from the iliac crest of OA subjects has been found to contain a higher content of the growth factors insulin-like growth factor types I and II (IGF-I and IGF-II) and transforming growth factor (TGF)-β, and an increased concentration of osteocalcin (OCN) protein, compared with that in control subjects (Dequeker *et al.*, 1993b; Gevers and Dequeker, 1987; Raymaekers *et al.*, 1992). The well-recognised anabolic effect of IGF-I, IGF-II, and TGF-β, together with a suggested role for them to link bone resorption to bone formation (Baylink *et al.*, 1990), also provide clues to the molecular mechanisms that lead to maintenance or increase of bone mass in OA. Furthermore, Hilal *et al.* (1998) have shown that osteoblast-like cells cultured from OA subchondral bone produce more IGF-I than cells from individuals without OA pathology. Interestingly, a recent study has shown that subchondral bone osteoblasts, from individuals with hip OA, produce a molecularly distinct collagen, type I collagen homotrimer (Bailey *et al.*, 2002). This finding was associated with a disorganised collagen matrix and reduced mineralisation, which could potentially significantly weaken the biomechanical properties of the bone matrix, resulting in collagen overproduction and thickening of the bone (Bailey and Knott, 1999).

Collectively, these reports of an altered trabecular bone structure and bone matrix in individuals with OA suggest that the bone changes may precede the joint degeneration of OA, or may arise secondarily to the joint pathology, or indeed may occur in parallel with the cartilage damage, driven by the same causative agent(s) that lead to cartilage disease. Whichever of these is the case, in order to devise effective treatments for OA, it is clearly important to consider the bony component of this disease and to develop an understanding of the cellular and molecular processes that lead to the bony changes. Thus, the aim of the work described in this chapter was to compare the expression of mRNA species

corresponding to a number of skeletally active molecules in OA bone, at a skeletal site distal to the degenerative joint changes in OA, with their expression in non-OA bone. It was hoped that these studies might give clues to the molecular mechanisms that lead to the altered bone structures in OA.

The cellular and molecular mechanisms that lead to particular trabecular structures in healthy bone, or in the pathology of OA, are not well understood. However, as detailed in Chapter 5.1, there is now a large amount of information about the factors that are capable of regulating the differentiation and activity of the cell types that are responsible for the remodelling of bone, the osteoblast and the osteoclast. It is understood that physiological bone remodelling is achieved by the initial activity of osteoclasts to resorb bone followed by the formation of new bone by osteoblasts, and that these processes are strongly inter-related. Signals that promote osteoclast differentiation appear to act *via* receptors expressed by cells of the osteoblast lineage (Martin and Ng, 1994), suggesting that *in situ,* localised activation of osteoclastogenesis leads to site-directed remodelling. Receptor activator of nuclear factor kappa B (RANK) ligand, RANK, and osteoprotegerin (OPG) are key molecular regulators of osteoclast development and activity. RANKL is expressed on the cell surface of stromal/osteoblastic cells and promotes osteoclast development by binding to its cognate receptor, RANK, which is expressed on the surface of osteoclasts and their precursors, with the required presence of macrophage colony stimulating factor (M-CSF) (Anderson *et al.*, 1997; Hsu *et al.*, 1999; Lacey *et al.*, 1998; Nakagawa *et al.*, 1998; Wong *et al.*, 1997; Yasuda *et al.*, 1998b). OPG is a natural antagonist for RANKL and inhibits osteoclast formation and bone resorption (Simonet *et al.*, 1997). Mice deficient in OPG develop extensive osteoporosis, associated with increased numbers of osteoclasts (Bucay *et al.*, 1998; Mizuno *et al.*, 1998). Likewise, RANKL-deficient mice are

severely osteopetrotic and lack osteoclasts (Kong *et al.*, 1999). Extensive bone marrow cell culture studies have shown that RANKL, OPG, and to a lesser extent, RANK, are modulated by growth factors, cytokines, peptide and steroid hormones, and drugs known to affect bone metabolism (Hofbauer *et al.*, 2000; Hofbauer and Heufelder, 2001; Horowitz *et al.*, 2001; Suda *et al.*, 1999).

This chapter describes investigation of the expression of mRNA corresponding to the key regulators of osteoclast biology and bone metabolism, RANKL, OPG and RANK, in trabecular bone from the proximal femur of individuals suffering from primary hip OA. In addition, expression of mRNA encoding the cytokines IL-6 and IL-11, both of which are involved in the regulation of the RANKL-RANK-OPG system of osteoclast development (as detailed in Chapter 5.1), together with the osteoblastic cell marker, osteocalcin (OCN), and the calcitonin receptor (CTR), which in bone is exclusively expressed by osteoclasts, was investigated in OA trabecular bone from the proximal femur. The specific skeletal site that the trabecular bone was sampled from was the intertrochanteric region of the proximal femur, as trabecular bone in this region has previously been shown to be structurally different between OA and control bone (Crane *et al.*, 1990). Further, the intertrochanteric region is remote from the subchondral bone that undergoes well-characterised secondary changes in severe OA (Fazzalari *et al.*, 1992). Moreover, a trabecular bone core biopsy from the intertrochanteric region is easily obtainable during total hip arthroplasty surgery, as this region is reamed and the bone usually discarded. The mRNA expression data from OA intertrochanteric bone is presented as a comparison to mRNA expression data from a skeletal site-matched control group, which is independently described in Chapter 5. The control group comprises a cohort of autopsy individuals, who had not suffered from conditions thought to affect their bone turnover status and in particular, macroscopic

examination of the femoral head showed no significant sign of joint degeneration according to the criteria of Collins (1949).

6.2 CHAPTER AIMS

- To describe the expression levels of mRNA corresponding to factors, known to have important regulatory roles in bone remodelling, in human trabecular bone tissue sampled from the intertrochanteric region of the proximal femur, a skeletal site distal to the degenerative joint changes in OA, in primary hip OA individuals.

- To seek gender or age-related differences in the pattern of mRNA expression in trabecular bone from the proximal femur in individuals with primary hip OA.

- To compare the pattern of mRNA expression of the skeletally active molecules, in trabecular bone from the intertrochanteric region, between individuals with primary hip OA and an autopsy control group (control data is independently described in Chapter 5).

6.3 METHODS

6.3.1 Case selection

Proximal femur surgical specimens, 8 from the left and 8 from the right anatomical side, were obtained from 16 patients, undergoing total hip arthroplasty surgery for advanced primary OA, at the Royal Adelaide Hospital (Table 6.1). The age of the OA cases, comprising 8 women (aged 49-84 years; mean ± SD [standard deviation] age, 68.5 ± 12.1 years) and 8 men (aged 50-85 years; 68.6 ± 12.4 years), varied between 49 and 85 years

(68.6 ± 11.8 years). There was no difference in the mean age between females and males. The control group comprised 14 postmortem cases, aged 20 to 85 years (61.6 ± 20.6 years), not known to have suffered from any disease affecting the skeleton (described in Chapter 5.3.1 and Table 5.1). The mean age of the OA group did not significantly differ from the control group. The clinical diagnosis of OA is based on radiological investigation (Kellgren and Lawrence, 1963), and patient history determines whether the OA is classified as primary in nature. In addition, the orthopaedic surgeon graded the macroscopic appearance of the femoral head and acetabulum at surgery by assessment of the location and degree of fibrillation and degeneration, according to the criteria of Collins (1949). For all OA cases selected in this thesis, the macroscopic grade of the femoral head and acetabulum at surgery was severe (Table 6.1). The most severe grade, grade 5, which is characterised by generalised eburnation of bone and bone remodelling, was found in 75% and 69% of OA cases for the femoral head and acetabulum, respectively. Patients suspected of having secondary OA, inflammatory joint disease, Paget's disease, drug-induced disease or other conditions, which may have affected the trabecular bone architecture and quality, were excluded from the OA group. The autopsy control femoral heads were also macroscopically graded for OA according to the criteria of Collins (1949). None of the selected autopsy femoral heads showed any significant sign of joint degeneration. Informed consent was obtained for the collection of these surgical specimens, with approval by the Royal Adelaide Hospital Human Ethics Committee.

Table 6.1 Profiles of surgical cases comprising the osteoarthritic (OA) group.

Case	Age *(years)*	Gender	Anatomical side	Femoral head *(Macroscopic grade at surgery)*	Acetabulum
OA1	49	Female	Right	4	4
OA2	59	Female	Left	5	5
OA3	60	Female	Right	3	3
OA4	66	Female	Right	4	3
OA5	72	Female	Right	5	5
OA6	78	Female	Right	5	5
OA7	80	Female	Right	5	5
OA8	84	Female	Left	5	5
OA9	50	Male	Right	5	5
OA10	54	Male	Left	5	5
OA11	62	Male	Right	5	5
OA12	69	Male	Left	5	5
OA13	73	Male	Left	5	4
OA14	77	Male	Left	5	5
OA15	79	Male	Left	5	4
OA16	85	Male	Left	4	5

OA, surgical osteoarthritic case.
The appearance of the femoral head and acetabulum were macroscopically graded at surgery according to the following criteria: [1] normal cartilage; [2] fibrillation of cartilage; [3] partial thickness cartilage loss; [4] localised bone exposed; [5] generalised eburnated bone exposed, remodelled.

6.3.2 Sampling of trabecular bone from the intertrochanteric region of the human proximal femur

At total hip arthroplasty surgery, a 10 mm internal diameter tube saw was used to take a trabecular bone core biopsy of the intertrochanteric region (Figure 2.1), taken in line with the femoral medullary canal (Fazzalari *et al.*, 1998b), from OA patients. The bone core

biopsies, 10 mm in diameter and 3-5 cm in length, were placed in cold (4°C) sterile RNase-free 0.85% saline and transported directly to the laboratory. Within 12 hours after retrieval at surgery, trabecular bone tissue was sampled as small fragments from an approximate tube saw length of 1-2 cm, using sterile bone cutters and/or a sterile scalpel blade. The trabecular bone tissue fragments were rinsed briefly in DEPC-treated water (the rinsed material contained trabecular bone and bone marrow) and then immersed in RNA lysis buffer (4 M guanidine isothiocyanate solution; 2 ml/250 mg wet weight). In addition, for each trabecular bone core biopsy of the intertrochanteric region from OA patients, a trabecular bone sample (10 mm in diameter and 2-3 cm in length), contiguous with the bone sampled for RNA isolation, was processed for undecalcified bone histomorphometry and microdamage assessment (Chapters 7 and 8; respectively). The trabecular bone was sampled from the intertrochanteric region of the proximal femur for each postmortem control case, as described in Chapter 5.3.2.

6.3.3 Semi-quantitative RT-PCR of total RNA isolated from human trabecular bone

Total RNA was isolated from the intertrochanteric trabecular bone tissue fragments (Chapter 2.2.2.1) for each surgical OA and postmortem control case. Semi-quantitative RT-PCR (Chapter 2.2.2.3), using the human-specific oligonucleotide primer pairs listed in Table 2.1 and primer conditions described in Chapter 2.2.2.3.2, was used to determine the relative expression levels of IL-6, IL-11, CTR, OCN, RANKL, OPG, and RANK mRNA in these bone RNA samples. Amplified PCR product corresponding to IL-6, IL-11, CTR, OCN, RANKL, OPG, and RANK mRNA are represented as a ratio of the respective PCR product/GAPDH PCR product. RT-PCR data for RANKL, OPG, and RANK mRNA could not be obtained for cases OA6 (78-year-old female), OA14 (77-year-old male), OA15 (79-

year-old male), C10 (65-year-old male), and C13 (73-year-old male) due to small quantities of total RNA recovered. In addition, RT-PCR data for RANK mRNA was not available for case OA12 (69-year-old male).

6.3.4 Statistical analysis of mRNA expression data

RT-PCR reactions were performed twice, from duplicate cDNA syntheses, which confirmed that repeated RT-PCR analysis of the same RNA samples yielded reproducible results. In addition, to minimise inter-assay variability for the comparison of OA and control cases, all PCR products for a given mRNA species ($n \leq 30$), were electrophoresed in a single 2% agarose gel. The Shapiro-Wilk statistic was used to test the semi-quantitative RT-PCR data for normality (PC-SAS software; SAS Institute). The semi-quantitative RT-PCR data were found to be normally distributed. Therefore, parametric statistical methods were used to analyse the data (Excel; Microsoft Corp.). The statistical significance of differences in mRNA expression between females and males, and between the control and OA groups, were determined by Student's *t*-test. The F-test was used to analyse differences in the variance of mRNA expression between the control and OA groups. The F-statistic represents the ratio of the variances of the control and OA groups. Linear regression analysis was used to describe age-related changes, and to examine the relationship between PCR products representing specific mRNA species. Student's *t*-test was used to compare the slopes and intercepts of significant linear regressions between the OA and control groups. If there was more than one significant independent factor associated with a specific mRNA species, multiple regression was performed to determine the contribution of each independent factor. The mRNA expression data is quoted as mean ± standard deviation. The critical value for significance was chosen as $p = 0.05$.

6.4 RESULTS

6.4.1 Pattern of mRNA expression in OA and control trabecular bone from the human proximal femur

The expression of IL-6, IL-11, CTR, OCN, RANKL, OPG, and RANK mRNA in trabecular bone sampled from the intertrochanteric region of the proximal femur from patients with severe hip OA and autopsy control individuals was assessed using semi-quantitative RT-PCR. The intertrochanteric region was chosen for sampling because the trabecular architecture in this region depends upon stresses in the proximal femoral shaft while being unaffected by the sclerotic and cystic changes of the subchondral bone in the OA femoral head (Fazzalari *et al.*, 1985). These mRNA species were chosen because they represent, in the case of IL-6 and IL-11, recognised skeletally-active cytokines capable of promoting osteoclast formation. CTR and OCN were chosen as specific markers of the presence of osteoclasts and osteoblasts, respectively. RANKL, OPG, and RANK were chosen for their central regulatory roles in controlling osteoclast development and activity.

Expression of mRNA corresponding to each of these seven mRNA species was found in all trabecular bone samples analysed from the proximal femur of both OA and control individuals. A typical pattern of mRNA expression for IL-6, IL-11, the CTR isoforms, OCN, RANKL, OPG, and RANK for two cases from each of the OA and control groups is shown in Figure 6.1. The PCR products were authenticated by comparison with the expected product size and by hybridisation to an internal detecting oligonucleotide probe (Atkins *et al.*, 2000). As observed for the control bone samples (described in Chapter 5.4.1), the insert-negative isoform of the CTR (732 bp PCR product) was consistently more abundant than the insert-positive isoform (780 bp PCR product) in the OA bone samples. Figure 6.1, representing the pattern of mRNA expression for two cases from each

of the OA and control groups, clearly illustrates a reduction in the expression level of IL-6 and IL-11 mRNA, and an enhancement in the expression level of OCN and RANK mRNA, in the OA bone samples, compared to the controls.

The number of PCR cycles employed for each of these mRNA transcripts was within the exponential phase of the amplification curve, enabling comparison of mRNA expression between bone samples. Relative levels of IL-6, IL-11, CTR, OCN, RANKL, OPG, and RANK mRNA were determined by normalising values to the GAPDH mRNA level determined for each sample. The individual values obtained for IL-6, IL-11, CTR, OCN, RANKL, OPG, and RANK mRNA are expressed as a ratio to GAPDH in Figures 6.2-6.10, 6.12-6.15, and 6.19-6.25. The two younger cases in the control cohort, cases C1 (20-year-old female) and C8 (24-year-old male), are indicated in Figures 6.2-6.8, 6.11, and 6.16-6.18, as the control group data is compared to the OA group data with and without these two cases.

6.4.2 Comparison of mRNA expression between females and males in the OA group

The student's *t*-test was used to assess whether there were any gender differences in the mean mRNA expression levels of IL-6, IL-11, CTR, OCN, RANKL, OPG, RANK, and the RANKL/OPG mRNA ratio in OA human trabecular bone from the proximal femur. The ratio of RANKL to OPG mRNA was included in the analysis as this ratio has been hypothesised, based upon a large amount of evidence, to be the main determinant of the pool size of active osteoclasts in the local bone environment (Hofbauer *et al.*, 2000). The ratio of RANKL/OPG mRNA was found to be significantly higher in the bone samples from females (5 of the 7 females were postmenopausal) than in males in the control cohort

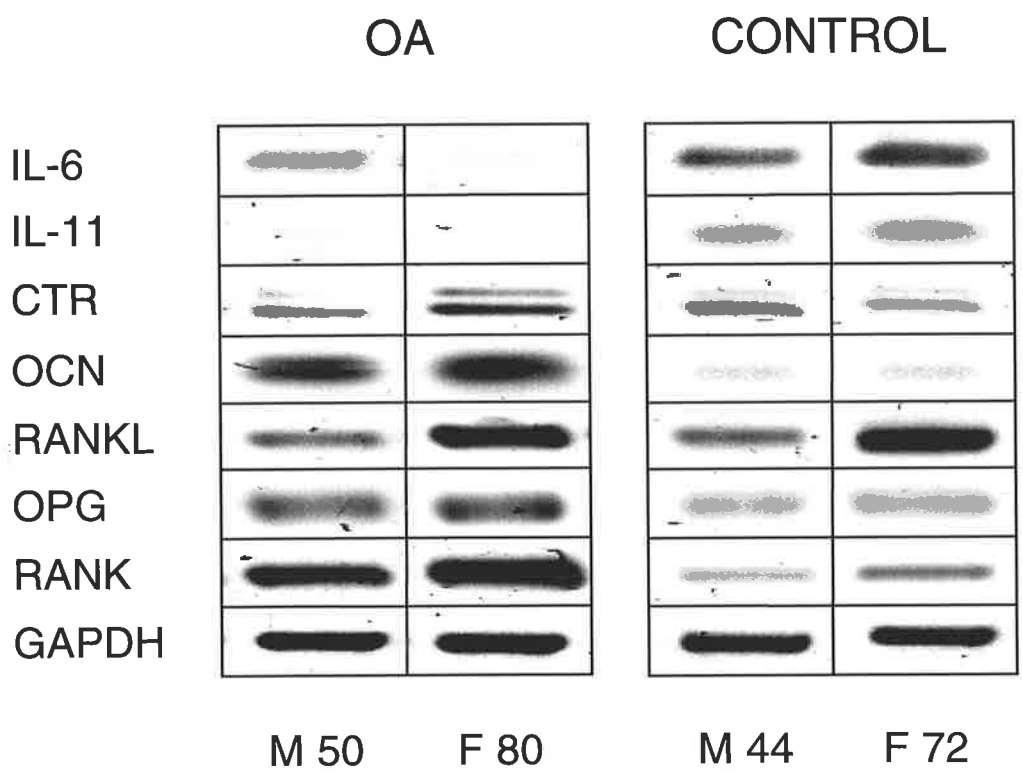

Figure 6.1: Expression of IL-6 (544 bp), IL-11 (289 bp), CTR isoforms (780/732 bp), OCN (255 bp), RANKL (665 bp), OPG (433 bp), RANK (702 bp), and GAPDH (415 bp) mRNA in total RNA extracted from intertrochanteric trabecular bone, as determined by RT-PCR (Chapter 2.2.2.3). Specimens were obtained from a 50-year-old male (M50) and an 80-year-old female (F80) undergoing total hip arthroplasty surgery for primary osteoarthritis (OA); and from a 44-year-old male (M44) and a 72-year-old female (F72), without any bone-related disease, at autopsy (control). PCR products representing each mRNA species were visualised on SYBR® Gold-stained 2% agarose gels.

($p < 0.05$; described in Chapter 5.4.2).

No significant differences were observed between OA females and OA males for the mean mRNA expression of IL-6/GAPDH, CTR/GAPDH, OCN/GAPDH, RANKL/GAPDH, OPG/GAPDH, RANK/GAPDH or the RANKL/OPG ratio (Table 6.2). A small difference that did reach statistical significance was found between OA females and OA males for IL-11/GAPDH mRNA expression ($p < 0.05$; Table 6.2). There was no difference in the RANKL/OPG mRNA ratio between OA females and OA males, despite 7 of the 8 OA females being postmenopausal, and thus likely to have an increased bone remodelling rate due to oestrogen deficiency.

Based on these comparisons between OA females and OA males for mRNA gene expression, further analyses of the data were made, independent of gender for the OA group, similar to the control group (described in Chapter 5.4.2).

6.4.3 Comparison of mRNA expression between OA and control trabecular bone from the human proximal femur

The individual values obtained for IL-6, IL-11, CTR, OCN, RANKL, OPG, and RANK mRNA expression in the OA and control groups are shown in Figures 6.2 to 6.8. The student's *t*-test was used to assess whether there were any differences in the mRNA expression levels between the OA and control groups. To enable comparison of age-matched control and OA groups, analysis was performed on complete data sets or after exclusion of the two younger control individuals (cases C1 (20-year-old female) and C8 (24-year-old male); Tables 6.3 and 6.4).

Table 6.2 Female and male RT-PCR product/GAPDH ratios in intertrochanteric trabecular bone from OA individuals.

Ratio	Female ($n = 8$)	Male ($n = 8$)
IL-6/GAPDH	0.11 ± 0.04	0.13 ± 0.08
IL-11/GAPDH	0.12 ± 0.04	0.09 ± 0.02 [a]
CTR/GAPDH	0.65 ± 0.32	0.55 ± 0.30
OCN/GAPDH	1.36 ± 0.57	1.14 ± 0.51
RANKL/GAPDH	0.45 ± 0.35; $n = 7$	0.56 ± 0.68; $n = 6$
OPG/GAPDH	0.33 ± 0.15; $n = 7$	0.27 ± 0.33; $n = 6$
RANK/GAPDH	0.64 ± 0.30; $n = 7$	0.78 ± 0.52; $n = 5$
RANKL/OPG	1.52 ± 1.17; $n = 7$	2.09 ± 0.69; $n = 6$

Values are mean ± standard deviation.
[a] $p < 0.05$.

In OA, the mean mRNA expression of IL-6/GAPDH and IL-11/GAPDH were significantly reduced in comparison to the control group ($p < 0.05$ and $p < 0.001$; Figures 6.2 and 6.3; respectively). This difference in IL-6/GAPDH mRNA expression was not observed between the OA group and the controls aged greater than 40 years (Table 6.3). Furthermore, Figure 6.2 shows that the outlier in the controls, case C5 (72-year-old female) with a high relative expression level of IL-6/GAPDH mRNA, influenced the mean expression level of IL-6/GAPDH mRNA in the control group. However, the reduction in the mean IL-11/GAPDH mRNA expression in OA remained significant when the OA data was compared to controls greater than 40 years of age ($p < 0.001$; Table 6.3). The stimulatory effects of IL-11 on osteoclast differentiation appear to be mediated by induction of RANKL expression by marrow stromal/osteoblastic cells (Nakashima *et al.*, 2000; Yasuda *et al.*, 1998b). Thus, the reduced expression of IL-11 mRNA in the OA group suggests a reduced promotion of osteoclastogenesis by osteoblasts in OA trabecular bone.

There was no significant difference in the mean expression of CTR/GAPDH mRNA between the OA and control groups (Figure 6.4), even when the OA data was compared to controls greater than 40 years of age (Table 6.3). In contrast, there was a highly significant elevation in both the mean and the variance of the expression of OCN/GAPDH mRNA in OA compared with the control samples ($p < 0.00001$; Figure 6.5; F-statistic = 26.5, representing the ratio of the OA variance to control variance, $p < 0.00001$), and compared with controls aged greater than 40 years ($p < 0.00001$; Table 6.3; F-statistic = 36.2, $p < 0.00001$). As OCN is regarded as an indicator of bone formation and a molecular marker for osteoblasts (Stein and Lian, 1993), the enhanced expression of OCN mRNA in the OA group suggests that there is an increase in bone formation and/or osteoblastic activity in

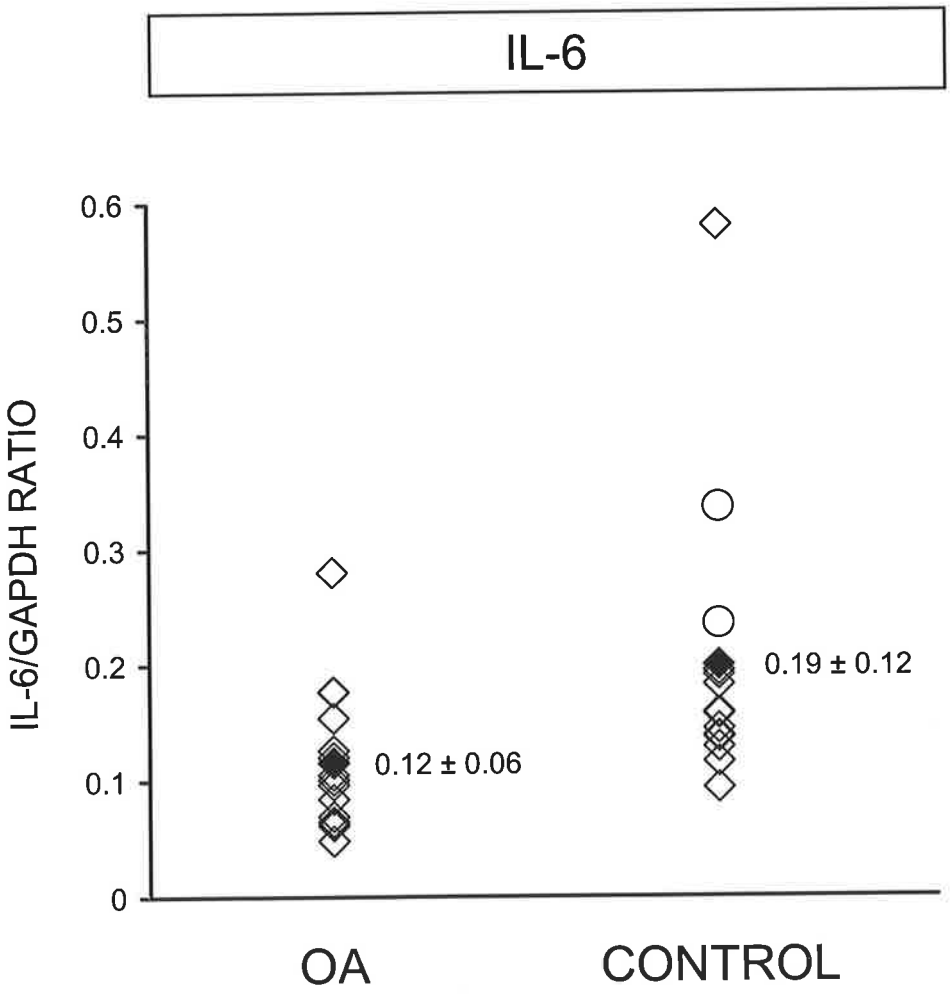

Figure 6.2: Relative ratio of IL-6/GAPDH mRNA expression in intertrochanteric trabecular bone from OA (n = 16) and control (n = 14) individuals. OA patients had significantly reduced IL-6/GAPDH mRNA ($p < 0.05$) versus controls. Two control cases, <40 years old, are indicated (○). The means are indicated (◆). Values are mean ± standard deviation.

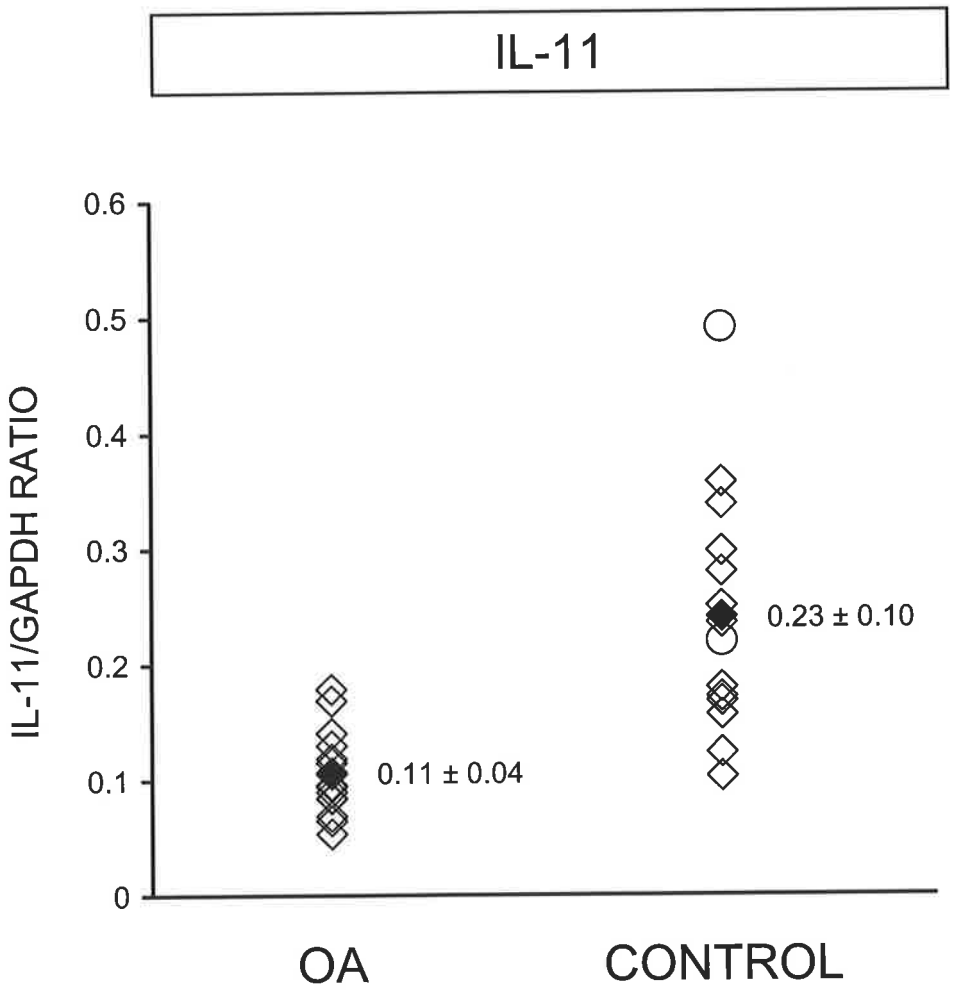

Figure 6.3: Relative ratio of IL-11/GAPDH mRNA expression in intertrochanteric trabecular bone from OA (n = 16) and control (n = 14) individuals. OA patients had significantly reduced IL-11/GAPDH mRNA ($p < 0.001$) versus controls. Two control cases, <40 years old, are indicated (○). The means are indicated (◆). Values are mean ± standard deviation.

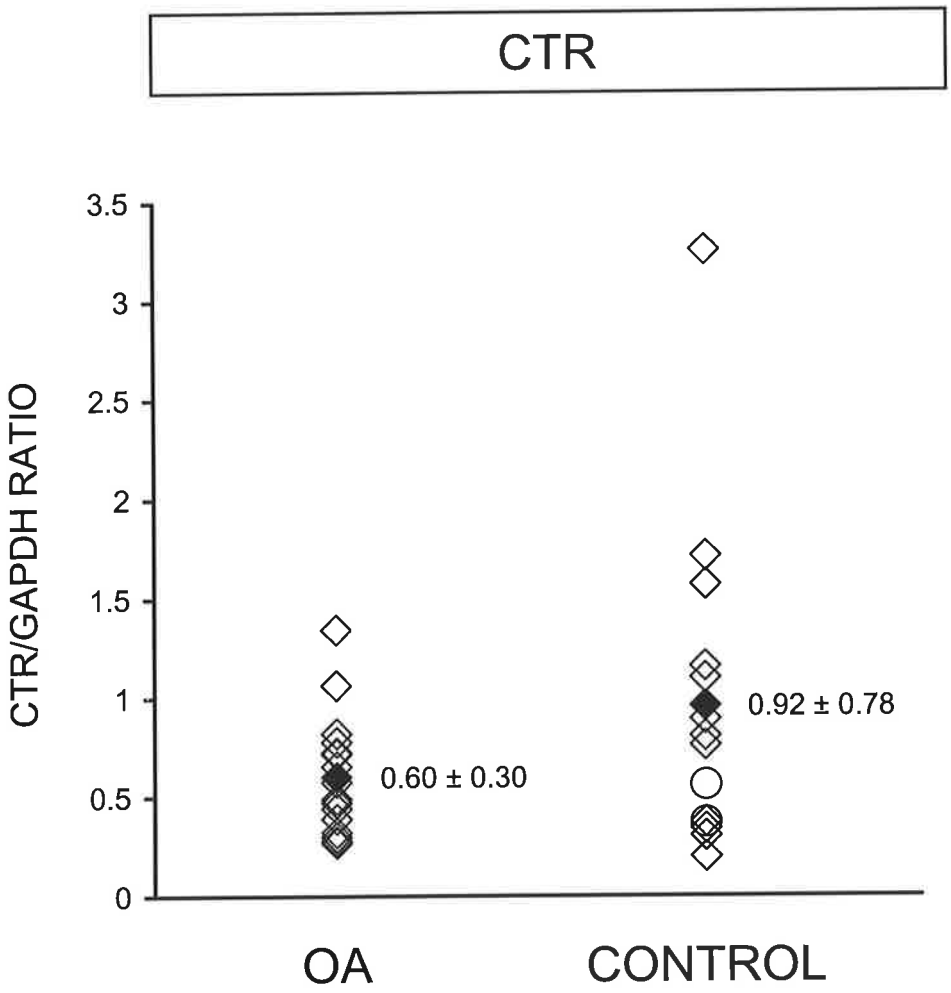

Figure 6.4: Relative ratio of CTR/GAPDH mRNA expression in intertrochanteric trabecular bone from OA (n = 16) and control (n = 14) individuals. No significant difference was observed for the ratio of CTR/GAPDH mRNA between OA and controls. Two control cases, <40 years old, are indicated (○). The means are indicated (◆). Values are mean ± standard deviation.

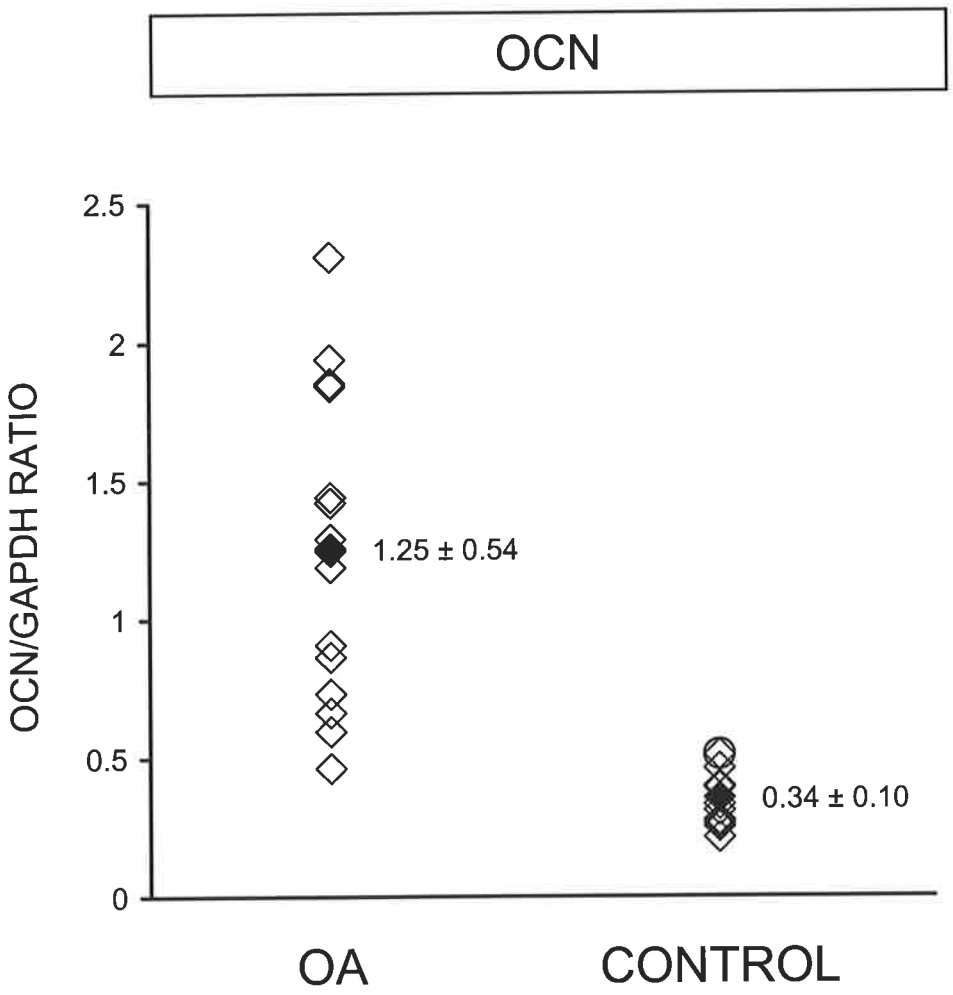

Figure 6.5: Relative ratio of OCN/GAPDH mRNA expression in intertrochanteric trabecular bone from OA (n = 16) and control (n = 14) individuals. The ratio of OCN/GAPDH mRNA was significantly elevated in OA versus controls ($p < 0.00001$). Two control cases, <40 years old, are indicated (○). The means are indicated (◆). Values are mean ± standard deviation.

intertrochanteric OA bone. This is consistent with a significant increase in mean osteoid volume, OV/TV, in OA bone compared to control bone, for trabecular bone sampled from the intertrochanteric region of the proximal femur (Tables 7.4 and 7.5; Chapter 7.4.5). However, the histomorphometric bone formation parameters of osteoid surface, OS/BS, and OV/BV, were not significantly different between the OA and control groups (Tables 7.4 and 7.5; Chapter 7.4.5). Interestingly, the enhanced expression of OCN mRNA in OA intertrochanteric bone supports a previous finding of increased OCN protein extracted from iliac crest bone of OA subjects (Gevers and Dequeker, 1987; Raymaekers *et al.*, 1992). It is important to note that it is not known whether the relative expression level of OCN mRNA is representative of the concentration of OCN protein in these trabecular bone samples.

Table 6.3 RT-PCR product/GAPDH ratios in intertrochanteric trabecular bone sampled from OA and control cases aged over 40 years.

Ratio	**OA** (***n*** **= 16**) *(aged 49-85 years)*	**Control >40 years** (***n*** **= 12**) *(aged 43-85 years)*
IL-6/GAPDH	0.12 ± 0.06	0.18 ± 0.12
IL-11/GAPDH	0.11 ± 0.04	0.21 ± 0.08 [a]
CTR/GAPDH	0.60 ± 0.30	1.00 ± 0.82
OCN/GAPDH	1.25 ± 0.54	0.32 ± 0.09 [b]
CTR/OCN	0.51 ± 0.21	3.51 ± 3.39 [c]

Values are mean ± standard deviation.
[a] $p < 0.001$, [b] $p < 0.00001$, [c] $p < 0.02$ vs. OA group.

There was no significant difference in mean RANKL/GAPDH or OPG/GAPDH mRNA expression levels between the OA and control groups (Figures 6.6 and 6.7), even when the OA data was compared to controls greater than 40 years of age (Table 6.4). There was comparable variance from the mean for RANKL mRNA in OA and the controls (Figure 6.6). Whereas the variance in the expression of OPG/GAPDH mRNA was significantly higher in OA compared with all control samples (F-statistic = 8.1, $p < 0.001$), or controls aged greater than 40 years (F-statistic = 8.0, $p < 0.003$). Interestingly, the mean expression of RANK/GAPDH mRNA was significantly elevated in OA compared to either the control group ($p < 0.02$; Figure 6.8), or controls aged greater than 40 years ($p < 0.02$; Table 6.4). RANK expression has been detected in pre-osteoclast, mature osteoclast, chondrocyte, dendritic, fibroblast, B, and T cells (Anderson *et al.*, 1997; Hsu *et al.*, 1999; Komuro *et al.*, 2001; Myers *et al.*, 1999; Nakagawa *et al.*, 1998). However, in the local bone microenvironment, it is not known whether immature and/or mature osteoclast cells are representative of the measured RANK mRNA, or whether the RANK mRNA expression is representative of the number of osteoclasts and/or the number of RANK receptors on each osteoclast. Further, a positive association was observed between the histomorphometric bone resorptive index, eroded surface, ES/BS, and RANK/GAPDH mRNA expression, in contiguous trabecular bone samples from the intertrochanteric region for controls (Figure 7.11; Chapter 7.4.3). However, there was no correlation between ES/BS and RANK/GAPDH mRNA expression in the OA group (Chapter 7.4.7). Additionally, it is important to note that it is not known whether the relative expression level of RANK mRNA is representative of the level of RANK protein in these trabecular bone samples.

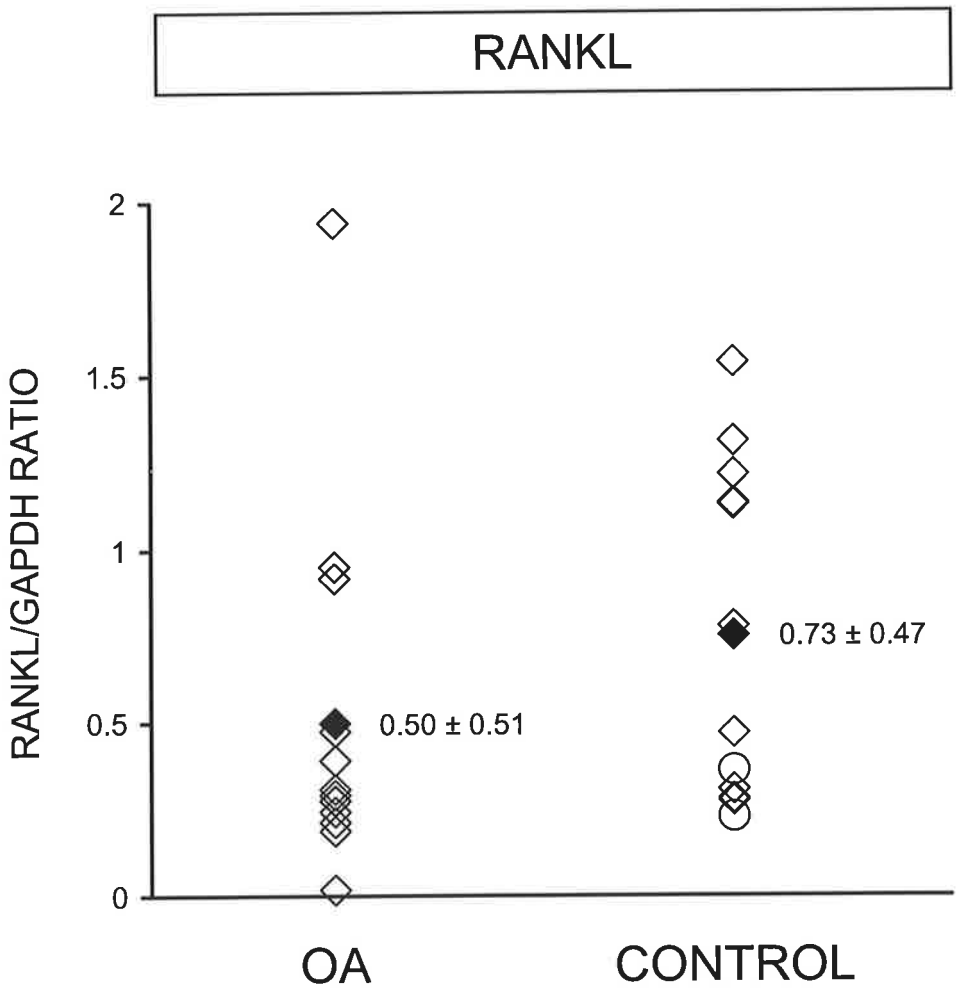

Figure 6.6: Relative ratio of RANKL/GAPDH mRNA expression in intertrochanteric trabecular bone from OA (n = 13) and control (n = 12) individuals. No significant difference was observed for the ratio of RANKL/GAPDH mRNA between OA and controls. Two control cases, <40 years old, are indicated (○). The means are indicated (◆). Values are mean ± standard deviation.

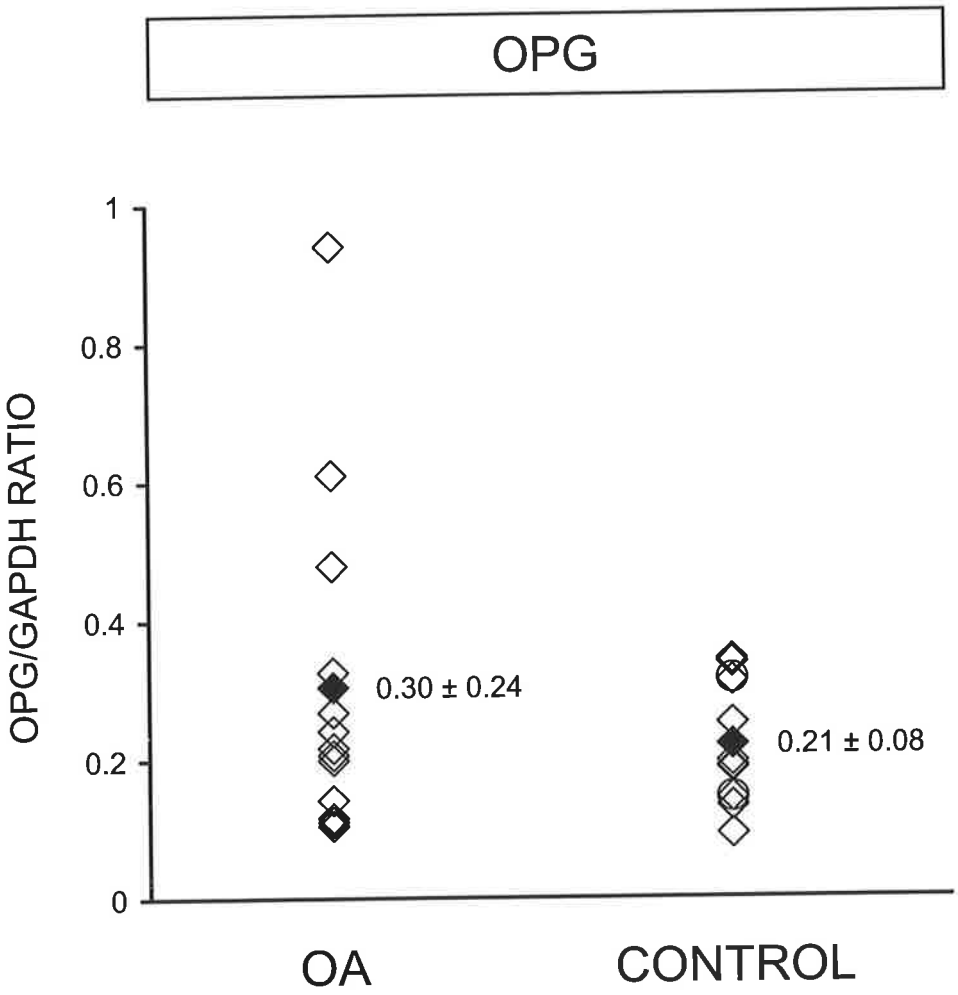

Figure 6.7: Relative ratio of OPG/GAPDH mRNA expression in intertrochanteric trabecular bone from OA (n = 13) and control (n = 12) individuals. No significant difference was observed for the ratio of OPG/GAPDH mRNA between OA and controls. Two control cases, <40 years old, are indicated (○). The means are indicated (◆). Values are mean ± standard deviation.

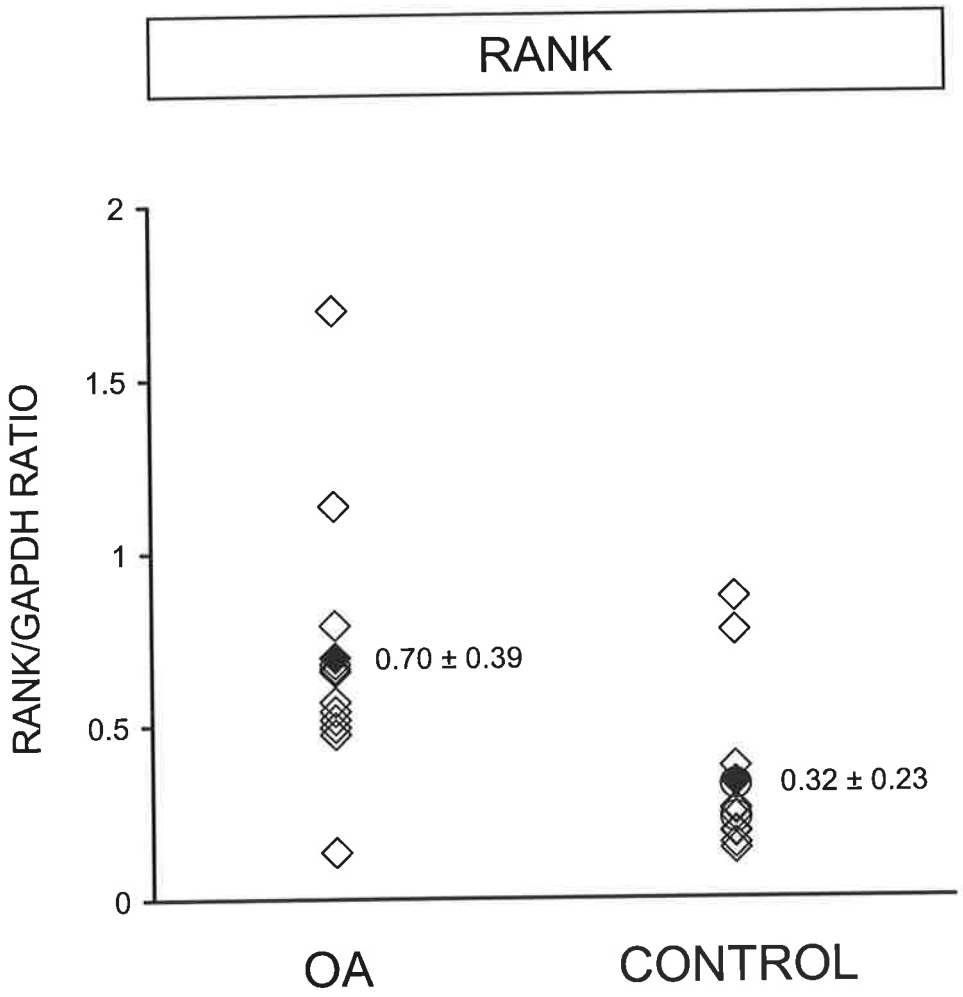

Figure 6.8: Relative ratio of RANK/GAPDH mRNA expression in intertrochanteric trabecular bone from OA (n = 12) and control (n = 12) individuals. The ratio of RANK/GAPDH mRNA was significantly elevated in OA versus controls ($p < 0.02$). Two control cases, <40 years old, are indicated (○). The means are indicated (◆). Values are mean ± standard deviation.

Table 6.4 RT-PCR product/GAPDH ratios in intertrochanteric trabecular bone sampled from OA and control cases aged over 40 years.

Ratio	OA (n = 13) *(aged 49-85 years)*	Control >40 years (n = 10) *(aged 43-85 years)*
RANKL/GAPDH	0.50 ± 0.51	0.82 ± 0.46
OPG/GAPDH	0.30 ± 0.24	0.21 ± 0.09
RANK/GAPDH	0.70 ± 0.39; n = 12	0.33 ± 0.25 [a]

Values are mean ± standard deviation.
[a] $p < 0.02$ vs. OA group.

6.4.4 Associations between expression of specific mRNA transcripts

As IL-6 and IL-11 are two cytokines that share many biological properties, including the ability to stimulate osteoclast development from their haematopoietic precursors (Martin *et al.*, 1998), the IL-6/GAPDH and IL-11/GAPDH mRNA ratios were co-plotted for the OA group, and analysed by linear regression analysis. No significant association was observed between the expression of IL-6/GAPDH and IL-11/GAPDH mRNA in the OA group (Figure 6.9), which is in contrast to the positive association between IL-6 and IL-11 mRNA observed in control bone samples (Figure 6.9; Chapter 5.4.3). Interestingly, the OA data points clustered at the lower end of the positive linear regression line for controls (Figure 6.9), which was consistent with the reduced mean IL-6/GAPDH and IL-11/GAPDH mRNA expression in the OA group (Figures 6.2 and 6.3, respectively; Table 6.3).

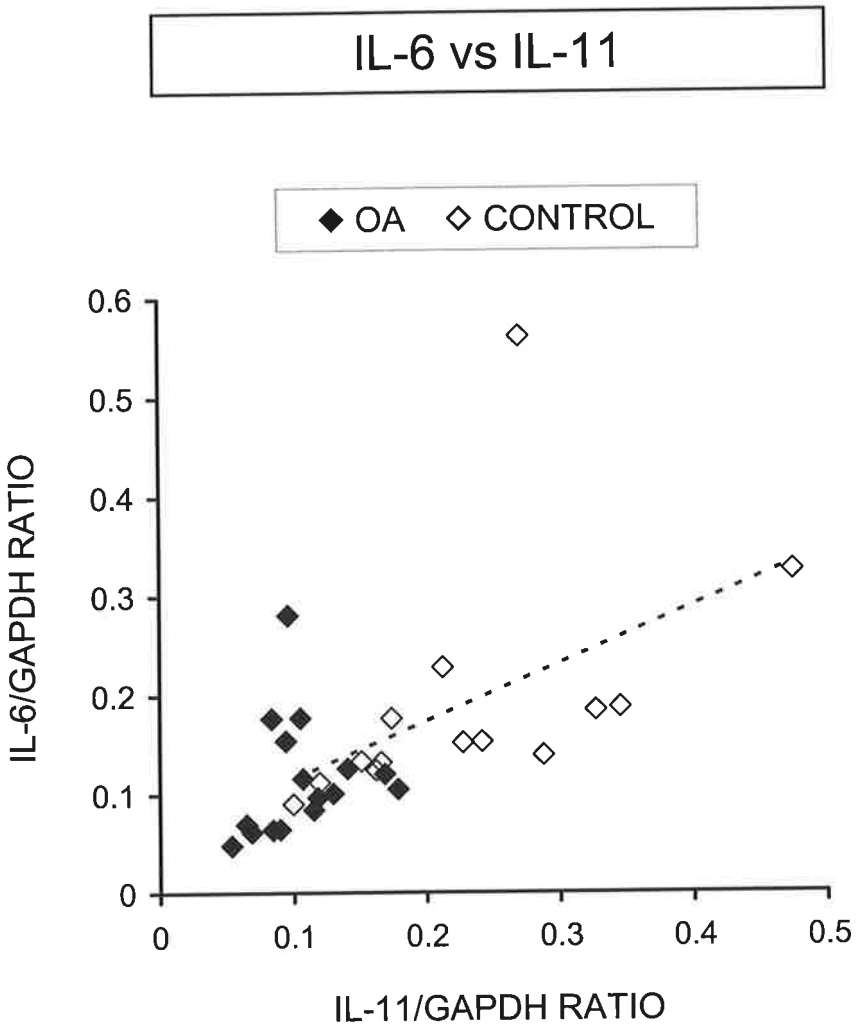

Figure 6.9: Associations between the relative ratio of IL-6/GAPDH mRNA and IL-11/GAPDH mRNA in intertrochanteric trabecular bone from OA (n = 16) and control (n = 14) individuals. No significant relationship was found for the OA group (IL-6/GAPDH = 0.26*IL-11/GAPDH + 0.09; r = 0.16 and p = NS). A positive association was observed between the two parameters in controls (IL-6/GAPDH = 0.58*IL-11/GAPDH + 0.06; r = 0.49 and $p < 0.05$ {broken line}). NS = not significant.

OCN is utilised as an indicator of bone formation as it is one of the marker genes for the progression of osteoblastic differentiation (Stein and Lian, 1993). The CTR in bone is uniquely expressed on the surface of mononuclear osteoclast precursor cells and multinuclear osteoclasts (Hattersley and Chambers, 1989; Quinn *et al.*, 1999). The plot of CTR/GAPDH versus OCN/GAPDH mRNA expression might be regarded as an index of the balance of resorption to formation in these bone samples. Interestingly, a significant positive association was found between CTR/GAPDH and OCN/GAPDH mRNA expression in the OA group ($r = 0.52$, $p < 0.05$; Figure 6.10), which was not present in the control group (Figure 6.10; Chapter 5.4.3). Furthermore, a significant reduction in the CTR/OCN mRNA ratio was observed in the OA group compared to the controls ($p < 0.01$; Figure 6.11), and controls aged greater than 40 years ($p < 0.02$; Table 6.3). The variance in the CTR/OCN mRNA ratio was significantly higher in the control samples compared with OA (F-statistic = 233.2, representing the ratio of the control variance to OA variance, $p < 0.00001$), and in the controls aged greater than 40 years compared with OA (F-statistic = 252.2, $p < 0.00001$). The reduced mean and variance in the expression of the CTR/OCN mRNA ratio in the OA group, compared with the control samples, is suggestive of a skewing of the remodelling process towards net bone formation in OA. In interpreting this result, it is important to note that it is not known whether immature and/or mature osteoclast cells are representative of the measured CTR mRNA, nor whether the CTR mRNA expression is representative of the number of osteoclasts and/or the number of calcitonin receptors on each osteoclast. However, a significant positive association was observed between the expression of CTR/GAPDH and RANK/GAPDH mRNA in the OA bone samples ($r = 0.89$, $p < 0.001$; Figure 6.12), which was not evident in the control bone samples. RANK is expressed on the surface of the same cell types as the CTR in bone, namely osteoclasts and their precursors (Hsu *et al.*, 1999; Myers *et al.*, 1999).

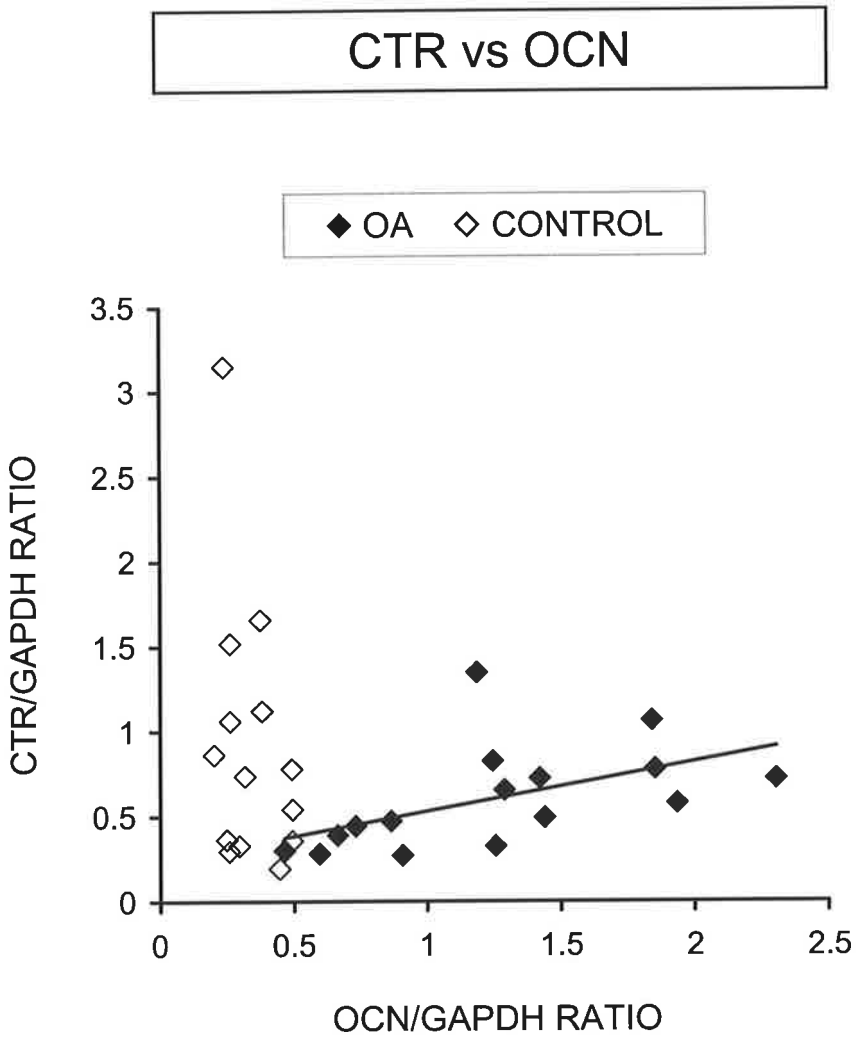

Figure 6.10: Associations between the relative ratio of CTR/GAPDH mRNA and OCN/GAPDH mRNA in intertrochanteric trabecular bone from OA (n = 16) and control (n = 14) individuals. A significant positive correlation was observed between the two parameters in OA patients (CTR/GAPDH = 0.29*OCN/GAPDH + 0.24; r = 0.52 and p < 0.05 {solid line}). No significant relationship was found for the control group (CTR/GAPDH = -2.44*OCN/GAPDH + 1.76; r = -0.32 and p = NS). NS = not significant.

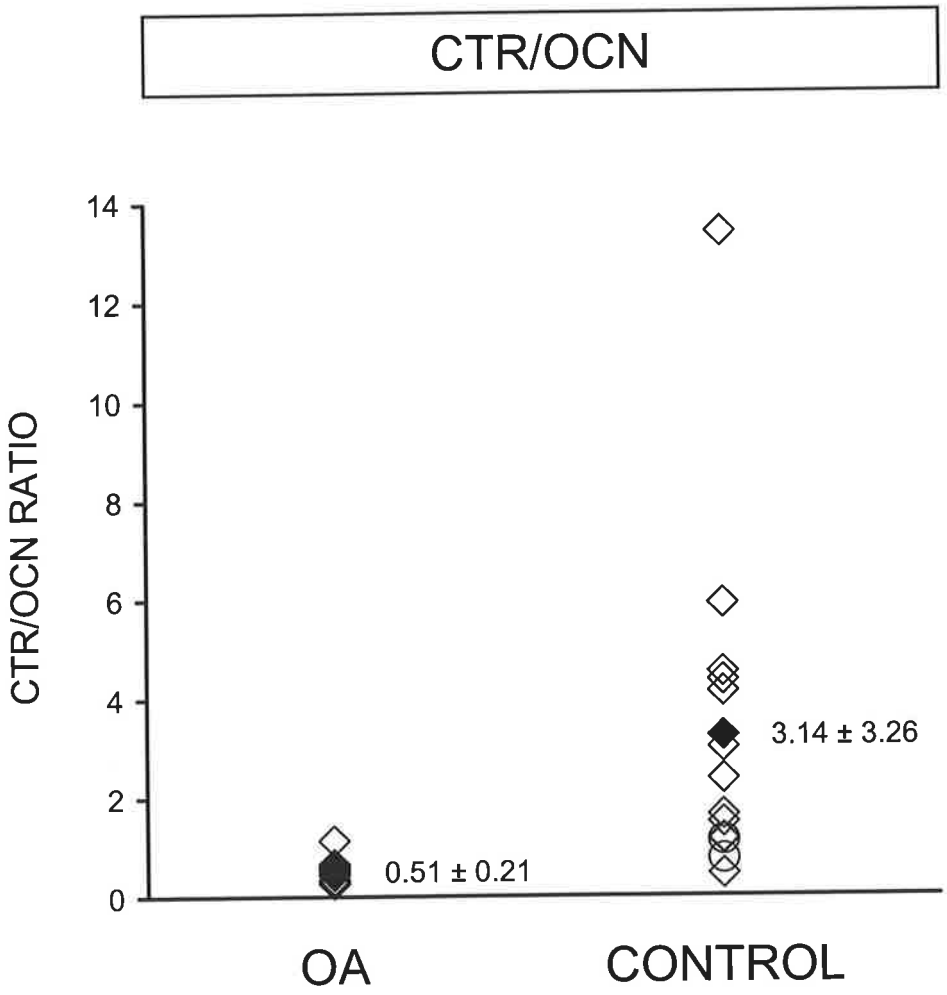

Figure 6.11: Relative ratio of CTR/OCN mRNA expression in intertrochanteric trabecular bone from OA (n = 16) and control (n = 14) individuals. The CTR/OCN mRNA ratio was significantly lower in OA patients versus controls ($p < 0.01$). Two control cases, <40 years old, are indicated (○). The means are indicated (◆). Values are mean ± standard deviation.

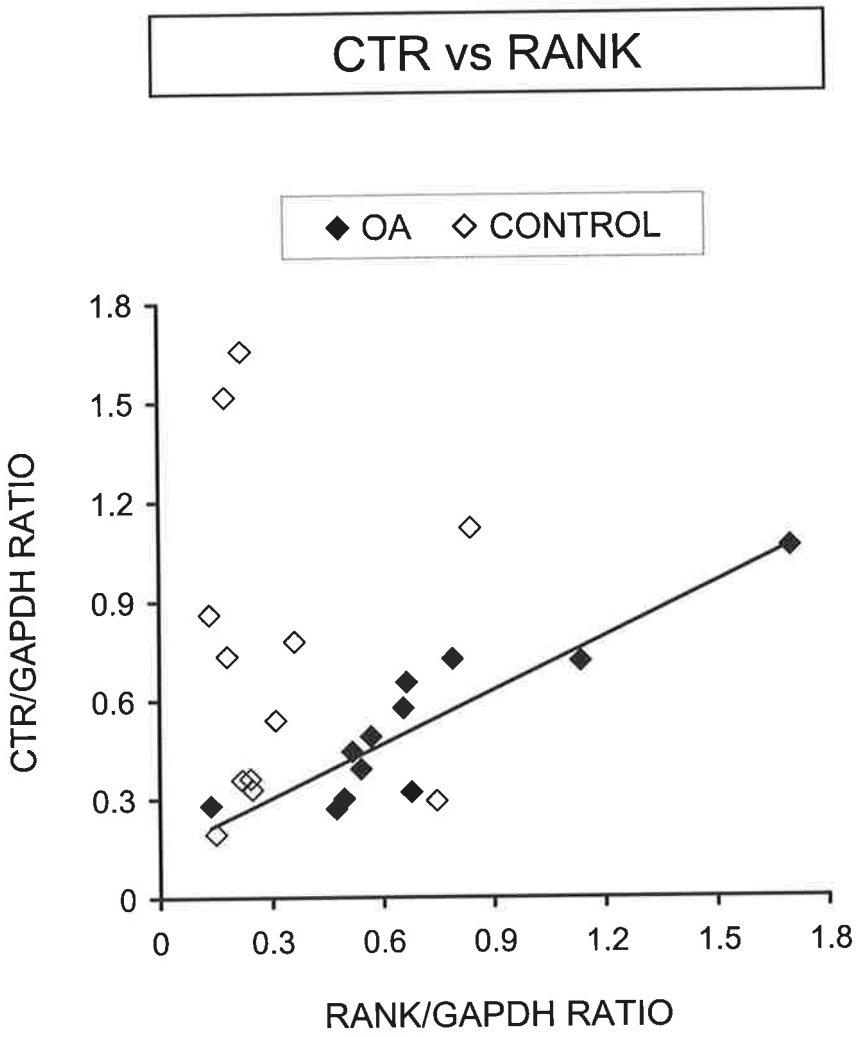

Figure 6.12: Associations between the relative ratio of CTR/GAPDH mRNA and RANK/GAPDH mRNA in intertrochanteric trabecular bone from OA (n = 12) and control (n = 12) individuals. A significant positive correlation was observed between the two parameters in OA patients (CTR/GAPDH = 0.54*RANK/GAPDH + 0.14; r = 0.89 and $p < 0.001$ {solid line}). No significant relationship was found for the control group (CTR/GAPDH = -0.03*RANK/GAPDH + 0.74; r = -0.01 and p = NS). NS = not significant.

Both IL-6 and IL-11 have been shown to stimulate the development of osteoclasts from their haematopoietic precursors (Martin *et al.*, 1998). Although the stimulatory effects of IL-11 on osteoclast differentiation appear to be mediated by inducing RANKL expression on marrow stromal/osteoblastic cells (Nakashima *et al.*, 2000; Yasuda *et al.*, 1998b), the reported effects of IL-6 on RANKL-RANK-promoted osteoclast development are conflicting (Brandstrom *et al.*, 1998; Hofbauer *et al.*, 1998; Hofbauer *et al.*, 1999b; Nakashima *et al.*, 2000; O'Brien *et al.*, 1999; Vidal *et al.*, 1998). When the IL-6/GAPDH or IL-11/GAPDH mRNA ratios were co-plotted with the RANKL/GAPDH, OPG/GAPDH or RANK/GAPDH mRNA ratios for these OA bone samples, no significant associations were observed (results not shown), consistent with the control group data (Chapter 5.4.3).

Extensive bone marrow cell culture studies have shown that growth factors, cytokines, and peptide and steroid hormones modulate the gene expression of RANKL, OPG, and to a lesser extent, RANK (Hofbauer *et al.*, 2000; Hofbauer and Heufelder, 2001; Horowitz *et al.*, 2001; Suda *et al.*, 1999). Therefore, the results for RANKL and OPG mRNA, RANKL and RANK mRNA, and RANK and OPG mRNA were co-plotted, as they were for the controls in Chapter 5.4.3, to identify whether any relationships exist in the local human bone microenvironment of the OA proximal femur. Firstly, RANKL/GAPDH mRNA versus OPG/GAPDH mRNA values were positively associated for the OA bone samples ($r = 0.79$, $p < 0.001$; Figure 6.13), consistent with the control group data (Figure 6.13; Chapter 5.4.3). It appears that this positive association between RANKL and OPG mRNA in OA bone is statistically reliant on two outliers, cases OA7 (80-year-old female) and OA13 (73-year-old male). However, both of these outliers consistently showed a high relative expression level of RANKL/GAPDH, OPG/GAPDH, and RANK/GAPDH mRNA,

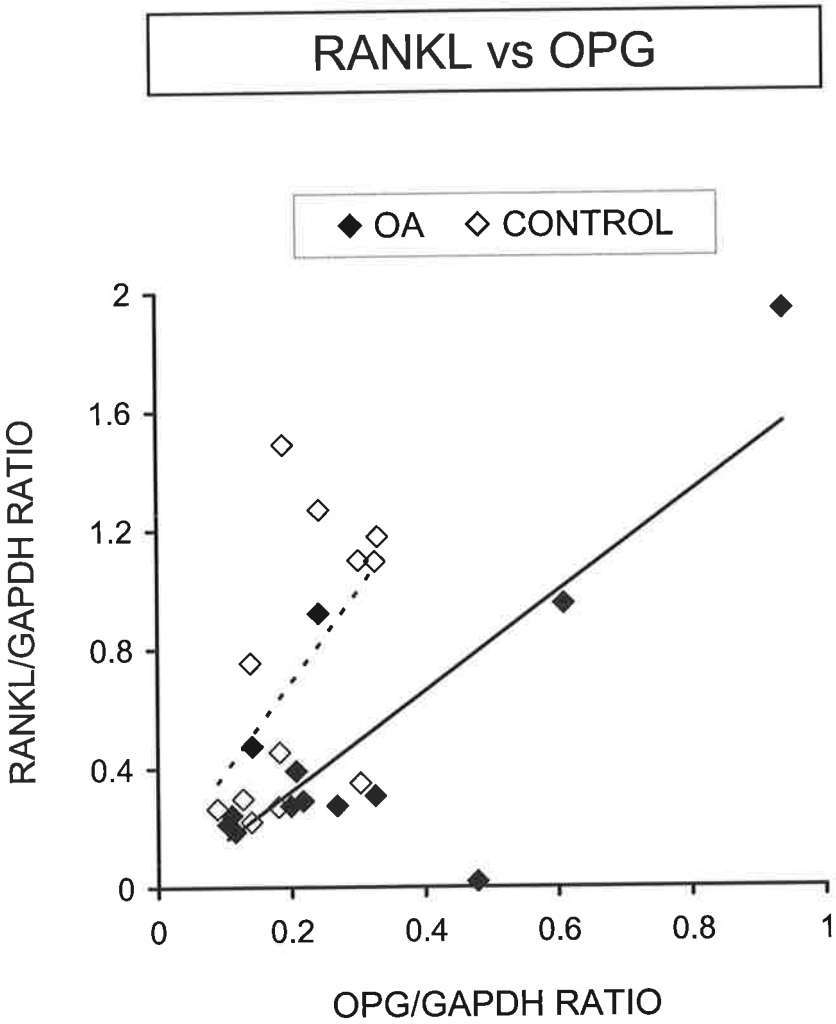

Figure 6.13: Associations between the relative ratio of RANKL/GAPDH mRNA and OPG/GAPDH mRNA in intertrochanteric trabecular bone from OA (n = 13) and control (n = 12) individuals. A significant positive correlation was observed between the two parameters in OA patients (RANKL/GAPDH = 1.67*OPG/GAPDH - 0.01; r = 0.79 and $p < 0.001$ {solid line}) and controls (RANKL/GAPDH = 3.06*OPG/GAPDH + 0.08; r = 0.55 and $p < 0.05$ {broken line}).

when compared to the other OA cases. Furthermore, the individual values for the RANKL/OPG mRNA ratio for the two outliers, OA7 and OA13 (relative ratio of RANKL/OPG mRNA = 1.56 and 2.06, respectively), lie close to the OA group mean (relative ratio of RANKL/OPG mRNA = 1.78; Figure 6.16). Interestingly, the slope of the linear regression line for the control samples was greater than for the OA samples ($p < 0.01$), so that for a given level of RANKL mRNA, the corresponding level of OPG mRNA was greater in OA samples (Figure 6.13). Per unit of OPG gene expression, the level of RANKL gene expression in OA was about half that in the controls (regression slopes = 1.67 for OA versus 3.06 for controls). Taken together, these results suggest that there is a relationship between the positive and negative osteoclastic influences in the bone microenvironment and that the inhibitory influence is relatively greater in OA. Secondly, when the RANKL/GAPDH mRNA levels were plotted versus RANK/GAPDH mRNA, the level of RANKL gene expression increased as the level of RANK gene expression increased for the OA bone samples ($r = 0.95$, $p < 0.001$; Figure 6.14), consistent with the control group data (Figure 6.14; Chapter 5.4.3). Although the slopes of the linear regression lines for the OA and control samples were parallel, the results segregated such that for a given level of RANK mRNA, the level of RANKL mRNA was higher in the control group ($p < 0.001$; Figure 6.14). Therefore, when combining Figures 6.13 and 6.14, for a given level of OPG or RANK gene expression, there was a lower level of RANKL gene expression in OA compared with controls. Finally, the plot of RANK/GAPDH mRNA versus OPG/GAPDH mRNA expression shows the level of RANK gene expression associated positively with OPG gene expression in OA bone samples ($r = 0.74$, $p < 0.003$; Figure 6.15), which is in contrast to no association between RANK and OPG mRNA in control bone samples (Figure 6.15; Chapter 5.4.3). The positive association between RANK and OPG mRNA in OA bone is statistically reliant on the same two outliers, cases

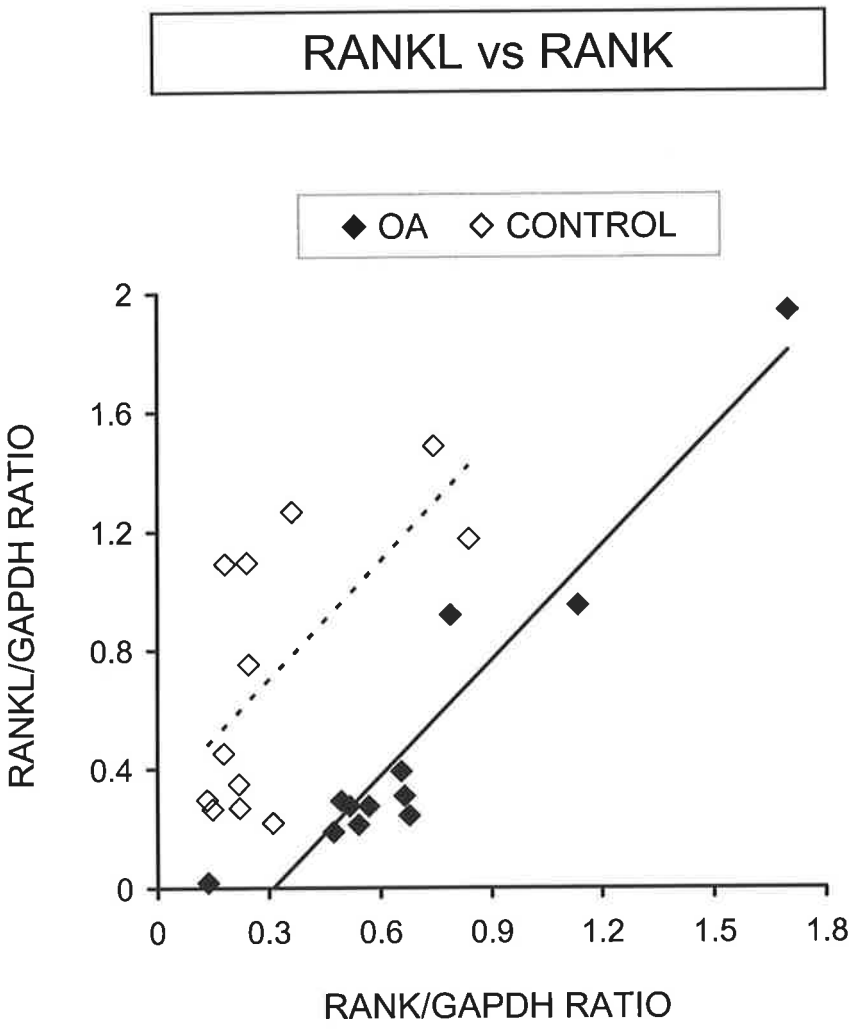

Figure 6.14: Associations between the relative ratio of RANKL/GAPDH mRNA and RANK/GAPDH mRNA in intertrochanteric trabecular bone from OA (n = 12) and control (n = 12) individuals. A significant positive correlation was observed between the two parameters in OA patients (RANKL/GAPDH = 1.30*RANK/GAPDH - 0.40; r = 0.95 and $p < 0.001$ {solid line}) and controls (RANKL/GAPDH = 1.34*RANK/GAPDH + 0.30; $r = 0.66$ and $p < 0.01$ {broken line}).

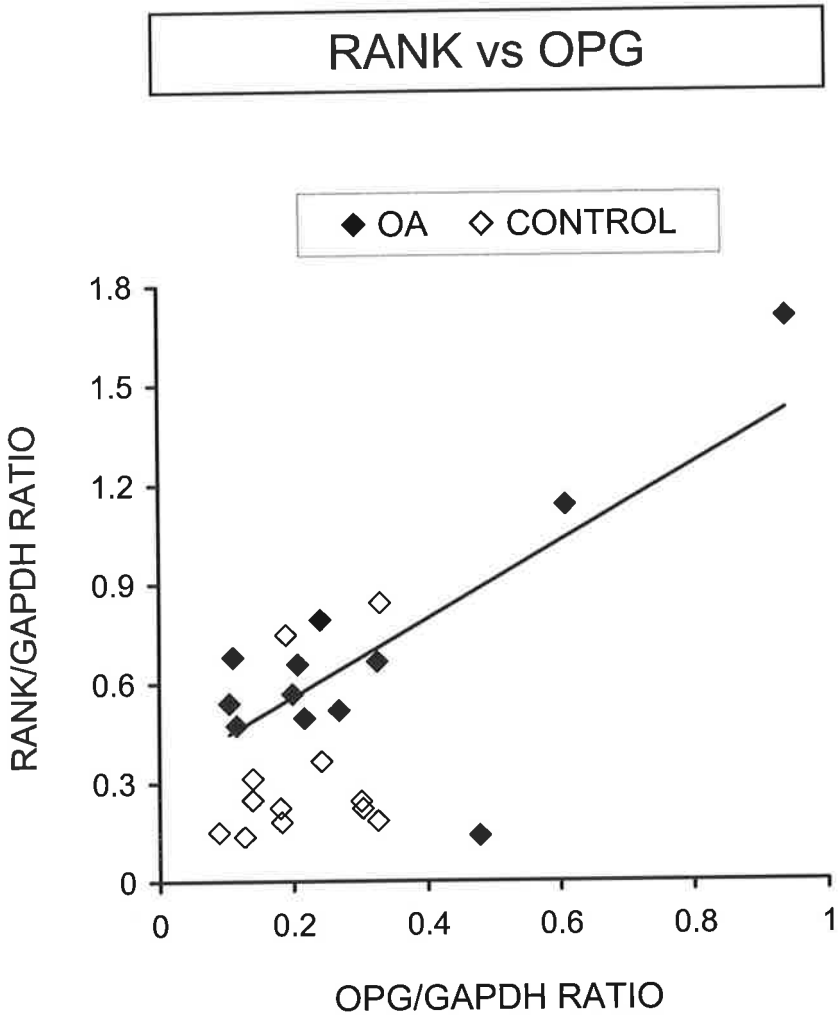

Figure 6.15: Associations between the relative ratio of RANK/GAPDH mRNA and OPG/GAPDH mRNA in intertrochanteric trabecular bone from OA (n = 12) and control (n = 12) individuals. A significant positive correlation was observed between the two parameters in OA patients (RANK/GAPDH = 1.17*OPG/GAPDH + 0.32; r = 0.74 and $p < 0.003$ {solid line}). No association was observed between the two parameters in controls (RANK/GAPDH = 0.90*OPG/GAPDH + 0.13; r = 0.33 and p = NS). NS = not significant.

OA7 (80-year-old female) and OA13 (73-year-old male), that influenced the RANKL versus OPG mRNA association in OA bone (Figure 6.13). It is reiterated that both of these outliers consistently showed a high relative expression level of the osteoclastogenic factors, RANKL, OPG, and RANK mRNA, when compared to the other OA cases. Furthermore, it is acknowledged that the number of cases in the OA and control groups is small, and increased cases in each study group are required to strengthen these relationships, observed in human bone samples.

As positive associations were observed between RANKL and OPG mRNA (in both OA and control bone; Figure 6.13), RANKL and RANK mRNA (in both OA and control bone; Figure 6.14), and RANK and OPG mRNA (in OA bone only; Figure 6.15), student's *t*-test was used to assess whether there were any differences between the OA and control groups for the RANKL/OPG, RANKL/RANK, and RANK/OPG mRNA ratios. The mean ratios of RANKL/OPG mRNA and RANKL/RANK mRNA were significantly lower in the OA group, compared to controls ($p < 0.02$ and $p < 0.001$; Figures 6.16 and 6.17; respectively). Conversely, the mean ratio of RANK/OPG mRNA was significantly increased in the OA group, compared to the control group ($p < 0.03$; Figure 6.18). The exclusion of the two younger control individuals did not affect the significant differences in the RANKL/OPG, RANKL/RANK, and RANK/OPG mRNA ratios between the OA and control groups (Table 6.5). The magnitude of the RANKL/RANK and RANK/OPG mRNA ratios in OA bone samples were directly influenced by the elevation in the mean expression of RANK/GAPDH mRNA in the OA group, compared to the controls (Figure 6.8; Table 6.4). The ratio of RANKL to OPG has been hypothesised, based upon a large amount of evidence, to be the main determinant of the pool size of active osteoclasts in the local bone microenvironment (Hofbauer *et al.*, 2000). The lower mean RANKL/OPG mRNA ratio in

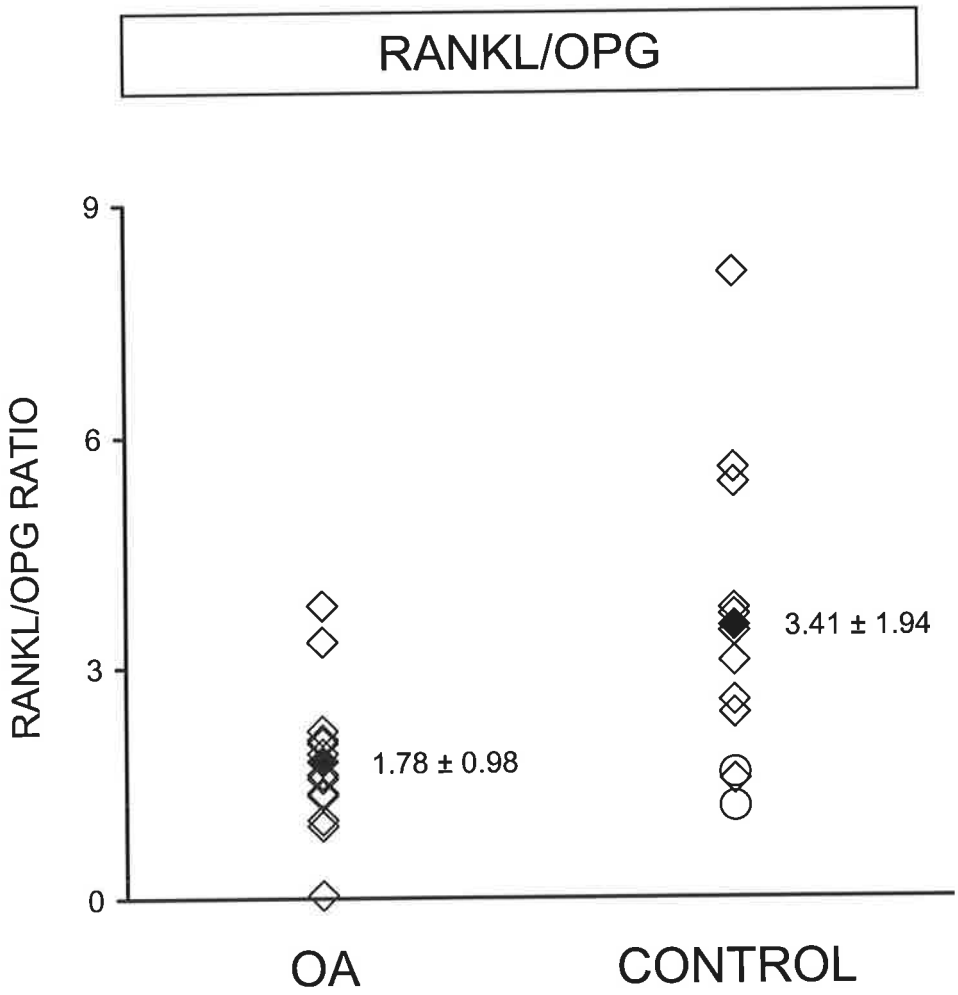

Figure 6.16: Relative ratio of RANKL/OPG mRNA expression in intertrochanteric trabecular bone from OA (n = 13) and control (n = 12) individuals. The RANKL/OPG mRNA ratio was significantly lower in OA patients versus controls ($p < 0.02$). Two control cases, <40 years old, are indicated (O). The means are indicated (◆). Values are mean ± standard deviation.

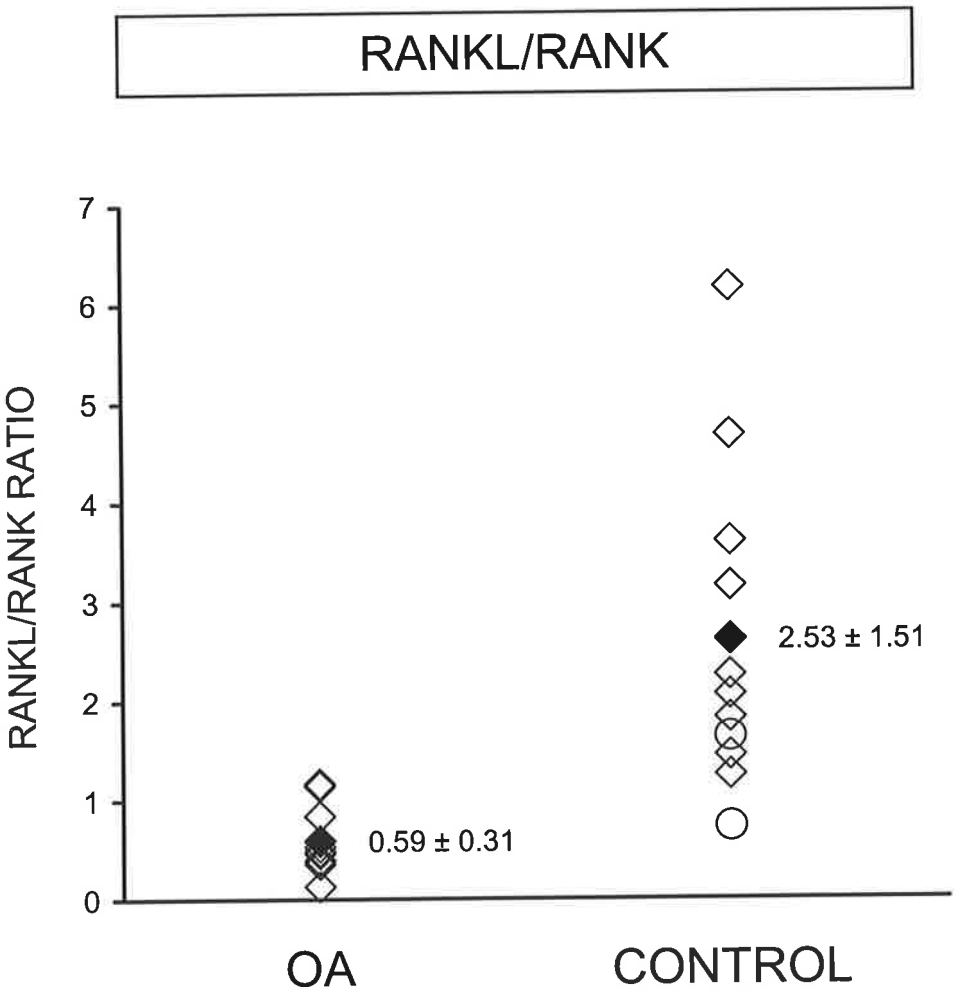

Figure 6.17: Relative ratio of RANKL/RANK mRNA expression in intertrochanteric trabecular bone from OA (n = 12) and control (n = 12) individuals. The RANKL/RANK mRNA ratio was significantly lower in OA patients versus controls ($p < 0.001$). Two control cases, <40 years old, are indicated (○). The means are indicated (◆). Values are mean ± standard deviation.

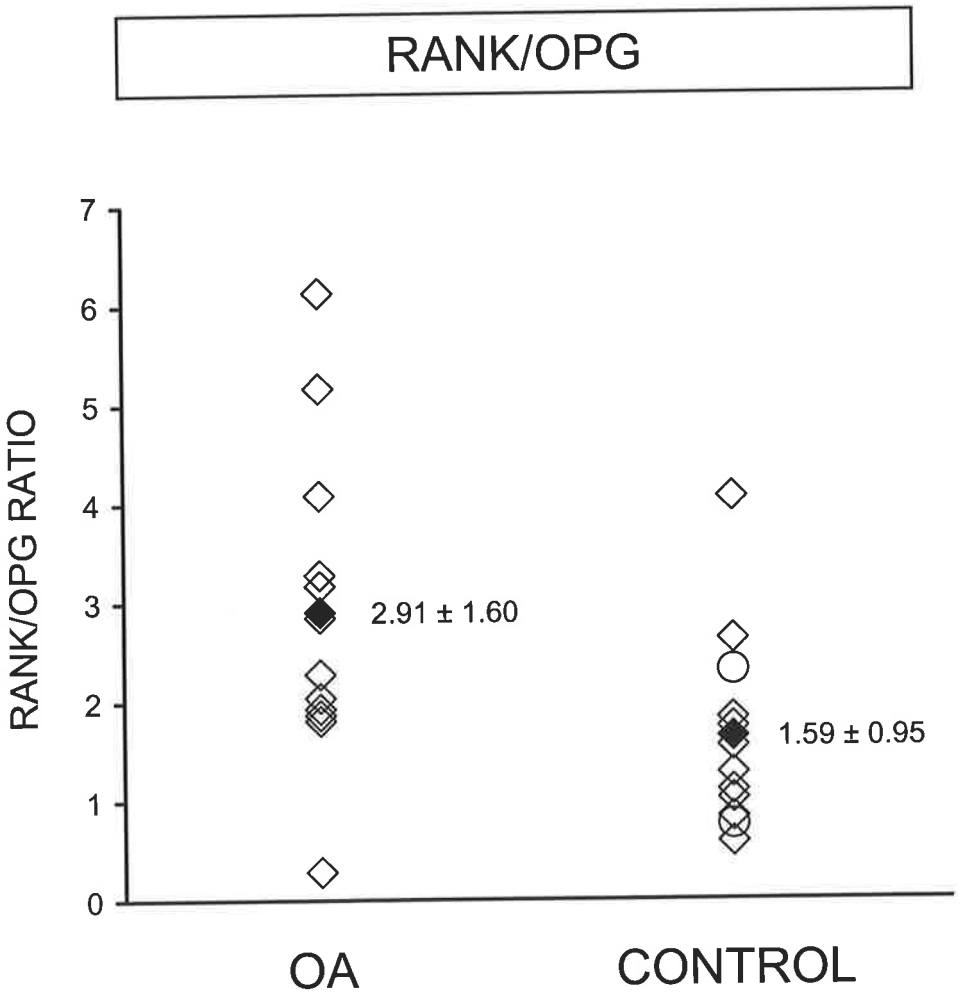

Figure 6.18: Relative ratio of RANK/OPG mRNA expression in intertrochanteric trabecular bone from OA (n = 12) and control (n = 12) individuals. The ratio of RANKL/OPG mRNA was significantly elevated in OA patients versus controls (p < 0.03). Two control cases, <40 years old, are indicated (○). The means are indicated (◆). Values are mean ± standard deviation.

OA bone suggests that the effective activity of RANKL to promote osteoclast formation and thus increase the pool size of active osteoclasts is reduced in the bone microenvironment of OA. In fact, the histomorphometric bone resorption index, eroded surface, ES/BS, measured in trabecular bone sampled from the intertrochanteric region of the proximal femur, was significantly reduced in the OA group compared to the controls (Tables 7.4 and 7.5; Chapter 7.4.5).

Table 6.5 RT-PCR product ratios in intertrochanteric trabecular bone sampled from OA and control cases aged over 40 years.

Ratio	OA (n = 13) *(aged 49-85 years)*	Control >40 years (n = 10) *(aged 43-85 years)*
RANKL/OPG	1.78 ± 0.98	3.82 ± 1.86 [a]
RANKL/RANK	0.59 ± 0.31; n = 12	2.81 ± 1.49 [b]
RANK/OPG	2.91 ± 1.60; n = 12	1.61 ± 0.99 [c]

Values are mean ± standard deviation.
[a] $p < 0.01$; [b] $p < 0.001$; [c] $p < 0.04$ vs. OA group.

6.4.5 Age-related changes in mRNA expression in OA and control trabecular bone from the human proximal femur

To investigate whether there are any age-related changes in the mRNA expression levels in OA human trabecular bone from the proximal femur, each PCR product/GAPDH mRNA ratio was plotted as a function of increasing age in years, and analysed by linear regression analysis, as for the controls in Chapter 5.4.4. IL-6/GAPDH mRNA expression was not dependent on age in the OA group (Figure 6.19), consistent with the control group data for

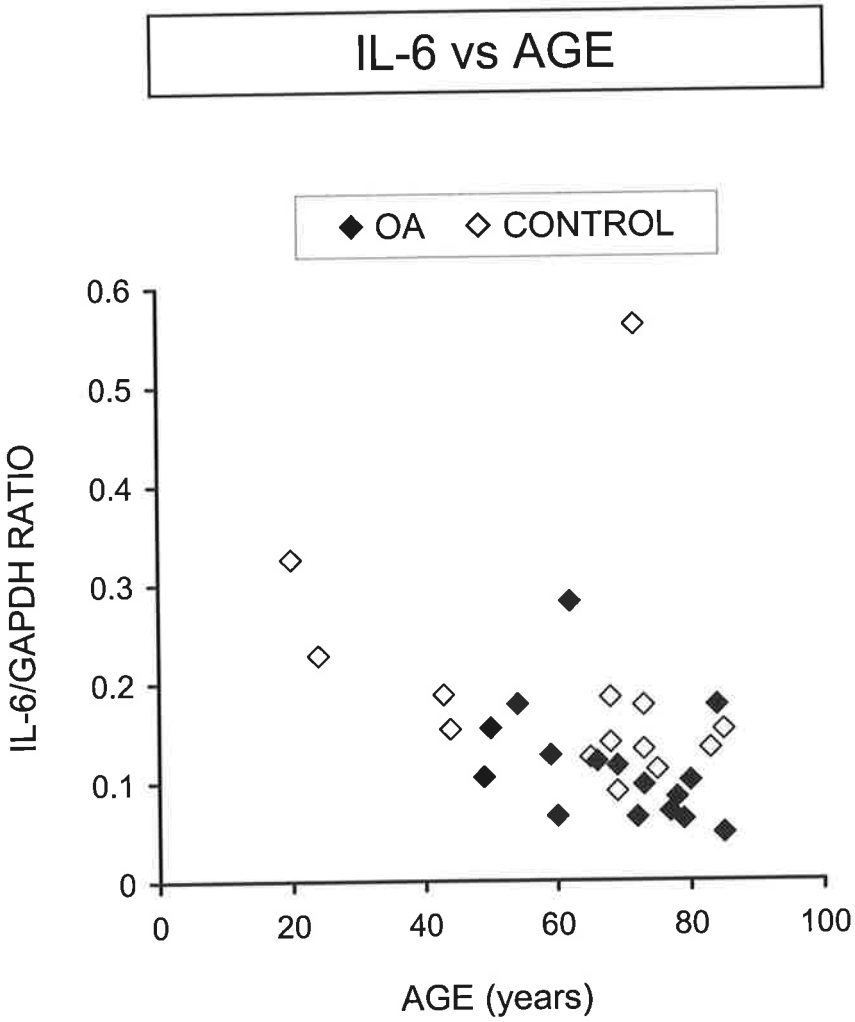

Figure 6.19: Changes in IL-6/GAPDH mRNA with age in intertrochanteric trabecular bone from OA (n = 16) and control (n = 14) individuals. No significant change in IL-6/GAPDH mRNA with age was found in either OA (IL-6/GAPDH = -0.002*AGE + 0.25; r = -0.38 and p = NS) or controls (IL-6/GAPDH = -0.001*AGE + 0.28; r = -0.24 and p = NS). NS = not significant.

IL-6 mRNA (Figure 6.19; Chapter 5.4.4). The IL-11/GAPDH mRNA ratio declined with age in the OA group (r = -0.50, $p < 0.04$; Figure 6.20), consistent with the control group data (Figure 6.20; Chapter 5.4.4). When plotted as a function of age, the OA and control values for IL-11 mRNA appeared to be two distinct groups with little overlap, with the OA bone samples containing significantly lower levels of IL-11 mRNA than controls across the entire age range investigated ($p < 0.001$; Figures 6.3 and 6.20; Table 6.3). Thus, the reduced expression of IL-11 mRNA in the OA group suggests a reduced promotion of osteoclastogenesis by osteoblasts in OA trabecular bone, with age and compared to control human bone.

There was a positive association and marked increase of CTR/GAPDH mRNA expression with age in the OA group (r = 0.60, $p < 0.01$; Figure 6.21), which is in contrast to no association between CTR mRNA and age in control bone samples (Figure 6.21; Chapter 5.4.4). As both age and RANK mRNA expression were significantly associated with CTR mRNA expression in OA bone (Figures 6.21 and 6.12, respectively), a multiple regression analysis was performed to determine the contribution of age and RANK mRNA expression to CTR mRNA expression. CTR mRNA expression was dependent on RANK mRNA expression and not age in OA bone ($p < 0.002$), suggesting that similar cells types, that is osteoclast precursors and/or mature osteoclasts, are contributing to the measured CTR and RANK mRNA expression in these OA bone samples. Intriguingly, when the OCN/GAPDH mRNA results were plotted against age for the OA bone samples, there was a positive association and marked increase in OCN mRNA with age (r = 0.63, $p < 0.01$; Figure 6.22). This age-related increase in OCN mRNA expression in the OA group was strikingly different to the control group, where OCN mRNA expression declined with age (Figure 6.22; Chapter 5.4.4), with the control bone samples containing significantly lower

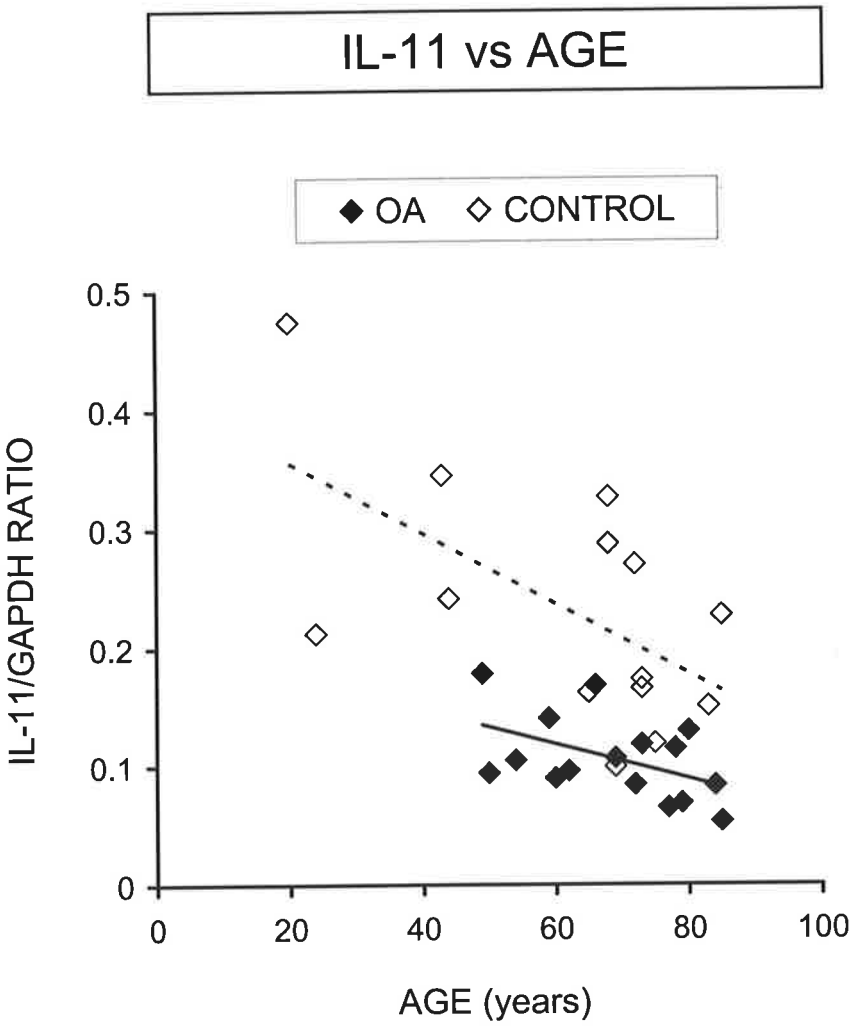

Figure 6.20: Changes in IL-11/GAPDH mRNA with age in intertrochanteric trabecular bone from OA (n = 16) and control (n = 14) individuals. There was a significant decline in IL-11/GAPDH mRNA for both OA (IL-11/GAPDH = -0.002*AGE + 0.21; r = -0.50 and $p < 0.04$ {solid line}) and control (IL-11/GAPDH = -0.003*AGE + 0.41; r = -0.60 and $p < 0.02$ {broken line}) groups with age.

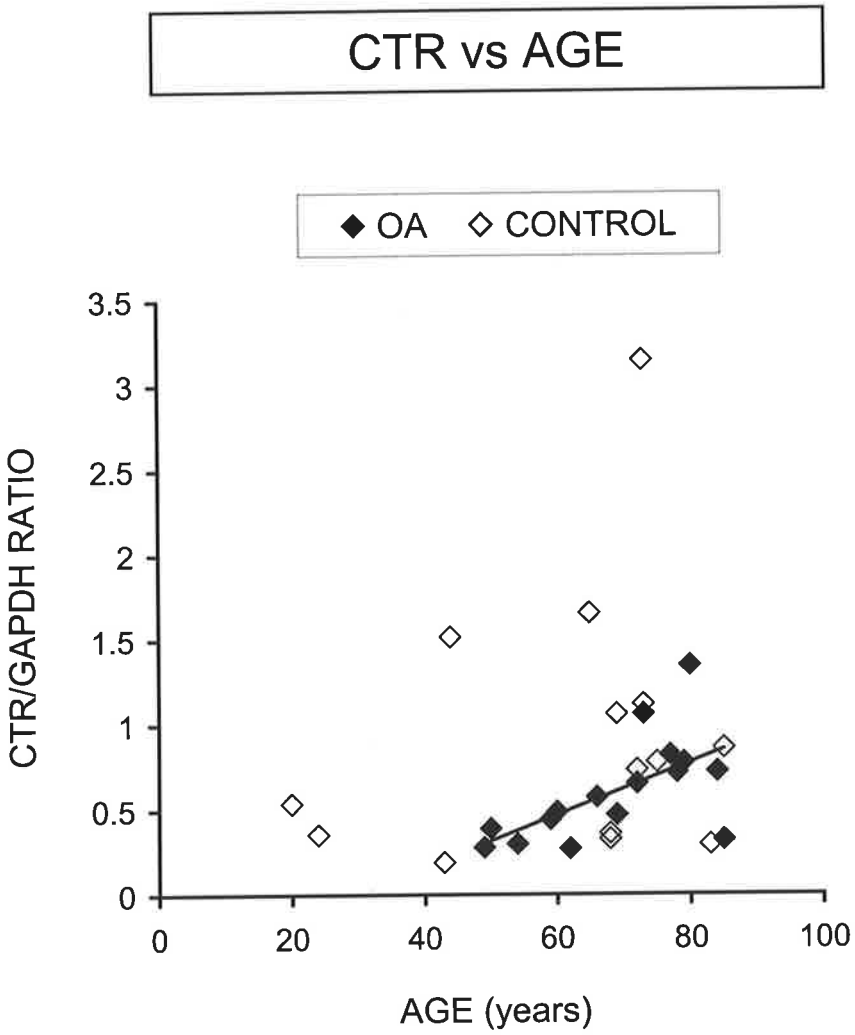

Figure 6.21: Changes in CTR/GAPDH mRNA with age in intertrochanteric trabecular bone from OA (n = 16) and control (n = 14) individuals. In OA, there was a significant increase in CTR/GAPDH mRNA with age (CTR/GAPDH = 0.02*AGE - 0.45; r = 0.60 and $p < 0.01$ {solid line}). There was no significant change in CTR/GAPDH mRNA with age in controls (CTR/GAPDH = 0.01*AGE + 0.42; r = 0.22 and p = NS). NS = not significant.

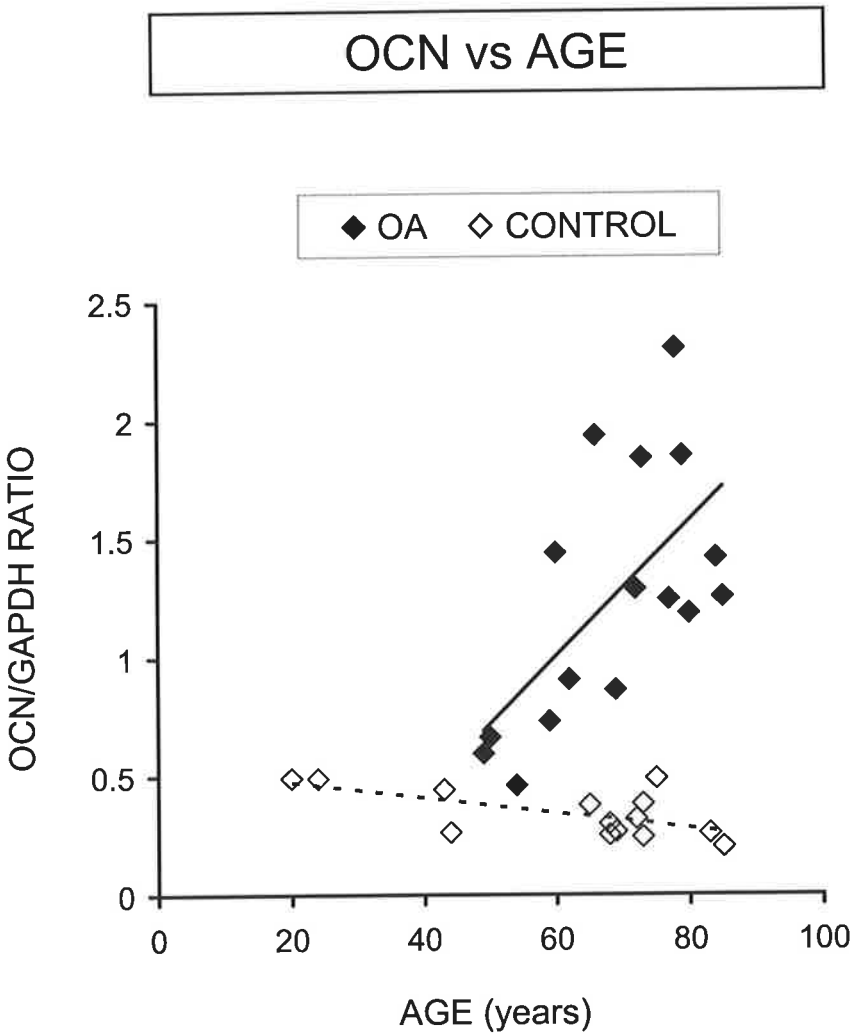

Figure 6.22: Changes in OCN/GAPDH mRNA with age in intertrochanteric trabecular bone from OA (n = 16) and control (n = 14) individuals. In OA, there was a significant increase in OCN/GAPDH mRNA with age (OCN/GAPDH = 0.03*AGE - 0.71; r = 0.63 and $p < 0.01$ {solid line}). In controls, there was a significant decline in OCN/GAPDH mRNA with age (OCN/GAPDH = -0.003*AGE + 0.54; r = -0.64 and $p < 0.01$ {broken line}).

levels of OCN mRNA than OA ($p < 0.00001$; Figure 6.5; Table 6.3). Furthermore, the OA group appeared to diverge from control OCN mRNA levels between the ages of 40 to 50 years. As OCN is regarded as an indicator of bone formation and a molecular marker for osteoblasts (Stein and Lian, 1993), the age-related increase in OCN mRNA expression in OA suggests that there is an increase in bone formation and/or osteoblastic activity with age. However, no correlation was observed between the histomorphometric bone formation index, osteoid surface, OS/BS, and age in the OA group (Figure 7.20; Chapter 7.4.6), for trabecular bone sampled from the intertrochanteric region of the proximal femur. Intriguingly, a positive association was observed between OS/BS and OCN/GAPDH mRNA expression, in contiguous trabecular bone samples from the intertrochanteric region for the OA group (Figure 7.30; Chapter 7.4.7), which was not evident for the controls. The CTR/OCN mRNA ratio was not dependent on age for either the OA or control group (results not shown). It is reiterated that it is not known whether the relative expression level of OCN mRNA is representative of the concentration of OCN protein in these trabecular bone samples.

The values corresponding to mRNA levels for RANKL, OPG, and RANK in OA trabecular bone from the proximal femur were plotted as a function of age. The expression of RANKL/GAPDH mRNA showed no statistical dependence on age for the OA group (Figure 6.23), in contrast to the age-related increase in RANKL mRNA in control bone samples (Figure 6.23; Chapter 5.4.4). However, when the outlier, case OA13 (73-year-old male), was removed from the OA data set, the RANKL/GAPDH mRNA expression ratio significantly increased with age in the OA group ($r = 0.70$, $p < 0.008$). OPG/GAPDH mRNA expression was not dependent on age in the OA group (Figure 6.24), consistent with the relatively constant expression of OPG mRNA with age in controls (Figure 6.24;

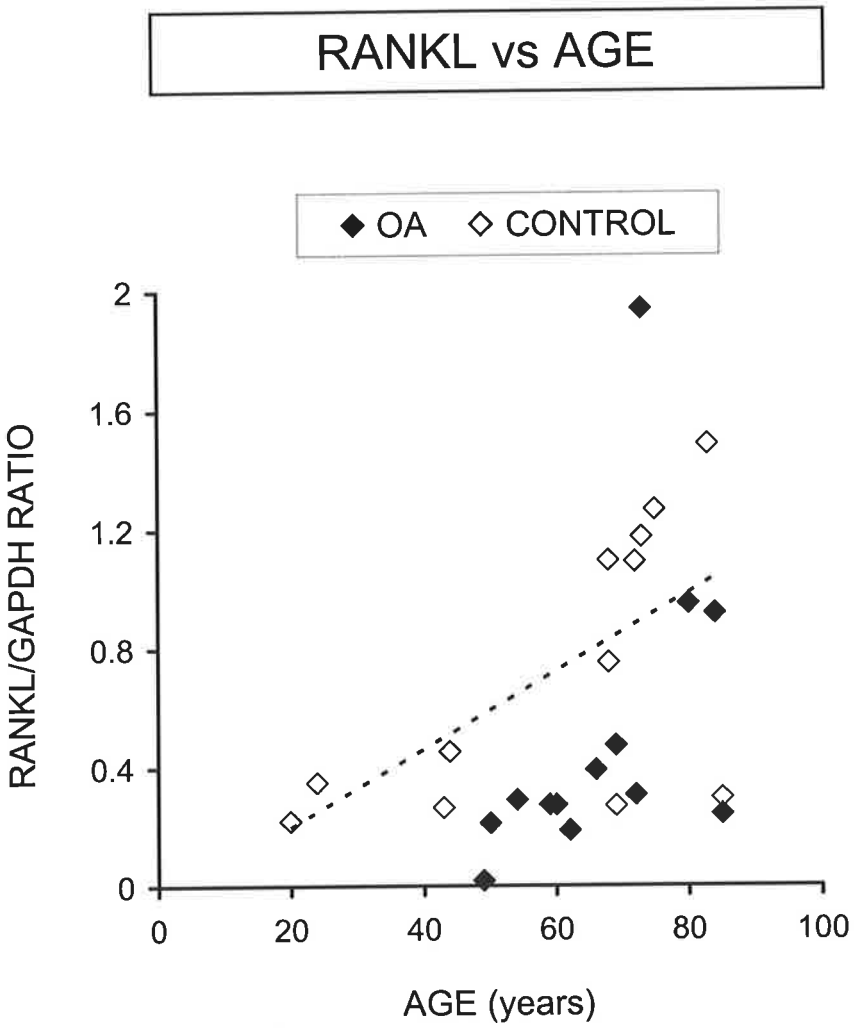

Figure 6.23: Changes in RANKL/GAPDH mRNA with age in intertrochanteric trabecular bone from OA (n = 13) and control (n = 12) individuals. There was no significant change in RANKL/GAPDH mRNA with age in OA (RANKL/GAPDH = 0.02*AGE - 0.91; r = 0.50 and p = NS; n = 12 (without outlier); RANKL/GAPDH = 0.02*AGE - 0.66; r = 0.70 and $p < 0.008$). There was a significant increase in RANKL/GAPDH mRNA with age in controls (RANKL/GAPDH = 0.01*AGE - 0.07; r = 0.62 and $p < 0.02$ {broken line}). NS = not significant.

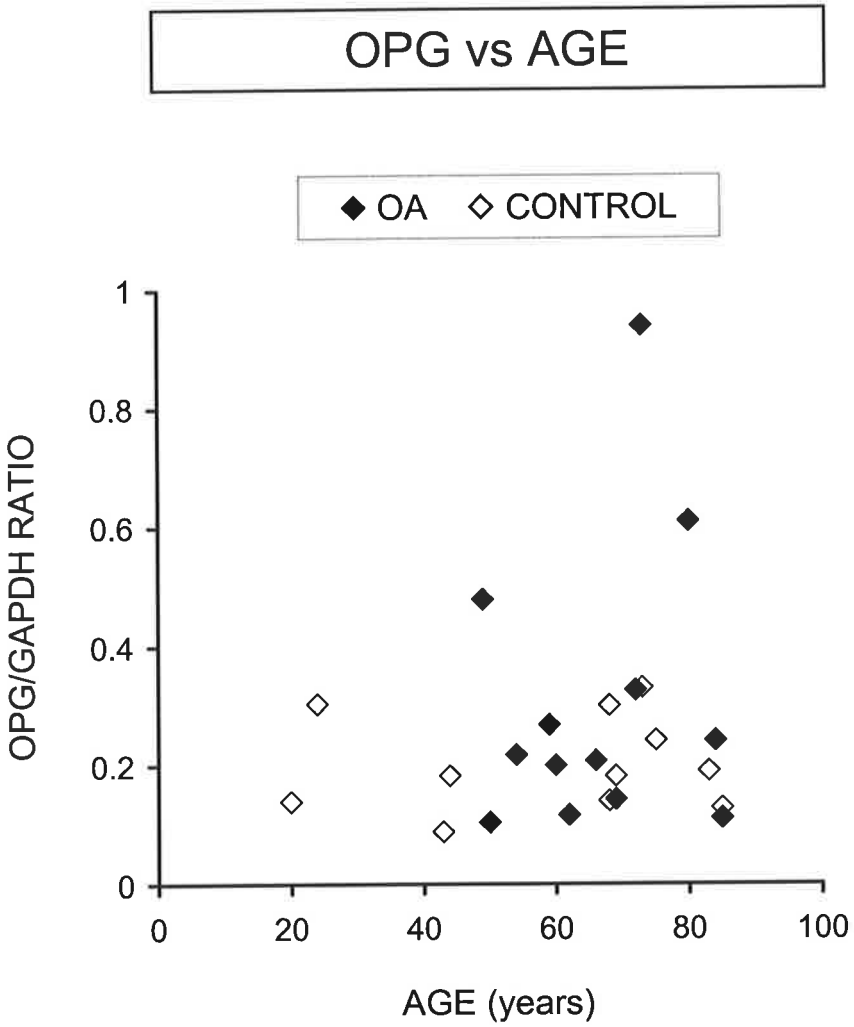

Figure 6.24: Changes in OPG/GAPDH mRNA with age in intertrochanteric trabecular bone from OA (n = 13) and control (n = 12) individuals. No significant change in OPG/GAPDH mRNA with age was found in either OA (OPG/GAPDH = 0.004*AGE + 0.06; r = 0.18 and p = NS) or controls (OPG/GAPDH = 0.0005*AGE + 0.18; r = 0.13 and p = NS). NS = not significant.

Chapter 5.4.4). There was a positive association between the expression of RANK/GAPDH mRNA and age for the OA bone samples ($r = 0.58$, $p < 0.04$; Figure 6.25), and the level of RANK gene expression tended to be higher than controls at each age (Figure 6.8; Table 6.4). Further, when the outlier, case OA13 (73-year-old male) with a high relative expression level of RANK/GAPDH mRNA, was removed from the OA data set, the positive association between RANK mRNA and age was statistically more significant ($r = 0.76$, $p < 0.005$). In contrast, there was no age-related change in RANK mRNA in control bone samples (Figure 6.25; Chapter 5.4.4). As age, and both the expression of CTR mRNA and RANKL mRNA, were significantly associated with RANK mRNA expression in OA bone (Figures 6.25, 6.12, and 6.14, respectively), multiple regression analyses were performed to determine the contribution of age and CTR mRNA expression, and age and RANKL mRNA expression, to RANK mRNA expression. Firstly, RANK mRNA expression was dependent on CTR mRNA expression and not age in OA bone ($p < 0.002$), suggesting that similar cells types, that is osteoclast precursors and/or mature osteoclasts, are contributing to the measured RANK and CTR mRNA expression in these OA bone samples. Secondly, RANK mRNA expression was dependent on RANKL mRNA expression and not age in OA bone ($p < 0.00002$), suggesting that either the same stimulus regulates the expression of both RANKL and RANK mRNA, or, more likely, that the same stimulus up-regulates RANKL and causes recruitment of RANK-expressing osteoclast precursor cells in OA bone.

The ratio of RANKL to OPG has been hypothesised, based upon a large amount of evidence, to be the main determinant of the pool size of active osteoclasts in the local bone microenvironment (Hofbauer *et al.*, 2000). Therefore, the RANKL/OPG mRNA ratio was investigated with age in the OA group. Interestingly, as observed for the controls (Figure

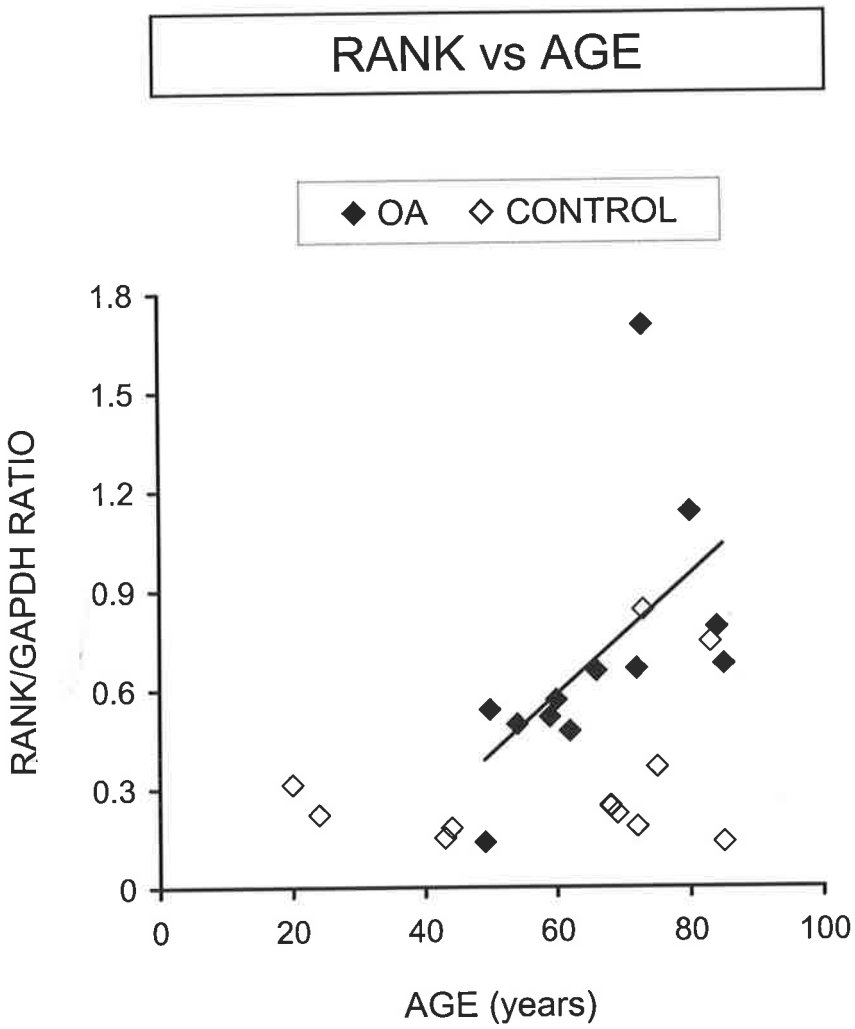

Figure 6.25: Changes in RANK/GAPDH mRNA with age in intertrochanteric trabecular bone from OA (n = 12) and control (n = 12) individuals. In OA, there was a significant increase in RANK/GAPDH mRNA with age (RANK/GAPDH = 0.02*AGE - 0.50; r = 0.58 and $p < 0.04$ {solid line}; n = 11 (without outlier); RANK/GAPDH = 0.01*AGE - 0.32; r = 0.76 and $p < 0.005$). There was no significant change in RANK/GAPDH mRNA with age in controls (RANK/GAPDH = 0.003*AGE + 0.12; r = 0.32 and p = NS). NS = not significant.

6.26; Chapter 5.4.4), the ratio of RANKL/OPG mRNA increased with age in the OA group ($r = 0.58$, $p < 0.03$; Figure 6.26). Importantly, the values segregated such that the RANKL/OPG mRNA levels in control bone were higher than for OA across the entire age range examined (Figures 6.16 and 6.26; Table 6.5). This suggests that the effective activity of RANKL to promote osteoclast formation and thus increase the pool size of active osteoclasts is reduced in the bone microenvironment of OA, consistent with the observation of reduced eroded bone surface, ES/BS, in OA (Tables 7.4 and 7.5; Chapter 7.4.5). The RANKL/RANK mRNA ratio increased with age in the OA group ($r = 0.58$, $p < 0.04$; Figure 6.27), which is in contrast to no age-dependence in controls (Figure 6.27; Chapter 5.4.4). The difference between the OA and control groups for RANKL/RANK mRNA expression with age is reflected in the 24 times greater variance in this value in controls than OA (F-statistic = 23.5, representing the ratio of the control variance to OA variance, $p < 0.00001$; Table 6.5). More importantly, the plot of RANKL/RANK mRNA versus age showed a clear segregation of values between control and OA individuals, such that the values for OA were lower than controls across the age range examined (Figures 6.17 and 6.27; Table 6.5). The RANK/OPG mRNA ratio, as observed for controls (Chapter 5.4.4), was not dependent on age for the OA group (results not shown).

6.5 DISCUSSION

OA of the hip is characterised by progressive degenerative damage to the articular joint cartilage and changes in the subchondral bone trabecular architecture. Trabecular bone structural changes are also present at sites distal to the joint articular surface, in the proximal femur and in the iliac crest (Crane *et al.*, 1990; Fazzalari *et al.*, 1992), suggesting that they are not solely reactive to the joint pathology. Very few studies have investigated the cellular and molecular processes or mechanisms that may lead to these structural

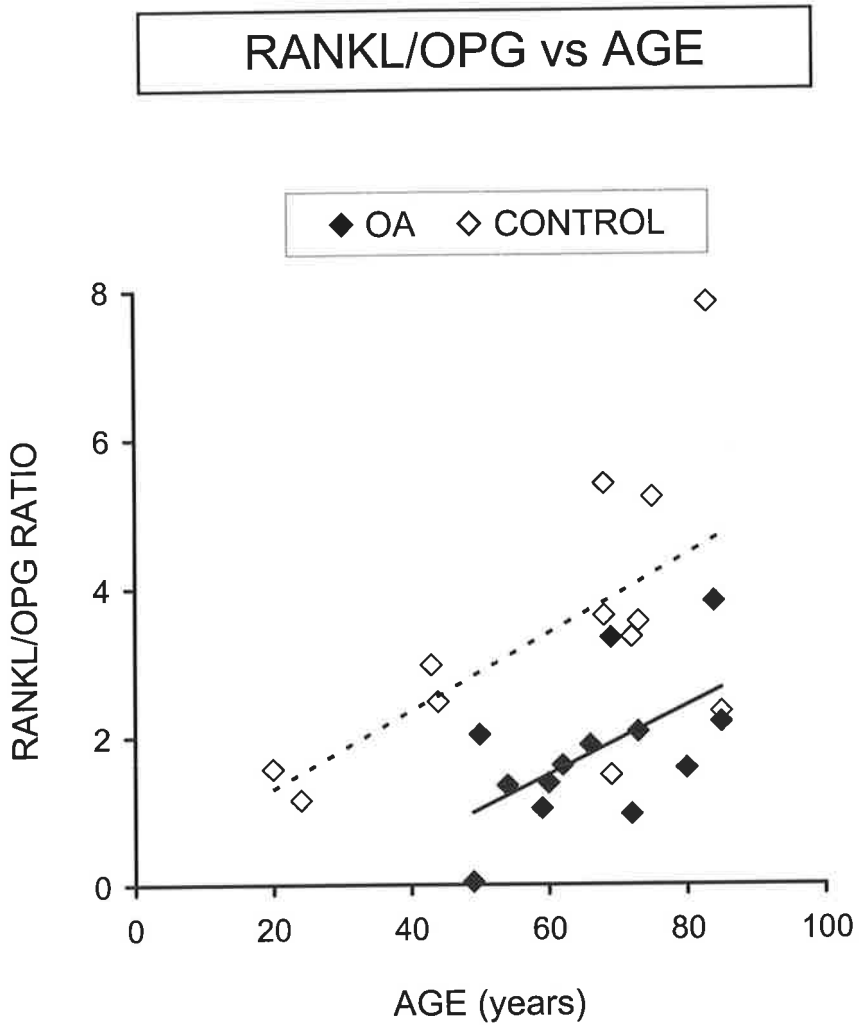

Figure 6.26: Changes in the RANKL/OPG mRNA ratio with age in intertrochanteric trabecular bone from OA (n = 13) and control (n = 12) individuals. There was a significant increase in the RANKL/OPG mRNA ratio for both OA (RANKL/OPG = 0.05*AGE - 1.31; r = 0.58 and $p < 0.03$ {solid line}) and control (RANKL/OPG = 0.05*AGE + 0.25; $r = 0.60$ and $p < 0.03$ {broken line}) groups with age.

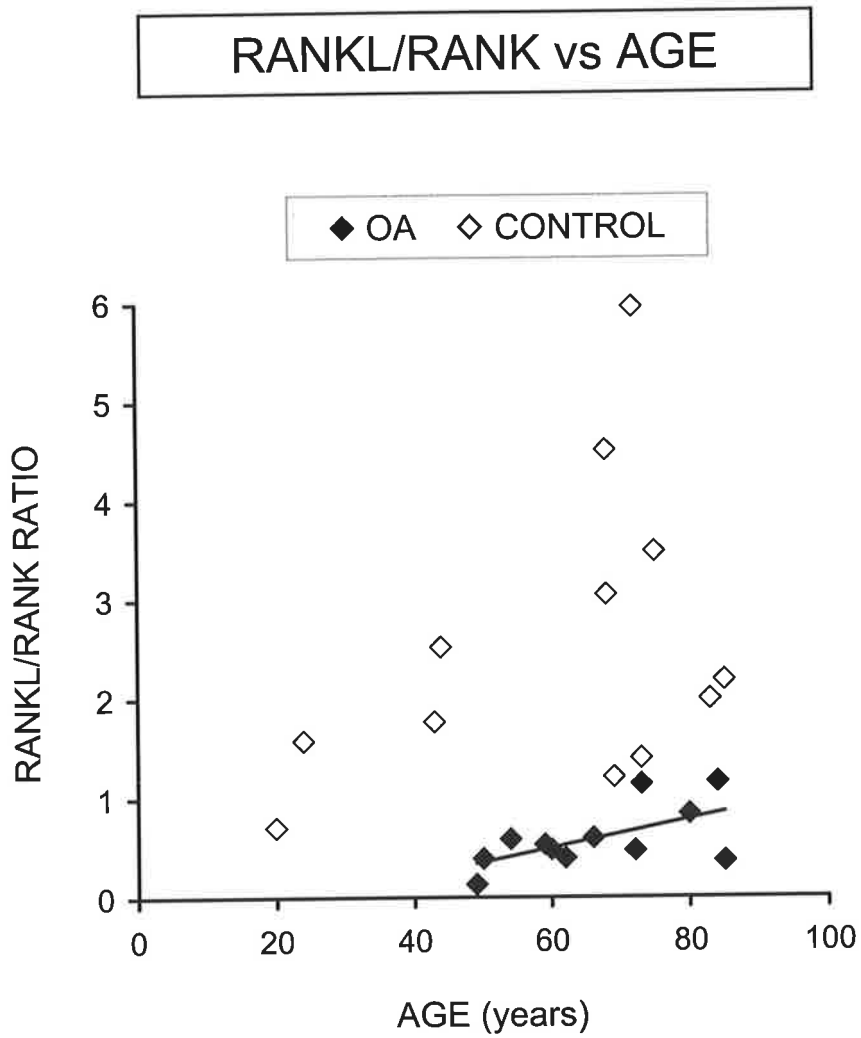

Figure 6.27: Changes in the RANKL/RANK mRNA ratio with age in intertrochanteric trabecular bone from OA (n = 12) and control (n = 12) individuals. In OA, there was a significant increase in the RANKL/RANK mRNA ratio with age (RANKL/RANK = 0.01*AGE - 0.36; r = 0.58 and $p < 0.04$ {solid line}). There was no significant change in the RANKL/RANK mRNA ratio with age in controls (RANKL/RANK = 0.03*AGE + 0.86; r = 0.40 and p = NS). NS = not significant.

changes in OA trabecular bone. The aim of the work described in this chapter was to investigate mRNA expression, corresponding to a select group of skeletally active molecules, in the human trabecular bone microenvironment of individuals suffering from primary OA of the hip in comparison to non-OA controls, at a skeletal site distal from the degenerative changes at the joint articular surface. The intertrochanteric region of the proximal femur was chosen for sampling of trabecular bone because characteristic architectural changes at this site in OA have been described previously (Crane *et al.*, 1990), while it is unaffected by the sclerotic and cystic changes of the OA femoral head (Fazzalari *et al.*, 1985), and therefore unlikely to be affected directly by any inflammatory cytokines in the synovial fluid.

The select group of skeletally active molecules chosen for investigation included the key regulators of osteoclast biology and bone metabolism, RANKL, OPG, and RANK, two cytokines capable of promoting osteoclast formation, IL-6 and IL-11, and the CTR and OCN, as cell specific markers of osteoclasts and osteoblasts, respectively. Striking differences were found in the pattern of mRNA expression of these skeletally active molecules in intertrochanteric trabecular bone from individuals with primary hip OA in comparison to non-OA control cases. The observed differences in mRNA expression between the OA and control groups are highly unlikely to be due to inherent differences in mRNA stability between surgical (OA) and postmortem (control) bone tissues, as total RNA and specific mRNA transcripts were found to be relatively stable in surgical bone tissues stored at 4°C up to 12 hours after retrieval, and in postmortem bone tissues stored at 4°C up to 3.5 days postmortem (as described in Chapter 3). Furthermore, differences in mRNA expression, corresponding to the skeletally active molecules described in this chapter, have been observed in intertrochanteric trabecular bone from 13 patients

undergoing total hip arthroplasty surgery for a fractured neck of femur (#NOF) in comparison to 23 postmortem control cases (H. Dassios *et al.*, unpublished observations). For instance, the expression of RANKL/GAPDH mRNA was significantly increased in #NOF patients in comparison to controls, whereas OPG/GAPDH mRNA expression did not differ between these groups. Consequently, there was a significant increase in the relative expression level of the RANKL/OPG mRNA ratio in the #NOF patients. Interestingly, there were no differences in the expression level of CTR/GAPDH and OCN/GAPDH mRNA between the #NOF patients and postmortem controls (H. Dassios *et al.*, unpublished observations).

6.5.1 Enhanced OCN mRNA expression in OA human trabecular bone from the intertrochanteric region of the proximal femur

OCN, the major non-collagenous protein of bone matrix, is utilised as an indicator of bone formation as it is one of the marker genes for the progression of osteoblastic differentiation (Stein and Lian, 1993). The enhanced mRNA expression of OCN in OA trabecular bone was the most striking difference between the OA and control groups (Figure 6.5; Table 6.3). This finding suggests that there may be an increase in bone formation and/or osteoblastic activity in intertrochanteric OA bone. Interestingly, mean osteoid volume, OV/TV, was significantly increased in intertrochanteric OA bone compared to control bone (Tables 7.4 and 7.5; Chapter 7.4.5). However, the histomorphometric bone formation parameters of osteoid surface, OS/BS, and osteoid volume, OV/BV, although higher in OA bone, were not significantly different between the OA and control groups (Tables 7.4 and 7.5; Chapter 7.4.5). Furthermore, trabecular bone volume, BV/TV, at the intertrochanteric region was not different between the OA and control groups (Tables 7.4 and 7.5; Chapter 7.4.5). The enhanced expression of OCN mRNA in OA intertrochanteric bone supports a

previous finding of increased OCN protein extracted from iliac crest bone of OA subjects (Gevers and Dequeker, 1987; Raymaekers *et al.*, 1992). However, it is not known whether the relative expression level of OCN mRNA is representative of the concentration of OCN protein in the intertrochanteric OA and control trabecular bone samples. In addition, it is not known whether there is a difference in the degree of carboxylation of OCN between the OA and control groups. This is important as the vitamin K-dependent gamma-carboxylated OCN has a high affinity for hydroxyapatite, whereas undercarboxylated OCN binds to hydroxyapatite with a low affinity, and is less likely to be incorporated into the bone matrix (Vermeer *et al.*, 1995).

The biological function of OCN in the bone microenvironment has not been precisely defined. Mice deficient in OCN have increased bone density, cortical thickness, and bone formation (Ducy *et al.*, 1996). However, osteoblast number was not altered in OCN deficient mice, suggesting that the role of OCN in the bone microenvironment is an inhibitor of osteoblast function (Ducy *et al.*, 1996). Subsequently, those investigators reported that bone mineral maturation was impaired in OCN-deficient mice, suggesting that OCN is involved in the regulation of bone mineral turnover (Boskey *et al.*, 1998). Interestingly, there were significantly more osteoclasts per unit surface in the OCN-deficient mice than in the wild-type mice (Ducy *et al.*, 1996). Conversely, OCN has been shown to be important for osteoclast recruitment both in *in vitro* and in animal models (Chenu *et al.*, 1994; DeFranco *et al.*, 1991; Glowacki *et al.*, 1989; Glowacki *et al.*, 1991; Ingram *et al.*, 1994; Liggett *et al.*, 1994).

Dequeker *et al.* (1993b) postulated that there may be an increased biosynthetic activity of osteoblasts in OA, a possibility supported by Hilal *et al.* (1998) showing that bone explants

and osteoblasts from OA subchondral bone produced more IGF-I than controls. Furthermore, Hilal *et al.* (1998) have shown an increase in *de novo* OCN synthesis, in response to 1,25-$(OH)_2D_3$ stimulation, by OA osteoblasts *in vitro*. Given that the phenotypic alterations in the OA subchondral osteoblast-like cells were observed in *ex vivo* and *in vitro* experiments, Hilal *et al.* (1998) have suggested that the altered OA osteoblast phenotype may be caused by a primary defect in these cells, rather than a secondary response to local chemical and/or systemic factors *in vivo*. The increased metabolic capacity of the OA osteoblast is unlikely to translate into increased mineralisation of OA bone, as a number of reports have shown OA bone to be hypomineralised (Brown *et al.*, 2002; Grynpas *et al.*, 1991; Helliwell *et al.*, 1996; Li and Aspden, 1997a; Li and Aspden, 1997b; Mansell and Bailey, 1998). Moreover, a recent study has shown that subchondral bone osteoblasts, from individuals with hip OA, produce a molecularly distinct collagen, type I collagen homotrimer (i.e., three $\alpha 1$ chains of type I collagen; Bailey *et al.*, 2002).

Alterations in the mechanical environment of the hip joint can adversely affect the direction and distribution of bone loading. Severe OA hip patients tend to have altered gait patterns due to joint pain and anatomical differences, which would result in abnormal directions of bone loading (Moore *et al.*, 1994), and perhaps an increase in local load amplitudes. Mechanical stimulation of rat caudal vertebrae resulted in an increase in the expression level of OCN mRNA on the trabecular bone surface (Lean *et al.*, 1995). Interestingly, osteoblast-like cells from OA hip patients were responsive to mechanical microstrain *in vitro*, of a physiological magnitude, in comparison to osteoblast-like cells from age-matched osteoporotic hip fracture patients, which were unresponsive to mechanical strain (Stanford *et al.*, 2000). Furthermore, a trend for an increased protein level of OCN was observed when the OA osteoblast-like cell cultures were subjected to

microstrain (Stanford *et al.*, 2000). Osteocytes are suggested to be the mechanosensing cells of the bone matrix (Burger and Klein-Nulend, 1999). In addition to OCN being a marker gene for the progression of osteoblastic differentiation (Stein and Lian, 1993), osteocytes have been shown to constitutively express OCN mRNA (Mason *et al.*, 1996). A limitation of the semi-quantitative RT-PCR analysis of OCN mRNA expression in the OA and control intertrochanteric trabecular bone samples is that the cellular origin(s) of the measured OCN mRNA is not known.

A significant age-related increase in the abundance of OCN mRNA was observed in intertrochanteric trabecular bone from individuals with severe primary OA, with onset between the ages of 40 and 50 years (Figure 6.22). This age-related increase in OCN mRNA in the OA group was strikingly different to the control group, where OCN mRNA expression declined with age (Figure 6.22; Chapter 5.4.4), with the control bone samples containing significantly lower levels of OCN mRNA than OA (Figure 6.5; Table 6.3). In addition, a significant reduction in the CTR/OCN mRNA ratio was observed in OA trabecular bone (Figure 6.11; Table 6.3), suggestive of a skewing of the remodelling process toward net bone formation in OA. These analyses are consistent with the known maintenance or increase of bone volume in OA versus the age-dependent bone loss found in the general population (Crane *et al.* 1990). Furthermore, trabecular bone volume, BV/TV, at the intertrochanteric region of the proximal femur, was maintained with age for the OA group, in comparison to an age-related decline in BV/TV in controls (Figure 7.17; Chapter 7.4.6). Interestingly, the number of mesenchymal stem cells with osteogenic potential, cultured from femoral neck bone marrow, did not change with age for OA hip patients (Oreffo *et al.*, 1998a). In interpreting the CTR/OCN mRNA data, it is important to note that it is not known whether immature and/or mature osteoclast cells are

representative of the measured CTR mRNA, nor whether the CTR mRNA expression is representative of the number of osteoclasts and/or the number of calcitonin receptors on each osteoclast. However, a positive association was observed between the expression of CTR and RANK mRNA in the OA bone samples (Figure 6.12), which was not evident in the control bone samples. Given that RANK is expressed on the surface of the same cell types as the CTR in bone, namely osteoclasts and their precursors (Hsu *et al.*, 1999; Myers *et al.*, 1999), similar cells types, that is osteoclast precursors and/or mature osteoclasts, are contributing to the measured RANK and CTR mRNA expression in the OA bone samples.

6.5.2 Reduced IL-6 and IL-11 mRNA expression in OA human trabecular bone from the intertrochanteric region of the proximal femur

IL-6 and IL-11 are two cytokines that share many biological properties, including the ability to stimulate osteoclast development from their haematopoietic precursors (Martin *et al.*, 1998). There was a significant reduction in the mRNA expression of both IL-6 and IL-11 in OA intertrochanteric trabecular bone in comparison to the control group (Figures 6.2 and 6.3, respectively; Table 6.3). However, the difference in IL-6 mRNA expression between the OA and control groups was dependent upon two control cases aged less than 40 years (Table 6.3). The reduced expression of IL-6 and IL-11 mRNA in the OA group suggests that there may be a reduced promotion of osteoclastogenesis by osteoblasts in OA trabecular bone. Although the stimulatory effects of IL-11 on osteoclast differentiation appear to be mediated by inducing RANKL expression on marrow stromal/osteoblastic cells (Nakashima *et al.*, 2000; Yasuda *et al.*, 1998b), the reported effects of IL-6 on RANKL-RANK-promoted osteoclast development are conflicting (Brandstrom *et al.*, 1998; Hofbauer *et al.*, 1998; Hofbauer *et al.*, 1999b; Nakashima *et al.*, 2000; O'Brien *et al.*, 1999; Vidal *et al.*, 1998). IL-6 and IL-11 mRNA expression did not correlate with

RANKL, OPG or RANK mRNA expression in either the OA or control bone samples. Given that IL-6 can be produced by a number of cell types in the bone microenvironment, including marrow stromal cells, monocyte-macrophages, osteoblasts, and osteoclasts (Girasole *et al.*, 1992; Kishimoto, 1989; Linkhart *et al.*, 1991; O'Keefe *et al.*, 1997), it is not known which cell types are contributing to the IL-6 mRNA levels measured in the OA and control bone samples. Interestingly, while expression of IL-6 mRNA in the bone is contributed by several cell types, IL-11 mRNA is likely to be expressed predominantly by cells of mesenchymal origin, namely, cells of the osteoblast lineage (Paul *et al.*, 1990).

A number of reports have described OA individuals to have a better preserved bone mass compared to age- and sex-matched controls, independent of body mass index (Gotfredsen *et al.*, 1990; Lethbridge-Cejku *et al.*, 1996; Nevitt *et al.*, 1995). A recent study has shown that elevated bone mineral density (BMD) is associated with a subsequent accelerated joint space narrowing rate (Goker *et al.*, 2000). Primary OA and osteoporosis are rarely both seen in the same patient, and clinical reports and epidemiological studies have suggested that there is a negative association between the two age-related diseases (Cooper *et al.*, 1991; Dequeker *et al.*, 1993a; Soloman *et al.*, 1982; Verstraeten *et al.*, 1991). Interestingly, a polymorphism in the IL-6 gene promoter, characterised by lower plasma levels of IL-6 (Fishman *et al.*, 1998), is associated with higher BMD at the femoral neck and lumbar spine in a longitudinal study of Caucasian young men, both during late puberty and after development of peak bone mass (Lorentzon *et al.*, 2000).

There was a significant decline with age in the expression of IL-11 mRNA in both the OA and control groups (Figure 6.20), suggesting that the effect of IL-11 to stimulate osteoclast development may decline with age in both groups. In the case of IL-6 mRNA, an observed

trend toward a decline with age in the OA and control groups did not reach statistical significance (Figure 6.19). IL-11 has been suggested to play a critical role in the hierarchy of osteoclastogenic factors, since *in vitro* its expression is induced by a number of hormone and local activators of osteoclast formation (Manolagas, 1995; Romas *et al.*, 1996; Yang and Yang, 1994). In addition, neutralisation of IL-11 has been shown *in vitro* to suppress osteoclast development induced by 1,25-$(OH)_2D_3$, PTH, IL-1, and TNF-α (Girasole *et al.*, 1994). Although the evidence to date suggests one major role for IL-11 in bone is to act as an upstream stimulatory signal for osteoclast differentiation (Martin *et al.*, 1998; as detailed in Chapter 5.1), the full role of this pleiotropic cytokine in the bone microenvironment is not completely understood. IL-11 has also been implicated as a suppressor of osteoblastic synthetic activity. For example, IL-11 dose-dependently inhibited nodule formation and reduced alkaline phosphatase expression in rat calvarial cell cultures (Hughes and Howells, 1993b). The reduced IL-11 mRNA expression in OA bone (Figure 6.3; Table 6.3) can be understood in terms of this dual activity of the cytokine to activate osteoclastogenesis and inhibit osteoblast synthetic activity.

When plotted as a function of age, the OA and control values for IL-11 mRNA appeared to be two distinct groups with little overlap, with the OA bone samples containing significantly lower levels of IL-11 mRNA than controls across the entire age range investigated (Figure 6.20). It is intriguing that there was no obvious age of onset of the difference between the IL-11 mRNA in OA and controls (Figure 6.20). That is, this difference between the two groups may be pre-existing. However, the expression level of OCN mRNA increased in OA between 40 and 50 years of age and diverged from the controls, in which OCN mRNA expression decreased with age (Figure 6.22). The latter result in non-OA controls is consistent with a reported decrease in OCN protein at the

femoral neck and iliac crest with age (Boonen *et al.*, 1997; Vanderschueren *et al.*, 1990). It is possible that the IL-11 data point to a *pre-existing* biochemical and genetic difference between the bone of OA individuals and the remainder of the population. This difference is likely to be of considerable magnitude, since it was clearly discernible in the data described in this chapter, with relatively small numbers of subjects and in which the control group was unselected apart from the exclusion criteria of evidence of OA or other bone-related diseases. The reduced expression of IL-11 mRNA may be a reflection of the genetic determinants that result in altered bone turnover in OA, leading eventually to the altered bone structure that is characteristic of OA.

6.5.3 Reduced expression of the RANKL/OPG mRNA ratio in OA human trabecular bone from the intertrochanteric region of the proximal femur

RANKL, OPG, and RANK are key regulators of osteoclast biology and bone metabolism. Extensive bone marrow cell culture studies have shown that growth factors, cytokines, and peptide and steroid hormones modulate the gene expression of RANKL, OPG, and to a lesser extent, RANK (Hofbauer *et al.*, 2000; Hofbauer and Heufelder, 2001; Horowitz *et al.*, 2001; Suda *et al.*, 1999). A significant positive association was observed between RANKL and OPG mRNA in both OA and control intertrochanteric trabecular bone (Figure 6.13). This finding suggests that the same stimuli/stimulus up-regulate/s both RANKL and OPG mRNA expression in these bone samples. Experiments *in vitro*, in which bone marrow stromal cells and osteoblast-like cells were treated with pro-resorptive agents such as IL-1β and TNF-α, have shown up-regulation of both RANKL and OPG mRNA (as detailed in Chapter 5.5.3; Hofbauer *et al.*, 1999b; Takami *et al.*, 2000). A significant positive association was also observed between the expression of RANKL and RANK mRNA in both OA and control intertrochanteric trabecular bone (Figure 6.14). This

finding suggests that either the same stimulus regulates the expression of both RANKL and RANK mRNA, or, more likely, that the same stimulus up-regulates RANKL and causes recruitment of RANK-expressing osteoclast precursor cells (as detailed in Chapter 5.5.3). Although the positive relationships between RANKL and OPG mRNA (Figure 6.13), and RANKL and RANK mRNA (Figure 6.14), were observed in both OA and control bone, the data show clear differences. For a given level of OPG or RANK mRNA expression, there was a lower level of RANKL mRNA expression in OA bone compared with controls. This finding suggests that there is a lower net osteoclastogenic influence in OA intertrochanteric trabecular bone. Furthermore, these data are consistent with lower levels of IL-6 and IL-11 mRNA in OA bone compared to controls (Figures 6.2 and 6.3, respectively; Table 6.3), both of which act on cells of the osteoblast lineage to promote osteoclast formation (Martin *et al.*, 1998).

RANKL and OPG are important downstream signals of osteoclast biology, onto which many hormonal, chemical, and biochemical signals converge (Hofbauer and Heufelder, 2001). Hofbauer *et al.* (2000) hypothesised that the ratio of RANKL to OPG is the main determinant of the pool size of active osteoclasts in the local bone microenvironment, acting as a final effector system to modulate differentiation, activation, and apoptosis of osteoclasts. The ratio of RANKL/OPG mRNA was positively associated with age in both the OA and control groups (Figure 6.26) and this is largely driven by the changing RANKL mRNA levels (compare Figures 6.23 and 6.24). This suggests that the effective activity of RANKL to promote osteoclast formation and thus increase the pool size of active osteoclasts, at the intertrochanteric region of the proximal femur, may be increased with age in both OA and control individuals. Moreover, the histomorphometric bone resorption index, eroded surface, ES/BS, was found to increase as the RANKL/OPG

mRNA ratio increased, in contiguous trabecular bone samples for the control group (Figure 7.8; Chapter 7.4.3). However, the plot of RANKL/OPG mRNA versus age showed a clear segregation of values between control and OA individuals, such that the values for OA were lower than controls across the entire age range examined (Figures 6.16 and 6.26; Table 6.5). This suggests that the effective activity of RANKL to promote osteoclast formation is reduced in the bone microenvironment of OA, consistent with the observation of reduced ES/BS in OA intertrochanteric bone (Tables 7.4 and 7.5; Chapter 7.4.5). The lower ratio of RANKL/OPG mRNA in OA bone (Figure 6.16; Table 6.5) occurs in the context of no statistical difference in the mean RANKL/GAPDH and OPG/GAPDH mRNA expression between the OA and control groups (Figures 6.6 and 6.7; respectively; Table 6.4). This is indicative of a robust and multidimensional control process operating to maintain the integrity of the skeleton.

As detailed in Chapter 5.5.3, the osteoclastogenic capacity of the stromal/osteoblast cell has been shown to depend upon the expression ratio of RANKL/OPG, reflecting the differentiation stage of the cell (Deyama *et al.*, 2000; Gori *et al.*, 2000; Nagai and Sato, 1999). Undifferentiated or pre-osteoblastic or bone marrow stromal cells reportedly express abundant RANKL and low levels of OPG, and, further, the increased RANKL/OPG ratio correlates with the cells capacity to support osteoclast formation and activation. Conversely, the RANKL/OPG ratio is lower in mature osteoblasts and their capacity to support osteoclast development is suppressed or lost (Deyama *et al.*, 2000; Gori *et al.*, 2000; Nagai and Sato, 1999). This suggests that the lower level of RANKL/OPG mRNA in OA intertrochanteric trabecular bone (Figure 6.16; Table 6.5) may be associated with a decreased number of stromal/osteoblast cells with an osteoclastogenic capacity.

In interpreting *in vivo* results, it is important to note that, while RANKL is expressed by a relatively restricted number of cell types, including stromal/osteoblastic cells and T cells, OPG is expressed more widely by several cell types (Collin-Osdoby *et al.* 2001; Kwon *et al.*, 1998; Simonet *et al.*, 1997; Tan *et al.*, 1997; Yasuda *et al.*, 1998b). Given that the cellular origin of the measured RANKL and OPG mRNA in the OA and control trabecular bone samples is not known, it was intriguing to observe a strong positive association between the bone resorption index, ES/BS, and the ratio of RANKL/OPG mRNA, measured in contiguous trabecular bone samples for the controls (Figure 7.8; Chapter 7.4.3). This association between ES/BS and RANKL/OPG mRNA was found to be almost entirely because of the RANKL component (compare Figures 7.9 and 7.10; Chapter 7.4.3). Thus, this relationship strongly supports the concept that the surrogate measures of RANKL and OPG mRNA levels relate directly to levels of expression of the corresponding proteins in the bone tissue.

As detailed in section 6.5.1, severe OA hip patients tend to have altered gait patterns due to joint pain and anatomical differences, which would result in abnormal directions of bone loading (Moore *et al.*, 1994), and perhaps an increase in local load amplitudes. Rubin *et al.* (1999) have shown that mechanical strain inhibits osteoclast formation in murine bone marrow cell cultures. Subsequently, those investigators reported that mechanical strain of murine bone stromal cells resulted in a reduction of RANKL mRNA expression and an associated inhibition of osteoclast formation (Rubin *et al.*, 2000). These reports are of interest given that the effective activity of RANKL to promote osteoclast formation is reduced in the bone microenvironment of OA (Figure 6.16; Table 6.5).

6.5.4 The potential use of gene expression profiles in trabecular bone biopsies for predicting development of OA: involvement of other skeletally active factors

The aetiology of OA is poorly understood, although it has both heritable and environmental components (Chitnavis *et al.*, 1997; Felson *et al.*, 1998; Spector *et al.*, 1996a). As detailed in section 6.1, numerous reports of an altered trabecular bone structure and bone matrix in individuals with OA (reviewed in Dequeker and Luyten, 2000) suggest that the bone changes may precede the joint degeneration of OA, or may arise secondarily to the joint pathology, or indeed may occur in parallel with the cartilage damage, driven by the same causative agent(s) that lead to cartilage disease. Interestingly, recent reports have shown that bone changes may precede cartilage changes in the onset and progression of primary OA (Bruno *et al.*, 1999; Goker *et al.*, 2000). The work described in this chapter has established that patients with primary hip OA have a different mRNA expression profile of several skeletally active molecules at the intertrochanteric region of the proximal femur. This skeletal site is remote from the subchondral bone that undergoes well-characterised secondary changes in severe OA (Fazzalari *et al.*, 1992). Specifically, the expression of IL-11 and OCN mRNA provided a clear discriminator between OA patients and controls (as detailed in sections 6.5.1 and 6.5.2). It is possible that these differences in gene expression point to *pre-existing* genetic and biochemical differences between the bone of OA individuals and the remainder of the population. Thus, the potential use of this type of gene expression data to identify individuals that will progress to OA needs to be explored. These types of predictive analyses may be possible, given that the mRNA expression of several skeletally active molecules was similar between the proximal femur (intertrochanteric and femoral neck regions) and iliac crest for a cohort of postmortem

individuals (as detailed in Chapter 4); with the latter skeletal site amenable to biopsy. It is not known whether this relationship holds for OA individuals.

A more complete gene profile in skeletal regions distal to the degenerative joint changes in patients with primary OA needs to be established. Specifically, a profile of gene expression in the iliac crest that is consistent with that in the proximal femur, such as at the intertrochanteric region, in the same OA individuals would be supportive of the hypothesis of a generalised skeletal involvement in OA. There are a large number of skeletally active molecules known to regulate the differentiation and activity of the cells of bone remodelling, osteoblasts and osteoclasts. To further explore the molecular mechanisms for the altered trabecular bone structure and bone turnover in OA, RT-PCR (semi-quantitative, as described in this thesis, or quantitative) could be used to determine the profile of expression of a greater number of genes known to be involved in bone metabolism, than those described in this chapter. Examples of molecular factors involved in the regulation of osteoclast formation, either as stimulatory or inhibitory factors, that would be of interest include IL-1α and IL-1β, IL-17, IL-18, macrophage colony stimulating factor (M-CSF), prostaglandin E_2 (PGE_2), PTH, and TNF-α (Martin and Udagawa, 1998; Roodman, 1999). The mRNA expression level of TNF-α in trabecular bone was similar between the iliac crest, femoral neck, and intertrochanteric region, for a cohort of postmortem individuals (Table 4.3; Chapter 4.4.2). Furthermore, a significant positive association was observed between IL-6 and TNF-α mRNA expression levels (Table 4.5; Chapter 4.4.4), suggesting the co-regulation of these pro-osteoclastic cytokines in the postmortem bone samples. Interestingly, Hilal *et al.* (2001) have shown that osteoblast-like cells cultured from OA subchondral bone produce more PGE_2 than controls, and that the OA osteoblasts are resistant to PTH stimulation. The data for CTR mRNA should be confirmed with the

analysis of other osteoclast cell markers, including carbonic anhydrase II, cathepsin K, and TRAP, which are highly expressed by osteoclasts (Martin and Udagawa, 1998). The mRNA expression level of TRAP in trabecular bone was similar between the iliac crest, femoral neck, and intertrochanteric region, for a cohort of postmortem individuals (Table 4.3; Chapter 4.4.2). Furthermore, significant positive associations were observed between CTR, TRAP, and RANK mRNA expression levels (Figures 4.1 and 4.2; Table 4.4; Chapter 4.4.4), suggesting that similar cells types, that is osteoclasts and their precursors, are contributing to the measured CTR, TRAP, and RANK mRNA expression in the postmortem bone samples. Bone anabolic factors, including the bone morphogenetic proteins, BMP-2, BMP-4, and BMP-7 (Rosen and Thies, 1992), and the growth factors TGF-β1, TGF-β2, TGF-β3, IGF-I, and IGF-II (Centrella *et al.*, 1994; Hayden *et al.*, 1995), would be of interest as the bone matrix from the iliac crest of OA subjects has been found to contain a higher content of IGF-I, IGF-II, and TGF-β compared with that in control subjects (Dequeker *et al.*, 1993b; Gevers and Dequeker, 1987). Furthermore, Hilal *et al.* (1998) have shown that osteoblast-like cells cultured from OA subchondral bone produce more IGF-I than cells from individuals without OA pathology. The mRNA expression level of TGF-β1 in trabecular bone was similar between the iliac crest, femoral neck, and intertrochanteric region, for a cohort of postmortem individuals (Table 4.3; Chapter 4.4.2). Given that OA subchondral femoral head and femoral neck trabecular bone have been shown to be hypomineralised (Brown *et al.*, 2002; Grynpas *et al.*, 1991; Helliwell *et al.*, 1996; Li and Aspden, 1997a; Li and Aspden, 1997b; Mansell and Bailey, 1998), and that a recent study has shown that subchondral bone osteoblasts, from individuals with hip OA, produce a molecularly distinct collagen, type I collagen homotrimer (Bailey *et al.*, 2002), the analysis of bone matrix protein genes would be of specific interest. This analysis would include type I collagen (α1 and α2 chains), osteonectin, osteopontin (OPN), and bone

sialoprotein (Karsenty, 1999). The mRNA expression level of OPN in trabecular bone was similar between the iliac crest, femoral neck, and intertrochanteric region, for a cohort of postmortem individuals (Table 4.3; Chapter 4.4.2). Furthermore, an interesting observation was a significant positive association between OCN and OPN mRNA expression levels (Figure 4.5; Table 4.7; Chapter 4.4.4), in the postmortem bone samples.

The use of gene array technology would allow a comparison of a larger number of genes between OA and control individuals, to determine whether consistent over- or under-expression of one or more genes is characteristic of OA. In addition to identifying a different profile of genes between OA and control individuals, gene array analysis may identify novel targets that are involved in the regulation of bone remodelling and thus the bony changes characteristic of OA. In a preliminary study, RNA isolated from intertrochanteric trabecular bone from three primary OA hip patients was compared with that from three age- and sex-matched non-OA controls, using a commercial cDNA microarray containing over 4000 known human genes. This microarray approach identified 24 genes that were consistently differentially expressed, showing a greater than 2-fold difference, in all three OA and control samples (S. Gronthos *et al.*, unpublished observations). Interestingly, a recent report has described the use of gene array technology to identify differentially expressed genes between normal and OA human cartilage (Aigner *et al.*, 2001).

6.5.5 Conclusions

Numerous reports of an altered trabecular bone structure and bone matrix in individuals with OA (reviewed in Dequeker and Luyten, 2000) suggest that the bone changes may precede the joint degeneration of OA, or may arise secondarily to the joint pathology, or

indeed may occur in parallel with the cartilage damage, driven by the same causative agent(s) that lead to cartilage disease. Whichever of these is the case, in order to devise effective treatments for OA, it is clearly important to consider the bony component of this disease and to develop an understanding of the cellular and molecular processes that lead to the bony changes. Striking differences were observed in the pattern of mRNA expression, corresponding to a number of skeletally active molecules, in trabecular bone from the intertrochanteric region of the proximal femur, between patients with severe primary hip OA and non-OA controls. The intertrochanteric region is remote from the subchondral bone that undergoes well-characterised secondary changes in severe OA. Specifically, the expression of factors associated with the development of the osteoclast, the RANKL/OPG mRNA ratio, IL-6 mRNA, and IL-11 mRNA, were all significantly reduced in OA bone compared to non-OA bone. Conversely, mRNA expression of the osteoblastic cell marker, OCN, was significantly enhanced in OA bone compared to non-OA bone, consistent with a previous finding of increased OCN protein in iliac crest bone from OA subjects (Gevers and Dequeker, 1987; Raymaekers *et al.*, 1992). The expression of IL-11 and OCN mRNA provided a clear discriminator between OA hip patients and controls. Thus, it is possible that these differences in gene expression point to *pre-existing* genetic and biochemical differences between the bone of OA individuals and the remainder of the population. Finally, the way in which the expression of these skeletally active molecules relates to trabecular bone structure and bone turnover in the OA and control human bone microenvironment needs to be established. Indeed, these data enabled the identification of a number of correlations between mRNA expression and trabecular bone volume and bone turnover indices, measured in contiguous human bone tissues sampled from the proximal femur. These results are presented in Chapter 7.

CHAPTER 7

MOLECULAR HISTOMORPHOMETRY OF CONTROL AND OSTEOARTHRITIC TRABECULAR BONE FROM THE HUMAN PROXIMAL FEMUR

7.1 INTRODUCTION

The mechanisms that lead to the particular shape and structure of bony trabeculae in general, and in the human proximal femur in particular, are clearly complex, involving both mechanical and biochemical inputs. There is a substantial amount of information about the molecular factors that are capable of regulating the differentiation and activity of the cell types that are responsible for the remodelling of bone, the osteoblast and the osteoclast (as detailed in Chapter 5.1). The process of bone remodelling is involved in both the maintenance and alteration of trabecular structures. The current knowledge of systemic and local regulation of bone remodelling has been developed primarily from studies utilising *in vitro* cell culture systems, human and predominantly murine, and animal studies such as the effects of gene deletion studies in mice (reviewed in Ducy *et al.*, 2000; Hofbauer and Heufelder, 2001; Raisz, 1999; Roodman, 1999; Suda *et al.*, 1999). However, it is important to investigate the mRNA expression of skeletally active genes in the local human bone microenvironment, where paracrine mediators of bone turnover can be measured with their local regulatory mechanisms intact. This led to investigation of the mRNA expression of a number of skeletally active molecules in non-diseased and osteoarthritic (OA) trabecular bone, sampled from the human proximal femur, which is described in Chapters 5 and 6 of this thesis. The way in which the expression of these skeletally active molecules relates to trabecular bone structure and bone turnover in the human bone microenvironment needs to be established.

Therefore, this chapter describes an innovative experimental approach, involving the analysis of the mRNA expression of molecular regulators of bone remodelling, in combination with histomorphometric assessment of trabecular bone structure and bone turnover, in contiguous human bone tissues sampled from the proximal femur. A similar

investigational approach has been reported by Abildgaard *et al.* (2000), where histomorphometric indices of bone resorption, in iliac crest biopsies from multiple myeloma patients, positively correlated with protein levels of IL-6, in marrow plasma aspirated from the bone biopsy area. Further, the concentration of transforming growth factor (TGF)-β1, extracted from the bone matrix of iliac crest biopsies (from breast cancer patients) and femoral head trabecular bone (from hip fracture patients), was shown to positively correlate with osteoblast- and osteoclast-covered surfaces in the same bone samples (Pheilschifter *et al.*, 1998). Similarly, histomorphometric parameters of bone formation and resorption positively correlated with the bone matrix concentration of insulin-like growth factor type I (IGF-I) in the same iliac crest biopsies from the Pheilschifter *et al.* (1998) study (Seck *et al.*, 1998). Interestingly, the concentration of bone matrix TGF-β1 did not correlate with trabecular bone volume in either iliac crest or femoral head bone samples (Pheilschifter *et al.*, 1998), whereas there was a positive correlation between the concentration of bone matrix IGF-I and trabecular bone volume in iliac crest bone (Seck *et al.*, 1998).

As detailed in Chapter 6.1, OA is characterised by progressive degenerative damage to the articular joint cartilage, and is associated with a conservation of bone mass and a different, more rigid structure of the subchondral bone (reviewed in Dequeker and Luyten, 2000). Although the major focus of research into the aetiology of OA has been on the articular cartilage, the disease is also consistently associated with marked changes in the subchondral bone. Fazzalari *et al.* (1992) have investigated the structural parameters of the trabecular bone in the proximal femur adjacent to OA hips. Typically, the subchondral bone is sclerotic, with increased trabecular bone volume, and altered trabecular size and spacing, compared to age-matched controls (Crane *et al.*, 1990; Fazzalari *et al.*, 1992). It

has been postulated that such changes are due to alteration of loading through the joint because of the articular disease (Bland and Cooper, 1984) or, alternatively, that they are secondary to pathology within the joint. However, similar structural changes are also present at sites distal to the joint articular surface, in the proximal femur and in the iliac crest (Crane *et al.*, 1990; Fazzalari *et al.*, 1992), suggesting that they are not merely reactive to the joint pathology. The different bone structure in hip OA is accompanied by a reduced incidence of trabecular microfracture (Fazzalari *et al.*, 1987), and altered mechanical properties, with a more rigid trabecular bone in the femoral neck (Li and Aspden, 1997b; Martens *et al.*, 1983). Since this more rigid bone would have a reduced ability to absorb shock, it has been postulated that the bone changes in OA might exacerbate the disease or could even precede and be causative of the cartilage degeneration (Radin *et al.*, 1972; Dequeker *et al.*, 1996).

Consistent with this concept of generalised bone structural changes in OA, bone matrix from the iliac crest of OA subjects has been found to contain a higher content of growth factors that may have important regulatory roles in bone turnover, IGF-I, IGF-II, and TGF-β, and an increased concentration of osteocalcin (OCN) protein, compared with that in control subjects (Dequeker *et al.*, 1993b; Gevers and Dequeker, 1987; Raymaekers *et al.*, 1992). Interestingly, a recent study has shown that osteoblasts isolated from subchondral bone of individuals with hip OA produce a molecularly distinct collagen, type I collagen homotrimer (Bailey *et al.*, 2002). This finding was associated with a disorganised collagen matrix and reduced mineralisation, which could potentially weaken the biomechanical properties of the bone matrix, resulting in collagen overproduction and thickening of the bone (Bailey and Knott, 1999).

These reports of an altered trabecular bone structure and bone matrix in individuals with OA suggest that the bone changes may precede the joint degeneration of OA, or may arise secondarily to the joint pathology, or indeed may occur in parallel with the cartilage damage, driven by the same causative agent(s) that lead to cartilage disease. Whichever of these is the case, in order to devise effective treatments for OA, it is clearly important to consider the bony component of this disease and to develop an understanding of the cellular and molecular processes that lead to the bony changes.

Striking differences were observed in the pattern of mRNA expression corresponding to a number of skeletally active molecules in human OA bone, at a skeletal site distal to the degenerative joint changes in OA, in comparison to skeletal site-matched non-OA bone (described in Chapter 6). For example, the expression of factors associated with the development of the osteoclast, the RANKL/OPG mRNA ratio, IL-6 mRNA, and IL-11 mRNA, were all significantly reduced in OA bone compared to non-OA bone (Figures 6.16, 6.2, and 6.3, respectively; Chapter 6.4.3). Conversely, mRNA expression of the osteoblastic cell marker, OCN, was significantly enhanced in OA bone compared to non-OA bone (Figure 6.5; Chapter 6.4.3), consistent with a previous finding of increased OCN protein in iliac crest bone from OA subjects (Gevers and Dequeker, 1987; Raymaekers *et al.*, 1992). This chapter describes investigation of histomorphometric parameters of trabecular bone structure and bone turnover in bone sampled from the proximal femur of individuals suffering from primary hip OA, compared to skeletal site-matched non-OA/control individuals. Further, the relationships between the histomorphometric parameters and the mRNA expression levels of skeletally active molecules (independently described in Chapters 5 and 6), measured in contiguous trabecular bone samples from both OA and control individuals, are examined. The skeletally active molecules in this

investigation include the key regulators of osteoclast biology and metabolism, RANKL, RANK, and OPG, the cytokines IL-6 and IL-11, both of which are involved in the regulation of the RANKL-RANK-OPG system of osteoclast development, the osteoblastic cell marker, OCN, and the bone osteoclastic cell marker, the calcitonin receptor (CTR) (as detailed in Chapter 5.1). The specific skeletal site that the trabecular bone was sampled from was the intertrochanteric region of the proximal femur, as trabecular bone in this region has previously been shown to be structurally different between OA and control bone (Crane *et al.*, 1990). Moreover, the intertrochanteric region is remote from the subchondral bone that undergoes well-characterised secondary changes in severe OA (Fazzalari *et al.*, 1992). The control group comprised a cohort of autopsy individuals, who had not suffered from conditions thought to affect their bone turnover status and in particular, macroscopic examination of the femoral head showed no significant sign of joint degeneration, according to the criteria of Collins (1949).

7.2 CHAPTER AIMS

- To investigate whether there are gender-related differences and age-related changes in the histomorphometric parameters describing trabecular structure and bone turnover in non-diseased/control human trabecular bone tissue, sampled from the intertrochanteric region of the proximal femur.

- To examine the relationship between the histomorphometric parameters describing trabecular structure and bone turnover, and the levels of expression of mRNA corresponding to factors known to have important regulatory roles in bone remodelling, measured in contiguous bone samples from the intertrochanteric region of the proximal

femur for non-diseased/control individuals (mRNA expression data for controls is independently described in Chapter 5).

- To investigate whether there are gender-related differences and age-related changes in the histomorphometric parameters describing trabecular structure and bone turnover in trabecular bone tissue sampled from the intertrochanteric region of the proximal femur, a skeletal site distal to the degenerative joint changes in OA, in individuals with primary hip OA.

- To compare the histomorphometric parameters describing trabecular structure and bone turnover, in trabecular bone sampled from the intertrochanteric region, between individuals with primary hip OA and an autopsy control group.

- To examine the relationship between the histomorphometric parameters describing trabecular structure and bone turnover, and the mRNA expression levels of the skeletally active molecules, measured in contiguous bone samples from the intertrochanteric region for primary hip OA individuals (mRNA expression data for the OA cases is independently described, as a comparison to controls, in Chapter 6).

- To compare the relationships between the histomorphometric parameters and mRNA levels of skeletally active molecules, measured in contiguous bone samples from the intertrochanteric region, between individuals with primary hip OA and an autopsy control group.

7.3 METHODS

7.3.1 Case selection

Proximal femurs were obtained from 14 routine autopsies performed at the Royal Adelaide Hospital. The postmortem case details, including age, gender, anatomical side, postmortem interval, and cause of death, are listed in Table 5.1. There were 12 postmortem cases available for undecalcified bone histomorphometric analysis. Trabecular bone tissue for histomorphometric analysis was not available from cases C11 (69-year-old male) and C13 (73-year-old male; Table 5.1) due to an inadequate amount of bone tissue remaining after RNA isolation. The age of the 12 postmortem cases for histomorphometric analysis, comprising 7 women (aged 20-83 years; mean ± SD [standard deviation] age, 61.3 ± 22.0 years) and 5 men (aged 24-85 years; 58.2 ± 24.3 years), varied between 20 and 85 years (60.0 ± 21.9 years). There was no difference in the mean age between females and males. These postmortem cases, which are categorized as *control* cases in this thesis, were selected from routine autopsies not known to have suffered from any disease affecting the skeleton and on macroscopic and radiological assessment of the proximal femur showed no significant sign of joint degeneration, according to the criteria of Collins (1949; described in Chapter 5.3.1 and Table 5.1).

Surgical specimens from the proximal femur were obtained from 16 patients undergoing total hip arthroplasty surgery for advanced primary OA at the Royal Adelaide Hospital. The surgical OA case details, including age, gender, anatomical side, and macroscopic grade of the femoral head and acetabulum, are listed in Table 6.1. There were 15 OA cases available for undecalcified bone histomorphometric analysis. Trabecular bone tissue for histomorphometric analysis was not available from case OA10 (54-year-old male; Table 6.1) due to an inadequate amount of bone tissue remaining after RNA isolation. An

additional 18 surgical OA cases were available for undecalcified bone histomorphometric analysis (Table 7.1). These additional OA cases were from an archive of human trabecular bone tissues stored in the Division of Tissue Pathology (Institute of Medical and Veterinary Science, Adelaide, SA, Australia). The additional OA proximal femur specimens were all obtained from patients undergoing total hip arthroplasty surgery for advanced primary OA, which were selected using the same criteria as described in Chapter 6.3.1. In brief, the selection of primary OA cases excluded patients suspected of having secondary OA, inflammatory joint disease, Paget's disease, drug-induced disease or other conditions, which may have affected the trabecular bone architecture and quality. The surgical case details, of anatomical side, and macroscopic grade of the femoral head and acetabulum, were not available for the additional 18 OA cases listed in Table 7.1. In total, there were 33 OA cases available for undecalcified bone histomorphometric analysis. The age of the 33 OA cases, comprising 18 women (aged 49-84 years; 71.5 ± 9.0 years) and 15 men (aged 37-85 years; 66.0 ± 14.2 years), varied between 37 and 85 years (69.0 ± 11.8 years). There was no difference in the mean age between OA females and OA males. The mean age of the OA group (n = 33) for bone histomorphometric analysis did not differ significantly from the control group (n = 12).

7.3.2 Sampling of trabecular bone from the intertrochanteric region of the human proximal femur

Trabecular bone was sampled from the intertrochanteric region of the proximal femur for each postmortem case. Initially, each proximal femur was sectioned in the coronal plane using a band saw, which had been cleaned with DEPC-treated water, to allow access to trabecular bone for sampling from the intertrochanteric site, which is enclosed within the femoral cortex (Figure 2.1). Trabecular bone tissue for RNA isolation, taken from the

Table 7.1 Profiles of additional surgical osteoarthritic (OA) cases for undecalcified bone histomorphometric analysis.

Case	Age *(years)*	Gender
OA17	64	Female
OA18	70	Female
OA19	71	Female
OA20	73	Female
OA21	74	Female
OA22	74	Female
OA23	75	Female
OA24	79	Female
OA25	79	Female
OA26	80	Female
OA27	37	Male
OA28	45	Male
OA29	56	Male
OA30	56	Male
OA31	74	Male
OA32	74	Male
OA33	75	Male
OA34	78	Male

OA, surgical osteoarthritic case.

intertrochanteric region, was sampled from an approximate 1.5 x 1.0 cm^2 area, to a specimen depth of 0.5 cm (described in Chapter 5.3.2). The remaining coronal half of each proximal femur was stored frozen until required for undecalcified histological analysis. Two 5 mm-thick coronal slices were cut from the remaining frozen coronal half of each proximal femur, using a diamond blade on the Exakt saw (Exakt Apparatebau GmbH & Co. KG). One coronal slice was used for bone histomorphometric analysis, and the other coronal slice for microdamage assessment (Chapter 8). A contact X-ray image of the 5 mm-thick coronal slice for undecalcified bone histomorphometric analysis was taken using a Faxitron X-ray cabinet (Hewlett-Packard). The X-ray image was used to enable reproducible sampling of trabecular bone from the intertrochanteric region as a 1.0 x 1.0 cm^2 block of tissue, using an Isomet 11-1180 low-speed diamond saw (Buehler Ltd.). The intertrochanteric trabecular bone tissue blocks (1.0 x 1.0 x 0.5 cm^3) were immediately fixed in 70% ethanol for 24 hours at room temperature.

At total hip arthroplasty surgery in OA patients, a 10 mm internal diameter tube saw was used to take a trabecular bone core biopsy of the intertrochanteric region (Figure 2.1), taken in line with the femoral medullary canal (Fazzalari *et al.*, 1998b). The bone core biopsies, 10 mm in diameter and 3-5 cm in length, were placed in cold (4°C) sterile RNase-free 0.85% saline and transported directly to the laboratory. Trabecular bone tissue was sampled from an approximate tube saw length of 1-2 cm for RNA isolation (described in Chapter 6.3.2). The remainder of each intertrochanteric bone core biopsy, 10 mm in diameter and 2-3 cm in length, was stored frozen until required for undecalcified histological analysis. These trabecular bone samples were X-rayed (Faxitron X-ray cabinet; Hewlett-Packard) before sampling for undecalcified histological analysis, to ensure the exclusion of any damaged tissue (particularly the ends of the biopsy). Each

undamaged tube saw biopsy, approximately 1-1.5 cm in length, was bisected lengthwise using an Isomet low-speed diamond saw (Buehler Ltd.). One half of the tube saw was processed for undecalcified bone histomorphometric analysis and the other half processed for microdamage assessment (Chapter 8). The trabecular bone tissue samples were immediately fixed in 70% ethanol for 24 hours at room temperature.

7.3.3 Undecalcified bone histomorphometric analysis

Trabecular bone samples from the intertrochanteric region, fixed in 70% ethanol, for autopsy control and surgical OA cases (section 7.3.2), were embedded undecalcified in methyl methacrylate (MMA; Chapter 2.2.3.3). Undecalcified bone sections, 5 μm-thick, were stained by the von Kossa silver method and counterstained with haematoxylin and eosin to distinguish between the mineralised bone, the osteoid, and the cellular components of the marrow (Chapter 2.2.3.4.1 and 2.2.3.5). Bone histomorphometric analysis was performed using an ocular-mounted Zeiss II Integration 100 point (10 x 10) graticule in a X10 eye-piece and an objective magnification of X10 on an Olympus BH-2 light microscope (Olympus; Chapter 2.2.3.6.1). The following standard histomorphometric parameters (Parfitt *et al.*, 1987) were calculated using formulae from Recker (1983):

Trabecular bone structural parameters:

(1)	Percentage of mineralised bone tissue volume	BV/TV
(2)	Surface density of bone in mm^2/mm^3	BS/TV
(3)	Specific surface of bone in mm^2/mm^3	BS/BV
(4)	Trabecular thickness in μm	Tb.Th
(5)	Trabecular separation in μm	Tb.Sp
(6)	Trabecular number per mm	Tb.N

Static indices of bone turnover:

(1)	Percentage of osteoid volume	OV/TV
(2)	Percentage of osteoid volume	OV/BV
(3)	Percentage of osteoid surface	OS/BS
(4)	Percentage of eroded surface	ES/BS

7.3.4 Semi-quantitative RT-PCR of total RNA isolated from human trabecular bone

Total RNA was isolated from intertrochanteric trabecular bone tissue (Chapter 2.2.2.1) sampled from the autopsy control and surgical OA cases listed in Tables 5.1 and 6.1. Semi-quantitative RT-PCR (Chapter 2.2.2.3), using the human-specific oligonucleotide primer pairs listed in Table 2.1 and primer conditions described in Chapter 2.2.2.3.2, was used to determine the relative levels of IL-6, IL-11, CTR, OCN, RANKL, OPG, and RANK mRNA in these bone RNA samples. Amplified PCR product corresponding to IL-6, IL-11, CTR, OCN, RANKL, OPG, and RANK mRNA are represented as a ratio of the respective PCR product/GAPDH PCR product (mRNA expression data for controls is independently described in Chapter 5; mRNA expression data for the OA cases is independently described, as a comparison to controls, in Chapter 6). RT-PCR data for RANKL, OPG, and RANK mRNA could not be obtained for cases C10 (65-year-old male), C13 (73-year-old male), OA6 (78-year-old female), OA14 (77-year-old male), and OA15 (79-year-old male) due to small quantities of total RNA recovered. In addition, RT-PCR data for RANK mRNA was not available for case OA12 (69-year-old male).

7.3.5 Statistical analysis of histomorphometric data

The Shapiro-Wilk statistic was used to test the bone histomorphometric data for normality (PC-SAS software; SAS Institute). The histomorphometric data for bone structural parameters and static indices of bone turnover were found to be normally distributed. Therefore, parametric statistical methods were used to analyse the data (Excel; Microsoft Corp.). The statistical significance of differences in the histomorphometric variables between females and males, and between the autopsy control and OA groups, were determined by Student's *t*-test. The F-test was used to analyse differences in the variance of the histomorphometric parameters between females and males. Linear regression analysis was used to describe age-related changes. Regression analysis was used to examine the relationship between histomorphometric parameters. Regression analysis was used to examine the relationship between PCR products representing specific mRNA species (section 7.3.4) and bone histomorphometric variables (section 7.3.3), measured in contiguous trabecular bone tissue samples. Student's *t*-test was used to compare the slopes and intercepts of significant linear regressions between the OA and control groups. If there was more than one significant independent factor associated with a specific histomorphometric variable, multiple regression was performed to determine the contribution of each independent factor. The histomorphometric data is quoted as mean ± standard deviation. The critical value for significance was chosen as $p = 0.05$.

7.4 RESULTS

7.4.1 Comparison of mean trabecular bone structure and bone turnover indices between females and males in the control group

The student's *t*-test was used to assess whether there were any gender differences in the histomorphometric parameters describing trabecular bone structure and bone turnover in

non-diseased (control) human trabecular bone, sampled from the intertrochanteric region of the proximal femur. Mean trabecular separation (Tb.Sp) was significantly increased in females compared to males ($p < 0.05$; Table 7.2). In addition, although not statistically significant, the mean values for trabecular thickness (Tb.Th) and trabecular number (Tb.N) were lower in females than in males (Table 7.2). The increased Tb.Sp in females is consistent with what has been reported in the literature for postmenopausal bone loss in women (Weinstein and Hutson, 1987). No significant differences were observed between females and males for any of the other histomorphometric parameters (Table 7.2). Based on these comparisons between females and males, and the small number of samples for the control cohort ($n = 12$), further analyses of the histomorphometric data were made independent of gender. In addition, the control group data is compared to the OA group data with and without inclusion of the two younger cases in this control cohort, cases C1 (20-year-old female) and C8 (24-year-old male), which are specifically indicated in Figures 7.5-7.16.

7.4.2 Age-related changes in trabecular bone structure and bone turnover indices in control individuals

To investigate age-related changes in the histomorphometric parameters describing trabecular bone structure and bone turnover in control human trabecular bone, sampled from the intertrochanteric region of the proximal femur, each histomorphometric parameter was plotted as a function of increasing age in years, and analysed by linear regression analysis. A significant decrease in BV/TV with age was observed ($r = -0.70$, $p < 0.008$; Figure 7.1), which is consistent with a previous report of an age-related decline in trabecular bone volume measured from a comparable region of the human proximal femur (Crane *et al.*, 1990). This age-related decline in BV/TV was dependent on inclusion of the

Table 7.2 Trabecular bone structure and bone turnover indices in female and male control intertrochanteric trabecular bone samples.

Histomorphometric parameter	Female ($n = 7$)	Male ($n = 5$)
BV/TV (%)	9.9 ± 6.5	10.8 ± 3.2
BS/TV (mm^2/mm^3)	1.7 ± 0.5	2.3 ± 0.5
BS/BV (mm^2/mm^3)	28.4 ± 8.7	20.9 ± 4.7
Tb.Th (μm)	77 ± 24	100 ± 19
Tb.Sp (μm)	1161 ± 302	814 ± 209 [a]
Tb.N (number/mm)	0.86 ± 0.24	1.14 ± 0.25
OV/TV (%)	0.08 ± 0.05	0.06 ± 0.03
OV/BV (%)	1.35 ± 0.91	0.62 ± 0.44
OS/BS (%)	9.2 ± 4.5	5.5 ± 1.9
ES/BS (%)	11.1 ± 4.8	7.4 ± 2.8

Values are mean ± standard deviation.
[a] $p < 0.05$.

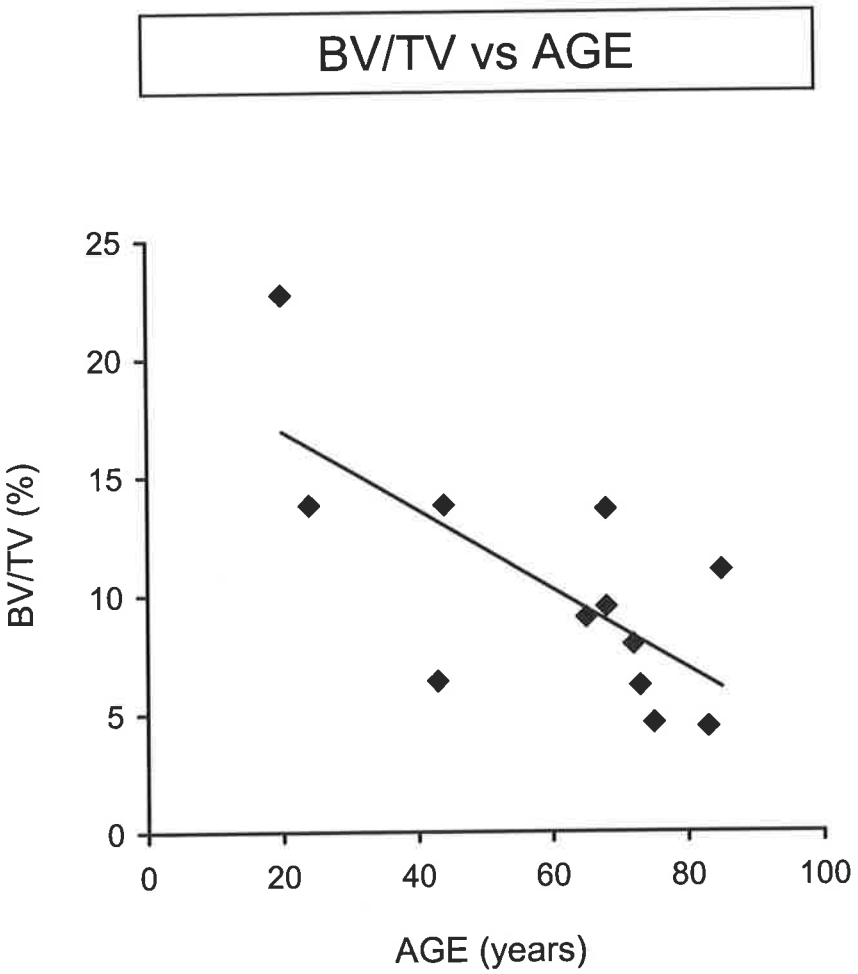

Figure 7.1: There was a significant decline in BV/TV with age in intertrochanteric trabecular bone from controls individuals (n = 12; BV/TV = -0.17*AGE + 20.25; r = -0.70 and $p < 0.008$).

two younger cases, cases C1 (20-year-old female) and C8 (24-year-old male). When Tb.Sp was plotted against age, variability increased for cases aged greater than 60 years, but nonetheless a positive association was seen ($r = 0.54$, $p < 0.05$; Figure 7.2). This age-related increase in Tb.Sp was dependent on inclusion of the two younger cases. This finding is consistent with a reported age-related increase in Tb.Sp, measured from the iliac crest, in a cohort of non-diseased autopsy cases with an age range of 20 to 80 years (49.5 ± 18.3 years; Weinstein and Hutson, 1987). There were no relationships with age for any of the other histomorphometric parameters describing trabecular bone structure, BS/TV, BS/BV, Tb.Th, and Tb.N, in control human trabecular bone sampled from the intertrochanteric region of the proximal femur (results not shown).

There was a significant increase in eroded bone surface (ES/BS) with age ($r = 0.65$, $p < 0.02$; Figure 7.3), indicating an increased extent of bone resorption with age in control human trabecular bone. This age-related increase in ES/BS was dependent on inclusion of the two younger cases. Croucher *et al.* (1991) have shown that ES/BS measured in iliac crest bone biopsies positively correlated with age in normal healthy individuals. In that study, the age-related increase in ES/BS was accompanied by an increase with age in the number of resorption cavities per mm of trabecular bone surface (Croucher *et al.*, 1991). When osteoid surface (OS/BS) was plotted against age, there was a positive association ($r = 0.61$, $p < 0.03$; Figure 7.4), indicating an increased extent of bone formation with age. The relationship between OS/BS and age was strengthened after exclusion of the two younger control individuals ($n = 10$; $r = 0.72$, $p < 0.01$). This, together with an age-dependent increase in ES/BS, indicates an increase in the rate of bone turnover with aging in control individuals, which is consistent with biochemical markers of bone turnover in healthy men and women (Khosla *et al.*, 1997; Krall *et al.*, 1997). Intriguingly, there was a

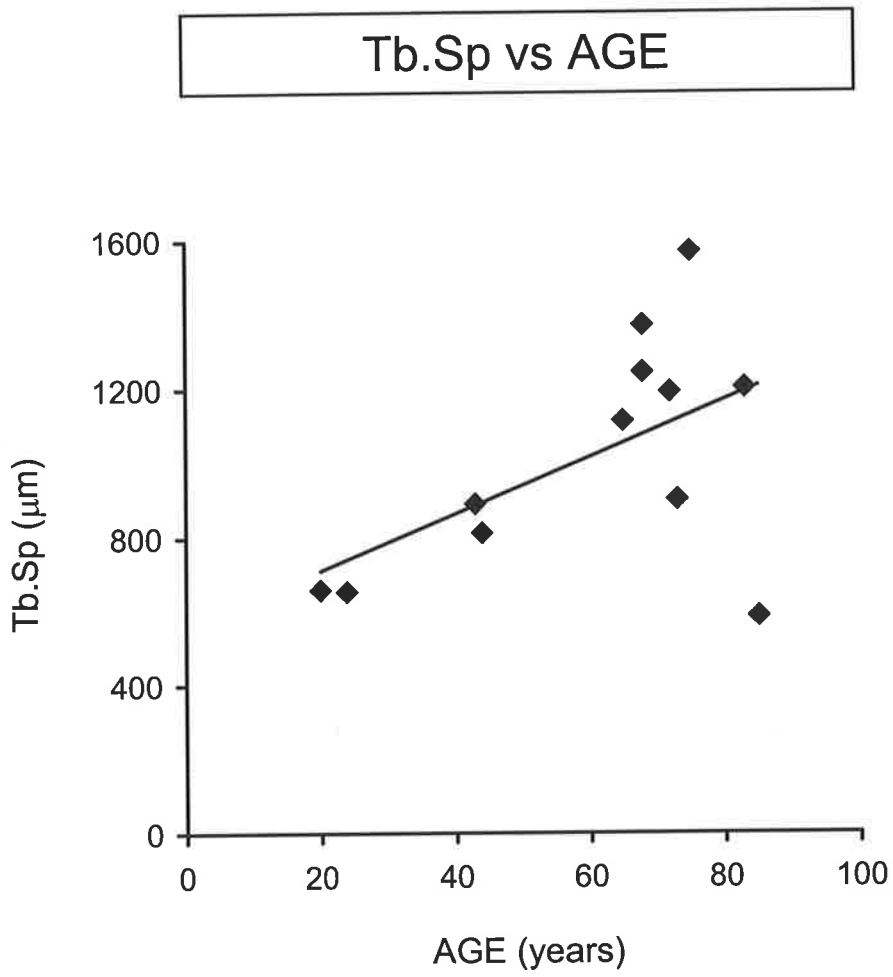

Figure 7.2: There was a significant increase in Tb.Sp with age in intertrochanteric trabecular bone from controls individuals (n = 12; Tb.Sp = 7.66*AGE + 556.93; r = 0.54 and $p < 0.05$).

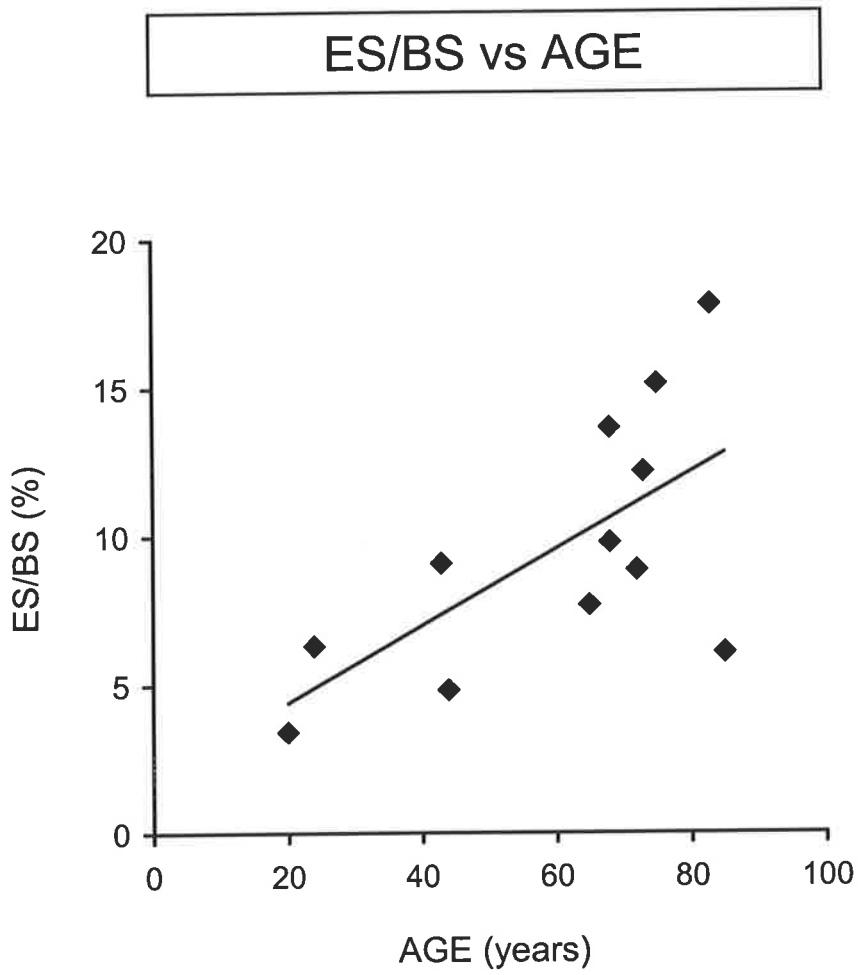

Figure 7.3: There was a significant increase in ES/BS with age in intertrochanteric trabecular bone from controls individuals (n = 12; ES/BS = 0.13*AGE + 1.83; r = 0.65 and $p < 0.02$).

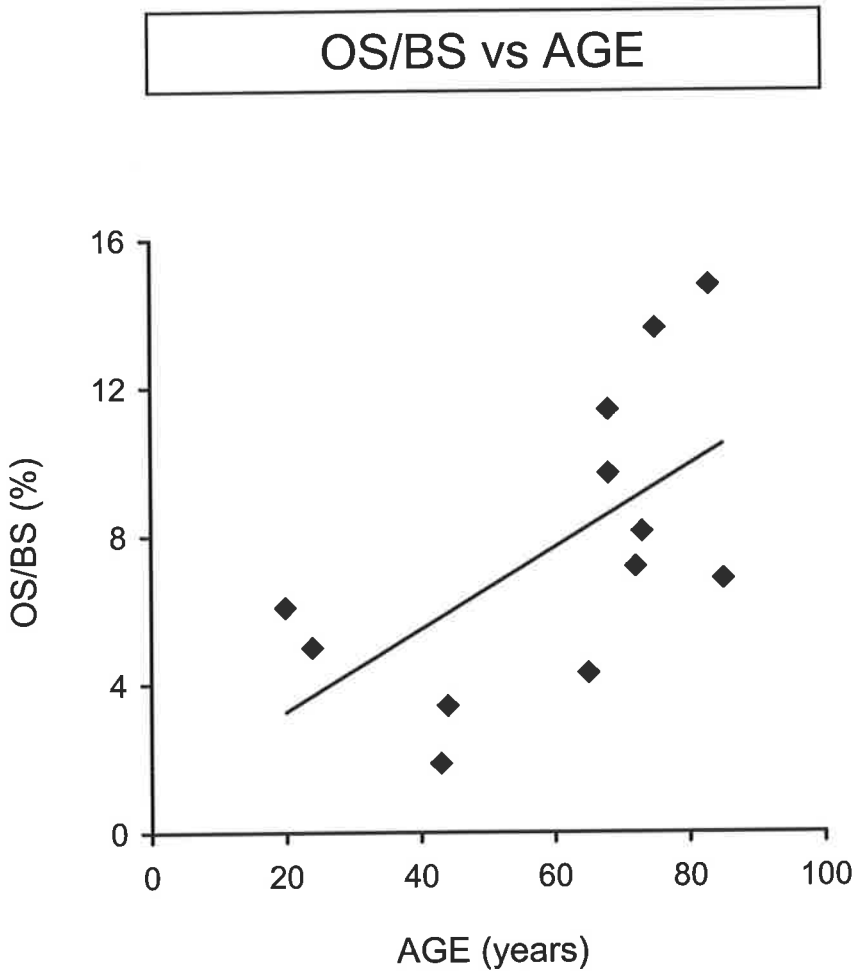

Figure 7.4: There was a significant increase in OS/BS with age in intertrochanteric trabecular bone from controls individuals (n = 12; OS/BS = 0.11*AGE + 1.03; r = 0.61 and $p < 0.03$).

significant positive correlation between ES/BS and OS/BS ($r = 0.79$, $p < 0.001$; Figure 7.5). This relationship was maintained even after exclusion of the two younger control individuals ($n = 10$; $r = 0.82$, $p < 0.002$). This finding indicates that the processes of bone resorption and bone formation are tightly coupled in control human trabecular bone sampled from the intertrochanteric region of the proximal femur.

The histomorphometric parameters describing the proportion of osteoid volume per total tissue volume and per mineralised bone tissue volume, OV/TV and OV/BV, respectively, were not age-dependent in control human trabecular bone (results not shown). Interestingly, a significant positive association was observed between two histomorphometric parameters representative of bone formation, OV/BV and OS/BS ($r = 0.64$, $p < 0.02$; Figure 7.6), which was maintained after exclusion of the two younger control cases ($n = 10$; $r = 0.62$, $p < 0.04$). No statistical association was observed between OV/TV and OS/BS (Figure 7.7). However, when the outlier, case C7 (83-year-old female) with low OV/TV and high OS/BS values (Figure 7.7), was removed, there was a significant positive association between OV/TV and OS/BS ($r = 0.70$, $p < 0.01$). The positive associations between OV/BV and OS/BS, and OV/TV and OS/BS, are not unexpected as osteoid volume and the extent of osteoid surface are linked by the temporal aspect of bone formation. That is, changes in osteoid volume and in the extent of osteoid surface may reflect variations in the rate of osteoid formation and/or variations in the rate of mineralisation. Furthermore, an increase in the birth-rate of new basic multicellular units (BMUs) may reflect greater osteoid volume and surface.

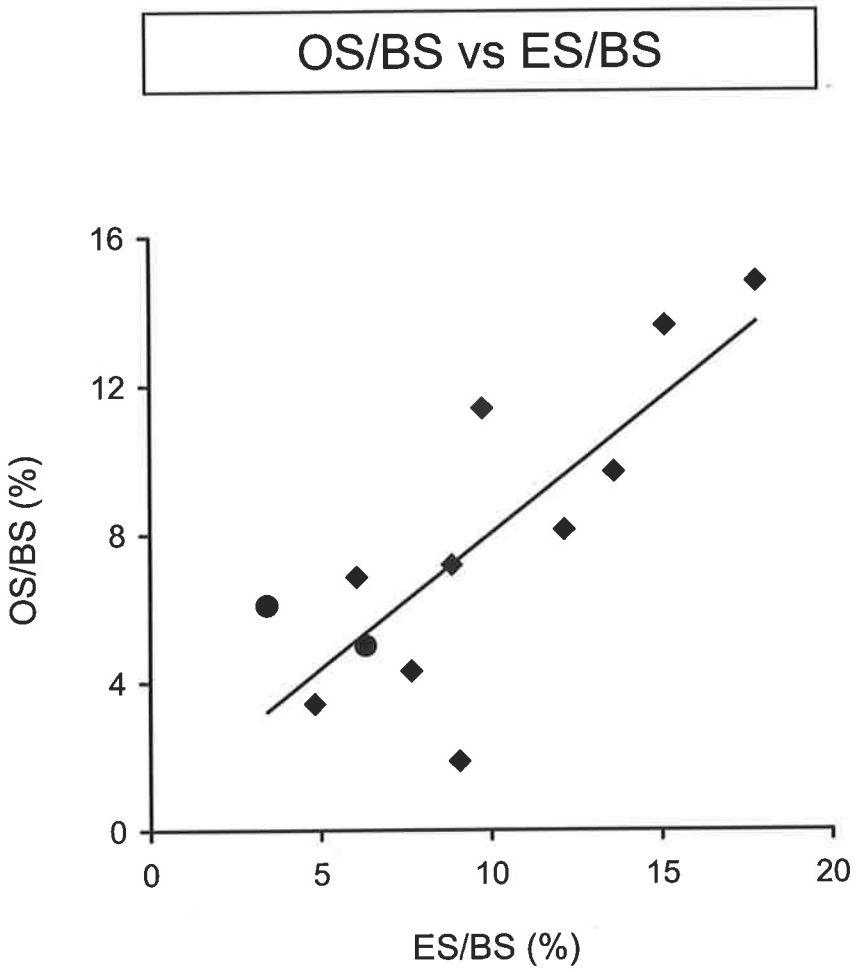

Figure 7.5: A positive association was observed between OS/BS and ES/BS in intertrochanteric trabecular bone from control individuals (n = 12; OS/BS = 0.73*ES/BS + 0.71; r = 0.79 and $p < 0.001$). Two cases, <40 years old, are indicated (●).

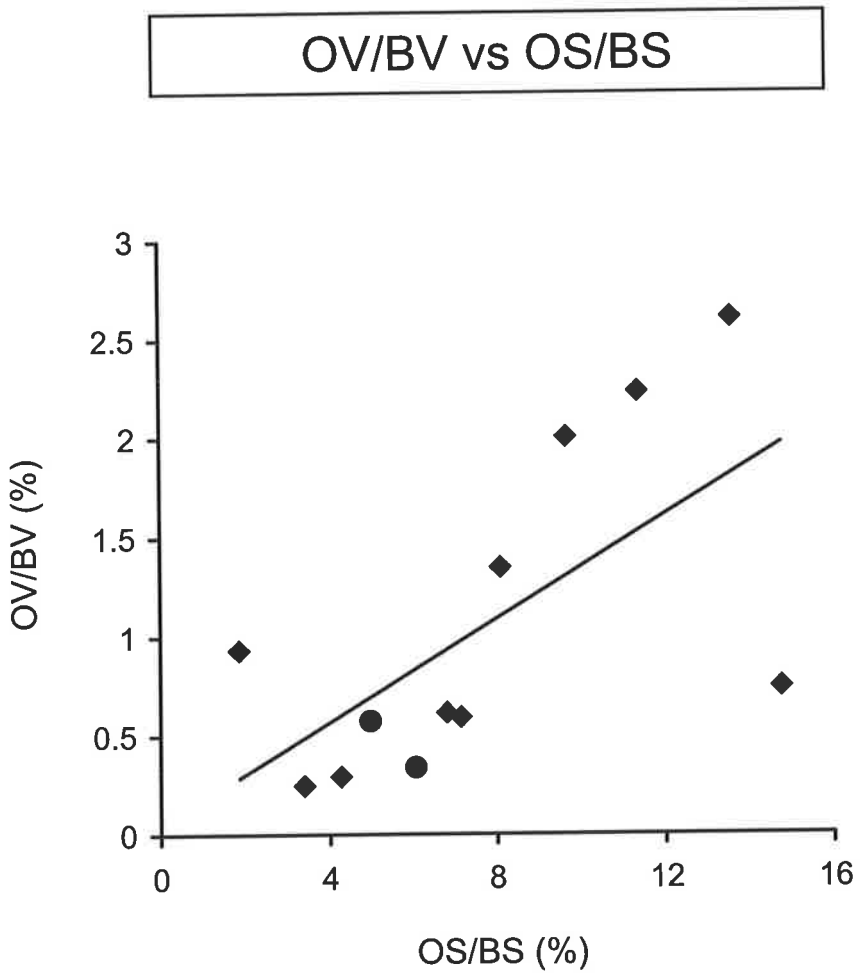

Figure 7.6: A positive association was observed between OV/BV and OS/BS in intertrochanteric trabecular bone from control individuals (n = 12; OV/BV = 0.13*OS/BS + 0.04; $r = 0.64$ and $p < 0.02$). Two cases, <40 years old, are indicated (●).

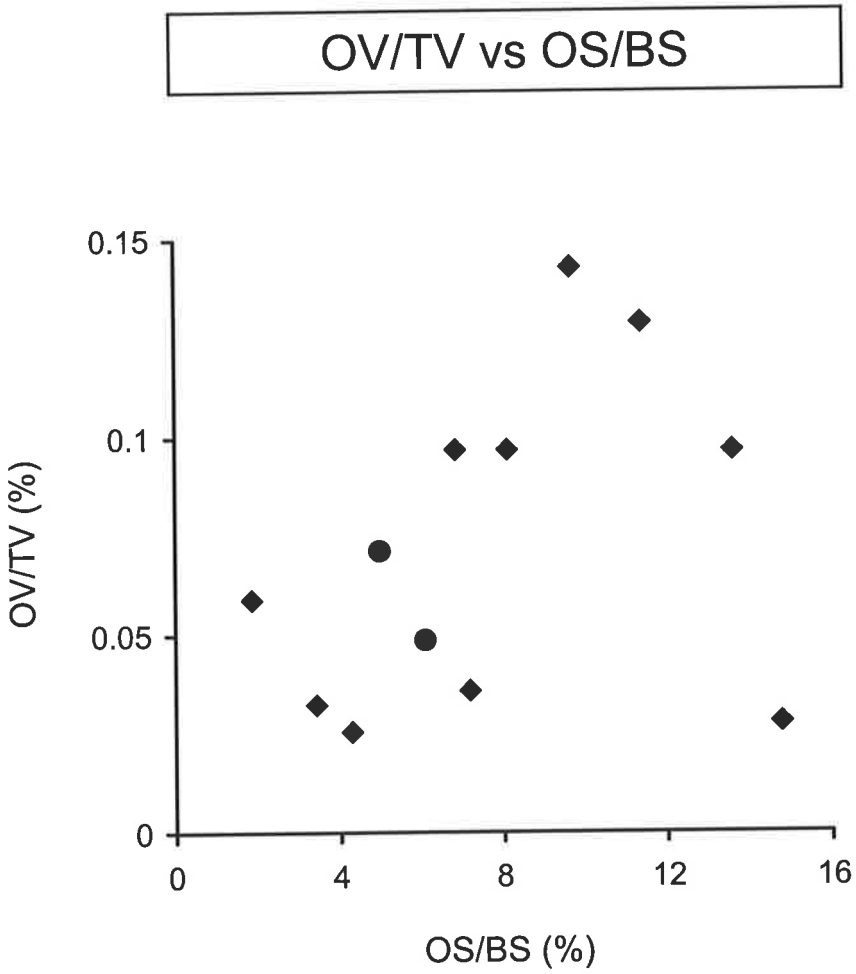

Figure 7.7: No association was observed between OV/TV and OS/BS in intertrochanteric trabecular bone from control individuals (n = 12; OV/TV = 0.004*OS/BS + 0.04; r = 0.36 and p = NS; n = 11 (without outlier); OV/TV = 0.008*OS/BS + 0.02; r = 0.70 and $p < 0.01$). Two cases, <40 years old, are indicated (●). NS = not significant.

7.4.3 Associations between bone histomorphometric parameters and mRNA levels of skeletally active molecules in control trabecular bone from the human proximal femur

Histomorphometric parameters describing trabecular bone structure and bone turnover, and the levels of mRNA corresponding to factors known to have important regulatory roles in bone remodelling, were measured in contiguous bone samples from the intertrochanteric region of the proximal femur for control individuals. Linear regression analysis was used to investigate whether there are any relationships between the histomorphometric parameters and mRNA levels of skeletally active molecules. RANKL and OPG are important downstream signals of osteoclast biology, onto which many hormonal, chemical, and biochemical signals converge (Hofbauer and Heufelder, 2001; detailed in Chapter 5.1). Hofbauer *et al.* (2000) hypothesised that the ratio of RANKL to OPG is the main determinant of the pool size of active osteoclasts in the local bone microenvironment, acting as a final effector system to modulate differentiation, activation, and apoptosis of osteoclasts. Thus, the relationship between the ratio of RANKL/OPG mRNA, as determined by semi-quantitative RT-PCR (section 7.3.4), and histomorphometric parameters describing trabecular bone structure and bone turnover (particularly eroded bone surface) was explored. There were 11 control cases, for which both semi-quantitative RT-PCR and histomorphometric data were available for analysis (refer to sections 7.3.1 and 7.3.4).

When eroded bone surface (ES/BS) and the ratio of RANKL/OPG mRNA, measured in contiguous bone samples from the human proximal femur, were co-plotted, a strong positive association was observed ($r = 0.93$, $p < 0.001$; Figure 7.8). This strong association was maintained even after exclusion of the two younger control individuals ($n = 9$; $r =$

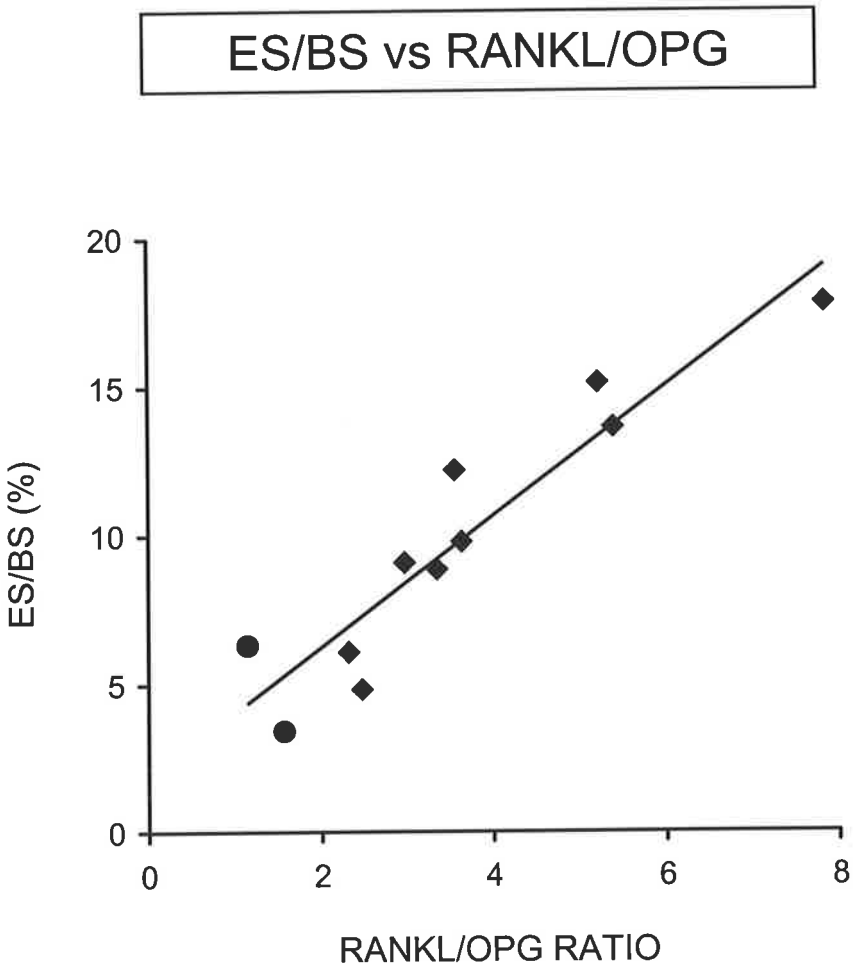

Figure 7.8: A positive association was observed between ES/BS and the RANKL/OPG mRNA ratio, measured in contiguous intertrochanteric trabecular bone samples, from control individuals (n = 11; ES/BS = 2.20*RANKL/OPG + 1.86; r = 0.93 and p < 0.001). Two cases, <40 years old, are indicated (●).

0.93, $p < 0.001$). Additionally, a significant positive association was found between ES/BS and RANKL/GAPDH mRNA expression in these control bone samples ($r = 0.83$, $p < 0.001$; Figure 7.9), which was maintained after exclusion of the two younger control cases ($n = 9$; $r = 0.77$, $p < 0.007$). No association was observed between ES/BS and OPG/GAPDH mRNA (Figure 7.10). Taken together, these observations suggest that the relationship between ES/BS and the ratio of RANKL/OPG mRNA (Figure 7.8) is determined by changes in the mRNA level of RANKL, independent of OPG mRNA levels (Figure 7.9).

When ES/BS and RANK/GAPDH mRNA expression were co-plotted, a positive association was observed ($r = 0.61$, $p < 0.04$; Figure 7.11), which was maintained after exclusion of the two younger control cases ($n = 9$; $r = 0.67$, $p < 0.03$). However, this positive association between ES/BS and RANK mRNA is statistically reliant on two outliers, cases C7 (83-year-old female) and C12 (73-year-old male). RANK is the cognate receptor for RANKL (Anderson *et al.*, 1997; Hsu *et al.*, 1999) and is expressed on the surface of osteoclasts and their precursors (Hsu *et al.*, 1999). Since age, the RANKL/OPG mRNA ratio, the relative level of RANKL/GAPDH mRNA, and the expression of RANK/GAPDH mRNA, were all significantly associated with ES/BS in control human trabecular bone (Figures 7.3, 7.8, 7.9, and 7.11, respectively), a multiple regression analysis was performed to determine the contribution of age, the RANKL/OPG mRNA ratio, RANKL mRNA, and RANK mRNA expression to ES/BS. ES/BS was found to be only dependent on the ratio of RANKL/OPG mRNA expression in control bone ($p < 0.02$), supporting the concept that the relative levels of RANKL and OPG mRNA measured in these human bone tissues relate directly to levels of expression of the corresponding proteins in the bone tissue. Moreover, these data suggest that the ratio of RANKL to OPG,

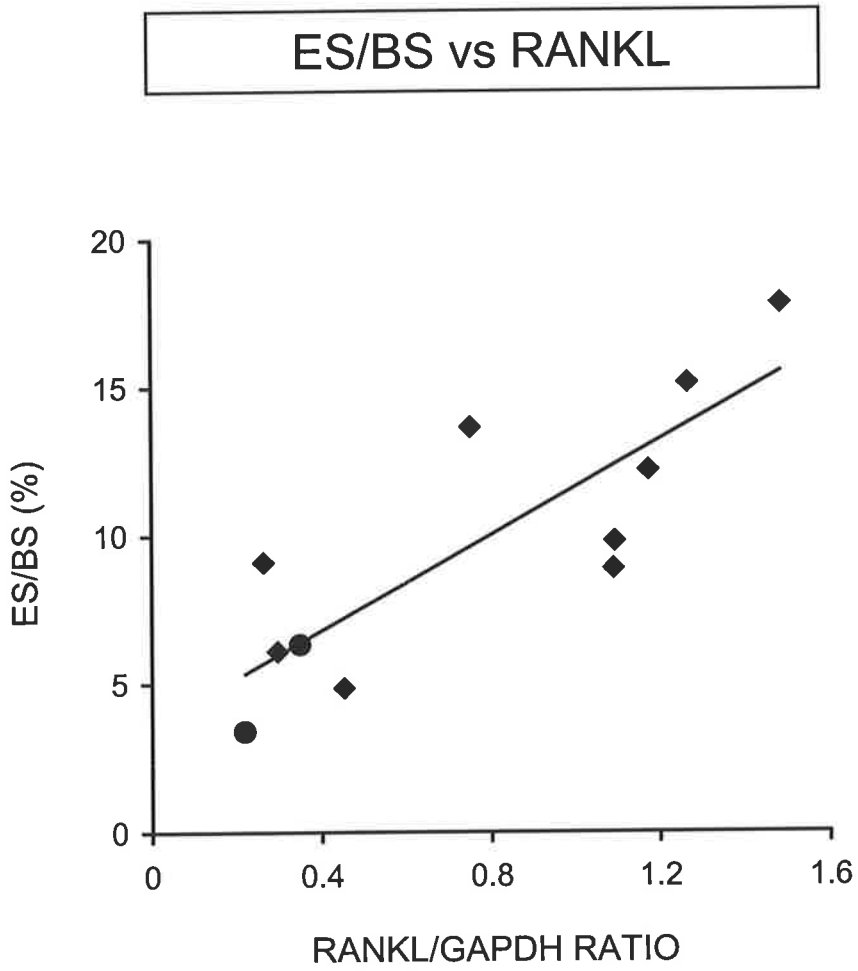

Figure 7.9: A positive association was observed between ES/BS and the relative ratio of RANKL/GAPDH mRNA, measured in contiguous intertrochanteric trabecular bone samples, from control individuals (n = 11; ES/BS = 8.04*RANKL/GAPDH + 3.57; r = 0.83 and $p < 0.001$). Two cases, <40 years old, are indicated (●).

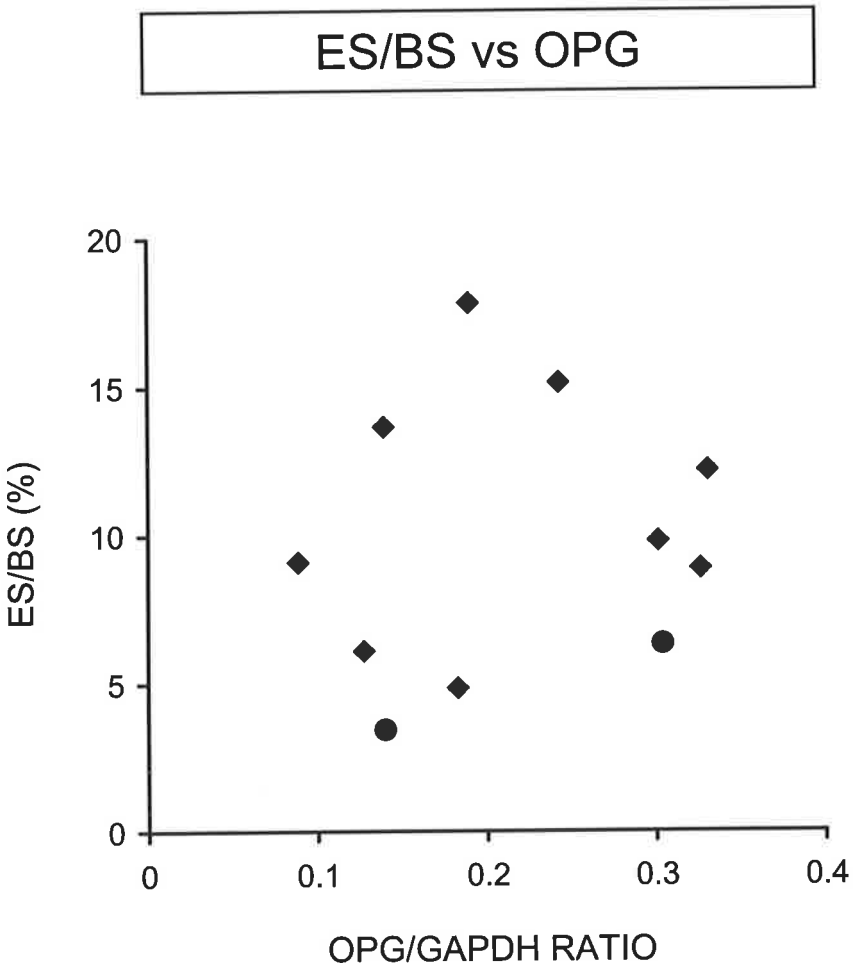

Figure 7.10: No association was observed between ES/BS and the relative ratio of OPG/GAPDH mRNA, measured in contiguous intertrochanteric trabecular bone samples, from control individuals (n = 11; ES/BS = 7.29*OPG/GAPDH + 8.17; r = 0.14 and p = NS). Two cases, <40 years old, are indicated (●). NS = not significant.

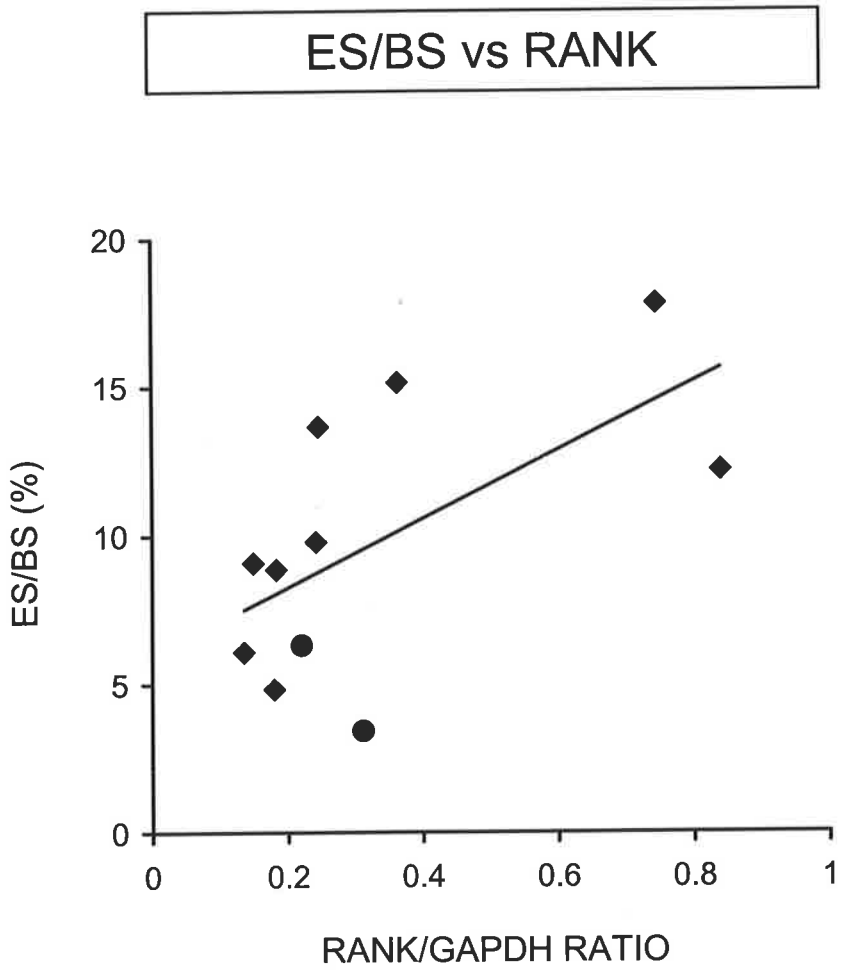

Figure 7.11: A positive association was observed between ES/BS and the relative ratio of RANK/GAPDH mRNA, measured in contiguous intertrochanteric trabecular bone samples, from control individuals (n = 11; ES/BS = 11.52*RANK/GAPDH + 5.95; r = 0.61 and $p < 0.04$). Two cases, <40 years old, are indicated (●).

which is likely to represent the actual local osteoclastic influence in bone, plays a central role in controlling the extent of bone resorption in human trabecular bone.

Analogous to the observations for ES/BS, there was a strong positive association between OS/BS and the ratio of RANKL/OPG mRNA in control human trabecular bone ($r = 0.80$, $p < 0.001$; Figure 7.12). Furthermore, this association was maintained after exclusion of the two younger control individuals ($n = 9$; $r = 0.80$, $p < 0.004$). A significant positive association was found between OS/BS and RANKL/GAPDH mRNA expression ($r = 0.84$, $p < 0.001$; results not shown). There was no significant association between OS/BS and OPG/GAPDH mRNA (results not shown). Thus, as for ES/BS, these observations suggest that the relationship between OS/BS and the ratio of RANKL/OPG mRNA (Figure 7.12) is determined by changes in the mRNA expression level of RANKL. The strong positive associations observed between both ES/BS and OS/BS with the ratio of RANKL/OPG mRNA in control human trabecular bone (Figures 7.8 and 7.12, respectively), suggest that the local ratio of RANKL/OPG may well be of central importance in bone remodelling. No associations were observed between the osteoid volume parameters, OV/TV and OV/BV, and the RANKL/OPG mRNA ratio (results not shown).

The only significant relationship that was observed between the ratio of RANKL/OPG mRNA and a histomorphometric parameter describing trabecular bone structure was a negative association between BV/TV and the ratio of RANKL/OPG mRNA ($r = -0.67$, $p < 0.05$; Figure 7.13). However, this association was dependent on inclusion of the two younger cases. A negative association was also found between BV/TV and RANKL/GAPDH mRNA expression ($r = -0.63$, $p < 0.03$; results not shown). No significant association was observed between BV/TV and OPG/GAPDH mRNA (results

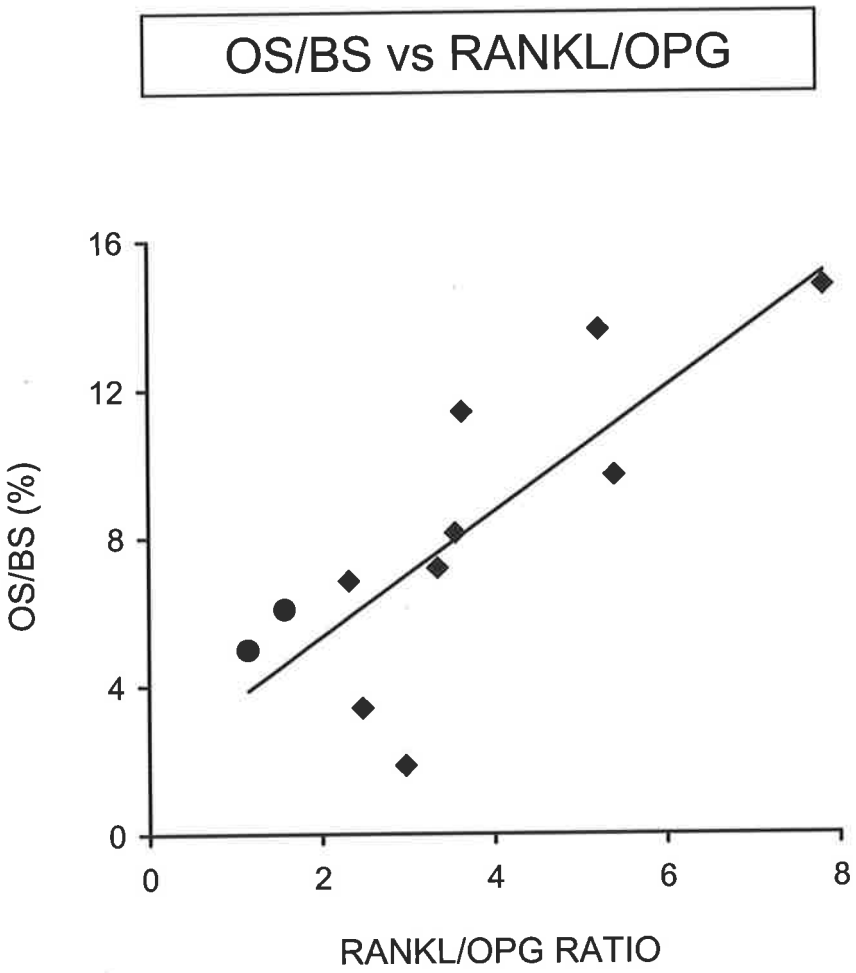

Figure 7.12: A positive association was observed between OS/BS and the RANKL/OPG mRNA ratio, measured in contiguous intertrochanteric trabecular bone samples, from control individuals (n = 11; OS/BS = 1.69*RANKL/OPG + 1.94; r = 0.80 and $p < 0.001$). Two cases, <40 years old, are indicated (●).

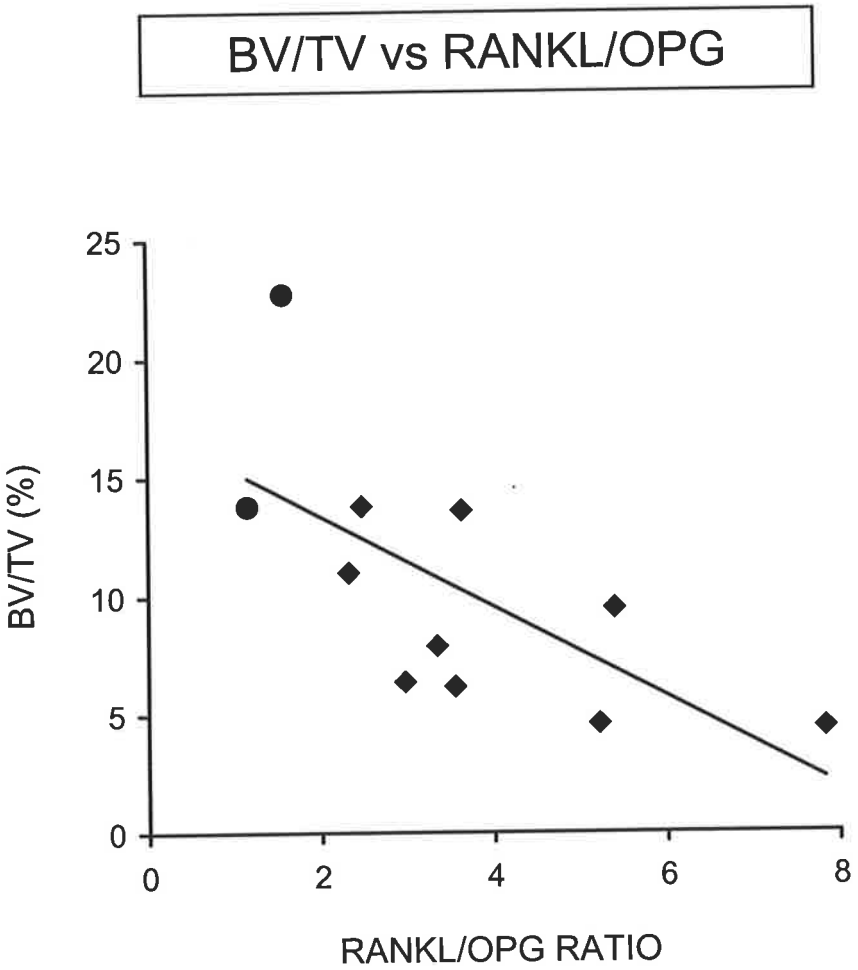

Figure 7.13: A negative association was observed between BV/TV and the RANKL/OPG mRNA ratio, measured in contiguous intertrochanteric trabecular bone samples, from control individuals (n = 11; BV/TV = -1.90*RANKL/OPG + 17.17; r = -0.67 and $p < 0.05$). Two cases, <40 years old, are indicated (●).

not shown). Thus, the negative association between BV/TV and the ratio of RANKL/OPG mRNA (Figure 7.13) is likely to be determined by changes in the mRNA expression level of RANKL, as observed for ES/BS and OS/BS. The processes of bone resorption and bone formation, represented by ES/BS and OS/BS, respectively, were shown to be tightly coupled in these control trabecular bone samples (Figure 7.5; section 7.4.2). However, the negative association between BV/TV and the ratio of RANKL/OPG mRNA (Figure 7.13) suggests that the coupled remodelling process may be in favour of net bone resorption in control human trabecular bone sampled from the intertrochanteric region of the proximal femur.

The cytokines IL-6 and IL-11 have both been shown to stimulate the development of osteoclasts from their haematopoietic precursors (Martin *et al.*, 1998). The stimulatory effects of IL-11 on osteoclast differentiation appear to be mediated by inducing RANKL expression on marrow stromal/osteoblastic cells (Nakashima *et al.*, 2000; Yasuda *et al.*, 1998b). However, the reported effects of IL-6 on RANKL-RANK-promoted osteoclast development are conflicting (Brandstrom *et al.*, 1998; Hofbauer *et al.*, 1998; Hofbauer *et al.*, 1999b; Nakashima *et al.*, 2000; O'Brien *et al.*, 1999; Vidal *et al.*, 1998). Thus, linear regression analysis was used to investigate potential relationships between the expression of IL-6 and IL-11 mRNA, as determined by semi-quantitative RT-PCR (section 7.3.4), and histomorphometric parameters describing trabecular bone structure and bone turnover in control human bone samples. There were 12 control cases, for which both semi-quantitative RT-PCR and histomorphometric data were available for analysis (refer to sections 7.3.1 and 7.3.4).

When ES/BS and IL-11/GAPDH mRNA expression, measured in contiguous bone samples from the human proximal femur, were co-plotted, a negative association was observed (r = -0.54, $p < 0.05$; Figure 7.14), which was dependent on inclusion of one younger case {case C1 (20-year-old female)}. Since IL-11 appears to stimulate osteoclast differentiation *via* induction of RANKL expression on marrow stromal/osteoblastic cells, albeit in murine cell lines (Nakashima *et al.*, 2000; Yasuda *et al.*, 1998b), the negative association between ES/BS and IL-11 mRNA in human bone is not consistent with the strong positive relationships shown between ES/BS and the ratio of RANKL/OPG mRNA (Figure 7.8) and RANKL mRNA expression (Figure 7.9). Moreover, IL-11 mRNA expression did not correlate with RANKL, OPG, or RANK mRNA expression in these control bone samples (Chapter 5.4.3). IL-11 has also been implicated as a suppressor of osteoblastic synthetic activity. For example, IL-11 dose-dependently inhibited nodule formation and reduced alkaline phosphatase expression in rat calvarial cell cultures (Hughes and Howells, 1993b). However, no association was observed between OS/BS and IL-11/GAPDH mRNA expression (Figure 7.15). Further, a positive association was observed between BV/TV and IL-11/GAPDH mRNA expression in these control bone samples (r = 0.73, $p < 0.005$; Figure 7.16), which was dependent on inclusion of one younger case {case C1 (20-year-old female)}. Interestingly, this finding is consistent with a recent report showing over-expression of IL-11 in transgenic mice resulted in an increase in bone mass, which was due to increased bone formation and increased numbers of osteoblasts, with no change in bone resorption or osteoclast number (Takeuchi *et al.*, 2002). Taken together, the negative association between ES/BS and IL-11 mRNA (Figure 7.14), and the positive association between BV/TV and IL-11 mRNA (Figure 7.16), suggest that local expression levels of IL-11 mRNA may be involved in inhibition of bone resorption in these intertrochanteric human trabecular bone samples. Although the evidence to date suggests that one major role

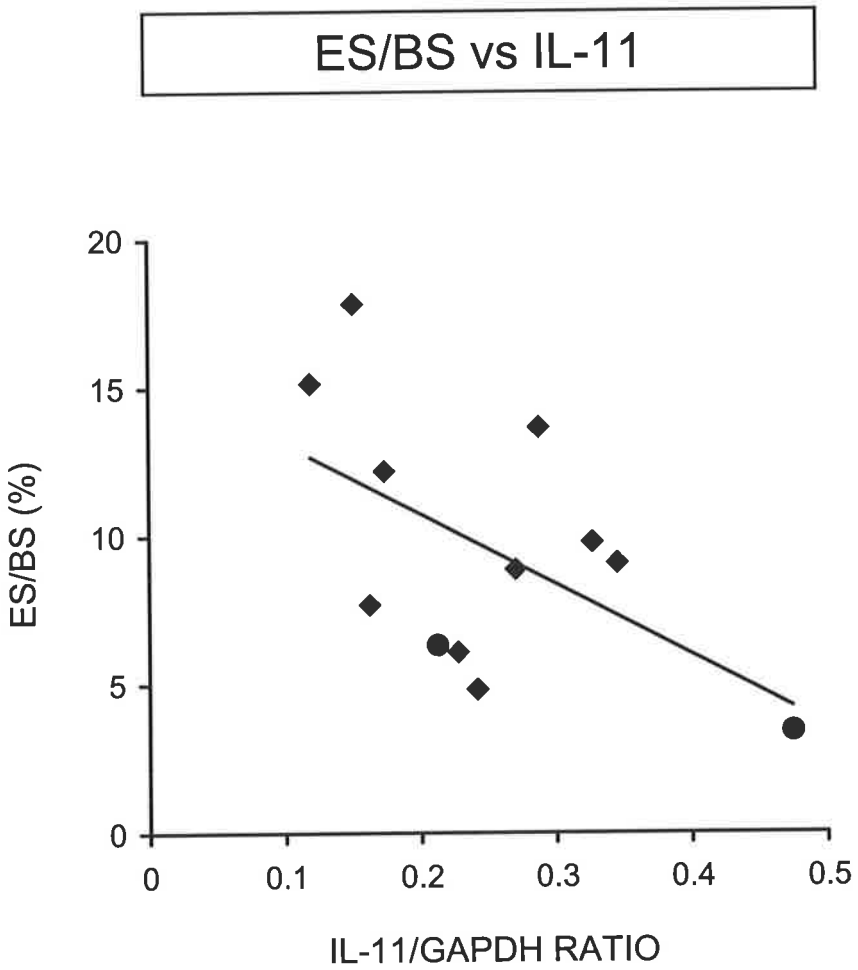

Figure 7.14: A negative association was observed between ES/BS and the relative ratio of IL-11/GAPDH mRNA, measured in contiguous intertrochanteric trabecular bone samples, from control individuals (n = 12; ES/BS = -23.79*IL-11/GAPDH + 15.51; r = -0.54 and $p < 0.05$). Two cases, <40 years old, are indicated (●).

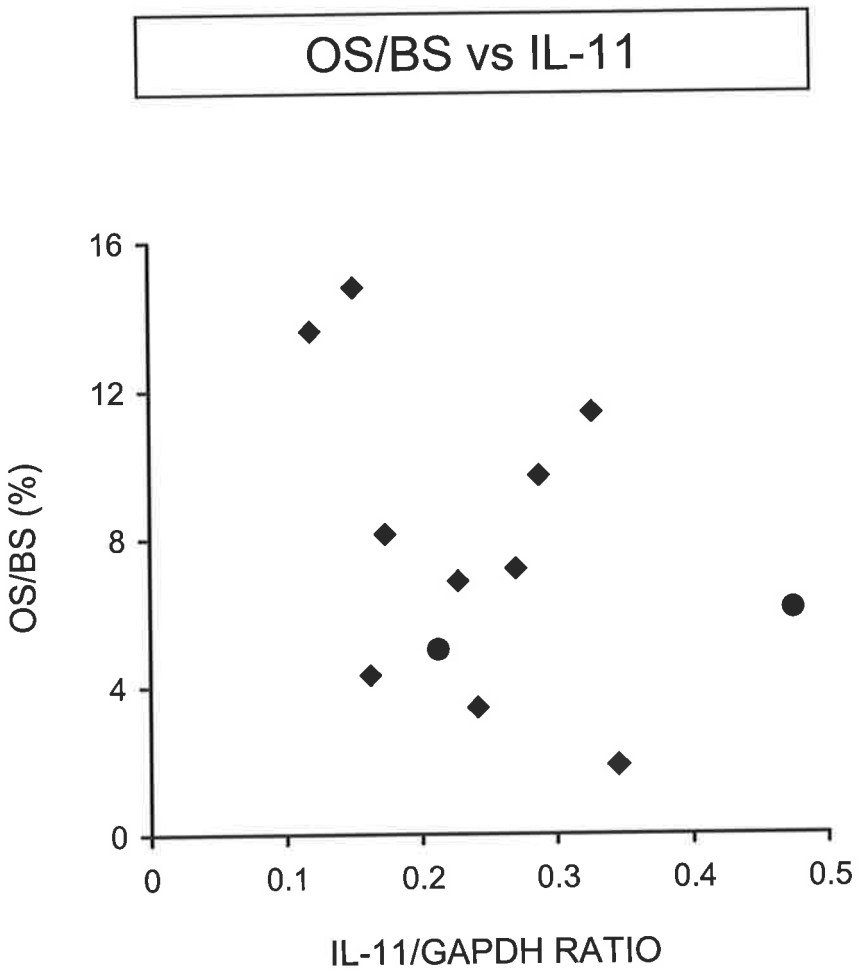

Figure 7.15: No association was observed between OS/BS and the relative ratio of IL-11/GAPDH mRNA, measured in contiguous intertrochanteric trabecular bone samples, from control individuals (n = 12; OS/BS = -14.79*IL-11/GAPDH + 11.37; r = -0.37 and p = NS). Two cases, <40 years old, are indicated (●). NS = not significant.

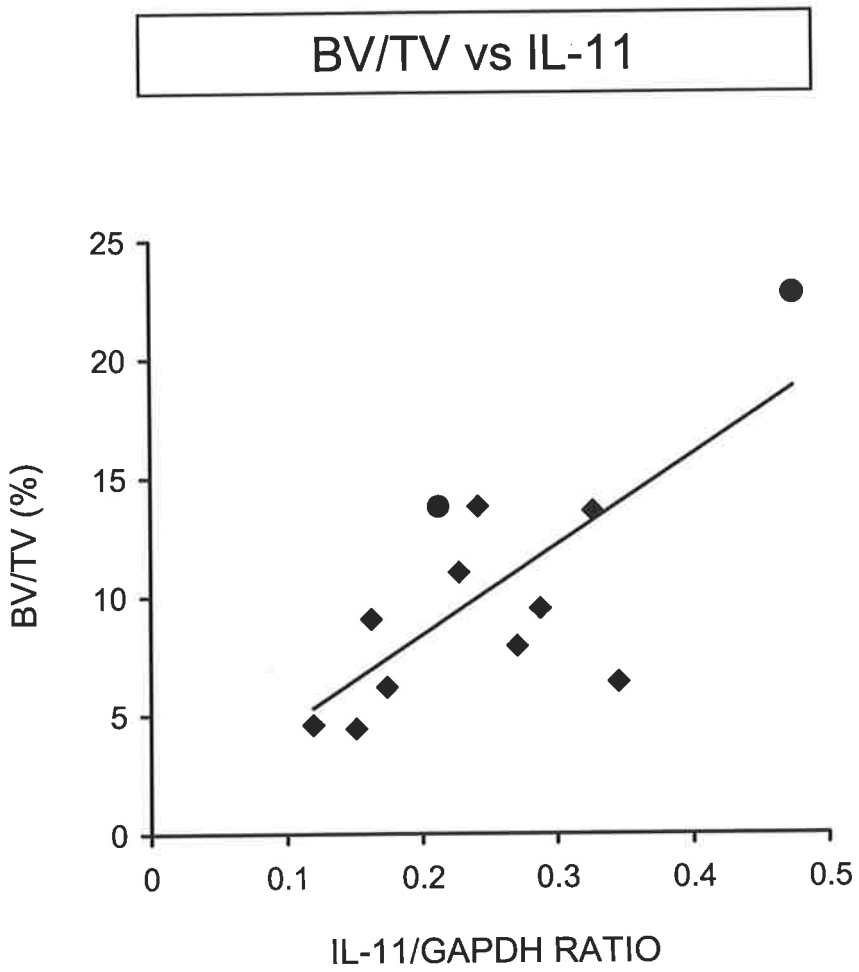

Figure 7.16: A positive association was observed between BV/TV and the relative ratio of IL-11/GAPDH mRNA, measured in contiguous intertrochanteric trabecular bone samples, from control individuals (n = 12; BV/TV = 37.99*IL-11/GAPDH + 0.76; r = 0.73 and $p < 0.005$). Two cases, <40 years old, are indicated (●).

for IL-11 in bone is to act as an upstream stimulatory signal for osteoclast differentiation (Martin *et al.*, 1998), the full role of this pleiotropic cytokine in the bone microenvironment is not yet understood. For this reason, and as the temporal relationship between local IL-11 mRNA expression and initiation of bone resorption in these bone samples is not known, interpretation of the findings described here is speculative. Furthermore, it is acknowledged that the associations between ES/BS and BV/TV with IL-11 mRNA may be effect rather than cause (i.e., bone resorption may somehow negatively influence IL-11 mRNA expression). Additionally, it is important to note that the cellular origin(s) of the measured IL-11 mRNA expression in these human trabecular bone samples are not known.

No significant associations were observed between ES/BS, OS/BS, or BV/TV and IL-6/GAPDH mRNA expression (results not shown). However, when an outlier result, case C5 (72-year-old female) with a high relative expression level of IL-6/GAPDH mRNA (described in Chapter 5), was removed, a negative association was observed between ES/BS and IL-6/GAPDH mRNA expression in these control bone samples (n = 11; r = -0.60, $p < 0.04$; results not shown). In addition, a positive association was observed between BV/TV and IL-6/GAPDH mRNA expression when the outlier, case C5, was removed (n = 11; r = 0.81, $p < 0.001$; results not shown). As a positive association was found between IL-6/GAPDH and IL-11/GAPDH mRNA expression in these control bone samples (Figure 5.4; Chapter 5.4.3), the similar relationships between ES/BS and BV/TV with either IL-6 or IL-11 mRNA expression are not unexpected. However, as for the IL-11 data, an explanation of these results remains elusive.

Linear regression analysis was used to investigate potential associations between the mRNA expression of the osteoblastic cell marker, osteocalcin (OCN), and a bone osteoclastic cell marker, the calcitonin receptor (CTR), as determined by semi-quantitative RT-PCR (section 7.3.4), and histomorphometric parameters describing trabecular bone structure and bone turnover in control human bone samples. There were 12 control cases, for which both semi-quantitative RT-PCR and histomorphometric data were available for analysis (refer to sections 7.3.1 and 7.3.4). No associations were observed between any of the histomorphometric parameters and either OCN/GAPDH mRNA or CTR/GAPDH mRNA expression, measured in contiguous bone samples from the human proximal femur (results not shown).

7.4.4 Comparison of mean trabecular bone structure and bone turnover indices between females and males in the OA group

Gender differences in the histomorphometric parameters describing trabecular bone structure and bone turnover in OA human trabecular bone, sampled from the intertrochanteric region of the proximal femur, were assessed using the student's *t*-test. The only significant difference between OA females and OA males for any of the histomorphometric parameters was an increase in mean osteoid surface (OS/BS) in females compared to males ($p < 0.02$; Table 7.3). In addition, the variance in OS/BS was significantly higher in females compared to males (F-statistic = 5.2, representing the ratio of the female variance to male variance, $p < 0.002$; Table 7.3), suggesting that in the study population the females are a more heterogeneous group with respect to OS/BS. Furthermore, the increased OS/BS in females is consistent with the postmenopausal skeletal changes in women. Based on these comparisons between OA females and OA

males, further analyses of the histomorphometric data were made, independent of gender for the OA group, as was described for the control group (section 7.4.1).

Table 7.3 Trabecular bone structure and bone turnover indices in female and male OA intertrochanteric trabecular bone samples.

Histomorphometric parameter	Female (n = 18)	Male (n = 15)
BV/TV (%)	8.9 ± 2.9	10.0 ± 3.0
BS/TV (mm^2/mm^3)	2.3 ± 0.4	2.1 ± 0.5
BS/BV (mm^2/mm^3)	26.0 ± 6.5	22.4 ± 7.6
Tb.Th (μm)	83 ± 22	98 ± 26
Tb.Sp (μm)	834 ± 179	895 ± 231
Tb.N (number/mm)	1.13 ± 0.21	1.06 ± 0.25
OV/TV (%)	0.14 ± 0.09	0.10 ± 0.05
OV/BV (%)	1.53 ± 1.00	1.15 ± 0.76
OS/BS (%)	11.4 ± 6.4	7.0 ± 2.8 [a]
ES/BS (%)	6.6 ± 2.9	5.5 ± 1.9

Values are mean ± standard deviation.
[a] $p < 0.02$.

7.4.5 Comparison of mean trabecular bone structure and bone turnover indices between OA and control individuals

Histomorphometric parameters describing trabecular bone structure and bone turnover were measured in OA human trabecular bone, sampled from the intertrochanteric region of

the proximal femur, a skeletal site distal to the degenerative joint changes in OA, and in skeletal site-matched non-OA (control) trabecular bone. The student's *t*-test was used to assess whether there were any differences in the histomorphometric parameters between the OA and control groups. To enable comparison of age-matched control and OA groups, analysis was also performed after exclusion of the two younger control individuals, cases C1 (20-year-old female) and C8 (24-year-old male), and one younger OA individual, case OA27 (37-year-old male; Table 7.5). The mean values for the structural parameters of trabecular bone at the intertrochanteric region were similar for the OA and control groups (Table 7.4). When the age-matched control and OA groups were compared, OA bone had significantly increased mean surface density of bone (BS/TV; $p < 0.05$), decreased mean trabecular separation (Tb.Sp; $p < 0.04$), and increased mean trabecular number (Tb.N; $p < 0.05$; Table 7.5). The observed increase in BS/TV and decrease in Tb.Sp in OA trabecular bone, sampled from the intertrochanteric region, is consistent with a previous report, which compared OA trabecular bone with control bone sampled from the subchondral principal compressive region of the femoral head, a skeletal site adjacent to the degenerative joint changes in OA (Fazzalari *et al.*, 1992). Fazzalari *et al.* (1992) did not provide data for Tb.N for OA and control trabecular bone sampled from this skeletal site.

The mean values for the static indices of bone turnover, OV/TV, OV/BV, OS/BS, and ES/BS, showed the same overall relationships between the OA and control groups, whether all samples were included in the analysis (Table 7.4), or only those from individuals aged greater than 40 years (Table 7.5). In both analyses, mean eroded bone surface (ES/BS) was significantly decreased in the OA group ($p < 0.03$, Table 7.4; $p < 0.01$, Table 7.5), indicating reduced bone resorption at the intertrochanteric region in OA. This reduction in ES/BS in OA bone is consistent with a previous report of OA trabecular bone sampled

from the subchondral principal tensile region of the femoral head and the iliac crest (Fazzalari *et al.*, 1992). Additionally, OA bone had significantly increased mean OV/TV, in both analyses ($p < 0.01$, Table 7.4; $p < 0.03$, Table 7.5). Although the mean values for the other parameters corresponding to bone formation, OV/BV and OS/BS, were higher in OA bone than in the controls, this difference did not reach statistical significance (Tables 7.4 and 7.5).

Table 7.4 Trabecular bone structure and bone turnover indices in OA and control intertrochanteric trabecular bone samples.

Histomorphometric parameter	**OA** (***n*** **= 33**) *(aged 37-85 years)*	**Control** (***n*** **= 12**) *(aged 20-85 years)*
BV/TV (%)	9.4 ± 3.0	10.2 ± 5.2
BS/TV (mm^2/mm^3)	2.2 ± 0.5	1.9 ± 0.5
BS/BV (mm^2/mm^3)	24.4 ± 7.1	25.3 ± 8.0
Tb.Th (μm)	90 ± 25	87 ± 24
Tb.Sp (μm)	862 ± 203	1016 ± 313
Tb.N (number/mm)	1.10 ± 0.23	0.97 ± 0.27
OV/TV (%)	0.12 ± 0.07	0.07 ± 0.04 [a]
OV/BV (%)	1.36 ± 0.90	1.05 ± 0.81
OS/BS (%)	9.4 ± 5.4	7.7 ± 4.0
ES/BS (%)	6.1 ± 2.5	9.6 ± 4.4 [b]

Values are mean ± standard deviation.
[a] $p < 0.01$, [b] $p < 0.03$ vs. OA group.

Table 7.5 Trabecular bone structure and bone turnover indices in intertrochanteric trabecular bone sampled from OA and control individuals aged over 40 years.

Histomorphometric parameter	OA >40 years (n = 32) *(aged 45-85 years)*	Control >40 years (n = 10) *(aged 43-85 years)*
BV/TV (%)	9.4 ± 3.0	8.6 ± 3.4
BS/TV (mm^2/mm^3)	2.2 ± 0.5	1.8 ± 0.5 [a]
BS/BV (mm^2/mm^3)	24.3 ± 7.3	26.4 ± 8.4
Tb.Th (μm)	90 ± 25	84 ± 25
Tb.Sp (μm)	861 ± 206	1089 ± 291 [b]
Tb.N (number/mm)	1.10 ± 0.24	0.90 ± 0.24 [a]
OV/TV (%)	0.12 ± 0.08	0.07 ± 0.04 [c]
OV/BV (%)	1.37 ± 0.92	1.16 ± 0.84
OS/BS (%)	9.4 ± 5.5	8.1 ± 4.3
ES/BS (%)	6.1 ± 2.5	10.5 ± 4.1 [d]

Values are mean ± standard deviation.
[a] $p < 0.05$, [b] $p < 0.04$, [c] $p < 0.03$, [d] $p < 0.01$ vs. OA group.

7.4.6 Age-related changes in trabecular bone structure and bone turnover indices in OA and control individuals

To investigate whether there are any age-related changes in the histomorphometric parameters describing trabecular bone structure and bone turnover in OA human trabecular bone, sampled from the intertrochanteric region of the proximal femur, each histomorphometric parameter was plotted as a function of increasing age in years, and analysed by linear regression analysis, as for the controls in section 7.4.2. In contrast to the

age-related decline in BV/TV in controls, BV/TV was not dependent on age in the OA group (Figure 7.17). This finding of no age-dependence for trabecular bone volume at the intertrochanteric region for the OA group is consistent with previous reports from a comparable region of the proximal femur and from the medial principal compressive region of the femoral head (Crane *et al.*, 1990; Fazzalari and Parkinson, 1998). Tb.Sp was not dependent on age in the OA group, in contrast to the age-related increase in Tb.Sp for controls (Figure 7.18). In addition, the plot of Tb.Sp versus age showed a segregation of values between control and OA individuals, such that the values for OA were, in general, lower than for the controls greater than 40 years of age (Figure 7.18; Table 7.5). There were no relationships with age for any of the other histomorphometric parameters describing trabecular bone structure, BS/TV, BS/BV, Tb.Th, and Tb.N, in OA human trabecular bone (results not shown), consistent with the control data (section 7.4.2).

The histomorphometric parameter describing eroded bone surface, ES/BS, was not dependent on age for the OA group, in contrast to the age-related increase in ES/BS for the controls (Figure 7.19). The OA values for ES/BS segregated such that they were, almost entirely, lower than the control values in each corresponding age range, which was consistent with the difference in mean values of ES/BS between the OA and control groups (Tables 7.4 and 7.5). Osteoid surface (OS/BS) showed no statistical dependence on age for the OA group (Figure 7.20). In contrast, there was a significant increase in OS/BS with age for controls (Figure 7.20). Despite the lack of correlation with age in OA for either ES/BS or OS/BS, there was a statistically significant positive correlation between ES/BS and OS/BS in OA ($r = 0.42$, $p < 0.02$; Figure 7.21), which was also observed for the control group data (Figure 7.21). However, both the slope and the intercept of the linear regression line for the OA samples was greater than for the control samples ($p < 0.05$ and $p < 0.001$,

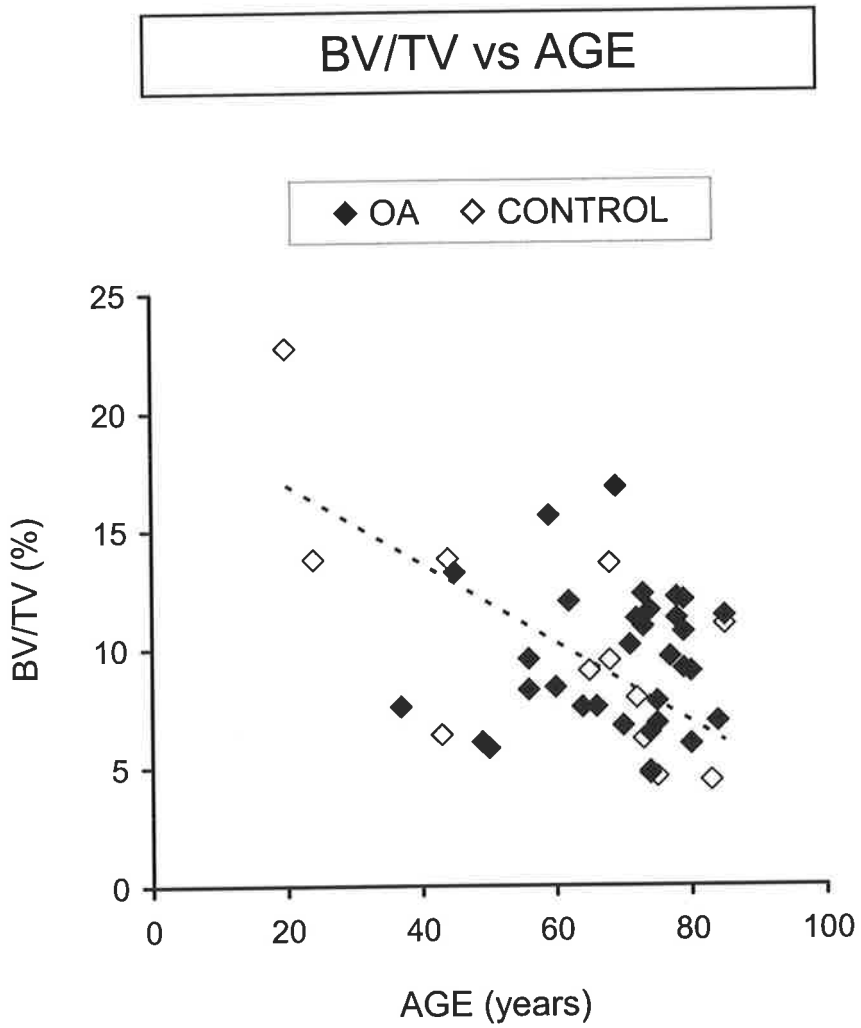

Figure 7.17: Changes in BV/TV with age in intertrochanteric trabecular bone from OA (n = 33) and control (n = 12) individuals. There was no significant change in BV/TV with age in OA (BV/TV = 0.009*AGE + 8.80; r = 0.03 and p = NS). There was a significant decline in BV/TV with age in controls (BV/TV = -0.17*AGE + 20.25; r = -0.70 and $p < 0.008$ {broken line}). NS = not significant.

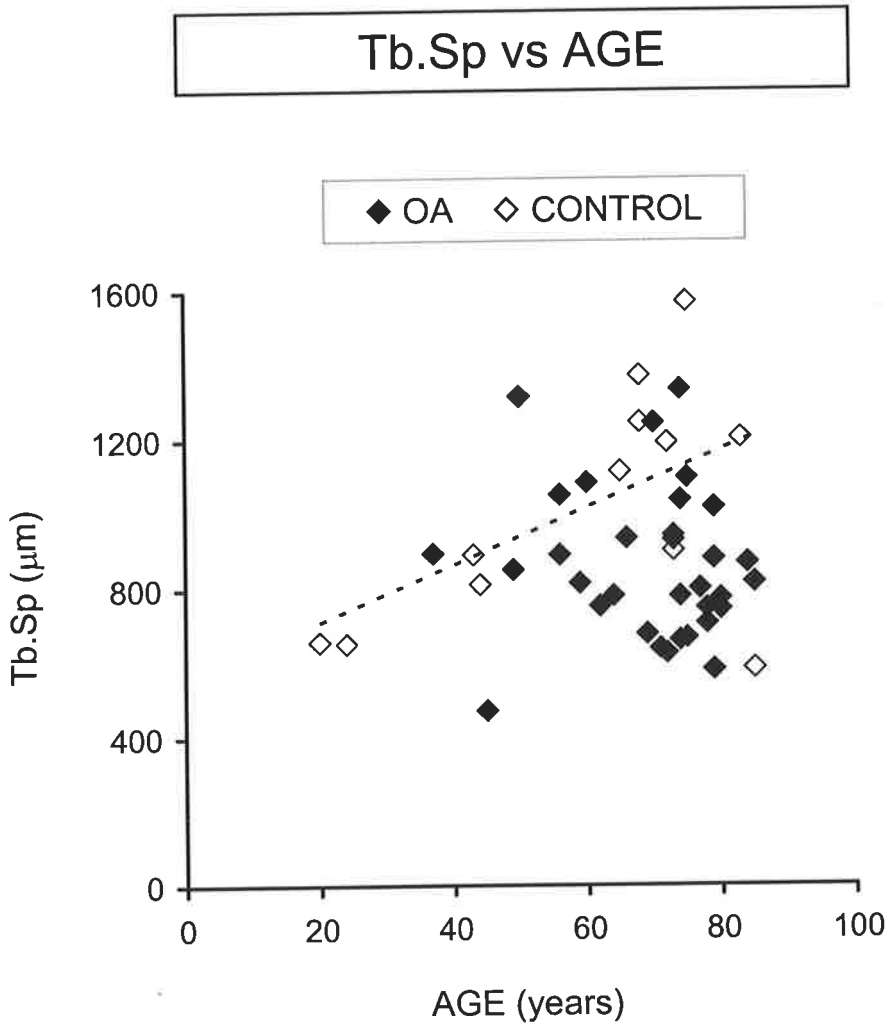

Figure 7.18: Changes in Tb.Sp with age in intertrochanteric trabecular bone from OA ($n = 33$) and control ($n = 12$) individuals. There was no significant change in Tb.Sp with age in OA (Tb.Sp = -1.88*AGE + 991.46; r = -0.11 and p = NS). There was a significant increase in Tb.Sp with age in controls (Tb.Sp = 7.66*AGE + 556.93; r = 0.54 and $p < 0.05$ {broken line}). NS = not significant.

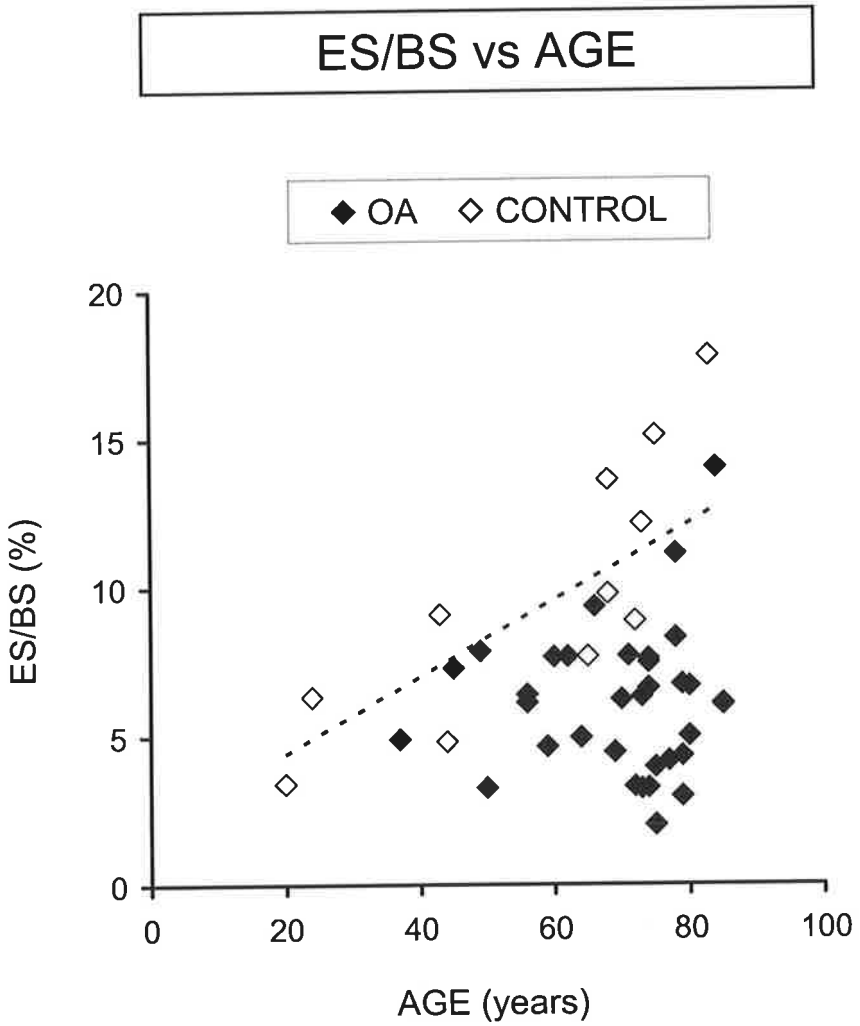

Figure 7.19: Changes in ES/BS with age in intertrochanteric trabecular bone from OA (n = 33) and control (n = 12) individuals. There was no significant change in ES/BS with age in OA (ES/BS = 0.02*AGE + 4.87; r = 0.08 and p = NS). There was a significant increase in ES/BS with age in controls (ES/BS = 0.13*AGE + 1.83; r = 0.65 and $p < 0.02$ {broken line}). NS = not significant.

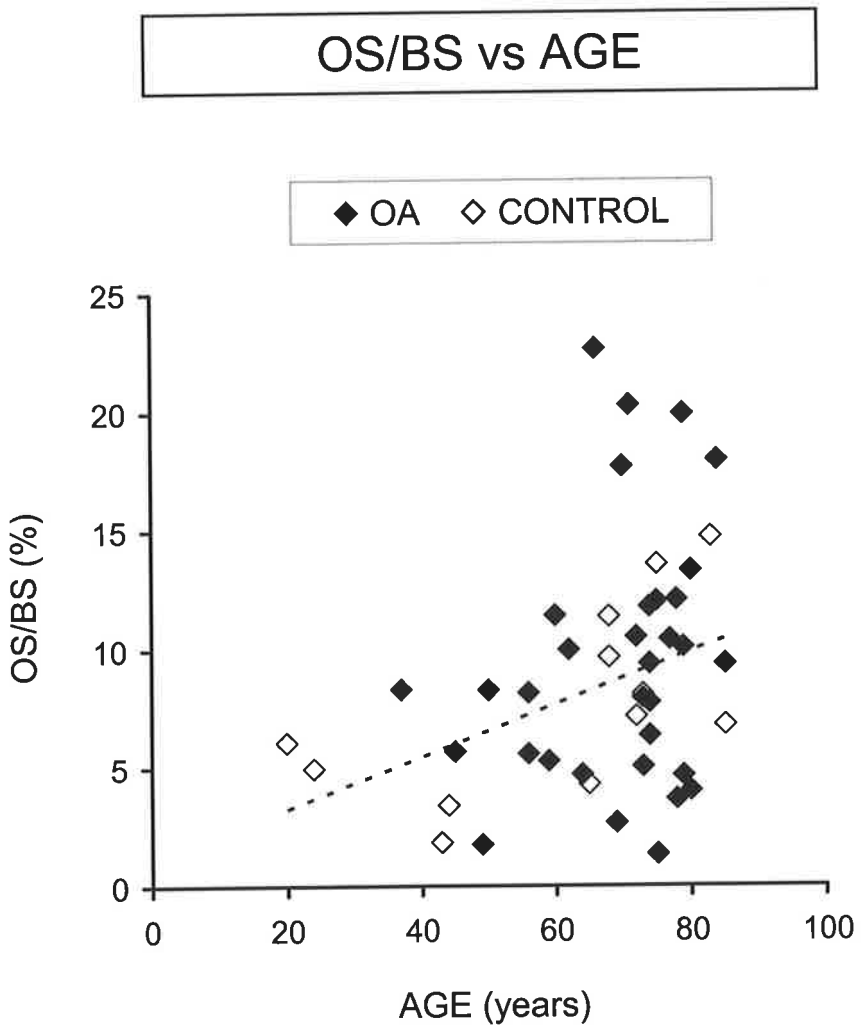

Figure 7.20: Changes in OS/BS with age in intertrochanteric trabecular bone from OA (n = 33) and control (n = 12) individuals. There was no significant change in OS/BS with age in OA (OS/BS = 0.11*AGE + 1.77; r = 0.24 and p = NS). There was a significant increase in OS/BS with age in controls (OS/BS = 0.11*AGE + 1.03; r = 0.61 and $p < 0.03$ {broken line}). NS = not significant.

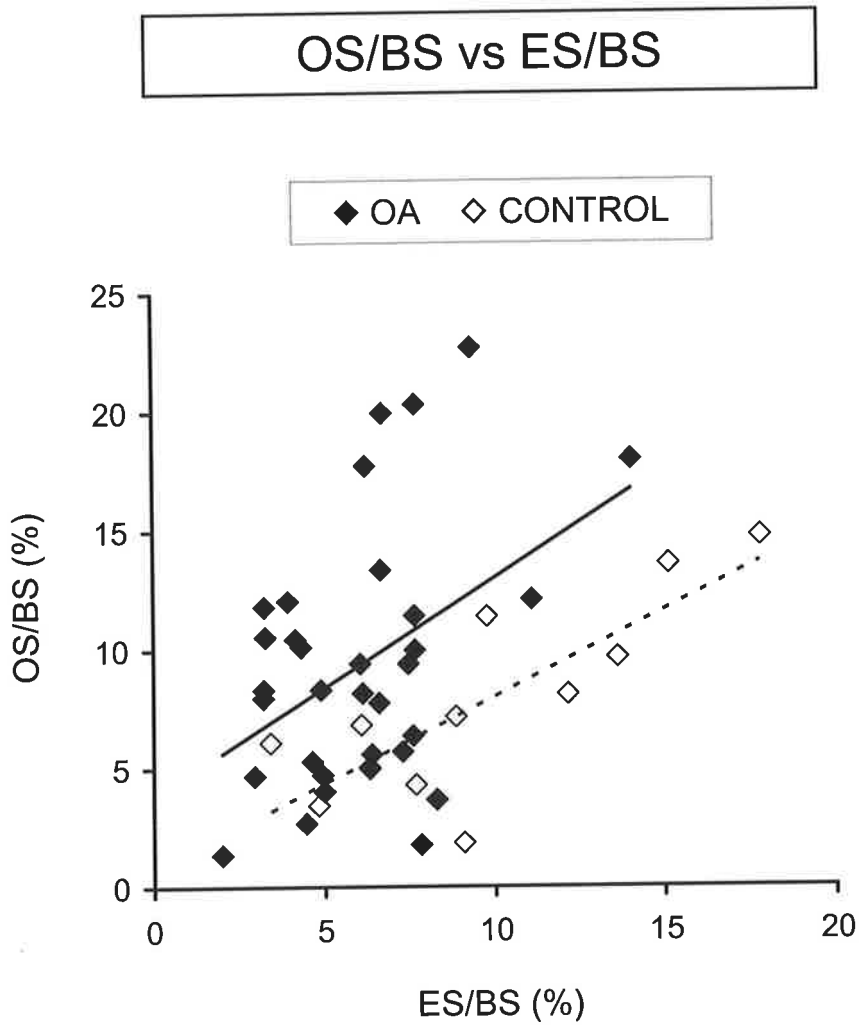

Figure 7.21: Associations between OS/BS and ES/BS in intertrochanteric trabecular bone from OA (n = 33) and control (n = 12) individuals. A significant positive correlation was observed between the two parameters in OA patients (OS/BS = 0.92*ES/BS + 3.77; r = 0.42 and $p < 0.02$ {solid line}) and controls (OS/BS = 0.73*ES/BS + 0.71; $r = 0.79$ and $p < 0.001$ {broken line}).

respectively), indicating that for a given amount of resorption there is more bone-forming surface in the OA group than for the controls (Figure 7.21). These results have important implications for bone remodelling in OA, at least at the intertrochanteric region of the proximal femur, a skeletal site distal to the degenerative joint changes in OA.

The histomorphometric parameters describing osteoid volume, OV/TV and OV/BV, were not age-dependent in OA trabecular bone (results not shown), consistent with the control data (section 7.4.2). A significant positive association was observed between two bone formation parameters, OV/BV and OS/BS, in OA bone ($r = 0.59$, $p < 0.001$; Figure 7.22), and in control bone (Figure 7.22). In addition, there was a significant positive association between OV/TV and OS/BS in the OA trabecular bone samples ($r = 0.65$, $p < 0.001$; Figure 7.23). A statistical association between OV/TV and OS/BS in the controls was only observed when the outlier, case C7 (83-year-old female) with low OV/TV and high OS/BS values, was removed (Figure 7.7; section 7.4.2). As detailed in section 7.4.2, the positive associations between OV/BV and OS/BS, and OV/TV and OS/BS, are not unexpected as osteoid volume and the extent of osteoid surface are linked by the temporal aspect of bone formation (i.e., changes in osteoid volume and in the extent of osteoid surface may reflect variations in the rate of osteoid formation and/or variations in the rate of mineralisation). Furthermore, an increase in the birth-rate of new BMUs may reflect greater osteoid volume and surface.

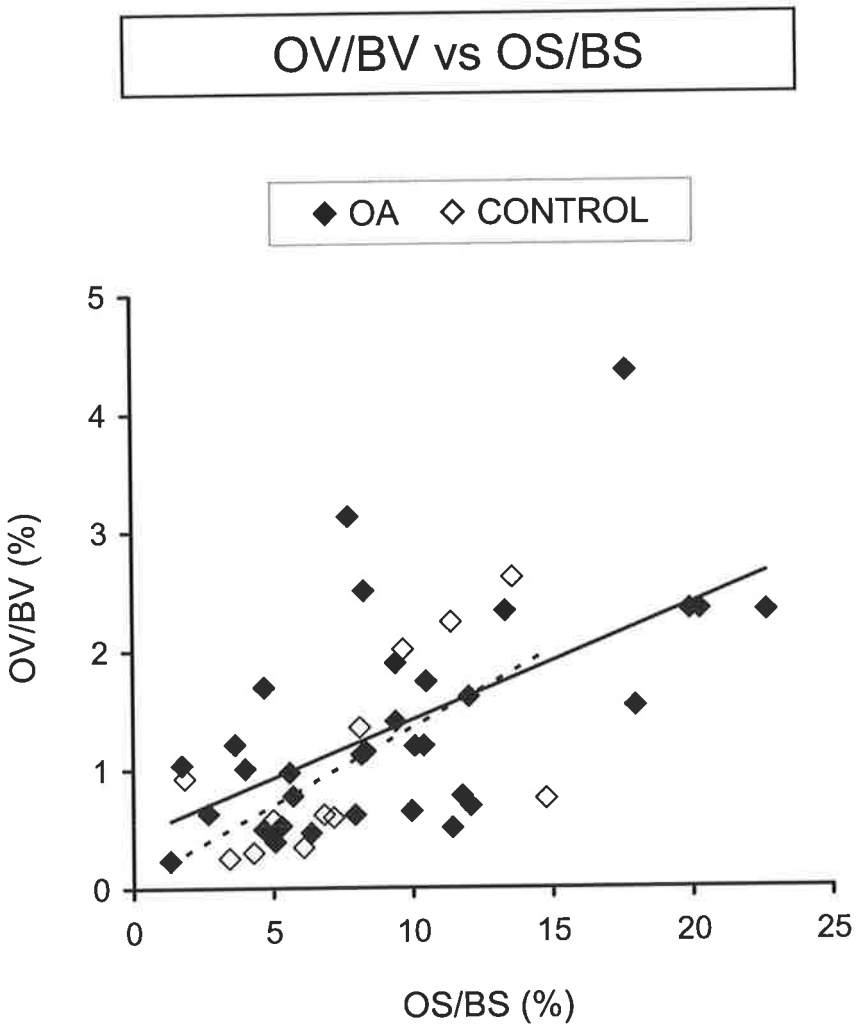

Figure 7.22: Associations between OV/BV and OS/BS in intertrochanteric trabecular bone from OA (n = 33) and control (n = 12) individuals. A significant positive correlation was observed between the two parameters in OA patients (OV/BV = 0.10*OS/BS + 0.44; r = 0.59 and $p < 0.001$ {solid line}) and controls (OV/BV = 0.13*OS/BS + 0.04; $r = 0.64$ and $p < 0.02$ {broken line}).

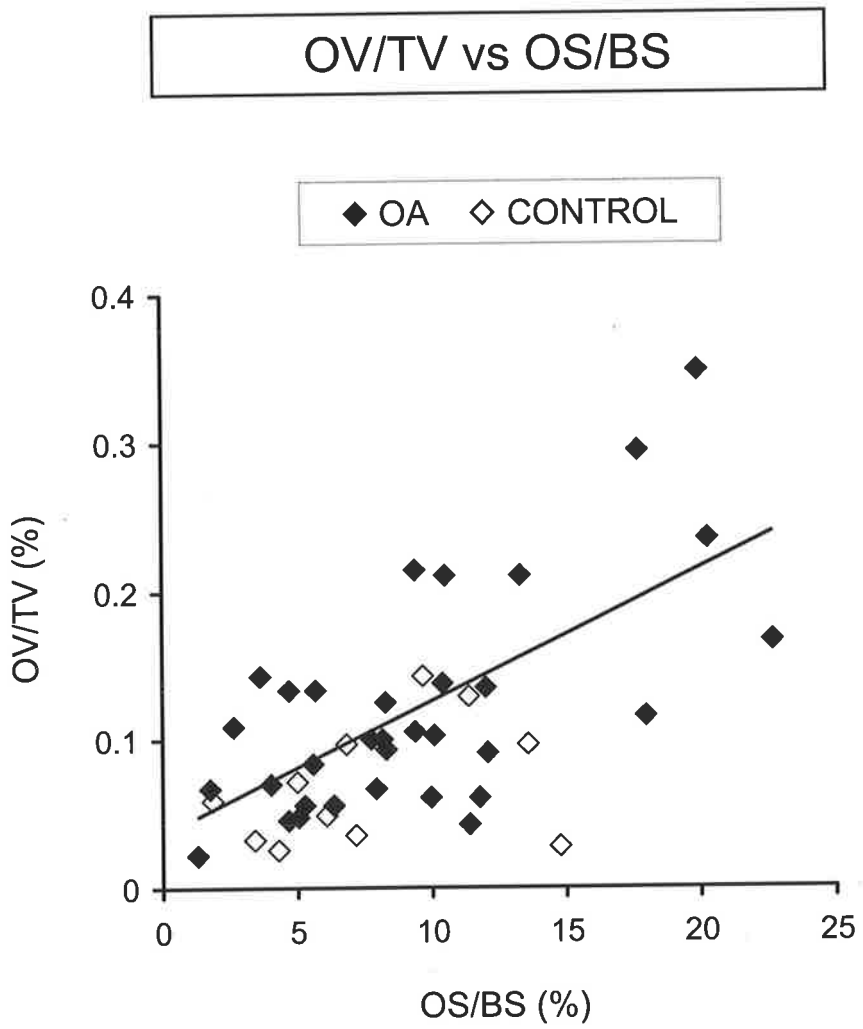

Figure 7.23: Associations between OV/TV and OS/BS in intertrochanteric trabecular bone from OA (n = 33) and control (n = 12) individuals. A significant positive correlation was observed between the two parameters in OA patients (OV/TV = 0.009*OS/BS + 0.04; r = 0.65 and $p < 0.001$ {solid line}). No association was observed between the two parameters in controls (OV/TV = 0.004*OS/BS + 0.04; r = 0.36 and p = NS). NS = not significant.

7.4.7 Associations between bone histomorphometric parameters and mRNA levels of skeletally active molecules in OA and control trabecular bone from the human proximal femur

Histomorphometric parameters describing trabecular bone structure and bone turnover, and the levels of mRNA corresponding to factors known to have important regulatory roles in bone remodelling, were measured in contiguous bone samples from the intertrochanteric region of the proximal femur for OA individuals. To investigate potential relationships between the histomorphometric parameters and mRNA levels of skeletally active molecules, the data were co-plotted, as for the controls in section 7.4.3, and analysed by linear regression analysis. Because of much evidence that the ratio of RANKL to OPG is the main determinant of the pool size of active osteoclasts in the local bone microenvironment (Hofbauer *et al.*, 2000), the relationship between the ratio of RANKL/OPG mRNA, as determined by semi-quantitative RT-PCR (section 7.3.4), and histomorphometric parameters describing trabecular bone structure and bone turnover (particularly eroded bone surface), was explored in OA bone. There were 12 OA cases, for which both semi-quantitative RT-PCR and histomorphometric data were available for analysis (refer to sections 7.3.1 and 7.3.4).

In contrast to the strong positive association between ES/BS and the ratio of RANKL/OPG mRNA in control trabecular bone (Figure 7.8; section 7.4.3), no statistical association was observed between ES/BS and the RANKL/OPG mRNA ratio in OA trabecular bone (Figure 7.24). Interestingly, the OA data points clustered at the lower end of the positive linear regression line for controls (Figure 7.24), which was consistent with the reduced mean ES/BS and reduced RANKL/OPG mRNA expression in the OA group, compared to the controls (Tables 7.4 and 7.5; Figure 6.16; Table 6.5; Chapter 6.4.4; respectively).

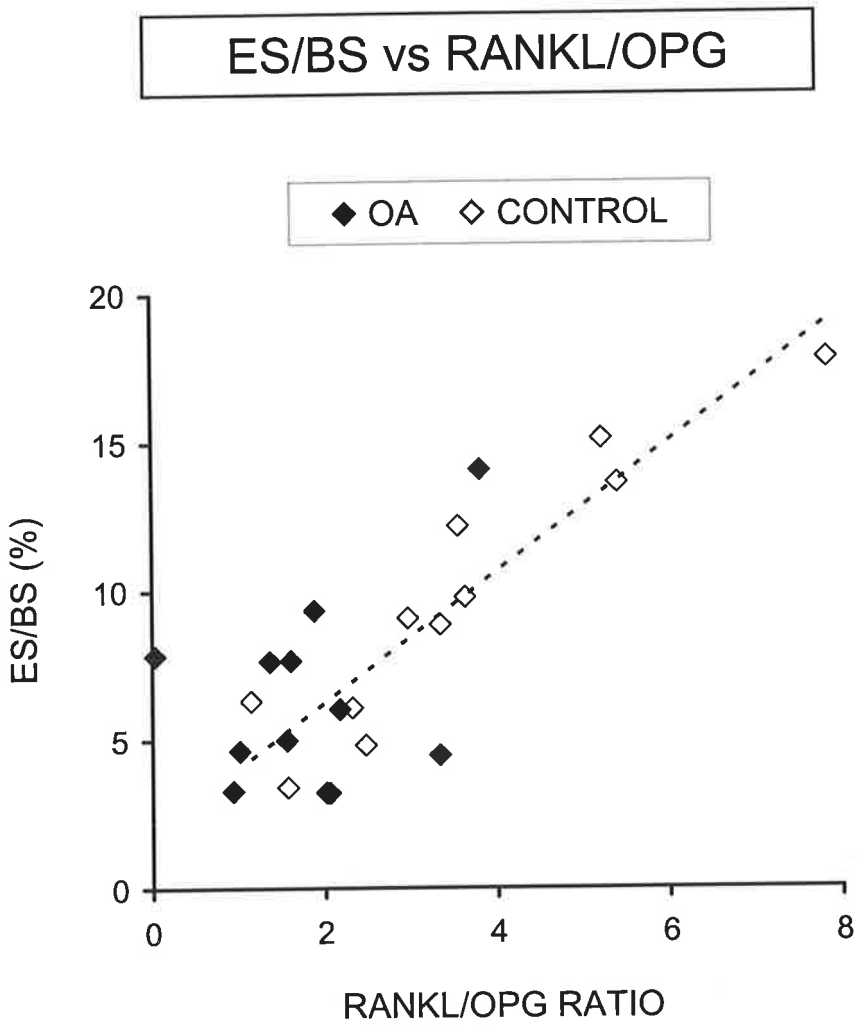

Figure 7.24: Associations between ES/BS and the RANKL/OPG mRNA ratio, measured in contiguous intertrochanteric trabecular bone samples, from OA (n = 12) and control (n = 11) individuals. No significant relationship was found for the OA group (ES/BS = 1.06*RANKL/OPG + 4.45; r = 0.34 and p = NS). A positive association was observed between the two parameters in controls (ES/BS = 2.20*RANKL/OPG + 1.86; r = 0.93 and $p < 0.001$ {broken line}). NS = not significant.

Further, no associations were observed between ES/BS and RANKL/GAPDH mRNA, OPG/GAPDH mRNA, or RANK/GAPDH mRNA expression in the OA bone samples (results not shown). There was no significant association between OS/BS and the RANKL/OPG mRNA ratio in OA bone (Figure 7.25), which is in contrast to the positive association between OS/BS and RANKL/OPG mRNA in the control bone samples (Figure 7.25; section 7.4.3). In addition, as for ES/BS, no associations were observed between OS/BS and RANKL/GAPDH mRNA or OPG/GAPDH mRNA expression, in OA bone (results not shown). When BV/TV values versus the RANKL/OPG mRNA ratio were plotted for the OA bone samples, no association was observed (Figure 7.26). In contrast, there was a negative association between BV/TV and RANKL/OPG mRNA expression in the controls (Figure 7.26; section 7.4.3). Further, no association was observed between the osteoid volume parameters, OV/TV and OV/BV, or any of the other bone structural parameters, BS/TV, BS/BV, Tb.Th, Tb.Sp, and Tb.N, with the RANKL/OPG mRNA ratio in the OA bone samples (results not shown), consistent with the control group data (section 7.4.3).

Current evidence suggests that one major role for IL-6 and IL-11 in bone is to act as an upstream stimulatory signal for osteoclast differentiation (Martin *et al.*, 1998; as detailed in Chapter 5.1). In addition, IL-6 and IL-11 have both been implicated as suppressors of osteoblastic synthetic activity (Hughes and Howells, 1993a; Hughes and Howells, 1993b). However, a recent report of over-expression of IL-11 in transgenic mice suggests that this cytokine functions as an anabolic factor for bone *in vivo* (Takeuchi *et al.*, 2002). The full role of these pleiotropic cytokines in the bone microenvironment is not completely understood. Linear regression analysis was used to investigate whether there are any associations between expression of IL-6 and IL-11 mRNA, as determined by semi-

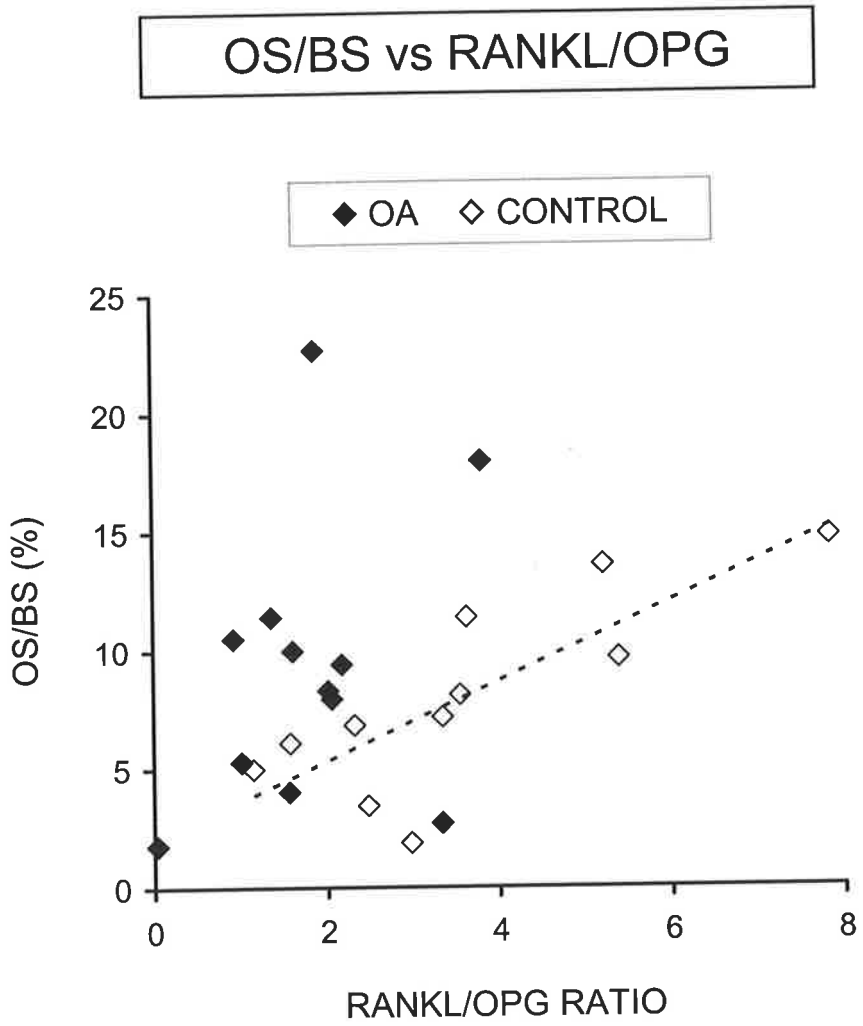

Figure 7.25: Associations between OS/BS and the RANKL/OPG mRNA ratio, measured in contiguous intertrochanteric trabecular bone samples, from OA (n = 12) and control (n = 11) individuals. No significant relationship was found for the OA group (OS/BS = 2.06*RANKL/OPG + 5.58; r = 0.34 and p = NS). A positive association was observed between the two parameters in controls (OS/BS = 1.69*RANKL/OPG + 1.94; r = 0.80 and $p < 0.001$ {broken line}). NS = not significant.

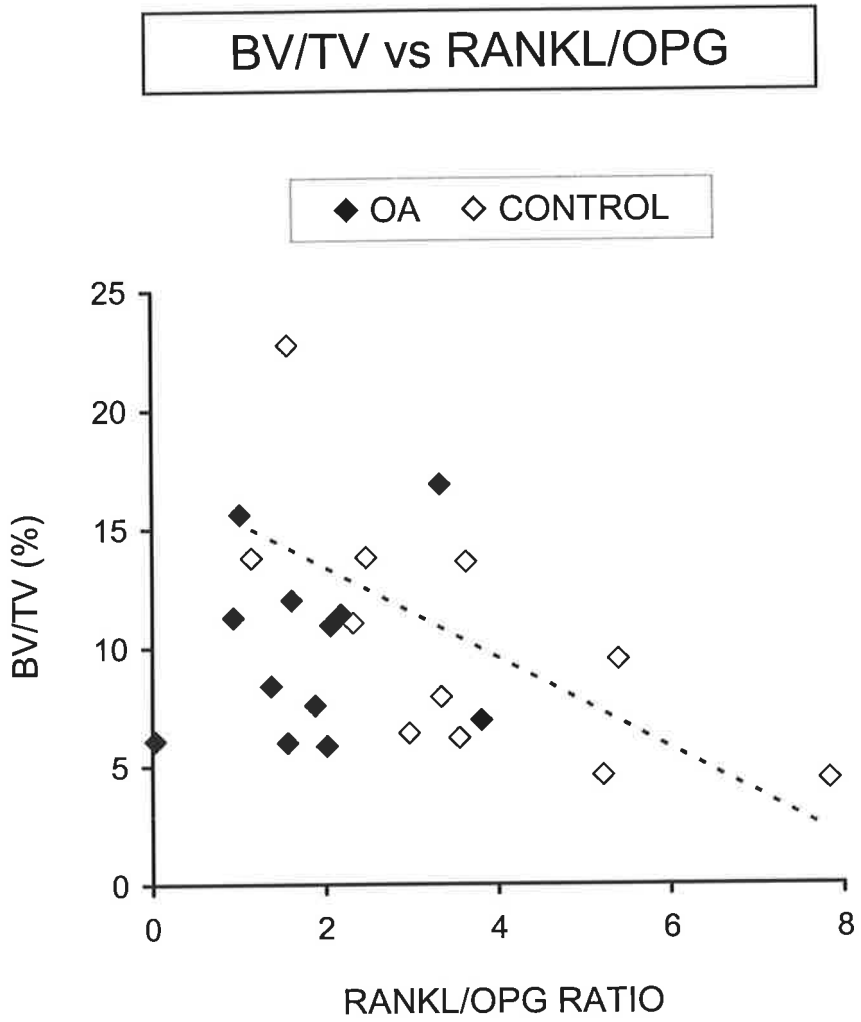

Figure 7.26: Associations between BV/TV and the RANKL/OPG mRNA ratio, measured in contiguous intertrochanteric trabecular bone samples, from OA (n = 12) and control (n = 11) individuals. No significant relationship was found for the OA group (BV/TV = 0.59*RANKL/OPG + 8.80; r = 0.16 and p = NS). A negative association was observed between the two parameters in controls (BV/TV = -1.90*RANKL/OPG + 17.17; r = -0.67 and $p < 0.05$ {broken line}). NS = not significant.

quantitative RT-PCR (section 7.3.4), and histomorphometric parameters describing trabecular bone structure and bone turnover in OA bone samples. There were 15 OA cases, for which both semi-quantitative RT-PCR and histomorphometric data were available for analysis (refer to sections 7.3.1 and 7.3.4). In contrast to the negative association between ES/BS and IL-11/GAPDH mRNA expression in control trabecular bone (Figure 7.14; section 7.4.3), no association was observed between ES/BS and IL-11/GAPDH mRNA, measured in contiguous bone samples from the intertrochanteric region, for the OA group (Figure 7.27). The OA data points were segregated from the controls on the plot of ES/BS versus IL-11/GAPDH mRNA, with lower ES/BS and lower IL-11 mRNA levels, which was consistent with the difference in mean values of ES/BS and IL-11/GAPDH mRNA expression between the OA and control groups (Tables 7.4 and 7.5; Figure 6.3; Table 6.3; Chapter 6.4.3; respectively). No association was observed between OS/BS and IL-11/GAPDH mRNA expression in the OA bone samples (Figure 7.28), consistent with the control group data (Figure 7.28; section 7.4.3). In addition, there was no association between BV/TV and IL-11/GAPDH mRNA expression in OA trabecular bone (Figure 7.29), which is in contrast to the positive association between BV/TV and IL-11/GAPDH mRNA expression observed in control bone samples (Figure 7.29; section 7.4.3). No significant associations were observed between ES/BS, OS/BS, or BV/TV and IL-6/GAPDH mRNA expression in these OA bone samples (results not shown).

Linear regression analysis was used to investigate associations between mRNA expression of the osteoblastic cell marker, OCN, and a bone osteoclastic cell marker, the CTR, as determined by semi-quantitative RT-PCR (section 7.3.4), and histomorphometric parameters describing trabecular bone structure and bone turnover, in contiguous bone samples from the intertrochanteric region, for OA individuals. There were 15 OA cases, for

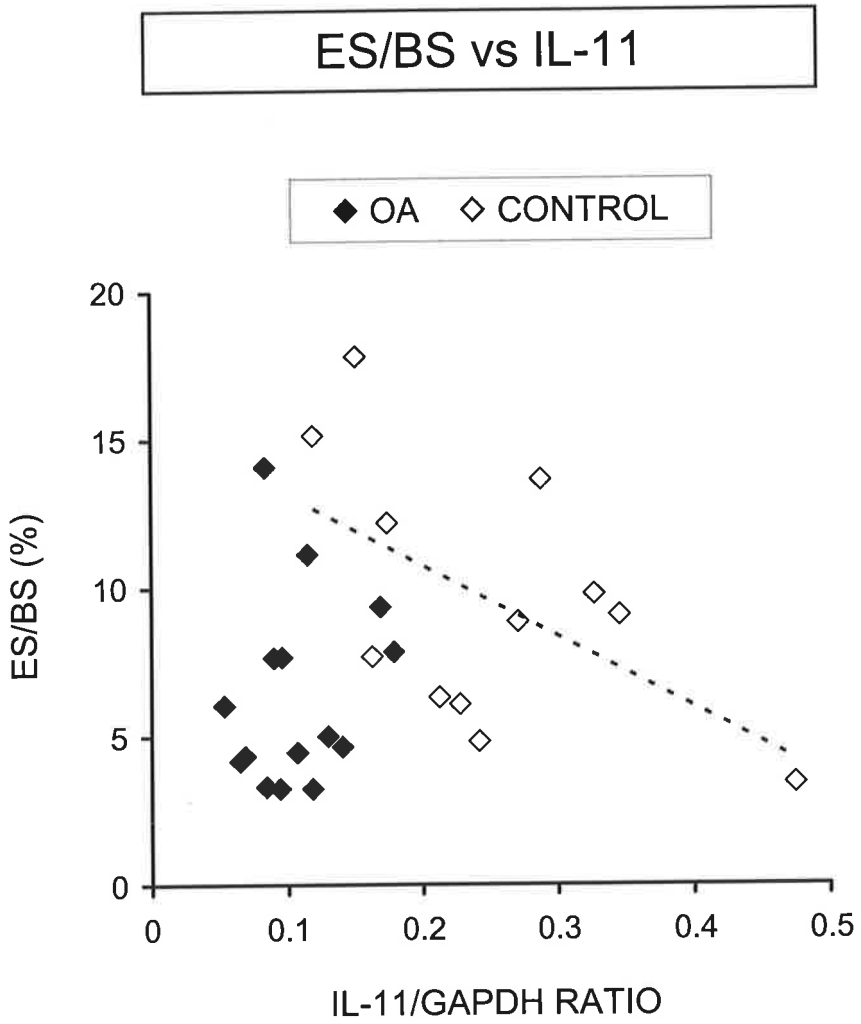

Figure 7.27: Associations between ES/BS and the relative ratio of IL-11/GAPDH mRNA, measured in contiguous intertrochanteric trabecular bone samples, from OA (n = 15) and control (n = 12) individuals. No significant relationship was found for the OA group (ES/BS = 15.36*IL-11/GAPDH + 4.78; r = 0.18 and p = NS). A negative association was observed between the two parameters in controls (ES/BS = -23.79*IL-11/GAPDH + 15.51; r = -0.54 and $p < 0.05$ {broken line}). NS = not significant.

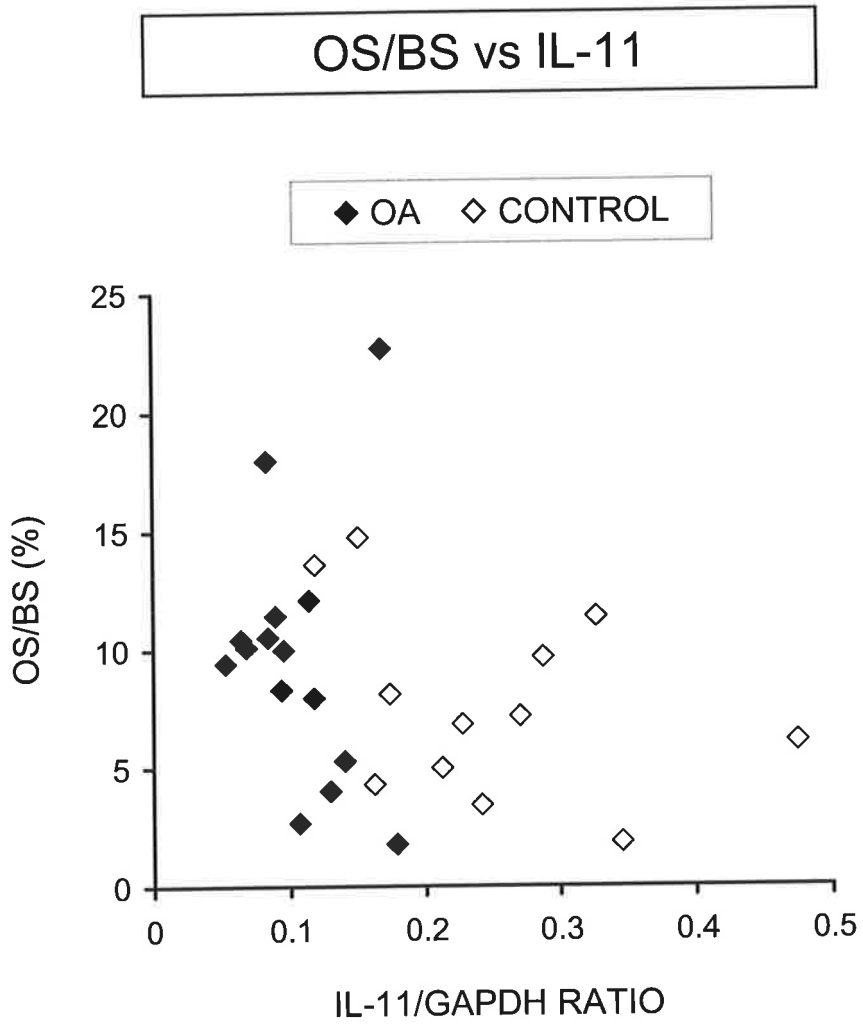

Figure 7.28: Associations between OS/BS and the relative ratio of IL-11/GAPDH mRNA, measured in contiguous intertrochanteric trabecular bone samples, from OA (n = 15) and control (n = 12) individuals. No significant relationship was observed between the two parameters in either the OA group (OS/BS = -16.44*IL-11/GAPDH + 11.39; r = -0.11 and p = NS) or controls (OS/BS = -14.79*IL-11/GAPDH + 11.37; r = -0.37 and p = NS). NS = not significant.

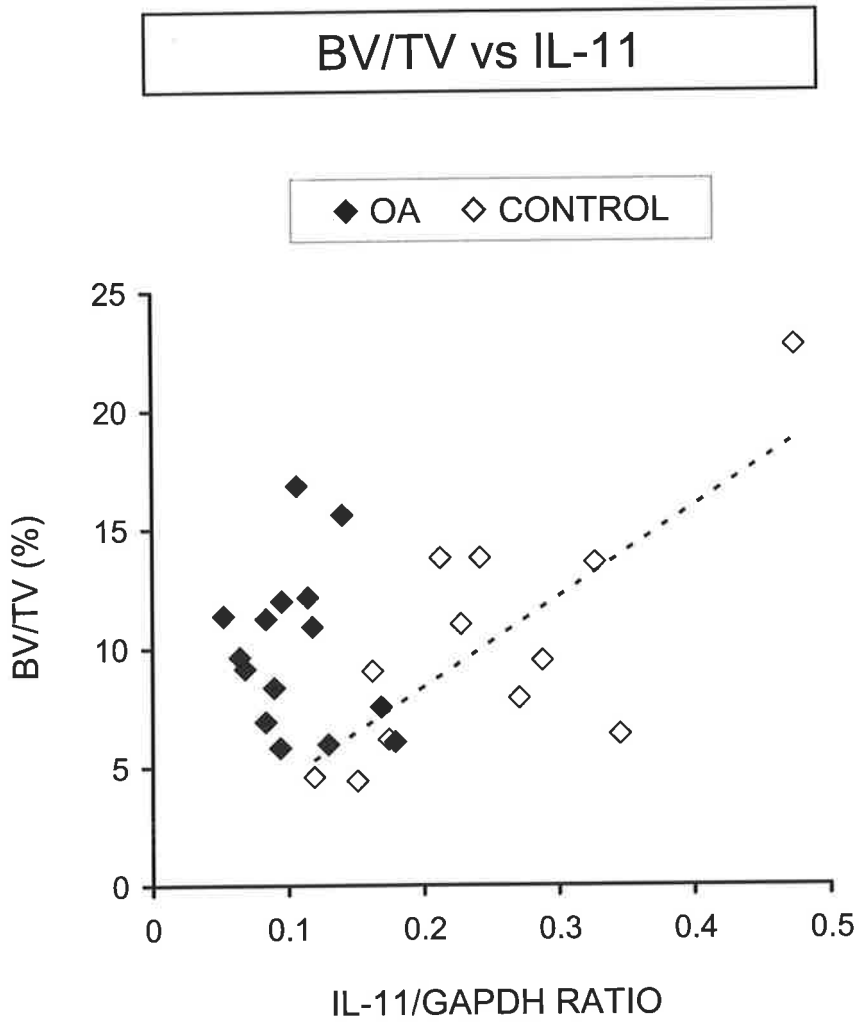

Figure 7.29: Associations between BV/TV and the relative ratio of IL-11/GAPDH mRNA, measured in contiguous intertrochanteric trabecular bone samples, from OA (n = 15) and control (n = 12) individuals. No significant relationship was found for the OA group (BV/TV = -12.60*IL-11/GAPDH + 11.30; r = -0.14 and p = NS). A positive association was observed between the two parameters in controls (BV/TV = 37.99*IL-11/GAPDH + 0.76; r = 0.73 and $p < 0.005$ {broken line}). NS = not significant.

which both semi-quantitative RT-PCR and histomorphometric data were available for analysis (refer to sections 7.3.1 and 7.3.4). A significant positive association was observed between the bone formation parameter, OS/BS, and expression of OCN/GAPDH mRNA in OA trabecular bone ($r = 0.61, p < 0.01$; Figure 7.30). This association between OS/BS and OCN mRNA expression was not observed in the controls (Figure 7.30). The correlation between OCN mRNA, which is regarded as an indicator of bone formation and a molecular marker for osteoblasts (Stein and Lian, 1993), and OS/BS in OA bone, suggests that the OCN mRNA expression level measured in each OA bone sample is likely to reflect the extent of bone formation in the tissue. Positive associations were found between the histomorphometric parameters describing osteoid volume, OV/BV and OV/TV, with OS/BS in the OA bone samples (Figures 7.22 and 7.23, respectively). However, no associations were observed between OV/BV or OV/TV and OCN/GAPDH mRNA expression in OA bone (results not shown). Further, no associations were observed between any of the histomorphometric structural parameters and OCN/GAPDH mRNA in the OA bone samples (results not shown). CTR/GAPDH mRNA expression was not associated with any of the histomorphometric parameters (results not shown), consistent with the control group data (section 7.4.3).

7.5 DISCUSSION

The mRNA expression of a select group of skeletally active molecules has been investigated in non-diseased/control and OA trabecular bone sampled from the human proximal femur. These data are described in Chapters 5 and 6 of this thesis. However, the way in which the expression of these skeletally active molecules relates to trabecular bone structure and bone turnover in the control and OA human bone microenvironment needs to be established. Thus, the aim of the work described in this chapter was to investigate the

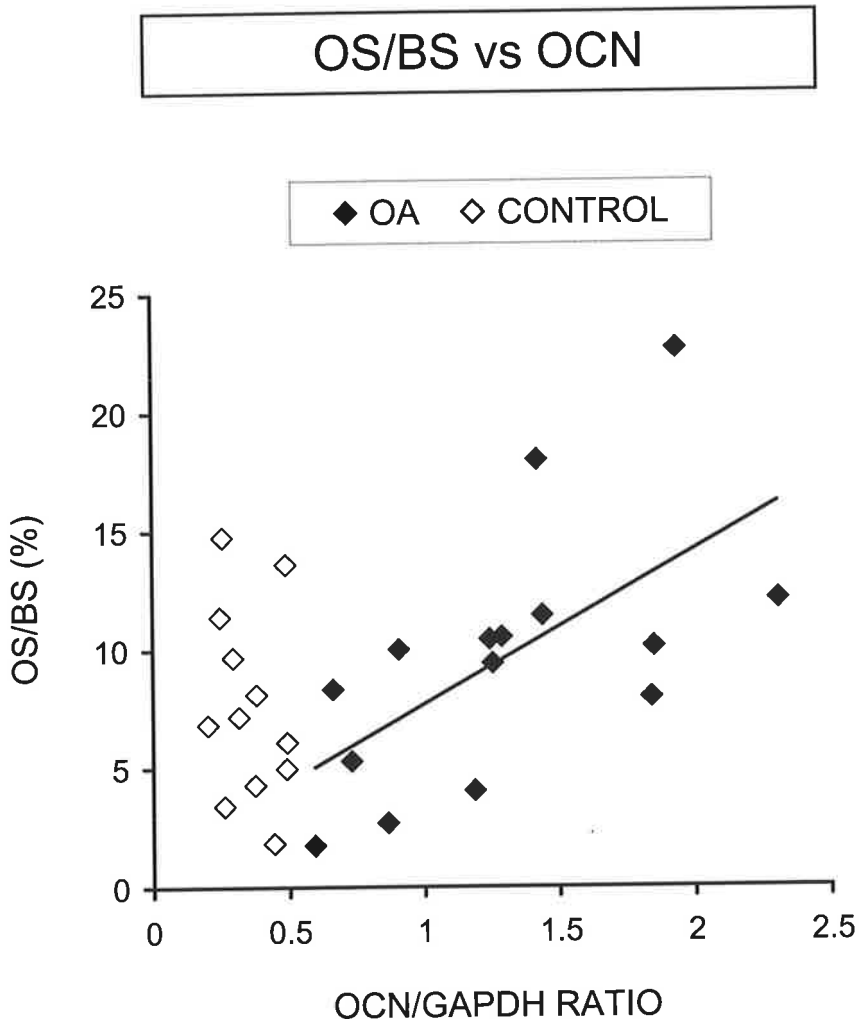

Figure 7.30: Associations between OS/BS and the relative ratio of OCN/GAPDH mRNA, measured in contiguous intertrochanteric trabecular bone samples, from OA (n = 15) and control (n = 12) individuals. A significant positive correlation was observed between the two parameters in OA patients (OS/BS = 6.53*OCN/GAPDH + 1.14; r = 0.61 and $p < 0.01$ {solid line}). No significant relationship was found for the control group (OS/BS = -8.25*OCN/GAPDH + 10.63; r = -0.22 and p = NS). NS = not significant.

relationships between histomorphometric parameters, describing trabecular bone structure and bone turnover, and mRNA expression levels of skeletally active molecules, measured in contiguous intertrochanteric trabecular bone samples from control and OA individuals. In addition, histomorphometric parameters of trabecular bone structure and bone turnover, measured in intertrochanteric bone samples, were compared between control and primary hip OA individuals. The intertrochanteric region of the proximal femur was chosen for sampling of trabecular bone because this region is remote from the subchondral bone that undergoes well-characterised secondary changes in severe OA (Fazzalari *et al.*, 1992). The skeletally active molecules in this investigation included the key regulators of osteoclast biology and bone metabolism, RANKL, OPG, and RANK, two cytokines capable of promoting osteoclast formation, IL-6 and IL-11, and the CTR and OCN, as cell specific markers of osteoclasts and osteoblasts, respectively.

7.5.1 The ratio of mRNA levels of RANKL to OPG correlates with bone remodelling indices in control trabecular bone from the human proximal femur

RANKL and OPG are important downstream signals of osteoclast biology, onto which many hormonal, chemical, and biochemical signals converge (Hofbauer and Heufelder, 2001; detailed in Chapter 5.1). RANKL is expressed on the cell surface of stromal/osteoblastic cells and promotes osteoclast development by binding to its cognate receptor, RANK, which is expressed on the surface of osteoclasts and their precursors, with the required presence of macrophage colony stimulating factor (M-CSF) (Anderson *et al.*, 1997; Hsu *et al.*, 1999; Lacey *et al.*, 1998; Nakagawa *et al.*, 1998; Wong *et al.*, 1997; Yasuda *et al.*, 1998b). OPG is a natural antagonist for RANKL and inhibits osteoclast formation and bone resorption (Simonet *et al.*, 1997). Hofbauer *et al.* (2000) hypothesised

that the ratio of RANKL to OPG is the main determinant of the pool size of active osteoclasts in the local bone microenvironment, acting as a final effector system to modulate differentiation, activation, and apoptosis of osteoclasts. Co-plots of the molecular measures of RANKL, OPG, and RANK mRNA and indices of trabecular bone structure and bone turnover revealed strong associations in contiguous intertrochanteric bone samples from control individuals (Figures 7.8-7.13). The bone resorption index, eroded bone surface (ES/BS), was strongly positively associated with RANKL/OPG mRNA levels (Figure 7.8) and this was found to be almost entirely because of the RANKL component (compare Figures 7.9 and 7.10). Furthermore, a multiple regression analysis found that ES/BS was statistically dependent on RANKL/OPG mRNA levels and not on the age of the control individuals (section 7.4.3). Given that the ratio of RANKL/OPG is likely to represent the actual local osteoclastogenic influence (Hofbauer *et al.*, 2000), the relationship between ES/BS and RANKL/OPG mRNA levels strongly supports the concept that these surrogate measures of RANKL and OPG relate directly to levels of expression of the corresponding proteins in the bone tissue. Moreover, the relationship between ES/BS and RANKL/OPG mRNA levels suggests that the effective concentration of RANKL is dominant in controlling the extent of bone resorption in non-diseased/control human trabecular bone.

The relationship between ES/BS and RANKL/OPG mRNA levels in human trabecular bone tissue is consistent with a number of *in vitro* and *in vivo* studies in rodents. For instance, soluble RANKL has been shown to concentration-dependently induce bone resorption in a fetal mouse long bone culture system (Tsukii *et al.*, 1998). Furthermore, this bone resorption was abolished when OPG was added concomitantly with soluble RANKL (Tsukii *et al.*, 1998). Mice subcutaneously injected with recombinant RANKL show a

reduction in trabecular bone volume at the proximal tibia (Lacey *et al.*, 1998). Interestingly, this reduction in bone volume was due to an increase in the osteoclast cell size, rather than a change in osteoclast number (Lacey *et al.*, 1998). Conversely, bone mineral density and trabecular bone volume increased in the distal femur from rats treated with recombinant human OPG, which was associated with a dose-dependent decrease in active osteoclast number (Yasuda *et al.*, 1998a).

Interestingly, the index of bone formation, osteoid surface (OS/BS), was also strongly positively associated with the RANKL/OPG mRNA ratio (Figure 7.12). This finding is consistent with the notion that bone resorption and bone formation are tightly coupled in the human bone microenvironment (Figure 7.5; section 7.4.2) and that bone turnover is initiated by bone resorption, which is in turn dependent on the effective levels of RANKL. It is important to note that the molecular indices (RANKL/OPG mRNA levels) are completely consistent with the histomorphometric parameters, a highly significant finding given the totally different means of assessing these two types of data.

OPG has been shown to play an important role as a regulator of postnatal bone mass in studies of OPG-deficient mice (Bucay *et al.*, 1998; Mizuno *et al.*, 1998). Mice, in which the OPG gene is deleted, develop extensive osteoporosis, associated with increased numbers of osteoclasts (Bucay *et al.*, 1998; Mizuno *et al.*, 1998). Furthermore, the OPG-deficient mice have increased bone turnover, associated with an increase in both osteoclast and osteoblast numbers, which is likely to reflect the coupling between osteoclast-mediated resorption and osteoblast-mediated bone formation (Bucay *et al.*, 1998). Interestingly, in patients with low bone turnover renal osteodystrophy, serum OPG levels, which were above the normal range, negatively correlated with the histomorphometric parameters of

bone resorption, ES/BS, and bone formation, osteoblast surface (Ob.S/BS), measured in iliac crest biopsies (Coen *et al.*, 2002).

As detailed in section 7.4.3, the evidence to date suggests that one major role for IL-6 and IL-11 in bone is to act as an upstream stimulatory signal for osteoclast differentiation (Martin *et al.*, 1998; as detailed in Chapter 5.1). In addition, IL-6 and IL-11 have both been implicated as suppressors of osteoblastic synthetic activity (Hughes and Howells, 1993a; Hughes and Howells, 1993b). However, a recent report of over-expression of IL-11 in transgenic mice suggests that this cytokine functions as an anabolic factor for bone *in vivo* (Takeuchi *et al.*, 2002). Thus, the full role of these pleiotropic cytokines in the bone microenvironment is not completely understood. Intriguingly, a negative association was observed between the bone resorption index, ES/BS, and IL-11 mRNA levels in contiguous intertrochanteric trabecular bone samples from control individuals (Figure 7.14). Further, trabecular bone volume, BV/TV, was positively associated with IL-11 mRNA levels (Figure 7.16). This latter finding is consistent with a recent report showing that over-expression of IL-11 in transgenic mice resulted in an increase in bone mass, which was due to increased bone formation and increased numbers of osteoblasts, with no change in bone resorption or osteoclast number (Takeuchi *et al.*, 2002). However, no association was observed between the index of bone formation, OS/BS, and IL-11 mRNA levels in these control human bone samples (Figure 7.15). Taken together, the negative association between ES/BS and IL-11 mRNA, and the positive association between BV/TV and IL-11 mRNA, suggest that local expression levels of IL-11 mRNA may be involved in inhibition of bone resorption in these intertrochanteric human trabecular bone samples. However, interpretation of these findings is speculative given that the cellular origin(s) of the measured IL-11 mRNA expression are not known, and that the temporal

relationship between local IL-11 mRNA expression and initiation of bone resorption in these human trabecular bone samples is not known. Interestingly, similar associations between ES/BS and BV/TV with IL-6 mRNA levels were observed in the human bone samples when an outlier result was removed (section 7.4.3). Collectively, these data draw attention to the fact that the full role of IL-6 and IL-11 in the bone microenvironment, under normal physiological conditions, is not completely understood, and may be different from that deduced from bone loss pathologies, as discussed below.

IL-6 has been implicated as playing a pathogenetic role in several conditions characterised by excessive osteoclastic bone resorption (including hyperparathyroidism, multiple myeloma, and rheumatoid arthritis), rather than a major involvement in normal physiological osteoclast development (Grey *et al.*, 1996; Kotake *et al.*, 1996; Manolagas and Jilka, 1995; Roodman *et al.*, 1992; Roodman, 1995). Histomorphometric indices of bone resorption, in iliac crest biopsies from multiple myeloma patients, have been shown to positively correlate with protein levels of IL-6, in marrow plasma aspirated from the bone biopsy area (Abildgaard *et al.*, 2000). Furthermore, Langub *et al.* (1996) have shown increased osteoclastic expression of IL-6 mRNA, detected by *in situ* hybridisation, associated with increased histomorphometric indices of bone resorption in the same iliac crest biopsies from seven patients with high bone turnover renal osteodystrophy.

7.5.2 Reduced eroded bone surface in OA human trabecular bone from the intertrochanteric region of the proximal femur

Previous studies have described the relative maintenance with age of trabecular bone volume in OA, compared with the well-known decrease in trabecular bone volume with age in non-OA controls (Crane *et al.* 1990). Although the relationship between BV/TV

with age for control subjects without progressive OA has been confirmed (Figure 7.1), comparison with OA subjects will require a greater sample size than for the data described in this chapter (Figure 7.17). In addition to the conservation of trabecular bone volume in OA, the femoral trabecular bone adjacent to the intertrochanteric region in OA is reported to have less well-mineralised bone than non-OA bone (Li and Aspden, 1997b; Mansell and Bailey, 1998). However, bone in OA with increased BV/TV is structurally more rigid (Crane *et al.* 1990; Li and Aspden 1997b; Martens *et al.*, 1983). The data presented in this chapter suggest that the principal reason for these differences in trabecular bone in OA may be an altered bone turnover balance, where a decrease in eroded surface (ES/BS), relative to bone formation (OS/BS; Figure 7.21; Tables 7.4 and 7.5), could result in maintenance of BV/TV. This suggestion would be consistent with other studies of the hip, iliac crest, and spine, which provided evidence that bone volume in OA is increased or maintained as a result of reduced bone turnover (Fazzalari *et al.*, 1992; Nevitt *et al.* 1995; Peel *et al.*, 1995). Given that those observations were made at sites distant from the joint, they were thought not to be subject to loading abnormalities or simply reactive to the joint pathology.

The decrease in the bone resorption index, ES/BS, relative to OS/BS, in OA intertrochanteric trabecular bone (Figure 7.21; Tables 7.4 and 7.5), is consistent with lower RANKL/OPG mRNA levels in intertrochanteric trabecular bone tissues from OA individuals (Figure 6.16; Table 6.5; Chapter 6.4.4). Furthermore, OA intertrochanteric bone has lower levels than control of mRNA for IL-6 and IL-11 (Figures 6.2 and 6.3, respectively; Table 6.3; Chapter 6.4.3), both of which can act on cells of the osteoblast lineage to promote osteoclast formation (Martin *et al.*, 1998).

The mean value for the bone formation parameter, osteoid volume (OV/TV), was significantly increased in OA intertrochanteric bone compared to control bone (Tables 7.4 and 7.5). Interestingly, there were positive associations between the bone formation parameters OV/BV and OS/BS, and OV/TV and OS/BS, in both OA and control bone samples (Figures 7.22 and 7.23, respectively). However, the mean values for OV/BV and OS/BS, although higher in OA bone, were not statistically different from controls (Tables 7.4 and 7.5). It is difficult to interpret the increased OV/TV in OA bone as it is not known whether this increase is a reflection of an increase in the birth-rate of new basic multicellular units (BMUs) and/or an increase in mineralisation lag time. Dynamic histomorphometry, using tetracycline double labelling (Frost, 1969), is needed to resolve whether there is a difference in the mineral apposition rate and/or the mineralisation lag time between OA and control bone. However, these studies would have to be performed with iliac crest bone biopsies to enable the comparison of primary OA hip patients to non-OA control individuals.

7.5.3 The relationships between the ratio of mRNA levels of RANKL to OPG with bone remodelling indices in controls are not evident for OA trabecular bone from the human proximal femur

Strong positive associations between both eroded bone surface (ES/BS) and osteoid surface (OS/BS) with RANKL/OPG mRNA levels were observed in contiguous intertrochanteric bone samples from control individuals (Figures 7.8 and 7.12). Given that the mean values for ES/BS and RANKL/OPG mRNA levels were both significantly lower in OA intertrochanteric bone (Tables 7.4 and 7.5; Figure 6.16; Table 6.5; Chapter 6.4.4; respectively), it was surprising that no relationship between ES/BS and RANKL/OPG mRNA levels was evident for OA bone (Figure 7.24). Interestingly, on the plot of ES/BS

versus RANKL/OPG mRNA, the OA data points clustered at the lower end of the positive linear regression line for controls (Figure 7.24). It is acknowledged that the number of cases in the OA and control groups for the molecular histomorphometric data is small. A greater sample size is required to explore whether there is any relationship between ES/BS and RANKL/OPG mRNA levels in OA intertrochanteric bone. In contrast to the control data, no relationship between OS/BS and RANKL/OPG mRNA levels was evident for OA bone (Figure 7.25). Given that the relationships between RANKL/OPG and bone turnover were not evident for the OA bone samples, at a skeletal site distal to the degenerative joint changes in OA, it can be hypothesised that the molecular mechanisms of bone turnover are fundamentally different in OA. Further, it can be speculated that the trabecular bone structures in OA arise by subversion of the physiological RANKL-controlled mechanisms.

OCN is utilised as an indicator of bone formation as it is one of the marker genes for the progression of osteoblastic differentiation (Stein and Lian, 1993). A significant positive association was observed between the index of bone formation, OS/BS, and OCN mRNA levels in contiguous intertrochanteric trabecular bone samples from OA individuals (Figure 7.30). This finding suggests that the OCN mRNA level measured in each OA bone sample is likely to reflect the extent of bone formation in the tissue. However, no relationship between OS/BS and OCN mRNA levels was evident for the control bone samples (Figure 7.30). Given that osteocytes have been shown to constitutively express OCN mRNA (Mason *et al.*, 1996), it is important that the cellular origin(s) of the measured OCN mRNA in these OA and control bone samples are elucidated. This can be resolved by the use of *in situ* hybridisation in combination with immunohistochemistry for the bone tissue localisation of OCN at the mRNA and protein level, respectively.

7.5.4 The potential use of molecular histomorphometric analysis of trabecular bone biopsies for predicting development of OA

The aetiology of OA is poorly understood, although it has both heritable and environmental components (Chitnavis *et al.*, 1997; Felson *et al.*, 1998; Spector *et al.*, 1996a). As detailed in section 7.1, numerous reports of an altered trabecular bone structure and bone matrix in individuals with OA (reviewed in Dequeker and Luyten, 2000) suggest that the bone changes may precede the joint degeneration of OA, or may arise secondarily to the joint pathology, or indeed may occur in parallel with the cartilage damage, driven by the same causative agent(s) that lead to cartilage disease. Interestingly, recent reports have shown that bone changes may precede cartilage changes in the onset and progression of primary OA (Bruno *et al.*, 1999; Goker *et al.*, 2000). This chapter describes an innovative experimental approach, involving the analysis of the mRNA expression of a select group of skeletally active molecules, in combination with histomorphometric assessment of trabecular bone structure and bone turnover, in contiguous human bone tissues sampled from the proximal femur. This experimental approach, termed "molecular histomorphometry", has provided strong evidence that effective levels of RANKL may be of central importance in determining the trabecular bone volume and bone turnover at the intertrochanteric region of the non-diseased/control human proximal femur (as detailed in sections 7.4.3 and 7.5.1). Furthermore, strikingly different results were obtained with intertrochanteric bone from individuals with severe primary hip OA (as detailed in sections 7.4.7 and 7.5.3). Given that the intertrochanteric region is remote from the subchondral bone that undergoes well-characterised secondary changes in severe OA (Fazzalari *et al.*, 1992), the data described in this chapter suggest that the use of molecular histomorphometry has great potential to elucidate mechanisms that lead to the altered bone structures found in OA. If the altered bone structure and composition is an early event in

the pathogenesis of OA, causing or exacerbating the condition, an understanding of the mechanisms, together with early recognition of potential OA sufferers, may enable preventative treatment of these individuals in the future.

A more complete gene profile, mapped to bone tissue morphology (i.e., molecular histomorphometry), in skeletal regions distal to the degenerative joint changes in patients with primary OA needs to be established. Specifically, a profile of gene expression mapped to bone tissue morphology in the iliac crest that is consistent with that in the proximal femur, such as at the intertrochanteric region, in the same OA individuals would be supportive of the hypothesis of a generalised skeletal involvement in OA. The use of the iliac crest for these studies is important for a number of reasons. Firstly, the iliac crest is a skeletal site accessible for bone biopsy and is the accepted bone biopsy site for histomorphometric assessment of skeletal change (Parfitt, 1983). Secondly, the iliac crest is not subject to loading abnormalities or joint pathological changes. Finally, the trabecular bone structure and bone matrix biochemistry of the iliac crest have been described in OA (Crane *et al.*, 1990; Dequeker *et al.*, 1993b; Fazzalari *et al.*, 1992; Gevers and Dequeker, 1987). For instance, the bone matrix from the iliac crest of OA subjects has been found to contain a higher content of the growth factors IGF-I, IGF-II, and TGF-β, and an increased concentration of OCN, compared with that in control subjects (Dequeker *et al.*, 1993b; Gevers and Dequeker, 1987). If the profile of gene expression mapped to bone tissue morphology in the iliac crest of severe primary hip OA individuals is consistently different to that of non-OA control subjects, the potential use of this molecular histomorphometric approach to identify individuals at risk of developing OA, before development of symptoms, could be explored. Other skeletally active factors that would be of specific

interest in these analyses, in addition to those described in this chapter, are detailed in Chapter 6.5.4.

7.5.5 Conclusions

The molecular determinants of trabecular bone structure and bone turnover are not understood in normal human bone or skeletal disease. However, a molecular histomorphometric experimental approach has provided strong evidence that effective levels of RANKL may be of central importance in determining the trabecular bone volume and bone turnover at the intertrochanteric region of the non-diseased/control human proximal femur. Strikingly different results were obtained with intertrochanteric bone from individuals with severe primary hip OA. Given that the intertrochanteric region is remote from the subchondral bone that undergoes well-characterised secondary changes in severe OA, the data described in this chapter suggest that the use of molecular histomorphometry has great potential to elucidate mechanisms that lead to the altered bone structures found in OA. If the altered bone structure and composition is an early event in the pathogenesis of OA, causing or exacerbating the condition, an understanding of the mechanisms, together with early recognition of potential OA sufferers, may enable preventative treatment of these individuals in the future.

CHAPTER 8

TRABECULAR BONE MICRODAMAGE IN THE HUMAN PROXIMAL FEMUR: REGIONAL DISTRIBUTION AND THE INFLUENCE OF AGE AND OSTEOARTHRITIS ON DAMAGE MORPHOLOGY

8.1 INTRODUCTION

Mechanical strain is an important stimulus for the maintenance of normal bone metabolism (Frost, 2000). However, repetitive loading causes skeletal fatigue or microdamage, resulting in the microscopic cracking of the ultra-structural bone matrix (Burr *et al.*, 1997). The accumulation of microdamage in bone has been shown to contribute to the loss of bone quality or biomechanical properties (Burr *et al.*, 1997; Carter *et al.*, 1981; Carter and Hayes, 1977; Forwood and Parker, 1989; Mashiba *et al.*, 2000; Pattin *et al.*, 1996; Schaffler *et al.*, 1989). However, the role of microdamage in the aetiology of fatigue fractures and bone adaptation is unknown. Microdamage created during testing, *ex vivo*, can increase the fragility of bone by decreasing the load necessary to cause fracture (Burr *et al.*, 1998; Carter and Hayes, 1977). *In vivo*, microdamage may accumulate in a bone faster than the bone's capacity to repair that damage. The effect of this residual microdamage on bone strength is unknown. However, microdamage is thought to play an important role in fractures attributed to aging or osteoporosis (Burr *et al.*, 1997). Microcrack accumulation is influenced by an individual's age (Fazzalari *et al.*, 1998b; Mori *et al.*, 1997; Schaffler *et al.*, 1995), cyclic loading (Schaffler *et al.*, 1989), and can influence bone remodelling (Mori and Burr, 1993).

Recently, bone microdamage has been described morphologically using laser scanning confocal microscopy and, in general, refers to discrete microcracks, cross-hatch staining, and diffuse staining (Fazzalari *et al.*, 1998a; O'Brien *et al.*, 2000). *In vivo*, microdamage is found in both cortical and trabecular human bone (Fazzalari *et al.*, 1998b; Schaffler *et al.*, 1995; Wenzel *et al.*, 1996). The distribution of microdamage in the human skeleton is unknown. The *in vivo* microdamage in human trabecular bone has been reported for the femoral head (Mori *et al.*, 1997), the intertrochanteric region of the proximal femur

(Fazzalari *et al.*, 1998b), vertebrae (Wenzel *et al.*, 1996), and in cortical bone of the femoral shaft (Schaffler *et al.*, 1995). There have been no reports of any difference in the morphology of microdamage (microcracks or cross-hatch staining or diffuse staining) found in cortical bone compared to trabecular bone. However, the distribution of microdamage in trabecular bone from different regions of the proximal femur from the same individual is unknown.

Microdamage repair is often confused with microfracture healing that involves microcallus formation (Fazzalari, 1993). These are quite distinct types of damage involving the initiation and progression of microscopic and ultra-structural damage on the one hand (Burr *et al.*, 1997), and trabecular fracture on the other (Fazzalari, 1993). Microdamage repair is not well understood but depends on targeted remodelling, which is distinct from fracture healing (Bentolila *et al.*, 1998; Burr *et al.*, 1997; Mori and Burr, 1993). Bone remodelling is achieved by initial activity of osteoclasts to resorb bone, followed by the formation of new bone by osteoblasts (Chapter 1.3.2). Bone remodelling fulfils metabolic functions, replacing bone matrix in a stochastic fashion throughout the skeleton. Superimposed on this is targeted remodelling of bone as a response to microdamage (Burr, 2002). These processes are regulated by factors that are produced and act locally in the bone microenvironment (Chapter 1.3.4). Thus, some basic multicellular units (BMUs) may be "targeted" to (i.e., initiated by, and in proximity to) microdamage, while others are involved in "stochastic" or "random" remodelling (Burr, 2002; Martin, 2000; Parfitt, 2002). Recently, microdamage has been shown to induce osteocyte apoptosis, which may provide an important local signal to remodel a damaged area of bone (Verborgt *et al.*, 2000). However, at this time, the nature and mechanism of the stimulus to recruit

osteoclasts to begin the targeted bone remodelling process, to remove the bone microdamage, is unknown.

As detailed in Chapter 6.1, osteoarthritis (OA) is characterised by progressive degenerative damage to the articular joint cartilage, and is associated with a conservation of bone mass and a different, more rigid structure of the subchondral bone (reviewed in Dequeker and Luyten, 2000). Although the major focus of research into the aetiology of OA has been on the articular cartilage, the disease is also associated with marked changes in the structure of subchondral trabecular bone (Fazzalari *et al.*, 1992), and changes in the structure of trabecular bone at sites distal to the joint articular surface, including the proximal femur and iliac crest (Crane *et al.*, 1990; Fazzalari *et al.*, 1992). Typically, the subchondral bone is sclerotic, with increased trabecular bone volume, and altered trabecular size and spacing, compared to age-matched controls (Crane *et al.*, 1990; Fazzalari *et al.*, 1992). These changes in trabecular bone structure in OA may develop to compensate for an altered bone matrix structure and composition in OA. For instance, OA subchondral femoral head and femoral neck trabecular bone have been shown to be hypomineralised (Brown *et al.*, 2002; Grynpas *et al.*, 1991; Helliwell *et al.*, 1996; Li and Aspden, 1997a; Li and Aspden, 1997b; Mansell and Bailey, 1998), and a recent study has shown that subchondral bone osteoblasts, from individuals with hip OA, produce a molecularly distinct collagen, type I collagen homotrimer (Bailey *et al.*, 2002). The different bone structure and bone matrix composition in OA is accompanied by altered biomechanical properties, with a more rigid trabecular bone in the subchondral and femoral neck regions (Li and Aspden, 1997a; Li and Aspden, 1997b; Martens *et al.*, 1983). Since this more rigid bone would have a reduced ability to absorb shock, it has been postulated that the bone changes in OA might exacerbate the disease or could even precede and be causative of the cartilage degeneration

(Radin *et al.*, 1972; Dequeker *et al.*, 1996). Given that the accumulation of microdamage in bone contributes to the loss of bone biomechanical properties (Burr *et al.*, 1997; Carter *et al.*, 1981; Carter and Hayes, 1977; Forwood and Parker, 1989; Mashiba *et al.*, 2000; Pattin *et al.*, 1996; Schaffler *et al.*, 1989), it is clearly important to describe the amount and morphological type of trabecular bone microdamage in OA.

It was hypothesised that the microdamage burden at specific skeletal regions of the human proximal femur, the subchondral principal compressive region, the medial principal compressive region, and the intertrochanteric region (Figure 2.3), would be similar, because these regions are loaded primarily in compression due to a combination of gravitational and muscle forces (Ling *et al.*, 1996). This chapter describes investigation of the *in vivo* distribution of trabecular bone microdamage in the proximal femur at autopsy for a cohort of individuals who show no macroscopic evidence of OA and have no medical record of disease affecting their bone turnover status. In addition, this chapter describes investigation of the amount and morphological type of *in vivo* trabecular bone microdamage at the intertrochanteric region of the proximal femur for individuals suffering from primary hip OA, compared to skeletal-site matched non-OA/control individuals. The intertrochanteric region of the proximal femur was chosen for investigation as the trabecular bone at this region has previously been shown to be structurally different between OA and controls (Crane *et al.*, 1990). Further, the intertrochanteric region is remote from the subchondral bone that undergoes well-characterised secondary changes in severe OA (Fazzalari *et al.*, 1992). In addition, striking differences in the pattern of mRNA expression, corresponding to a number of skeletally active molecules, were observed at the intertrochanteric region between patients with severe primary hip OA and non-OA/control individuals (described in Chapter 6). The nature and mechanism of the stimulus to recruit

osteoclasts to begin the targeted bone remodelling process, to repair bone microdamage, is unknown. Thus, relationships were examined between mRNA expression levels of skeletally active molecules, with known regulatory roles in osteoclastogenesis (IL-6, IL-11, RANKL, and OPG; independently described in Chapters 5 and 6), and microdamage morphometric parameters, measured in contiguous intertrochanteric trabecular bone samples from both OA and control individuals.

8.2 CHAPTER AIMS

- To investigate whether there are regional differences in the morphometric parameters describing the extent of microdamage in trabecular bone sampled from the subchondral principal compressive, medial principal compressive, and intertrochanteric regions of the non-diseased/control human proximal femur.

- To investigate whether there are gender differences and age-related changes in the morphometric parameters describing the extent of microdamage, in trabecular bone tissue sampled from the intertrochanteric region of the proximal femur, in individuals with primary hip OA and an autopsy control group.

- To compare the morphometric parameters describing the extent of microdamage, in trabecular bone from the intertrochanteric region of the proximal femur, a skeletal site distal to the degenerative joint changes in OA, between individuals with primary hip OA and an autopsy control group.

- To examine the relationship between the levels of expression of mRNA corresponding to factors known to have important regulatory roles in bone remodelling, and the morphometric parameters describing the extent of microdamage, measured in contiguous bone samples from the intertrochanteric region of the proximal femur for control and OA individuals (mRNA expression data for control and OA cases is independently described in Chapters 5 and 6).

8.3 METHODS

8.3.1 Case selection

Proximal femurs were obtained from 12 routine autopsies performed at the Royal Adelaide Hospital. Samples from the 12 postmortem cases were also used for undecalcified bone histomorphometric analysis (described in Chapter 7). The postmortem case details, including age, gender, anatomical side, postmortem interval, and cause of death, are listed in Table 5.1 (trabecular bone tissue was not available for microdamage assessment from cases C11 and C13; refer to Chapter 7.3.1). The age of the 12 postmortem cases for microdamage assessment, comprising 7 women (aged 20-83 years; mean ± SD [standard deviation] age, 61.3 ± 22.0 years) and 5 men (aged 24-85 years; 58.2 ± 24.3 years), varied between 20 and 85 years (60.0 ± 21.9 years). There was no difference in the mean age between females and males. These postmortem cases, which are categorized as *control* cases in this thesis, were selected from routine autopsies not known to have suffered from any disease affecting the skeleton and on macroscopic and radiological assessment of the proximal femur showed no significant sign of joint degeneration, according to the criteria of Collins (1949; described in Chapter 5.2.1 and Table 5.1).

Surgical specimens from the proximal femur were obtained from 33 patients undergoing total hip arthroplasty surgery for advanced primary OA at the Royal Adelaide Hospital. The 33 surgical OA cases were also used for undecalcified bone histomorphometric analysis (described in Chapter 7). The OA case details, including age, gender, and for a subset of cases, anatomical side, and macroscopic grade of the femoral head and acetabulum, are listed in Tables 6.1 and 7.1 (trabecular bone tissue for microdamage assessment was not available from case OA10; refer to Chapter 7.3.1). These surgical OA cases were selected using the same criteria as described in Chapter 6.3.1. In brief, the selection of primary OA cases excluded patients suspected of having secondary OA, inflammatory joint disease, Paget's disease, drug-induced disease or other conditions, which may have affected the trabecular bone architecture and quality. The age of the 33 OA cases, comprising 18 women (aged 49-84 years; 71.5 ± 9.0 years) and 15 men (aged 37-85 years; 66.0 ± 14.2 years), varied between 37 and 85 years (69.0 ± 11.8 years). There was no difference in the mean age between OA females and OA males. The mean age of the OA group did not differ significantly from the control group.

8.3.2 Sampling of trabecular bone from the human proximal femur

Trabecular bone was sampled from the subchondral principal compressive (SPC), medial principal compressive (MPC), and intertrochanteric (IT) regions of the proximal femur for each postmortem case (Figure 2.3). Initially, as detailed in Chapter 7.3.2, each proximal femur was sectioned in the coronal plane using a band saw, which had been cleaned with DEPC-treated water, to allow access to trabecular bone for sampling from the IT site, which is enclosed within the femoral cortex (Figure 2.1). Trabecular bone tissue for RNA isolation, taken from the IT region, was sampled from an approximate 1.5 x 1.0 cm^2 area, to a specimen depth of 0.5 cm (described in Chapter 5.3.2). The remaining coronal half of

each proximal femur was stored frozen until required for undecalcified microdamage assessment and histological analysis. Two 5 mm-thick coronal slices were cut from the remaining frozen coronal half of each proximal femur, using a diamond blade on the Exakt saw (Exakt Apparatebau GmbH & Co. KG). One coronal slice was used for microdamage assessment, and the other coronal slice for histomorphometric analysis (Chapter 7). A contact X-ray image of the 5 mm-thick coronal slice for microdamage assessment was taken using a Faxitron X-ray cabinet (Hewlett-Packard). The X-ray image was used to enable reproducible sampling of trabecular bone from the SPC, MPC, and IT regions (Figure 2.3), as a 1.0 x 1.0 cm^2 block of tissue, using an Isomet 11-1180 low-speed diamond saw (Buehler Ltd.). The SPC, MPC, and IT trabecular bone tissue blocks (1.0 x 1.0 x 0.5 cm^3) were immediately fixed in 70% ethanol for 24 hours at room temperature.

As detailed in Chapter 7.3.2, at total hip arthroplasty surgery in OA patients, a 10 mm internal diameter tube saw was used to take a trabecular bone core biopsy of the IT region (Figure 2.1), taken in line with the femoral medullary canal (Fazzalari *et al.*, 1998b). The bone core biopsies, 10 mm in diameter and 3-5 cm in length, were placed in cold (4°C) sterile RNase-free 0.85% saline and transported directly to the laboratory. Trabecular bone tissue was sampled from an approximate tube saw length of 1-2 cm for RNA isolation (described in Chapter 6.3.2). The remainder of each IT bone core biopsy, 10 mm in diameter and 2-3 cm in length, was stored frozen until required for undecalcified microdamage assessment and histological analysis. These trabecular bone samples were X-rayed (Faxitron X-ray cabinet; Hewlett-Packard) before sampling for microdamage assessment, to ensure the exclusion of any damaged tissue (particularly the ends of the biopsy). Each undamaged tube saw biopsy, approximately 1-1.5 cm in length, was bisected lengthwise using an Isomet low-speed diamond saw (Buehler Ltd.). One half of the tube

saw was processed for microdamage assessment and the other half processed for undecalcified bone histomorphometric analysis (Chapter 7). The trabecular bone tissue samples were immediately fixed in 70% ethanol for 24 hours at room temperature.

8.3.3 Morphometric analysis of microdamage in undecalcified basic fuchsin bulk-stained trabecular bone tissue

Trabecular bone samples for microdamage assessment, from the SPC, MPC, and IT regions for autopsy control cases, and from the IT region for surgical OA cases (section 8.3.2), fixed in 70% ethanol, were bulk-stained in basic fuchsin according to the protocols of Burr and Hooser (1995) and Fazzalari *et al.* (1998b; Chapter 2.2.3.2). The bulk-stained trabecular bone samples were then embedded undecalcified in methyl methacrylate (MMA; Chapter 2.2.3.3). A diamond wire saw (Ahlburg Technical Equipment) was used to cut 70 μm-thick sections from each MMA embedded bone sample (Chapter 2.2.3.4.2), for quantitation of morphometric parameters describing the extent of microdamage. Microdamage is identified histologically by discrete microcracks, cross-hatch staining, and diffuse staining (Burr and Stafford, 1990; Fazzalari *et al.*, 1998b; Figures 2.7A and 2.7B; Chapter 2.2.3.6.2). To avoid edge artifacts, only microdamage further than 1 mm from the edge of the sample was measured (Fyhrie and Schaffler, 1994). Morphometric analysis was performed by point counting and by using a semi-automated digitizing system (Bioquant, R & M Biometrics), at a magnification of X250, on a Nikon Optiphot II microscope (Nikon; Chapter 2.2.3.6.2). The following morphometric parameters were measured:

Microdamage parameters:

(1) Trabecular bone area in mm^2 B.Ar

(2) Total tissue area in mm^2 TT.Ar

(3) Number of microcracks Cr.N

(4) Mean microcrack length in μm Cr.Le

(5) Area of trabecular bone damage in mm^2 Dx.Ar

The above measurements were used to calculate the following morphometric parameters describing the extent of bone microdamage:

Morphometric parameters describing the extent of microdamage:

(1) Percentage of mineralised bone tissue volume BV/TV

BV/TV = B.Ar/TT.Ar

(2) Numerical microcrack density in number/mm^2 Cr.Dn

Cr.Dn = Cr.N/B.Ar

(3) Microcrack surface density in μm/mm^2 Cr.S.Dn

Cr.S.Dn = Cr.Le*Cr.Dn

(4) Percentage of damaged bone volume DxV/BV

DxV/BV = Dx.Ar/B.Ar

(5) Percentage of damaged bone volume DxV/TV

DxV/TV = Dx.Ar/TT.Ar

8.3.4 Semi-quantitative RT-PCR of total RNA isolated from human trabecular bone

Total RNA was isolated from trabecular bone tissue (Chapter 2.2.2.1) sampled from the IT region for the autopsy control and surgical OA cases listed in Tables 5.1 and 6.1. Semi-quantitative RT-PCR (Chapter 2.2.2.3), using the human-specific oligonucleotide primer

pairs listed in Table 2.1 and primer conditions described in Chapter 2.2.2.3.2, was used to determine the relative levels of IL-6, IL-11, RANKL, and OPG mRNA in these bone RNA samples. Amplified PCR product corresponding to IL-6, IL-11, RANKL, and OPG mRNA are represented as a ratio of the respective PCR product/GAPDH PCR product (mRNA expression data for controls is independently described in Chapter 5; mRNA expression data for the OA cases is independently described, as a comparison to controls, in Chapter 6).

8.3.5 Statistical analysis of microdamage morphometric data

The Shapiro-Wilk statistic was used to test the bone microdamage morphometric data for normality (PC-SAS software; SAS Institute). The morphometric parameters describing the extent of bone microdamage were found to be both normally and non-normally distributed. Therefore, both parametric and non-parametric statistical methods were used to analyse the data (Excel; Microsoft Corp.; PC-SAS software; SAS Institute). Differences in the microdamage morphometric parameters between the proximal femur regions, SPC, MPC, and IT, were tested by one-way analysis of variance (ANOVA) for the means (parametric) or by the Kruskal-Wallis one-way ANOVA by ranks for the medians (non-parametric). If significant differences were indicated, comparison between proximal femur region means or medians was tested by Student's *t*-test (parametric) or the Mann-Whitney *U*-test (non-parametric), respectively. The statistical significance of differences in the microdamage parameters between females and males, and between the autopsy control and OA groups, were determined by Student's *t*-test or the Mann-Whitney *U*-test. Linear regression analysis was used to describe age-related changes. The F-test was used to analyse differences in the variance of the microdamage morphometric parameters between individuals (OA or control) less than 60 years of age and greater or equal to 60 years of

age. Regression analysis was used to examine the relationship between bone microdamage morphometric parameters. The Spearman rank correlation (r_s) was used to test for an association between two non-normally distributed microdamage parameters. Regression analysis was used to examine the relationship between PCR products representing specific mRNA species (section 8.3.4) and bone microdamage morphometric parameters (section 8.3.3), measured in contiguous trabecular bone tissue samples. Parametric data is quoted as mean ± standard deviation and non-parametric data quoted as the median (quartiles). The critical value for significance was chosen as $p = 0.05$.

8.4 RESULTS

8.4.1 Comparison of bone microdamage morphometric parameters between females and males at each proximal femur skeletal site in control individuals

The morphometric parameters describing the extent of bone microdamage, at each site in the proximal femur in control individuals, were found to be both normally (BV/TV and Cr.Le) and non-normally (Cr.Dn, Cr.S.Dn, DxV/BV, and DxV/TV) distributed (the Shapiro-Wilk statistic; PC-SAS software; SAS Institute). The non-normal distribution of microdamage morphometric data from human trabecular bone tissues has been reported previously for the femoral head (Mori *et al.*, 1997) and vertebral bone (Vashishth *et al.*, 2000a). Therefore, the student's *t*-test or the Mann-Whitney *U*-test was used to assess whether there were any gender differences in the morphometric parameters describing the extent of bone microdamage in non-diseased (control) human trabecular bone sampled from the subchondral principal compressive (SPC), medial principal compressive (MPC), and intertrochanteric (IT) regions of the proximal femur. Mean trabecular bone volume (BV/TV) was significantly reduced in females compared to males at the SPC region ($p < 0.04$; Table 8.1). In addition, the variance in BV/TV was significantly higher in females

Microdamage parameter	SPC		MPC		IT	
	Female (n = 7)	Male (n = 5)	Female (n = 7)	Male (n = 5)	Female (n = 7)	Male (n = 5)
BV/TV (%)	18.4 ± 8.5	27.3 ± 2.9 [a]	23.2 ± 8.2	25.5 ± 4.7	12.9 ± 10.1	11.0 ± 5.4
Cr.Dn (number/mm^2)	0.49 (0.30-1.40)	0.51 (0.31-0.54)	0.54 (0.30-0.87)	0.26 (0.23-0.38)	0.46 (0.20-1.33)	0.51 (0.27-0.71)
Cr.Le (μm)	56 ± 12	62 ± 15	86 ± 37	68 ± 11	68 ± 13	55 ± 9
Cr.S.Dn (μm/mm^2)	26.3 (19.8-88.0)	25.0 (23.3-29.5)	41.9 (26.5-50.6)	16.8 (14.6-21.9)	32.9 (13.7-92.2)	23.9 (16.6-37.1)
DxV/BV (%)	1.26 (0.07-1.93)	1.05 (0.43-1.18)	1.03 (0.09-2.30)	0 (0-0.40)	0.47 (0.08-2.11)	0 (0-1.73)
DxV/TV (%)	0.09 (0.02-0.28)	0.29 (0.10-0.31)	0.25 (0.02-0.36)	0 (0-0.07)	0.08 (0.01-0.14)	0 (0-0.27)

Proximal femur skeletal regions: SPC, subchondral principal compressive; MPC, medial principal compressive; IT, intertrochanteric region.
Parametric data reported as mean ± standard deviation, and non-parametric data as median (quartiles).
[a] $p < 0.04$.

Table 8.1 Microdamage morphometric parameters in female and male control trabecular bone sampled from the subchondral principal compressive, medial principal compressive, and intertrochanteric regions of the human proximal femur.

compared to males (F-statistic = 8.4, representing the ratio of the female variance to male variance, $p < 0.03$; Table 8.1), suggesting that the females are a more heterogeneous group with respect to BV/TV at the SPC region. In comparison, Crane *et al.* (1990) and Fazzalari *et al.* (1989) reported no gender difference for BV/TV at the SPC region in autopsy control cases. No significant differences in BV/TV were observed between females and males at the MPC or IT regions (Table 8.1). There were no significant differences in the microdamage parameters Cr.Dn, Cr.Le, Cr.S.Dn, DxV/BV, and DxV/TV between females and males at the SPC, MPC, and IT regions (Table 8.1). Based on these comparisons between females and males at each skeletal region, and the small number of samples for the control cohort ($n = 12$), further analyses of the microdamage morphometric data were made independent of gender. In addition, the control group data is analysed between the three skeletal regions and in comparison to the OA group data with and without inclusion of the two younger cases in this control cohort, cases C1 (20-year-old female) and C8 (24-year-old male), which are specifically indicated in Figures 8.2 and 8.3.

8.4.2 Comparison of bone microdamage morphometric parameters between proximal femur skeletal sites in control individuals

Morphometric parameters describing the extent of microdamage were measured in non-diseased (control) human trabecular bone sampled from the SPC, MPC, and IT regions of the proximal femur (Figure 2.3). These three skeletal regions are loaded primarily in compression due to a combination of gravitational and muscles forces (Ling *et al.*, 1996). Thus, it was hypothesised that the microdamage burden at these regions would be similar. One-way analysis of variance (ANOVA) for the means or Kruskal-Wallis one-way ANOVA by ranks for the medians was used to assess whether there were any differences in the microdamage morphometric parameters between the three skeletal regions. Further,

if significant differences were indicated, comparison between proximal femur region means or medians was assessed by student's *t*-test or the Mann-Whitney *U*-test. Analysis was also performed after exclusion of the two younger control individuals, cases C1 (20-year-old female) and C8 (24-year-old male; results not shown).

Mean trabecular bone volume (BV/TV) was significantly lower at the IT region ($p < 0.002$) in comparison to both the SPC and MPC regions ($p < 0.007$ and $p < 0.001$, respectively; Table 8.2). This observation of reduced BV/TV at the IT region was maintained after exclusion of the two younger control cases ($n = 10$; SPC, 20.7 ± 8.1 vs. MPC, 22.5 ± 6.0 vs. IT, 9.8 ± 5.9, $p < 0.0005$). Moreover, when the two younger cases were excluded, BV/TV at the IT region was significantly reduced in comparison to both the SPC and MPC regions ($n = 10$; $p < 0.004$ and $p < 0.0002$, respectively). BV/TV was similar between the SPC and MPC regions, whether all samples were included in the analysis (Table 8.2), or only those from individuals aged greater than 40 years (results not shown). The similar magnitude of mean BV/TV between the SPC and MPC regions, together with the decreased mean BV/TV at the IT region, is consistent with two previous reports of normal human proximal femur histomorphometry (Crane *et al.*, 1990; Fazzalari *et al.*, 1989). The higher mean BV/TV at the SPC and MPC regions is consistent with the trabecular bone network being subjected to higher compressive stress at these regions (Carter *et al.*, 1989). This is in comparison to the lower mean BV/TV at the IT region, where finite element modelling of stress distributions in the human femur demonstrated that trabecular bone only supports 20% of the compressive load during gait, at this region (Lotz *et al.*, 1995).

Table 8.2 Microdamage morphometric parameters in subchondral principal compressive, medial principal compressive, and intertrochanteric trabecular bone sampled from the proximal femur of 12 control individuals aged 20-85 years.

Microdamage parameter	SPC	MPC	IT
BV/TV (%)	22.1 ± 8.0	24.2 ± 6.8	12.1 ± 8.2 [a,b]
Cr.Dn (number/mm^2)	0.50 (0.30-0.73)	0.36 (0.25-0.77)	0.49 (0.23-0.96)
Cr.Le (μm)	59 ± 13	78 ± 29 [c]	63 ± 13
Cr.S.Dn (μm/mm^2)	25.6 (21.9-48.4)	26.5 (18.0-51.1)	28.4 (15.3-65.7)
DxV/BV (%)	1.11 (0.10-2.02)	0.29 (0-1.61)	0.32 (0-2.28)
DxV/TV (%)	0.14 (0.03-0.36)	0.05 (0-0.35)	0.05 (0-0.24)

Proximal femur skeletal regions: SPC, subchondral principal compressive; MPC, medial principal compressive; IT, intertrochanteric region.
Parametric data reported as mean ± standard deviation, and non-parametric data as median (quartiles).
[a] $p < 0.007$ vs. SPC region, [b] $p < 0.001$ vs. MPC region, [c] $p < 0.05$ vs. SPC region.

As hypothesised, microdamage (Cr.Dn, Cr.S.Dn, DxV/BV, and DxV/TV) was observed to be quantitatively similar in all proximal femoral skeletal regions, with the exception of reduced mean microcrack length (Cr.Le) in the SPC region ($p < 0.05$; Table 8.2). However, mean Cr.Le in the SPC region was only significantly reduced in comparison to the MPC region ($p < 0.05$), but not when compared to the IT region (Table 8.2). This reduction in mean Cr.Le in the SPC region was dependent on inclusion of the two younger cases (results not shown). Interestingly, this difference in mean Cr.Le between the SPC and MPC regions was apparent even though there was no difference in BV/TV between the regions (Table 8.2). The significantly reduced Cr.Le in the subchondral bone, compared with a region (MPC) distal to the articular surface, may be indicative of different bone material properties, such as bone tissue mineralisation, and/or differential bone remodelling rates between these regions (Ampe *et al.*, 1986; Fazzalari *et al.*, 1989; Li and Aspden, 1997a).

8.4.3 Age-related changes in bone microdamage morphometric parameters at each proximal femur skeletal site in control individuals

To investigate whether there are any age-related changes in the morphometric parameters describing the extent of bone microdamage in the SPC, MPC, and IT regions of the non-diseased (control) human proximal femur, each microdamage parameter, for each skeletal region, was plotted as a function of increasing age in years, and analysed by linear regression analysis. Trabecular bone volume (BV/TV) declined with age at all three skeletal regions (SPC, $p < 0.05$; MPC, $p < 0.001$; IT, $p < 0.01$; Figures 8.1A-8.1C). The age-related decline in BV/TV at the SPC and IT regions was dependent on inclusion of the two younger cases. However, the significant decrease in BV/TV with age at the MPC region was maintained when the two younger cases were excluded from the analysis ($n =$

Figure 8.1: Changes in BV/TV with age in subchondral principal compressive (SPC; A), medial principal compressive (MPC; B), and intertrochanteric (IT; C) trabecular bone from control individuals (n = 12). There was a significant decline in BV/TV with age at the SPC (BV/TV = -0.20*AGE + 33.89; r = -0.54 and $p < 0.05$), MPC (BV/TV = -0.26*AGE + 39.84; r = -0.84 and $p < 0.001$), and IT (BV/TV = -0.25*AGE + 27.35; r = -0.68 and $p < 0.01$) regions of the proximal femur.

BV/TV vs AGE

A

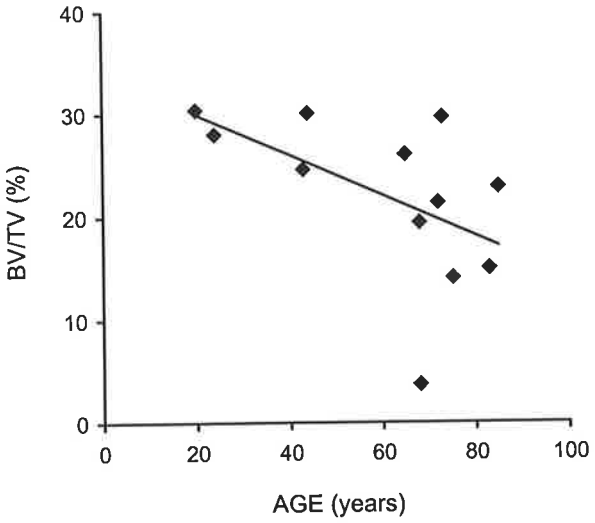

SPC

B

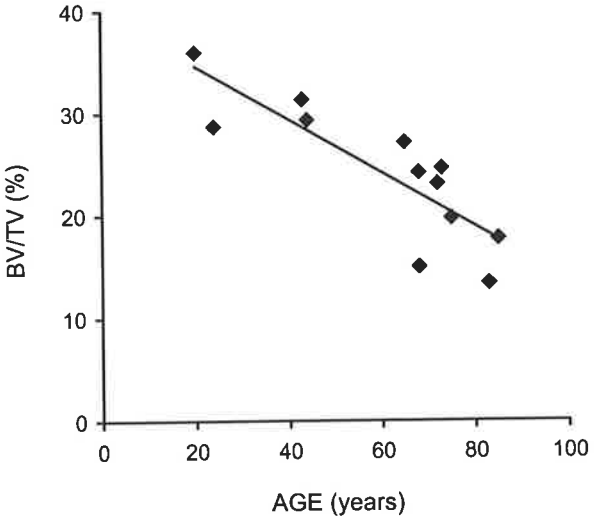

MPC

C

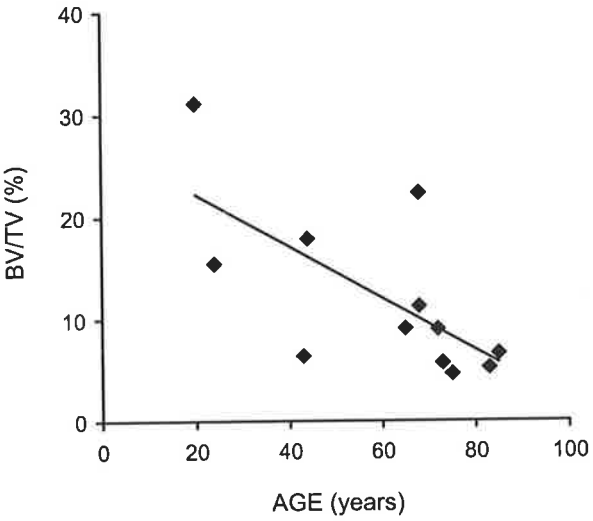

IT

10; r = -0.81, $p < 0.002$). The age-related decline in BV/TV at the SPC, MPC, and IT regions of the human proximal femur is consistent with the results shown in Figure 7.1 for the IT region from control individuals (Chapter 7.4.2) and with a previous report, which described these changes for a larger autopsy control cohort (n = 69; Crane *et al.*, 1990). The microdamage morphometric parameters, Cr.Dn, Cr.Le, Cr.S.Dn, DxV/BV, and DxV/TV, did not show any age-dependence at the SPC, MPC, or IT regions of the proximal femur (results not shown).

8.4.4 Associations between bone microdamage morphometric parameters at each proximal femur skeletal site in control individuals

Linear regression analysis was used to investigate whether there are any relationships between the morphometric parameters describing the extent of bone microdamage in the SPC, MPC, and IT regions of the non-diseased (control) human proximal femur. In addition, the Spearman rank correlation (r_s) was used to test for an association between two non-normally distributed microdamage parameters. When microcrack density (Cr.Dn) and BV/TV were co-plotted, a significant negative association was observed at the SPC and MPC regions ($p < 0.001$ and $p < 0.02$; Figures 8.2A and 8.2B, respectively). These associations between Cr.Dn and BV/TV were maintained when the two younger cases were excluded from the analysis (n = 10; SPC, r = -0.81, $p < 0.002$; MPC, r = -0.67, $p <$ 0.02). However, the negative association between Cr.Dn and BV/TV at the SPC region is statistically reliant on the two outliers, cases C3 (68-year-old female) and C7 (83-year-old female), with high Cr.Dn and low BV/TV values (Figure 8.2A). No association was observed between Cr.Dn and BV/TV at the IT region (Figure 8.2C). Similarly, a significant negative association was observed between microcrack surface density (Cr.S.Dn) and BV/TV at the SPC and MPC regions ($p < 0.001$ and $p < 0.05$; Figures 8.3A

Figure 8.2: Associations between Cr.Dn and BV/TV in subchondral principal compressive (SPC; A), medial principal compressive (MPC; B), and intertrochanteric (IT; C) trabecular bone from control individuals (n = 12). A significant negative association was observed between the two parameters at the SPC (Cr.Dn = -0.08*BV/TV + 2.56; r = -0.81 and $p < 0.001$) and MPC (Cr.Dn = -0.03*BV/TV + 1.15; r = -0.64 and $p < 0.02$) regions of the proximal femur. No association was observed between the two parameters at the IT region (Cr.Dn = -0.02*BV/TV + 1.20; r = -0.14 and p = NS). Two cases, <40 years old, are indicated (●). NS = not significant.

Cr.Dn vs BV/TV

A

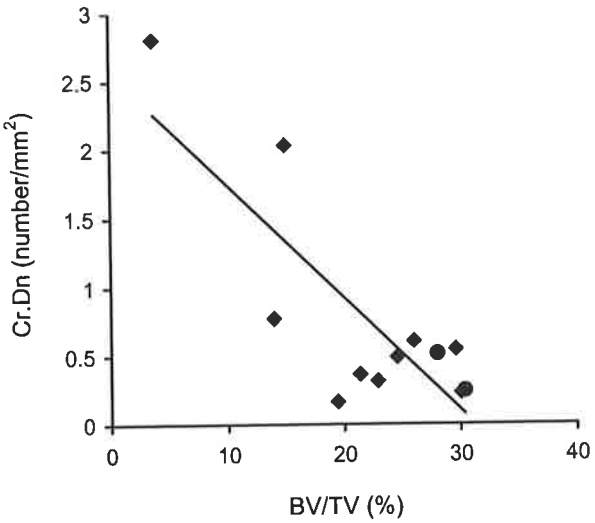

SPC

B

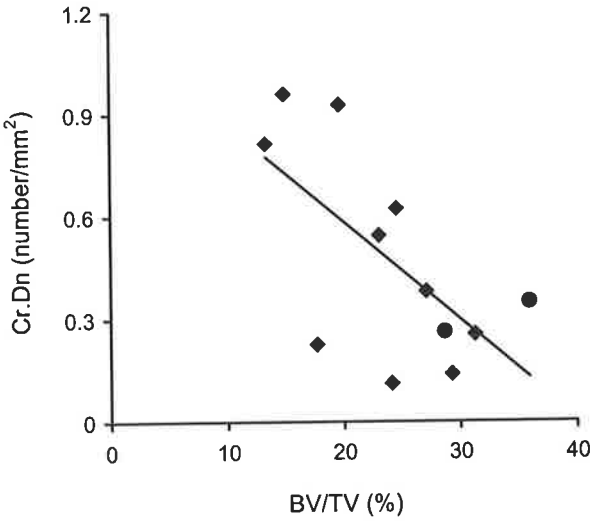

MPC

C

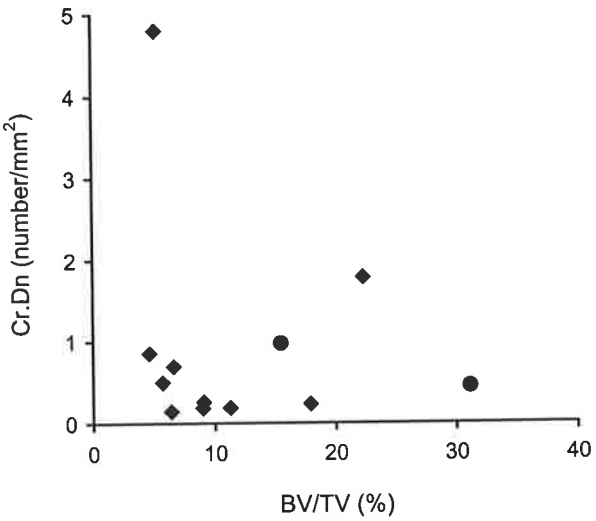

IT

Figure 8.3: Associations between Cr.S.Dn and BV/TV in subchondral principal compressive (SPC; A), medial principal compressive (MPC; B), and intertrochanteric (IT; C) trabecular bone from control individuals (n = 12). A significant negative association was observed between the two parameters at the SPC (Cr.S.Dn = -4.03*BV/TV + 130.83; r = -0.80 and $p < 0.001$) and MPC (Cr.S.Dn = -1.50*BV/TV + 69.33; r = -0.56 and $p < 0.05$) regions of the proximal femur. No association was observed between the two parameters at the IT region (Cr.S.Dn = -0.96*BV/TV + 68.97; r = -0.10 and p = NS). Two cases, <40 years old, are indicated (●). NS = not significant.

Cr.S.Dn vs BV/TV

A

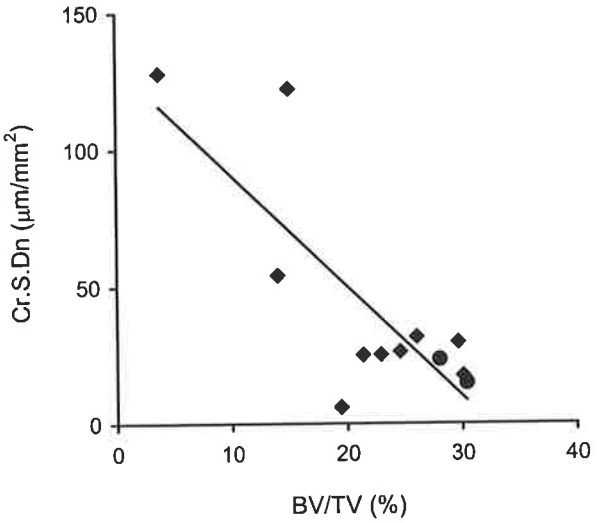

SPC

B

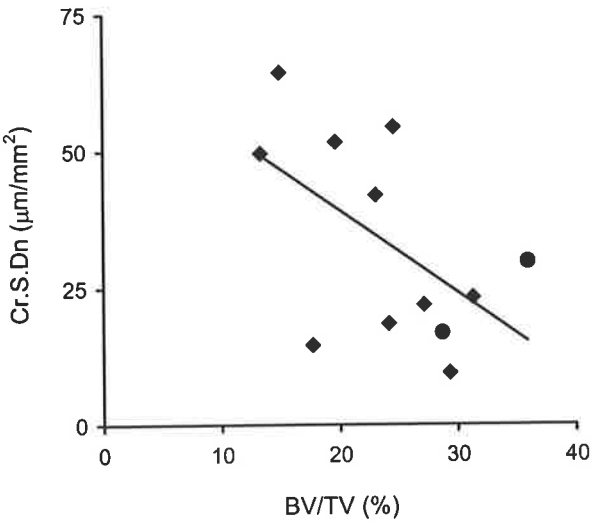

MPC

C

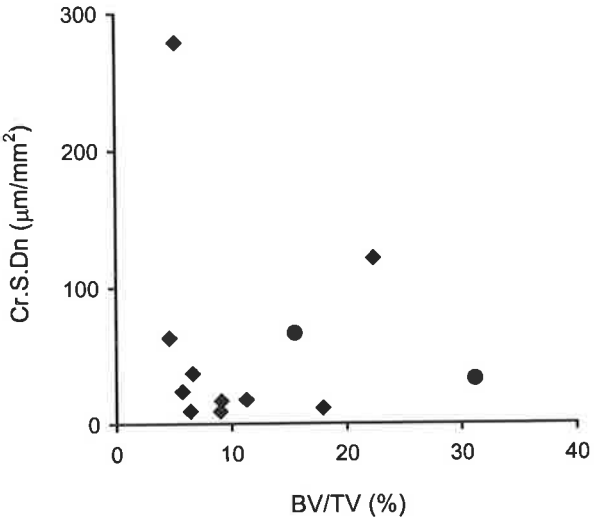

IT

and 8.3B, respectively), which was maintained after exclusion of the two younger cases (n = 10; SPC, r = -0.79, $p < 0.003$; MPC, r = -0.59, $p < 0.05$). At the SPC region, as observed for Cr.Dn vs. BV/TV (Figure 8.2A), the negative association between Cr.S.Dn and BV/TV is statistically reliant on the two outliers, cases C3 (68-year-old female) and C7 (83-year-old female), with high Cr.S.Dn and low BV/TV values (Figure 8.3A). No association was observed between Cr.S.Dn and BV/TV at the IT region (Figure 8.3C). Taken together, these observations suggest that in some circumstances changes in the magnitude of Cr.Dn and Cr.S.Dn are dependent upon the amount of trabecular bone at the SPC and MPC regions of the human proximal femur. Interestingly, the negative association between either Cr.Dn or Cr.S.Dn and BV/TV was not evident at the IT region. This non-uniformity between the proximal femoral regions is consistent with the difference in mean BV/TV between the IT region and the SPC and MPC regions (Table 8.2), and with the higher compressive loads supported by the trabecular bone at the SPC and MPC regions in comparison to the IT region, where the femoral cortices support most of the load (Carter *et al.*, 1989; Lotz *et al.*, 1995). A negative power-law relationship between bone volume and microcrack density has been found in human femoral head subchondral bone and vertebral bone (Mori *et al.*, 1997; Wenzel *et al.*, 1996). The morphometric parameters describing the volume fraction of bone microdamage, DxV/BV and DxV/TV, did not associate with changes in BV/TV at the SPC, MPC, or IT regions of the proximal femur (results not shown).

Positive associations were observed between Cr.Dn with both DxV/BV and DxV/TV at the IT region (r_s = 0.80, $p < 0.002$; r_s = 0.73, $p < 0.007$; respectively; Table 8.3). In addition, Cr.Dn and DxV/BV were positively associated at the MPC region (r_s = 0.59, $p < 0.05$; Table 8.3). However, the association between Cr.Dn and DxV/TV at the MPC region did

Table 8.3 Associations between the microdamage morphometric parameters Cr.Dn and Cr.S.Dn with DxV/BV and DxV/TV in subchondral principal compressive, medial principal compressive, and intertrochanteric trabecular bone sampled from the proximal femur of 12 control individuals aged 20-85 years.

Association	SPC	MPC	IT
Cr.Dn vs DxV/BV	$r_s = 0.37$ p = NS	$r_s = 0.59$ $p < 0.05$	$r_s = 0.80$ $p < 0.002$
Cr.Dn vs DxV/TV	$r_s = 0.11$ p = NS	$r_s = 0.51$ p = NS	$r_s = 0.73$ $p < 0.007$
Cr.S.Dn vs DxV/BV	$r_s = 0.29$ p = NS	$r_s = 0.65$ $p < 0.03$	$r_s = 0.88$ $p < 0.0003$
Cr.S.Dn vs DxV/TV	$r_s = -0.01$ p = NS	$r_s = 0.59$ $p < 0.05$	$r_s = 0.82$ $p < 0.002$

Proximal femur skeletal regions: SPC, subchondral principal compressive; MPC, medial principal compressive; IT, intertrochanteric region.
r_s, Spearman rank correlation; NS, not significant.

not reach statistical significance (Table 8.3). Similarly, positive associations were observed between Cr.S.Dn with both DxV/BV and DxV/TV at the IT and MPC regions (IT: r_s = 0.88, $p < 0.0003$; $r_s = 0.82$, $p < 0.002$; respectively; MPC: $r_s = 0.65$, $p < 0.03$; $r_s = 0.59$, $p <$ 0.05; respectively; Table 8.3). No associations between Cr.Dn and Cr.S.Dn with DxV/BV and DxV/TV were observed at the SPC region (Table 8.3). Collectively, these positive associations between the morphometric parameters describing microcracks, Cr.Dn and Cr.S.Dn, with the damaged bone volume parameters, DxV/BV and DxV/TV, which predominantly represent the volume fraction of diffuse staining, for the first time suggest that linear microcracks and diffuse microdamage are linked at the MPC and IT regions of the human proximal femur. In contrast, no correlation between microcrack density and diffuse microdamage was observed in human vertebral bone (Vashishth *et al.*, 2000a). Interestingly, the positive associations between Cr.Dn and Cr.S.Dn with DxV/BV and DxV/TV at the MPC and IT regions were not evident at the SPC region, which may relate to reported differences in bone material properties, such as bone tissue mineralisation, and/or differential bone remodelling rates between these regions (Ampe *et al.*, 1986; Fazzalari *et al.*, 1989; Li and Aspden, 1997a). No association was observed between Cr.Le and DxV/BV or DxV/TV at the SPC, MPC, and IT regions of the proximal femur (results not shown).

8.4.5 Comparison of bone microdamage morphometric parameters between females and males in the OA group

The morphometric parameters describing the extent of bone microdamage in OA human trabecular bone, sampled from the intertrochanteric (IT) region of the proximal femur, were found to be both normally (BV/TV and Cr.Le) and non-normally (Cr.Dn, Cr.S.Dn, DxV/BV, and DxV/TV) distributed (the Shapiro-Wilk statistic; PC-SAS software; SAS

Institute). Therefore, gender differences in the microdamage morphometric parameters in OA human trabecular bone, sampled from the IT region of the proximal femur, were assessed using the student's *t*-test or the Mann-Whitney *U*-test. There were no significant differences between OA females and OA males for any of the microdamage morphometric parameters; BV/TV, Cr.Dn, Cr.Le, Cr.S.Dn, DxV/BV, and DxV/TV (Table 8.4). Based on these comparisons between OA females and OA males, further analyses of the microdamage morphometric data were made, independent of gender for the OA group, as was described for the control group (section 8.4.1).

Table 8.4 Microdamage morphometric parameters in female and male OA intertrochanteric trabecular bone samples.

Microdamage parameter	Female (n = 18)	Male (n = 15)
BV/TV (%)	8.3 ± 3.3	9.3 ± 2.8
Cr.Dn (number/mm^2)	1.24 (0.50-1.86)	0.50 (0.46-1.36)
Cr.Le (μm)	53 ± 19	48 ± 16
Cr.S.Dn (μm/mm^2)	59.9 (27.9-123.1)	29.1 (22.4-61.8)
DxV/BV (%)	5.3 (2.1-7.8)	1.9 (1.2-3.9)
DxV/TV (%)	0.39 (0.19-0.58)	0.14 (0.09-0.40)

Parametric data reported as mean ± standard deviation, and non-parametric data as median (quartiles).

8.4.6 Comparison of bone microdamage morphometric parameters between OA and control individuals

Morphometric parameters describing the extent of microdamage were measured in OA human trabecular bone, sampled from the IT region of the proximal femur, a skeletal site distal to the degenerative joint changes in OA, and in skeletal site-matched non-OA (control) trabecular bone. The student's *t*-test or the Mann-Whitney *U*-test was used to assess whether there were any differences in the microdamage morphometric parameters between the OA and control groups. To enable comparison of age-matched control and OA groups, analysis was also performed after exclusion of the two younger control individuals, cases C1 (20-year-old female) and C8 (24-year-old male), and one younger OA individual, case OA27 (37-year-old male; Table 8.6). The mean values for trabecular bone volume (BV/TV) at the IT region were similar for the OA and control groups (Table 8.5), and for the age-matched control and OA groups (Table 8.6). Microcrack density (Cr.Dn) and microcrack surface density (Cr.S.Dn) were not significantly different between the OA and control groups (Tables 8.5 and 8.6). The average microcrack length (Cr.Le) was significantly less in OA bone compared to the controls ($p < 0.03$; Table 8.5). However, when the age-matched control and OA groups were compared, Cr.Le was not significantly different (Table 8.6). The median values for the morphometric parameters describing the volume fraction of bone microdamage (representing discrete microcracks, cross-hatch staining, and diffuse staining), DxV/BV and DxV/TV, were significantly increased in the OA group compared to the control group ($p < 0.003$ and $p < 0.008$, respectively; Table 8.5). In addition, when the age-matched control and OA groups were compared, the observed increase in DxV/BV and DxV/TV in the OA group remained significant ($p < 0.004$; Table 8.6). The decreased Cr.Le and increased DxV/BV and DxV/TV in the OA proximal femur compared with the controls may be indicative of a more effective

inhibition of microcrack propagation in OA. Further, these differences in bone microdamage morphometric parameters between the OA and control groups may be related to reports of a different bone matrix structure and composition in OA, given that mean BV/TV was not different between the groups. Reported differences include hypomineralisation and loosely packed collagen fibres in OA bone (Bailey *et al.*, 2002; Li and Aspden, 1997a; Li and Aspden, 1997b; Mansell and Bailey, 1998).

Table 8.5 Microdamage morphometric parameters in OA and control intertrochanteric trabecular bone samples.

Microdamage parameter	**OA** (***n*** **= 33**) *(aged 37-85 years)*	**Control** (***n*** **= 12**) *(aged 20-85 years)*
BV/TV (%)	8.7 ± 3.1	12.1 ± 8.2
Cr.Dn (number/mm^2)	0.61 (0.46-1.70)	0.49 (0.23-0.96)
Cr.Le (μm)	51 ± 18	63 ± 13 [a]
Cr.S.Dn (μm/mm^2)	34.1 (22.7-111.8)	28.4 (15.3-65.7)
DxV/BV (%)	3.63 (1.56-7.34)	0.32 (0-2.28) [b]
DxV/TV (%)	0.25 (0.12-0.53)	0.05 (0-0.24) [c]

Parametric data reported as mean ± standard deviation, and non-parametric data as median (quartiles).
[a] $p < 0.03$, [b] $p < 0.003$, [c] $p < 0.008$ vs. OA group.

Table 8.6 Microdamage morphometric parameters in intertrochanteric trabecular bone sampled from OA and control individuals aged over 40 years.

Microdamage parameter	OA >40 years (n = 32) *(aged 45-85 years)*	Control >40 years (n = 10) *(aged 43-85 years)*
BV/TV (%)	8.8 ± 3.1	9.8 ± 5.9
Cr.Dn (number/mm^2)	0.65 (0.46-1.79)	0.39 (0.21-0.75)
Cr.Le (μm)	51 ± 18	61 ± 14
Cr.S.Dn (μm/mm^2)	38.0 (22.5-117.1)	20.9 (12.8-43.6)
DxV/BV (%)	3.67 (1.66-7.46)	0.08 (0-1.94)[a]
DxV/TV (%)	0.26 (0.12-0.54)	0.01 (0-0.09)[a]

Parametric data reported as mean ± standard deviation, and non-parametric data as median (quartiles).
[a] $p < 0.004$ vs. OA group.

8.4.7 Age-related changes in bone microdamage morphometric parameters in OA and control individuals

To investigate whether there are any age-related changes in the morphometric parameters describing the extent of bone microdamage in OA human trabecular bone, sampled from the IT region of the proximal femur, and in skeletal site-matched non-OA (control) trabecular bone, each microdamage parameter was plotted as a function of increasing age in years, and analysed by linear regression analysis. In contrast to the age-related decline in BV/TV in controls ($p < 0.01$; Figure 8.1C), BV/TV was not dependent on age in the OA group (results not shown; as described in Chapter 7.4.6). The relationships between Cr.Dn, Cr.S.Dn, DxV/BV, and DxV/TV with age could not be described by linear regression

analysis (Figures 8.4-8.7). A non-linear increase with age was observed for Cr.Dn and Cr.S.Dn in the OA group, and the control group, although limited by sample size, appeared to also follow this pattern of a non-linear increase with age (Figures 8.4 and 8.5, respectively). Before the age of 60 years the variance in Cr.Dn and Cr.S.Dn (for OA and controls) was relatively constant for each age decade, after the age of 60 years there was a significant increase in the variance (Cr.Dn: OA, F-statistic = 7.0, representing the ratio of the variance in cases aged ≥ 60 years to the variance in cases aged < 60 years, $p < 0.02$; controls, F-statistic = 17.2, $p < 0.02$; Cr.S.Dn: OA, F-statistic = 6.9, $p < 0.02$; controls, F-statistic = 11.9, $p < 0.04$). Beyond 60 years of age some cases had Cr.Dn and Cr.S.Dn values that are within the range of those cases aged less than 60 years, but many cases showed considerably increased Cr.Dn and Cr.S.Dn (Figures 8.4 and 8.5, respectively). The non-linear age-related increase in Cr.Dn and Cr.S.Dn is consistent with a previous report of an exponential increase with age in Cr.Dn and Cr.S.Dn in trabecular bone sampled from the IT region for severe OA hip cases (Fazzalari *et al.*, 1998b). Furthermore, microcracks have been shown to accumulate exponentially with age in femoral head subchondral bone, from women with and without femoral neck fracture (Mori *et al.*, 1997), and in femoral diaphyseal bone (Schaffler *et al.*, 1995).

As for Cr.Dn and Cr.S.Dn, a similar non-linear increase with age was observed for DxV/BV in the OA group, but this was not evident in the control group (Figure 8.6). As for Cr.Dn and Cr.S.Dn, before the age of 60 years the variance in DxV/BV for the OA group was relatively constant for each age decade; after the age of 60 years there was a significant increase in the variance (F-statistic = 8.0, $p < 0.008$; Figure 8.6). There was no relationship between DxV/TV with age in either the OA or control group, nor any significant difference in the variance of DxV/TV between individuals (OA or control) less

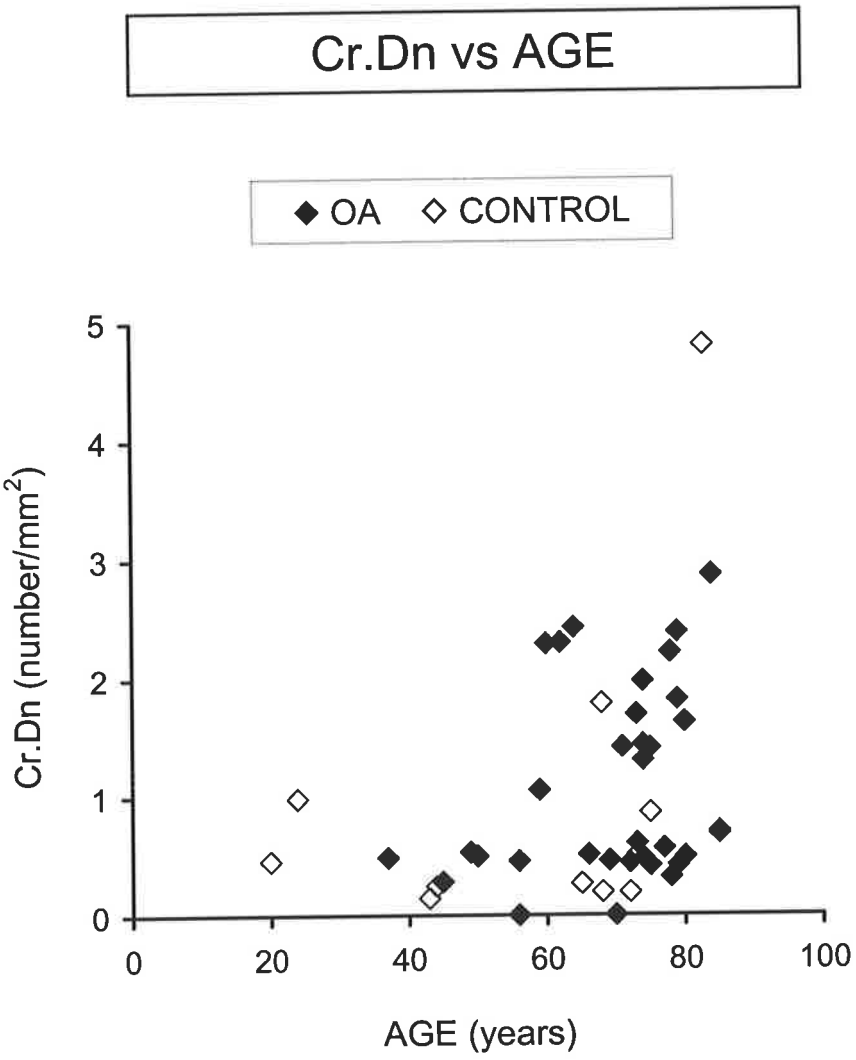

Figure 8.4: Changes in Cr.Dn with age in intertrochanteric trabecular bone from OA (n = 33) and control (n = 12) individuals. There was a non-linear increase in Cr.Dn with age for the OA and control groups.

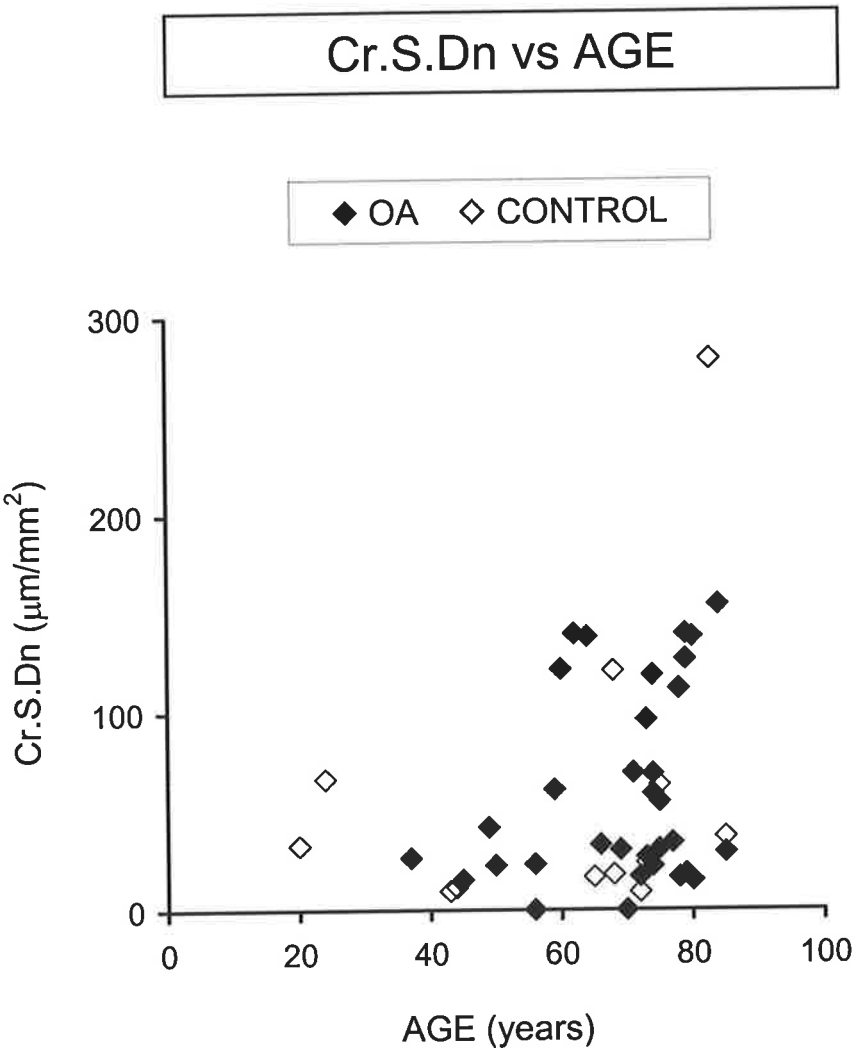

Figure 8.5: Changes in Cr.S.Dn with age in intertrochanteric trabecular bone from OA (n = 33) and control (n = 12) individuals. There was a non-linear increase in Cr.S.Dn with age for the OA and control groups.

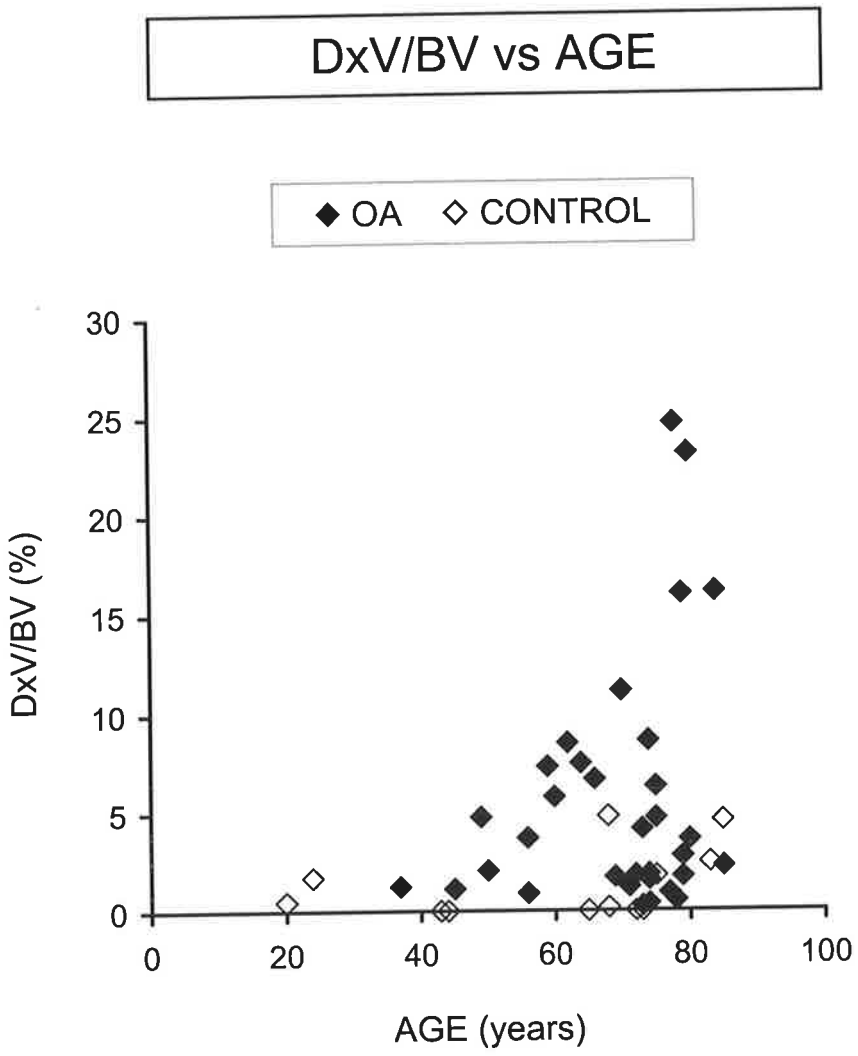

Figure 8.6: Changes in DxV/BV with age in intertrochanteric trabecular bone from OA (n = 33) and control (n = 12) individuals. There was a non-linear increase in DxV/BV with age for the OA group. There was no change in DxV/BV with age for the controls.

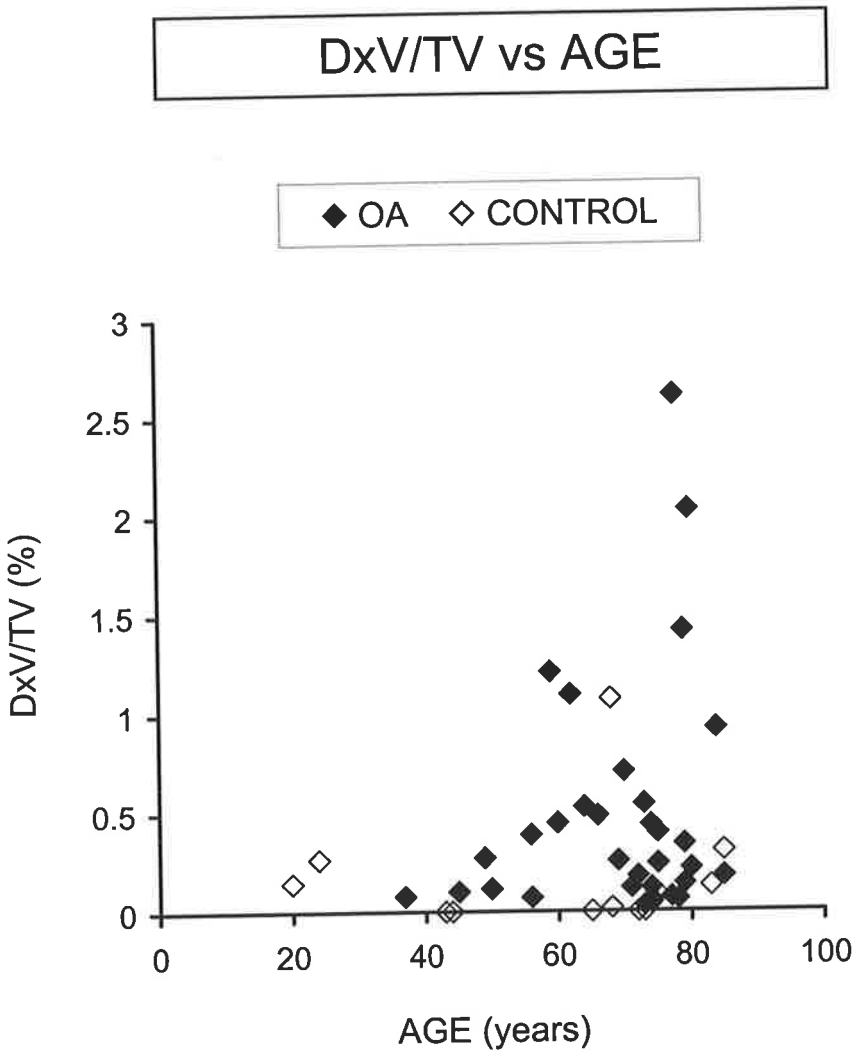

Figure 8.7: Changes in DxV/TV with age in intertrochanteric trabecular bone from OA (n = 33) and control (n = 12) individuals. There was no change in DxV/TV with age for the OA and control groups.

than 60 years of age and greater or equal to 60 years of age (Figure 8.7). The control data was clearly embedded in the distribution of OA data for the DxV/BV and DxV/TV versus age plots (Figures 8.6 and 8.7, respectively). However, as described in section 8.4.6, it was apparent that the OA group had significantly greater DxV/BV and DxV/TV than the controls (Tables 8.4 and 8.5). The observation that DxV/BV and DxV/TV, which predominantly represent the volume fraction of diffuse staining, were not age-dependent in the control trabecular bone samples is consistent with a previous report of diffuse microdamage in human vertebral bone (Vashishth *et al.*, 2000a). Cr.Le was not age-dependent in OA or control trabecular bone, sampled from the IT region of the proximal femur (results not shown).

8.4.8 Associations between bone microdamage morphometric parameters in OA and control individuals

Linear regression analysis was used to investigate whether there are any relationships between the morphometric parameters describing the extent of bone microdamage in OA human trabecular bone, sampled from the IT region of the proximal femur, and in skeletal site-matched non-OA (control) trabecular bone. In addition, the Spearman rank correlation (r_s) was used to test for an association between two non-normally distributed microdamage parameters. No associations were observed between any of the morphometric parameters describing microcracks, Cr.Dn, Cr.Le, and Cr.S.Dn, or the damaged bone volume parameters, DxV/BV and DxV/TV, with BV/TV in the OA and control groups (Cr.Dn, Figure 8.8; DxV/BV, Figure 8.9; results not shown). The co-plot of DxV/BV versus BV/TV (Figure 8.9) showed that for the controls DxV/BV was relatively constant and independent of BV/TV, while for the OA group the amount of DxV/BV was very heterogeneous but still independent of BV/TV. These observations suggest that the

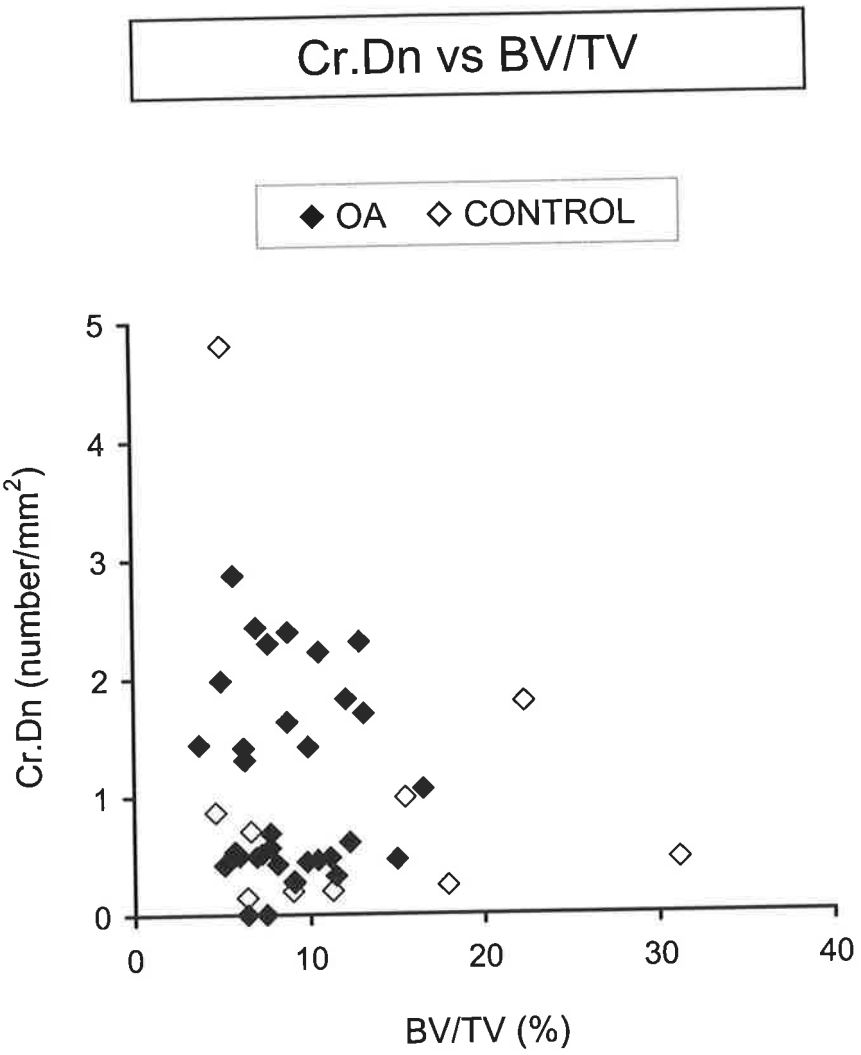

Figure 8.8: Associations between Cr.Dn and BV/TV in intertrochanteric trabecular bone from OA (n = 33) and control (n = 12) individuals. No association was observed between the two parameters in either the OA group (Cr.Dn = 0.003*BV/TV + 1.06; r = 0.01 and p = NS) or controls (Cr.Dn = -0.02*BV/TV + 1.20; r = -0.14 and p = NS). NS = not significant.

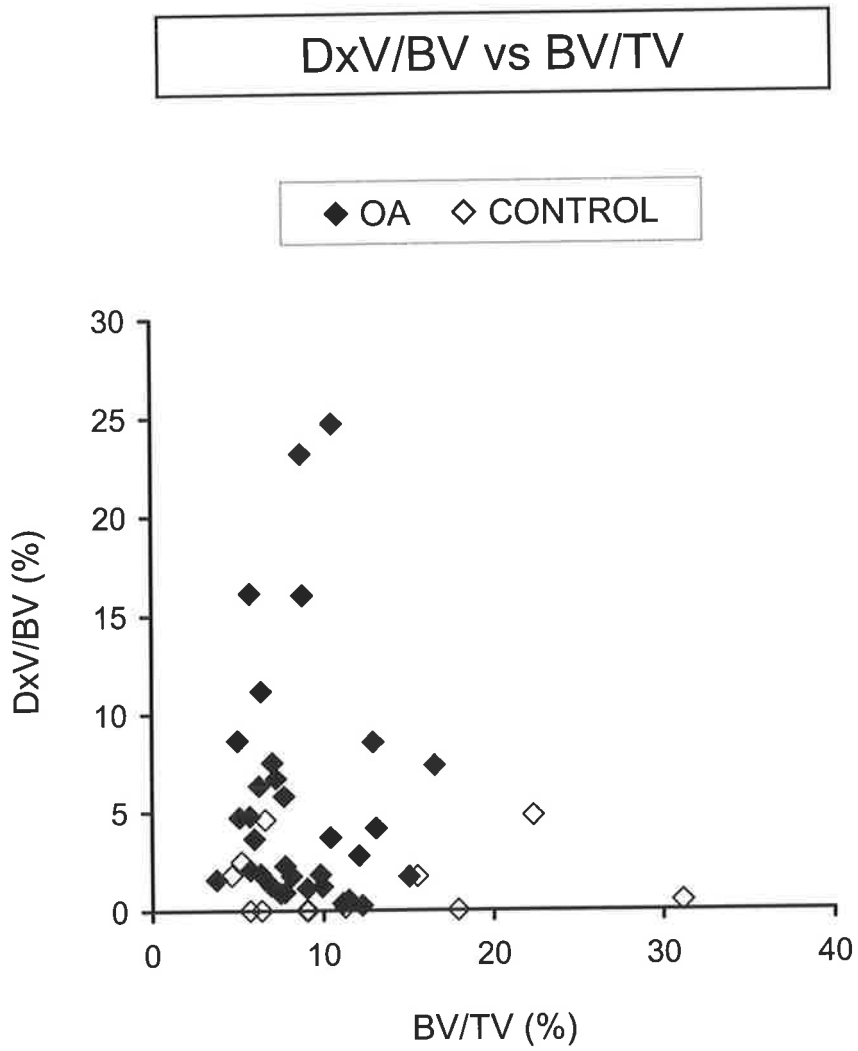

Figure 8.9: Associations between DxV/BV and BV/TV in intertrochanteric trabecular bone from OA (n = 33) and control (n = 12) individuals. No association was observed between the two parameters in either the OA group (DxV/BV = -0.08*BV/TV + 6.32; r = -0.04 and p = NS) or controls (DxV/BV = 0.01*BV/TV + 1.18; r = 0.06 and p = NS). NS = not significant.

differences in Cr.Le, DxV/BV, and DxV/TV, between the OA and control groups (Tables 8.4 and 8.5; section 8.4.6) are not dependent on changes in trabecular bone volume, but may be related to differences in the material property of trabecular bone in OA individuals (Li and Aspden, 1997a; Li and Aspden, 1997b; Mansell and Bailey, 1998).

Positive associations were observed between Cr.Dn with both DxV/BV and DxV/TV in the OA and control bone samples (OA: $r_s = 0.56$, $p < 0.0007$; $r_s = 0.55$, $p < 0.002$; respectively; controls: $r_s = 0.80$, $p < 0.002$; $r_s = 0.73$, $p < 0.007$; respectively; Table 8.7). Similarly, positive associations were observed between Cr.S.Dn with both DxV/BV and DxV/TV in the OA and control bone samples (OA: $r_s = 0.61$, $p < 0.0003$; $r_s = 0.62$, $p < 0.0002$; respectively; controls: $r_s = 0.88$, $p < 0.0003$; $r_s = 0.82$, $p < 0.002$; respectively; Table 8.7). Collectively, these positive associations between the morphometric parameters describing microcracks, Cr.Dn and Cr.S.Dn, with the damaged bone volume parameters, DxV/BV and DxV/TV, which predominantly represent the volume fraction of diffuse staining, for the first time suggest that linear microcracks and diffuse microdamage are linked, for both OA and controls, at the IT region of the proximal femur. In contrast, no correlation between microcrack density and diffuse microdamage was observed in trabecular bone sampled from the IT region for 18 severe OA hip cases (Fazzalari *et al.*, 1998b) and in human vertebral bone (Vashishth *et al.*, 2000a). No association was observed between Cr.Le and DxV/BV or DxV/TV in the OA and control groups (results not shown).

Table 8.7 Associations between the microdamage morphometric parameters Cr.Dn and Cr.S.Dn with DxV/BV and DxV/TV in OA and control intertrochanteric trabecular bone samples.

Association	**OA** (***n*** **= 33**) *(aged 37-85 years)*	**Control** (***n*** **= 12**) *(aged 20-85 years)*
Cr.Dn vs DxV/BV	$r_s = 0.56$ $p < 0.0007$	$r_s = 0.80$ $p < 0.002$
Cr.Dn vs DxV/TV	$r_s = 0.55$ $p < 0.002$	$r_s = 0.73$ $p < 0.007$
Cr.S.Dn vs DxV/BV	$r_s = 0.61$ $p < 0.0003$	$r_s = 0.88$ $p < 0.0003$
Cr.S.Dn vs DxV/TV	$r_s = 0.62$ $p < 0.0002$	$r_s = 0.82$ $p < 0.002$

r_s, Spearman rank correlation.

8.4.9 Associations between mRNA levels of skeletally active molecules and microdamage morphometric parameters in OA and control trabecular bone from the human proximal femur

Microdamage is repaired by stimulating a local bone remodelling response (Bentolila *et al.*, 1998; Mori and Burr, 1993), and has been shown to induce osteocyte apoptosis, which may provide an important local signal to remodel a damaged area of bone (Verborgt *et al.*, 2000). However, at this time, the nature and mechanism of the stimulus to recruit osteoclasts to begin the bone remodelling process, to remove the bone microdamage, is unknown. Morphometric parameters describing the extent of bone microdamage, and the levels of mRNA corresponding to factors known to have important regulatory roles in bone remodelling, were measured in contiguous bone samples from the IT region of the human proximal femur for control and OA individuals. Current evidence suggests that one major role for the cytokines IL-6 and IL-11 in bone is to act as an upstream stimulatory signal for osteoclasts to differentiate from their haematopoietic precursors (Martin *et al.*, 1998; as detailed in Chapter 5.1). Thus, linear regression analysis was used to investigate whether there are any associations between the expression of IL-6 and IL-11 mRNA, as determined by semi-quantitative RT-PCR (section 8.3.4), and morphometric parameters describing the extent of bone microdamage in control and OA bone samples. There were 12 control and 15 OA cases, for which both semi-quantitative RT-PCR and microdamage morphometric data were available for analysis (refer to section 8.3.1, and Chapter 7.3.1 and 7.3.4). When the control and OA data were pooled, a significant positive association was observed between IL-11/GAPDH mRNA expression and average microcrack length (Cr.Le; $n = 27$; $r = 0.44$, $p < 0.02$; Figure 8.10). This positive association between mRNA expression of a pro-resorptive cytokine, IL-11, and Cr.Le, is consistent with microdamage (represented by

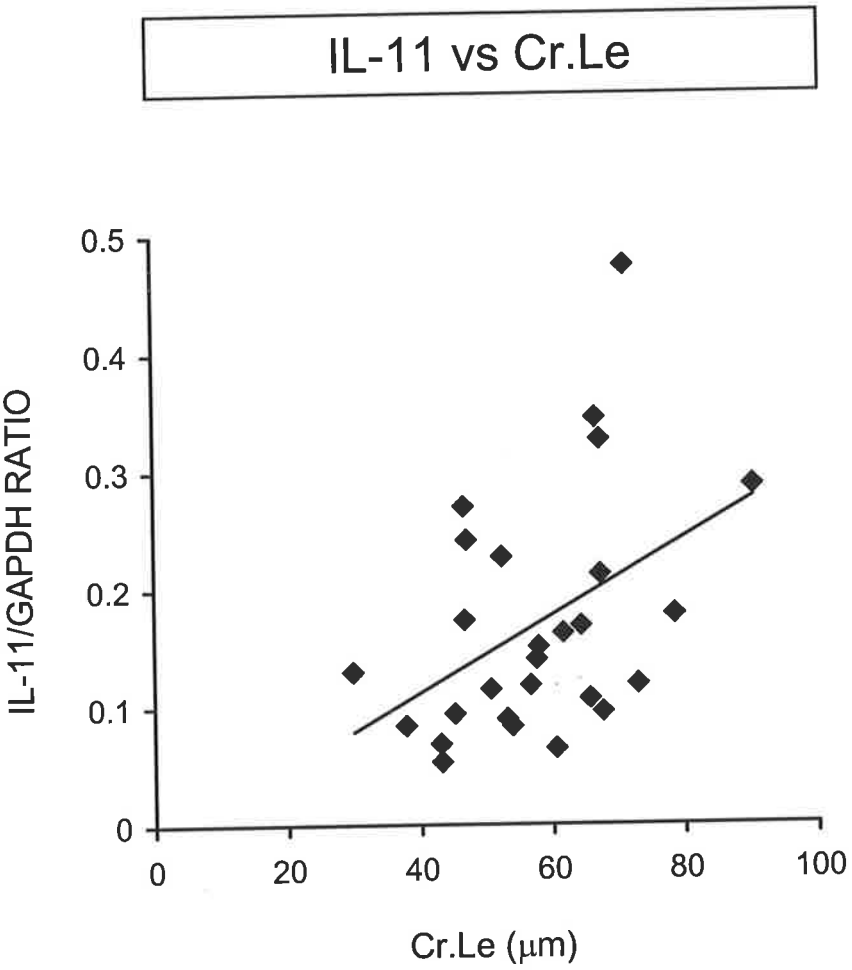

Figure 8.10: A positive association was observed between the relative ratio of IL-11/GAPDH mRNA and Cr.Le, measured in contiguous intertrochanteric trabecular bone samples, from the pooled data set of OA and control individuals (n = 27; IL-11/GAPDH = 0.003*Cr.Le - 0.02; r = 0.44 and $p < 0.02$).

changes in average microcrack length) providing a stimulus for osteoclastic bone resorption. However, when the OA and control data were analysed independently, no significant association between IL-11/GAPDH mRNA expression and Cr.Le was observed (Figure 8.11). Interestingly, the OA data points were segregated from the controls on the plot of IL-11/GAPDH mRNA versus Cr.Le, with lower IL-11 mRNA levels for the OA samples, which was consistent with the lower mean value of IL-11/GAPDH mRNA expression in OA compared with controls (Figure 6.3 and Table 6.3; Chapter 6.4.3). There was no significant association between IL-6/GAPDH mRNA expression and Cr.Le in the pooled data set of OA and control individuals (Figure 8.12). However, when the outlier, control case C5 (72-year-old female) with a high relative expression level of IL-6/GAPDH mRNA (described in Chapter 5), was removed, a positive association was observed between IL-6/GAPDH mRNA expression and Cr.Le in the pooled OA and control data ($n = 26$; $r = 0.40$, $p < 0.05$; Figure 8.12). As for IL-11 mRNA, this positive association between mRNA expression of a pro-resorptive cytokine, IL-6, and Cr.Le, is consistent with microdamage providing a stimulus for osteoclastic bone resorption. No significant association was observed between IL-6/GAPDH mRNA expression and Cr.Le when the OA and control data were analysed independently (Figure 8.13). However, the plot of IL-6/GAPDH mRNA versus Cr.Le suggests a segregation of the data points such that the OA values for IL-6 mRNA are lower than the controls, which was consistent with the difference in the mean value of IL-6/GAPDH mRNA expression between the OA and control groups (Figure 6.2; Chapter 6.4.3). No associations were observed between IL-6/GAPDH or IL-11/GAPDH mRNA expression and any of the other morphometric parameters describing microcracks, Cr.Dn, and Cr.S.Dn, or the damaged bone volume parameters, DxV/BV and DxV/TV, in the pooled or independent control and OA data sets (results not shown).

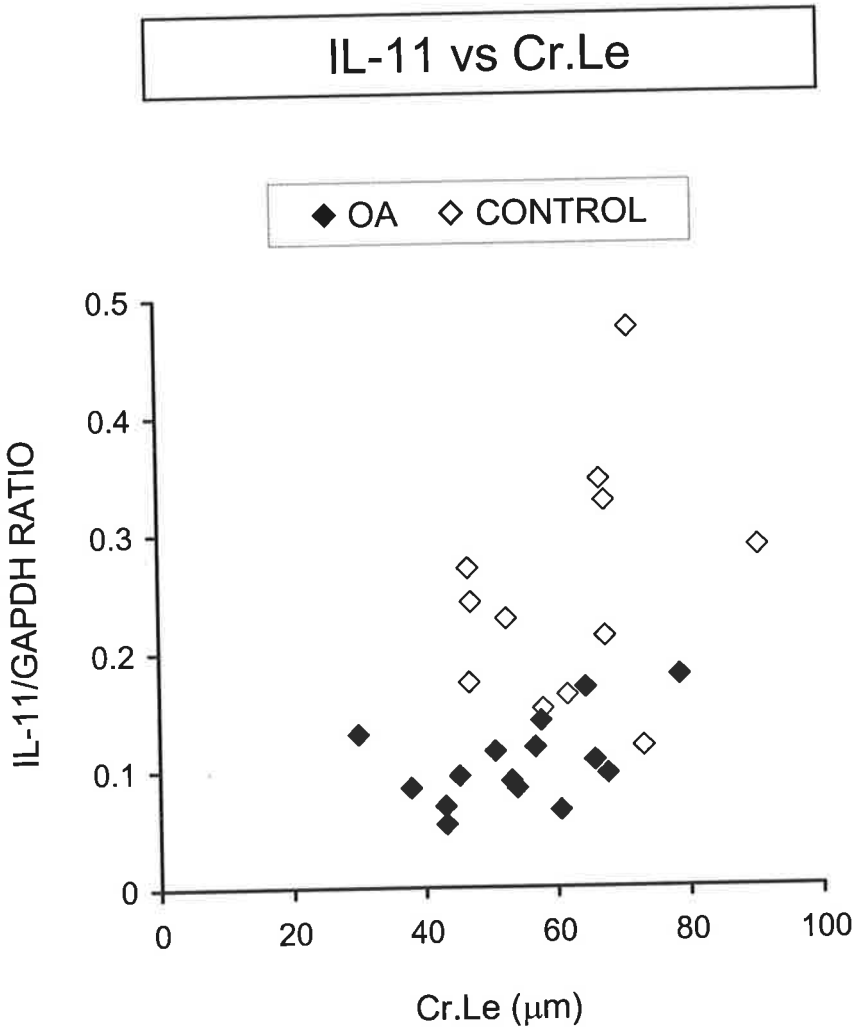

Figure 8.11: Associations between the relative ratio of IL-11/GAPDH mRNA and Cr.Le, measured in contiguous intertrochanteric trabecular bone samples, from OA (n = 15) and control (n = 12) individuals. No association was observed between the two parameters in either the OA group (IL-11/GAPDH = 0.001*Cr.Le + 0.03; r = 0.47 and p = NS) or controls (IL-11/GAPDH = 0.002*Cr.Le + 0.12; r = 0.28 and p = NS). NS = not significant.

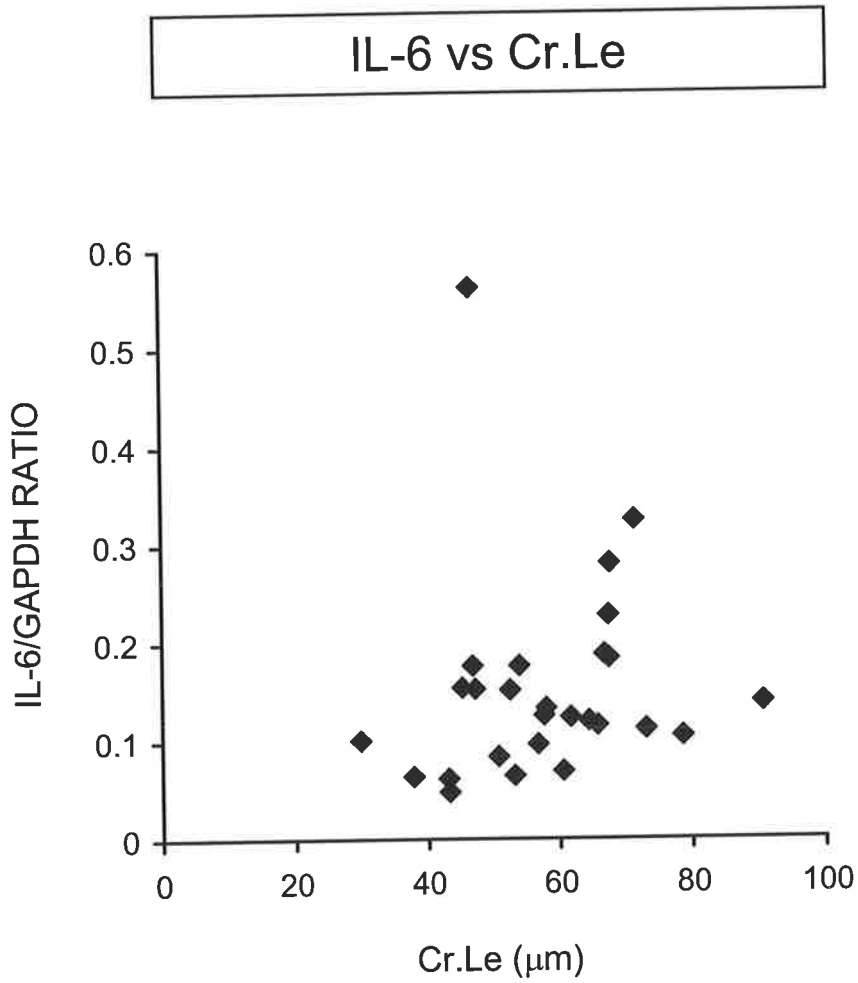

Figure 8.12: No association was observed between the relative ratio of IL-6/GAPDH mRNA and Cr.Le, measured in contiguous intertrochanteric trabecular bone samples, from the pooled data set of OA and control individuals (n = 27; IL-6/GAPDH = 0.0009*Cr.Le + 0.10; r = 0.12 and p = NS; n = 26 (without outlier); IL-6/GAPDH = 0.002*Cr.Le + 0.02; r = 0.40 and $p < 0.05$). NS = not significant.

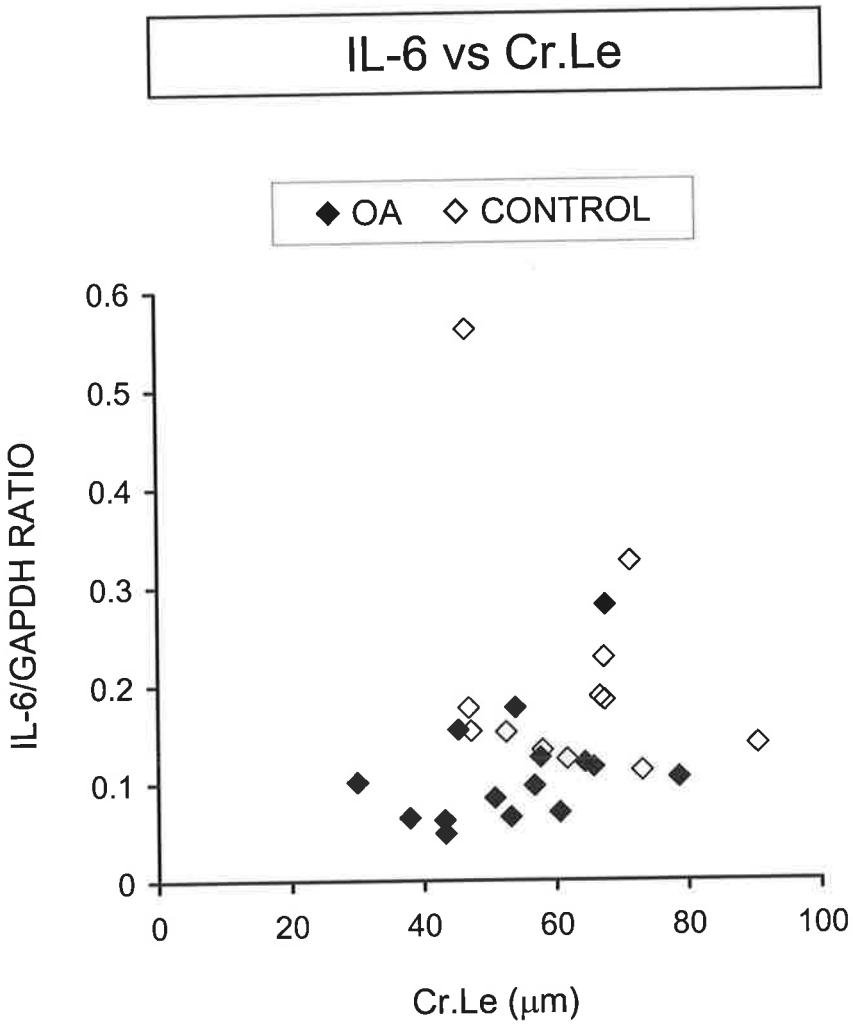

Figure 8.13: Associations between the relative ratio of IL-6/GAPDH mRNA and Cr.Le, measured in contiguous intertrochanteric trabecular bone samples, from OA (n = 15) and control (n = 12) individuals. No association was observed between the two parameters in either the OA group (IL-6/GAPDH = 0.002*Cr.Le + 0.02; r = 0.38 and p = NS) or controls (IL-6/GAPDH = -0.003*Cr.Le + 0.38; r = -0.29 and p = NS). NS = not significant.

RANKL and OPG are important downstream signals of osteoclast biology, onto which many hormonal, chemical, and biochemical signals converge (Hofbauer and Heufelder, 2001; detailed in Chapter 5.1). Hofbauer *et al.* (2000) hypothesised that the ratio of RANKL to OPG is the main determinant of the pool size of active osteoclasts in the local bone environment. Furthermore, a strong positive association was observed between eroded bone surface, ES/BS, and the ratio of RANKL/OPG mRNA, measured in contiguous trabecular bone samples from the IT region of the proximal femur, for non-diseased/control individuals (Figure 7.8; Chapter 7.4.3). Thus, linear regression analysis was used to investigate whether there are any associations between the expression of the RANKL/OPG mRNA ratio, as determined by semi-quantitative RT-PCR (section 8.3.4), and morphometric parameters describing the extent of bone microdamage in control and OA bone samples. There were 11 control and 12 OA cases, for which both semi-quantitative RT-PCR and microdamage morphometric data were available for analysis (refer to section 8.3.1, and Chapter 7.3.1 and 7.3.4). When the control and OA data were pooled or analysed independently, no significant association between the ratio of RANKL/OPG mRNA and any of the morphometric parameters describing microcracks, Cr.Dn, Cr.Le, and Cr.S.Dn, or the damaged bone volume parameters, DxV/BV and DxV/TV, was observed (results not shown). Further, no associations were observed between RANKL/GAPDH or OPG/GAPDH mRNA expression and any of the microdamage morphometric parameters, in the pooled or independent control and OA data sets (results not shown).

8.5 DISCUSSION

Repetitive loading causes skeletal fatigue or microdamage, resulting in the microscopic cracking of the ultra-structural bone matrix (Burr *et al.*, 1997). Microdamage has been identified as discrete microcracks and ultra-microcracking that is described as cross-hatch or diffuse microdamage (Figures 2.7A and 2.7B; Burr *et al.*, 1997; Fazzalari *et al.*, 1998a). The distribution of microdamage in trabecular bone from different regions of the proximal femur from the same individual is unknown. OA is characterised by progressive degenerative damage to the articular joint cartilage and changes in the subchondral bone trabecular architecture, which may develop to compensate for an altered bone matrix structure (loosely packed collagen fibres) and composition (hypomineralisation) in OA (Bailey *et al.*, 2002; Li and Aspden, 1997a; Li and Aspden, 1997b; Mansell and Bailey, 1998). The different bone structure and bone matrix composition in OA is accompanied by altered biomechanical properties, with a more rigid trabecular bone in the subchondral and femoral neck regions (Li and Aspden, 1997a; Li and Aspden, 1997b; Martens *et al.*, 1983). The accumulation of microdamage in bone contributes to the loss of bone quality (i.e., bone biomechanical properties; Burr *et al.*, 1997; Carter *et al.*, 1981; Carter and Hayes, 1977; Forwood and Parker, 1989; Mashiba *et al.*, 2000; Pattin *et al.*, 1996; Schaffler *et al.*, 1989). Thus, it is important to describe the amount and morphological type of trabecular bone microdamage in OA.

The aim of the work described in this chapter was threefold. First, to investigate the *in vivo* distribution of trabecular bone microdamage in the human proximal femur, for a cohort of autopsy individuals, without any joint disease or any medical condition predicted to affect the skeletal status. Second, to investigate the amount and morphological type of *in vivo* trabecular bone microdamage at the intertrochanteric region of the proximal femur, for

individuals suffering from primary hip OA, compared to skeletal-site matched non-OA/control individuals. The intertrochanteric region of the proximal femur was chosen for sampling of trabecular bone because characteristic architectural changes at this site in OA have been described previously (Crane *et al.*, 1990), while it is remote from the subchondral bone that undergoes well-characterised secondary changes in severe OA (Fazzalari *et al.*, 1992). Third, to investigate the relationship between mRNA expression levels of skeletally active molecules, with known regulatory roles in osteoclastogenesis (IL-6, IL-11, RANKL, and OPG), and microdamage morphometric parameters, measured in contiguous intertrochanteric trabecular bone samples from both OA and control individuals. These final data were of particular interest as the nature and mechanism of the stimulus to recruit osteoclasts to begin the targeted bone remodelling process, to repair bone microdamage, is unknown.

8.5.1 Regional distribution of trabecular bone microdamage in the human proximal femur

In vivo bone microdamage in the human proximal femur was similar in magnitude at the subchondral principal compressive region, the medial principal compressive region, and the intertrochanteric region (Table 8.2). These skeletal sites are regions of principal compressive loading due to muscular forces and involvement in the transfer of upper body weight to the cortex of the femur (Ling *et al.*, 1996). This relatively uniform distribution of microdamage suggests that the principal components of the femoral trabecular bone network are equally exposed to deformations resulting in microdamage independent of bone volume (BV/TV). These findings support the hypothesis that normal trabecular bone architecture acquires a structure able to sustain a level of deformation and associated microdamage that can be repaired by bone remodelling. There must be a balance between

the repair of microdamage by bone remodelling to ensure that microdamage does not accumulate and put the bone at risk of fatigue failure. However, the significantly reduced microcrack length (Cr.Le) in the subchondral bone, compared to a site distal to the articular surface, the medial principal compressive region (Table 8.2), may be indicative of different bone material properties, such as bone tissue mineralisation, and/or differential bone remodelling rates between these regions (Ampe *et al.*, 1986; Fazzalari *et al.*, 1989; Li and Aspden, 1997a). In addition, the subchondral region's proximity to the spherical articular surface may influence the local deformation characteristics of the trabecular bone (Harrison *et al.*, 1953).

8.5.2 Influence of age and osteoarthritis on trabecular bone microdamage morphology at the intertrochanteric region of the human proximal femur

Few computational algorithms for adaptive skeletal changes have been developed for microdamage because methods have not been available to recognise the different morphological manifestations of microdamage and to quantify the magnitude of local damage in the bone (Huiskes *et al.*, 2000; Prendergast and Taylor, 1994). To the present, stained microcracks are the only criteria to have been correlated with bone biomechanics (Burr *et al.*, 1998; Forwood and Parker, 1989; Schaffler *et al.*, 1989), leaving the influence of *in vivo* ultra-structural damage (cross-hatch and diffuse microdamage) on bone fragility open for scrutiny. Few attempts have been made to investigate diffuse microdamage and its influence on bone biomechanics. In the vertebral body, Fyhrie and Schaffler (1994) showed that the failure mechanism of horizontal and vertical trabeculae is different. The horizontal trabeculae fail as a result of microcrack propagation, whereas vertical trabeculae remained grossly intact but show diffuse microdamage within the bone matrix. Subsequently, those investigators reported that *in vivo* diffuse staining was located

primarily in vertically oriented trabeculae of the vertebral body (Wenzel *et al.*, 1996). Schaffler *et al.* (1994) described diffuse microdamage associated with microcracks as the "damage process zone", a zone wherein the features of the bone matrix ultra-structure, such as the collagen fibre-bone mineral inter-relationship may minimise the formation of larger cracks and encourage the formation of numerous smaller cracks (Fazzalari *et al.*, 1998a).

In the OA proximal femur, decreased microcrack length (Cr.Le) and an increased volume fraction of bone microdamage (predominantly representing cross-hatch and diffuse staining), DxV/BV and DxV/TV, may be indicative of a more effective inhibition of microcrack propagation (Tables 8.5 and 8.6). Further, these differences in Cr.Le, DxV/BV, and DxV/TV between the OA and control proximal femur, given that mean BV/TV was not different between OA and controls (Tables 8.5 and 8.6), may be related to reports of a different bone matrix structure and composition in OA, such as hypomineralisation and loosely packed collagen fibres (Bailey *et al.*, 2002; Brown *et al.*, 2002; Grynpas *et al.*, 1991; Helliwell *et al.*, 1996; Li and Aspden, 1997a; Li and Aspden, 1997b; Mansell and Bailey, 1998). Interestingly, a recent study by Bailey *et al.* (2002) has shown that subchondral bone osteoblasts, from individuals with hip OA, produce a molecularly distinct collagen, type I collagen homotrimer (i.e., three $\alpha 1$ chains of type I collagen). A decreased enthalpy (i.e., the energy required to denature the triple helix) of the type I collagen homotrimer fibre indicated that the homotrimer molecules are more loosely packed in the fibre (Bailey *et al.*, 2002). Furthermore, the collagen fibres appeared to be narrower and aligned in a disorganised manner in OA subchondral bone (Bailey *et al.*, 2002). The type I collagen homotrimer is suggested to be mechanically weaker and less mineralised in bone (McBride *et al.*, 1998; Misof *et al.*, 1997). Subchondral and femoral

neck trabecular bone from hip OA subjects has been reported to be materially weaker (i.e., less stiff and dense) compared with age-matched controls (Li and Aspden, 1997a). However, biomechanical studies of OA subchondral and femoral neck trabecular bone cores have shown the bone to be stiffer or more rigid (Li and Aspden, 1997a; Li and Aspden, 1997b; Martens *et al.*, 1983). The biomechanical properties of a trabecular bone core are influenced by the bone matrix composition and trabecular bone architecture. The more rigid subchondral trabecular bone in OA is associated with trabecular bone architectural changes, such as increased trabecular bone volume, and altered trabecular size and spacing (Crane *et al.*, 1990; Fazzalari *et al.*, 1992).

Microdamage repair is not well understood but depends on targeted remodelling (Bentolila *et al.*, 1998; Burr *et al.*, 1997; Mori and Burr, 1993). Therefore, the accumulation of microdamage in bone may depend upon the rate at which the bone is remodelled. However, the bone remodelling rate is representative of both stochastic remodelling, essential for maintaining mineral homeostasis, and targeted remodelling as a response to microdamage (Burr, 2002). The increased volume fraction of bone microdamage (predominantly representing cross-hatch and diffuse staining), DxV/BV and DxV/TV, at the intertrochanteric region of the OA proximal femur (Tables 8.5 and 8.6), may be related to a reduction in bone turnover at this skeletal site. Interestingly, a decrease in eroded bone surface, ES/BS, was observed in OA intertrochanteric trabecular bone in comparison to age-matched controls (Table 7.5; Chapter 7.4.5). However, the repair of diffuse microdamage has not been elucidated. Bentolila *et al.* (1998) reported only a trend between diffuse microdamage and intracortical remodelling resorption spaces in adult rat long bone after fatigue loading.

The increased volume fraction of bone microdamage, DxV/BV and DxV/TV, at the intertrochanteric region of the OA proximal femur (Tables 8.5 and 8.6), may relate to an increase in load amplitude, the number of load cycles, or the direction of the load on the trabecular bone. Fazzalari *et al.* (1998b) reported a trend for microcrack density (Cr.Dn) and DxV/BV to increase as the trabecular bone anisotropy decreases with respect to the bone specimen loading axis. The authors suggested that loading trabecular bone on an axis not aligned to the principal trabecular alignment may lead to increased microdamage (Fazzalari *et al.*, 1998b). Alterations in the mechanical environment of the hip joint can adversely affect the direction and distribution of bone loading. Severe OA hip patients tend to have altered gait patterns due to joint pain and anatomical differences, which would result in abnormal directions of bone loading (Moore *et al.*, 1994).

Although the age-distribution of microcrack density (Cr.Dn) in OA, as described in section 8.4.7 (Figure 8.4), is similar to the age-distribution of Cr.Dn reported in women with and without subcapital osteoporotic fracture (Mori *et al.*, 1997), the epidemiological evidence indicates that patients with OA have a very low incidence of osteoporotic fracture (Dequeker *et al.*, 1993a; Verstraeten *et al.*, 1991; Chapter 1.2.2). Furthermore, it has been suggested that OA and osteoporotic fracture are mutually exclusive (Dequeker *et al.*, 1996). The DxV/BV age-distribution in OA is non-linear and similar to Cr.Dn (Figure 8.6). Beyond the age of 60 years, the DxV/BV distribution is heterogeneous, with some patients having DxV/BV data comparable to those patients less than 60 years of age, but with other patients having significantly increased DxV/BV (Figure 8.6). It is hypothesised that increased DxV/BV is related to increased bone toughness; i.e., increased energy input is required for bone failure. Diffuse damage may be a more effective energy-absorbing mechanism than microcracking (Fazzalari *et al.*, 1998a). Zioupos (2001) recently reported

that it was necessary to re-evaluate the fragility of aging human bone. It is possible that more emphasis should be placed on bone's energy-related resistance to fracture than on its stiffness or strength (Zioupos, 2001). A recent animal study using high-dose bisphosphonates has indicated the need to understand more fully the causal relationship and interaction between microcracks and bone tissue toughness (Mashiba *et al.*, 2000).

The average microcrack length (Cr.Le) for the OA and control groups was not age-dependent, being constant with age and less than about 100 μm. In addition, Cr.Le was not dependent on DxV/BV. These results highlight that Cr.Le appears to have an upper limit that may be characteristic of bone material structure. In the case of bisphosphonate treatment, the mean degree of bone mineralisation was shown to increase over time (Boivin *et al.*, 2000), and this was associated with increases in microcrack length in cortical bone (Mashiba *et al.*, 2000). In the OA proximal femur, numerical microcrack density (Cr.Dn) and microcrack surface density (Cr.S.Dn) were not dependent on BV/TV (Figure 8.8; section 8.4.8), a measure linked to bone architecture, but may be closely associated with reported changes in the material properties of bone in OA (Brown *et al.*, 2002; Grynpas *et al.*, 1991; Helliwell *et al.*, 1996; Li and Aspden, 1997a; Li and Aspden, 1997b; Mansell and Bailey, 1998). In addition, there was no evidence for any dependence of DxV/BV or DxV/TV on BV/TV for either the OA or control group data (Figure 8.9; section 8.4.8). Nevertheless, the co-plot of DxV/BV versus BV/TV (Figure 8.9) showed that the control group had similar DxV/BV independent of BV/TV, even though the OA group had a heterogeneous distribution of DxV/BV, which was still independent of BV/TV. Again, these results may be indicative of a differing bone material structure between OA and control cases. Interestingly, the microcrack parameters, Cr.Dn and Cr.S.Dn, positively correlated with the damaged bone volume parameters, DxV/BV and

DxV/TV, which predominantly represent the volume fraction of diffuse staining, in both the OA and control groups (Table 8.7). These data suggest, for the first time, that linear microcracks and diffuse microdamage are linked in both OA and normal individuals, at the intertrochanteric region of the proximal femur.

8.5.3 Association between cytokine mRNA expression and microcrack length in human trabecular bone from the proximal femur: potential role of IL-11 in the initiation of microdamage repair

As detailed in Chapter 1.3.3.1, Mori and Burr (1993) first demonstrated that microdamage initiates its repair by targeted bone remodelling, by fatigue loading dog long bones and observing a subsequent increase in osteoclastic resorption. Bentolila *et al.* (1998) tested the hypothesis that bone fatigue loading *in vivo*, which induces *in vivo* microdamage, can activate the remodelling process in adult rat long bones, in which haversian remodelling characteristically does not occur. Ten days after fatigue loading of adult rat ulnae, intracortical resorption was activated (Bentolila *et al.* 1998). Moreover, numerical microcrack density was reduced by almost 40% by ten days after fatigue loading. Intriguingly, intracortical resorption was associated with both bone microdamage and regions of altered osteocyte and canalicular integrity (Bentolila *et al.* 1998). Subsequently, those investigators reported that microdamage induced osteocyte apoptosis, which may provide an important local signal to remodel a damaged area of bone (Verborgt *et al.*, 2000; Verborgt *et al.*, 2002). Osteocyte apoptosis has been implicated in the local control of bone resorption (Noble *et al.*, 1997; Tomkinson *et al.*, 1997; Tomkinson *et al.*, 1998). Verborgt *et al.* (2000) have suggested that osteocyte apoptosis induced by bone microdamage may occur by direct injury to osteocytes or disruption of canaliculi, which would result in an alteration of canalicular flow and impairment of the nutrition and

metabolic activities of osteocytes. A number of mechanisms by which apoptotic osteocytes could provide a targeting signal for bone resorption have been proposed. These include apoptotic osteocytes exposing specific cell surface markers that are preferentially targeted by osteoclast precursor cells, apoptotic cell fragmentation products moving through bone canaliculi to provide a potential transmissible signal(s) to bone lining surface cells, and the release of proteases and cytokines with pro-resorptive roles, such as IL-1, by apoptotic osteocytes (Bronckers *et al.*, 1996; Hogquist *et al.*, 1991; Verborgt *et al.*, 2000). However, at this time, the nature and mechanism of the stimulus to recruit osteoclasts to begin the targeted bone remodelling process, to remove the bone microdamage, is unknown.

There is a lack of information regarding the repair of microdamage in trabecular bone and in human bone tissues. Osteocytes are located in lacunae (cavities) and are extensively connected to one another as well as to the bone lining surface cells by cytoplasmic processes inside the canaliculi. Osteocytes are suggested to be the mechanosensing cells of the bone matrix (Chapter 1.3.1.3; Burger and Klein-Nulend, 1999). A decline in osteocyte lacunar density in human cortical and trabecular bone has been shown to associate with an accumulation of microcracks with age (Mori *et al.*, 1997; Vashishth *et al.*, 2000b). These studies suggest that an impaired osteocyte network is associated with the failure of microdamage repair. Interestingly, sites of bone microdamage were often seen in close association to an eroded bone surface in intertrochanteric trabecular bone sampled from the OA and control proximal femur, for the cases described in this chapter (Figure 8.14).

Current evidence suggests that one major role for the cytokines IL-6 and IL-11 in bone is to act as an upstream stimulatory signal for osteoclasts to differentiate from their haematopoietic precursors (Martin *et al.*, 1998; as detailed in Chapter 5.1). A significant

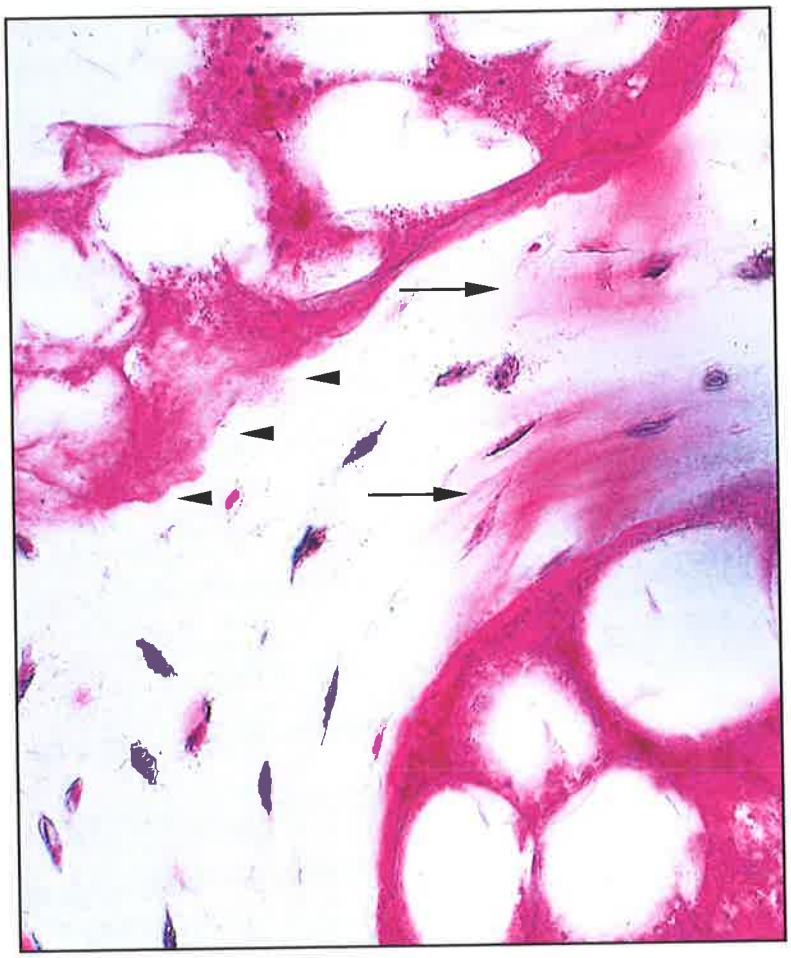

Figure 8.14: Photomicrograph of human femoral 70 µm-thick section of trabecular bone bulk-stained with basic fuchsin which shows microdamage in association with an eroded bone surface. Arrows identify diffuse patches of basic fuchsin staining. Arrow heads identify an eroded trabecular bone surface (objective magnification: X20).

positive association was observed between IL-11/GAPDH mRNA expression and microcrack length (Cr.Le), measured in contiguous trabecular bone samples from the intertrochanteric region, for the pooled OA and control data (Figure 8.10). In addition, IL-6/GAPDH mRNA expression positively associated with Cr.Le in the pooled OA and control data, when an outlier data point was removed (Figure 8.12; Chapter 8.4.9). This positive association between mRNA expression of a pro-resorptive cytokine, IL-11 more so than IL-6, with Cr.Le, is consistent with microdamage providing a stimulus for osteoclastic bone resorption. Increased microcrack length has the potential to cause increased disruption of the osteocytic canalicular network, which may provide an increased stimulus for the initiation of bone remodelling. When the OA and control data were analysed independently, no significant associations between IL-11 and IL-6 mRNA expression with Cr.Le were observed (Figures 8.11 and 8.13, respectively). Even though the sample sizes are small (OA, n = 15; controls, n = 12), the OA data points are segregated from the controls on the plots of IL-11/GAPDH and IL-6/GAPDH mRNA versus Cr.Le, with lower IL-11 and IL-6 mRNA levels for the OA samples (Figures 8.11 and 8.13, respectively). These data suggest that the reparative response to microcracks, hypothesised to be represented by bone tissue levels of IL-11 mRNA, is reduced in OA trabecular bone. However, as the full role of the pleiotropic cytokine IL-11 in the bone microenvironment is not understood, the cellular origin(s) of the measured IL-11 mRNA expression in these human bone samples are not known, and as the temporal relationship between the appearance of *in vivo* microdamage and IL-11 mRNA expression is not known, interpretation of these findings is speculative. Furthermore, it is recognised that there are many other candidate molecules that may have roles in the molecular regulation of the microdamage repair process.

A hypothesis of how microdamage is repaired by stimulating a targeted bone remodelling response in trabecular bone is presented in Figures 8.15A and 8.15B. A microcrack in the trabecular bone matrix damages osteocytic canalicular processes and induces local osteocyte apoptosis. This disruption of the osteocytic network triggers a signalling cascade of molecular factors, postulated to be inflammatory cytokines with pro-resorptive roles in the bone microenvironment, such as TNF-α, IL-1, IL-6, and IL-11, and/or growth factors, resulting in the recruitment of osteoclast and osteoblast precursor cells from the bone marrow to the site of microdamage (Figure 8.15A). The osteoclast and osteoblast precursor cells differentiate into mature bone resorbing osteoclasts and bone forming osteoblasts, respectively. This local bone remodelling response results in the removal of the bone microdamage and a subsequent restoration of the osteocytic network (Figure 8.15B). Further studies are needed in the adult rat model of microdamage creation (Bentolila *et al.*, 1998) to elucidate the temporal relationship between the appearance of microdamage, gene expression, and subsequent activation of targeted osteoclastic resorption.

8.5.4 Conclusions

The accumulation of microdamage in bone contributes to the loss of bone quality. The work described in this chapter has identified a relatively uniform distribution of microdamage in the proximal femur for an autopsy control group, which suggests that the principal components of the femoral trabecular bone network are equally exposed to deformations resulting in microdamage independent of bone volume (BV/TV). Furthermore, these findings support the hypothesis that trabecular bone architecture adapts to sustain normal physiological deformations that result in a uniform distribution of microdamage; this microdamage does not usually accumulate and is able to be repaired by bone remodelling. Differences were found in the amount and morphological type of *in vivo*

Figure 8.15: A hypothesis of how microdamage is repaired by stimulating a targeted bone remodelling response. (A) A microcrack in the trabecular bone matrix damages osteocytic canalicular processes and induces local osteocyte apoptosis. This disruption of the osteocytic network triggers a signalling cascade of molecular factors, postulated to be inflammatory cytokines such as TNF-α, IL-1, IL-6, and IL-11, and/or growth factors, resulting in the recruitment of osteoclast and osteoblast precursor cells from the bone marrow to the site of microdamage. (B) The osteoclast and osteoblast precursor cells differentiate into mature bone resorbing osteoclasts and bone forming osteoblasts, respectively. This local bone remodelling response results in the removal of the bone microdamage and a subsequent restoration of the osteocytic network.

A

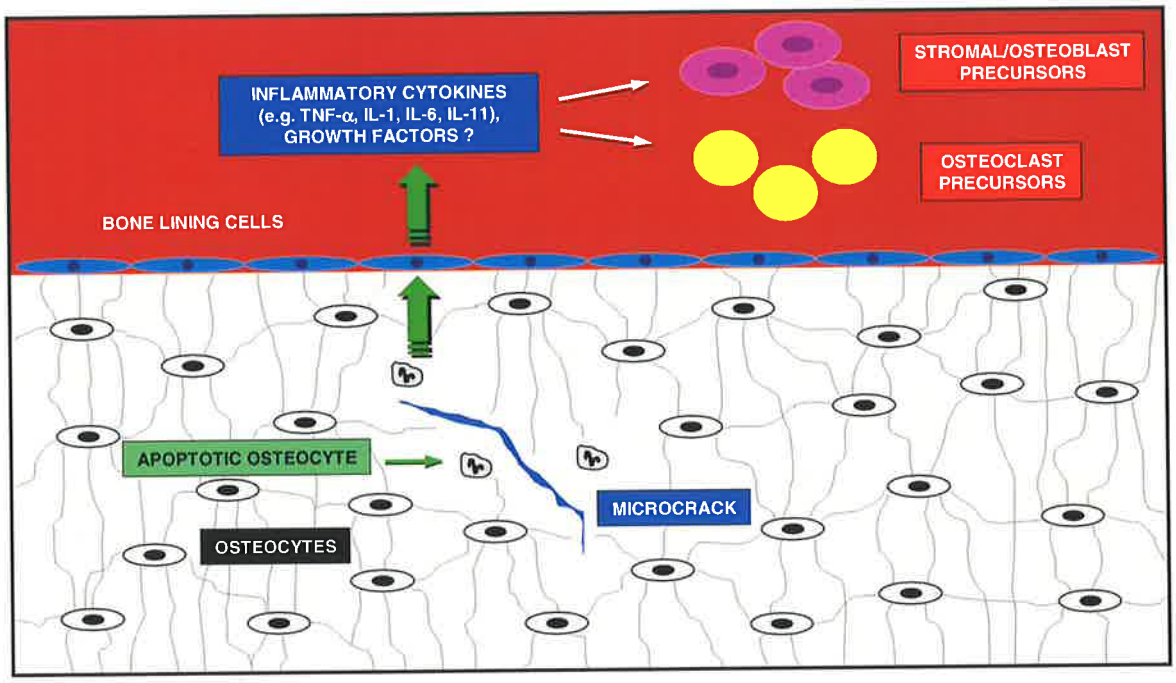
INFLAMMATORY CYTOKINES
(e.g. TNF-α, IL-1, IL-6, IL-11),
GROWTH FACTORS ?
STROMAL/OSTEOBLAST
PRECURSORS
OSTEOCLAST
PRECURSORS
BONE LINING CELLS
APOPTOTIC OSTEOCYTE
MICROCRACK
OSTEOCYTES

B

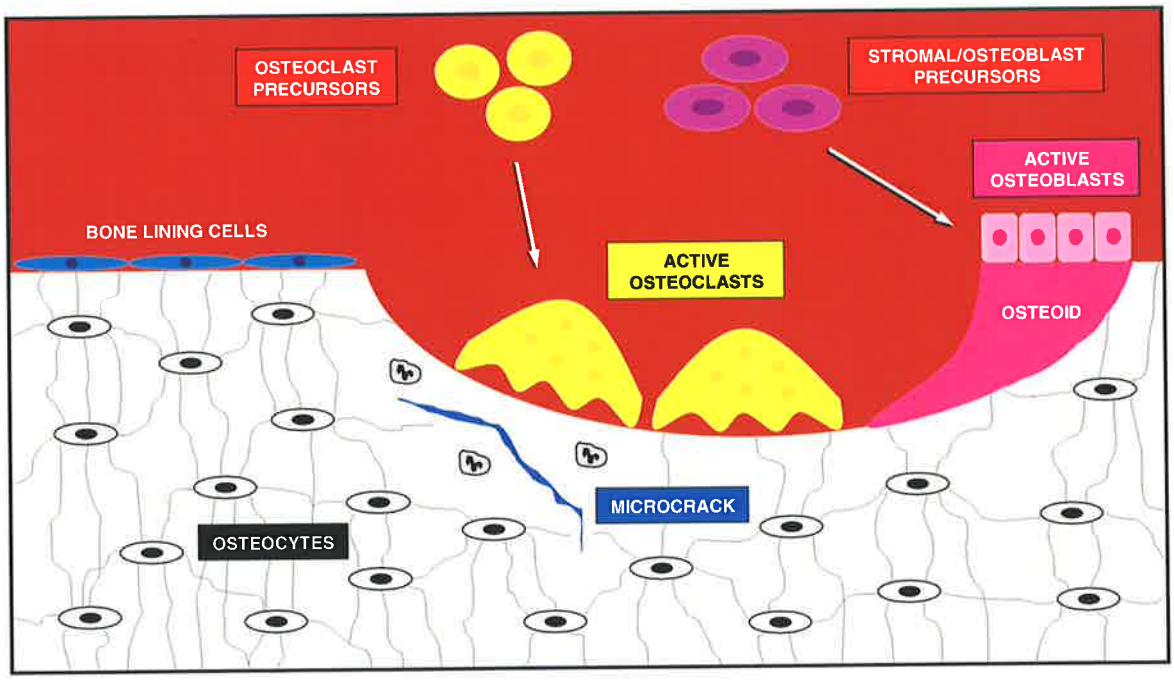
OSTEOCLAST
PRECURSORS
STROMAL/OSTEOBLAST
PRECURSORS
ACTIVE
OSTEOBLASTS
BONE LINING CELLS
ACTIVE
OSTEOCLASTS
OSTEOID
MICROCRACK
OSTEOCYTES

trabecular bone microdamage between individuals suffering from primary hip OA and non-OA/control cases, at the intertrochanteric region of the proximal femur. The intertrochanteric region is remote from the subchondral bone that undergoes well-characterised secondary changes in severe OA. The microdamage characteristics of intertrochanteric OA bone include the non-linear increase in the volume fraction of bone microdamage (DxV/BV) with increasing age and a heterogeneous distribution of DxV/BV when compared with controls. In addition, microcrack length (Cr.Le) was significantly reduced in the OA group. These findings are consistent with the reported bone material property differences for OA, such as hypomineralisation and loosely packed collagen fibres. Microdamage is repaired by stimulating a local (targeted) bone remodelling response. However, at this time, the nature and mechanism of the stimulus to recruit osteoclasts to begin the targeted bone remodelling process, to remove bone microdamage, is unknown. Intriguingly, a positive association was observed between mRNA expression of a pro-resorptive cytokine, IL-11, and Cr.Le, measured in contiguous trabecular bone samples from the intertrochanteric region, for the pooled OA and control data. This observation is consistent with microdamage providing a stimulus for osteoclastic bone resorption. However, further studies are needed in the adult rat model of microdamage creation to elucidate the temporal relationship between the appearance of microdamage, gene expression, and subsequent activation of targeted osteoclastic resorption. Further study into the factors that influence the accumulation and skeletal distribution of microdamage is fundamental to understanding skeletal health.

CHAPTER 9

SUMMARY AND FUTURE RESEARCH DIRECTIONS

9.1 SUMMARY

Research into the aetiology of osteoarthritis (OA) has predominantly focussed on understanding the mechanism of breakdown and loss of articular cartilage. However, there is now substantial evidence from spontaneous OA animal models that there is a change in the density and metabolism of subchondral bone before any signs of cartilage fibrillation. Furthermore, in primary human OA, alterations in bone density, trabecular bone structure, bone mineralisation, bone growth factor content, and osteoblast cell activity have been observed in subchondral bone and at skeletal sites distal to the joint articular surface. Collectively, these studies suggest that the bone changes may precede the joint degeneration of OA, or may arise secondarily to the joint pathology, or indeed may occur in parallel with the cartilage damage, driven by the same causative agent(s) that lead to cartilage disease. Whichever of these is the case, in order to devise effective treatments for OA, it is clearly important to consider the bony component of this disease and to develop an understanding of the cellular and molecular processes that lead to the bony changes.

The principal aim of this thesis was to describe trabecular bone remodelling, from both a molecular and histomorphometric perspective, at a skeletal site distal to the subchondral bone, the intertrochanteric region of the proximal femur, from OA patients undergoing joint replacement surgery for primary OA of the hip, and age-matched adults, at autopsy, without any overt/known joint disease or any medical condition predicted to affect their bone turnover status.

Contiguous trabecular bone samples were analysed for mRNA expression of a selection of molecular factors involved in the regulation of bone remodelling, together with the histomorphometric quantitation of static indices of bone turnover, bone structural

parameters, and microdamage parameters. High quality undegraded RNA was extracted from trabecular bone retrieved surgically (OA) and at autopsy (control), and semi-quantitative RT-PCR analysis was performed using a panel of oligonucleotides designed to amplify mRNA encoding a number of skeletally active molecules.

At first, it was established that total RNA and specific mRNA transcripts were relatively stable in bone tissues stored at 4°C up to 3.5 days postmortem. Secondly, the mRNA expression pattern of a number of bone cell markers and regulatory molecules of bone remodelling was not different between the proximal femur (intertrochanteric and femoral neck regions) and iliac crest, for a cohort of postmortem individuals. This finding was unexpected, given the known heterogeneity of bone turnover and architecture in the human skeleton.

Striking differences were observed in gene expression between OA and control trabecular bone at the intertrochanteric region of the proximal femur. Specifically, the expression of factors associated with the development of the osteoclast, the RANKL/OPG mRNA ratio, IL-6 mRNA, and IL-11 mRNA, were all significantly reduced in OA bone compared to control bone. There is extensive evidence from cell culture experiments that the local ratio of RANKL to OPG determines the effective activity of RANKL to promote osteoclast formation. Thus, the lower expression level of RANKL/OPG mRNA in OA bone suggests that osteoclast formation may be reduced at the intertrochanteric region in OA. Furthermore, the bone resorption index, eroded surface (ES/BS), relative to the bone formation index, osteoid surface (OS/BS), was significantly reduced in OA bone compared to controls, consistent with reports of lower bone turnover in OA. In contrast, an age-dependent elevation in the mRNA expression of an osteoblastic cell marker, osteocalcin

(OCN), was observed in OA bone compared with control bone. This finding is consistent with a reported increase in OCN protein in OA iliac crest bone, and also that at the intertrochanteric region there is maintenance of trabecular bone volume in OA.

Intriguingly, when the histomorphometric and molecular analyses on contiguous bone samples were combined, there was a strong positive correlation between ES/BS and the RANKL/OPG mRNA ratio, independent of age, in controls. This finding suggests that, as more RANKL becomes available to promote osteoclast formation, there is an increase in bone resorption. Further, trabecular bone volume (BV/TV) was inversely correlated to the ratio of RANKL/OPG mRNA. In addition, a strong positive association was found between OS/BS and the ratio of RANKL/OPG mRNA in the controls. This is the first direct evidence that RANKL and OPG are involved in human bone remodelling, consistent with the roles of RANKL and OPG in osteoclast development established from *in vitro* murine and human cell systems and *in vivo* murine gene deletion studies. Moreover, RANKL has been shown to be of central importance in determining the trabecular bone volume and turnover in the human bone microenvironment of the proximal femur. These relationships between the RANKL/OPG mRNA ratio and ES/BS, BV/TV, and OS/BS, observed in controls, were not evident in trabecular bone from severe primary OA, suggesting that bone turnover in the proximal femur may be regulated differently in this disease. Further, it can be speculated that the trabecular bone structures in OA arise by subversion of the physiological RANKL-controlled mechanisms.

Recent reports have shown that OA bone is less mineralised and the matrix collagen is disorganised, which could potentially significantly weaken the biomechanical properties of the bone matrix, resulting in collagen overproduction and thickening of the bone.

Interestingly, the length and type of microscopic cracks in the bone matrix, specifically bone microdamage, differed between OA and control bone sampled from the intertrochanteric region of the proximal femur. Intriguingly, the proportion of bone matrix containing diffuse microdamage, focal collections of very fine microcracks, was higher in OA bone. Bone microdamage is targeted for repair, and thus subsequent removal, by stimulating a local bone remodelling response, *via* an unknown molecular mechanism. As the length of the microcracks increased, for the pooled OA and control data, there was an associated elevation in the mRNA expression of the pro-resorptive cytokine IL-11, measured in contiguous bone samples. This finding is consistent with an increased stimulus for bone resorption in response to microdamage.

The experimental approach of *molecular histomorphometry*, to compare gene expression with trabecular bone structure and bone turnover, has provided the first description of the molecular events in the local bone microenvironment in OA. The data presented in this thesis support, but do not prove, the hypothesis that altered bone architecture may be the cause of primary OA. Furthermore, the experimental approach has great potential to uncover the mechanisms of normal bone turnover and of those that lead to the altered bone structures found in OA. If OA is caused or exacerbated by altered bone structure, it may be possible to find ways to modify or prevent the bone changes and thus delay joint degeneration. Such a finding would have important implications for the current treatment of OA, which is the surgical replacement of diseased joints.

9.2 LIMITATIONS

The sample sizes of the surgical OA and autopsy control groups, particularly for the semi-quantitative RT-PCR data, are small. A greater sample size is required for each study group to strengthen the observed age relationships, associations between expression of specific mRNA transcripts, associations between histomorphometric parameters and mRNA expression, and the differential mRNA expression between the OA and control bone samples. Bone tissues from advanced or end-stage OA patients are readily available from joint replacement surgery. It is difficult, or rarely possible, to obtain suitable non-diseased/control bone tissues at surgery. A valuable resource of skeletal site-matched control tissue is postmortem bone tissue. However, it is becoming more difficult to obtain bone tissues for research from postmortem cases primarily due to declining autopsy rates at most hospitals/institutions and restrictive government legislation.

A limitation of the data presented in this thesis is the extent of linear regression analysis performed on sample sizes that are small. It is a well-established fact that the more analyses performed on a data set, the more results will meet "by chance" the significance level of $p < 0.05$. However, the associations between expression of specific mRNA transcripts, and the associations between histomorphometric parameters and mRNA expression have been presented and interpreted based upon the existing knowledge of the role(s) of these molecular factors in the regulation of bone remodelling. Furthermore, the degree of scatter of the observations around the regression line was generally not large, which indicated a close relationship between the variables. It is acknowledged that these associations, for example the strong positive association between ES/BS and RANKL/OPG mRNA levels in control bone (which suggests that the effective

concentration of RANKL is related causally to bone resorption), do not establish cause and effect relationships in the human bone microenvironment.

One limitation of semi-quantitative RT-PCR analysis of mRNA expression in homogenised bone tissue samples is that the data provide no information about the cellular origin(s) of each mRNA transcript. Another limitation is that it is not known whether the gene expression patterns are representative of the corresponding protein levels in the bone tissue. This can be resolved by the use of *in situ* hybridisation in combination with immunohistochemistry for the bone tissue localisation of each molecular factor of interest at the mRNA and protein level, respectively. The advantage of semi-quantitative RT-PCR analysis of mRNA expression in bone tissue over cell culture techniques is that no *a priori* assumptions about participation of various cell types are required and thus, factors/mediators of bone turnover can be analysed with their local regulatory mechanisms intact. Furthermore, there remains much to be learnt about the roles of various cell types in physiological and pathological bone turnover in the actual local bone microenvironment.

9.3 FUTURE RESEARCH DIRECTIONS

An innovative experimental approach, termed "molecular histomorphometry", has been described in this thesis, involving the analysis of the mRNA expression of a select group of skeletally active molecules, in combination with histomorphometric assessment of trabecular bone structure and bone turnover, in contiguous human bone tissues sampled from the OA and non-diseased/control proximal femur. A more complete gene profile, mapped to bone tissue morphology (i.e., molecular histomorphometry), in skeletal regions distal to the degenerative joint changes in patients with primary OA needs to be established. Specifically, a profile of gene expression mapped to bone tissue morphology in the iliac crest that is consistent with that in the proximal femur, such as at the intertrochanteric region, in the same OA individuals would be supportive of the hypothesis of a generalised skeletal involvement in OA. The use of the iliac crest for these studies is important for a number of reasons. Firstly, the iliac crest is a skeletal site accessible for bone biopsy and is the accepted bone biopsy site for histomorphometric assessment of skeletal change. Secondly, the iliac crest is not subject to loading abnormalities or joint pathological changes. Finally, the trabecular bone structure and bone matrix biochemistry of the iliac crest have been described in OA. If the profile of gene expression mapped to bone tissue morphology in the iliac crest of severe primary hip OA individuals is consistently different to that of non-OA control subjects, the potential use of this molecular histomorphometric approach to identify individuals at risk of developing OA, before development of symptoms, could be explored. Other skeletally active factors that would be of specific interest in these analyses, in addition to those described in this thesis, are detailed in Chapter 6.5.4.

In more general terms, the experimental approach of molecular histomorphometry described in this thesis can be applied to study pathogenetic mechanisms of other musculoskeletal diseases, such as osteoporosis (which is characterised by atrophied trabecular bone architecture). In addition, molecular histomorphometry has clear advantages over other methods to investigate genetic causes of musculoskeletal diseases. For example, linkage analysis cannot discern *levels of gene products* in tissues, which could arise by mutations in the promoter region of the gene and/or the effects of other gene products. The use of gene expression profiles mapped to tissue morphology have the potential to bridge the gap between cell culture studies and human pathophysiology, and may thus provide important new information in the rational design of treatments for a variety of musculoskeletal diseases.

BIBLIOGRAPHY

CITED REFERENCES

Abildgaard N., Glerup H., Rungby J., Bendix-Hansen K., Kassem M., Brixen K., Heickendorff L., Nielsen J.L., and Eriksen E.F. (2000) Biochemical markers of bone metabolism reflect osteoclastic and osteoblastic activity in multiple myeloma. *European Journal of Haematology* 64: 121-129.

Abrahamsen B., Shalhoub V., Larson E.K., Eriksen E.F., Beck-Nielsen H., and Marks Jr S.C. (2000) Cytokine RNA levels in transiliac bone biopsies from healthy early postmenopausal women. *Bone* 26: 137-145.

Adebanjo O.A., Moonga B.S., Yamate T., Sun L., Minkin C., Abe E., and Zaidi M. (1998) Mode of action of interleukin-6 on mature osteoclasts. Novel interactions with extracellular Ca^{2+} sensing in the regulation of osteoclastic bone resorption. *Journal of Cell Biology* 142: 1347-1356.

Aerssens J., Boonen S., Joly J., and Dequeker J. (1997) Variations in trabecular bone composition with anatomical site and age: potential implications for bone quality assessment. *Journal of Endocrinology* 155: 411-421.

Aerssens J., Dequeker J., Peeters J., Breemans S., and Boonen S. (1998) Lack of association between osteoarthritis of the hip and gene polymorphisms of VDR, COL1A1, and COL2A1 in postmenopausal women. *Arthritis and Rheumatism* 41: 1946-1950.

Ahlen J., Andersson S., Mukohyama H., Roth C., Backman A., Conaway H.H., and Lerner U.H. (2002) Characterization of the bone-resorptive effect of interleukin-11 in cultured mouse calvarial bones. *Bone* 31: 242-251.

Aigner T., Zien A., Gehrsitz A., Gebhard P.M., and McKenna L. (2001) Anabolic and catabolic gene expression pattern analysis in normal versus osteoarthritic cartilage using complementary DNA-array technology. *Arthritis and Rheumatism* 44: 2777-2789.

Amling M., Herden S., Posl M., Hahn M., Ritzel H., and Delling G. (1996) Heterogeneity of the skeleton: comparison of the trabecular microarchitecture of the spine, the iliac crest, the femur, and the calcaneus. *Journal of Bone and Mineral Research* 11: 36-45.

Ampe J., Dequeker J., and Gevers G. (1986) Regional variation of bone matrix components in osteoarthrotic and normal femoral heads. *Clinical Rheumatology* 5: 225-230.

Anderson D.M., Maraskovsky E., Billingsley W.L., Dougall W.C., Tometsko M.E., Roux E.R., Teepe M.C., DuBose R.F., Cosman D., and Galibert L. (1997) A Homologue of the TNF receptor and its ligand enhance T-cell growth and dendritic cell function. *Nature* 390: 175-179.

Anderson-MacKenzie J.M., Billingham M.E., and Bailey A.J. (1999) Collagen remodeling in the anterior cruciate ligament associated with developing spontaneous murine osteoarthritis. *Biochemical and Biophysical Research Communications* 258: 763-767.

Anderson-MacKenzie J.M., Quasnichka H.L., Starr R., Lewis E.J., Billingham M.E.J., and Bailey A.J. (2002) Fundamental bone remodelling in guinea pig osteoarthritis development. *Osteoarthritis and Cartilage* 10(Suppl A): S54-S55.

Arner E.C., Pratta M.A., Trzaskos J.M., Decicco C.P., and Tortorella M.D. (1999) Generation and characterization of aggrecanase. A soluble, cartilage-derived aggrecan-degrading activity. *Journal of Biological Chemistry* 274: 6594-6601.

Arrighi H., Khosla S., Melton L.J., Riggs B., Bekker P., and Dunstan C.R. (2000) The relationship between circulating osteoprotegerin and estrogen in postmenopausal women. *Journal of Bone and Mineral Research* 15(Suppl 1): M344.

Asou Y., Rittling S.R., Yoshitake H., Tsuji K., Shinomiya K., Nifuji A., Denhardt D.T., and Noda M. (2001) Osteopontin facilitates angiogenesis, accumulation of osteoclasts, and resorption in ectopic bone. *Endocrinology* 142: 1325-1332.

Atkins G.J., Haynes D.R., Graves S.E., Evdokiou A., Hay S., Bouralexis S., and Findlay D.M. (2000) Expression of osteoclast differentiation signals by stromal elements of giant cell tumors. *Journal of Bone and Mineral Research* 15: 640-649.

Azuma Y., Kaji K., Katogi R., Takeshita S., and Kudo A. (2000) Tumor necrosis factor-alpha induces differentiation of and bone resorption by osteoclasts. *Journal of Biological Chemistry* 275: 4858-4864.

Bahn S., Augood S.J., Ryan M., Standaert D.G., Starkey M., and Emson P.C. Gene expression profiling in the post-mortem human brain - no cause for dismay. (2001) *Journal of Chemical Neuroanatomy* 22: 79-94.

Bailey A.J. and Knott L. (1999) Molecular changes in bone collagen in osteoporosis and osteoarthritis in the elderly. *Experimental Gerontology* 34: 337-351.

Bailey A.J., Sims T.J., and Knott L. (2002) Phenotypic expression of osteoblast collagen in osteoarthritic bone: production of type I homotrimer. *International Journal of Biochemistry and Cell Biology* 34: 176-182.

Baylink D., Linkhart T., Farley J., Mohan S., Linkhart S., and Fitzsimmons R. (1990) The potential role(s) of bone-derived growth factors as determinants of local bone formation. In: Rosenfeld R. and Grumbach M. (editors.) Turner Syndrome. Marcel Dekker, New York.

Bekker P.J., Holloway D., Nakanishi A., Arrighi M., Leese P.T., and Dunstan C.R. (2001) The effect of a single dose of osteoprotegerin in postmenopausal women. *Journal of Bone and Mineral Research* 16: 348-360.

Bendele A.M. and Hulman J.F. (1988) Spontaneous cartilage degeneration in guinea pigs. *Arthritis and Rheumatism* 31: 561-565.

Bentolila V., Boyce T.M., Fyhrie D.P., Drumb R., Skerry T.M., and Schaffler M.B. (1998) Intracortical remodelling in adult rat long bones after fatigue loading. *Bone* 23: 275-281.

Beresford J.N., Bennett J.H., Devlin C., Leboy P.S., and Owen M.E. (1992) Evidence for an inverse relationship between the differentiation of adipocytic and osteogenic cells in rat marrow stromal cell cultures. *Journal of Cell Science* 102: 341-351.

Beuf O., Ghosh S., Newitt D.C., Link T.M., Steinbach L., Ries M., Lane N., and Majumdar S. (2002) Magnetic resonance imaging of normal and osteoarthritic trabecular bone structure in the human knee. *Arthritis and Rheumatism* 46: 385-393.

Billingham M.E.J. (1998) Advantages afforded by the use of animal models for evaluation of potential disease-modifying osteoarthritis drugs (DMOADs). In: Brandt K.D., Doherty M., and Lohmander L.S. (editors). Osteoarthritis. Oxford University Press, New York, pp. 429-438.

Billinghurst R.C., Dahlberg L., Ionescu M., Reiner A., Bourne R., Rorabeck C., Mitchell P., Hambor J., Diekmann O., Tschesche H., Chen J., Van Wart H., and Poole A.R. (1997) Enhanced cleavage of type II collagen by collagenases in osteoarthritic articular cartilage. *Journal of Clinical Investigation* 99: 1534-1545.

Bland J.H. and Cooper S.M. (1984) Osteoarthritis: a review of the cell biology involved and evidence for reversibility. Management rationally related to known genesis and pathophysiology. *Seminars in Arthritis and Rheumatism* 14: 106-133.

Boivin G.Y., Chavassieux P.M., Santora A.C., Yates J., and Meunier P.J. (2000) Alendronate increases bone strength by increasing the mean degree of mineralization of bone tissue in osteoporotic women. *Bone* 27: 687-694.

Boonen S., Aerssens J., Dequeker J., Nicholson P., Cheng X., Lowet G., Verbeke G., and Bouillon R. (1997) Age-associated decline in human femoral neck cortical and trabecular content of insulin-like growth factor I: potential implications for age-related (type II) osteoporotic fracture occurrence. *Calcified Tissue International* 61: 173-178.

Boskey A.L. (1996) Matrix proteins and mineralization: an overview. *Connective Tissue Research* 5: 357-363.

Boskey A.L., Gadaleta S., Gundberg C., Doty S.B., Ducy P., and Karsenty G. (1998) Fourier transform infrared microspectroscopic analysis of bones of osteocalcin-deficient mice provides insight into the function of osteocalcin. *Bone* 23: 187-196.

Brandstrom H., Jonsson K.B., Vidal O., Ljunghall S., Ohlsson C., and Ljunggren O. (1998) Tumor necrosis factor-alpha and -beta upregulate the levels of osteoprotegerin mRNA in human osteosarcoma MG-63 cells. *Biochemical and Biophysical Research Communications* 248: 454-457.

Bronckers A.L., Goei W., Luo G., Karsenty G., D'Souza R.N., Lyaruu D.M., and Burger E.H. (1996) DNA fragmentation during bone formation in neonatal rodents assessed by transferase-mediated end labeling. *Journal of Bone and Mineral Research* 11: 1281-1291.

Brown S.J., Pollintine P., Powell D.E., Davie M.W., and Sharp C.A. (2002) Regional differences in mechanical and material properties of femoral head cancellous bone in health and osteoarthritis. *Calcified Tissue International* 71: 227-234.

Bruno R.J., Sauer P.A., Rosenberg A.G., Block J., and Sumner D.R. (1999) The pattern of bone mineral density in the proximal femur and radiographic signs of early joint degeneration. *Journal of Rheumatology* 26: 636-640.

Bucay N., Sarosi I., Dunstan C.R., Morony S., Tarpley J., Capparelli C., Scully S., Tan H.L., Xu W., Lacey D.L., Boyle W.J., and Simonet W.S. (1998) Osteoprotegerin-deficient mice develop early onset osteoporosis and arterial calcification. *Genes & Development* 12: 1260-1268.

Buckwalter J.A., Stanish W.D., Rosier R.N., Schenck R.C. Jr, Dennis D.A., and Coutts R.D. (2001) The increasing need for nonoperative treatment of patients with osteoarthritis. *Clinical Orthopaedics and Related Research* 385: 36-45.

Burger E.H. and Klein-Nulend J. (1999) Mechanotransduction in bone-role of the lacuno-canalicular network. *FASEB Journal* 13 Suppl: S101-S112

Burke W.J., O'Malley K.L., Chung H.D., Harmon S.K., Miller J.P., and Berg L. Effect of pre- and postmortem variables on specific mRNA levels in human brain. (1991) *Molecular Brain Research* 11: 37-41.

Burkhardt R., Kettner G., Bohm W., Schmidmeier M., Schlag R., Frisch B., Mallmann B., Eisenmenger W., and Gilg T. (1987) Changes in trabecular bone, hematopoiesis and bone marrow vessels in aplastic anemia, primary osteoporosis, and old age: a comparative histomorphometric study. *Bone* 8: 157-164.

Burr D.B. and Stafford T. (1990) Validity of the bulk-staining technique to separate artifactual from *in vivo* bone microdamage. *Clinical Orthopaedics and Related Research* 260: 305-308.

Burr D.B. and Hooser M. (1995) Alterations to the en bloc basic fuchsin staining protocol for the demonstration of microdamage produced *in vivo*. *Bone* 17: 431-433.

Burr D.B., Forwood M.R., Fyhrie D.P., Martin R.B., Schaffler M.B., and Turner C.H. (1997) Bone microdamage and skeletal fragility in osteoporotic and stress fractures. *Journal of Bone and Mineral Research* 12: 6-15.

Burr D.B., Turner C.H., Naick P., Forwood M.R., Ambrosius W., Hasan M.S., and Pidaparti R. (1998) Does microdamage accumulation affect the mechanical properties of bone? *Journal of Biomechanics* 31: 337-345.

Burr D.B. (2002) Targeted and nontargeted remodeling. *Bone* 30: 2-4.

Calvo M.S., Eyre D.R., and Gundberg C.M. (1996) Molecular basis and clinical application of biological markers of bone turnover. *Endocrine Reviews* 17: 333-368.

Carlson C.S., Loeser R.F., Jayo M.J., Weaver D.S., Adams M.R., and Jerome C.P. (1994) Osteoarthritis in cynomolgus macaques: a primate model of naturally occurring disease. *Journal of Orthopaedic Research* 12: 331-339.

Carlson C.S., Loeser R.F., Johnstone B., Tulli H.M., Dobson D.B., and Caterson B. (1995) Osteoarthritis in cynomolgus macaques. II. Detection of modulated proteoglycan epitopes in cartilage and synovial fluid. *Journal of Orthopaedic Research* 13: 399-409.

Carlson C.S., Loeser R.F., Purser C.B., Gardin J.F., and Jerome C.P. (1996) Osteoarthritis in cynomolgus macaques. III: Effects of age, gender, and subchondral bone thickness on the severity of disease. *Journal of Bone and Mineral Research* 11: 1209-1217.

Carney S.L. and Muir H. (1988) The structure and function of cartilage proteoglycans. *Physiological Reviews* 68: 858-910.

Carter D.R. and Hayes W.C. (1977) The compressive behaviour of bone as a two-phase porous structure. *Journal of Bone and Joint Surgery* 59-A: 954-962.

Carter D.R., Caler W.E., Spengler D.M., and Frankel V.H. (1981) Fatigue behaviour of adult cortical bone: the influence of mean strain and strain range. *Acta Orthopaedica Scandinavica* 52: 481-490.

Carter D.R., Orr T.E., and Fyhrie D.P. (1989) Relationships between loading history and femoral cancellous bone architecture. *Journal of Biomechanics* 22: 231-244.

Cawston T., Billington C., Cleaver C., Elliott S., Hui W., Koshy P., Shingleton B., and Rowan A. (1999) The regulation of MMPs and TIMPs in cartilage turnover. *Annals of the New York Academy of Sciences* 878: 120-129.

Centrella M., Horowitz M.C., Wozney J.M., and McCarthy T.L. (1994) Transforming growth factor-beta gene family members and bone. *Endocrine Reviews* 15: 27-39.

Chambers T.J., Darby J.A., and Fuller K. (1985) Mammalian collagenase predisposes bone surfaces to osteoclastic resorption. *Cell and Tissue Research* 241: 671-675.

Chenu C., Colucci S., Grano M., Zigrino P., Barattolo R., Zambonin G., Baldini N., Vergnaud P., Delmas P.D., and Zallone A.Z. (1994) Osteocalcin induces chemotaxis, secretion of matrix proteins, and calcium-mediated intracellular signaling in human osteoclast-like cells. *Journal of Cell Biology* 127: 1149-1158.

Chitnavis J., Sinsheimer J.S., Clipsham K., Loughlin J., Sykes B., Burge P.D., and Carr A.J. (1997) Genetic influences in end-stage osteoarthritis. Sibling risks of hip and knee replacement for idiopathic osteoarthritis. *Journal of Bone and Joint Surgery* 79: 660-664.

Chomczynski P. and Sacchi N. (1987) Single-step method of RNA isolation by acid guanidinium thiocyanate-phenol-chloroform extraction. *Analytical Biochemistry* 162: 156-159.

Coen G., Ballanti P., Balducci A., Calabria S., Fischer M.S., Jankovic L., Manni M., Morosetti M., Moscaritolo E., Sardella D., and Bonucci E. (2002) Serum osteoprotegerin and renal osteodystrophy. *Nephrology, Dialysis, Transplantation* 17: 233-238.

Collin-Osdoby P., Rothe L., Anderson F., Nelson M., Maloney W., and Osdoby P. (2001) Receptor activator of NF-kappa B and osteoprotegerin expression by human microvascular endothelial cells, regulation by inflammatory cytokines, and role in human osteoclastogenesis. *Journal of Biological Chemistry* 276: 20659-20672.

Collins D. (1949) The Pathology of Articular and Spinal Diseases. Edward Arnold and Co., London, pp. 74-115.

Collins C., Evans R.G., Ponsford F., Miller P., and Elson C.J. (1994) Chondro-osseous metaplasia, bone density and patellar cartilage proteoglycan content in the osteoarthritis of STR/ORT mice. *Osteoarthritis and Cartilage* 2: 111-118.

Cooper C., Cook P.L., Osmond C., Fisher L., and Cawley M.I. (1991) Osteoarthritis of the hip and osteoporosis of the proximal femur. *Annals of the Rheumatic Diseases* 50: 540-542.

Crandall C. (2002) Parathyroid hormone for treatment of osteoporosis. *Archives of Internal Medicine* 162: 2297-2309.

Crane G.J., Fazzalari N.L., Parkinson I.H., and Vernon-Roberts B. (1990) Age-related changes in femoral trabecular bone in arthrosis. *Acta Orthopaedica Scandinavica* 61: 421-426.

Croucher P.I., Garrahan N.J., Mellish R.W., and Compston J.E. (1991) Age-related changes in resorption cavity characteristics in human trabecular bone. *Osteoporosis International* 1: 257-261.

Davey R.A., Hahn C.N., May B.K., and Morris H.A. (2000) Osteoblast gene expression in rat long bones: effects of ovariectomy and dihydrotestosterone on mRNA levels. *Calcified Tissue International* 67: 75-79.

DeFranco D.J., Glowacki J., Cox K.A., and Lian J.B. (1991) Normal bone particles are preferentially resorbed in the presence of osteocalcin-deficient bone particles *in vivo*. *Calcified Tissue International* 49: 43-50.

Demissie S., Cupples L.A., Myers R., Aliabadi P., Levy D., and Felson D.T. (2002) Genome scan for quantity of hand osteoarthritis: the Framingham Study. *Arthritis and Rheumatism* 46: 946-952.

Dempster D.W., Cosman F., Parisien M., Shen V., and Lindsay R. (1993) Anabolic actions of parathyroid hormone on bone. *Endocrine Reviews* 14: 690-709.

Denhardt D.T. and Noda M. (1998) Osteopontin expression and function: role in bone remodeling. *Journal of Cellular Biochemistry Supplement* 30-31: 92-102.

Dequeker J., Johnell O., and The MEDOS Study Group. (1993a) Osteoarthritis protects against femoral neck fracture: the MEDOS study experience. *Bone* 14(Suppl 1): S51-S56.

Dequeker J., Mohan S., Finkelman R.D., Aerssens J., and Baylink D.J. (1993b) Generalized osteoarthritis associated with increased insulin-like growth factor types I and II and transforming growth factor beta in cortical bone from the iliac crest. Possible mechanism of increased bone density and protection against osteoporosis. *Arthritis and Rheumatism* 36: 1702-1708.

Dequeker J., Boonen S., Aerssens J., and Westhovens R. (1996) Inverse relationship osteoarthritis - osteoporosis: What is the evidence? What are the consequences? *British Journal of Rheumatism* 35: 813-820.

Deyama Y., Takeyama S., Koshikawa M., Shirai Y., Yoshimura Y., Nishikata M., Suzuki K., and Matsumoto A. (2000) Osteoblast maturation suppressed osteoclastogenesis in coculture with bone marrow cells. *Biochemical and Biophysical Research Communications* 274: 249-254.

D'Ippolito G., Schiller P.C., Ricordi C., Roos B.A., and Howard G.A. (1999) Age-related osteogenic potential of mesenchymal stromal stem cells from human vertebral bone marrow. *Journal of Bone and Mineral Research* 14: 1115-1122.

Disler D.G., McCauley T.R., Kelman C.G., Fuchs M.D., Ratner L.M., Wirth C.R., and Hospodar P.P. (1996) Fat-suppressed three-dimensional spoiled gradient-echo MR imaging of hyaline cartilage defects in the knee: comparison with standard MR imaging and arthroscopy. *AJR American Journal of Roentgenology* 167: 127-132.

Dodds R.A., Connor J.R., James I.E., Rykaczewski E.L., Appelbaum E., Dul E., and Gowen M. (1995) Human osteoclasts, not osteoblasts, deposit osteopontin onto resorption surfaces: an *in vitro* and ex vivo study of remodeling bone. *Journal of Bone and Mineral Research* 10: 1666-1680.

Dougados M., Gueguen A., Nguyen M., Thiesce A., Listrat V., Jacob L., Nakache J.P., Gabriel K.R., Lequesne M., and Amor B. (1992) Longitudinal radiologic evaluation of osteoarthritis of the knee. *Journal of Rheumatology* 19: 378-384.

Dougall W.C., Glaccum M., Charrier K., Rohrbach K., Brasel K., De Smedt T., Daro E., Smith J., Tometsko M.E., Maliszewski C.R., Armstrong A., Shen V., Bain S., Cosman D., Anderson D., Morrissey P.J., Peschon J.J., and Schuh J. (1999) RANK is essential for osteoclast and lymph node development. *Genes & Development* 13: 2412-2424.

Drury R.A.B. and Wallington E.A. (1980) Bone and decalcification. In: Carleton's Histological Techniques. (5th edition) Oxford University, Oxford, pp. 217.

Ducy P., Desbois C., Boyce B., Pinero G., Story B., Dunstan C., Smith E., Bonadio J., Goldstein S., Gundberg C., Bradley A., and Karsenty G. (1996) Increased bone formation in osteocalcin-deficient mice. *Nature* 382: 448-452.

Ducy P., Zhang R., Geoffroy V., Ridall A.L., and Karsenty G. (1997) Osf2/Cbfa1: a transcriptional activator of osteoblast differentiation. *Cell* 89: 747-754.

Ducy P., Schinke T., and Karsenty G. (2000) The osteoblast: a sophisticated fibroblast under central surveillance. *Science* 289: 1501-1504.

Eckstein F., Adam C., Sittek H., Becker C., Milz S., Schulte E., Reiser M., and Putz R. (1997) Non-invasive determination of cartilage thickness throughout joint surfaces using magnetic resonance imaging. *Journal of Biomechanics* 30: 285-289.

Eikmans M., Baelde H.J., de Heer E., and Bruijn J.A. (2001) Effect of age and biopsy site on extracellular matrix mRNA and protein levels in human kidney biopsies. *Kidney International* 60: 974-981.

Eriksen E.F. (1986) Normal and pathological remodeling of human trabecular bone: three dimensional reconstruction of the remodeling sequence in normals and in metabolic bone disease. *Endocrine Reviews* 7: 379-408.

Eventov I., Frisch B., Cohen Z., and Hammel I. (1991) Osteopenia, hematopoiesis, and bone remodelling in iliac crest and femoral biopsies: a prospective study of 102 cases of femoral neck fractures. *Bone* 12: 1-6.

Everts V., Delaisse J.M., Korper W., Jansen D.C., Tigchelaar-Gutter W., Saftig P., and Beertsen W. (2002). The bone lining cell: its role in cleaning Howship's lacunae and initiating bone formation. *Journal of Bone and Mineral Research* 17: 77-90.

Fazzalari N.L., Darracott J., and Vernon-Roberts B. (1985) Histomorphometric changes in the trabecular structure of a selected stress region in the femur in patients with osteoarthritis and fracture of the femoral neck. *Bone* 6: 125-133.

Fazzalari N.L., Moore R.J., Manthey B.A., and Vernon-Roberts B. (1989) Comparative study of iliac crest and proximal femur histomorphometry in normal patients. *Journal of Clinical Pathology* 42: 745-748.

Fazzalari N.L., Moore R.J., Manthey B.A., and Vernon-Roberts B. (1992) Comparative study of iliac crest and subchondral femoral bone in osteoarthritic patients. *Bone* 13: 331-315.

Fazzalari N.L. (1993) Trabecular microfracture. *Calcified Tissue International* 53(Suppl 1): S143-S146.

Fazzalari N.L. and Parkinson I.H. (1998) Femoral trabecular bone of osteoarthritic and normal subjects in an age and sex matched group. *Osteoarthritis and Cartilage* 6: 377-382.

Fazzalari N.L., Forwood M.R., Manthey B.A., Smith K., and Kolesik P. (1998a) Three-dimensional confocal images of microdamage in cancellous bone. *Bone* 23: 373-378.

Fazzalari N.L., Forwood M.R., Smith K., Manthey B.A., and Herreen P. (1998b) Assessment of cancellous bone quality in severe osteoarthrosis: bone mineral density, mechanics, and microdamage. *Bone* 22: 381-388.

Felson D.T., Hannan M.T., Naimark A., Berkeley J., Gordon G., Wilson P.W., and Anderson J. (1991) Occupational physical demands, knee bending, and knee osteoarthritis: results from the Framingham Study. *Journal of Rheumatology* 18: 1587-1592.

Felson D.T., Zhang Y., Hannan M.T., Naimark A., Weissman B., Aliabadi P., and Levy D. (1997) Risk factors for incident radiographic knee osteoarthritis in the elderly: the Framingham Study. *Arthritis and Rheumatism* 40: 728-733.

Felson D.T. (1998) Epidemiology of osteoarthritis. In: Brandt K.D., Doherty M., and Lohmander L.S. (editors). Osteoarthritis. Oxford University Press, New York, pp. 13-22.

Felson D.T. and Zhang Y. (1998) An update on the epidemiology of knee and hip osteoarthritis with a view to prevention. *Arthritis and Rheumatism* 41: 1343-1355.

Felson D.T., Couropmitree N.N., Chaisson C.E., Hannan M.T., Zhang Y., McAlindon T.E., LaValley M., Levy D., and Myers R.H. (1998) Evidence for a Mendelian gene in a segregation analysis of generalized radiographic osteoarthritis: the Framingham Study. *Arthritis and Rheumatism* 41: 1064-1071.

Fishman D., Faulds G., Jeffery R., Mohamed-Ali V., Yudkin J.S., Humphries S., and Woo P. (1998) The effect of novel polymorphisms in the interleukin-6 (IL-6) gene on IL-6 transcription and plasma IL-6 levels, and an association with systemic-onset juvenile chronic arthritis. *Journal of Clinical Investigation* 102: 1369-1376.

Flores R.H. and Hochberg M.C. (1998) Definition and classification of osteoarthritis. In: Brandt K.D., Doherty M., and Lohmander L.S. (editors). Osteoarthritis. Oxford University Press, New York, pp. 1-12.

Forwood M.R. and Parker A.W. (1989) Microdamage in response to repetitive torsional loading in the rat tibia. *Calcified Tissue International* 45: 47-53.

Forwood M.R. and Turner C.H. (1995) Skeletal adaptations to mechanical usage: results from tibial loading studies in rats. *Bone* 17: S197-S205.

Forwood M.R., Burr D.B., Takano Y., Eastman D.F., Smith P.N., and Schwardt J.D. (1995) Risedronate treatment does not increase microdamage in the canine femoral neck. *Bone* 16: 643-650.

Frenkel B., Capparelli C., Van Auken M., Baran D., Bryan J., Stein J.L., Stein G.S., and Lian J.B. (1997) Activity of the osteocalcin promoter in skeletal sites of transgenic mice and during osteoblast differentiation in bone marrow-derived stromal cell cultures: effects of age and sex. *Endocrinology* 138: 2109-2116.

Frost H.M. (1969) Tetracycline-based histological analysis of bone remodeling. *Calcified Tissue Research* 3: 211-237.

Frost H.M. (2000) The utah paradigm of skeletal physiology: an overview of its insights for bone, cartilage and collagenous tissue organs. *Journal of Bone and Mineral Metabolism* 18: 305-316.

Fyhrie D.P. and Schaffler M.B. (1994) Failure mechanisms in human vertebral cancellous bone. *Bone* 15: 105-109.

Gelber A.C., Hochberg M.C., Mead L.A., Wang N.Y., Wigley F.M., and Klag M.J. (2000) Joint injury in young adults and risk for subsequent knee and hip osteoarthritis. *Annals of Internal Medicine* 133: 321-328.

Gevers G. and Dequeker J. (1987) Collagen and non-collagenous protein content (osteocalcin, sialoprotein, proteoglycan) in the iliac crest bone and serum osteocalcin in women with and without hand osteoarthritis. *Collagen and Related Research* 7: 435-442.

Gevers G., Dequeker J., Geusens P., Nyssen-Behets C., and Dhem A. (1989a) Physical and histomorphological characteristics of iliac crest bone differ according to the grade of osteoarthritis at the hand. *Bone* 10: 173-177.

Gevers G., Dequeker J., Martens M., Van Audekercke R., Nyssen-Behets C., and Dhem A. (1989b) Biomechanical characteristics of iliac crest bone in elderly women according to osteoarthritis grade at the hand joints. *Journal of Rheumatology* 16: 660-663.

Girasole G., Jilka R., Passeri G., Boswell S., Boder G., Williams D., and Manolagas S. (1992) 17b-Estradiol inhibits interleukin-6 production by bone marrow-derived stromal cells and osteoblasts *in vitro*: a potential mechanism for the antiosteoporotic effect of estrogens. *Journal of Clinical Investigation* 89: 883-891.

Girasole G., Passeri G., Jilka R., and Manolagas S. (1994) Interleukin-11: a new cytokine critical for osteoclast development. *Journal of Clinical Investigation* 93: 1516-1524.

Glowacki J., Cox K.A., and Wilcon S. (1989) Impaired osteoclast differentiation in subcutaneous implants of bone particles in osteopetrotic mutants. *Journal of Bone and Mineral Metabolism* 5: 271-278.

Glowacki J., Rey C., Glimcher M.J., Cox K.A., and Lian J. (1991) A role for osteocalcin in osteoclast differentiation. *Journal of Cellular Biochemistry* 45: 292-302.

Goker B., Sumner D.R., Hurwitz D.E., and Block J.A. (2000) Bone mineral density varies as a function of the rate of joint space narrowing in the hip. *Journal of Rheumatology* 27: 735-738.

Gori F., Hofbauer L.C., Dunstan C.R., Spelsberg T.C., Khosla S., and Riggs B.L. (2000) The expression of osteoprotegerin and RANK ligand and the support of osteoclast formation by stromal-osteoblast lineage cells is developmentally regulated. *Endocrinology* 141: 4768-4776.

Gotfredsen A., Riis B.J., Christiansen C., and Rodbro P. (1990) Does a single local absorptiometric bone measurement indicate the overall skeletal status? Implications for osteoporosis and osteoarthritis of the hip. *Clinical Rheumatology* 9: 193-203.

Grey A., Mitnick M.A., Shapses S., Ellison A., Gundberg C., and Insogna K. (1996) Circulating levels of interleukin-6 and tumor necrosis factor-alpha are elevated in primary hyperparathyroidism and correlate with markers of bone resorption-a clinical research center study. *Journal of Clinical Endocrinology and Metabolism* 81: 3450-3454.

Gronthos S., Zannettino A., Graves S., Ohta S., Hay S., and Simmons P. (1999) Differential cell surface expression of the STRO-1 and alkaline phosphatase antigens on discrete developmental stages in primary cultures of human bone cells. *Journal of Bone and Mineral Research* 14: 47-56.

Grubbs F.E. (1948) On estimating precision of measuring instruments and product variability. *J Am Statist Ass* 43: 243-264.

Grynpas M.D., Alpert B., Katz I., Lieberman I., and Pritzker K.P. (1991) Subchondral bone in osteoarthritis. *Calcified Tissue International* 49: 20-26.

Hadler N.M., Gillings D.B., Imbus H.R., Levitin P.M., Makuc D., Utsinger P.D., Yount W.J., Slusser D., and Moskovitz N. (1978) Hand structure and function in an industrial setting. *Arthritis and Rheumatism* 21: 210-220.

Harris S.E., Bonewald L.F., Harris M.A., Sabatini M., Dallas S., Feng J.Q., Ghosh-Choudhury N., Wozney J., and Mundy G.R. (1994) Effects of transforming growth factor beta on bone nodule formation and expression of bone morphogenetic protein 2, osteocalcin, osteopontin, alkaline phosphatase, and type I collagen mRNA in long-term cultures of fetal rat calvarial osteoblasts. *Journal of Bone and Mineral Research* 9: 855-863.

Harris S.E., Sabatini M., Harris M.A., Feng J.Q., Wozney J., and Mundy G.R. (1994) Expression of bone morphogenetic protein messenger RNA in prolonged cultures of fetal rat calvarial cells. *Journal of Bone and Mineral Research* 9: 389-394.

Harrison M.H., Schajowicz F., and Trueta J. (1953) Osteoarthritis of the hip: a study of the nature and evolution of the disease. *Journal of Bone and Joint Surgery* 35B: 598-626.

Harrison P.J., Heath P.R., Eastwood S.L., Burnet P.W.J., McDonald B., and Pearson R.C.A. (1995) The relative importance of premortem acidosis and postmortem interval for human brain gene expression studies: selective mRNA vulnerability and comparison with their encoded proteins. *Neuroscience Letters* 200: 151-154.

Hart D.J., Doyle D.V., and Spector T.D. (1999) Incidence and risk factors for radiographic knee osteoarthritis in middle-aged women: the Chingford Study. *Arthritis and Rheumatism* 42: 17-24.

Hart D.J., Cronin C., Daniels M., Worthy T., Doyle D.V., and Spector T.D. (2002) The relationship of bone density and fracture to incident and progressive radiographic osteoarthritis of the knee: the Chingford Study. *Arthritis and Rheumatism* 46: 92-99.

Hattersley G. and Chambers T.J. (1989) Calcitonin receptors as markers for osteoclastic differentiation: correlation between generation of bone-resorptive cells and cells that express calcitonin receptors in mouse bone marrow cultures. *Endocrinology* 125: 1606-1612.

Hayden J.M., Mohan S., and Baylink D.J. (1995) The insulin-like growth factor system and the coupling of formation to resorption. *Bone* 17(Suppl 2): S93-S98.

Helliwell T.R., Kelly S.A., Walsh H.P., Klenerman L., Haines J., Clark R., and Roberts N.B. (1996) Elemental analysis of femoral bone from patients with fractured neck of femur or osteoarthrosis. *Bone* 18: 151-157.

Henssge C. (1995) Temperature-based methods II. In: Henssge C., Knight B., Krompecher T., Madea B., and Nokes L. The Estimation of the Time Since Death in the Early Postmortem Period. Edward Arnold, London, pp. 46-105.

Hilal G., Martel-Pelletier J., Pelletier J.P., Ranger P., and Lajeunesse D. (1998) Osteoblast-like cells from human subchondral osteoarthritic bone demonstrate an altered phenotype *in vitro*: possible role in subchondral bone sclerosis. *Arthritis and Rheumatism* 41: 891-899.

Hilal G., Massicotte F., Martel-Pelletier J., Fernandes J.C., Pelletier J.P., and Lajeunesse D. (2001) Endogenous prostaglandin E_2 and insulin-like growth factor 1 can modulate the levels of parathyroid hormone receptor in human osteoarthritic osteoblasts. *Journal of Bone and Mineral Research* 16: 713-721.

Hildebrand T., Laib A., Muller R., Dequeker J., and Ruegsegger P. (1999) Direct three-dimensional morphometric analysis of human cancellous bone: microstructural data from spine, femur, iliac crest, and calcaneus. *Journal of Bone and Mineral Research* 14: 1167-1174.

Hirsch R., Lethbridge-Cejku M., Hanson R., Scott W.W. Jr, Reichle R., Plato C.C., Tobin J.D., and Hochberg M.C. (1998) Familial aggregation of osteoarthritis: data from the Baltimore Longitudinal Study on Aging. *Arthritis and Rheumatism* 41: 1227-1232.

Hofbauer L.C., Dunstan C.R., Spelsberg T.C., Riggs B.L., and Khosla S. (1998) Osteoprotegerin production by human osteoblast lineage cells is stimulated by vitamin D, bone morphogenetic protein-2, and cytokines. *Biochemical and Biophysical Research Communications* 250: 776-781.

Hofbauer L.C., Gori F., Riggs B.L., Lacey D.L., Dunstan C.R., Spelsberg T.C., and Khosla S. (1999a) Stimulation of osteoprotegerin ligand and inhibition of osteoprotegerin production by glucocorticoids in human osteoblastic lineage cells: potential paracrine mechanisms of glucocorticoid-induced osteoporosis. *Endocrinology* 140: 4382-4389.

Hofbauer L.C., Lacey D.L., Dunstan C.R., Spelsberg T.C., Riggs B.L., and Khosla S. (1999b) Interleukin-1beta and tumor necrosis factor-alpha, but not interleukin-6, stimulate osteoprotegerin ligand gene expression in human osteoblastic cells. *Bone* 25: 255-259.

Hofbauer L.C., Khosla S., Dunstan C.R., Lacey D.L., Boyle W.J., and Riggs B.L. (2000) The roles of osteoprotegerin and osteoprotegerin ligand in the paracrine regulation of bone resorption. *Journal of Bone and Mineral Research* 15: 2-12.

Hofbauer L.C. and Heufelder A.E. (2001) Role of receptor activator of nuclear factor-κB ligand and osteoprotegerin in bone cell biology *Journal of Molecular Medicine* 79: 243-253.

Hofbauer L.C., Shui C., Riggs B.L., Dunstan C.R., Spelsberg T.C., O'Brien T., and Khosla S. (2001) Effects of immunosuppressants on receptor activator of NF-kappaB ligand and osteoprotegerin production by human osteoblastic and coronary artery smooth muscle cells. *Biochemical and Biophysical Research Communications* 280: 334-339.

Hogquist K.A., Nett M.A., Unanue E.R., and Chaplin D.D. (1991) Interleukin 1 is processed and released during apoptosis. *Proceedings of the National Academy of Sciences of the USA* 88: 8485-8489.

Horowitz M.C., Xi Y., Wilson K., and Kacena M.A. (2001) Control of osteoclastogenesis and bone resorption by members of the TNF family of receptors and ligands. *Cytokine & Growth Factor Reviews* 12: 9-18.

Horwood N.J., Elliot J., Martin T.J., and Gillespie M.T. (1998) Osteotropic agents regulate the expression of osteoclast differentiation factor and osteoprotegerin in osteoblastic stromal cells. *Endocrinology* 139: 4743-4746.

Hruska K.A. and Teitelbaum S.L. (1995) Renal osteodystrophy. *The New England Journal of Medicine* 333: 166-174.

Hsu H., Lacey D.L., Dunstan C.R., Solovyev I., Colombero A., Timms E., Tan H.L., Elliott G., Kelley M.J., Sarosi I., Wang L., Xia X.Z., Elliott R., Chiu L., Black T., Scully S., Capparelli C., Morony S., Shimamoto G., Bass M.B., and Boyle W.J. (1999) Tumor necrosis factor receptor member RANK mediates osteoclast differentiation and activation induced by osteoprotegerin ligand. *Proceedings of the National Academy of Sciences of the USA* 96: 3540-3545.

Huebner J.L., Hanes M.A., Beekman B., TeKoppele J.M., and Kraus V.B. (2002) A comparative analysis of bone and cartilage metabolism in two strains of guinea-pig with varying degrees of naturally occurring osteoarthritis. *Osteoarthritis and Cartilage* 10: 758-67.

Hughes D.E., Dai A., Tiffee J.C., Li H.H., Mundy G.R., and Boyce B.F. (1996) Estrogen promotes apoptosis of murine osteoclasts mediated by TGF-beta. *Nature Medicine* 2: 1132-1136.

Hughes F.J. and Howells G.L. (1993a) Interleukin-6 inhibits bone formation *in vitro*. *Journal of Bone and Mineral Metabolism* 21: 21-28.

Hughes F. and Howells G. (1993b) Interleukin-11 inhibits bone formation *in vitro*. *Calcified Tissue International* 53: 362-364.

Huiskes R., Ruimerman R., Harry van Lenthe G., and Janssen J.D. (2000) Effects of mechanical forces on maintenance and adaptation of form in trabecular bone. *Nature* 405: 704-706.

Humphreys-Beyer M.G., King F.K., Bunnel B., and Brody B. (1986) Isolation of biologically active RNA from human autopsy for the study of cystic fibrosis. *Biotechnology and Applied Biochemistry* 8: 392-403.

Ikeda T., Nagai Y., Yamaguchi A., Yokose S., and Yoshiki S. (1995) Age-related reduction in bone matrix protein mRNA expression in rat bone tissues: application of histomorphometry to in situ hybridization. *Bone* 16: 17-23.

Ikeda T., Utsuyama M., and Hirokawa K. (2001) Expression profiles of receptor activator of nuclear factor kappaB ligand, receptor activator of nuclear factor kappaB, and osteoprotegerin messenger RNA in aged and ovariectomized rat bones. *Journal of Bone and Mineral Research* 16: 1416-1425.

Ingram R.T., Park Y.K., Clarke B.L., and Fitzpatrick L.A. (1994) Age- and gender-related changes in the distribution of osteocalcin in the extracellular matrix of normal male and female bone. Possible involvement of osteocalcin in bone remodeling. *Journal of Clinical Investigation* 93: 989-997.

Ingvarsson T. (2000) Prevalence and inheritance of hip osteoarthritis in Iceland. *Acta Orthopaedica Scandinavica* 298(Suppl): 1-46

Ishida K., Zhu B., and Maeda H. (2000) Novel approach to quantitative reverse transcription PCR assay of mRNA component in autopsy material using the TaqMan fluorogenic detection system: dynamics of pulmonary surfactant apoprotein A. *Forensic Science International* 113: 127-131.

Ishimi Y., Miyaura C., Jin C.H., Akatsu T., Abe E., Nakamura Y., Yamaguchi A., Yoshiki S., Matsuda T., Hirano T., Kishimoto T., and Suda T. (1990) IL-6 is produced by osteoblasts and induces bone resorption. *Journal of Immunology* 145: 3297-3303.

Jeffery A.K. (1973) Osteogenesis in the osteoarthritic femoral head. A study using radioactive ^{32}P and tetracycline bone markers. *Journal of Bone and Joint Surgery British Volume* 55: 262-272.

Jilka R., Hangoc G., Girasole G., Passeri G., Williams D., Abrams J., Boyce B., Broxmeyer H., and Manolagas S. (1992) Increased osteoclast development after estrogen loss: mediation by interleukin-6. *Science* 257: 88-91.

Jilka R.L. (1998) Cytokines, bone remodeling, and estrogen deficiency: a 1998 update. *Bone* 23: 75-81.

Jimi E., Nakamura I., Duong L.T., Ikebe T., Takahashi N., Rodan G.A., and Suda T. (1999) Interleukin 1 induces multinucleation and bone-resorbing activity of osteoclasts in the absence of osteoblasts/stromal cells. *Experimental Cell Research* 247: 84-93.

Karsenty G. (1999) The genetic transformation of bone biology. *Genes & Development* 13: 3037-3051.

Kasperk C., Wergedal J., Strong D., Farley J., Wangerin K., Gropp H., Ziegler R., and Baylink D.J. (1995) Human bone cell phenotypes differ depending on their skeletal site of origin. *Journal of Clinical Endocrinology and Metabolism* 80: 2511-2517.

Kawashima I., Ohsumi J., Mita-Honjo K., Shimoda-Takano K., Ishikawa H., Sakakibara S., Miyadai K., and Takiguchi Y. (1991) Molecular cloning of cDNA encoding adipogenesis inhibitory factor and identity with interleukin-11. *FEBS Letters* 283: 199-202.

Keen R.W., Hart D.J., Lanchbury J.S., and Spector T.D. (1997) Association of early osteoarthritis of the knee with a Taq I polymorphism of the vitamin D receptor gene. *Arthritis and Rheumatism* 40: 1444-1449.

Kellgren J.H. and Moore R. (1952) Generalized osteoarthritis and Heberden's nodes. *British Medical Journal* 1: 181-187.

Kellgren J.H. and Lawrence J.S. (1963) Atlas of Standard Radiographs: the Epidemiology of Chronic Rheumatism. Vol. 2. Blackwell Scientific Publications, Oxford.

Khosla S., Atkinson E.J., Melton L.J. 3rd, and Riggs B.L. (1997) Effects of age and estrogen status on serum parathyroid hormone levels and biochemical markers of bone turnover in women: a population-based study. *Journal of Clinical Endocrinology and Metabolism* 82: 1522-1527.

Kielty C.M., Hopkinson I., and Grant M.E. (1994) The collagen family: structure, assembly and organization in the extracellular matrix. In: Royce P.M. and Steinmann B. (editors) Connective Tissue and its Heritable Disorders. Wiley-Liss, New York, pp. 103-147.

Kim G., Kim C., Choi C., Park J., and Lee K. (1997) Involvement of different second messengers in parathyroid hormone- and interleukin-1-induced interleukin-6 and interleukin-11 production in human bone marrow stromal cells. *Journal of Bone and Mineral Research* 12: 896-902.

Kishimoto T. (1989) The biology of interleukin-6. *Blood* 74: 1-10.

Kishimoto T., Akira S., Narazaki M., and Taga T. (1995) Interleukin-6 family of cytokines and gp130. *Blood* 86: 1243-1254.

Kleiner D.E., Emmert-Buck M.R., and Liotta L.A. (1995) Necropsy as a research method in the age of molecular pathology. *The Lancet* 346: 945-948.

Klein-Nulend J., Semeins C.M., Ajubi N.E., Nijweide P.J., and Burger E.H. (1995) Pulsating fluid flow increases nitric oxide (NO) synthesis by osteocytes but not periosteal fibroblasts-correlation with prostaglandin upregulation. *Biochemical and Biophysical Research Communications* 217: 640-648.

Klein-Nulend J., Burger E.H., Semeins C.M., Raisz L.G., and Pilbeam C.C. (1997) Pulsating fluid flow stimulates prostaglandin release and inducible prostaglandin G/H synthase mRNA expression in primary mouse bone cells. *Journal of Bone and Mineral Research* 12: 45-51.

Kodama Y., Takeuchi Y., Suzawa M., Fukumoto S., Murayama H., Yamato H., Fujita T., Kurokawa T., and Matsumoto T. (1998) Reduced expression of interleukin-11 in bone marrow stromal cells of senescence-accelerated mice (SAMP6): relationship to osteopenia with enhanced adipogenesis. *Journal of Bone and Mineral Research* 13: 1370-1377.

Komine M., Kukita A., Kukita T., Ogata Y., Hotokebuchi T., and Kohashi O. (2001) Tumor necrosis factor-alpha cooperates with receptor activator of nuclear factor kappaB ligand in generation of osteoclasts in stromal cell-depleted rat bone marrow cell culture. *Bone* 28: 474-483.

Komori T., Yagi H., Nomura S., Yamaguchi A., Sasaki K., Deguchi K., Shimizu Y., Bronson R.T., Gao Y.H., Inada M., Sato M., Okamoto R., Kitamura Y., Yoshiki S., and Kishimoto T. (1997) Targeted disruption of Cbfa1 results in a complete lack of bone formation owing to maturational arrest of osteoblasts. *Cell* 89: 755-764.

Komuro H., Olee T., Kühn K., Quach J., Brinson D.C., Shikhman A., Valbracht J., Creighton-Achermann L., and Lotz M. (2001) The osteoprotegerin/receptor activator of nuclear factor kappaB/receptor activator of nuclear factor kappaB ligand system in cartilage. *Arthritis and Rheumatism* 44: 2768-2776.

Kong Y.Y., Yoshida H., Sarosi I., Tan H.L., Timms E., Capparelli C., Morony S., Oliveira-dos-Santos A.J., Van G., Itie A., Khoo W., Wakeham A., Dunstan C.R., Lacey D.L., Mak T.W., Boyle W.J., and Penninger J.M. (1999) OPGL is a key regulator of osteoclastogenesis, lymphocyte development and lymph-node organogenesis. *Nature* 397: 315-323.

Kotake S., Sato K., Kim K.J., Takahashi N., Udagawa N., Nakamura I., Yamaguchi A., Kishimoto T., Suda T., and Kashiwazaki S. (1996) Interleukin-6 and soluble interleukin-6 receptors in the synovial fluids from rheumatoid arthritis patients are responsible for osteoclast-like cell formation. *Journal of Bone and Mineral Research* 11: 88-95.

Krall E.A., Dawson-Hughes B., Hirst K., Gallagher J.C., Sherman S.S., and Dalsky G. (1997) Bone mineral density and biochemical markers of bone turnover in healthy elderly men and women. *The Journals of Gerontology. Series A, Biological Sciences and Medical Sciences* 52: M61-M67.

Kuestner R., Elrod R., Grant F., Hagen F., Kuijper J., Matthewes S., O'Hara P., Sheppard P., Stroop S., Thompson D., Whitmore T., Findlay D., Houssami S., Sexton P., and Moore E. (1994) Cloning and characterization of an abundant subtype of the human calcitonin receptor. *Molecular Pharmacology* 46: 246-255.

Kujala U.M., Kettunen J., Paananen H., Aalto T., Battie M.C., Impivaara O., Videman T., and Sarna S. (1995) Knee osteoarthritis in former runners, soccer players, weight lifters, and shooters. *Arthritis and Rheumatism* 38: 539-546.

Kurokouchi K., Kambe F., Yasukawa K., Izumi R., Ishiguro N., Iwata H., and Seo H. (1998) TNF-alpha increases expression of IL-6 and ICAM-1 genes through activation of NF-kappaB in osteoblast-like ROS17/2.8 cells. *Journal of Bone and Mineral Research* 13: 1290-1299.

Kwon B.S., Wang S., Udagawa N., Haridas V., Lee Z.H., Kim K.K., Oh K.O., Greene J., Li Y., Su J., Gentz R., Aggarwal B.B., and Ni J. (1998) TR1, a new member of the tumor necrosis factor receptor superfamily, induces fibroblast proliferation and inhibits osteoclastogenesis and bone resorption. *FASEB Journal* 12: 845-854.

Lacey D.L., Timms E., Tan H.L., Kelley M.J., Dunstan C.R., Burgess T., Elliott R., Colombero A., Elliott G., Scully S., Hsu H., Sullivan J., Hawkins N., Davy E., Capparelli C., Eli A., Qian Y.X., Kaufman S., Sarosi I., Shalhoub V., Senaldi G., Guo J., Delaney J., and Boyle W.J. (1998) Osteoprotegerin ligand is a cytokine that regulates osteoclast differentiation and activation. *Cell* 93: 165-176.

Lai C.F. and Cheng S.L. (2002) Signal transductions induced by bone morphogenetic protein-2 and transforming growth factor-beta in normal human osteoblastic cells. *Journal of Biological Chemistry* 277: 15514-15522.

Laiho K. and Penttila A. (1981) Autolytic changes in blood cells and other tissue cells of human cadavers. *Forensic Science International* 17: 109-120.

Langub M.C. Jr, Koszewski N.J., Turner H.V., Monier-Faugere M.C., Geng Z., and Malluche H.H. (1996) Bone resorption and mRNA expression of IL-6 and IL-6 receptor in patients with renal osteodystrophy. *Kidney International* 50: 515-520.

Langub M.C. and Malluche H.H. (2002) Patients with renal osteodystrophy have increased RANKL expression in bone. Proceedings of the IXth Congress of the International Society of Bone Morphometry. pp. 28.

Lanyon P., Muir K., Doherty S., and Doherty M. (2000) Assessment of a genetic contribution to osteoarthritis of the hip: sibling study. *British Medical Journal* 321: 1179-1183.

Larsen S., Rygaard K., Asnaes S., and Spang-Thomsen M. (1992) Northern and southern blot analysis of human RNA and DNA in autopsy material. *APMIS* 100: 498-502.

Lean J.M., Jagger C.J., Chambers T.J., and Chow J.W. (1995) Increased insulin-like growth factor I mRNA expression in rat osteocytes in response to mechanical stimulation. *American Journal of Physiology* 268: E318-E327.

Lee S.K. and Lorenzo J.A. (1999) Parathyroid hormone stimulates TRANCE and inhibits osteoprotegerin messenger ribonucleic acid expression in murine bone marrow cultures: correlation with osteoclast-like cell formation. *Endocrinology* 140: 3552-3561.

Leonard S., Logel J., Luthman D., Casanova M., Kirch D., and Freedman R. (1993) Biological stability of mRNA isolated from human postmortem brain collections. *Biological Psychiatry* 33: 456-466.

Lethbridge-Cejku M., Tobin J.D., Scott W.W. Jr, Reichle R., Roy T.A., Plato C.C., and Hochberg M.C. (1996) Axial and hip bone mineral density and radiographic changes of osteoarthritis of the knee: data from the Baltimore longitudinal study of aging. *Journal of Rheumatology* 23: 1943-1947.

Li B. and Aspden R.M. (1997a) Composition and mechanical properties of cancellous bone from the femoral head of patients with osteoporosis or osteoarthritis. *Journal of Bone and Mineral Research* 12: 641-651.

Li B. and Aspden R.M. (1997b) Material properties of bone from the femoral neck and calcar femorale of patients with osteoporosis or osteoarthritis. *Osteoporosis International* 7: 450-456.

Li J., Sarosi I., Yan X.Q., Morony S., Capparelli C., Tan H.L., McCabe S., Elliott R., Scully S., Van G., Kaufman S., Juan S.C., Sun Y., Tarpley J., Martin L., Christensen K., McCabe J., Kostenuik P., Hsu H., Fletcher F., Dunstan C.R., Lacey D.L., and Boyle W.J. (2000) RANK is the intrinsic hematopoietic cell surface receptor that controls osteoclastogenesis and regulation of bone mass and calcium metabolism. *Proceedings of the National Academy of Sciences of the USA* 97: 1566-1571.

Liaw L., Skinner M.P., Raines E.W., Ross R., Cheresh D.A., Schwartz S.M., and Giachelli C.M. (1995) The adhesive and migratory effects of osteopontin are mediated via distinct cell surface integrins. Role of $\alpha_v\beta_3$ in smooth muscle cell migration to osteopontin *in vitro*. *Journal of Clinical Investigation* 95: 713-724.

Liggett W.H. Jr, Lian J.B., Greenberger J.S., and Glowacki J. (1994) Osteocalcin promotes differentiation of osteoclast progenitors from murine long-term bone marrow cultures. *Journal of Cellular Biochemistry* 55: 190-199.

Lin J., Kawano H., Paparella M.M., and Ho S.B. (1999) Improved RNA analysis for immediate autopsy of temporal bone soft tissues. *Acta Oto-laryngologica (Stockh)* 119: 787-795.

Lind M., Eriksen E.F., and Bunger C. (1996) Bone morphogenetic protein-2 but not bone morphogenetic protein-4 and -6 stimulates chemotactic migration of human osteoblasts, human marrow osteoblasts, and U2-OS cells. *Bone* 18: 53-57.

Lindberg H. (1986) Prevalence of primary coxarthrosis in siblings of patients with primary coxarthrosis. *Clinical Orthopaedics and Related Research* 203: 273-275.

Ling R.S.M., O'Connor J.J., Lu T., and Lee A.J.C. (1996) Muscular activity and the biomechanics of the hip. *Hip International* 6: 91-105.

Linkhart T., Linkhart S., MacCharles D., Long D., and Strong D. (1991) Interleukin-6 messenger RNA expression and interleukin-6 protein secretion in cells isolated from normal human bone: regulation by interleukin-1. *Journal of Bone and Mineral Research* 6: 1285-1294.

Linkhart T.A., Mohan S., and Baylink D.J. (1996) Growth factors for bone growth and repair: IGF, TGF beta and BMP. *Bone* 19(Suppl 1): S1-S12.

Lohmander L.S. and Felson D.T. (1998) Defining and validating the clinical role of molecular markers in osteoarthritis. In: Brandt K.D., Doherty M., and Lohmander L.S. (editors) Osteoarthritis. Oxford University Press, New York, pp. 519-530.

Lorentzon M., Lorentzon R., and Nordstrom P. (2000) Interleukin-6 gene polymorphism is related to bone mineral density during and after puberty in healthy white males: a cross-sectional and longitudinal study. *Journal of Bone and Mineral Research* 15: 1944-1949.

Lotz J.C., Cheal E.J., and Hayes W.C. (1995) Stress distributions within the proximal femur during gait and falls: implications for osteoporotic fracture. *Osteoporosis International* 5: 252-261.

Madea B., Krompecher T., and Knight B. (1995) Muscle and tissue changes after death. In: Henssge C., Knight B., Krompecher T., Madea B., and Nokes L. The Estimation of the Time Since Death in the Early Postmortem Period. Edward Arnold, London, pp. 138-220.

Malchau H., Herberts P., Eisler T., Garellick G., and Soderman P. (2002) The Swedish Total Hip Replacement Register. *Journal of Bone and Joint Surgery American Volume* 84-A Suppl 2: 2-20.

Malyankar U.M., Scatena M., Suchland K.L., Yun T.J., Clark E.A., and Giachelli C.M. (2000) Osteoprotegerin is an alpha vbeta 3-induced, NF-kappa B-dependent survival factor for endothelial cells. *Journal of Biological Chemistry* 275: 20959-20962.

Manolagas S.C. (1995) Role of cytokines in bone resorption. *Bone* 17(Suppl 2): S63-S67.

Manolagas S.C. and Jilka R.L. (1995) Bone marrow, cytokines, and bone remodeling. Emerging insights into the pathophysiology of osteoporosis. *The New England Journal of Medicine* 332: 305-311.

Mansell J.P., Tarlton J.F., and Bailey A.J. (1997) Biochemical evidence for altered subchondral bone collagen metabolism in osteoarthritis of the hip. *British Journal of Rheumatology* 36: 16-19.

Mansell J.P. and Bailey A.J. (1998) Abnormal cancellous bone collagen metabolism in osteoarthritis. *Journal of Clinical Investigation* 101: 1596-1603.

Marcelli C., Yates A.J., and Mundy G.R. (1990) *In vivo* effects of human recombinant transforming growth factor beta on bone turnover in normal mice. *Journal of Bone and Mineral Research* 5: 1087-1096.

Marchuk L., Sciore P., Reno C., Frank C.B., and Hart D.A. (1998) Postmortem stability of total RNA isolated from rabbit ligament, tendon and cartilage. *Biochimica et Biophysica Acta* 1379: 171-177.

Maroudas A.I. (1976) Balance between swelling pressure and collagen tension in normal and degenerate cartilage. *Nature* 260: 808-809.

Martens M., Van Audekercke R., Delport P., Meester P., and Mulier J. (1983) The mechanical characteristics of cancellous bone at the upper femoral region. *Journal of Biomechanics* 16: 971-983.

Martin T.J. and Ng K.W. (1994) Mechanisms by which cells of the osteoblast lineage control osteoclast formation and activity. *Journal of Cellular Biochemistry* 56: 357-366.

Martin T.J. and Udagawa N. (1998) Hormonal regulation of osteoclast function. *TEM* 9: 6-12.

Martin T.J., Romas E., and Gillespie M.T. (1998) Interleukins in the control of osteoclast differentiation. *Critical Reviews of Eukaryotic Gene Expression* 8: 107-123.

Martin R.B. (2000) Toward a unifying theory of bone remodeling. *Bone* 26: 1-6.

Mashiba T., Hirano T., Turner C.H., Forwood M.R., Johnston C.C., and Burr D.B. (2000) Suppressed bone turnover by bisphosphonates increases microdamage accumulation and reduces some biomechanical properties in dog rib. *Journal of Bone and Mineral Research* 15: 613-620.

Mason D.J., Hillam R.A., and Skerry T.M. (1996) Constitutive *in vivo* mRNA expression by osteocytes of beta-actin, osteocalcin, connexin-43, IGF-I, c-fos and c-jun, but not TNF-alpha nor tartrate-resistant acid phosphatase. *Journal of Bone and Mineral Research* 11: 350-357.

McBride D.J Jr, Shapiro J.R., and Dunn M.G. (1998) Bone geometry and strength measurements in aging mice with the oim mutation. *Calcified Tissue International* 62: 172-176.

McKane W.R., Khosla S., Peterson J.M., Egan K., and Riggs B.L. (1994) Circulating levels of cytokines that modulate bone resorption: effects of age and menopause in women. *Journal of Bone and Mineral Research* 9: 1313-1318.

Meacock S.C., Bodmer J.L., and Billingham M.E. (1990) Experimental osteoarthritis in guinea-pigs. *International Journal of Experimental Pathology* 71: 279-293.

Merry K., Dodds R., Littlewood A., and Gowen M. (1993) Expression of osteopontin mRNA by osteoclasts and osteoblasts in modelling adult human bone. *Journal of Cell Science* 104: 1013-1020.

Meulenbelt I., Bijkerk C., Miedema H.S., Breedveld F.C., Hofman A., Valkenburg H.A., Pols H.A., Slagboom P.E., and van Duijn C.M. (1998) A genetic association study of the IGF-1 gene and radiological osteoarthritis in a population-based cohort study (the Rotterdam Study). *Annals of the Rheumatic Diseases* 57: 371-374.

Milgram J.W. and Jasty M. (1982) Osteopetrosis. A morphological study of twenty-one cases. *Journal of Bone and Joint Surgery* 64: 912-929.

Minisola S., Rosso R., Romagnoli E., D'Erasmo E., Manfredi G., Damiani C., De Antoni F., and Mazzuoli G. (1997) Serum osteocalcin and bone mineral density at various skeletal sites: a study performed with three different assays. *Journal of Laboratory and Clinical Medicine* 129: 422-429.

Minkin C. (1982) Bone acid phosphatase: tartrate-resistant acid phosphatase as a marker of osteoclast function. *Calcified Tissue International* 34: 285-290.

Misof K., Landis W.J., Klaushofer K., and Fratzl P. (1997) Collagen from the osteogenesis imperfecta mouse model (oim) shows reduced resistance against tensile stress. *Journal of Clinical Investigation* 100: 40-45.

Mizuno A., Amizuka N., Irie K., Murakami A., Fujise N., Kanno T., Sato Y., Nakagawa N., Yasuda H., Mochizuki S., Gomibuchi T., Yano K., Shima N., Washida N., Tsuda E., Morinaga T., Higashio K., and Ozawa H. (1998) Severe osteoporosis in mice lacking osteoclastogenesis inhibitory factor/osteoprotegerin. *Biochemical and Biophysical Research Communications* 247: 610-615.

Moore R.J., Fazzalari N.L., Manthey B.A., and Vernon-Roberts B. (1994) The relationship between head-neck-shaft angle, calcar width, articular cartilage thickness and bone volume in arthrosis of the hip. *British Journal of Rheumatology* 33: 432-436.

Moore E.E., Kuestner R.E., Stroop S.D., Grant F.J., Matthewes S.L., Brady C.L., Sexton P.M., and Findlay D.M. (1995) Functionally different isoforms of the human calcitonin receptor result from alternative splicing of the gene transcript. *Journal of Molecular Endocrinology* 9: 959-968.

Mori S. and Burr D.B. (1993) Increased intracortical remodeling following fatigue damage. *Bone* 14: 103-109.

Mori S., Harruff R., Ambrosius W., and Burr D.B. (1997) Trabecular bone volume and microdamage accumulation in the femoral heads of women with and without femoral neck fracture. *Bone* 21: 521-526.

Mosavin R. and Mellon W.S. (1996) Posttranscriptional regulation of osteocalcin mRNA in clonal osteoblast cells by 1,25-dihydroxyvitamin D_3. *Archives of Biochemistry and Biophysics* 332: 142-152.

Muir H. (1995) The chondrocyte, architect of cartilage. Biomechanics, structure, function and molecular biology of cartilage matrix macromolecules. *Bioessays* 17: 1039-1048.

Mukohyama H., Ransjo M., Taniguchi H., Ohyama T., and Lerner U.H. (2000) The inhibitory effects of vasoactive intestinal peptide and pituitary adenylate cyclase-activating polypeptide on osteoclast formation are associated with upregulation of osteoprotegerin and downregulation of RANKL and RANK. *Biochemical and Biophysical Research Communications* 271: 158-163.

Munasinghe J.P., Tyler J.A., Carpenter T.A., and Hall L.D. (1995) High resolution MR imaging of joint degeneration in the knee of the STR/ORT mouse. *Journal of Magnetic Resonance Imaging* 13: 421-428.

Mundy G.R. (1996) Regulation of bone formation by bone morphogenetic proteins and other growth factors. *Clinical Orthopaedics and Related Research* 323: 24-28.

Mundy G.R. (1999) Cellular and molecular regulation of bone turnover. *Bone* 24(Suppl): 35S-38S.

Myers D.E., Collier F.M., Minkin C., Wang H., Holloway W.R., Malakellis M., and Nicholson G.C. (1999) Expression of functional RANK on mature rat and human osteoclasts. *FEBS Letters* 463: 295-300.

Nagai M. and Sato N. (1999) Reciprocal gene expression of osteoclastogenesis inhibitory factor and osteoclast differentiation factor regulates osteoclast formation. *Biochemical and Biophysical Research Communications* 257: 719-723.

Nakagawa N., Kinosaki M., Yamaguchi K., Shima N., Yasuda H., Yano K., Morinaga T., and Higashio K. (1998) RANK is the essential signaling receptor for osteoclast differentiation factor in osteoclastogenesis. *Biochemical and Biophysical Research Communications* 253: 395-400.

Nakashima T., Kobayashi Y., Yamasaki S., Kawakami A., Eguchi K., Sasaki H., and Sakai H. (2000) Protein expression and functional difference of membrane-bound and soluble receptor activator of NF-kappaB ligand: modulation of the expression by osteotropic factors and cytokines. *Biochemical and Biophysical Research Communications* 275: 768-775.

Nakchbandi I.A., Mitnick M.A., Masiukiewicz U.S., Sun B.H., and Insogna K.L. (2001) IL-6 negatively regulates IL-11 production *in vitro* and *in vivo*. *Endocrinology* 142: 3850-3856.

Nevitt M.C., Lane N.E., Scott J.C., Hochberg M.C., Pressman A.R., Genant H.K., and Cummings S.R. (1995) Radiographic osteoarthritis of the hip and bone mineral density. The study of osteoporotic fractures research group. *Arthritis and Rheumatism* 38: 907-916.

Neyret P., Donell S.T., and Dejour H. (1993) Results of partial meniscectomy related to the state of the anterior cruciate ligament. Review at 20 to 35 years. *Journal of Bone and Joint Surgery British Volume* 75: 36-40.

Nijweide P.J., Burger E.H., Klein-Nulend J., and van der Pluijm G. (1996) The Osteocyte. In: Bilezikian J.P., Raisz L.G., and Rodan G.A. (editors) Principles of Bone Biology. Academic Press, San Diego, pp. 115-126.

Noble B.S., Stevens H., Loveridge N., and Reeve J. (1997) Identification of apoptotic changes in osteocytes in normal and pathological human bone. *Bone* 20: 273-282.

Noda M. and Camilliere J.J. (1989) *In vivo* stimulation of bone formation by transforming growth factor-beta. *Endocrinology* 124: 2991-2994.

O'Brien C.A., Gubrij I., Lin S.C., Saylors R.L., and Manolagas S.C. (1999) STAT3 activation in stromal/osteoblastic cells is required for induction of the receptor activator of NF-kappaB ligand and stimulation of osteoclastogenesis by gp130-utilizing cytokines or interleukin-1 but not 1,25-dihydroxyvitamin D_3 or parathyroid hormone. *Journal of Biological Chemistry* 274: 19301-19308.

O'Brien F.J., Taylor D., Dickson G.R., and Lee T.C. (2000) Visualisation of three-dimensional microcracks in compact bone. *Journal of Anatomy* 197 Pt 3: 413-420.

O'Keefe R., Teot L., Singh D., Puzas J., Rosier R., and Hicks D. (1997) Osteoclasts constitutively express regulators of bone resorption: an immunohistochemical and in situ hybridization study. *Laboratory Investigation* 76: 457-465.

Oliveria S.A., Felson D.T., Reed J.I., Cirillo P.A., and Walker A.M. (1995) Incidence of symptomatic hand, hip, and knee osteoarthritis among patients in a health maintenance organization. *Arthritis and Rheumatism* 38: 1134-1141.

Oreffo R.O., Bennett A., Carr A.J., and Triffitt J.T. (1998a) Patients with primary osteoarthritis show no change with ageing in the number of osteogenic precursors. *Scandinavian Journal of Rheumatology* 27: 415-424.

Oreffo R.O., Bord S., and Triffitt J.T. (1998b) Skeletal progenitor cells and ageing human populations. *Clinical Science (London)* 94: 549-555.

Pacifici R. (1998) Cytokines, estrogen, and postmenopausal osteoporosis--the second decade *Endocrinology* 139: 2659-2661.

Palmqvist P., Persson E., Conaway H.H., and Lerner U.H. (2002) IL-6, leukemia inhibitory factor, and oncostatin M stimulate bone resorption and regulate the expression of receptor activator of NF-kappa B ligand, osteoprotegerin, and receptor activator of NF-kappa B in mouse calvariae. *Journal of Immunology* 169: 3353-3362.

Parfitt A.M. (1977) The cellular basis of bone turnover and bone loss: a rebuttal of the osteocytic resorption-bone flow theory. *Clinical Orthopaedics and Related Research* 127: 236-247.

Parfitt A.M., Drezner M.K., Glorieux F.H., Kanis J.A., Malluche H., Meunier P.J., Ott S.M., and Recker R.R. (1987) Bone histomorphometry: standardization of nomenclature, symbols, and units. Report of the ASBMR Histomorphometry Nomenclature Committee. *Journal of Bone and Mineral Research* 2: 595-610.

Parfitt A.M. (1994) Osteonal and hemi-osteonal remodeling the spatial and temporal framework for signal traffic in adult human bone. *Journal of Cellular Biochemistry* 55: 273-286.

Parfitt A.M., Villanueva A.R., Foldes J., and Rao D.S. (1995) Relations between histologic indices of bone formation: implications for the pathogenesis of spinal osteoporosis. *Journal of Bone and Mineral Research* 10: 466-473.

Parfitt A.M. (1996) Skeletal heterogeneity and the purposes of bone remodelling: Implications for the understanding of osteoporosis. In: Marcus R., Feldman D., and Kelsey J. (editors) Academic, San Diego, pp. 315-329.

Parfitt A.M. (2002) Targeted and nontargeted bone remodeling: relationship to basic multicellular unit origination and progression. *Bone* 30: 5-7.

Pattin C.A., Caler W.E., and Carter D.R. (1996) Cyclic mechanical property degradation during fatigue loading of cortical bone. *Journal of Biomechanics* 29: 69-79.

Paul S., Bennett F., Calvetti J., Kelleher K., Wood C., O'Hara Jr R., Leary A., Sibley B., Clark S., Williams D., and Yang Y. (1990) Molecular cloning of a cDNA encoding interleukin 11, a stromal cell-derived lymphopoietic cytokine. *Proceedings of the National Academy of Sciences of the USA* 87: 7512-7516.

Peel N.F., Barrington N.A., Blumsohn A., Colwell A., Hannon R., and Eastell R. (1995) Bone mineral density and bone turnover in spinal osteoarthrosis. *Annals of the Rheumatic Diseases* 54: 867-871.

Perry V.P., Stevenson R.E., McFarland W., and Zink G.A. (1960) Motility studies of human post-mortem bone marrow. *Blood* 16: 1020-1028.

Pfeilschifter J. and Mundy G.R. (1987) Modulation of type beta transforming growth factor activity in bone cultures by osteotropic hormones. *Proceedings of the National Academy of Sciences of the USA* 84: 2024-2028.

Pfeilschifter J., Bonewald L., and Mundy G.R. (1990a) Characterization of the latent transforming growth factor beta complex in bone. *Journal of Bone and Mineral Research* 5: 49-58.

Pfeilschifter J., Wolf O., Naumann A., Minne H.W., Mundy G.R., and Ziegler R. (1990b) Chemotactic response of osteoblastlike cells to transforming growth factor beta. *Journal of Bone and Mineral Research* 5: 825-830.

Pfeilschifter J., Diel I., Scheppach B., Bretz A., Krempien R., Erdmann J., Schmid G., Reske N., Bismar H., Seck T., Krempien B., and Ziegler R. (1998) Concentration of transforming growth factor beta in human bone tissue: relationship to age, menopause, bone turnover, and bone volume. *Journal of Bone and Mineral Research* 13: 716-730.

Pirskanen A., Jaaskelainen T., and Maenpaa P.H. (1994) Effects of transforming growth factor beta 1 on the regulation of osteocalcin synthesis in human MG-63 osteosarcoma cells. *Journal of Bone and Mineral Research* 9: 1635-1642.

Pitsillides A.A., Rawlinson S.C., Suswillo R.F., Bourrin S., Zaman G., and Lanyon L.E. (1995) Mechanical strain-induced NO production by bone cells: a possible role in adaptive bone (re)modeling? *FASEB Journal* 9: 1614-1622.

Poli V., Balena R., Fattori E., Markatos A., Yamamoto M., Tanaka H., Ciliberto G., Rodan G., and Costantini F. (1994) Interleukin-6 deficient mice are protected from bone loss caused by estrogen depletion. *EMBO* 13: 1189-1196.

Porteous I.B. (1961) Persistence of motility in bone-marrow cells from the cadaver. *Nature* 192: 569-570.

Prendergast P.J. and Taylor D. (1994) Prediction of bone adaptation using damage accumulation. *Journal of Biomechanics* 27: 1067-1076.

Quasnichka H.L., Anderson-MacKenzie J.M., Billingham M.E.J., and Bailey A.J. (2002) Biomechanical, biochemical and ultrastructural changes in the cruciate ligaments of osteoarthritic knees. *Osteoarthritis and Cartilage* 10(Suppl A): S54.

Quinn J.M., Morfis M., Lam M.H., Elliott J., Kartsogiannis V., Williams E.D., Gillespie M.T., Martin T.J., and Sexton P.M. (1999) Calcitonin receptor antibodies in the identification of osteoclasts. *Bone* 25: 1-8.

Radin E.L., Paul I.L., and Rose R.B. (1972) Role of mechanical factors in pathogenesis of primary osteoarthritis. *The Lancet* 1: 519-520.

Radin E., Abernethy P., Townsend P., and Rose R. (1978) The role of bone changes in the degeneration of articular cartilage in osteoarthrosis. *Acta Orthopaedica Belgica* 44: 55-63.

Radin E., Burr D., Caterson B., Fyhrie D., Brown T., and Boyd R. (1991) Mechanical determinants of osteoarthrosis. *Seminars in Arthritis and Rheumatism* 21: S12-S21.

Raisz L.G. (1999) Physiology and pathophysiology of bone remodeling. *Clinical Chemistry* 45: 1353-1358.

Ralston S.H. (1994) Analysis of gene expression in human bone biopsies by polymerase chain reaction: evidence for enhanced cytokine expression in postmenopausal osteoporosis. *Journal of Bone and Mineral Research* 9: 883-890.

Raymaekers G., Aerssens J., Van den Eynde R., Peeters J., Geusens P., Devos P., and Dequeker J. (1992) Alterations of the mineralization profile and osteocalcin concentrations in osteoarthritic cortical iliac crest bone. *Calcified Tissue International* 51: 269-275.

Recker R.R. (1983) Bone Histomorphometry - Techniques and Interpretation. CRC Press, Florida.

Reinholt F.P., Hultenby K., Oldberg A., and Heinegard D. (1990) Osteopontin-a possible anchor of osteoclasts to bone. *Proceedings of the National Academy of Sciences of the USA* 87: 4473-4475.

Ritter N.M., Farach-Carson M.C., and Butler W.T. (1992) Evidence for the formation of a complex between osteopontin and osteocalcin. *Journal of Bone and Mineral Research* 7: 877-885.

Roggia C., Gao Y., Cenci S., Weitzmann M.N., Toraldo G., Isaia G., and Pacifici R. (2001) Up-regulation of TNF-producing T cells in the bone marrow: a key mechanism by which estrogen deficiency induces bone loss *in vivo*. *Proceedings of the National Academy of Sciences of the USA* 98: 13960-13965.

Romas E., Udagawa N., Zhou H., Tamura T., Saito M., Taga T., Hilton D., Suda T., Ng K., and Martin T. (1996) The role of gp130-mediated signals in osteoclast development: regulation of interleukin 11 production by osteoblasts and distribution of its receptor in bone marrow cultures. *Journal of Experimental Medicine* 183: 2581-2591.

Roodman G., Kurihara N., Ohsaki Y., Kukita A., Hosking D., Smith J., and Singer F. (1992) Interleukin 6. A potential autocrine/paracrine factor in Paget's disease of bone. *Journal of Clinical Investigation* 89: 46-52.

Roodman G. (1995) Osteoclast function in Paget's disease and multiple myeloma. *Bone* 17: S57-S61.

Roodman G.D. (1996) Advances in bone biology: the osteoclast. *Endocrine Reviews* 17: 308-332.

Roodman G.D. (1999) Cell biology of the osteoclast. *Experimental Hematology* 27: 1229-1241.

Rosen V. and Thies R.S. (1992) The BMP proteins in bone formation and repair. *Trends in Genetics* 8: 97-102.

Rosen V., Cox K., and Hattersley G. (1996) Bone morphogenetic proteins. In: Bilezikian J.P., Raisz L.G., and Rodan G.A. (editors) Principles of Bone Biology. Academic Press, San Diego, pp. 661-671.

Ross B.M., Knowler J.T., and McCulloch J. (1992) On the stability of messenger RNA and ribosomal RNA in the brains of control human subjects and patients with Alzheimer's disease. *Journal of Neurochemistry* 58: 1810-1819.

Rozman C., Feliu E., Berga L., Reverter J.C., Climent C., and Ferran M.J. (1989) Age-related variations of fat tissue fraction in normal human bone marrow depend both on size and number of adipocytes: a stereological study. *Experimental Hematology* 17: 34-37.

Rubin J., Fan X., Biskobing D.M., Taylor W.R., and Rubin C.T. (1999) Osteoclastogenesis is repressed by mechanical strain in an *in vitro* model. *Journal of Orthopaedic Research* 17: 639-645.

Rubin J., Murphy T., Nanes M.S., and Fan X. (2000) Mechanical strain inhibits expression of osteoclast differentiation factor by murine stromal cells. *American Journal of Physiology. Cell Physiology* 278: C1126-C1132.

Sachs A.B. (1993) Messenger RNA degradation in eukaryotes. *Cell* 74: 413-421.

Sambrook J. and Russell D.W. (2001) Molecular Cloning: a Laboratory Manual. (3rd edition) Cold Spring Harbor, New York.

Samura A., Wada S., Suda S., Iitaka M., and Katayama S. (2000) Calcitonin receptor regulation and responsiveness to calcitonin in human osteoclast-like cells prepared *in vitro* using receptor activator of nuclear factor-kappaB ligand and macrophage colony-stimulating factor. *Endocrinology* 141: 3774-3782.

Scatena M., Almeida M., Chaisson M.L., Fausto N., Nicosia R.F., and Giachelli C.M. (1998) NF-kappaB mediates $\alpha_v\beta_3$ integrin-induced endothelial cell survival. *Journal of Cell Biology* 141: 1083-1093.

Schaffler M.B., Radin E.L., and Burr D.B. (1989) Mechanical and morphological effects of strain rate on fatigue of compact bone. *Bone* 10: 207-214.

Schaffler M.B., Pitchford W.C., Choi K., and Riddle J.M. (1994) Examination of compact bone microdamage using back-scattered electron microscopy. *Bone* 15: 483-488.

Schaffler M.B., Choi K., and Milgrom C. (1995) Aging and matrix microdamage accumulation in human compact bone. *Bone* 17: 521-525.

Schnitzler C.M., Biddulph S.L., Mesquita J.M., and Gear K.A. (1996) Bone structure and turnover in the distal radius and iliac crest: a histomorphometric study. *Journal of Bone and Mineral Research* 11: 1761-1768.

Seck T., Scheppach B., Scharla S., Diel I., Blum W.F., Bismar H., Schmid G., Krempien B., Ziegler R., and Pfeilschifter J. (1998) Concentration of insulin-like growth factor (IGF)-I and -II in iliac crest bone matrix from pre- and postmenopausal women: relationship to age, menopause, bone turnover, bone volume, and circulating IGFs. *Journal of Clinical Endocrinology and Metabolism* 83: 2331-2337.

Seck T., Diel I., Bismar H., Ziegler R., and Pfeilschifter J. (2001) Serum parathyroid hormone, but not menopausal status, is associated with the expression of osteoprotegerin and RANKL mRNA in human bone samples. *European Journal of Endocrinology* 145: 199-205.

Sharma L., Song J., Felson D.T., Cahue S., Shamiyeh E., and Dunlop D.D. (2001) The role of knee alignment in disease progression and functional decline in knee osteoarthritis. *Journal of the American Medical Association* 286: 188-195.

Shur I., Lokiec F., Bleiberg I., and Benayahu D. (2001) Differential gene expression of cultured human osteoblasts. *Journal of Cellular Biochemistry* 83: 547-553.

Simonet W.S., Lacey D.L., Dunstan C.R., Kelley M., Chang M.S., Luthy R., Nguyen H.Q., Wooden S., Bennett L., Boone T., Shimamoto G., DeRose M., Elliott R., Colombero A., Tan H.L., Trail G., Sullivan J., Davy E., Bucay N., Renshaw-Gegg L., Hughes T.M., Hill D., Pattison W., Campbell P., Sander S., Van G., Tarpley J., Derby P., Lee R., and Boyle W.J. (1997) Osteoprotegerin: a novel secreted protein involved in the regulation of bone density. *Cell* 89: 309-319.

Slemenda C., Heilman D.K., Brandt K.D., Katz B.P., Mazzuca S.A., Braunstein E.M., and Byrd D. (1998) Reduced quadriceps strength relative to body weight: a risk factor for knee osteoarthritis in women? *Arthritis and Rheumatism* 41: 1951-1959.

Sodek J., Chen J., Nagata T., Kasugai S., Todescan R. Jr, Li I.W., and Kim R.H. (1995) Regulation of osteopontin expression in osteoblasts. *Annals of the New York Academy of Sciences* 760: 223-241.

Sokoloff L. (1956) Natural history of degenerative joint disease in small laboratory animals. 1. Pathological anatomy of degenerative joint disease in mice. *Archives of Pathology* 62: 118-128.

Solomon L. (1976) Patterns of osteoarthritis of the hip. *Journal of Bone and Joint Surgery British Volume* 58: 176-183.

Solomon L., Schnitzler C.M., Browett J.P. (1982) Osteoarthritis of the hip: the patient behind the disease. *Annals of the Rheumatic Diseases* 41: 118-125.

Spector T.D., Hart D.J., and Doyle D.V. (1994) Incidence and progression of osteoarthritis in women with unilateral knee disease in the general population: the effect of obesity. *Annals of the Rheumatic Diseases* 53: 565-568.

Spector T.D., Cicuttini F., Baker J., Loughlin J., and Hart D. (1996a) Genetic influences on osteoarthritis in women: a twin study. *British Medical Journal* 312: 940-943.

Spector T.D., Harris P.A., Hart D.J., Cicuttini F.M., Nandra D., Etherington J., Wolman R.L., and Doyle D.V. (1996b) Risk of osteoarthritis associated with long-term weight-bearing sports: a radiologic survey of the hips and knees in female ex-athletes and population controls. *Arthritis and Rheumatism* 39: 988-995.

Stammberger T., Eckstein F., Englmeier K.H., and Reiser M. (1999) Determination of 3D cartilage thickness data from MR imaging: computational method and reproducibility in the living. *Magnetic Resonance in Medicine* 41: 529-536.

Stanford C.M., Welsch F., Kastner N., Thomas G., Zaharias R., Holtman K., and Brand R.A. (2000) Primary human bone cultures from older patients do not respond at continuum levels of *in vivo* strain magnitudes. *Journal of Biomechanics* 33: 63-71.

Stein G.S. and Lian J.B. (1993) Molecular mechanisms mediating proliferation/differentiation interrelationships during progressive development of the osteoblast phenotype. *Endocrine Reviews* 14: 424-442.

Stuart C.A., Wen G., and Jiang J. (1999) GLUT3 protein and mRNA in autopsy muscle specimens. *Metabolism* 48: 876-880.

Suda T., Nakamura I., Jimi E., and Takahashi N. (1997) Regulation of osteoclast function. *Journal of Bone and Mineral Research* 12: 869-879.

Suda T., Takahashi N., Udagawa N., Jimi E., Gillespie M.T., and Martin T.J. (1999) Modulation of osteoclast differentiation and function by the new members of the tumor necrosis factor receptor and ligand families. *Endocrine Reviews* 20: 345-357.

Szulc P., Hofbauer L.C., Heufelder A.E., Roth S., and Delmas P.D. (2001) Osteoprotegerin serum levels in men: correlation with age, estrogen, and testosterone status. *Journal of Clinical Endocrinology and Metabolism* 86: 3162-3165.

Takai H., Kanematsu M., Yano K., Tsuda E., Higashio K., Ikeda K., Watanabe K., and Yamada Y.J. (1998) Transforming growth factor-beta stimulates the production of osteoprotegerin/osteoclastogenesis inhibitory factor by bone marrow stromal cells. *Biological Chemistry* 273: 27091-27096.

Takami M., Takahashi N., Udagawa N., Miyaura C., Suda K., Woo J.T., Martin T.J., Nagai K., and Suda T. (2000) Intracellular calcium and protein kinase C mediate expression of receptor activator of nuclear factor-kappaB ligand and osteoprotegerin in osteoblasts. *Endocrinology* 141: 4711-4719.

Takeshita S., Arai S., and Kudo A. (2001) Identification and characterization of mouse bone marrow stromal cell lines immortalized by temperature-sensitive SV40 T antigen: supportive activity for osteoclast differentiation. *Bone* 29: 236-241.

Takeuchi Y., Watanabe S., Ishii G., Takeda S., Nakayama K., Fukumoto S., Kaneta Y., Inoue D., Matsumoto T., Harigaya K., and Fujita T. (2002) Interleukin-11 as a stimulatory factor for bone formation prevents bone loss with advancing age in mice. *Journal of Biological Chemistry* 277: 49011-49018.

Tan K.B., Harrop J., Reddy M., Young P., Terrett J., Emery J., Moore G., and Truneh A. (1997) Characterization of a novel TNF-like ligand and recently described TNF ligand and TNF receptor superfamily genes and their constitutive and inducible expression in hematopoietic and non-hematopoietic cells. *Gene* 204: 35-46.

Terai K., Takano-Yamamoto T., Ohba Y., Hiura K., Sugimoto M., Sato M., Kawahata H., Inaguma N., Kitamura Y., and Nomura S. (1999) Role of osteopontin in bone remodeling caused by mechanical stress. *Journal of Bone and Mineral Research* 14: 839-849.

Tetlow L.C., Adlam D.J., and Woolley D.E. (2001) Matrix metalloproteinase and proinflammatory cytokine production by chondrocytes of human osteoarthritic cartilage: associations with degenerative changes. *Arthritis and Rheumatism* 44: 585-594.

Tomkinson A., Reeve J., Shaw R.W., and Noble B.S. (1997) The death of osteocytes via apoptosis accompanies estrogen withdrawal in human bone. *Journal of Clinical Endocrinology and Metabolism* 82: 3128-3135.

Tomkinson A., Gevers E.F., Wit J.M., Reeve J., and Noble B.S. (1998) The role of estrogen in the control of rat osteocyte apoptosis. *Journal of Bone and Mineral Research* 13: 1243-1250.

Tong D., Schneeberger C., Leodolter S., and Zeillinger R. (1997) Quantitative determination of gene expression by competitive reverse transcription-polymerase chain reaction in degraded RNA samples. *Analytical Biochemistry* 251: 173-177.

Tsukii K., Shima N., Mochizuki S., Yamaguchi K., Kinosaki M., Yano K., Shibata O., Udagawa N., Yasuda H., Suda T., and Higashio K. (1998) Osteoclast differentiation factor mediates an essential signal for bone resorption induced by 1 alpha,25-dihydroxyvitamin D_3, prostaglandin E_2, or parathyroid hormone in the microenvironment of bone. *Biochemical and Biophysical Research Communications* 246: 337-341.

Udagawa N., Takahashi N., Jimi E., Matsuzaki K., Tsurukai T., Itoh K., Nakagawa N., Yasuda H., Goto M., Tsuda E., Higashio K., Gillespie M.T., Martin T.J., and Suda T. (1999) Osteoblasts/stromal cells stimulate osteoclast activation through expression of osteoclast differentiation factor/RANKL but not macrophage colony-stimulating factor: receptor activator of NF-kappa B ligand. *Bone* 25: 517-523.

Uitterlinden A.G., Burger H., Huang Q., Odding E., Duijn C.M., Hofman A., Birkenhager J.C., van Leeuwen J.P., and Pols H.A. (1997) Vitamin D receptor genotype is associated with radiographic osteoarthritis at the knee. *Journal of Clinical Investigation* 100: 259-263.

van der Rest M. and Garrone R. (1991) Collagen family of proteins. *FASEB Journal* 5: 2814-2823.

Vanderschueren D., Gevers G., Raymaekers G., Devos P., and Dequeker J. (1990) Sex- and age-related changes in bone and serum osteocalcin. *Calcified Tissue International* 46: 179-182.

van Saase J.L., van Romunde L.K., Cats A., Vandenbroucke J.P., and Valkenburg H.A. (1989) Epidemiology of osteoarthritis: Zoetermeer survey. Comparison of radiological osteoarthritis in a Dutch population with that in 10 other populations. *Annals of the Rheumatic Diseases* 48: 271-280.

Vashishth D., Koontz J., Qiu S.J., Lundin-Cannon D., Yeni Y.N., Schaffler M.B., and Fyhrie D.P. (2000a) *In vivo* diffuse damage in human vertebral trabecular bone. *Bone* 26: 147-152.

Vashishth D., Verborgt O., Divine G., Schaffler M.B., and Fyhrie D.P. (2000b) Decline in osteocyte lacunar density in human cortical bone is associated with accumulation of microcracks with age. *Bone* 26: 375-380.

Verborgt O., Gibson G.J., and Schaffler M.B. (2000) Loss of osteocyte integrity in association with microdamage and bone remodelling after fatigue *in vivo*. *Journal of Bone and Mineral Research* 15: 60-67.

Verborgt O., Tatton N.A., Majeska R.J., and Schaffler M.B. (2002) Spatial distribution of Bax and Bcl-2 in osteocytes after bone fatigue: complementary roles in bone remodeling regulation? *Journal of Bone and Mineral Research* 17: 907-914.

Vermeer C., Jie K.S., and Knapen M.H. (1995) Role of vitamin K in bone metabolism. *Annual Review of Nutrition* 15: 1-22.

Verstraeten A., Van Ermen H., Haghebaert G., Nijs J., Geusens P., and Dequeker J. (1991) Osteoarthrosis retards the development of osteoporosis. Observation of the coexistence of osteoarthrosis and osteoporosis. *Clinical Orthopaedics and Related Research* 264: 169-177.

Vidal O.N., Sjogren K., Eriksson B.I., Ljunggren O., and Ohlsson C. (1998) Osteoprotegerin mRNA is increased by interleukin-1 alpha in the human osteosarcoma cell line MG-63 and in human osteoblast-like cells. *Biochemical and Biophysical Research Communications* 248: 696-700.

Vikkula M., Palotie A., Ritvaniemi P., Ott J., Ala-Kokko L., Sievers U., Aho K., and Peltonen L. (1993) Early-onset osteoarthritis linked to the type II procollagen gene. Detailed clinical phenotype and further analyses of the gene. *Arthritis and Rheumatism* 36: 401-409.

Wada S., Udagawa N., Akatsu T., Nagata N., Martin T.J., and Findlay D.M. (1997) Regulation by calcitonin and glucocorticoids of calcitonin receptor gene expression in mouse osteoclasts. *Endocrinology* 138: 521-529.

Wada S., Yasuda S., Nagai T., Maeda T., Kitahama S., Suda S., Findlay D.M., Iitaka M., and Katayama S. (2001) Regulation of calcitonin receptor by glucocorticoid in human osteoclast-like cells prepared *in vitro* using receptor activator of nuclear factor-kappaB ligand and macrophage colony-stimulating factor. *Endocrinology* 142: 1471-1478.

Wakabayashi H., Hirata H., Onodera K., Yamamoto T., Tanizawa T., and Kusana T. (2000) The levels of vitamin K analogues in bone and serum of osteoporotic and osteoarthritic patients determined by the high performance liquid chromatography with ECD method. *Journal of Bone and Mineral Research* 15: S303.

Walton M. (1977a) Degenerative joint disease in the mouse knee; radiological and morphological observations. *Journal of Pathology* 123: 97-107.

Walton M. (1977b) Degenerative joint disease in the mouse knee; histological observations. *Journal of Pathology* 123: 109-122.

Walton M. and Elves M.W. (1979) Bone thickening in osteoarthrosis. Observations of an osteoarthrosis-prone strain of mouse. *Acta Orthopaedica Scandinavica* 50: 501-506.

Watson P.J., Hall L.D., Malcolm A., and Tyler J.A. (1996) Degenerative joint disease in the guinea pig. Use of magnetic resonance imaging to monitor progression of bone pathology. *Arthritis and Rheumatism* 39: 1327-1337.

Weinbaum S., Cowin S.C., and Zeng Y. (1994) A model for the excitation of osteocytes by mechanical loading-induced bone fluid shear stresses. *Journal of Biomechanics* 27: 339-360.

Weinstein R.S. and Hutson M.S. (1987) Decreased trabecular width and increased trabecular spacing contribute to bone loss with aging. *Bone* 8: 137-142.

Weitzmann M.N., Roggia C., Toraldo G., Weitzmann L., and Pacifici R. (2002) Increased production of IL-7 uncouples bone formation from bone resorption during estrogen deficiency. *Journal of Clinical Investigation* 110: 1643-1650.

Wenzel T.E., Schaffler M.B., and Fyhrie D.P. (1996) *In vivo* trabecular microcracks in human vertebral bone. *Bone* 19: 89-95.

Westacott C.I., Webb G.R., Warnock M.G., Sims J.V., and Elson C.J. (1997) Alteration of cartilage metabolism by cells from osteoarthritic bone. *Arthritis and Rheumatism* 40: 1282-1291.

Wong B.R., Rho J., Arron J., Robinson E., Orlinick J., Chao M., Kalachikov S., Cayani E., Bartlett F.S., Frankel W.N., Lee S.Y., and Choi Y. (1997) TRANCE is a novel ligand of the tumor necrosis factor receptor family that activates c-Jun N-terminal kinase in T cells. *Journal of Biological Chemistry* 272: 25190-25194.

Yang L. and Yang Y.C. (1994) Regulation of interleukin (IL)-11 gene expression in IL-1 induced primate bone marrow stromal cells. *Journal of Biological Chemistry* 269: 32732-32739.

Yano K., Tsuda E., Washida N., Kobayashi F., Goto M., Harada A., Ikeda K., Higashio K., and Yamada Y. (1999) Immunological characterization of circulating osteoprotegerin/osteoclastogenesis inhibitory factor: increased serum concentrations in postmenopausal women with osteoporosis. *Journal of Bone and Mineral Research* 14: 518-527.

Yasojima K., McGeer E.G., and McGeer P.L. (2001) High stability of mRNAs postmortem and protocols for their assessment by RT-PCR. *Brain Research Protocols* 8: 212-218.

Yasuda H., Shima N., Nakagawa N., Mochizuki S.I., Yano K., Fujise N., Sato Y., Goto M., Yamaguchi K., Kuriyama M., Kanno T., Murakami A., Tsuda E., Morinaga T., and Higashio K. (1998a) Identity of osteoclastogenesis inhibitory factor (OCIF) and osteoprotegerin (OPG): a mechanism by which OPG/OCIF inhibits osteoclastogenesis *in vitro*. *Endocrinology* 139: 1329-1337.

Yasuda H., Shima N., Nakagawa N., Yamaguchi K., Kinosaki M., Mochizuki S.I., Tomoyasu A., Yano K., Goto M., Murakami A., Tsuda E., Morinaga T., Higashio K., Udagawa N., Takahashi N., and Suda T. (1998b) Osteoclast differentiation factor is a ligand for osteoprotegerin/osteoclastogenesis-inhibitory factor and is identical to TRANCE/RANKL. *Proceedings of the National Academy of Sciences of the USA* 95: 3597-3602.

Young R.D., Vaughan-Thomas A., Wardale R.J., and Duance V.C. (2002) Type II collagen deposition in cruciate ligament precedes osteoarthritis in the guinea pig knee. *Osteoarthritis and Cartilage* 10: 420-428.

Zhang Y., Glynn R.J., and Felson D.T. (1996) Musculoskeletal disease research: should we analyze the joint or the person? *Journal of Rheumatology* 23: 1130-1134.

Zioupos P. (2001) Accumulation of in-vivo fatigue microdamage and its relation to biomechanical properties in ageing human cortical bone. *Journal of Microscopy* 201: 270-278.